UIS: INTRODUCTION TO ORGANIC SPECTROSCOPY



University of Illinois, Springfield

LibreTexts™

University of Illinois, Springfield

UIS: Introduction to Organic Spectroscopy

This text is disseminated via the Open Education Resource (OER) LibreTexts Project (https://LibreTexts.org) and like the thousands of other texts available within this powerful platform, it is freely available for reading, printing, and "consuming."

The LibreTexts mission is to bring together students, faculty, and scholars in a collaborative effort to provide and accessible, and comprehensive platform that empowers our community to develop, curate, adapt, and adopt openly licensed resources and technologies; through these efforts we can reduce the financial burden born from traditional educational resource costs, ensuring education is more accessible for students and communities worldwide.

Most, but not all, pages in the library have licenses that may allow individuals to make changes, save, and print this book. Carefully consult the applicable license(s) before pursuing such effects. Instructors can adopt existing LibreTexts texts or Remix them to quickly build course-specific resources to meet the needs of their students. Unlike traditional textbooks, LibreTexts' web based origins allow powerful integration of advanced features and new technologies to support learning.



LibreTexts is the adaptable, user-friendly non-profit open education resource platform that educators trust for creating, customizing, and sharing accessible, interactive textbooks, adaptive homework, and ancillary materials. We collaborate with individuals and organizations to champion open education initiatives, support institutional publishing programs, drive curriculum development projects, and more.

The LibreTexts libraries are Powered by NICE CXone Expert and was supported by the Department of Education Open Textbook Pilot Project, the California Education Learning Lab, the UC Davis Office of the Provost, the UC Davis Library, the California State University Affordable Learning Solutions Program, and Merlot. This material is based upon work supported by the National Science Foundation under Grant No. 1246120, 1525057, and 1413739.

Any opinions, findings, and conclusions or recommendations expressed in this material are those of the author(s) and do not necessarily reflect the views of the National Science Foundation nor the US Department of Education.

Have questions or comments? For information about adoptions or adaptions contact info@LibreTexts.org or visit our main website at https://LibreTexts.org.

This text was compiled on 06/07/2025

TABLE OF CONTENTS

Licensing

1: Introduction to Organic Spectroscopy

- 1.1: 12.0 Introduction
- 1.2: 12.5 Spectroscopy and the Electromagnetic Spectrum
- 1.3: Electromagnetic Radiation
- 1.4: Introduction to Spectroscopy
- 1.5: The Power of the Fourier Transform for Spectroscopists
- 1.6: Time-resolved vs. Frequency Resolved

2: Mass Spectrometry

- 2.1: Introduction to Mass Spectrometry
- 2.2: Mass Spectrometry
- 2.3: How the Mass Spectrometer Works
  - Electrospray Ionization Mass Spectrometry
  - Injection Stage
  - MALDI-TOF
  - Mass Analyzers (Mass Spectrometry)
- 2.4: Interpretation of Mass Spectra
  - 13C
  - Br and Cl
  - Fragmentation
  - Fragmentation Patterns in Mass Spectra
  - Molecular Ions
  - Molecular Ion and Nitrogen
  - Organic Compounds Containing Halogen Atoms
  - The Molecular Ion (M^+) Peak
  - The M 1 Peak
- 2.5: Mass Spectrometry Problems
  - LEGO Exercise
- 2.6: ESI-QTOF-MS Coupled to HPLC and its Application for Food Safety

3: Infrared Spectroscopy

- 3.1: Infrared Spectroscopy
- 3.2: IR Spectroscopy
- 3.3: Theory
  - How an FTIR Spectrometer Operates
  - Theory
- 3.4: ATR-FTIR
- 3.5: Instrumentation
- 3.6: Sample Handling
- 3.7: Interpreting Infrared Spectra
- 3.8: Interpreting Infrared Spectra
  - Carbon Nitrogen Bonds
  - IR10. More Practice with IR Spectra

- IR2. Hydrocarbon Spectra
- IR3. Subtle Points of IR Spectroscopy
- IR4. Carbon Carbon Multiple Bonds
- IR5. Carbon Oxygen Single Bonds
- IR6. Carbon Oxygen Double Bonds
- IR8. More Complicated IR Spectra
- IR9. Misleading Peaks
- IR Table of Organic Compounds
- What Does an IR Spectrum Look Like?

- 3.9: Interpretation
- 3.10: Identifying the Presence of Particular Groups
- 3.11: Infrared Spectra of Some Common Functional Groups
- 3.12: Application

4: Conjugated Compounds and Ultraviolet Spectroscopy

- 4.1: Chapter Objectives
- 4.2: 14.0 Introduction
- 4.3: Molecular Orbital Theory
- 4.4: Allylic Carbocations
- 4.5: 14.3 Kinetic vs. Thermodynamic Control of Reactions
- 4.6: 14.4 The Diels-Alder Cycloaddition Reaction
- 4.7: 14.5 Characteristics of the Diels-Alder Reaction
- 4.8: Natural and Synthetic Rubbers
- 4.9: Ultraviolet Spectroscopy
- 4.10: The Effect of Conjugation
- 4.11: 14.9 Conjugation, Color, and the Chemistry of Vision
- 4.12: UV-Visible Spectroscopy
- Index

5: Proton Nuclear Magnetic Resonance Spectroscopy (NMR)

- 5.1: Nuclear Magnetic Resonance Spectroscopy
- 5.2: Introduction
- 5.3: NMR Spectroscopy
- 5.4: Theory
  - Bloch Equations
  - Larmor Precession
  - NMR Interactions
  - Quantum Mechanic Treatment
  - Relaxation
  - Rotations and Irreducible Tensor Operators
- 5.5: The Nature of NMR Absorptions
- 5.6: Interpretation
- 5.7: Interpretation
  - Integration in NMR
  - Pascal's Triangle
- 5.8: Structural Assignment
  - (n 1) Rule
  - Background to C-13 NMR
  - Determine Structure with Combined Spectra
  - High Resolution Proton NMR Spectra

- Integration in Proton NMR
- Interpreting C-13 NMR Spectra
- Introduction to Proton NMR
- Low Resolution Proton NMR Spectra
- More About Electronics
- Multiplicity in Proton NMR
- NMR11. More About Multiplicity
- NMR14. More Practice with NMR Spectroscopy
- NMR2. Carbon-13 NMR
- NMR3. Symmetry in NMR
- NMR4. 13C NMR and Geometry
- NMR5. 13C NMR and Electronics
- NMR8. Chemical Shift in 1H NMR
- NMR Appendix. Useful Charts for NMR identification

- 5.9: Active Learning with NMR
  - In-Class Questions
    - Set 1 – Basic Concepts
    - Set 2 – Energy Transition and Population
    - Set 3 – Electron Shielding
    - Set 4 – Nuclear Coupling
    - Set 5 – Exchange Effects
    - Set 6 – Classical Description
  - Instructor's Manual
  - Learning Objectives
  - Text
- 5.10: Chemical Shifts
- 5.11: \(^1H\) NMR Spectroscopy and Proton Equivalence
- 5.12: Chemical Shifts in \(^1H\) NMR Spectroscopy
- 5.13: Integration of Proton Spectra
- 5.14: Spin-Spin Splitting in \(^1H\) NMR Spectra
- 5.15: Chemical Equivalence
- 5.16: More Complex Spin-Spin Splitting Patterns
- 5.17: Uses of \(^1H\) NMR Spectroscopy

6: Carbon-13 NMR Spectroscopy

- 13.4 \(^13C\) NMR Spectroscopy: Signal Averaging and FT-NMR
- 13.5 Characteristics of \(^13C\) NMR Spectroscopy
- 13.7 Uses of \(^13C\) NMR Spectroscopy
- 6.1: Interpreting C-13 NMR Spectra

7: Two-Dimensional NMR Spectroscopy

- 13.6: DEPT ^{13}C NMR Spectroscopy
- 7.1: 2D NMR
  - 2D NMR Background
  - 2D NMR Basics
  - 2D NMR Experiments
  - 2D NMR Introduction
  - Heteronuclear Correlations
  - Homonuclear Correlations
  - Indirect Detection

- 7.2 J-Resolved

8: Multinuclear Magnetic Resonance Spectroscopy

Index

Glossary

Detailed Licensing

Licensing

*A detailed breakdown of this resource's licensing can be found in **Back Matter/Detailed Licensing**.*

CHAPTER OVERVIEW

1: Introduction to Organic Spectroscopy

1.1: 12.0 Introduction
1.2: 12.5 Spectroscopy and the Electromagnetic Spectrum
1.3: Electromagnetic Radiation
1.4: Introduction to Spectroscopy
1.5: The Power of the Fourier Transform for Spectroscopists
1.6: Time-resolved vs. Frequency Resolved

1: Introduction to Organic Spectroscopy is shared under a CC BY-NC-SA 4.0 license and was authored, remixed, and/or curated by LibreTexts.

1.1: 12.0 Introduction

Objective

After completing this section, you should be able to recognize the various spectroscopic techniques used to identify and characterize organic compounds.

Key Terms

Make certain that you can define, and use in context, the key term below.

- spectroscopy

Study Notes

The term spectroscopy is used to describe a number of techniques used by chemists to obtain information about the structure and bonding of chemical compounds. Four types of spectroscopy are described in the course:

1. mass spectroscopy (also called mass spectrometry, Chapter 12).
2. infrared spectroscopy (often simply called IR, Chapter 12).
3. nuclear magnetic resonance spectroscopy (usually referred to as NMR, Chapter 13).
4. ultraviolet spectroscopy (abbreviated UV, Chapter 14).

Of these four techniques, we shall spend the least time on ultraviolet spectroscopy, as it is much less powerful than the other three. If you do any reading on chemistry outside of the course materials, you will almost certainly see references to other spectroscopic techniques, such as Raman spectroscopy, electron spin resonance (ESR) spectroscopy, and atomic absorption (AA) spectroscopy. Even a description of these techniques and the information they can provide is beyond the scope of this course.

Contributors and Attributions

- Dr. Dietmar Kennepohl FCIC (Professor of Chemistry, Athabasca University)

1.1: 12.0 Introduction is shared under a CC BY-NC-SA 4.0 license and was authored, remixed, and/or curated by LibreTexts.

1.2: 12.5 Spectroscopy and the Electromagnetic Spectrum

Objectives

After completing this section, you should be able to

1. write a brief paragraph discussing the nature of electromagnetic radiation.
2. write the equations that relate energy to frequency, frequency to wavelength and energy to wavelength, and perform calculations using these relationships.
3. describe, in general terms, how absorption spectra are obtained.

Key Terms

Make certain that you can define, and use in context, the key terms below.

- electromagnetic radiation
- electromagnetic spectrum
- hertz (Hz)
- infrared spectroscopy
- photon
- quantum

Study Notes

From your studies in general chemistry or physics, you should be familiar with the idea that electromagnetic radiation is a form of energy that possesses wave character and travels through space at a speed of $3.00 \times 10^8 \text{m} \cdot \text{s}^{-1}$. However, such radiation also displays some of the properties of particles, and on occasion it is more convenient to think of electromagnetic radiation as consisting of a stream of particles called *photons*.

In spectroscopy, the frequency of the electromagnetic radiation being used is usually expressed in *hertz* (*Hz*), that is, cycles per second. Note that $1 \text{ Hz} = \text{s}^{-1}$.

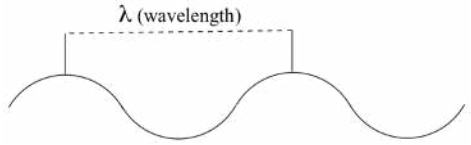
A *quantum* is a small, definite quantity of electromagnetic radiation whose energy is directly proportional to its frequency. (The plural is "quanta.") If you wish, you can read about the properties of electromagnetic radiation and the relationships among wavelength, frequency and energy, or refer to your general chemistry textbook if you still have it.

Note also that in SI units, Planck's constant is $6.626 \times 10^{-34} \text{ J} \cdot \text{s}$.

The electromagnetic spectrum

Electromagnetic radiation, as you may recall from a previous chemistry or physics class, is composed of electrical and magnetic waves which oscillate on perpendicular planes. Visible light is electromagnetic radiation. So are the gamma rays that are emitted by spent nuclear fuel, the x-rays that a doctor uses to visualize your bones, the ultraviolet light that causes a painful sunburn when you forget to apply sun block, the infrared light that the army uses in night-vision goggles, the microwaves that you use to heat up your frozen burritos, and the radio-frequency waves that bring music to anybody who is old-fashioned enough to still listen to FM or AM radio.

Just like ocean waves, electromagnetic waves travel in a defined direction. While the speed of ocean waves can vary, however, the speed of electromagnetic waves – commonly referred to as the speed of light – is essentially a constant, approximately 300 million meters per second. This is true whether we are talking about gamma radiation or visible light. Obviously, there is a big difference between these two types of waves – we are surrounded by the latter for more than half of our time on earth, whereas we hopefully never become exposed to the former to any significant degree. The different properties of the various types of electromagnetic radiation are due to differences in their wavelengths, and the corresponding differences in their energies: *shorter wavelengths correspond to higher energy.*



High-energy radiation (such as gamma- and x-rays) is composed of very short waves – as short as 10^{-16} meter from crest to crest. Longer waves are far less energetic, and thus are less dangerous to living things. Visible light waves are in the range of 400 – 700 nm (nanometers, or 10^{-9} m), while radio waves can be several hundred meters in length.

The notion that electromagnetic radiation contains a quantifiable amount of energy can perhaps be better understood if we talk about light as a stream of *particles*, called **photons**, rather than as a wave. (Recall the concept known as 'wave-particle duality': at the quantum level, wave behavior and particle behavior become indistinguishable, and very small particles have an observable 'wavelength'). If we describe light as a stream of photons, the energy of a particular wavelength can be expressed as:

$$E = \frac{hc}{\lambda} \tag{12.5.1}$$

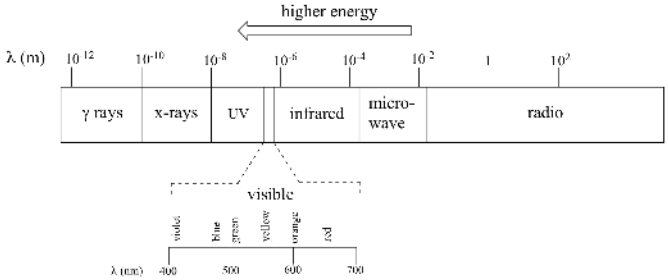
where E is energy in J, **λ** (the Greek letter *lambda*) is wavelength in meters, *c* is 3.00 x 10^8 m/s (the speed of light), and *h* is 6.626 × 10^{-34} J · s, a number known as Planck's constant.

Because electromagnetic radiation travels at a constant speed, each wavelength corresponds to a given frequency, which is the number of times per second that a crest passes a given point. Longer waves have lower frequencies, and shorter waves have higher frequencies. Frequency is commonly reported in hertz (Hz), meaning 'cycles per second', or 'waves per second'. The standard unit for frequency is s^{-1}.

When talking about electromagnetic waves, we can refer either to wavelength or to frequency - the two values are interconverted using the simple expression:

$$\lambda\nu = c \tag{12.5.2}$$

where **ν** (the Greek letter '*nu*') is frequency in s^{-1}. Visible red light with a wavelength of 700 nm, for example, has a frequency of 4.29 x 10^{14} Hz, and an energy of 2.84 x 10^{-19} J per photon or 171 kJ per mole of photons (remember Avogadro's number = 6.02 × 10^{23} mol^{-1}). The full range of electromagnetic radiation wavelengths is referred to as the **electromagnetic spectrum**.



Notice in the figure above that visible light takes up just a narrow band of the full spectrum. White light from the sun or a light bulb is a mixture of all of the visible wavelengths. You see the visible region of the electromagnetic spectrum divided into its different wavelengths every time you see a rainbow: violet light has the shortest wavelength, and red light has the longest.

Example 12.5.1

Visible light has a wavelength range of about 400-700 nm. What is the corresponding frequency range? What is the corresponding energy range, in kJ mol^{-1} of photons?

Answer

Add texts here. Do not delete this text firstFor light with a wavelength of 400 nm, the frequency is 7.50 × 10^{14} Hz:

$$\nu = \frac{3 \times 10^8 \text{ m s}^{-1}}{400 \times 10^{-9} \text{ m}} = 7.50 \times 10^{14} \text{ s}^{-1}$$

In the same way, we calculate that light with a wavelength of 700 nm has a frequency of 4.29 × 10^{14} Hz.

To calculate corresponding energies using hc/λ. We find for light at 400 nm:

$$E = \frac{(6.626 \times 10^{-34}\ \text{J s mol}^{-1})(3.00 \times 10^{8}\ \text{m s}^{-1})}{400 \times 10^{-9}\ \text{m}}$$

$$= 4.97 \times 10^{-19}\ \text{J per photon}$$

$$E\ (\text{one mole}) = E \times N$$

$$= (4.97 \times 10^{-19}\ \text{J})(6.02 \times 10^{23}\ \text{mol}^{-1})$$

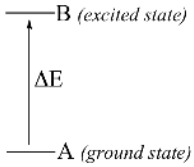
$$= 299\ \text{kJ mol}^{-1}$$

Using the same equation, we find that light at 700 nm corresponds to 171 kJ mol^{-1}.

Molecular spectroscopy – the basic idea

In a spectroscopy experiment, electromagnetic radiation of a specified range of wavelengths is allowed to pass through a sample containing a compound of interest. The sample molecules absorb energy from some of the wavelengths, and as a result jump from a low energy 'ground state' to some higher energy 'excited state'. Other wavelengths are *not* absorbed by the sample molecule, so they pass on through. A detector on the other side of the sample records which wavelengths were absorbed, and to what extent they were absorbed.

Here is the key to molecular spectroscopy: *a given molecule will specifically absorb only those wavelengths which have energies that correspond to the energy difference of the transition that is occurring.* Thus, if the transition involves the molecule jumping from ground state A to excited state B, with an energy difference of **Δ**E, the molecule will specifically absorb radiation with wavelength that corresponds to **Δ**E, while allowing other wavelengths to pass through unabsorbed.



By observing which wavelengths a molecule absorbs, and to what extent it absorbs them, we can gain information about the nature of the energetic transitions that a molecule is able to undergo, and thus information about its structure.

These generalized ideas may all sound quite confusing at this point, but things will become much clearer as we begin to discuss specific examples.

Exercises

? Exercise 1.2.1

Which of the following frequencies/wavelengths are higher energy

A. $\lambda = 2.0 \times 10^{-6}$ m or $\lambda = 3.0 \times 10^{-9}$ m

B. $\upsilon = 3.0 \times 10^{9}$ Hz or $\upsilon = 3.0 \times 10^{-6}$ Hz

Answer

A. $\lambda = 3.0 \times 10^{-9}$ m

B. $\upsilon = 3.0 \times 10^{9}$ Hz

Exercise 1.2.2

Calculate the energies (J) for the following;

A – Gamma Ray $\lambda = 4.0 \times 10^{-11}$ m

B – X-Ray $\lambda = 4.0 \times 10^{-9}$ m

C – UV light $\upsilon = 5.0 \times 10^{15}$ Hz

D – Infrared Radiation $\lambda = 3.0 \times 10^{-5}$ m

E – Microwave Radiation $\upsilon = 3.0 \times 10^{11}$ Hz

Answer

The following are in joules.

A – 4.96×10^{-15}

B – 4.96×10^{-17}

C – 3.31×10^{-18}

D – 6.62×10^{-21}

E – 1.99×10^{-22}

Contributors and Attributions

- Dr. Dietmar Kennepohl FCIC (Professor of Chemistry, Athabasca University)
- Prof. Steven Farmer (Sonoma State University)
- William Reusch, Professor Emeritus (Michigan State U.), Virtual Textbook of Organic Chemistry

1.2: 12.5 Spectroscopy and the Electromagnetic Spectrum is shared under a CC BY-NC-SA 4.0 license and was authored, remixed, and/or curated by LibreTexts.

1.3: Electromagnetic Radiation

As you read the print off this computer screen now, you are reading pages of fluctuating energy and magnetic fields. Light, electricity, and magnetism are all different forms of electromagnetic radiation.

Introduction

Electromagnetic radiation is a form of energy that is produced by oscillating electric and magnetic disturbance, or by the movement of electrically charged particles traveling through a vacuum or matter. The electric and magnetic fields come at right angles to each other and combined wave moves perpendicular to both magnetic and electric oscillating fields thus the disturbance. Electron radiation is released as photons, which are bundles of light energy that travel at the speed of light as quantized harmonic waves. This energy is then grouped into categories based on its wavelength into the electromagnetic spectrum. These electric and magnetic waves travel perpendicular to each other and have certain characteristics, including amplitude, wavelength, and frequency.

General Properties of all electromagnetic radiation:

1. Electromagnetic radiation can travel through empty space. Most other types of waves must travel through some sort of substance. For example, sound waves need either a gas, solid, or liquid to pass through in order to be heard.
2. The speed of light is always a constant. (Speed of light : 2.99792458 x 10^8 m s^{-1})
3. Wavelengths are measured between the distances of either crests or troughs. It is usually characterized by the Greek symbol λ.

Waves and their Characteristics

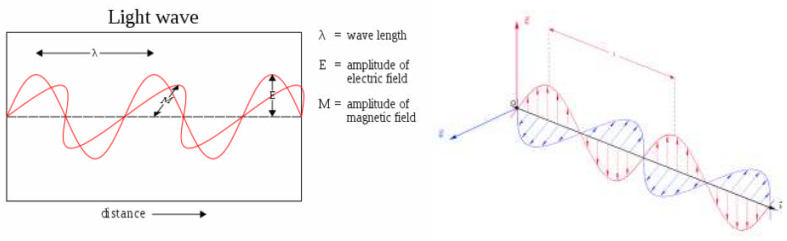


Fig. 1 & 2: Electromagnetic Waves

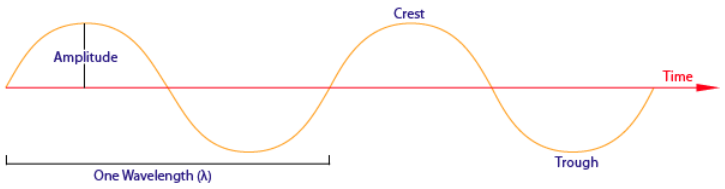


Fig. 3: An EM Wave

Amplitude

Amplitude is the distance from the maximum vertical displacement of the wave to the middle of the wave. This measures the magnitude of oscillation of a particular wave. In short, the amplitude is basically the height of the wave. Larger amplitude means higher energy and lower amplitude means lower energy. Amplitude is important because it tells you the intensity or brightness of a wave in comparison with other waves.

Wavelength

Wavelength (λ) is the distance of one full cycle of the oscillation. Longer wavelength waves such as radio waves carry low energy; this is why we can listen to the radio without any harmful consequences. Shorter wavelength waves such as x-rays carry higher energy that can be hazardous to our health. Consequently lead aprons are worn to protect our bodies from harmful radiation when we undergo x-rays. This wavelength frequently relationship is characterized by:

$$c = \lambda\nu \tag{1.3.1}$$

where

- c is the speed of light,
- λ is wavelength, and
- ν is frequency.

Shorter wavelength means greater frequency, and greater frequency means higher energy. Wavelengths are important in that they tell one what type of wave one is dealing with.

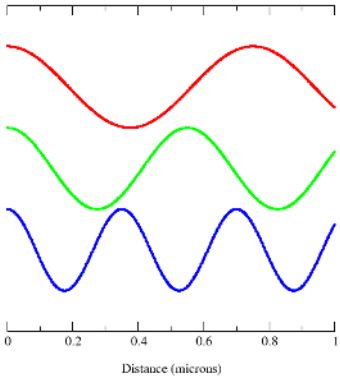


Fig. 4: Different Wavelengths and Frequencies

Remember, **Wavelength tells you the type of light** and **Amplitude tells you about the intensity of the light**

Frequency

Frequency is defined as the number of cycles per second, and is expressed as sec^{-1} or Hertz (Hz). Frequency is directly proportional to energy and can be express as:

$$E = h\nu \tag{1.3.2}$$

where

- E is energy,
- h is Planck's constant, (h= 6.62607 x 10^{-34} J), and
- ν is frequency.

Period

Period (T) is the amount of time a wave takes to travel one wavelength; it is measured in seconds (s).

Velocity

The velocity of wave in general is expressed as:

$$velocity = \lambda\nu \tag{1.3.3}$$

For Electromagnetic wave, the velocity in vacuum is $2.99 \times 10^8\ m/s$ or $186,282$miles/second.

Electromagnetic spectrum

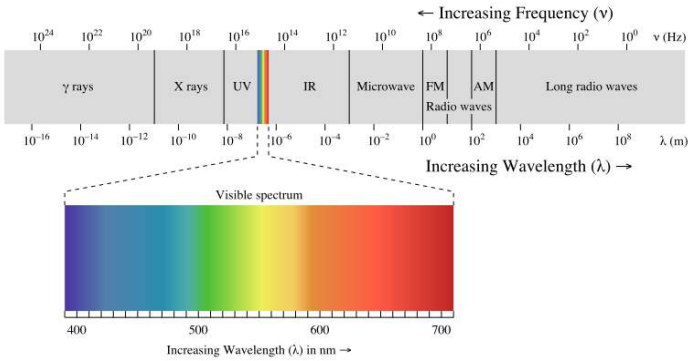


***Figure 24.5.1**: Electromagnetic spectrum with light highlighted. from Wikipedia.*

As a wave's wavelength increases, the frequency decreases, and as wave's wavelength decreases, the frequency increases. When electromagnetic energy is released as the energy level increases, the wavelength decreases and frequency decreases. Thus, electromagnetic radiation is then grouped into categories based on its wavelength or frequency into the electromagnetic spectrum. The different types of electromagnetic radiation shown in the electromagnetic spectrum consists of radio waves, microwaves, infrared waves, visible light, ultraviolet radiation, X-rays, and gamma rays. The part of the electromagnetic spectrum that we are able to see is the visible light spectrum.

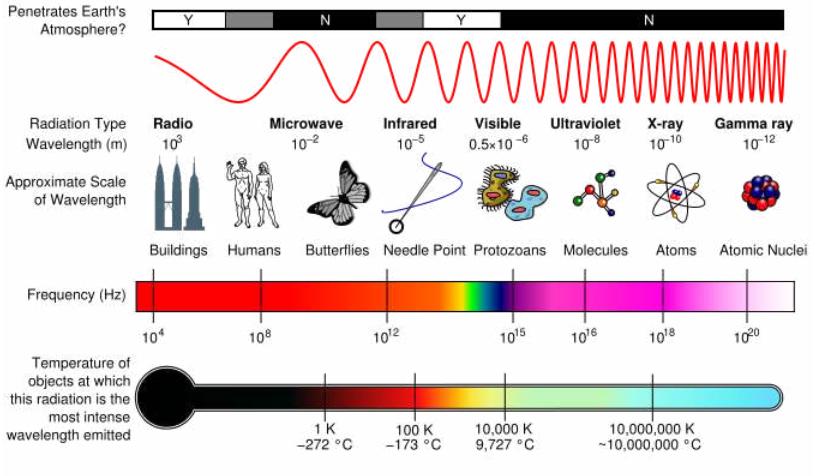


Fig. 6: Electromagnetic Spectrum with Radiation Types

Radiation Types

Radio Waves are approximately 10^{3} m in wavelength. As the name implies, radio waves are transmitted by radio broadcasts, TV broadcasts, and even cell phones. Radio waves have the lowest energy levels. Radio waves are used in remote sensing, where hydrogen gas in space releases radio energy with a low frequency and is collected as radio waves. They are also used in radar systems, where they release radio energy and collect the bounced energy back. Especially useful in weather, radar systems are used to can illustrate maps of the surface of the Earth and predict weather patterns since radio energy easily breaks through the atmosphere. ;

Microwaves can be used to broadcast information through space, as well as warm food. They are also used in remote sensing in which microwaves are released and bounced back to collect information on their reflections.

Microwaves can be measured in centimeters. They are good for transmitting information because the energy can go through substances such as clouds and light rain. Short microwaves are sometimes used in Doppler radars to predict weather forecasts.

Infrared radiation can be released as heat or thermal energy. It can also be bounced back, which is called near infrared because of its similarities with visible light energy. Infrared Radiation is most commonly used in remote sensing as infrared sensors collect thermal energy, providing us with weather conditions.

This picture represents a snap shot in mid-infrared light.

Visible Light is the only part of the electromagnetic spectrum that humans can see with an unaided eye. This part of the spectrum includes a range of different colors that all represent a particular wavelength. Rainbows are formed in this way; light passes through matter in which it is absorbed or reflected based on its wavelength. Thus, some colors are reflected more than other, leading to the creation of a rainbow.

Color Region	Wavelength (nm)

Violet	380-435
Blue	435-500
Cyan	500-520
Green	520-565
Yellow	565-590
Orange	590-625
Red	625-740

Fig. 7: The color regions of the Visible Spectrum

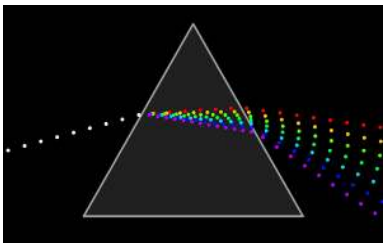


Fig. 8: Dispersion of Light Through A Prism

Ultraviolet, Radiation, X-Rays, and Gamma Rays are all related to events occurring in space. UV radiation is most commonly known because of its severe effects on the skin from the sun, leading to cancer. X-rays are used to produce medical images of the body. Gamma Rays can used in chemotherapy in order to rid of tumors in a body since it has such a high energy level. The shortest waves, Gamma rays, are approximately 10^{-12} m in wavelength. Out this huge spectrum, the human eyes can only detect waves from 390 nm to 780 nm.

Equations of Waves

The mathematical description of a wave is:

$$y = A\sin(kx - \omega t) \tag{1.3.4}$$

where A is the amplitude, k is the wave number, x is the displacement on the x-axis.

$$k = \frac{2\pi}{\lambda} \tag{1.3.5}$$

where λ is the wavelength. Angular frequency described as:

$$\omega = 2\pi\nu = \frac{2\pi}{T} \tag{1.3.6}$$

where ν is frequency and period (T) is the amount of time for the wave to travel one wavelength.

Interference

An important property of waves is the ability to combine with other waves. There are two type of interference: constructive and destructive. Constructive interference occurs when two or more waves are in phase and and their displacements add to produce a higher amplitude. On the contrary, destructive interference occurs when two or more waves are out of phase and their displacements negate each other to produce lower amplitude.

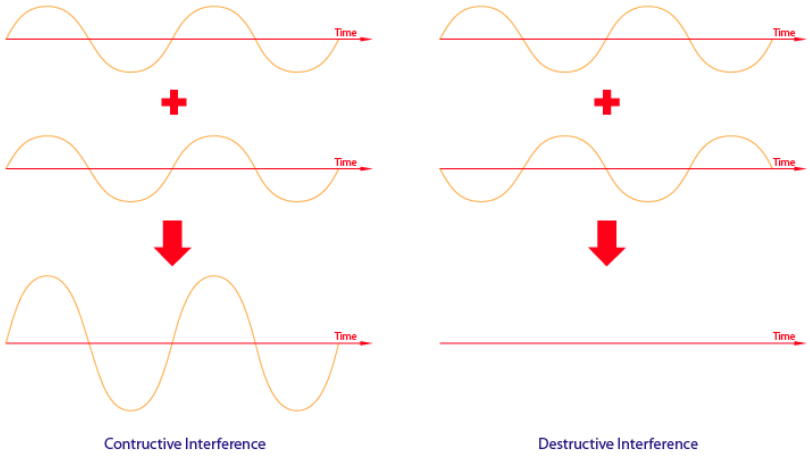


Figure 9 & 10: Constructive and Destructive Interference

Interference can be demonstrated effectively through the double slit experiment. This experiment consists of a light source pointing toward a plate with one slit and a second plate with two slits. As the light travels through the slits, we notice bands of alternating intensity on the wall behind the second plate. The banding in the middle is the most intense because the two waves are perfectly in phase at that point and thus constructively interfere. The dark bands are caused by out of phase waves which result in destructive interference. This is why you observe nodes on figure 4. In a similar way, if electrons are used instead of light, electrons will be represented both as waves and particles.

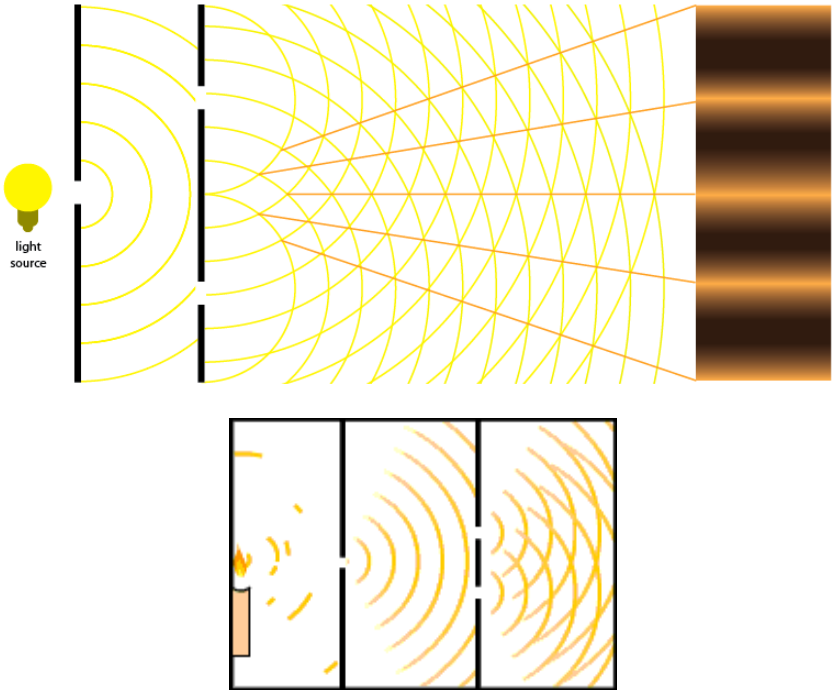


Fig. 11 & 12: Double-Slit Interference Experiment

Wave-Particle Duality

Electromagnetic radiation can either acts as a wave or a particle, a photon. As a wave, it is represented by velocity, wavelength, and frequency. Light is an EM wave since the speed of EM waves is the same as the speed of light. As a particle, EM is represented as a photon, which transports energy. When a photon is absorbed, the electron can be moved up or down an energy level. When it moves up, it absorbs energy, when it moves down, energy is released. Thus, since each atom has its own distinct set of energy

levels, each element emits and absorbs different frequencies. Photons with higher energies produce shorter wavelengths and photons with lower energies produce longer wavelengths.

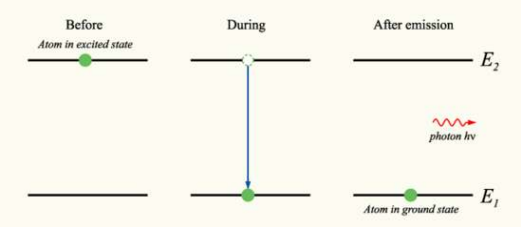


Fig. 13: Photon Before and After Emission

Ionizing and Non-Ionizing Radiation

Electromagnetic Radiation is also categorized into two groups based, ionizing and non-ionizing, on the severity of the radiation. Ionizing radiation holds a great amount of energy to remove electrons and cause the matter to become ionized. Thus, higher frequency waves such as the X-rays and gamma-rays have ionizing radiation. However, lower frequency waves such as radio waves, do not have ionizing radiation and are grouped as non-ionizing.

Electromagnetic Radiation and Temperature

Electromagnetic radiation released is related to the temperature of the body. Stephan-Boltzmann Law says that if this body is a black body, one which perfectly absorbs and emits radiation, the radiation released is equal to the temperature raised to the fourth power. Therefore, as temperature increases, the amount of radiation released increases greatly. Objects that release radiation very well also absorb radiation at certain wavelengths very well. This is explained by the Kirchhoff's Law. Wavelengths are also related to temperature. As the temperature increases, the wavelength of maximum emission decreases.

Problems

1. What is the wavelength of a wave with a frequency of 4.28 Hz?
2. What is the frequency of a wave with a wavelength of 200 cm?
3. What is the frequency of a wave with a wavelength of 500 pm?
4. What is the wavelength of a wave with a frequency of 2.998×10^5 Hz?
5. A radio transmits a frequency of 100 Hz. What is the wavelength of this wave?

Answers:

1. 700m
2. 1.5×10^8 Hz
3. 4.0×10^{17} Hz
4. 100m
5. 2.998×10^6 m

References

1. Atkins, Peter and Julio de Paula. Physical Chemistry for the Life Sciences. New York: Oxford University Press, 2006.
2. Chang, Raymond. Physical Chemistry for the Biosciences. USA: University Science Books, 2005.
3. McQuarrie, Donald and Simon, John. Physical Chemistry: A Molecular Approach. Sausalito, CA: University Science Books, 1997.
4. Price, Nicholas and Dwek, Raymond and Wormald, Mark. Principles and Problems in Physical Chemistry for Biochemists. R. G. Ratcliffe. New York: Oxford University Press, 1997.

1.3: Electromagnetic Radiation is shared under a CC BY-NC-SA 4.0 license and was authored, remixed, and/or curated by LibreTexts.

- **Electromagnetic Radiation** by Kevin Vo, Mateo Hernandez, Nikita Patel is licensed CC BY 4.0.

1.4: Introduction to Spectroscopy

Realizing that light may be considered to have both wave-like and particle-like characteristics, it is useful to consider that a given frequency or wavelength of light is associated with a "light quanta" of energy we now call a **photon**. As noted in the following equations, frequency and energy change proportionally, but wavelength has an inverse relationship to these quantities.

$$\nu = \frac{c}{\lambda} \tag{1.4.1}$$

and

$$\Delta E = h\nu \tag{1.4.2}$$

with

- ν is the frequency of light
- λ is the wavelength of ligt
- c is the speed of light ($3 \times 10^8\ m/sec$)
- ΔE is the transition energy (difference of energies between the initial and final states)
- h is Planck's constant ($h = 6.626069 \times 10^{-34}\ J\,s$)

To "see" a molecule, we must use light having a wavelength smaller than the molecule itself (roughly 1 to 15 angstroms). Such radiation is found in the X-ray region of the spectrum, and the field of **X-ray crystallography** yields remarkably detailed pictures of molecular structures amenable to examination. The chief limiting factor here is the need for high quality crystals of the compound being studied. The methods of X-ray crystallography are too complex to be described here; nevertheless, as automatic instrumentation and data handling techniques improve, it will undoubtedly prove to be the procedure of choice for structure determination. The spectroscopic techniques described below do not provide a three-dimensional picture of a molecule, but instead yield information about certain characteristic features. A brief summary of this information follows:

- **Ultraviolet-Visible Spectroscopy**: Absorption of this relatively high-energy light causes electronic excitation. The easily accessible part of this region (wavelengths of 200 to 800 nm) shows absorption only if conjugated π electron systems are present.
- **Infrared Spectroscopy**: Absorption of this lower energy radiation causes vibrational and rotational excitation of groups of atoms. within the molecule. Because of their characteristic absorptions, identification of functional groups is easily accomplished.
- **Nuclear Magnetic Resonance (NMR) Spectroscopy**: Absorption in the low-energy radio-frequency part of the spectrum causes excitation of nuclear spin states. NMR spectrometers are tuned to certain nuclei (e.g. ^{1}H, ^{13}C, ^{19}F & ^{31}P). For a given type of nucleus, high-resolution spectroscopy distinguishes and counts atoms in different locations in the molecule.

1.4: Introduction to Spectroscopy is shared under a CC BY-NC-SA 4.0 license and was authored, remixed, and/or curated by LibreTexts.

- **Introduction to Spectroscopy** by William Reusch is licensed CC BY-NC-SA 4.0.

1.5: The Power of the Fourier Transform for Spectroscopists

Fourier transform is a mathematical technique that can be used to transform a function from one real variable to another. It is a unique powerful tool for spectroscopists because a variety of spectroscopic studies are dealing with electromagnetic waves covering a wide range of frequency. In Fourier transform term $e^{-2\pi ixy}$, when x represents frequency, the corresponding y is time. This provides an alternate way to process signal in time domain instead of the conventional frequency domain. To realize this idea, Fourier transform from time domain to frequency domain is the essential process that enable us to translate raw data to readable spectra. Recent prosperity of Fourier transform in spectroscopy should also attribute to the development of efficient Fast Fourier Transform algorithm.

Introduction

The nature of trigonometric function enables Fourier transform to convert a function from the domain of one variable to another and reconstruct it later on. This is a robust mathematical tool to process data in different domains under different circumstances. Taking this principal idea and applying it in spectroscopy showed many impressive results in the early stage, which in other ways are very difficult to resolve. These benefits triggered a wide exploration of Fourier transform based methodology in a variety of spectroscopic techniques. At the same time, Fourier transform spectroscopic instruments are developed with great efforts by physicists and engineers. All these factors give rise to the wide use of Fourier transform spectroscopy.

In the following topics, the relevant mathematical background, the implementation of Fourier transform in spectroscopy and a brief overview of various Fourier transform Spectrometers will be addressed in sequence.

Fourier Series

The motivation of Fourier transform arises from Fourier series, which was proposed by French mathematician and physicist Joseph Fourier when he tried to analyze the flow and the distribution of energy in solid bodies at the turn of the 19th century. He claimed that the temperature distribution could be described as an infinite series of sines and cosines of the form shown in equation (1):

$$f(x) = \frac{a_0}{2} + \sum_{n=1}^{\infty} \left(a_n \cos \frac{n\pi x}{L} + b_n \sin \frac{n\pi x}{L} \right) \tag{1}$$

It turns out that this combination of sines and cosines series can be used to express any periodical function. As n increases, the series will approach to the original function more closely.

If we use Euler's Identity (equation 2), as well as the exponential representations of sine (equation 3} and cosine (equation 4) in our Fourier Series, we will find a natural redefinition of our coefficients a_n and b_n into a single complex coefficient C_n (equation 5).

$$e^{i\theta} = \cos\theta + i\sin\theta \tag{2}$$

$$\cos\theta = \frac{1}{2}(e^{i\theta} + e^{-i\theta}) \tag{3}$$

$$\sin\theta = \frac{1}{2i}(e^{i\theta} - e^{-i\theta}) \tag{4}$$

$$C_n = \frac{1}{2}(C_n - ib_n) \tag{5}$$

Using a bit of clever mathematics (complex conjugation, properties of odd function, rearranging summation set) we can represent our original Fourier series in terms of a complex exponential, shown as equation 6.

$$f(x) = \sum_{n=-\infty}^{\infty} C_n e^{i\theta} \tag{6a}$$

$$\theta = \frac{2\pi n x}{L} \tag{6b}$$

Writing the Fourier series in this exponential form helps to simplify many formulas and expressions involved in the transformation.

Fourier Transform

Then we can consider an extreme case, when L in equation 1, the summation becomes an integral as shown in equation (4)

$$f(x) = \sum_{-\infty}^{\infty} c_n e^{n\frac{i\pi x}{L}} = \int_{-\infty}^{\infty} c_n e^{n\frac{i\pi x}{L}} dn = \int_{-\infty}^{\infty} c_n e^{\frac{i\pi xn}{L}} dn \tag{7}$$

This naturally gives the Fourier transform pair of f(x) and F(y). The relationships are shown below :

$$F(y) = \int_{-\infty}^{+\infty} f(x) e^{-i2\pi yx} dx \tag{8a}$$

$$f(x) = \int_{-\infty}^{+\infty} F(y) e^{i2\pi xy} dx \tag{8b}$$

Another important formula widely used to benefit In other cases, it is used to simplify the integral in the Fourier transform based on the symmetry of the function. But so far, all these are just about mathematics. Its story with spectroscopy should start from the mathematical description of electromagnetic waves.

Mathematical description of electromagnetic waves

Maxwell–Faraday equation and Ampère's circuital law give us electromagnetic wave equations to describe the characteristics of an electromagnetic wave.[1] Using the linearity of Maxwell's equations in a vacuum, the solutions of the equation can be decomposed into a superposition of sinusoids as shown below[3]:

$$E(r,t) = \overrightarrow{E_0} \cos(2\pi ft - \overrightarrow{k} \cdot r + \phi_0) \tag{9a}$$

$$B(r,t) = \overrightarrow{B_0} \cos(2\pi ft - \overrightarrow{k} \cdot r + \phi_0) \tag{9b}$$

Where t is time, f is the frequency, k=(k_x,k_y,k_z) is the wave vector and ϕ is the phase angle.

This indicates that electromagnetic wave can be written as the sum of trigonometric functions with specific frequencies. Scientists already discovered the fact that frequency and time is a classic Fourier transform pair in Fourier transform relationship. All the Fourier transform pairs are connected by the Fourier transform term $e^{-i2\pi yx}$. Regarding this case, we can use the term to transform between two variables in this pair, namely time and frequency. In this way, we can measure the properties of the electromagnetic wave in both conventional frequency domain and somehow more robust time domain.

Applying Fourier Transform-Fourier Transform Spectroscopy

Fourier transform are widely involved in spectroscopy in all research areas that require high accuracy, sensitivity, and resolution. All these spectroscopic techniques using Fourier transform are considered Fourier transform spectroscopy. By definition, Fourier transform spectroscopy is a spectroscopic technique where interferograms are collected by measurements of the coherence of an electromagnetic radiation source in the time-domain or space-domain, and translated into frequency domain through Fourier transform.

Interferometer-What it is used for and how it works?

How to introduce a time-domain or space-domain variable in the spectrometer is the primary question that needed to be addressed when we consider constructing a Fourier transform spectrometer. In the experimental set-up, a Michelson interferometer is commonly used to solve this problem. Different from the classical Michelson interferometer with two fixed mirrors (***Figure 1.a***), the interferometer used in Fourier transform spectrometer has a moving mirror at one arm (***Figure 1.b***).

a. b.

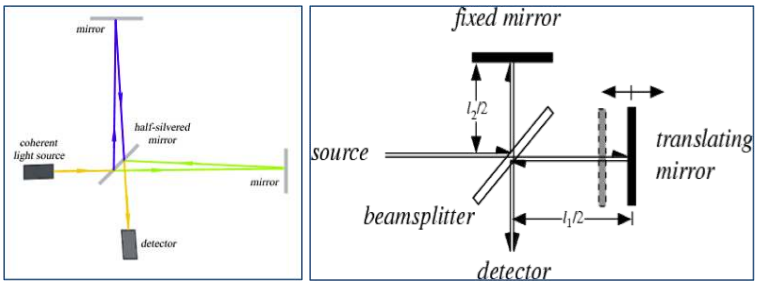


Figure 1. Scheme for Michelson interferometer [components: coherent light source; half-silvered beam-splitting mirror; two highly polished reflective mirrors; detector] ***(a)*** Stationary version [two fixed mirrors] ***(b)*** Movable version [One movable mirror and one movable mirror]

As shown in Figure 1.b, when a parallel beam of coherent light hits a half-silvered mirror, it is divided into two beams of equal intensities by partial reflection and transmission. After being reflected back, the two beams meet at the half-silvered mirror and recombine to produce an interference pattern, which is later detected by the detector. Manipulating the difference between these two paths of light is the core of Michelson interferometer. If these two paths differ by a whole number of wavelengths, the resulting constructive interference will give a strong signal at the detector. If they differ by a whole number and a half of wavelengths, destructive interference will cancel the intensity of the signal.

Measuring Interferograms

With a Fourier transform spectrometer equipped with an interferometer, we can easily vary the parameter in time domain or spatial domain by changing the position of the movable mirror.

But how data are collected by a Fourier transform spectrometer? A quick comparison between a conventional spectrometer and a Fourier transform Spectrometer may help to find the answer.

- Conventional spectrometer:

Monochromator is commonly used. It can block off all other wavelengths except for a certain wavelength of interest. Then measuring the intensity of a monochromic light with that particular wavelength becomes practical. To collect the full spectrum over a wide wavelength range, monochromator needs to vary the wavelength setting every time.

- Fourier transform spectrometer:

Rather than allowing only one wavelength to pass through the sample at a time, an interferometer can let through a beam with the whole wavelength range at once, and measure the intensity of the total beam at that optical path difference. Then by changing the position of the moving mirror, a different optical path difference is modified and the detector can measure another intensity of the total beam as the second data point. If the beam is modified for each new data point by scanning the moving mirror along the axis of the moving arm, a series of intensity versus each optical path length difference are collected.

So instead of obtaining a scan spectrum directly, raw data recorded by the detector in a Fourier transform spectrometer is less intuitive to reveal the property of the sample. The raw data is actually the intensity of the interfering wave versus the optical path difference (also called Interferogram). The spectrum of the sample is actually encoded into this interferogram.

Extracting the spectrum from raw data

Based on the previous discussion, it is predictable that, without further translation, the raw data collected on a Fourier transform spectrometer will be quite difficult to read. A Fourier transform needs to be performed to decode interferogram and extract actual spectrum I($\bar{v}$) from it. The following shows how to conduct a Fourier transform to decode:

The intensity collected by the detector is a function of the path length differences in the interferometer p and wavenumber $\bar{v}$[3]:

$$I(p,\bar{v}) = I(\bar{v})[1+\cos(2\pi\bar{v}p)] \tag{9}$$

Thus, the total intensity measured at a certain optical path length difference (for each data point at a certain optical pathlength difference p) is:

$$I(p) = \int_0^\infty I(p,\bar{v}) = I(\bar{v})[1+\cos(2\pi\bar{v}p)]\cdot d\bar{v} \tag{10}$$

It shows that they have a cosine Fourier transform relationship. So by computing an inverse Fourier transform, we can resolve the desired spectrum in terms of the measured raw data I(p) (10):

$$I(\bar{v}) = 4\int_0^{\infty} [I(p) - \frac{1}{2}I(p=0)]\cos(2\pi\bar{v}p)\cdot dp \tag{11}$$

An example to illustrate the raw data and the resolved spectrum is also shown in ***Figure 2***.

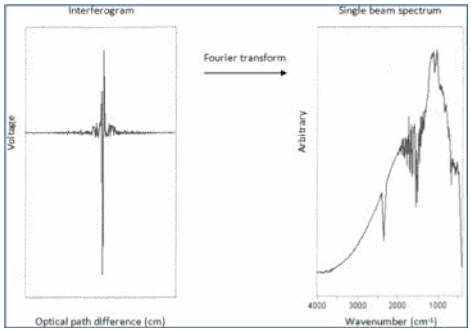


Figure 2. Fourier transform between interferogram and actual spectrum[4]

The Fast Fourier Transform (FFT)

Fast Fourier Transform (FFT) is a very efficient algorithm to compute Fourier transform. It applies to Discrete Fourier Transform (DFT) and its inverse transform. DFT is a method that decomposes a sequence of signals into a series of components with different frequency or time intervals. This operation is useful in many fields, but in most cases computing it directly from definition is too slow to be practical. Fast Fourier Transform algorithm can help to reduce DFT computation time by several orders of magnitude without losing the accuracy of the result. This benefit becomes more significant when the number of the components is very large. FFT is considered a huge improvement to make many DFT-based algorithms practical. In Fourier transform spectrometer, signals are often collected by a series of optical or digital channels at the detector. Then FFT is of great importance to quickly achieve the following signal processing and data extraction based on DFT method.

Combining all these steps together, we can take a look at how the data from the sample are processed. The diagram is shown in ***Figure 3***.

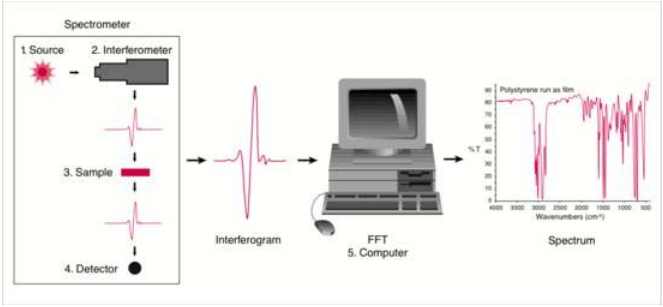


Figure 3. *Data processing in FTIR*

(Figure from ThermoNiolet at *mmrc.caltech.edu/FTIR/FTIRintro.pdf*)

Different operating modes in Fourier Transform Spectrometer

- *Continuous/Scanning FTS*

Continuous Fourier transform spectroscopy refers to the scanning form of FTS, in which by step moving one mirror, the whole range of optical path difference is measured. This is the most widely used mode in FTS, like most absorption spectra and emission spectra obtained by FTS.

- *Pulsed FTS*

In some Fourier transform spectrometers, depending on the feature of the involved spectroscopic technique and purpose of measurement, a pulsed Fourier transform technique may be applied instead of the scanning mode.

Pulsed FTS is different from conventional continuous FTS. It is not based on the transmittance technique, which is widely used in the absorption spectra, like FTIR. Instead, in pulse FTS, the idea is that the sample is first exposed to an energizing event, and this pulse induces a periodic response. The frequency of this response relative to the field strength is determined by the properties of the sample. Using Fourier transform to resolve the frequency will tell the information about the targeted analyte.

Pulse FTS is a relatively new improvement of FTS. Some examples are from pulse-Fourier Transform-Nuclear Magnetic Resonnance (FT-NMR), pulse-Fourier Transform-Electron Paramagnetic Resonnance (FFT-EPR) and Fourier Transform-Mass Spectrometry (FT-MS). Please refer to the following topics for more details about how they work.

- *Stationary FTS*

In addition to the continuous/scanning mode of FTS, a number of stationary Fourier transform spectrometers are also available to meet special needs.

The principle of the interferometer and the analysis of its output signal is similar to the typical scanning FTS. But the signal is collected at certain optical path length differences rather than scanning over the whole range of the path difference.

An overview of various FTS techniques

Fourier transform spectroscopy can be applied to a variety of regions of spectroscopy and it continues to grow in application and utilization including optical spectroscopy, infrared spectroscopy (IR), nuclear magnetic resonance, electron paramagnetic resonance spectroscopy, mass spectrometry, and magnetic resonance spectroscopic imaging (MRSI). Among them, Fourier Transform Infrared Spectroscopy (FTIR) has been most intensively developed, which uses scanning Fourier transform to measure the mid-IR absorption spectra. .

Nuclear Magnetic Resonance (NMR) and Electron Spin Resonance Spectroscopy (EPR) are two magnetic techniques that use pulse Fourier transform mode. A Radio Frequency Pulse (RF Pulse) in a strong ambient magnetic field background is used as the energizing event. This RF Pulse directs the magnetic particles at an angle to the ambient strong magnetic field, causing gyration of the particle. Then the resulting gyrating spin induces a periodic current in the detector coil. This periodic current is recorded as the signal. Each gyrating spin has a characteristic frequency relative to the strength of the ambient magnetic field, which is also governed by the properties of the sample.

Fourier Transform Mass Spectrometry (MS) is also operated at pulse Fourier transform mode. Different from NMR and EPR, the injection of the charged sample into the strong electromagnetic field of a cyclotron acts as the energizing event in MS. The injected charged particles travel in circles under the strong electromagnetic field. The circular pathway will thus induce a current in a fixed coil at one point in their circle. Each traveling particle exhibits a characteristic cyclotron frequency relative to the field strength, which is determined by the masses in the sample.

References

1. R.A. Serway, J.W. Jewett.*Principles of physics: a calculus-based text (4th edition)*, 809
2. Maxwell; James Clerk, *A Dynamical Theory of the Electromagnetic Field*, Philosophical Transactions of the Royal Society of London 155, 459-512 (1865).
3. Peter Atkins, Julio De Paula. 2006. Physical Chemistry, 8th ed. Oxford University Press: Oxford, UK.
4. Smith, B.C. *Fourier Transform Infrared Spectroscopy.* Boca Raton: CRC Press Inc,1996
5. Bernhard Jaun, Analytische Chemie IV-Structure determination by NMR, 1. Practical aspects of pulse Fourier transform NMR spectroscopy, 1.1-1.21

Outside Links

- Please visit the free source for a consice introductory liquid pulse FT-NMR textbook[5] : www.analytik.ethz.ch/praktika...nmr/ft-nmr.pdf
- Fourier Series en.Wikipedia.org/wiki/Fourier_series
- Electromagnetic wave equation en.Wikipedia.org/wiki/Electro..._wave_equation
- Fourier Transform en.Wikipedia.org/wiki/Fourier_transform
- Fourier Transform Spectroscopy en.Wikipedia.org/wiki/Fourier...m_spectroscopy
- Fast Fourier Transform en.Wikipedia.org/wiki/Fast_Fourier_transform
- Discrete Fourier Transform en.Wikipedia.org/wiki/Discret...rier_transform

Problems

1. Search literatures to find the advantages and the limitations of Fourier transform spectroscopic techniques.
2. Perform a Fourier transform to show how to extract spectrum, equation (11), from the raw data in equation (10).
3. Compare interferometer with monochromator (at least two aspects).
4. What are the important components to make Fourier transform spectrometer practical? What are they used for?
5. Based on the information introduced in this module, design any one of the Fourier transform spectrometers mentioned in the context.

Solutions

1. *Advantages*

Firstly, Fourier transform spectrometers have a multiplex advantage (Fellgett advantage) over dispersive spectral detection techniques for signal, but a multiplex disadvantage for noise; Moreover, measurement of a single spectrum is faster(in the FTIR technique) because the information at all frequencies is collected simultaneously. This allows multiple samples to be collected and averaged together also resulting in an improvement in sensitivity; In addition, FT spectrometers are cheaper than conventional spectrometers because building of interferometers is easier than the fabrication of a monochromator (in the FTIR technique). So most commercial IR spectrometers are built based on FTIR techniques.

Limitations: practical frequency regions limited (FT UV-vis is not quite practical)

2. See the following figure for the solution:

$$
\begin{aligned}
&2.\textit{Given: } I(p) = \int_0^\infty I(p,\bar{\nu})\cdot d\bar{\nu} = \int_0^\infty I(\bar{\nu})\cdot[1+\cos(2\pi\bar{\nu}\mathrm{p})]\cdot d\bar{\nu}\\
&\quad = \int_0^\infty I(\bar{\nu})\cdot d\bar{\nu} + \int_0^\infty I(\bar{\nu})\cdot\cos(2\pi\bar{\nu}\mathrm{p})\cdot d\bar{\nu}\\
&\quad = \int_0^\infty I(\bar{\nu})\cdot\cos(2\pi\bar{\nu}\cdot 0)\,d\bar{\nu} + \int_0^\infty I(\bar{\nu})\cdot\cos(2\pi\bar{\nu}\mathrm{p})\cdot d\bar{\nu}\\
&\quad = \frac{1}{2}\int_{-\infty}^\infty I(\bar{\nu})\cdot\cos(2\pi\bar{\nu}\cdot 0)\,d\bar{\nu} + \frac{1}{2}\int_{-\infty}^\infty I(\bar{\nu})\cdot\cos(2\pi\bar{\nu}\mathrm{p})\cdot d\bar{\nu}\\
&\quad = \frac{1}{2}I(p=0) + \frac{1}{2}\int_{-\infty}^\infty I(\bar{\nu})\cdot\cos(2\pi\bar{\nu}\mathrm{p})\cdot d\bar{\nu}
\end{aligned}
$$

If we look at the second term in the last equation, it is just a cosine Fourier Transform!
So by moving $I(p=0)$ to the other side,
we will just have this desired cosince Fourier Transform term left:

$$\int_{-\infty}^\infty I(\bar{\nu})\cdot cos(2\pi\bar{\nu}\mathrm{p})\cdot d\bar{\nu} = 2\cdot[I(p) - \frac{1}{2}\cdot I(p=0)]$$

Then to extract $I(\bar{\nu})$:

$$
\begin{aligned}
I(\bar{\nu}) &= \int_{-\infty}^\infty 2\left[I(p) - \frac{1}{2}\cdot I(p=0)\right]\cdot\cos(2\pi\bar{\nu}\mathrm{p})\cdot d\bar{\nu}\\
&= 2\int_0^\infty 2\left[I(p) - \frac{1}{2}\cdot I(p=0)\right]\cdot\cos(2\pi\bar{\nu}\mathrm{p})\cdot d\bar{\nu}\\
&= 4\int_0^\infty [I(p) - \frac{1}{2}\cdot I(p=0)]\cdot cos(2\pi\bar{\nu}\mathrm{p})\cdot d\bar{\nu}
\end{aligned}
$$

3. Interferometer vs. Monochromator

Interometer: a. Collect signal in time or spatial domain; b. Measure all frequencies in the incident beam at one time; c. Determined by the interferometer, raw data from FT spectrometer is an interogram, which needs to be Fourier Transform back to get spectrum.

Monochromator: a. Collect signal in frequency domain; b. Scan each wavelength and measure the intensity for each single wavelength at a time; c. Determined by the feasure of monochromator, spectrum can be directly collected from the spectrometer;

4. Interferometer and Fast Fourier Transform Data Analyzer

Interferometer: to generate continuous optical path length difference and enable the idea to collect data in the time or spatial domain;

Fast Fourier Transform Data Analyzer: to quickly transform the raw data (interferogram) to spectrum by using fast Fourier transform algorithm;

5. FTIR instrumentation: ***Figure 4***

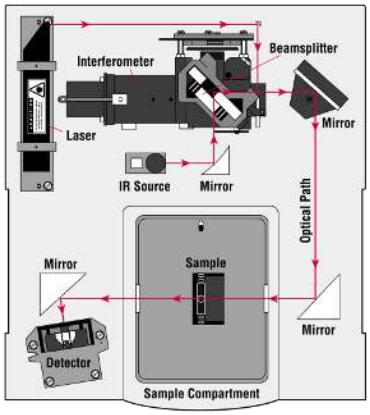


Figure 4. A FTIR Spectrometer Layout (Figure from ThermoNiolet at *mmrc.caltech.edu/FTIR/FTIRintro.pdf*)

FT-NMR instrumentation:

A modern high resolution liquid FT-NMR instrumentation is shown in ***Figure 5***:

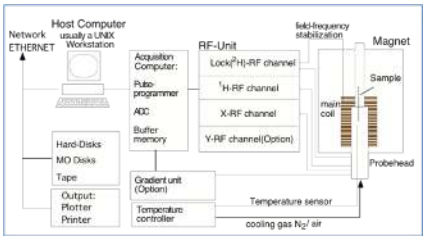


Figure 5. A schematic diagram of liquid FT-NMR[5]

1.5: The Power of the Fourier Transform for Spectroscopists is shared under a CC BY-NC-SA 4.0 license and was authored, remixed, and/or curated by LibreTexts.

- **The Power of the Fourier Transform for Spectroscopists** by Jing Zhao is licensed CC BY 4.0.

1.6: Time-resolved vs. Frequency Resolved

Spectroscopic measurements are typically taken in one of two domains: frequency or time. These measurements are given the terms frequency-resolved or time-resolved. Frequency-resolved measurements are the most familiar forms of spectroscopy. UV/Visible, IR, Raman, and X-ray spectroscopy are typically done in the frequency domain. This type of spectroscopy acquires data across a range of frequencies (or wavelengths). The data acquired is typically in the form of an light intensity which can in turn be interpreted as absorbance, transmittance, reflectance, or photon scattering depending on the instrument and technique being used.

Introduction

The less familiar time-resolved spectroscopy includes Ultrafast laser spectroscopy and florescence. In this form of spectroscopy data is acquired over a range of time. This data can be at a single wavelength or at multiple wavelengths, depending on the specific technique. Some spectroscopic techniques, such as Ultrafast laser spectroscopy, FT-NMR and FT-IR, span both frequency and time domains. In the case of Ultrafast laser spectroscopy, useful data is acquired in both the time and frequency domains. FT-NMR and FT-IR acquire data in the time domain. That data is then converted into a signal in the frequency domain using a process called Fourier Transform. This is covered in more detail below.

Frequency Resolution

Frequency is defined as inverse time. The unit is typically given in inverse seconds(s^{-1}) or hertz(hz). Frequency is used to represent the number of cycles occurring in a given time period. These cycles could be any repetitive process including: the periodic motion of a harmonic oscillator, the sinusoidal propagation of electromagnetic radiation, or the rotation of a rigid rotator. The most relevant for spectroscopy is the propagation or electromagnetic radiation, or light. This is often represented in many different forms that, though not technically frequency, are related to frequency, and therefore fall into the frequency domain. These include representing frequency as wavelength (nm), wavenumber (cm^{-1}), and photon energy (eV). These are all connected by a few simple equations given below. (c=speed of light, E=energy, v=frequency, w=wavenumber, h=Planck's constant,lambda=wavelength)

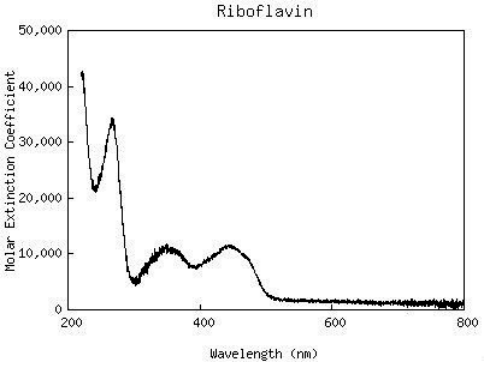
$$\lambda = \frac{c}{\nu}$$

$$E = h\nu$$

$$w = \frac{1}{\lambda}$$

The frequency domain is the most familiar domain in spectroscopy. UV/visible, infrared, photoelectron, microwave, and X-ray spectroscopy all have applications in the frequency domain. The results of these spectroscopic techniques are typically given in some form of intensity versus wavelength. The most familiar is likely the steady state ultraviolet/visible absorption spectrum(an example is shown below).

Frequency Resolved Visible Absorption Spectrum



The energy of absorbed light corresponds to the energy of transition between two eigen states of the system. In the case of visible spectroscopy these states are electronic states.

Time Resolution

Spectra can also be acquired in the time domain. Rather than acquiring spectra by averaging data over a relatively long time range, data is acquired over discrete time intervals or, in some cases, continuously. This may be done over one or many wavelengths. Time resolved spectroscopy observes the change in eigenstates with respect to time. In order for data from time-resolved spectroscopy to be useful, the spectroscopy must be suited to the time scale of the process of interest. Below is a table of the approximate time scales and spectral ranges of physical processes that may be interesting.

Process	Time	Applicable Spectral Range
Singlet Electronic Excited State Lifetime	femto-nanoseconds	Visible
Triplet Electronic Excited State Lifetime	nanoseconds-minutes	Visible
Molecular Vibration Excited State Lifetime	pico-milliseconds	Infrared
Nuclear Rotation	pico-microseconds	Radio
Molecular Reaction Kinetics	eons-picoseconds	Varies

If a spectroscopy with suitable spectral region and time resolution is available, time resolved spectroscopy can be used to study kinetics, reactions, and lifetimes. Common applications of time-resolved spectroscopy include ultrafast laser spectroscopy and time-resolved florescence.

Fourier Transform

The process of Fourier Transform is a mathematical process used to move from one set of coordinates to another. The most spectroscopically relevant fourier transform is from the time domain to the frequency domain. In this case, a signal originally measured in the time domain can be converted into a signal in the frequency domain. This is done via the mathematical process shown below.

$$F(v) = \int_{-\infty}^{\infty} f(t) e^{-2i\pi vt} dt$$

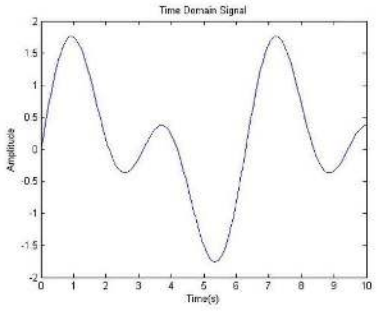
$$f(t) = \int_{-\infty}^{\infty} F(v) e^{-2i\pi vt} dv$$

A mathematical relation known as Euler's Formula is an important identity when using Fourier Transform, particularly with sine and cosine functions. This is shown below.

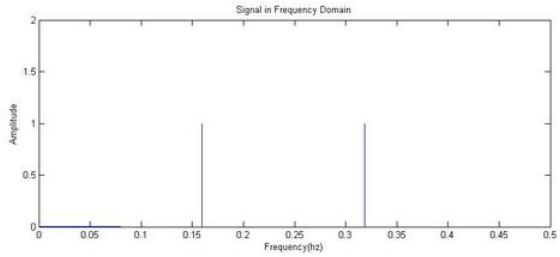
$$e^{\pm ix} = cos(x) \pm isin(x)$$

A simple graphic representation of Fourier Transform is shown below.

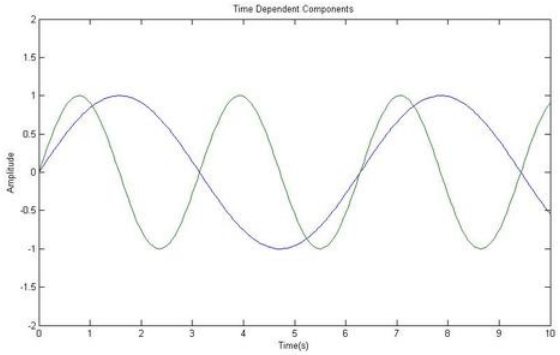
Original Signal in Time Domain



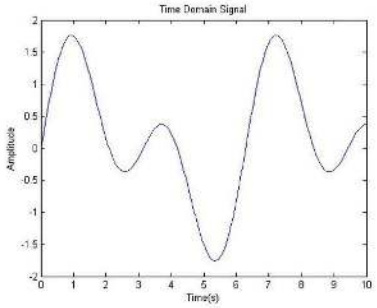
Fourier Transformed: Signal in Frequency Domain



Fourier Transformed Again: Signal in Time Domain (The Components of the Original Signal)



Sum of the Components(Equivalent to the Original Signal)



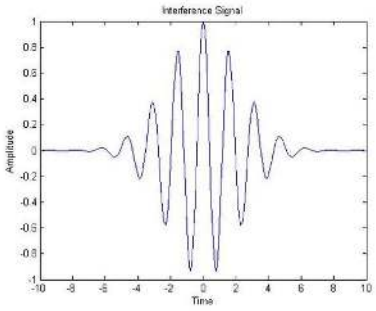
An example fourier transform with sine is given in the links section.

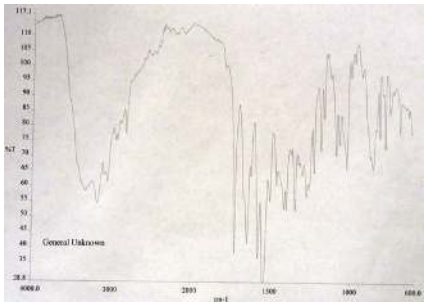
Common Application of Fourier Transform

Some fields of spectroscopy use measurements taken in the time domain to gain information about the frequency domain. These spectroscopies include Nuclear Magnetic Resonance, Fourier Transform Ion Cyclotron Resonance Mass Spectroscopy(FT-ICR MS) and Fourier Transform Infrared spectroscopy(FT-IR). Unlike the above graphic representation of Fourier Transform, these systems yield transforms that are impossible to compute by hand. Computer algorithms must be used.

The initial signal typically forms a beat pattern. This can be in the form of an interferogram or a free induction decay(FID), in the cases of FT-IR and NMR, respectively. Graphic representations of an interferogram and FID are shown below alongside IR and NMR spectra.

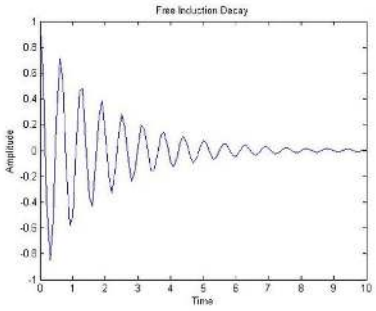
FT-IR Spectra

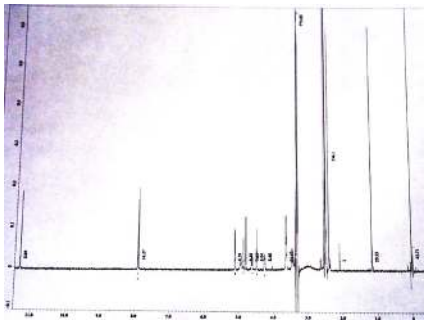




Interferogram(*X-axis: Time*|Y-Axis:Amplitude) Infrared Spectrum(*X-axis: Wave Number (cm^{-1})*|*Y-axis: Percent Transmission*)

FT-NMR Spectra



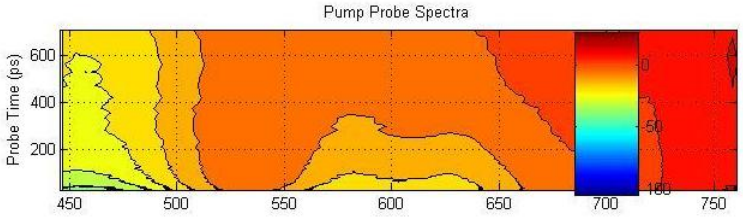


Free Induction Decay(*X-axis: Time*|*Y-axis: Amplitude*) NMR Spectrum(*X-axis: Chemical Shift (ppm)*|*Y-axis: Amplitude*)

Spectroscopy in Both Time and Frequency Domains

Some spectroscopies yield data in both time and frequency domains. The most prominent of these techniques is time-resolved laser spectroscopy. By measuring complete spectra at discrete time intervals, spectral evolution with respect to time can be monitored. This technique is unique in it's ability to collect data in multiple domains with femtosecond time resolution. This allows electronic states to be monitored both as they evolve over time and statically at any particular time along the time scale of the instrument. Below is an example of a typical ultrafast spectrum, notice both wavelength and time domains. This three-dimensional spectrum can be deconstructed to yield either time or frequency dependent results in two-dimensions. This is also shown below.

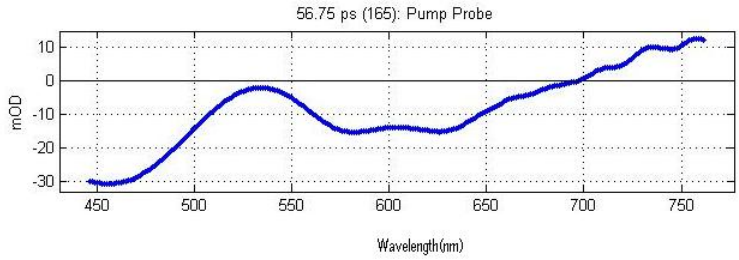
Time Resolved Visible Absorbance Spectrum



(X-axis:Wavelength(nm)|*Y-axis:Time(ps)*|*Z-axis:(ABS)[Shown as color]*)

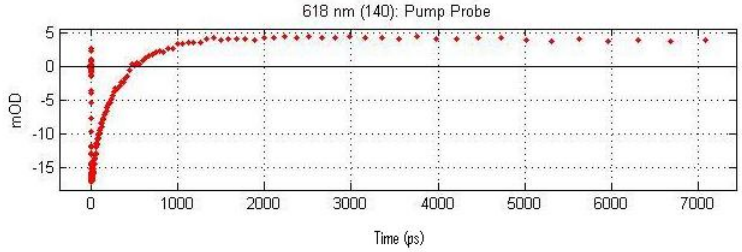
The time resolved spectrum shown above is plotted as a contour plot showing the Z-axis as a color gradient from red(low signal) to blue(high signal). This contour plot contains a multitude of information, but is by itself not terribly useful. It is most easily analyzed by taking crossections at a single wavelength or time. Each is shown below.

Frequency Domain Signal (A crossection of the Time Resolved Spectrum constant time)



The above spectrum is a crossection of the complete time resolved spectrum. This particular crossection is the frequency domain signal at 56.75 picoseconds after the sample has been excited by a laser pulse.

Time Domain Signal (A crossection of the Time Resolved Spectrum at a single Wavelength)



The above spectrum is a crossection of the complete time resolved spectrum. This crossection is the time resolved signal at 618 nanometers. This crossection contains kinetic data on the eigen state that absorbs at 618nm.

References

1. Skoog, Douglas A. Principles of Instrumental Analysis. 5th ed. New York:Thompson Learning Incorporated,1998.
2. Atkins, Peter. Physical Chemistry. 7th ed. New York: W.H. Freeman, 2002.

Outside Links

- For a more in-depth/mathematical look at fourier transform: en.Wikipedia.org/wiki/Fourier_transform
- Fourier transform of a sine function: http://mathworld.wolfram.com/FourierTransformSine.html
- For a more in depth look at Euler's Formula: http://en.Wikipedia.org/wiki/Euler%27s_formula
- Use of Fourier Transform in FT-ICR Mass Spectroscopy: www.youtube.com/watch?v=7EHngA4S3Ws

1.6: Time-resolved vs. Frequency Resolved is shared under a CC BY-NC-SA 4.0 license and was authored, remixed, and/or curated by LibreTexts.

- **Time-resolved vs. Frequency Resolved** is licensed CC BY 4.0.

CHAPTER OVERVIEW

2: Mass Spectrometry

Learning Objectives

This chapter will define construction and use of multiple types of mass spectrometers including GCMS and LCMS systems. Interpretation of the resulting data will be an important focus.

- describe the design of differing types of mass spectrometers
- explain how gas chromatography and liquid chromatography are used in tandem with mass spectrometers
- explain common ionization methods
- describe the function of common mass analyzers
- interpret mass spectra

2.1: Introduction to Mass Spectrometry
2.2: Mass Spectrometry
2.3: How the Mass Spectrometer Works
Electrospray Ionization Mass Spectrometry
Injection Stage
MALDI-TOF
Mass Analyzers (Mass Spectrometry)
2.4: Interpretation of Mass Spectra
13C
Br and Cl
Fragmentation
Fragmentation Patterns in Mass Spectra
Molecular Ions
Molecular Ion and Nitrogen
Organic Compounds Containing Halogen Atoms
The Molecular Ion (M^+) Peak
The M 1 Peak
2.5: Mass Spectrometry Problems
LEGO Exercise
2.6: ESI-QTOF-MS Coupled to HPLC and its Application for Food Safety

2: Mass Spectrometry is shared under a CC BY-NC-SA 4.0 license and was authored, remixed, and/or curated by LibreTexts.

2.1: Introduction to Mass Spectrometry

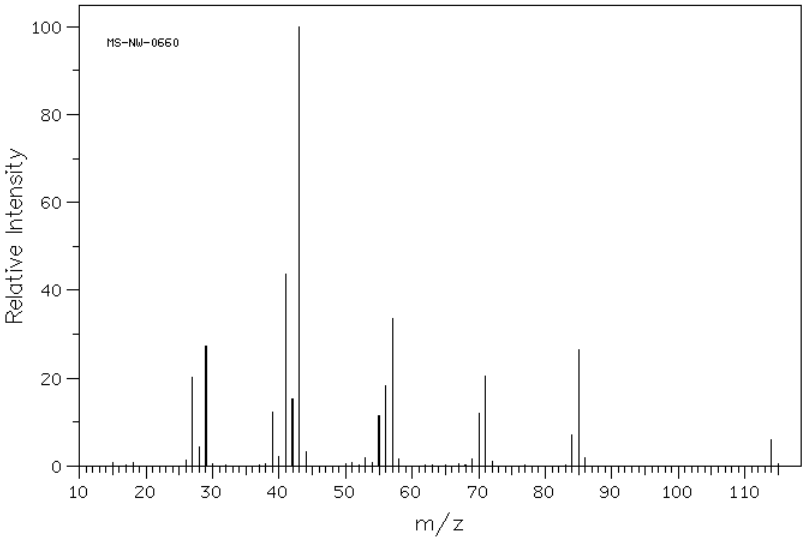
hexane

Figure MS1. Mass spectrum of hexane. Source: SDBSWeb : http://riodb01.ibase.aist.go.jp/sdbs/ (National Institute of Advanced Industrial Science and Technology of Japan, 22 August 2008)

- The y-axis is usually labeled "abundance" or "relative intensity". This axis shows how the relative ratios of molecules in the sample that have a particular mass.
- The x-axis is labeled "m/z" and corresponds to molecular mass. The designation m/z refers to the fact that this technique really measures the ratio of an ion's mass to its charge.
- A mass spectrum does not show the results from one molecule, but from millions of molecules. Because it is displaying results for a population of molecules, more than one mass is shown
- Many of the molecules in the sample fall apart during the experiment.
- A mass spectrum is a bar graph showing the weights of entire molecules as well as smaller pieces of molecules. The entire molecule must have the largest mass, the one farthest to the right, because if a molecule falls into pieces the pieces would be smaller than the whole.

Problem MS1.

The following figure shows the mass spectrum of a saturated hydrocarbon (containing only carbon and hydrogen with only single bonds between carbons, not double bonds).



1. Draw five different structures that would have the molecular weight of this compound.
2. Choose four smaller m/z values from the spectrum and draw one structure for each of them. Note that these fragments will not have complete Lewis structures.

Contributor

- Chris P Schaller, Ph.D., (College of Saint Benedict / Saint John's University)

This page titled 2.1: Introduction to Mass Spectrometry is shared under a CC BY-NC 3.0 license and was authored, remixed, and/or curated by Chris Schaller.

- **Introduction to Mass Spectrometry** by Chris Schaller is licensed CC BY-NC 3.0.

2.2: Mass Spectrometry

Principles of Mass Spectrometry and Modern Applications

Mass spectrometry (MS) is a powerful characterization technique used for the identification of a wide variety of chemical compounds. At its simplest, MS is merely a tool for determining the molecular weight of the chemical species in a sample. However, with the high resolution obtainable from modern machines, it is possible to distinguish isomers, isotopes, and even compounds with nominally identical molecular weights. Libraries of mass spectra have been compiled which allow rapid identification of most known compounds, including proteins as large as 100 kDa (100,000 amu).

Mass spectrometers separate compounds based on a property known as the mass-to-charge ratio. The sample to be identified is first ionized, and then passed through some form of magnetic field. Based on parameters such as how long it takes the molecule to travel a certain distance or the amount of deflection caused by the field, a mass can be calculated for the ion. As will be discussed later, there are a wide variety of techniques for ionizing and detecting compounds.

Limitations of MS generally stem from compounds that are not easily ionizable, or which decompose upon ionization. Geometric isomers can generally be distinguished easily, but differences in chirality are not easily resolved. Complications can also arise from samples which are not easily dissolved in common solvents.

Ionization Techniques

Electron Impact (EI)

In electon impact ionization, a vaporized sample is passed through a beam of electrons. The high energy (typically 70 eV) beam strips electrons from the sample molecules leaving a positively charged radical species. The molecular ion is typically unstable and undergoes decomposition or rearrangement to produce fragment ions. Because of this, electron impact is classified as a “hard” ionization technique. With regards to metal-containing compounds, fragments in EI will almost always contain the metal atom (i.e., $[ML_n]^{+\bullet}$fragments to $[ML_{n-1}]^+ + L^\bullet$, not $ML_{n-1}^\bullet + L^+$). One of the main limitations of EI is that the sample must be volatile and thermally stable.

Chemical Ionization (CI)

In chemical ionization, the sample is introduced to a chamber filled with excess reagent gas (such as methane). The reagent gas is ionized by electrons, forming a plasma with species such as CH_5^+, which react with the sample to form the pseudomolecular ion $[M+H]^+$. Because CI does not involve radical reactions, fragmentation of the sample is generally much lower than that of EI. CI can also be operated in negative mode (to generate anions) by using different reagent gases. For example, a mixture of CH_4 and NO_2 will generate hydroxide ions, which can abstract protons to yield the $[M-H]^-$ species. A related technique, atmospheric pressure chemical ionization (APCI) delivers the sample as a neutral spray, which is then ionized by corona discharge, producing ions in a similar manner as described above. APCI is particularly suited for low molecular weight, nonpolar species that cannot be easily analyzed by other common techniques such as ESI.

Field Ionization/Desorption

Field ionization and desorption are two closely related techniques which use quantum tunneling of electrons to generate ions. Typically, a highly positive potential is applied to an electrode with a sharp point, resulting in a high potential gradient at the tip Figure 2.2.1. As the sample reaches this field, electron tunneling occurs to generate the cation, which is repelled into the mass analyzer. Field ionization utilizes gaseous samples whereas in field desorption the sample is adsorbed directly onto the electrode. Both of these techniques are *soft*, resulting in low energy ions which do not easily fragment.

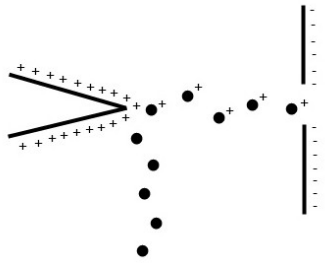


Figure 2.2.1 Schematic of field ionization.

Electrospray Ionization (ESI)

In ESI, a highly charged aerosol is generated from a sample in solution. As the droplets shrink due to evaporation, the charge density increases until a *coulombic explosion* occurs, producing daughter droplets that repeat the process until individualized sample ions are generated (Figure 2.2.2. One of the limitations of is the requirement that the sample be soluble. ESI is best applied to charged, polar, or basic compounds.

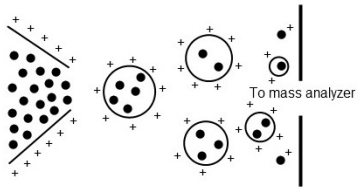


Figure 2.2.2 Schematic of electrospray ionization.

Matrix Assisted Laser Desorption Ionization (MALDI)

Laser desorption ionization generates ions by ablation from a surface using a pulsed laser. This technique is greatly improved by the addition of a matrix co-crystallized with the sample. As the sample is irradiated, a plume of desorbed molecules is generated. It is believed that ionization occurs in this plume due to a variety of chemical and physical interactions between the sample and the matrix (Figure 2.2.3). One of the major advantages of MALDI is that it produces singly charged ions almost exclusively and can be used to volatilize extremely high molecular weight species such as polymers and proteins. A related technique, desorption ionization on silicon (DIOS) also uses laser desorption, but the sample is immobilized on a porous silicon surface with no matrix. This allows the study of low molecular weight compounds which may be obscured by matrix peaks in conventional MALDI.

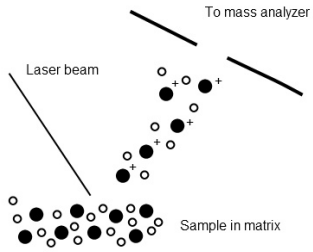


Figure 2.2.3 Schematic of matrix assisted laser desorption ionization.

Inductively Coupled Plasma Mass Spectrometry (ICP-MS)

A plasma torch generated by electromagnetic induction is used to ionize samples. Because the effective temperature of the plasma is about 10,000 °C, samples are broken down to ions of their constituent elements. Thus, all chemical information is lost, and the technique is best suited for elemental analysis. ICP-MS is typically used for analysis of trace elements.

Fast Atom Bombardment (FAB) and Secondary Ion Mass Spectrometry (SIMS)

Both of these techniques involve sputtering a sample to generate individualized ions; FAB utilizes a stream of inert gas atoms (argon or xenon) whereas SIMS uses ions such as Cs^+. Ionization occurs by charge transfer between the ions and the sample or by protonation from the matrix material (Figure 2.2.4). Both solid and liquid samples may be analyzed. A unique aspect of these techniques for analysis of solids is the ability to do depth profiling because of the destructive nature of the ionization technique.

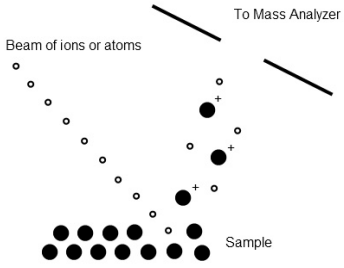


Figure 2.2.4 Schematic of fast atom bombardment ionization.

Choosing an Ionization Technique

Depending on the information desired from mass spectrometry analysis, different ionization techniques may be desired. For example, a hard ionization method such as electron impact may be used for a complex molecule in order to determine the component parts by fragmentation. On the other hand, a high molecular weight sample of polymer or protein may require an ionization method such as MALDI in order to be volatilized. Often, samples may be easily analyzed using multiple ionization methods, and the choice is simplified to choosing the most convenient method. For example, electrospray ionization may be easily coupled to liquid chromatography systems, as no additional sample preparation is required. Table 2.2.1 provides a quick guide to ionization techniques typically applied to various types of samples.

Table 2.2.1 Strengths of various ionization techniques

Information Desired	**Ionization Technique**
Elemental analysis	Inductively coupled plasma
Depth profiling	Fast atom bombardment/secondary ion mass spectroscopy
Chemical speciation/component analysis (fragmentation desired)	Electron impact
Molecular species identification of compounds soluble in common solvents	Electrospray ionization
Molecular species identification of hydrocarbon compounds	Field ionization
Molecular species identification of high molecular weight compounds	Matrix assisted laser desorption ionization
Molecular species identification of halogen containing compounds	Chemical ionization (negative mode)

Mass Analyzers

Sectors

A magnetic or electric field is used to deflect ions into curved trajectories depending on the *m*/*z* ratio, with heavier ions experiencing less deflection (Figure 2.2.5). Ions are brought into focus at the detector slit by varying the field strength; a mass spectrum is generated by scanning field strengths linearly or exponentially. Sector mass analyzers have high resolution and sensitivity, and can detect high mass ranges, but are expensive, require large amounts of space, and are incompatible with the most popular ionization techniques MALDI and ESI.

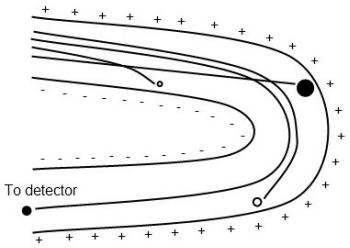


Figure 2.2.5 Schematic of a magnetic sector mass analyzer.

Time of Flight (TOF)

The amount of time required for an ion to travel a known distance is measured (Figure 2.2.6). A pulse of ions is accelerated through and electric analyzer such that they have identical kinetic energies. As a result, their velocity is directly dependent on their mass. Extremely high vacuum conditions are required to extend the mean free path of ions and avoid collisions. TOF mass analyzers are fastest, have unlimited mass ranges, and allow simultaneous detection of all species, but are best coupled with pulsed ionization sources such as MALDI.

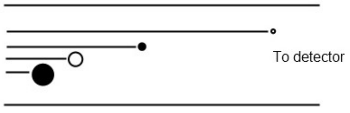


Figure 2.2.6 Schematic of a time-of-flight (TOF) mass analyzer.

Quadropole

Ions are passed through four parallel rods which apply a varying voltage and radiofrequency potential (Figure 2.2.7). As the field changes, ions respond by undergoing complex trajectories. Depending on the applied voltage and RF frequencies, only ions of a certain *m*/*z* ratio will have stable trajectories and pass through the analyzer. All other ions will be lost by collision with the rods. Quadrupole analyzers are relatively inexpensive, but have limited resolution and low mass range.

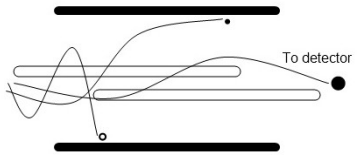


Figure 2.2.7 Schematic of a quadrupole mass analyzer.

Ion Trap

Ion traps operate under the same principle as quadrupole, but contain the ions in space. Electrodes can be manipulated to selectively eject ions of desired *m*/*z* ratios, allowing for mass analysis. Ion traps are uniquely suited for repeated cycles of mass spectrometry because of their ability to retain ions of desired *m*/*z* ratios. Selected fragments can be further fragmented by collision induced dissociation with helium gas. Ion traps are compact, relatively inexpensive, and can be adapted to many hybrid instruments.

Coupling Mass Spectrometry to Other Instruments

Mass spectrometry is a powerful tool for identification of compounds, and is frequently combined with separation techniques such as liquid or gas chromatography for rapid identification of the compounds within a mixture. Typically, liquid chromatography systems are paired with ESI-quadrupole mass spectrometers to take advantage of the solvated sample. GC-MS systems usually employ electron impact ionization and quadrupole or ion trap mass analyzers to take advantage of the gas-phase molecules and fragmentation libraries associated with EI for rapid identification.

Mass spectrometers are also often coupled in tandem to form MS-MS systems. Typically the first spectrometer utilizes a hard ionization technique to fragment the sample. The fragments are passed on to a second mass analyzer where they may be further fragmented and analyzed. This technique is particularly important for studying large, complex molecules such as proteins.

Fast Atom Bombardment

Fast atom bombardment (FAB) is an ionization technique for mass spectroscopy employing secondary ion mass spectroscopy (SIMS). Before the appearance of this technique, there was only limited way to obtain the mass spectrum of the intact oligopeptide which is not easy to be vaporized. Prior to 1970, electron ionization (EI) or chemical ionization (CI) was widely used but those methods require the destructive vaporization of the sample. Field desorption of ions with nuclear fission overcame this problem though due to the necessity of special technique and nuclear fission of ^{252}Cf limits the generality of this approach. FAB became prevalent solving those underlying problems by using bombardment of fast atom or ion which has high kinetic energy onto the sample in matrix.

Principle

The FAB utilizes the bombardment of accelerated atom or ion beams and the ionized sample is emitted by the collision of the beams and the sample in matrix. In this section, the detail of each step is discussed.

Atom Beam

Although ions can be accelerated by electric field relatively easily, that is not the case for the neutral atom. Therefore, in the FAB conversion of neutral atom into ion is significant to generate the accelerated species. The fast atom such as xenon used for the bombardment is produced through three steps (Figure 2.2.8):

1. Ionization of the atom by collision with electron.
2. Acceleration of the generated ion through high electric potential.
3. Electron transfer from the accelerated ion to another slow atom, affording the desired accelerated atom.

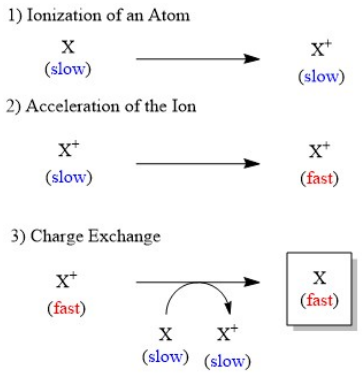


Figure 2.2.8 Process of generation of fast atom.

Ion Beam

In the same way as the atom beam, a fast ion beam also can be used. Although cesium ion (Cs^+) cheaper and heavier than xenon is often employed, they have drawback that the mass spectroscopy can be contaminated by the ions.

Bombardment

The obtained fast atom or ion is then bombarded to the sample in matrix which is a type of solvent having high boiling point, resulting in momentum transfer and vaporization of the sample (Figure 2.2.9). The fast atom used for the bombardment is called primary beam of atoms or ions while secondary beam of atoms or ions corresponds to the sputtered ions and neutrals. The ionized sample is directed by ion optics, leading to the detection of those ion in mass analyzer.

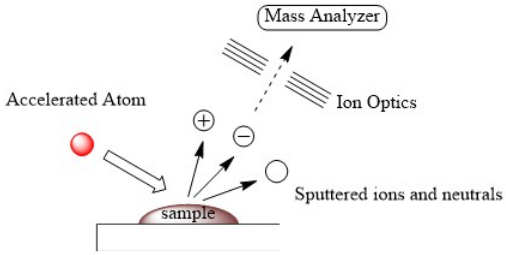


Figure 2.2.9 Bombardment of accelerated atom into sample. Only sputtered species with charge is introduced into ion optics and detected by analyzer.

Matrices

One of the crucial characteristics of FAB is using liquid matrix. For example, long-lived signal in FAB is responsible for using matrix. Due to the high vacuum condition, usual solvent for chemistry laboratory such as water and other common organic solvent is precluded for FAB and, therefore, solvent with high boiling point called matrix is necessary to be employed. Table 2.2.1 shows examples of matrix.

Table 2.2.1 Typical examples of matrices. Data from C. G. Herbert and R. A. W. Johnstone, *Mass Spectrometry Basics*, CRC Press, New York (2002)

Matrix	**Observed Ions (m/z)**
Glycerol	93
Thioglycerol	109
3-Nitrobenzyl alcohol (3-NOBA)	154
n-Octyl-3-nitrophenylether (NOP)	252
Triethanolamine	150
Diethanolamine	106
Polyethylene glycol (mixtures)	Dependent on the glycol used

Instrument

An image of a typical instrument for fast atom bombardment mass spectrometry is shown in Figure 2.2.10.



Figure 2.2.10 Instrumentation of fast atom bombardment mass spectrometry.

Spectra

The obtained spectrum by FAB has information of structure or bond nature of the compound in addition to the mass. Here, three spectrum are shown as examples.

Glycerol

Typical FAB mass spectrum of glycerol alone is shown in Figure 2.2.11.

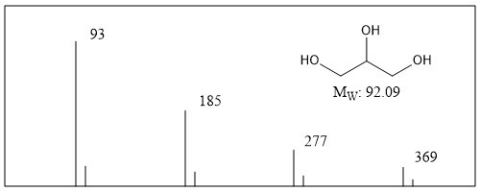


Figure 2.2.11 A simplified FAB mass spectrum of glycerol.

Glycerol shows signal at *m/z* 93 which is corresponding to the protonated glycerol with small satellite derived from isotope of carbon (^{13}C). At the same time, signals for cluster of protonated glycerol are also often observed at *m/z* 185, 277, and 369. As is seen in this example, signal from aggregation of the sample also can be detected and this will provide the information of the sample.

Sulfonated Azo Compound

Figure 2.2.12 shows positive FAB spectrum of sulfonated azo compound X and structure of the plausible fragments in the spectrum. The signal of the target compound X (M_w = 409) was observed at *m/z* 432 and 410 as an adduct with sodium and proton, respectively. Because of the presence of some type of relatively weak bonds, several fragmentation was observed. For example, signal at m/z 352 and 330 resulted from the cleavage of aryl-sulfonate bond. Also, nitrogen-nitrogen bond cleavage in the azo moiety occurred, producing the fragment signal at *m/z* 267 and 268. Furthermore, taking into account the fact that favorable formation of nitrogen-nitrogen triple bond from azo moiety, aryl-nitrogen bond can be cleaved and in fact those were detected at *m/z* 253 and 252. As is shown in these example, fragmentation can be used for obtaining information regarding structure and bond nature of desired compound.

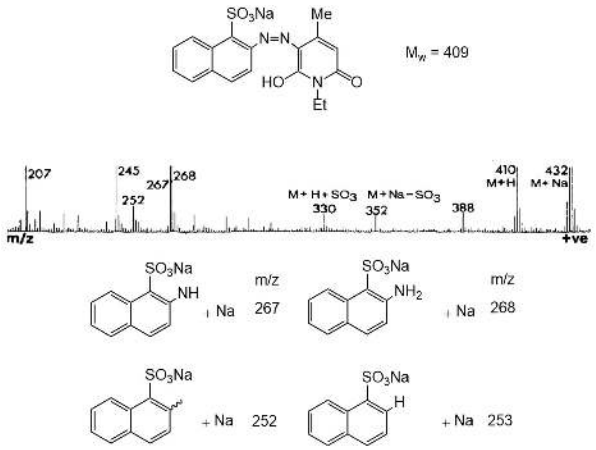


Figure 2.2.12 Positive FAB spectrum of sulfonated azo compound X. Adapted from J. J. Monaghan, M. Barber, R. S. Bordoli, R. D. Sedgwick, and A. N. Tyler, *Int. J. Mass. Spectrom.*, 1983, **46**, 447. Copyright: Elsevier (1983)

Bradykinin Potentiator C

The mass spectrum of protonated molecule (MH^+ = *m/z* 1052) of bradykinin potentiator C is shown in Figure 2.2.13. In this case fragmentation occurs between certain amino acids, affording the information of peptide sequence. For example, signal at *m/z* 884 is corresponding to the fragment as a result of scission of Gly-Leu bond. It should be noted that the pattern of fragmentation is not only done by one type of bond cleavage. Fragmentation at the bond between Gly-Pro is a good example; two type of fragment (*m/z* 533 and 520) are observed. Thus, pattern of fragmentation can afford the information of sequence of peptide.

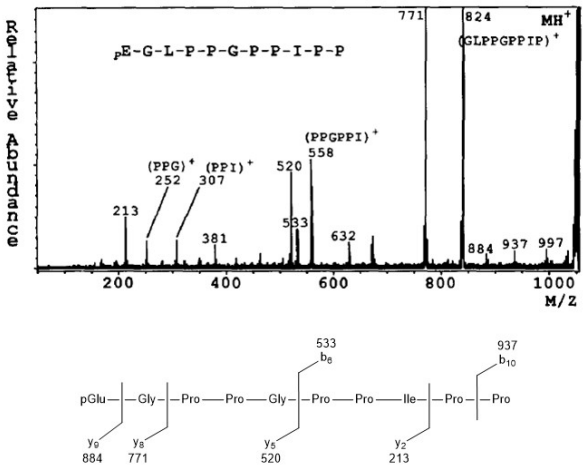


Figure 2.2.13 FAB spectrum of Bradykinin Potentiator C (above) and pattern of fragmentation (below). Adapted from J. T. Watson, D. S. Wagner, Y.-S. Chang, J. R. Strahler, S. M. Hanash, and D. A. Gage, *Int. J. Mass. Spectrom.*, 1991, **111**, 191. Copyright: Elsevier (1991).

Secondary Ion Mass Spectrometry (SIMS)

Secondary ion mass spectrometry (SIMS) is an analytical method which has very low detection limits, is capable of analyzing over a broad dynamic range, has high sensitivity, and has high mass resolution. In this technique, *primary ions* are used to sputter a solid (and sometimes a liquid) surface of any composition. This causes the emission of electrons, ions, and neutral species, so called *secondary particles*, from the solid surface. The secondary ions are then analyzed by a mass spectrometer. Depending on the operating mode selected, SIMS can be used for surface composition and chemical structure analysis, depth profiling, and imaging.

Theory

Of all the secondary particles that are sputtered from the sample surface, only about 1 in every 1,000 is emitted as an ion. Because only the ions may be detected by mass spectrometry, an understanding of how these secondary ions form is important.

Sputtering Models

Sputtering can be defined as the emission of atoms, molecules, or ions from a target surface as a result of particle bombardment of the surface. This phenomenon has been described by two different sets of models.

The first approach to describe sputtering, called linear collision cascade theory, compares the atoms to billiard balls and assumes that atomic collisions are completely elastic. Although there are a few different types of sputtering defined by this model, the type which is most important to SIMS is slow collisional sputtering. In this type of sputtering, the primary ion collides with the surface of the target and causes a cascade of random collisions between the atoms in the target. Eventually, these random collisions result in the emission of an atom from the target surface, as can be seen in Figure 2.2.14 This model does not take into account the location of atoms- it only requires that the energy of the incoming ion be higher than the energy required to sublimate atoms from the target surface.

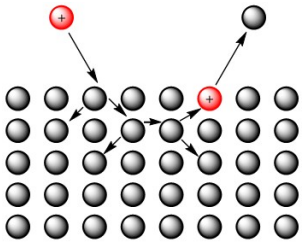


Figure 2.2.14 A diagram that illustrates linear collision cascade theory. The primary ion collides with an atom on the surface of the target, causing other elastic collisions to occur within the target. Eventually, a target atom or molecule is ejected from the surface.

Despite that fact that this method makes oversimplifications regarding atomic interactions and structure, its predicted sputter yield data is actually fairly close to the experimental data for elements such as Cu, Zn, Ag, and Au, which have high sputter yields. However, for low sputter yield elements, the model predicts three times more sputtered ions than what is actually observed.

The second method to describe sputtering uses computer-generated three-dimensional models of the atoms and molecules in the sample to predict the effect of particle bombardment. All models under this category describe the target solid in terms of its constituent atoms and molecules and their interactions with one another. However, these models only take into account atomic forces (not electronic forces) and describe atomic behavior using classical mechanics (not quantum mechanics). Two specific examples of this type of model are:

1. The molecular dynamics model
2. The binary collision approximation.

Ionization Models

The ionization models of sputtering can be divided into two categories, theories that predict ionization outside the target and theories that predict that they are generated inside the target. In the theories that describe ionization outside of the target, the primary particle strikes the target, causing the emission of an excited atom or molecule from the target. This particle relaxes by emitting an Auger electron, thus becoming an ion. Because no simple mathematical equation has been described for this theory, it is of little practical use. For this reason, ionization inside the target models are used more often. Additionally, it has been shown that ionization occurs more often inside the target. Although there are many models that describe ionization within the target, two representative models of this type are the bond-breaking model and the local thermal equilibrium theory.

In the bond breaking model, the primary particle strikes the target and causes the heterolytic cleavage of a bond in the target. So, either an anion or a cation is emitted directly from the target surface. This is an important model to mention because it has useful implications. Stated simply, the yield of positive ions can be increased by the presence of electronegative atoms in the target, in the primary ion beam, or in the sample chamber in general. The reverse is also true- the negative ion yield may be increased by the presence of electropositive atoms.

The local thermal equilibrium theory can be described as an expansion of the bond breaking model. Here, the increase in yield of positive ions when the target is in the presence of electronegative atoms is said to be the result of the high potential barrier of the metal oxide which is formed. This results in a low probability of the secondary ion being neutralized by an electron, thus giving a high positive ion yield.

Instrumentation

Primary Ion Sources

The primary ions in a SIMS instrument (labeled “Primary ion source” in Figure 2.2.15) are generated by one of three types of ion guns. The first type, called an electron bombardment plasma source, uses accelerating electrons (produced from a heated filament) to bombard an anode. If the energy of these electrons is two to three times higher than the ionization energy of the atom, ionization

occurs. Once a certain number of ions and electrons are obtained, a plasma forms. Then, an extractor is used to make a focused ion beam from the plasma.

In the second type of source, called the liquid metal source, a liquid metal film flows over a blunt needle. When this film is subjected to a strong electric field, electrons are ejected from the atoms in the liquid metal, leaving them ionized. An extractor then directs the ions out of the ion gun.

The last source is called a surface ionization source. Here, atoms of low ionization energy are absorbed onto a high work function metal. This type of system allows for the transfer of electrons from the surface atoms to the metal. When the temperature is increased, more atoms (or ions) leave the surface than absorb on the surface, causing an increase in absorbed ions compared to absorbed atoms. Eventually, nearly all of the atoms that leave the surface are ionized and can be used as an ion beam.

The type of source used depends on the type of SIMS experiment which is going to be run as well as the composition of the sample to be analyzed. A comparison of the three different sources is given in Table 2.2.2.

Table 2.2.2 A comparison of primary ion sources. Data from J.C. Vickerman, A. Brown, N.M. Reed, *Secondary ion mass spectrometry: Principles and applications*, Clarendon Press, Oxford, 1989.

Source	Spot Size (μm)	Brightness (A/m^2Sr)	Energy Speed (eV)	Ion Type
Electron Bombardment Plasma	1	10^4-10^7	<10	Ar^+, Xe^+, O_2^+
Liquid Metal	0.05	10^{10}	>10	Ga^+, In^+,Cs^+
Surface Ionization	0.1	10^7	<1	Cs^+

Of the three sources, electron bombardment plasma has the largest spot size. Thus, this source has a high-diameter beam and does not have the best spatial resolution. For this reason, this source is commonly used for bulk analysis such as depth profiling. The liquid metal source is advantageous for imaging SIMS because it has a high spatial resolution (or low spot size). Lastly, the surface ionization source works well for dynamic SIMS (see above)

because its very small energy spread allows for a uniform etch rate.

In addition to the ion gun type, the identity of the primary ion is also important. O_2^+ and Cs^+ are commonly used because they enhance the positive or negative secondary ion yield, respectively. However, use of the inert gas plasma source is advantageous because it allows for surface studies without reacting with the surface itself. Using the O_2^+ plasma source allows for an increased output of positively charged secondary ions, but it will alter the surface that is being studied. Also, a heavy primary ion allows for better depth resolution because it does not penetrate as far into the sample as a light ion.

Sputtering

The sputter rate, or the number of secondary ions that are removed from the sample surface by bombardment by one primary ion, depends both on the properties of the target and on the parameters of the primary beam.

There are many target factors that affect the sputter rate. A few examples are crystal structure and the topography of the target. Specifically, hexagonal close-packed crystals and rough surfaces give the highest sputter yield. There are many other properties of the target which effect sputtering, but they will not be discussed here.

As was discussed earlier, different primary ion sources are used for different SIMS applications. In addition to the source used, the manner in which the source is used is also important. First, the sputter rate can be increased by increasing the energy of the beam. For example, using a beam of energy greater than 10 keV gives a maximum of 10 sputtered particles per primary ion impact. Second, increasing the primary ion mass will also increase the secondary ion yield. Lastly, the angle of incidence is also important. It has been found that a maximum sputter rate can be achieved if the angle of impact is 70° relative to the surface normal.

Mass Spectrometers

The detector which measures the amount and type of secondary ions sputtered from the sample surface is a mass spectrometer. See Figure 2.2.15 for a diagram that shows where the mass spectrometer is relative to the other instrument components. The type of analysis one wishes to do determines which type of spectrometer is used. Both dynamic and static SIMS usually use a magnetic sector mass analyzer because it has a high mass resolution. Static SIMS (as well as imaging SIMS) may also use a time-of-flight system, which allows for high transmission. A description of how each of these mass spectrometers works and how the ions are

detected can be found elsewhere (see https://cnx.org/contents/kl4gTdhf@1/Principles-of-Mass-Spectrometry-and-Modern-Applications).

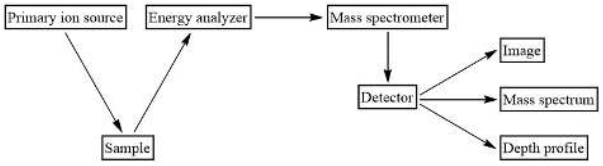


Figure 2.2.15 A diagram that shows the main components of a SIMS instrument. Diagram adapted from Wilson R.G. Wilson, F.A. Stevie, and C.W. Magee, *Secondary ion mass spectrometry: A practical handbook for depth profiling and bulk impurity analysis*, John Wiley & Sons Inc., New York, 1989.

Samples

SIMS can be used to analyze the surface and about 30 µm below the surface of almost any solid sample and some liquid samples. Depending on the type of SIMS analysis chosen, it is possible to obtain both qualitative and quantitative data about the sample.

Technique Selection

There are three main types of SIMS experiments: Dynamic SIMS, static SIMS, and imaging SIMS.

In dynamic SIMS analysis, the target is sputtered at a high rate. This allows for bulk analysis when the mass spectrometer is scanned over all mass ranges to get a mass spectrum and multiple measurements in different areas of the sample are taken. If the mass spectrometer is set to rapidly analyze individual masses sequentially as the target is eroded rapidly, it is possible to see the depth at which specific atoms are located up to 30 µm below the sample surface. This type of analysis is called a depth profile. Depth profiling is very useful because it is a quantitative method- it allows for the calculation of concentration as a function of depth so long as ion-implanted standards are used and the crater depth is measured. See the previous section for more information on ion-implants.

SIMS may also be used to obtain an image in a way similar to SEM while giving better sensitivity than SEM. Here, a finely focused ion beam (rather than an electron beam, as in SEM) is raster-scanned over the target surface and the resulting secondary ions are analyzed at each point. Using the identity of the ions at each analyzed spot, an image may be assembled based on the distributions of these ions.

In static SIMS, the surface of the sample is eroded very slowly so that the ions which are emitted are from areas which have not already been altered by the primary ion. By doing this, it is possible to identify the atoms and some of the molecules just on the surface of the sample.

An example that shows the usefulness of SIMS is the analysis of fingerprints using this instrument. Many other forms of analysis have been employed to characterize the chemical composition of fingerprints such as GC-MS. This is important in forensics to determine fingerprint degradation, to detect explosives or narcotics, and to help determine age of the person who left the print by analyzing differences in sebaceous secretions. Compared to GC-MS, SIMS is a better choice of analysis because it is relatively less destructive. In order to do a GC-MS, the fingerprint must be dissolved. SIMS, on the other hand, is a solid state method. Also, because SIMS only erodes through a few monolayers, the fingerprint can be kept for future analysis and for record-keeping. Additionally, SIMS depth profiling allows the researcher to determine the order in which substances were touched. Lastly, an image of the fingerprint can be obtained using the imaging SIMS analysis.

Sample Preparation

As with any other instrumental analysis, SIMS does require some sample preparation. First, rough samples may require polishing because the uneven texture will be maintained as the surface is sputtered. Because surface atoms are the analyte in imaging and static SIMS, polishing is obviously not required. However, it is required for depth profiling. Without polishing, layers beneath the surface of the sample will appear to be mixed with the upper layer in the spectrum, as can be seen in Figure 2.2.16.

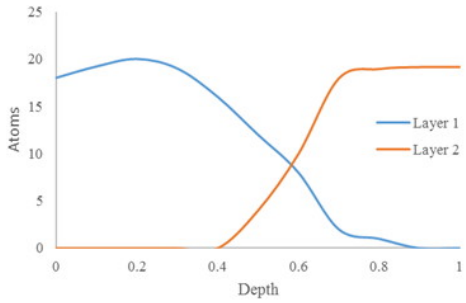


Figure 2.2.16 An example of what a poorly resolved depth profile would look like. A better depth profile would show steep slopes at the layer transition, rather than the gradual slopes seen here.

But, polishing before analysis does not necessarily guarantee even sputtering. This is because different crystal orientations sputter at different rates. So, if the sample is polycrystalline or has grain boundaries (this is often a problem with metal samples), the sample may develop small cones where the sputtering is occurring, leading to an inaccurate depth profile, as is seen in Figure 2.2.17.

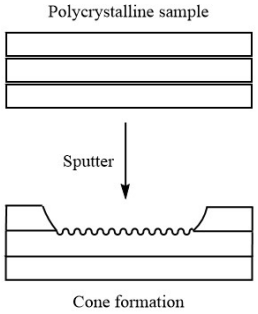


Figure 2.2.17 A diagram that shows cone formation during sputtering as a result of the polycrystalline nature of the sample. This leads to depth resolution degredation. Diagram adapted from R.G. Wilson, F.A. Stevie, and C.W. Magee, *Secondary ion mass spectrometry: A practical handbook for depth profiling and bulk impurity analysis*,John Wiley & Sons Inc., New York, 1989.

Analyzing insulators using SIMS also requires special sample preparation as a result of electrical charge buildup on the surface (since the insulator has no conductive path to diffuse the charge through). This is a problem because it distorts the observed spectra. To prevent surface charging, it is common practice to coat the sample with a conductive layer such as gold.

Once the sample has been prepared for analysis, it must be mounted to the sample holder. There are a few methods to doing this. One way is to place the sample on a spring loaded sample holder which pushes the sample against a mask. This method is advantageous because the researcher doesn't have to worry about adjusting the sample height for different samples (see below to find out why sample height is important). However, because the mask is on top of the sample, it is possible to accidentally sputter the mask. Another method used to mount samples is to simply glue them to a backing plate using silver epoxy. This method requires drying under a heat lamp to ensure that all volatiles are evaporated off the glue before analysis. Alternatively, the sample can be pressed in a soft metal like indium. The last two methods are especially useful for mounting of insulating samples, since they provide a conductive path to help prevent charge buildup.

When loading the mounted sample into the instrument, it is important that the sample height relative to the instrument lens is correct. If the sample is either too close or too far away, the secondary ions will either not be detected or they will be detected at the edge of the crater being produced by the primary ions (see Figure 2.2.18). Ideally, the secondary ions that are analyzed should be those resulting from the center of the primary beam where the energy and intensity are most uniform.

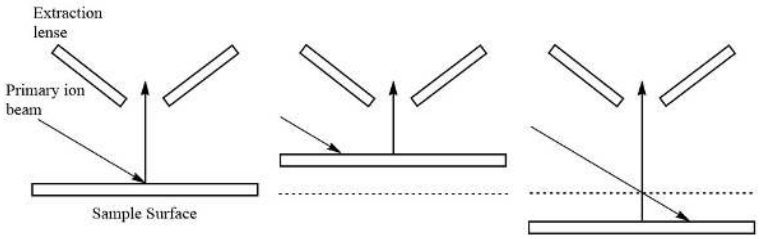


Figure 2.2.18 A diagram showing the importance of sample height in the instrument. If it is too high or too low, the sputtered ions will not make it through the extraction lense. Diagram adapted from R.G. Wilson, F.A. Stevie, and C.W. Magee, *Secondary ion mass spectrometry: A practical handbook for depth profiling and bulk impurity analysis*, John Wiley & Sons Inc., New York, 1989.

Standards

In order to do quantitative analysis using SIMS, it is necessary to use calibration standards since the ionization rate depends on both the atom (or molecule) and the matrix. These standards are usually in the form of ion implants which can be deposited in the sample using an implanter or using the primary ion beam of the SIMS (if the primary ion source is mass filtered). By comparing the known concentration of implanted ions to the number of sputtered implant ions, it is possible to calculate the relative sensitivity factor (RSF) value for the implant ion in the particular sample. By comparing this RSF value to the value in a standard RSF table and adjusting all the table RSF values by the difference between them, it is possible to calculate the concentrations of other atoms in the sample. For more information on RSF values, see above.

When choosing an isotope to use for ion implantation, it is important take into consideration possible mass interferences. For example, ^{11}B, ^{16}O, and ^{27}Al have the same overall masses and will interfere with each others ion intensity in the spectra. Therefore, one must chose an ion implant that does not have the same mass as any other species in the sample which are of interest.

Also, the depth at which the implant is deposited is also important. The implanted ion must be lower than the equilibration depth, above which, chaotic sputtering occurs until a sputter equilibrium is reached. However, care should be taken to ensure that the implanted ions do not pass the layer of interest in the sample- if the matrix changes, the implanted ions will no longer sputter at the same rate, causing concentrations to be inaccurate.

Matrix Effects

In SIMS, matrix effects are common and originate from changes in the ionization efficiency (the number of ionized species compared to totally number of sputtered species) and the sputtering yield. One of the main causes of matrix effects is the primary beam. As was discussed earlier, electronegative primary ions increases the number of positively charged secondary ions, while electropositive primary ions increases the number of negatively charged secondary ions. Matrix effects can also be caused by species present in the sample. The consequences of these matrix effects depends on the identity of the effecting species and the composition of the sample. To correct for matrix effects, it is necessary to use a standards and compare the results with RSFs (see above).

Detection Limits

For most atoms, SIMS can accurately detect down to a concentration of 1ppm. For some atoms, a concentration of 10 ppb may be achieved. The detection limit in this instrument is set by the count rate (how many ions may be counted per second) rather than by a limitation due to the mass of the ion. So, to decrease detection limit, the sample can be sputtered at a higher rate.

Sensitivity

The sensitivity of SIMS analysis depends on the element of interest, the matrix the element is in, and what primary ion is used. The sensitivity of SIMS towards a particular ion may easily be determined by looking at an RSF table. So, for example, looking at an RSF table for an oxygen primary ion and positive secondary ions shows that the alkali metals have the highest sensitivity (they have low RSF values). This makes sense, since these atoms have the lowest electron affinities and are the easiest to ionize. Similarly, looking at the RSF table for a cesium primary ion beam and negative secondary ions shows that the halogens have the highest sensitivity. Again, this makes sense since the halogens have the highest electron affinities and accept electrons easily.

Data Interpretation

Three types of spectra can be obtained from a SIMS analysis. From static SIMS, a mass spectrum is produced. From dynamic SIMS, a depth profile or mass spectrum is produced. And, not surprisingly, an image is produced from imaging SIMS.

Mass Spectra

As with a typical mass spectrum, the mass to charge ratio (*m/z*) is compared to the ion intensity. However, because SIMS is capable of a dynamic range of 9 orders of magnitude, the intensity of the SIMS mass spectra is displayed on a logarithmic scale. From this data, it is possible to observe isotopic data as well as molecular ion data and their relative abundances on the sample surface.

Depth Profile

A depth profile displays the intensity of one or more ions with respect to the depth (or, equivalently, time). Caution should be taken when interpreting this data- if ions are collected off the wall of the crater rather than from the bottom, it will appear that the layer in question runs deeper in the sample than it actually does.

Matrix Assisted Laser Desorption Ionization (MALDI)

Development of MALDI

As alluded to in previous sections, laser desorption (LD) was originally developed to produce ions in the gas phase. This is accomplished by pulsing a laser on the sample surface to ablate material causing ionization and vaporization of sample particles. However, the probability of attaining a valuable mass spectrum is highly dependent on the properties of the analyte. Furthermore, masses observed in the spectrum were products of the molecular fragmentation if the molecular weight was above 500 Da. Clearly, this was not optimal instrumentation for analyzing large biomolecules and bioinorganic compounds that do not ionize well and samples were degraded during the process. Matrix-assisted laser desorption ionization (MALDI) was developed and alleviated many issues associated with LD techniques. The MALDI technique allows proteins with masses up to 300,000 Da to be detected. This is important to bioinorganic chemistry when visualizing products resulting from catalytic reactions, metalloenzyme modifications, and other applications.

MALDI as a process decreases the amount of damage to the sample by protected the individual analytes within a matrix (more information of matrices later). The matrix itself absorbs much of the energy introduced by the laser during the pulsing action. Plus, energy absorbed by the matrix in subsequently transferred to the analyte (Figure 2.2.19). Once, energized, the analyte ionized and is released into a plume of ions containing common cations (Na^+, K^+, etc.), matrix ions, and analyte ions. These ions then enter the flight tube where they are sent to the detector. Different instrumental modes adjust for differences in ion flight time (Figure 2.2.19). The MALDI technique is also more sensitive and universal since readjustments to match absorption frequency is not necessary due to the matrix absorption. Many of the commonly used matrices have similar wavelength absorptions Table 2.2.3.

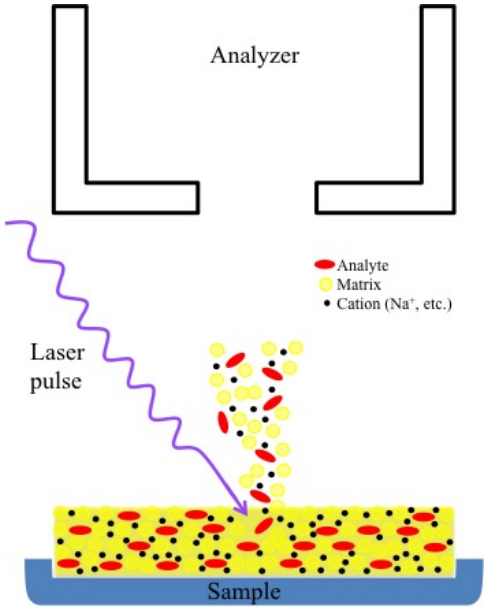
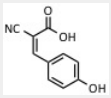
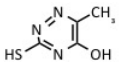
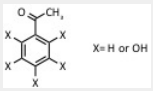
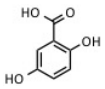
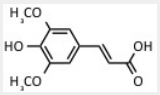
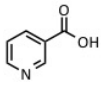
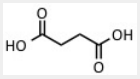
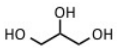


Figure 2.2.19 Schematic representation of the MALDI process. The laser strikes the surface of the matrix-analyte sample causing a "plume" of matrix and analyte ions that are received by the analyzer. Yellow circles represent the matrix, red ovals represent the sample/analyte, and the small black circles represent cations.

Table 2.2.3 Table of different small molecules used as MALDI matrices.

Matrix	Wavelength	Application	Structure

Cyano-4-hydroxycinnamic acid	UV: 337nm, 353 nm	Peptides	
6-Aza-2-thiothymine	UV: 337 nm, 353 nm	Proteins, peptides, non-covalent complexes	
k,m,n-Di(tri)hydroxy-acetophenone	UV: 337 nm, 353 nm	Proteins, peptides, non-covalent complexes	
2,5-Dihydroxybenzoic acid (requires 10% 2-hydroxy-5-methoxybenzoic acid)	UV: 337 nm, 353 nm	Proteins, peptides, carbohydrates, synthetic polymers	
Sinapinic acid	UV: 337 nm, 353 nm	Proteins, peptides	
Nicotinic acid	UV: 266 nm	Proteins, peptides, adduct formation	
Succinic acid	IR: 2.94 µm, 2.79 µm	Proteins, peptides	
Glycerol	IR: 2.94 µm, 2.79 µm	Proteins, peptides	

Collection of MALDI Spectra

The process of MALDI takes place in 2 steps:

1. Sample preparation.
2. Sample ablation

Sample Preparation

The sample for analysis is combined with a matrix (a solvent containing small organic molecules that have a strong absorbance at the laser wavelength) and added to the MALDI plate (Figure 2.2.18). The sample is then dried to the surface of the plate before it is analyzed, resulting in the matrix doped with the analyte of interest as a "solid solution". Figure 2.2.20 shows the loading of a peptide in water in cyano-4-hydroxycinnamic acid matrix.

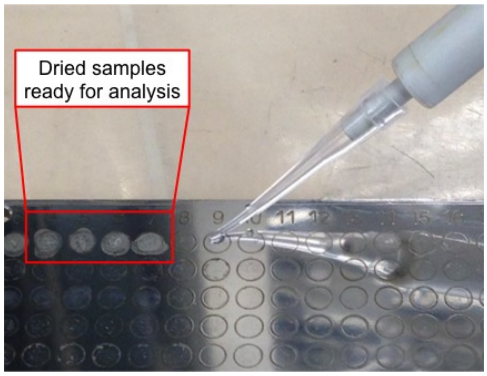


Figure 2.2.20 The addition of the sample and matrix on to a MALDI plate, the samples are left until completely dry.

Prior to insertion of the plate into the MALDI instrument, the samples *must be fully dried*. The MALDI plate with the dry samples is placed on a carrier and is inserted into the vacuum chamber (Figure 2.2.21a-b). After the chamber is evacuated, it is ready to start the step of sample ablation.



Figure 2.2.21 (a) Image of the MALDI carrier released for sample loading. (b-c) Image of the sample plate loaded into the MALDI carrier and insertion onto the instrument.

After the sample is loaded into the instrument, the instrument camera will show activate to show a live feed from inside of the chamber. The live feed allows the controller to view the location where the spectrum is being acquired. This becomes especially important when the operator manually fires the laser pulses.

Collection of a Spectrum

When the sample is loaded into the vacuum chamber of the instrument, there are several options for taking a mass spectrum. First, there are several modes for the instrument, two of which are described here: axial and reflectron modes.

Axial Mode

In the axial (or linear) mode, only a very short ion pulse is required before the ions go down the flight tube and hit the detector. This mode is often used when exact accuracy is not required since the mass accuracy has an error of about +/- 2-5%. Sources of these errors are found in the arrival time of different ions through the flight tube to the detector. Errors in the arrival time are caused by the difference in initial velocity with which the ions travel based on their size. The larger ions have a lower initial velocity, thus they reach the detector after a longer period of time. This decreases the mass detection resolution.

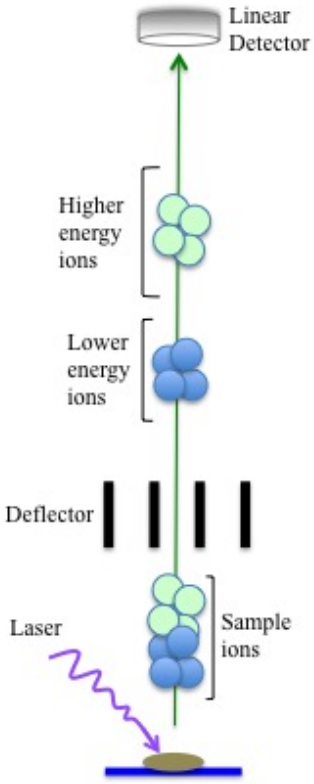


Figure 2.2.22 MALDI instrument diagram depicting the axial mode. The laser strikes the surface of the matrix-analyte sample and a plume of ions is released into the detector. The ions with higher energy travel faster compared to those with lower energy but the same mass. These ions will hit the detector at different times causing some loss in resolution.

Reflectron Mode

In the reflectron (“ion mirror”) mode, ions are refocused before they hit the detector. The reflectron itself is actually a set of ring electrodes that create an electric field that is constant near the end of the flight tube. This causes the ions to slow and reverse

direction towards a separate detector. Smaller ions are then brought closer to large ions before the group of ions hit the detector. This assists with improving detection resolution and decreases accuracy error to +/- 0.5%.

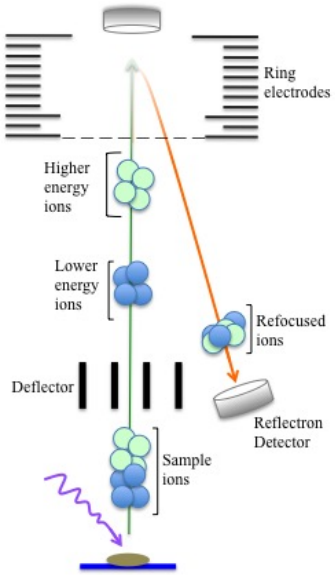


Figure 2.2.23 MALDI instrument diagram depicting the reflectron mode. The laser strikes the surface of the matrix-analyte sample and a plume of ions is released into the analyzer. Higher energy ions of the same mass travel down the flight tube faster than lower energy ion of a similar mass, however in the reflectron mode this difference in corrected. Ring electrodes are activated and create a uniform electric field. This slows the ions and redirects them into the reflectron detector. This increases resolution by refocusing the ions to reach the detector at a similar time.

Example of MALDI Application

While MALDI is used extensively in analyzing proteins and peptides, it is also used to analyze nanomaterials. The following example describes the analysis of fullerene analogues synthesized for a high performance conversion system for solar power. The fullerene C_{60} is a spherical carbon molecule consisting of 60 sp^2carbon atoms, the properties of which may be altered through functionalization. A series of *tert*-butyl-4-C61-benzoate (t-BCB) functionalized fullerenes were synthesized and isolated. MALDI was not used extensively as a method for observing activity, but instead was used as a conformative technique to determine the presence of desired product. Three fullerene derivatives were synthesized (Figure 2.2.24).The identity and number of functional groups were determined using MALDI (Figure 2.2.25).

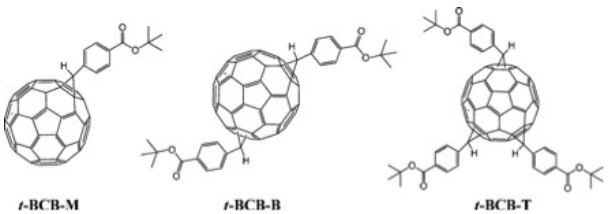


Figure 2.2.24 A series of *tert*-butyl-4-C61-benzoate (*t*-BCB) functionalized fullerenes were synthesized and isolated. These compounds were characterized by using MALDI to confirm desired product and isolation.

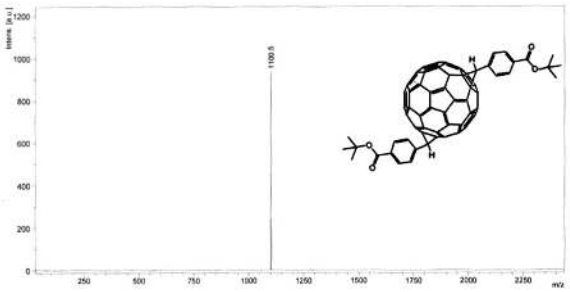


Figure 2.2.25 Mass for t-BCB-B (M_W = 1100) was determined by using MALDI.

Surface-Assisted Laser Desorption/Ionization Mass Spectrometry (SALDI-MS)

Surface-assisted laser desorption/ionization mass spectrometry, which is known as SALDI-MS, is a soft mass spectrometry technique capable of analyzing all kinds of small organic molecules, polymers and large biomolecules. The essential principle of this method is similar to (matrix-assisted laser desorption/ionization mass spectrometry) MALDI-MS (see http://cnx.org/contents/925e204d-d85...3e4d60057b37@1), but the organic matrix commonly used in MALDI has been changed into the surface of certain substrates, usually inorganic compounds. This makes SALDI a matrix-free ionization technique that avoids the interference of matrix molecules.

SALDI is considered to be a three-step process shown in Figure 2.2.26

- Samples are mixed with the substrates that provide large surface area to support sample molecule.
- The samples are irradiated with IR of UV laser pulses when the energy of laser pulses are absorbed by the substrates and transferred to the sample molecules.
- Desorption and ionization process are initiated, which produces ions that are accelerated into the analyzer.

Since the bulk of energy input goes to substrates instead of the sample molecules, it is thought to be a soft ionization technique useful in chemistry and chemical biology fields.

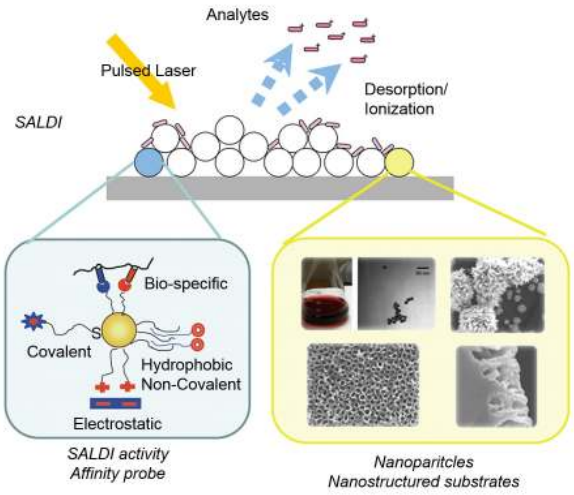


Figure 2.2.26 Schematic representations of SALDI-MS using various nanoparticles and nanostructures substrates, and an affinity probe. Reproduced from: R. Arakawa, and H. Kawasaki, *Anal. Sci.*, 2010, **26**, 1229. Copyright: Japan Society for Analytical Chemistry.

The most important characteristic of the substrate in SALDI is a large surface areas. In the past 30 years, efforts have been made to explore novel substrate materials that increase the sensitivity and selectivity in SALDI-MS. Depending on the substrate compounds being used, the interaction between the substrate materials and sample molecules could be covalent, non-covalent such as hydrophobic effect, bio-specific such as recognition between biotins and avidins, and between antigens and antibodies, or electrostatic. With the unique characteristics stated above, SALDI is able to combine the advantages of both hard and soft ionization techniques. On one hand, low molecular weight (LMW) molecules could be analyzed and identified in SALDI-MS, which resembles the function of most hard ionization techniques. On the other hand, molecular or quasi-molecular ions would dominate the spectra as what we commonly see in the spectra prepared by soft ionization techniques.

History

The SALDI technique actually emerged from its well-known rival technique, MALDI. The development of soft ionization techniques, which mainly included MALDI and ESI, enabled chemists and chemical biologists to analyze large polymers and biomolecules using mass spectrometry. This should be attributed to the soft ionization process which prohibited large degree of fragmentation that complicated the spectra, and resultant ions were dominantly molecular ions or quasi-molecular ions. In other words, tolerance of impurities would be increased since the spectra became highly simplified. While it was effective in determining molecular weight of the analytes, the matrix peaks would also appear in low mass range, which seriously interfered with the analysis of LMW analytes. As a result, the SALDI method emerged to resolve the problem by replacing matrix with surface that was rather stationary.

The original idea of SALDI was raised by Tanaka (Figure 2.2.27) in 1988. Ultra-fine cobalt powders with an average diameter of about 300 Å that were mixed in the sample were responsible of "rapid heating" due to its high photo-absorption and low heat capacity. With a large surface area, the cobalt powders were able to conduct heat to large numbers of surrounding glycerol liquid and analyte molecules, which indeed resulted in a thermal desorption/ionization mechanism. The upper mass limit was increased up to 100 kDa, which is shown in Figure 2.2.28 for the analysis of lysozymes from chicken egg white.



Figure 2.2.27 Japanese engineer Koichi Tanaka, recipient of the Nobel Prize in Chemistry in 2002.

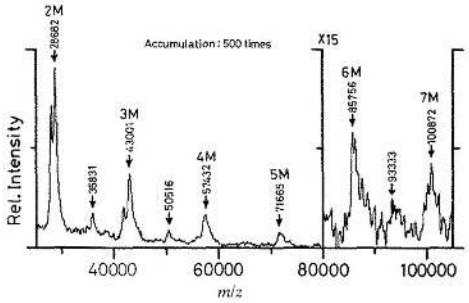


Figure 2.2.28 Laser ionization mass spectrum of lysozyme (enzymes that are able to damage bacteria cell walls) from chicken egg white. Molecular weight 14306 Da.Reproduced from: K. Tanaka, H. Waki, Y. Ido, S. Akita, and Y. Yoshida, and T. Yoshida, *Rapid Commun. Mass Spectrom.*, 1988, **2**, 151. Copyright: John Wiley and Sons.

The low mass range was not paid much attention at the beginning, and the concept of "surface-assisted" was not proposed until Sunner (Figure 2.2.29) and co-workers reported the study on graphite SALDI in 1995. And that was the first time the term "SALDI" was used by chemists. They achieved obtaining mass spectra of both proteins and LWM analytes by irradiating mixture of 2-150 μm graphite particles and solutions of analytes in glycerol. Although fragmentation of the LMW glycerol molecules was relatively complicated (Figure 2.2.30), it was still considered as a significant improvement in ionizing small molecules by soft ionization methods.



Figure 2.2.29 American chemist Jan Sunner.

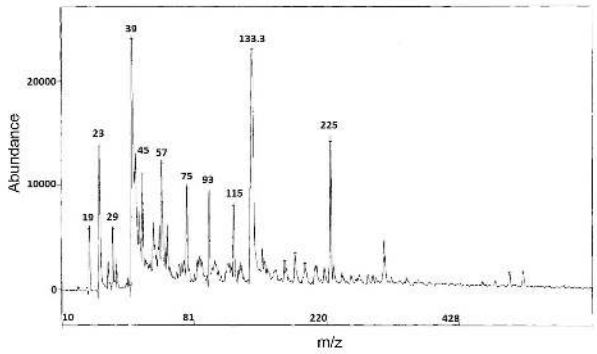


Figure 2.2.30 Graphite surface-assisted laser desorption mass spectrum (337 nm) of glycerol. Average of 82 laser shots. The ions at m/z=93 is protonated glycerol. The ions at m/z= 75, 57, 45, 29, and 19 are all fragments of GI. The ions at m/z= 23, 39, and 133 are Na^+, K^+, and Cs^+. The ions at 115, 131, and 225 are alkali ion/glycerol adducts, Na^+(glycerol), K^+(glycerol), and Cs^+(glycerol). Reproduced from J. Sunner, E. Dratz, and T. Chen, *Anal Chem*, 1995, **67**, 4335. Copyright: American Chemical Society.

Despite the breakthrough mentioned above, SALDI did not widely interest chemists. Regardless of its drawbacks in upper mass limit for the analysis of large molecules, the sensitivity was far from being satisfactory compared to hard ionization techniques in terms of testing LMW molecules. This situation has been changed ever since nanomaterials were introduced as the substrates, especially for the successful development of desorption/ionization on porous silicon (DIOS) shown in Figure 2.2.31. In fact, majority of research on SALDI-MS has been focusing on exploiting novel nanomaterial substrates, aiming at further broadening the mass range, improving the reproducibility, enhancing the sensitivity and extending the categories of compounds that were able to be analyzed. So far, a variety of nanomaterials have been utilized in SALDI-MS, including carbon-based nanomaterials, metal-based nanomaterials, semiconductor-based nanomaterials, etc.

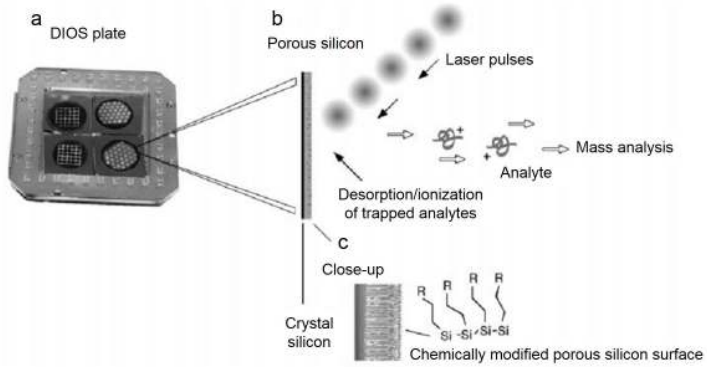


Figure 2.2.31 Experimental configuration for the DIOS-MS experiments. (a) Four porous silicon plates are placed on a MALDI plate. Each of the porous silicon plates contains photopatterned spots or grids prepared through illumination of n-type silicon with a 300-W tungsten filament through a mask and an f/50 reducing lens. (b) The silicon-based laser desorption/ionization process, in which the sample is placed on the porous silicon plate and allowed to dry, followed by laser-induced desorption/ionization mass spectrometry. (c) Cross-section of porous silicon, and the surface functionalities after hydrosilylation; R represents phenyl or alkyl chains. Reproduced from J. Wei, J. M. Buriak, and G. Siuzdak *Nature*, 1999, **399**, 243. Copyright: Nature Publishing Group.

Basic Principles of SALDI

Mechanism of Desorption and Ionization

As a soft ionization technique, SALDI is expected to produce molecular or quasi-molecular ions in the final mass spectra. Since this requires the ionization process to be both effective and controllable, which means sufficient sample molecules could be ionized while further fragmentation should be mostly avoided.

While the original goal mentioned above has been successfully accomplished for years, the study on desorption and ionization mechanism in detail is still one of the most popular and controversial research areas of SALDI at present. It is mostly agreed that the substrate material has played a significant role of both activating and protecting the analyte molecules. The schematic picture describing the entire process is shown in Figure 2.2.33. Energy input from the pulsed laser is largely absorbed by the substrate material, which is possibly followed by complicated energy transfer from the substrate material to the absorbed analyte molecules. As a result, both thermal and non-thermal desorption could be triggered, and for different modes of SALDI experiments, the specific desorption and ionization process greatly differs.

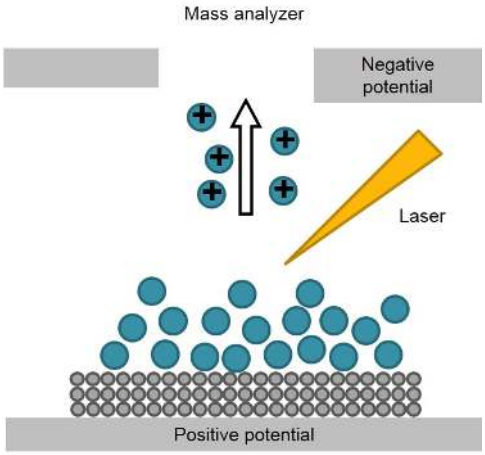


Figure 2.2.33 Schematic picture of surface assisted laser desorption/ionization. The gray spheres and blue spheres represent substrate materials and analyte molecules, respectively.

The mechanism for porous silicon surface as a SALDI substrate has been widely studied by researchers. In general, the process can be subdivided into the following steps:

1. Adsorption of neutral analyte molecules takes places by formation of hydrogen bonds with surface silanol groups;
2. Electronic excitation of the substrate under the influence of the laser pulse generates a free electron/“hole” pair. This separation causes enrichment of positive charges near the surface layer; as a result, the acidity of the silanol groups increases and proton transfer to analytes becomes easier;
3. Analyte ions are thermally activated and thus dissociated from the surface.

When no associated proton donor is present in the vicinity of analyte molecules, desorption might occur without ionization. Subsequently, the desorbed analyte molecule is ionized in the gas phase by collision with incoming ions.

Signal Enhancement Factors on SALDI Substrates

Since it is the active surface responsible for adsorption, desorption and ionization of analyte molecules that features the technique, the surface chemistry of substrate material is undoubtedly crucial for SALDI performance. But it is rather difficult to draw a general conclusion due to the fact that the affinity between different classes of substrates and analytes is considerably versatile. Basically, the interaction between those two components has an impact on trapping and releasing the analyte molecules, as well as the electronic surface state of the substrate and energy transfer coefficiency.

Another important aspect is the physical properties of the substrates which could alter desorption and ionization process directly, especially for the thermally activated pathway. This is closely related to rapid temperature increase on the substrate surface. Those properties include optical absorption coefficiency, heat capacity and heat conductivity (or heat diffusion rate). First, higher optical absorption coefficiency enables the substrate to absorb and generate more heat when certain amount of energy is provided by the laser source. Moreover, a lower heat capacity usually leads to larger temperature increase upon the same amount of heat. In addition, a lower hear conductivity helps the substrate to maintain a high temperature that will further result in a higher temperature peak. Therefore, the thermal desorption and ionization could occur more rapidly and effectively.

Instrumentation

The instrument involved in SALDI shown in Figure 2.2.34 is similar with in MALDI to large extent. It contains a laser source which generates pulsed laser that excites the sample mixture. There is a sample stage that places the sample mixture of substrate materials and analytes. Usually the mass analyzer and ion detector are on the other side to let the ions go through and become separated and detected based on different m/z value. Recent progress has been made that incorporates direct analysis in real time (DART) ion source into SALDI-MS system which makes it possible to perform the analysis in ambient conditions. Figure 2.2.35 shows their ambient SALDI-MS method.

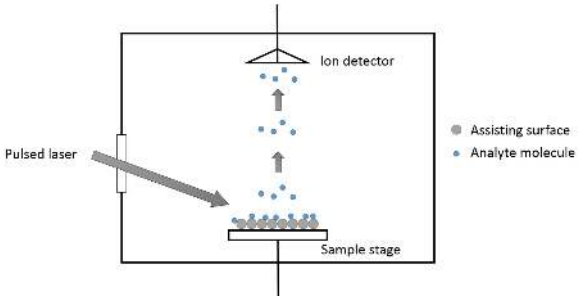


Figure 2.2.34 Schematic illistration of SALDI instrument.

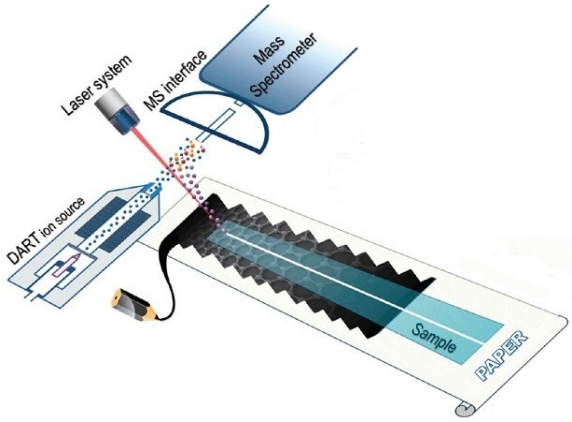


Figure 2.2.35 Schematic illustration of the performance of the ambient SALDI-MS. Reproduced from J. Zhang, Z. Li, C. Zhang, B. Feng, Z. Zhou, Y. Bai, and H. Liu, *Anal. Chem.*, 2012, **84**, 3296. Copyright: American Chemical Society, 2012.

Examples of Nanomaterials Used For Analysis of LMW Analytes in SALDI-MS

Porous Silicon as a Substrate Material

Porous silicon with large surface area could be used to trap certain analyte molecules for matrix-free desorption and ionization process. More interestingly, a large ultraviolet absorption coefficiency was found for this porous material, which also improved the ionization performance. It has been reported that using porous silicon as the substrate in SALDI-MS was able to work at femtomole and attomole levels of analytes including as peptides, caffeine, an antiviral drug molecule (WIN), reserpine and *N*-octyl-*β*-D-glucopyranoside . Compared to conventional MALDI-MS, the DIOS-MS (which was the specific type of SALDI in this research) successfully eliminated the matrix interference and displayed much higher quasi-molecular peak (MH^+), which could be observed in Figure 2.2.36. What's more, chemical modification of the porous silicon was able to further optimize the ionization characteristics.

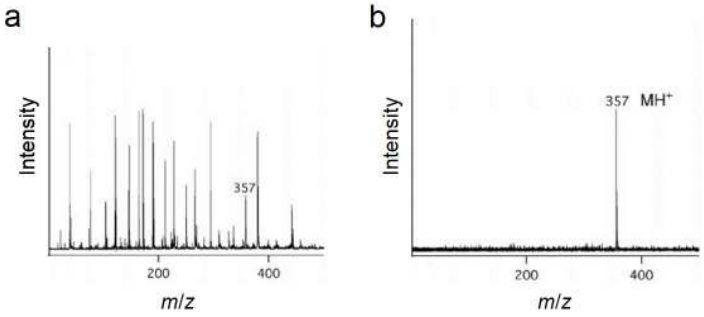


Figure 2.2.36 Analysis of WIN antiviral drug (500 fmol) using different desorption/ionization techniques. (a) MALDI-MS of same amount of antiviral drug usinga-cyano-4-hydroxycinnamic matrix. (b) DIOS-MS spectrum of WIN. Accurate mass measurements were obtained on WIN with a time-of-flight reflectron instrument, typically to within 10 ppm (the limit of accuracy of this instrument in this mass range). The inset spectrum represents post-source decay fragmentation measurements on WIN. These results are consistent with results from electrospray ionization tandem mass spectrometry experiments. Reproduced from J. Wei, J. M. Buriak, and G. Siuzdak, *Nature*, 1999, **399**, 243. Copyright: Nature Publishing Group, 1999.

Graphene as a Surface Material

Graphene is a type of popular carbon nanomaterial discovered in 2004. It has a large surface area that could effectively attach the analyte molecules. On the other hand, the efficiency of desorption/ionization for analytes on a layer of graphene can be enhanced for its simple monolayer structure and unique electronic properties. Polar compounds including amino acids, polyamines, anticancer drugs, and nucleosides can be successfully analyzed. In addition, nonpolar molecules can be analyzed with high resolution and sensitivity due to the hydrophobic nature of graphene itself. Compared with a conventional matrix, graphene exhibited a high desorption/ionization efficiency for nonpolar compounds. The graphene substrate functions as a substrate to trap analytes, and it transfers energy to the analytes upon laser irradiation, which allows for the analytes to be readily desorbed/ionized and the interference of matrix to be eliminated. It has been demonstrated that the use of graphene as a substrate material avoids the fragmentation of analytes and provides good reproducibility and a high salt tolerance, underscoring the potential application of graphene as a matrix for MALDI-MS analysis of practical samples in complex sample matrixes. It is also proved that the use of graphene as an adsorbent for the solid-phase extraction of squalene could improve greatly the detection limit.

Combination with GC

Gas-phase SALDI-MS analysis has a relatively high ionization efficiency, which leads to a high sensitivity. In 2009, gas chromatography (GC) was first used with SALDI-MS, where the SALDI substrate was amorphous silicon and the analyte was N-alkylated phenylethylamines. Detection limits were in the range of attomoles, but improvements are expected in the future. The combination with GC is expected to expand the use of SALDI-MS even more that SALDI could be applied to separation and identification of samples with more complexity. The instrumental setup is shown in Figure 2.2.37.

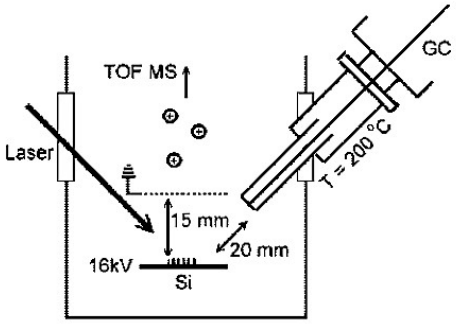


Figure 2.2.37 Instrument setup of GC-SALDI-MS. Reproduced from: S. Alimpiev, A. Grechnikov, J. Sunner, A. Borodkov, V. Karavanskii, Y. Simanovsky, and S. Nikiforov, *Anal. Chem.*, 2009, **81**, 1255. Copyright: American Chemical Society, 2009.

Differential Electrochemical Mass Spectrometry

In the study of electrochemistry, it had always been a challenge to obtain immediate and continuous detection of electrochemical products due to the limited formation on the surface of the electrode, until the discovery of differential electrochemical mass spectrometry. Scientists initially tested the idea by combining porous membrane and mass spectrometry for product analysis in the study of oxygen generation from $HClO_4$ using porous electrode in 1971. In 1984, another similar experiment was performed using a porous Teflon membrane with 100 μm of lacquers at the surface between the electrolytes and the vacuum system. Comparing to previous experiment, this experiment has demonstrated a vacuum system with improved time derivative that showed nearly immediate detection of volatile electrochemical reaction products, with high sensitivity of detecting as small as “one monolayer” at the electrode. In summary, the experiment demonstrated in 1984 not only showed continous sample detection in mass spectrometry but also the rates of formation, which distinguished itself from the technique performed previously in 1971. Hence, this method was called differential electrochemical mass spectrometry (DEMS). During the past couple decades, this technique has evolved from using classic electrode to rotating disc electrode (RDE), which provides a more homogeneous and faster transport of reaction species to the surface of the electrode.

Described in basic terms, differential electrochemical mass spectrometry is a characterization technique that analyzes specimens using both the electrochemical half-cell experimentation and mass spectrometry. It uses non-wetting membrane to separate the aqueous electrolyte and gaseous electrolyte, which gaseous electrolyte will permeate through the membrane and will be ionized and detected in the mass spectrometer using continuous, two-stage vacuum system. This analytical method can detect gaseous or volatile electrochemical reactants, reaction products, and even reaction intermediates. The instrument consists of three major

components: electrochemical half-cell, PTFE (polytetrafluoroethylene) membrane interface, and quadrupole mass spectrometer (QMS), which is a part of the vacuum system.

DEMS Operations

The entire assembly of the instrument is shown in Figure 2.2.38, which consists of three major components: an electrochemical half-cell, a PTFE membrane interface, and the quadrupole mass spectrometer. In this section, each component will be explained and its functionality will be explored, and additional information will be provided at the end of this section. The PTFE membrane is micro-porous membrane that separates the aqueous electrolyte from volatile electrolyte which will be drawn to the high vacuum portion. Using the high vacuum suction, the gaseous or volatile species will be allowed to permeate through the membrane using differential pressure, leaving the aqueous materials on the surface due to hydrophobic nature of the membrane. The selection of the membrane material is very important to maintain both the hydrophobicity and proper diffusion of volatile species. The species permeated to QMS will be monitored and measured, and the kinetics of formation will be determined at the end. Depending on the operating condition, different vacuum pumps might be required.

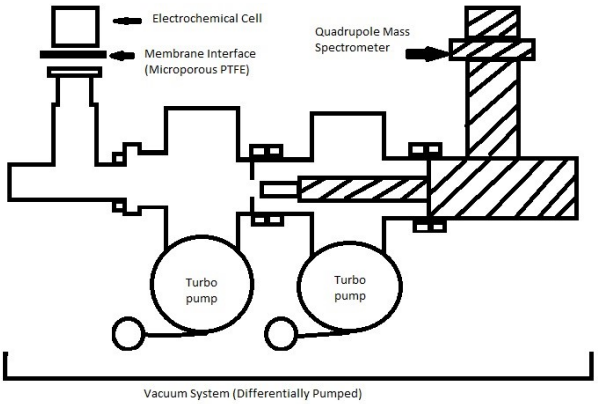


Figure 2.2.38 Mechanical setup of the entire differential electrochemical mass spectrometry. Adapted from Aston, S.J., “Design, Construction and Research Application of a Differential Electrochemical Mass Spectrometer (DEMS)”, Springer, 2011, 9-27.

Electrochemical Cells

First major component of the DEMS instrument is the design of electrochemical cells. There are many different designs that have been developed for the past several decades, depending on the types of electrochemical reactions, the types and sizes of electrodes. However, only the classic cell will be discussed in this chapter.

DEMS method was first demonstrated using the classical method. A conventional setup of electrochemical cell is showed in Figure 2.2.39. The powdered electrode material is deposited on the porous membrane to form the working electrode, shown as Working Electrode Material in Figure 2.2.39. In the demonstration by Wolber and Heitbaum, the electrode was prepared by having small Pt particles deposited onto the membrane by painting a lacquer. It was later in other experimentations evolved to use sputtering electro-catalyst layer for a more homogenous surface. The aqueous cell electrolyte is shielded with an upside down glass body with vertical tunnel opening to the PTFE membrane. The working electrode material lies above the PTFE membrane, where it is supported mechanically by stainless steel frit inside vacuum flange. Both the working electrode material and PTFE membrane are compressed between vacuum castings and PTFE spacer, which is a ring that prevents the electrolyte from leakage. The counter electrode (CE) and reference electrode (RE) made from platinum wire are placed on top of the working electrode material to create the electrical contact. One of the main advantages of the classical design is fast respond time, with high efficiency of “0.5 for lacquer and 0.9 with the sputter electrode”. However, this method poses certain difficulties. First, the electrolyte materials will be absorbed on the working electrode before it permeates through the membrane. Due to the limitation of absorption rate, the concentration on the surface of the electrode will be lower than bulk. Second, the aqueous volatile electrolyte must be absorbed onto working electrode, and then followed by evaporation through the membrane. Therefore, the difference in rates of absorption and evaporation will create a shift in equilibrium. Third, this method is also limited to the types of material that can be deposited on the surface, such as single crystals or even some polycrystalline electrode surfaces. Lastly, the way RE is position could potentially introduce impurity into the system, which will interfere with the experiment.

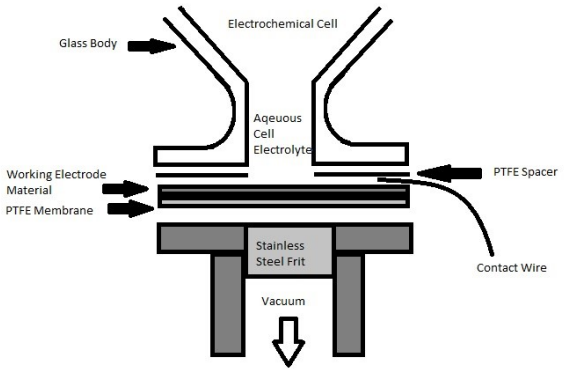


Figure adapted from J. S. Aston, *Design, Construction and Research Application of a Differential Electrochemical Mass Spectrometer (DEMS)*, Springer-Verlag, Berlin Heidelberg (2011).

Membrane Interface

PTFE membrane is placed between the aqueous electrolyte cell and the high vacuum system on the other end. It acts as a barrier that prevents aqueous electrolyte from passing through, while its selectivity allows the vaporized electrochemical species to transport to the high vacuum side, which the process is similar to vacuum membrane distillation shown in Figure 2.2.41. In order to prevent the aqueous solution from penetrating through the membrane, the surface of the membrane must be hydrophobic, which is a material property that repels water or aqueous fluid. Therefore, at each pore location, there is vapor and liquid interface where the liquid will remain on the surface while the vapor will penetrate into the membrane. Then the transportation of the material in vapor phase is triggered by the pressure difference created from the vacuum on the other end of the membrane. Therefore, the size of the pore is crucial in controlling its hydrophobic properties and the transfer rate through the membrane. When the pore size is less than 0.8 μm, the hydrophobic property is activated. This number is determined by calculating the surface tension of liquid, the contact angle and the applied pressure. Therefore, a membrane with relatively small pore sizes and large pore distribution is desired. In general membrane materials used are "typically 0.02 μm in size with thickness between 50 and 110 μm". In terms of materials, there are other materials such as polypropylene and polyvinylidene fluoride (PVDF)(Figure 2.2.41) have been tested; however, PTFE material (Figure 2.2.42) as membrane has demonstrated better durability and chemical resistance to electrochemical environment. Therefore, PTFE is shown to be the better candidate for such application, and is usually laminated onto polypropylene for enhanced mechanical properties. Despite the hydrophobic property of PTFE material, a significant amount aqueous material penetrates through the membrane due to the large pressure drop. Therefore, the correct sizing of the vacuum pumps is crucial to maintain the flux of gas to be transported to the mass spectrometry at the desire pressure. More information regarding the vacuum system will be discussed. In addition, capillary has been used in replacement of the membrane; however, this method will not be discussed here.

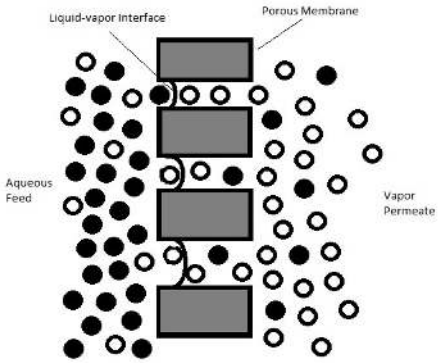


Figure 2.2.41 A illustration of the vacuum membrane distillation process. Adapted from J. S. Aston, *Design, Construction and Research Application of a Differential Electrochemical Mass Spectrometer (DEMS)*, Springer-Verlag, Berlin Heidelberg (2011).

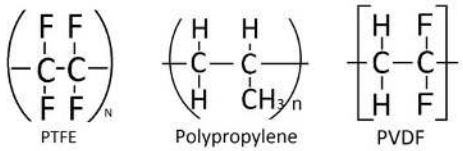


Figure 2.2.42 Chemical structures of polytetrafluoroethylene (PTFE), polypropylene and polyvinylidene fluoride (polyvinylidene difluoride, PVDF).

Vacuum and QMS

The correctly sized vacuum system can ensure the maximum amount of vapor material to be transported across the membrane. When the pressure drop is not adequate, part of the vapor material may be remain on the aqueous side as shown Figure 2.2.43. However, when the pressure drop is too large, too much aqueous electrolyte will be pulled from the liquid-vapor interface, subsequently increasing load on the vacuum pumps. In the cases of improper sized pumps can reduce pump efficiency and lower pump life-time if such problem is not corrected immediately. In addition, in order for mass spectrometry operate properly, the gas flux will need to maintain at a certain flow. Therefore, the vacuum pumps should provide steady flux of gas around 0.09 mbar/s.cm2 consisting mostly with gaseous or volatile species and other species that will be sent to mass spectrometry for analyzing. In additional, due to the limitation of pump speed of single vacuum pump, vacuum system with two or more pumps will be needed. For example, if 0.09 mbar/s.cm^2 is required and pump speed of 300 s^{-1} that operates at 10^{-5} mbar, the acceptable membrane geometrical area is 0.033 cm^{-2}. In order to increase the membrane area, addition pumps will be required in order to achieve the same gas flux.

Additional Information

There are several other analytical techniques such as cyclic voltammetry, potential step and galvanic step that can be combined with DEMS experiment. Cyclic voltammetry can provide both quantitative and qualitative results using the potential dependence. As a result, both the ion current of interested species and faradaic electrode current (the current generated by the reduction or oxidation of some chemical substance at an electrode) will be recorded when combining cyclic voltammetry and DEMS.

Applications

The lack of commercialization of this technique has limited it to only academic research. The largest field of application of DEMS is on electro-catalytic reactions. In addition, it is also used fuel cell research, detoxification reactions, electro-chemical gas sensors or more fundamental relevant research such as decomposition of ionic liquids etc.

Fuel Cell Differential Electrochemical Mass Spectrometry: Ethanol Electro-oxidation

The ethanol oxidation reaction was studied using alkaline membrane electrode assemblies (MEAs), constructed using nanoparticle Pt catalyst and alkaline polymeric membrane. DEMS will be use to study the mechanics of the ethanol oxidation reaction on the pt-based catalysts. The relevant products of the oxidation reaction are carbon dioxide, acetaldehyde and acetic acid. However, both carbon dioxide and acetaldehyde has the same molecular weight, which 44 g/mole. One approach is to monitor the major fragments where ionized CO_2^{2+} at m/z = 22 and COH^+ at m/z = 29 were used. Differential electrochemical mass spectrometry can detect volatile products of the electrochemical reaction; however, detections can be varied by solubility or boiling point. CO_2 is very volatile, but also soluble in water. If KOH is present, DEMS will not detect any CO_2traces. Therefore, all extra alkaline impurities should be removed before measurements are taken. The electrochemical characteristics can also be measured under various conditions and examples shown in Figure 2.2.43. In addition, the CCE (CO_2 current efficiency) was measured under different potentials. Using the CCE, the study concluded that the ethanol undergoes more complete oxidation using alkaline MEA than acidic MEA.

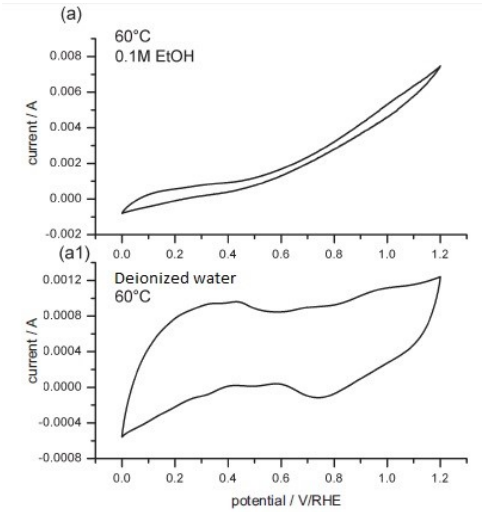


Figure 2.2.43 CV for the alkaline MEA are shown with 0.1 M EtOH solution in (a) for only de-ionized water in analyte (a1) both at 60 °C. Adapted from V. Rao, Hariyanto, C. Cremers, and U. Stimming, *Fuel Cells*, 2007, **5**, 417.

Studies on the Decomposition of Ionic Liquids

Ionic liquids (IL) have several properties such as high ionic conductivity, low vapor pressure, high thermal and electrochemical stability, which make them great candidate for battery electrolyte. Therefore, it is important to have better understanding of the stability of the reaction and of the products formed during decomposition behavior. DEMS is a powerful method where it can provide online detection of the volatile products; however, it runs into problems with high viscosity of ILs and low permeability due to the size of the molecules. Therefore, researchers modified the traditional setup of DEMS, which the modified method made use of the low vapor pressure of ILs and have electrochemical cell placed directly into the vacuum system. This experiment shows that this technique can be designed for very specific application and can be modified easily.

Conclusion

DEMS technique can provide on-line detection of products for electrochemical reactions both analytically and kinetically. In addition, the results are delivered with high sensitivity where both products and by-products can be detected as long as they are volatile. It can be easily assembled in the laboratory environment. For the past several decades, this technique has demonstrated advanced development and has delivered good results for many applications such as fuel cells, gas sensors etc. However, this technique has its limitation. There are many factors that need to be considered when designing this system such as half-cell electrochemical reaction, absorption rate and etc. Due to these constraints, the type of membrane should be selected and pump should be sized accordingly. Therefore, this characterization method is not one size fits all and will need to be modified base on the experimental parameters. Therefore, next step of development for DEMS is not only to improve its functions, but also to be utilized beyond the academic laboratory.

This page titled 2.2: Mass Spectrometry is shared under a CC BY license and was authored, remixed, and/or curated by Pavan M. V. Raja & Andrew R. Barron (OpenStax CNX) .

- **4.11: Mass Spectrometry** by Pavan M. V. Raja & Andrew R. Barron is licensed CC BY 4.0. Original source: http://cnx.org/contents/ba27839d-5042-4a40-afcf-c0e6e39fb45425.2.

2.3: How the Mass Spectrometer Works

This page describes how a mass spectrum is produced using a mass spectrometer.

How a mass spectrometer works

If something is moving and you subject it to a sideways force, instead of moving in a straight line, it will move in a curve - deflected out of its original path by the sideways force. Suppose you had a cannonball traveling past you and you wanted to deflect it as it went by you. All you've got is a jet of water from a hose-pipe that you can squirt at it. Frankly, its not going to make a lot of difference! Because the cannonball is so heavy, it will hardly be deflected at all from its original course. But suppose instead, you tried to deflect a table tennis ball traveling at the same speed as the cannonball using the same jet of water. Because this ball is so light, you will get a huge deflection.

The amount of deflection you will get for a given sideways force depends on the mass of the ball. If you knew the speed of the ball and the size of the force, you could calculate the mass of the ball if you knew what sort of curved path it was deflected through. The less the deflection, the heavier the ball. You can apply exactly the same principle to atomic sized particles.

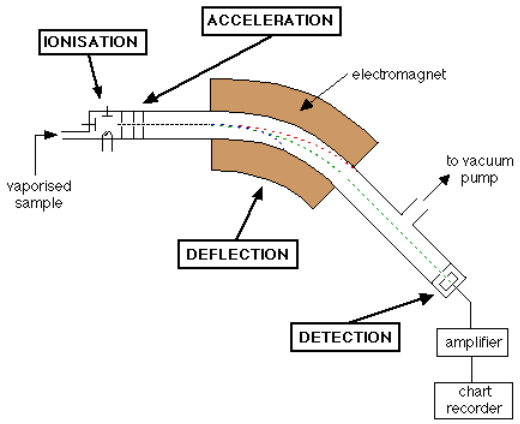
An outline of what happens in a mass spectrometer

Atoms can be deflected by magnetic fields - provided the atom is first turned into an ion. Electrically charged particles are affected by a magnetic field although electrically neutral ones aren't.

The sequence is :

- **Stage 1: Ionization**: The atom is ionised by knocking one or more electrons off to give a positive ion. This is true even for things which you would normally expect to form negative ions (chlorine, for example) or never form ions at all (argon, for example). Mass spectrometers always work with positive ions.
- **Stage 2: Acceleration:** The ions are accelerated so that they all have the same kinetic energy.
- **Stage 3: Deflection:** The ions are then deflected by a magnetic field according to their masses. The lighter they are, the more they are deflected. The amount of deflection also depends on the number of positive charges on the ion - in other words, on how many electrons were knocked off in the first stage. The more the ion is charged, the more it gets deflected.
- **Stage 4: Detection**: The beam of ions passing through the machine is detected electrically.

A full diagram of a mass spectrometer



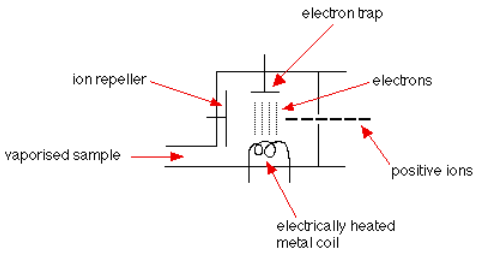
Understanding what's going on

The need for a vacuum

It's important that the ions produced in the ionization chamber have a free run through the machine without hitting air molecules.

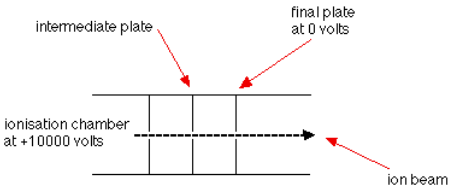
Ionization

The vaporized sample passes into the ionization chamber. The electrically heated metal coil gives off electrons which are attracted to the electron trap which is a positively charged plate.



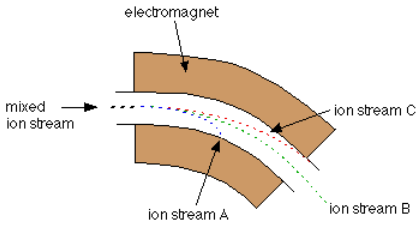
The particles in the sample (atoms or molecules) are therefore bombarded with a stream of electrons, and some of the collisions are energetic enough to knock one or more electrons out of the sample particles to make positive ions. Most of the positive ions formed will carry a charge of +1 because it is much more difficult to remove further electrons from an already positive ion. These positive ions are persuaded out into the rest of the machine by the ion repeller which is another metal plate carrying a slight positive charge.

Acceleration



The positive ions are repelled away from the very positive ionization chamber and pass through three slits, the final one of which is at 0 volts. The middle slit carries some intermediate voltage. All the ions are accelerated into a finely focused beam.

Deflection



Different ions are deflected by the magnetic field by different amounts. The amount of deflection depends on:

- the mass of the ion. Lighter ions are deflected more than heavier ones.
- the charge on the ion. Ions with 2 (or more) positive charges are deflected more than ones with only 1 positive charge.

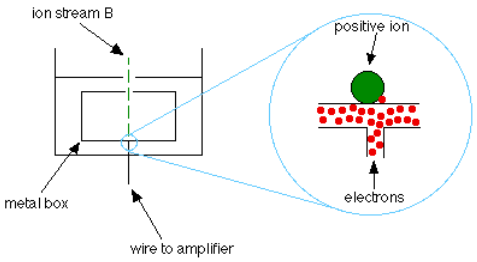
These two factors are combined into the mass/charge ratio. Mass/charge ratio is given the symbol m/z (or sometimes m/e). For example, if an ion had a mass of 28 and a charge of 1+, its mass/charge ratio would be 28. An ion with a mass of 56 and a charge of 2+ would also have a mass/charge ratio of 28.

In the last diagram, ion stream A is most deflected - it will contain ions with the smallest mass/charge ratio. Ion stream C is the least deflected - it contains ions with the greatest mass/charge ratio.

It makes it simpler to talk about this if we assume that the charge on all the ions is 1+. Most of the ions passing through the mass spectrometer will have a charge of 1+, so that the mass/charge ratio will be the same as the mass of the ion. Assuming 1+ ions, stream A has the lightest ions, stream B the next lightest and stream C the heaviest. Lighter ions are going to be more deflected than heavy ones.

Detection

Only ion stream B makes it right through the machine to the ion detector. The other ions collide with the walls where they will pick up electrons and be neutralised. Eventually, they get removed from the mass spectrometer by the vacuum pump.



When an ion hits the metal box, its charge is neutralized by an electron jumping from the metal on to the ion (right hand diagram). That leaves a space amongst the electrons in the metal, and the electrons in the wire shuffle along to fill it. A flow of electrons in the wire is detected as an electric current which can be amplified and recorded. The more ions arriving, the greater the current.

Detecting the other ions

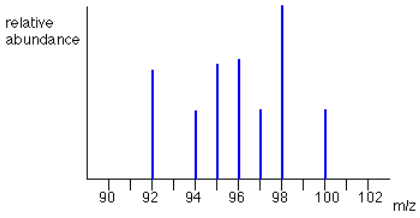
How might the other ions be detected - those in streams A and C which have been lost in the machine?

Remember that stream A was most deflected - it has the smallest value of m/z (the lightest ions if the charge is 1+). To bring them on to the detector, you would need to deflect them less - by using a smaller magnetic field (a smaller sideways force). To bring those with a larger m/z value (the heavier ions if the charge is +1) on to the detector you would have to deflect them more by using a larger magnetic field.

If you vary the magnetic field, you can bring each ion stream in turn on to the detector to produce a current which is proportional to the number of ions arriving. The mass of each ion being detected is related to the size of the magnetic field used to bring it on to the detector. The machine can be calibrated to record current (which is a measure of the number of ions) against m/z directly. The mass is measured on the ^{12}C scale.

What the mass spectrometer output looks like

The output from the chart recorder is usually simplified into a "stick diagram". This shows the relative current produced by ions of varying mass/charge ratio. The stick diagram for molybdenum looks like this:



You may find diagrams in which the vertical axis is labeled as either "relative abundance" or "relative intensity". Whichever is used, it means the same thing. The vertical scale is related to the current received by the chart recorder - and so to the number of ions arriving at the detector: the greater the current, the more abundant the ion.

As you will see from the diagram, the commonest ion has a mass/charge ratio of 98. Other ions have mass/charge ratios of 92, 94, 95, 96, 97 and 100. That means that molybdenum consists of 7 different isotopes. Assuming that the ions all have a charge of 1+, that means that the masses of the 7 isotopes on the carbon-12 scale are 92, 94, 95, 96, 97, 98 and 100.

Contributors and Attributions

- Jim Clark (Chemguide.co.uk)

This page titled 2.3: How the Mass Spectrometer Works is shared under a CC BY-NC 4.0 license and was authored, remixed, and/or curated by Jim Clark.

- **How the Mass Spectrometer Works** by Jim Clark is licensed CC BY-NC 4.0.

Electrospray Ionization Mass Spectrometry

Electrospray ionization is a soft ionization technique that is typically used to determine the molecular weights of proteins, peptides, and other biological macromolecules. Soft ionization is a useful technique when considering biological molecules of large molecular mass, such as the aformetioned, because this process does not fragment the macromolecules into smaller charged particles, rather it turns the macromolecule being ionized into small droplets. These droplets will then be further desolvated into even smaller droplets, which creates molecules with attached protons. These protonated and desolvated molecular ions will then be passed through the mass analyzer to the detector, and the mass of the sample can be determined.

Introduction

Electrospray ionization mass spectrometry is a desorption ionization method. Desorption ionization methods can be performed on solid or liquid samples, and allows for the sample to be nonvolatile or thermally unstable. This means that ionization of samples such as proteins, peptides, olgiopeptides, and some inorganic molecules can be performed. Electrospray ionization mass spectrometry requires that a molecule be of a fairly large mass. The instrument has a small mass range that it is able to detect, so therefore the mass of the unknown injected sample can easily be determined; as it must be in the range of the instrument. This quantitative analysis is done by considering the mass to charge ratios of the various peaks in the spectrum (Figure 1). The spectrum is shown with the mass-to-charge (m/z) ratio on the x-axis, and the relative intensity (%) of each peak shown on the y-axis. Calculations to determine the unknown mass, M_r, from the spectral data can then be performed using

$$p = \frac{m}{z} \tag{1}$$

$$p_1 = \frac{M_r + z_1}{z_1} \tag{2}$$

$$p_2 = \frac{M_r + (z_1 - 1)}{z_1 - 1} \tag{3}$$

where p_1 and p_2 are adjacent peaks. Peak p_1 comes before peak p_2 in the spectrum, and has a lower m/z value. The z_1 value represents the charge of peak one. It should be noted that as the m/z value increases, the number of protons attached to the molecular ion decreases. Figure 1 below illustrates these concepts. Electrospray ionization mass spectrometry research was pioneered by the analytical chemistry professor John Bennet Fenn, who shared the Nobel Prize in Chemistry with Koichi Tanaka in 2002 for his work on the subject.

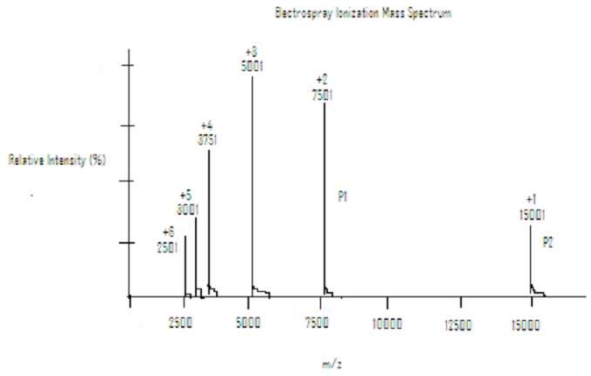


Figure 1. Mass Spectrum Example

Calculations for m/z in spectrum

$[M + 6H]^{6+}$ $[M + 5H]^{5+}$ $[M + 4H]^{4+}$

m/z = 15006/6 = 2501 m/z = 15005/5 = 3001 m/z = 15004/4 = 3751

$$[M + 3H]^{3+}\ [M + 2H]^{2+}\ [M + H]^{1+}$$

$$m/z = 15003/3 = 5001\ m/z = 15002/2 = 7501\ m/z = 15001/1 = 15001$$

Sample Preparation

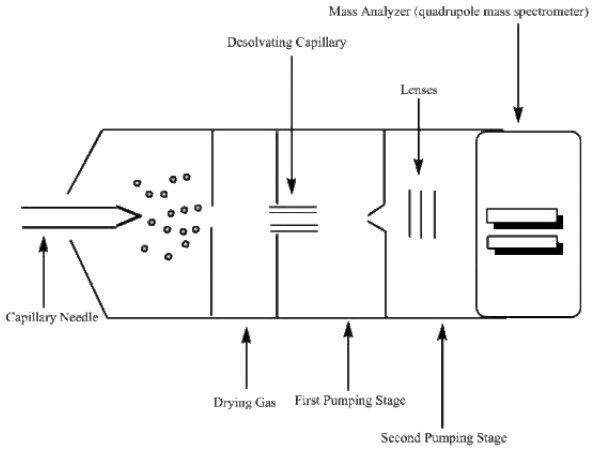
Samples for injection into the electrospray ionization mass spectrometer work the best if they are first purified. The reason purity in a sample is important is because this technique does not work well when mixtures are used as the analyte. For this reason a means of purification is often employed to inject a homogeneous sample into the capillary needle. High performance liquid chromatography, Capillary Electrophoresis, and Liquid-Solid Column Chromatography are methods of choice for this purpose. The chosen purification method is then attached to the capillary needle, and the sample can be introduced directly.

Advantages and Disadvantages

There are some clear advantages to using electrospray ionization mass spectrometry as an analytical method. One advantage is its ability to handle samples that have large masses. Another advantage is that this ionization method is one of the softest ionization methods available, therefore it has the ability to analyze biological samples that are defined by non-covalent interactions. A quadrupole mass analyzer can also be used for this method, which means that a sample's structure can be determined fairly easily. The m/z ratio range of the quadrupole instrument is fairly small, which means that the mass of the sample can be determined to with a high amount of accuracy. Finally, the sensitivity for this instrument is impressive and therefore can be useful in accurate quantitative and qualitative measurements.

Some disadvantages to electrospray ionization mass spectrometry are present as well. A major disadvantage is that this technique cannot analyze mixtures very well, and when forced to do so, the results are unreliable. The apparatus is also very difficult to clean and has a tendency to become overly contaminated with residues from previous experiments. Finally, the multiple charges that are attached to the molecular ions can make for confusing spectral data. This confusion is further fueled by use of a mixed sample, which is yet another reason why mixtures should be avoided when using an electrospray ionization mass spectrometer.

Apparatus



Capillary Needle

The capillary needle is the inlet into the apparatus for the liquid sample. Once in the capillary needle, the liquid sample is nebulized and charged. There is a large amount of pressure being applied to the capillary needle, which in effect nebulizes the liquid sample forming a mist. The stainless steel capillary needle is also surrounded by an electrode that retains a steady voltage of around 4000 volts. This applied voltage will place a charge on the droplets. Therefore, the mist that is ejected from the needle will be comprised of charged molecular ions.

Desolvating Capillary

The molecular ions are oxidized upon entering the desolvating capillary, and a continual voltage is applied to the gas chamber in which this capillary is located. Here the desolvation process begins, through the use of a dry gas or heat, and the desolvation process continues through various pumping stages as the molecular ion travels towards the mass analyzer. An example of a dry gas would be an N_2 gas that has been dehydrated. The gas or heat then provides means of evaporation, or desolvation, for the ionized droplets. As the droplets become smaller in size, their electric field densities become more concentrated. The increase in electric

field density causes the like charges to repel one another, which induces an increase in surface tension. The point where the droplet can no longer support this increase in surface tension is known as the Rayleigh limit. At this point, the droplet divides into smaller droplets of either positive or negative chrage. This process is refered to as either a coulombic explosion or the ions are described as exiting the droplet through the "Taylor cone". Once the molecular ions have reached the entrance to the mass analyzer, they have been effectively reduced through protonation.

Mass Analyzer

Mass Analyzers (Mass Spectrometry) are used to determine the mass-to-charge ratio (m/z), this ratio is used to differentiate between molecular ions that were formed in the desolvating capillary. In order for a mass-to-charge ratio to be determined, the mass analyzer must be able to separate even the smallest masses. The ability of the analyzer to resolve the mass peaks can be defined with the following equation;

$$R = \frac{m}{\Delta m} \tag{4}$$

This equation represents the mass of the first peak (m), divided by the difference between the neighboring peaks Δm. The better the resolution, the more useful the data. The mass analyzer must also be able to measure the ion currents produced by the multiply charged particles that are created in this process.

Mass analyzers use electrostatic lenses to direct the beam of molecular ions to the analyzer. A vacuum system is used to maintain a low pressure environment in order to prevent unwanted interactions between the molecular ions and any components that may be present in the atmosphere. These atmospheric components can effect the determined mass-to-charge ratio, so it is best to keep them to a minimum. The mass-to-charge ratio is then used to determine quantitative and qualitative properties of the liquid sample.

The mass analyzer used for electrospray ionization is a quadrupole mass spectrometer. A quadrupole mass spectrometer uses four charged rods, two negatively charged and two positively charged, that have alternating AC and DC currents. The rods are connected to both the positive terminal of the DC voltage and the negative terminal. Each pair of rods contains a negatively charged rod and a positively charged rod. The molecular ions are then sped through the chamber between these pairs of oppositely charged rods making use of a potential difference to do so. To maintain charge, and ultimately be readable by the detector, the molecular ions must travel through the quadrupole chamber without touching any of the four charged rods. If a molecular ion does run into one of the rods it will deem it neutral and undetectable.

Detector

The molecular ions pass through the mass analyzer to the detector. The detector most commonly used in conjunction with the quadrupole mass analyzer is a high energy dynode (HED), which is a electron multiplier with some slight variations. In an HED detector, the electrons are passed through the system at a high voltage and the electrons are measured at the end of the funnel shaped apparatus; otherwise known as the anode. A HED detector differs from the electron multiplier in that it operates at a much higher sensitivity for samples with a large mass than does the electron multiplier detector. Once the analog signal of the mass-to-charge ratio is recorded, it is then converted to a digital signal and a spectrum representing the data run can be analyzed.

References

1. Skoog, D.A.; Holler, F.J.; Crouch, S.R. Principles of Instrumental Analysis. Sixth Edition, Thomson Brooks/Cole, USA (2007).
2. Siuzdak, G. Mass Spectrometry for Biotechnology. Academic Press, Inc., USA (1996).
3. Chapman, J.R. Mass Spectrometry of Proteins and Peptides. Methods in Molecular Biology volume 146,Humana Press, Totowa, NJ (2000).
4. Snyder, A. P. Biochemical and Biotechnological Applications of Electrospray Ionization Mass Spectrometry. American Chemical Society, Washington, DC (1996).

Problems

Using the above spectrum, calculate the mass of the protein. For $p_{1,}$ shown in spectrum, the m/z is 7501 and for p_2 the m/z is 15001. (Hint: Use the above equations, and the charge of p_1 for z_1)

Contributors and Attributions

- Jennifer Murphy

Electrospray Ionization Mass Spectrometry is shared under a CC BY-NC-SA 4.0 license and was authored, remixed, and/or curated by LibreTexts.

- **Electrospray Ionization Mass Spectrometry** is licensed CC BY-NC-SA 4.0.

Injection Stage

The principle components of a mass spectrometer are an inlet, ion source, mass analyzer, detector, and data analysis. The function of an inlet system is to introduce a small amount of sample into the ion source with minimal loss of vacuum. However, many mass spectrometers contain more than one inlet system to accommodate a variety of samples. These include batch inlets, direct probe inlets, and chromatographic and capillary electrophoretic inlet systems.

Batch Inlets

The batch inlet system is considered the most common and simplest inlet system. Normally, the inside of the system is lined with glass to elude losses of polar analytes by adsorption. This system externally volatizes the sample which leaks into an empty ionization region. Boiling points up to 500 degrees C of gaseous and liquid samples can be used on typical systems. The system's vacuum contains a sample pressure of 10^{-4} to 10^{-5} Torr. Liquids are introduced using a microliter syringe into a reservoir; gases are enclosed in a metering area that is confined between two valves before being expanded into a reservoir container. Liquids that have boiling points lower than 500 degrees C can not be used in the system because the reservoir and tubing need to be kept at high temperatures by ovens and heating tapes. This is to ensure that the liquid samples are transformed to the gaseous phase and then leaked through a metal or glass diaphragm containing pinholes to the ionization area.

Direct Probe Inlets

A direct probe inlet is for small quantities of sample, solids, and nonvolatile liquids. Solids and nonvolatile liquids are injected through a probe, or sample holder. The probe is inserted through a vacuum lock which is designed to limit the volume of air needed to pump from the system after the probe has been inserted into the ionization section. Unlike the batch inlet, the sample will need to be cooled and/or heated on the probe. The probe is placed extremely close (a few millimeters) to the ionization source, where the slit leads to the spectrometer, and the sample is held in place on the surface of a glass or aluminum capillary tube or a small cup. This position makes it possible for thermally unstable compounds to be analyzed before decomposition because of the low pressure in the ionization area which is in close proximity to the sample. Do to the probe, nonvolatile samples such as carbohydrates, steroids, and metal-organic species can be studied because the low pressures lead to increased concentrations of the nonvolatile samples. The principle sample requirement is attainment of an analyte partial pressure of at least 10^{-8} torr before the onset of decomposition.[1]

Chromatographic and Capillary Electrophoretic Inlets

Chromatographic systems and Capillary Electrophoretic units are often coupled with mass spectrometers in order to allow separation and identification of the components in the sample. If these systems and units are linked with a mass spectrometer, then other specialized inlets, electrokinetic and pressure injection, are required. Electrokinetic and pressure injection controls the amount of volume injected by the duration of the injection, which typically range between 5 to 50 nL.

Electrokinetic Injection

The electrokinetic injection method involves one end of the capillary and electrode in a small cup removed from the buffer. Ionic migration and electroosmotic flow of the sample in the capillary are a result of a voltage applied for a recorded time. After this voltage is applied, the capillary end and electrode are placed back into the regular buffer solution for the remainder of the separation. The electrokinetic Injection technique injects larger quantities of the mobile ions versus the slower moving ions.

Pressure Injection

The pressure injection method is similar to the electrokinetic injection because the capillary end and electrode are removed from the buffer and placed into a small cup. However, instead of a voltage being applied, a pressure difference drives the sample into the capillary. A vacuum is applied at the detector end which produces the potential difference by pressurizing the sample or elevating the sample end. Pressure injection does not discriminate because of ion mobility, but it cannot be used in gel-filled capillaries.[1]

References

1. Skoog, D., Holler, J., Crouch, S. Principles of Instrumental Analysis, 6th Ed.; Thomson Brooks/Cole: Belmont, 2007

Injection Stage is shared under a CC BY-NC-SA 4.0 license and was authored, remixed, and/or curated by LibreTexts.

- **Injection Stage** is licensed CC BY-NC-SA 4.0.

MALDI-TOF

Proteins and peptides have been characterized by high pressure liquid chromatography (HPLC) or SDS PAGE by generating peptide maps. These peptide maps have been used as fingerprints of protein or as a tool to know the purity of a known protein in a known sample. Mass spectrometry gives a peptide map when proteins are digested with amino end specific, carboxy end specific, or amino acid specific digestive enzymes. This peptide map can be used to search a sequence database to find a good match from the existing database. This is because the more accurately the peptide masses are known, the less chance there is of bad matches.

Contributors and Attributions

- Basir Syed

MALDI-TOF is shared under a CC BY-NC-SA 4.0 license and was authored, remixed, and/or curated by LibreTexts.

- **MALDI-TOF** is licensed CC BY-NC-SA 4.0.

Mass Analyzers (Mass Spectrometry)

Mass spectrometry is an analytic method that employs ionization and mass analysis of compounds to determine the mass, formula and structure of the compound being analyzed. A mass analyzer is the component of the mass spectrometer that takes ionized masses and separates them based on charge to mass ratios and outputs them to the detector where they are detected and later converted to a digital output.

Introduction

There are six general types of mass analyzers that can be used for the separation of ions in a mass spectrometry.

1. Quadrupole Mass Analyzer
2. Time of Flight Mass Analyzer
3. Magnetic Sector Mass Analyzer
4. Electrostatic Sector Mass Analyzer
5. Quadrupole Ion Trap Mass Analyzers
6. Ion Cyclotron Resonance

Quadrupole Mass Analyzer

The DC bias will cause all the charged molecules to accelerate and move away from the center line, the rate being proportional to their charge to mass ratio. If their course goes off too far they will hit the metal rods or the sides of the container and be absorbed. So the DC bias acts like the magnetic field B of the mass spec and can be tuned to specific charge to mass ratios hitting the detector.

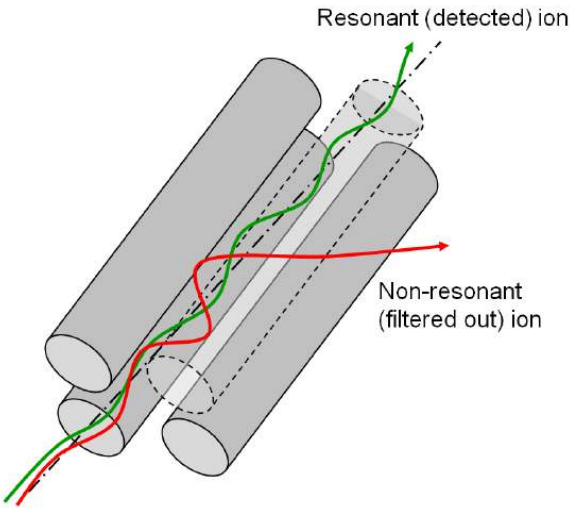


Figure 1: A quadrupole

The two sinusoidal electric fields at 90 orientation and 90 degrees degrees phase shift will cause an electric field which oscillates as a circle over time. So as the charged particles fly down toward the detector, they will be traveling in a spiral, the diameter of the spiral being determined by the charge to mass ratio of the molecule and the frequency and strength of the electric field. The combination of the DC bias and the circularly rotating electric field will be the charge particles will travel in a spiral which is curved. So by timing the peak of the curved spiral to coincide with the position of the detector at the end of the quadrupole, a great deal of selectivity to molecules charge to mass ratio can be obtained.

TOF (Time of Flight) Mass Analyzer

TOF Analyzers separate ions by time without the use of an electric or magnetic field. In a crude sense, TOF is similar to chromatography, except there is no stationary/ mobile phase, instead the separation is based on the kinetic energy and velocity of the ions.

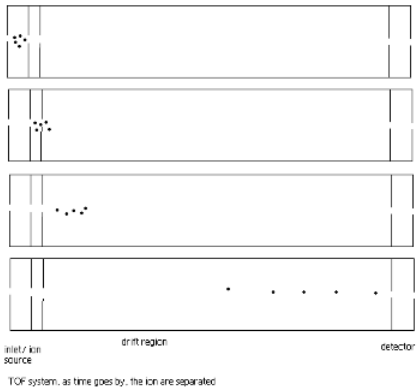


Figure 2: A TOF system. As time evolves, the ions (formed at the source) are separated.

Ions of the same charges have equal kinetic energies; kinetic energy of the ion in the flight tube is equal to the kinetic energy of the ion as it leaves the ion source:

$$KE = \frac{mv^2}{2} = zV \tag{1}$$

The time of flight, or time it takes for the ion to travel the length of the flight tube is:

$$T_f = \frac{L}{v} \tag{2}$$

- with L is the length of tube and
- v is the velocity of the ion

Substituting Equation 1 for kinetic energy in Equation 2 for time of flight:

$$T_f = L\sqrt{\frac{m}{z}}\sqrt{\frac{1}{2V}} \propto \sqrt{\frac{m}{z}} \tag{3}$$

During the analysis, L, length of tube, the Voltage from the ion source V are held constant, which can be used to say that time of flight is directly proportional to the root of the mass to charge ratio.

Unfortunately, at higher masses, resolution is difficult because flight time is longer. Also at high masses, not all of the ions of the same m/z values reach their ideal TOF velocities. To fix this problem, often a **reflectron** is added to the analyzer. The reflectron consists of a series of ring electrodes of very high voltage placed at the end of the flight tube. When an ion travels into the reflectron, it is reflected in the opposite direction due to the high voltage. The reflectron increases resolution by narrowing the broadband range of flight times for a single m/z value. Faster ions travel further into the reflectrons, and slower ions travel less into the reflector. This way both slow and fast ions, of the same m/z value, reach the detector at the same time rather then at different times, narrowing the bandwidth for the output signal.

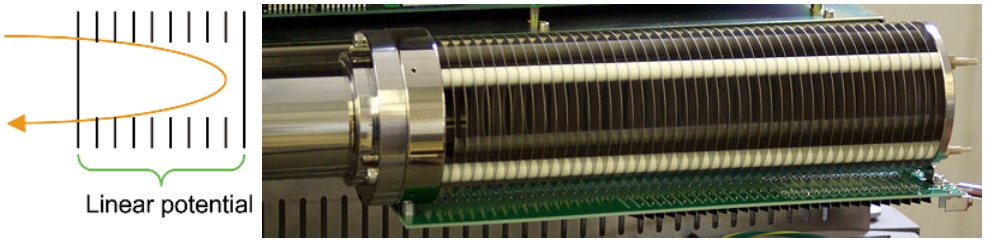


Figure 3: (left) A reflection. from Wikipedia. (right) 4. A photo of a reflectron. An ion mirror (right) attached to a flight tube (left) of the reflectron. Voltages applied to a stack of metal plates create the electric field reflecting the ions back to the flight tube. In this particular design, gaps between the mirror electrodes are too large. This can lead to a distortion of the field inside the mirror caused by a proximity of metal surface of the enveloping vacuum tube. from Wikipedia.

Magnetic Sector Mass Analyzer

Similar to time of flight (TOF) analyzer mentioned earlier,in magnetic sector analyzers ions are accelerated through a flight tube, where the ions are separated by charge to mass ratios. The difference between magnetic sector and TOF is that a magnetic field is

used to separate the ions. As moving charges enter a magnetic field, the charge is deflected to a circular motion of a unique radius in a direction perpendicular to the applied magnetic field. Ions in the magnetic field experience two equal forces; force due to the magnetic field and centripetal force.

$$F_B = zvB = F_c = \frac{mv^2}{r} \tag{4}$$

The above equation can then be rearranged to give:

$$v = \frac{Bzr}{m} \tag{5}$$

If this equation is substituted into the kinetic energy equation:

$$KE = zV = \frac{mv^2}{2} \tag{6}$$

$$\frac{m}{z} = \frac{B^2 r^2}{2V} \tag{7}$$

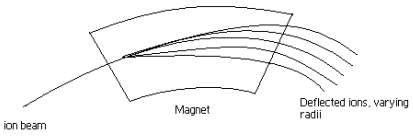


Figure 4: A magnetic sector separator.

Basically the ions of a certain m/z value will have a unique path radius which can be determined if both magnetic field magnitude B, and voltage difference V for region of acceleration are held constant. when similar ions pass through the magnetic field, they all will be deflected to the same degree and will all follow the same trajectory path. Those ions which are not selected by V and B values, will collide with either side of the flight tube wall or will not pass through the slit to the detector. Magnetic sector analyzers are used for mass focusing, they focus angular dispersions.

Electrostatic Sector Mass Analyzer

Is similar to time of flight analyzer in that it separates the ions while in flight, but it separates using an electric field. Electrostatic sector analyzer consists of two curved plates of equal and opposite potential. As the ion travels through the electric field, it is deflected and the force on the ion due to the electric field is equal to the centripetal force on the ion. Here the ions of the same kinetic energy are focused, and ions of different kinetic energies are dispersed.

$$KE = zV = \frac{mv^2}{2} \tag{8}$$

$$F_E = zE = F_c = \frac{mv^2}{R} \tag{9}$$

Electrostatic sector analyzers are energy focusers, where an ion beam is focused for energy. Electrostatic and magnetic sector analyzers when employed individually are single focusing instruments. However when both techniques are used together, it is called a double focusing instrument., because in this instrument both the energies and the angular dispersions are focused.

Quadrupole Ion Trap Mass Analyzers

This analyzer employs similar principles as the quadrupole analyzer mentioned above, it uses an electric field for the separation of the ions by mass to charge ratios. The analyzer is made with a ring electrode of a specific voltage and grounded end cap electrodes. The ions enter the area between the electrodes through one of the end caps. After entry, the electric field in the cavity due to the electrodes causes the ions of certain m/z values to orbit in the space. As the radio frequency voltage increases, heavier mass ion orbits become more stabilized and the light mass ions become less stabilized, causing them to collide with the wall, and eliminating the possibility of traveling to and being detected by the detector.

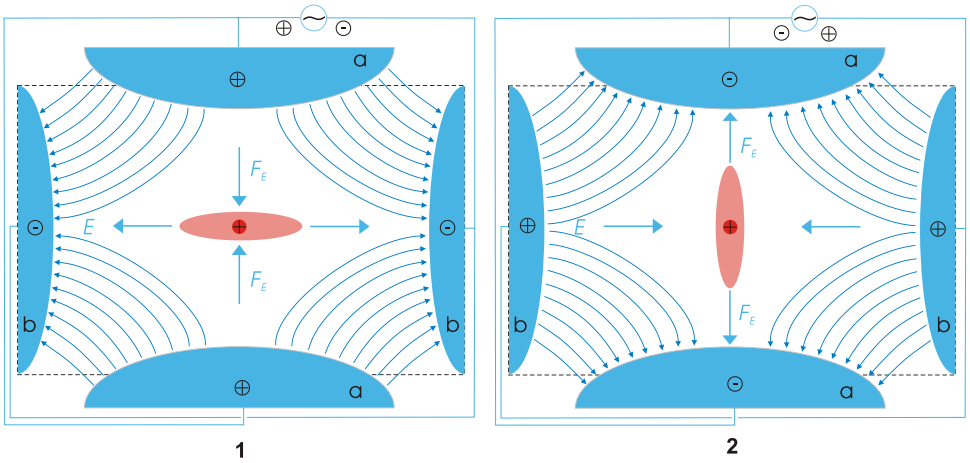


Figure 5: Scheme of a Quadrupole ion trap of classical setup with a particle of positive charge (dark red), surrounded by a cloud of similarly charged particles (light red). The electric field E (blue) is generated by a quadrupole of endcaps (a, positive) and a ring electrode (b). Picture 1 and 2 show two states during an AC cycle. (CC BY 2.5; Arian Kriesch Akriesch via Wikipedia).

The quadrupole ion trap usually runs a mass selective ejection, where selectively it ejects the trapped ions in order of in creasing mass by gradually increasing the applied radio frequency voltage.

Ion Cyclotron Resonance (ICR)

ICR is an ion trap that uses a magnetic field in order to trap ions into an orbit inside of it. In this analyzer there is no separation that occurs rather all the ions of a particular range are trapped inside, and an applied external electric field helps to generate a signal. As mentioned earlier, when a moving charge enters a magnetic field, it experiences a centripetal force making the ion orbit. Again the force on the ion due to the magnetic field is equal to the centripetal force on the ion.

$$zvB = \frac{mv^2}{r} \tag{10}$$

Angular velocity of the ion perpendicular to the magnetic field can be substituted here $w_c = v/r$

$$zB = mw_c \tag{11}$$

$$w_c = \frac{zB}{m} \tag{12}$$

Frequency of the orbit depends on the charge and mass of the ions, not the velocity. If the magnetic field is held constant, the charge to mass ratio of each ion can be determined by measuring the angular velocity ω_c. The relationship is that, at high w_c, there is low m/z value, and at low ω_c, there is a high m/z value. Charges of opposite signs have the same angular velocity, the only difference is that they orbit in the opposite direction.

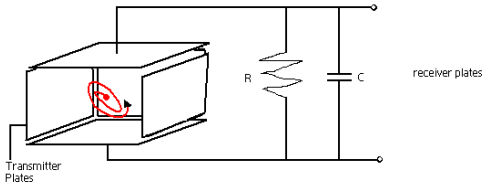


Figure 6: An ICR trap.

To generate an electric signal from the trapped ions, a vary electric field is applied to the ion trap

$$E = E_o \cos(\omega_c t) \tag{13}$$

When the ω_c in the electric field matches the ω_c of a certain ion, the ion absorbs energy making the velocity and orbiting radius of the ion increase. In this high energy orbit, as the ion oscillates between two plates, electrons accumulate at one of the plates over the other inducing an oscillating current, or current image. The current is directly proportional to the number of ions in the cell at a certain frequency.

In a Fourier Transform ICR, all of the ions within the cell are excited simultaneously so that the current image is coupled with the image of all of the individual ion frequencies. A Fourier transform is used to differential the summed signals to produce the desired results.

References

1. K. Downard, *Mass Spectrometry: A Foundation Course*, The Royal Society of Chemistry: UK 2004, Chapter 3
2. Skoog, Holler, Grouch, *Principles of Instrumental Analysis*, Thomson Brooks/Cole 2007, chapter 20
3. C. Herbert, R. Johnstone, *Mass Spectrometry Basics*, CRC Press LLC, 2003 chapter 25, 26, 39
4. E. De Hoffman, V. Stroobant, *Mass Spectrometry: Principles and Applications*, 2nd ed.;Wiley: England, 2001, chapter 2

Contributors and Attributions

- Ommaima Khan

Mass Analyzers (Mass Spectrometry) is shared under a CC BY-NC-SA 4.0 license and was authored, remixed, and/or curated by LibreTexts.

- **Mass Analyzers (Mass Spectrometry)** is licensed CC BY-NC-SA 4.0.

2.4: Interpretation of Mass Spectra

Your page has been created!

Remove this content and add your own.

Edit page

Click the Edit page button in your user bar. You will see a suggested structure for your content. Add your content and hit Save.

Tips:

Drag and drop

Drag one or more image files from your computer and drop them onto your browser window to add them to your page.

Classifications

Tags are used to link pages to one another along common themes. Tags are also used as markers for the dynamic organization of content in the CXone Expert framework.

Working with templates

CXone Expert templates help guide and organize your documentation, making it flow easier and more uniformly. Edit existing templates or create your own.

Visit for all help topics.

2.4: Interpretation of Mass Spectra is shared under a CC BY-NC-SA 4.0 license and was authored, remixed, and/or curated by LibreTexts.

13C

Isotopomers or isotopic isomers are isomers with isotopic atoms, having the same number of each isotope of each element but differing in their positions.

Isotopomers

If you look closely at the mass spectrum of an organic compound, 2-butanone, you see a line at m/z 72, which corresponds to 4 carbons, an oxygen and 8 hydrogens.

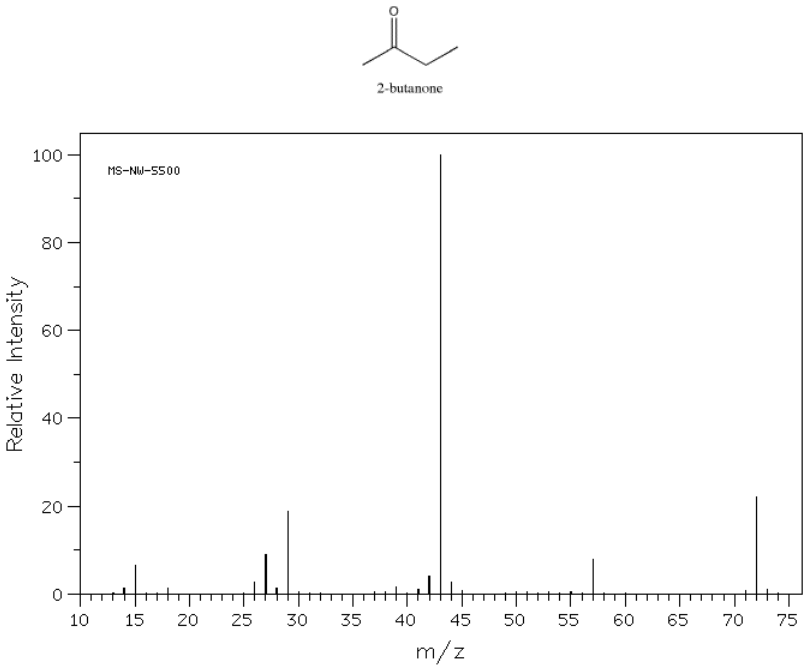


Figure MS3. Mass spectrum of 2-butanone. Source: SDBSWeb : http://riodb01.ibase.aist.go.jp/sdbs/ (National Institute of Advanced Industrial Science and Technology of Japan, 22 August 2008)

- Usually, whole numbers are used for molecular weights in mass spectrometry.
- The atomic masses in the periodic table, out to 4 decimal places, are the average masses including different possible isotopes.
- Because mass spectrometry examines individual molecules, individual atomic masses are needed, not average ones. Usually that means using a whole number.

In addition, there are a number of other lines at lower values of m/z; these correspond to the masses of smaller pieces of those 2-butanone molecules that fall apart during the experiment. We won't look too closely at how those arise until we get to radical reactions later in the course. However, we will look at some factors that make cations stable later in this chapter.

If you look closely at the mass spectrum of 2-butanone, you'll also see another little peak at m/z 73. This is referred to as the M+1 peak (one greater than the molecular ion), and it arises because of ^{13}C. This compound is referred to as an isotopomer; that means the same compound with a different isotope.

- ^{12}C is about 99% abundant; 99% of carbon atoms have a mass of 12 amu.
- ^{13}C is about 1% abundant; 1% of carbon atoms have a mass of 13 amu.
- Compounds that contain a ^{13}C atom have a mass one larger than expected.

The chance that a molecule in a sample contains a ^{13}C atom is related to the number of carbons present. If there is just one carbon atom in the molecule, it has a 1% chance of being a ^{13}C. That means the M+1 peak would be only 1/100th as tall as M+, the peak for the molecular ion.

- The M+1 peak from a ^{13}C atom is very small.
- The more carbons there are in a molecule, the bigger the M+1 peak.
- If there are 10 carbon atoms in the molecule, there is a 10% chance of a ^{13}C atom being present. The M+1 peak is about 1/10th the size of the M+ peak.

- If there are 100 carbons in the molecule, there is a very good chance that a ^{13}C atom is present. At that point, the M+1 peak is actually much larger than the M+. peak

Contributor

- Chris P Schaller, Ph.D., (College of Saint Benedict / Saint John's University)

This page titled 13C is shared under a CC BY-NC 3.0 license and was authored, remixed, and/or curated by Chris Schaller.

- **Isotopes: 13C** by Chris Schaller is licensed CC BY-NC 3.0.



bromoethane

Figure MS5. Mass spectrum of chlorobenzene.

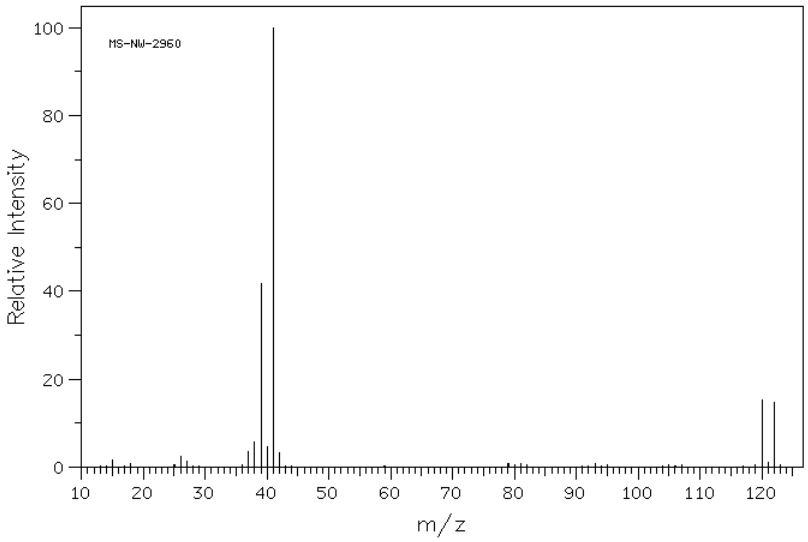
Source: SDBSWeb : http://riodb01.ibase.aist.go.jp/sdbs/ (National Institute of Advanced Industrial Science and Technology of Japan, 22 August 2008)

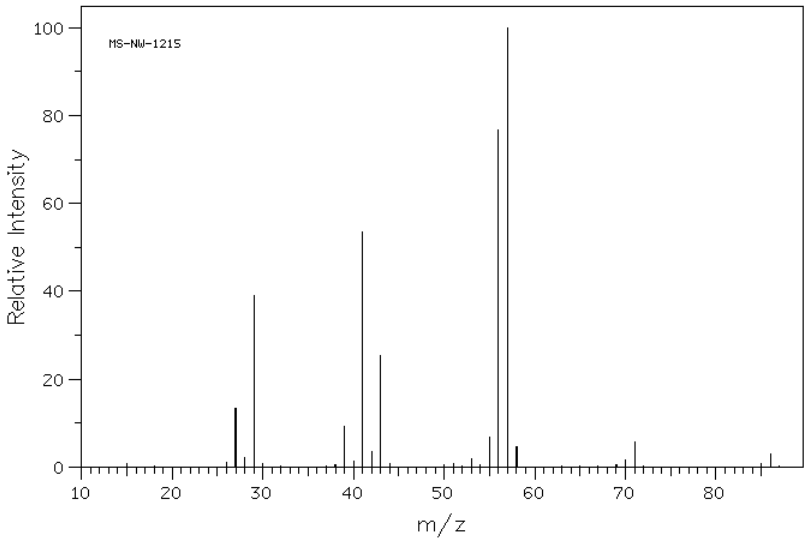
- Chlorinated compounds show an M+2 peak that is 1/3 as large as the M+ peak.

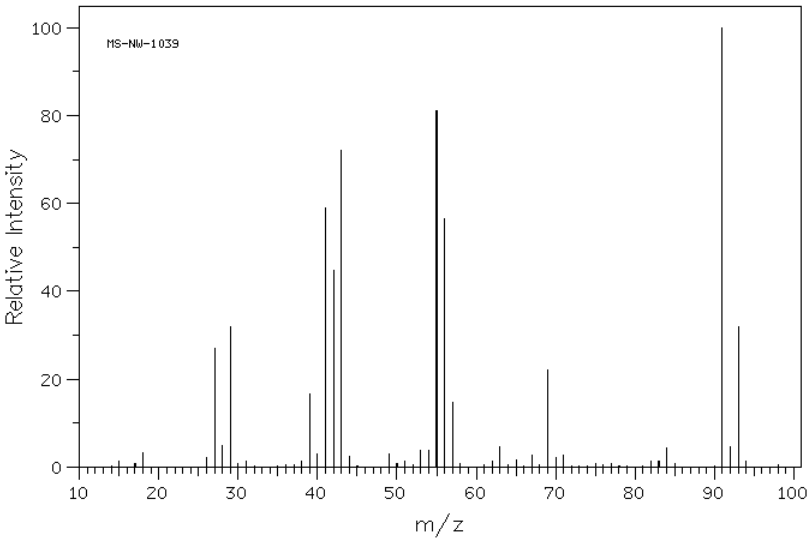
Note also that halogens are easily lost during mass spectrometry. If you subtract the mass of the halogen from the molecular ion mass, you will often find a peak that corresponds to the remainder of the structure.

Problem MS4.

Draw one possible structure for the compound in each of the following mass spectra.





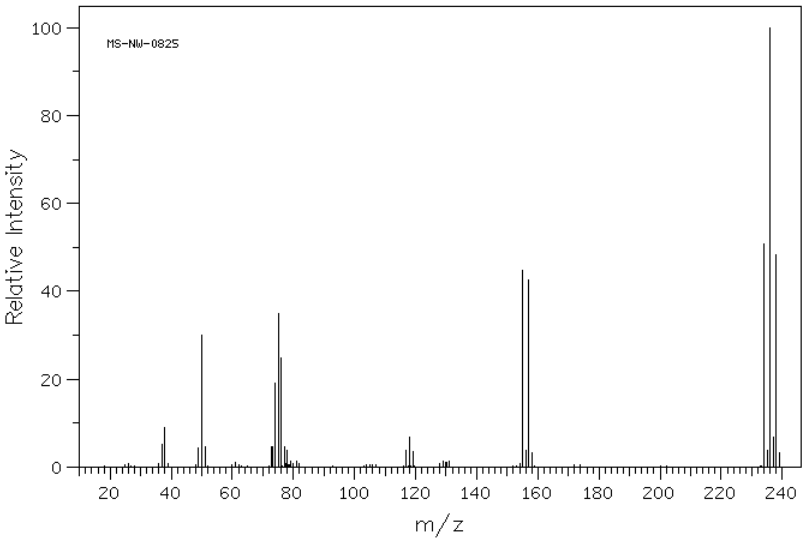


Source: SDBSWeb : http://riodb01.ibase.aist.go.jp/sdbs/ (National Institute of Advanced Industrial Science and Technology of Japan, 25 August 2008)

Problem MS5.

In the following mass spectrum, more than one halogen atom is present.

1. What is a possible structure of the compound?
2. Show why this pattern of molecular ions is observed.



Source: SDBSWeb : http://riodb01.ibase.aist.go.jp/sdbs/ (National Institute of Advanced Industrial Science and Technology of Japan, 25 August 2008)

Contributor

Chris P Schaller, Ph.D., (College of Saint Benedict / Saint John's University)

This page titled Br and Cl is shared under a CC BY-NC 3.0 license and was authored, remixed, and/or curated by Chris Schaller.

- **Isotopes: Br and Cl** by Chris Schaller is licensed CC BY-NC 3.0.

Fragmentation

When molecules go through a mass spectrometer, some of them arrive intact at the detector, but many of them break into pieces in a variety of different ways. To establish a charge on a molecule, an electron had to be removed; removal of that electron is effected through a collision, usually with a high-energy electron. During that collision, energy is transferred from the high-energy electron to the molecule, and that energy has to go somewhere. Part of it gets partitioned into various bond vibrations, so bonds start to vibrate quite a lot, until some of them snap completely. The molecular ion breaks apart and forms a fragment ion.

Some fragment ions are very common in mass spectrometry. These ions are seen frequently for either of two reasons:

- there is not a pathway available to break the ion down.
- the ion is relatively stable, so it forms easily.

Fragmentations occur through well-defined pathways or mechanisms. A mechanism is a step-by-step series of events that happens in a reaction. It is important to understand how reactions happen, but we will look at fragmentations when we study radical reactions.

However, it is useful to know what factors make cations stable.

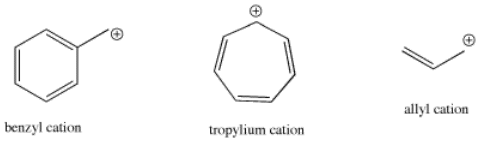
Some Common Ions

There are a number of ions commonly seen in mass spectrometry that tell you a little bit about the structure. Just like with anions, there are a couple of common factors influence cation stability:

- Electronegativity plays a role. More electronegative atoms are less likely to be cations.
- Polarizability also plays a role. More polarizable atoms are more likely to be cations.

However, in most cases, we will be looking at carbon with a positive charge, and there are additional factors to distinguish between them

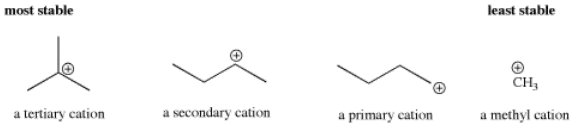
- Delocalization stabilizes a cation by spreading out the charge onto two or more different atoms.
- In Lewis structure terms, the easiest way to delocalize charge is via resonance.
- Resonance can involve other carbons, like in allyl and benzyl cations.



- Resonance can also involve other atoms, like in acylium or iminium cations.



- Delocalization can also be accomplished through inductive effects. The trend in carbocations is that the more substituents on teh carbocation, the greater the stability.
- Tertiary cations, with three substituents on the carbocation, are more stable than secondary cations, with two substituents on the carbocation. Secondary cations are more stable than primary ones. Primary cations are more stable than methyl cations.



Molecular orbital calculations suggest that the cation is stabilized through interaction with neighboring C-H bonds in the alkyl groups. Specifically, a C-H sigma bonding orbital has symmetry similar to the empty p orbital on the positive carbon. The lobes on the two orbitals can overlap such that they are in phase, and that allows electrons to be donated from the C-H bond to the central, electron-deficient carbon. Formally, there is a bonding interaction and an antibonding interaction between these two orbitals. Since one of these orbitals is empty, the antibonding combination remains unoccupied. The bonding combination is populated, however,

and since it is lower in energy than either the p orbital or the C-H sigma bond (all bonding combinations are lower in energy than the orbitals that combine to form them), there is a net decrease in energy.

Problem MS8.

Draw as many resonance structures as you can that help explain teh stability of the following cations:

a) allyl cation b) benzyl cation c) tropylium cation d) an acylium ion e) an iminium ion

Contributor

Chris P Schaller, Ph.D., (College of Saint Benedict / Saint John's University)

This page titled Fragmentation is shared under a CC BY-NC 3.0 license and was authored, remixed, and/or curated by Chris Schaller.

- **Fragmentation** by Chris Schaller is licensed CC BY-NC 3.0.

Fragmentation Patterns in Mass Spectra

This page looks at how fragmentation patterns are formed when organic molecules are fed into a mass spectrometer, and how you can get information from the mass spectrum.

The formation of molecular ions

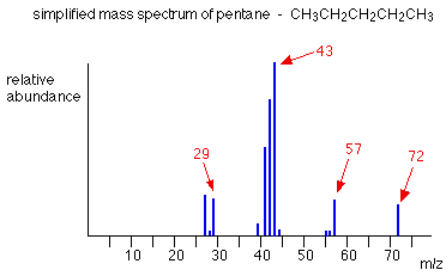
When the vaporized organic sample passes into the ionization chamber of a mass spectrometer, it is bombarded by a stream of electrons. These electrons have a high enough energy to knock an electron off an organic molecule to form a positive ion. This ion is called the **molecular ion - or sometimes the parent ion.** The molecular ion is often given the symbol M^+ or $M^{\cdot+}$ - the dot in this second version represents the fact that somewhere in the ion there will be a single unpaired electron. That's one half of what was originally a pair of electrons - the other half is the electron which was removed in the ionization process.

Fragmentation

The molecular ions are energetically unstable, and some of them will break up into smaller pieces. The simplest case is that a molecular ion breaks into two parts - one of which is another positive ion, and the other is an uncharged free radical.

$$M^{\cdot+} \rightarrow X^+ + Y^{\cdot}$$

The uncharged free radical won't produce a line on the mass spectrum. Only charged particles will be accelerated, deflected and detected by the mass spectrometer. These uncharged particles will simply get lost in the machine - eventually, they get removed by the vacuum pump. The ion, X^+, will travel through the mass spectrometer just like any other positive ion - and will produce a line on the stick diagram. All sorts of fragmentations of the original molecular ion are possible - and that means that you will get a whole host of lines in the mass spectrum. For example, the mass spectrum of pentane looks like this:



It's important to realize that the pattern of lines in the mass spectrum of an organic compound tells you something quite different from the pattern of lines in the mass spectrum of an element. With an element, each line represents a different isotope of that element. With a compound, each line represents a different fragment produced when the molecular ion breaks up.

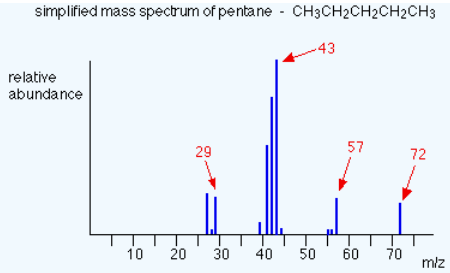
In the stick diagram showing the mass spectrum of pentane, the line produced by the heaviest ion passing through the machine (at m/z = 72) is due to the molecular ion. The tallest line in the stick diagram (in this case at m/z = 43) is called the **base peak**. This is usually given an arbitrary height of 100, and the height of everything else is measured relative to this. The base peak is the tallest peak because it represents the commonest fragment ion to be formed - either because there are several ways in which it could be produced during fragmentation of the parent ion, or because it is a particularly stable ion.

Using fragmentation patterns

This section will ignore the information you can get from the molecular ion (or ions). That is covered in three other pages which you can get at via the mass spectrometry menu. You will find a link at the bottom of the page.

Example 1: Mass Spectrum of Pentane

Let's have another look at the mass spectrum for pentane:



What causes the line at m/z = 57?

Solution

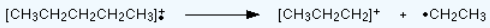
How many carbon atoms are there in this ion? There can't be 5 because 5 x 12 = 60. What about 4? 4 x 12 = 48. That leaves 9 to make up a total of 57. How about $C_4H_9^+$ then?

$C_4H_9^+$ would be $[CH_3CH_2CH_2CH_2]^+$, and this would be produced by the following fragmentation:

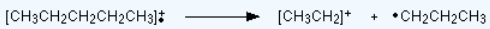


The methyl radical produced will simply get lost in the machine.

The line at m/z = 43 can be worked out similarly. If you play around with the numbers, you will find that this corresponds to a break producing a 3-carbon ion:



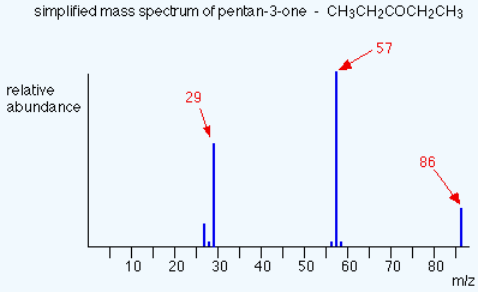
The line at m/z = 29 is typical of an ethyl ion, $[CH_3CH_2]^+$:



The other lines in the mass spectrum are more difficult to explain. For example, lines with m/z values 1 or 2 less than one of the easy lines are often due to loss of one or more hydrogen atoms during the fragmentation process.

Example 2: Pentan-3-one

This time the base peak (the tallest peak - and so the commonest fragment ion) is at m/z = 57. But this isn't produced by the same ion as the same m/z value peak in pentane.

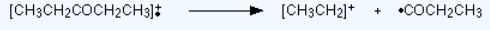


If you remember, the m/z = 57 peak in pentane was produced by $[CH_3CH_2CH_2CH_2]^+$. If you look at the structure of pentan-3-one, it's impossible to get that particular fragment from it.

Work along the molecule mentally chopping bits off until you come up with something that adds up to 57. With a small amount of patience, you'll eventually find $[CH_3CH_2CO]^+$ - which is produced by this fragmentation:



You would get exactly the same products whichever side of the CO group you split the molecular ion. The m/z = 29 peak is produced by the ethyl ion - which once again could be formed by splitting the molecular ion either side of the CO group.



Peak heights and the stability of ions

The more stable an ion is, the more likely it is to form. The more of a particular sort of ion that's formed, the higher its peak height will be. We'll look at two common examples of this.

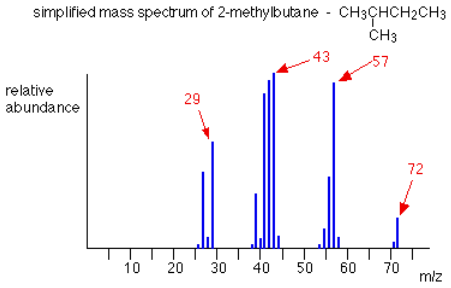
Examples involving carbocations (carbonium ions)

Summarizing the most important conclusion from the page on carbocations:

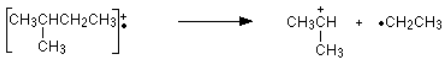
Order of stability of carbocations

primary < secondary < tertiary

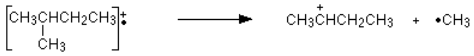
Applying the logic of this to fragmentation patterns, it means that a split which produces a secondary carbocation is going to be more successful than one producing a primary one. A split producing a tertiary carbocation will be more successful still. Let's look at the mass spectrum of 2-methylbutane. 2-methylbutane is an isomer of pentane - isomers are molecules with the same molecular formula, but a different spatial arrangement of the atoms.



Look first at the very strong peak at m/z = 43. This is caused by a different ion than the corresponding peak in the pentane mass spectrum. This peak in 2-methylbutane is caused by:



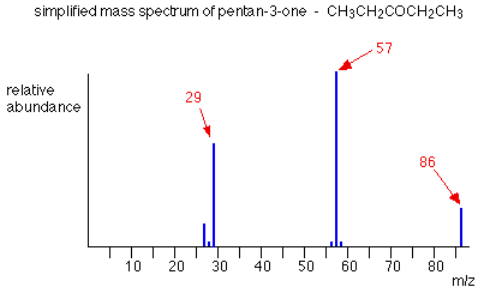
The ion formed is a secondary carbocation - it has two alkyl groups attached to the carbon with the positive charge. As such, it is relatively stable. The peak at m/z = 57 is much taller than the corresponding line in pentane. Again a secondary carbocation is formed - this time, by:



You would get the same ion, of course, if the left-hand CH_3 group broke off instead of the bottom one as we've drawn it. In these two spectra, this is probably the most dramatic example of the extra stability of a secondary carbocation.

Examples involving acylium ions, $[RCO]^+$

Ions with the positive charge on the carbon of a carbonyl group, C=O, are also relatively stable. This is fairly clearly seen in the mass spectra of ketones like pentan-3-one.



The base peak, at m/z=57, is due to the $[CH_3CH_2CO]^+$ ion. We've already discussed the fragmentation that produces this.

Using mass spectra to distinguish between compounds

Suppose you had to suggest a way of distinguishing between pentan-2-one and pentan-3-one using their mass spectra.

pentan-2-one		$CH_3COCH_2CH_2CH_3$
pentan-3-one		$CH_3CH_2COCH_2CH_3$

Each of these is likely to split to produce ions with a positive charge on the CO group. In the pentan-2-one case, there are two different ions like this:

- $[CH_3CO]^+$
- $[COCH_2CH_2CH_3]^+$

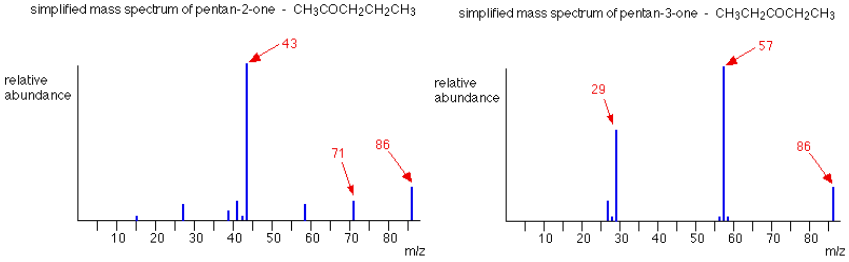
That would give you strong lines at m/z = 43 and 71.

With pentan-3-one, you would only get one ion of this kind:

- $[CH_3CH_2CO]^+$

In that case, you would get a strong line at 57. You don't need to worry about the other lines in the spectra - the 43, 57 and 71 lines give you plenty of difference between the two. The 43 and 71 lines are missing from the pentan-3-one spectrum, and the 57 line is missing from the pentan-2-one one.

The two mass spectra look like this:



Computer matching of mass spectra

As you've seen, the mass spectrum of even very similar organic compounds will be quite different because of the different fragmentations that can occur. Provided you have a computer data base of mass spectra, any unknown spectrum can be computer analysed and simply matched against the data base.

Contributors and Attributions

- Jim Clark (Chemguide.co.uk)

This page titled Fragmentation Patterns in Mass Spectra is shared under a CC BY-NC 4.0 license and was authored, remixed, and/or curated by Jim Clark.

- **Fragmentation Patterns in Mass Spectra** by Jim Clark is licensed CC BY-NC 4.0.

Molecular Ions

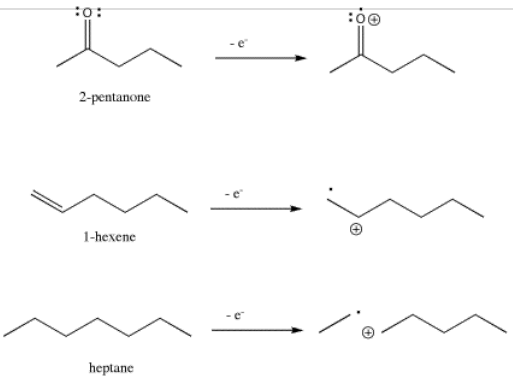
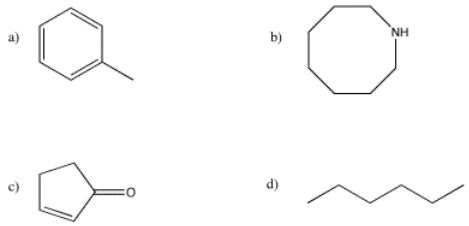


Figure MS4. Ionization in three different organic compounds.

Problem MS3.

Draw an equation for the formation of a molecular ion from each of the following compounds.



Contributor

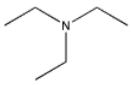
Chris P Schaller, Ph.D., (College of Saint Benedict / Saint John's University)

This page titled Molecular Ions is shared under a CC BY-NC 3.0 license and was authored, remixed, and/or curated by Chris Schaller.

- **Molecular Ions** by Chris Schaller is licensed CC BY-NC 3.0.

Molecular Ion and Nitrogen

Molecular Weight: Even or Odd?



triethylamine

Figure MS6. Mass spectrum of triethylamine. Source: SDBSWeb : http://riodb01.ibase.aist.go.jp/sdbs/ (National Institute of Advanced Industrial Science and Technology of Japan, 22 August 2008)

This phenomenon is a result of the fact that the most common elements in organic compounds, carbon and oxygen, have even atomic weights (12 and 16, respectively), so any number of carbons and oxygens will have even weights. The most common isotope of hydrogen has an odd molecular weight, but because carbon and oxygen both have even valences (carbon forms four bonds and oxygen forms two), there is always an even number of hydrogen atoms in an organic compound containing those elements, so they also add up to an even numbered weight.

Nitrogen has an even atomic weight (14), so any number of nitrogen atoms will add up to an even molecular weight. Nitrogen, however, has an odd valence (it forms three bonds), and as a result there will be an odd number of hydrogens in a nitrogenous compound, and the molecular weight will be odd because of the presence of an extra hydrogen.

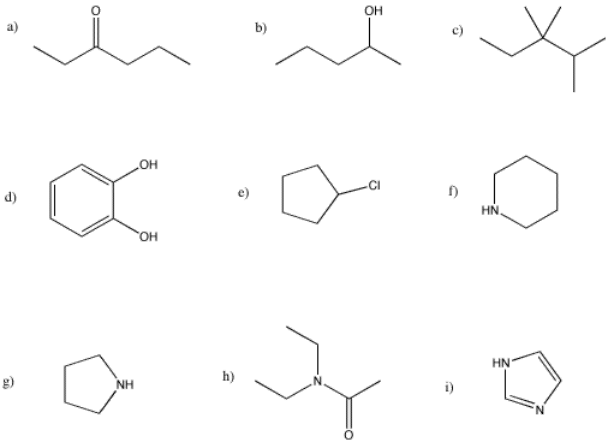
Of course, if there are two nitrogens in a molecule, there will be two extra hydrogens, so the molecular weight will actually be even. That means the rule about molecular weight and nitrogen should really be expressed as:

- odd numbers of nitrogen atoms in a molecule in an odd molecular weight.

What about those other atoms that sometimes show up in organic chemistry, such as the halogens? Halogens all have odd molecular weights (19 amu for fluorine, 35 or 37 for chlorine, 79 or 81 for bromine, and X for iodine). However, halogens all have a valence of 1, just like hydrogen. As a result, to add a halogen to methane, we would need to erase one of the hydrogen atoms and replace it with the halogen. Since we are just substituting one odd numbered atomic weight for another, the total weight remains even.

Problem MS6.

Calculate molecular weights for the following compounds.



Contributor

Chris P Schaller, Ph.D., (College of Saint Benedict / Saint John's University)

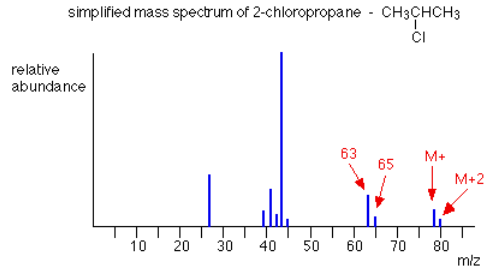
This page titled Molecular Ion and Nitrogen is shared under a CC BY-NC 3.0 license and was authored, remixed, and/or curated by Chris Schaller.

- **Molecular Ion and Nitrogen** by Chris Schaller is licensed CC BY-NC 3.0.

Organic Compounds Containing Halogen Atoms

This page explains how the M+2 peak in a mass spectrum arises from the presence of chlorine or bromine atoms in an organic compound. It also deals briefly with the origin of the M+4 peak in compounds containing two chlorine atoms.

One chlorine atom in a compound



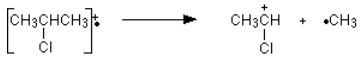
The molecular ion peaks (M+ and M+2) each contain one chlorine atom - but the chlorine can be either of the two chlorine isotopes, ^{35}Cl and ^{37}Cl.

The molecular ion containing the ^{35}Cl isotope has a relative formula mass of 78. The one containing ^{37}Cl has a relative formula mass of 80 - hence the two lines at m/z = 78 and m/z = 80.

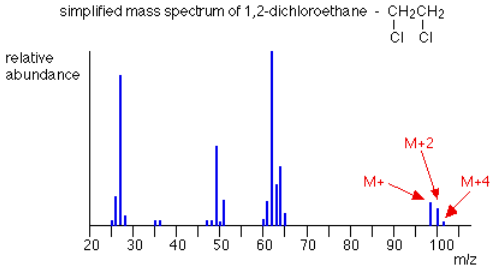
Notice that the peak heights are in the ratio of 3 : 1. That reflects the fact that chlorine contains 3 times as much of the ^{35}Cl isotope as the ^{37}Cl one. That means that there will be 3 times more molecules containing the lighter isotope than the heavier one.

So . . . if you look at the molecular ion region, and find two peaks separated by 2 m/z units and with a ratio of 3 : 1 in the peak heights, that tells you that the molecule contains 1 chlorine atom.

You might also have noticed the same pattern at m/z = 63 and m/z = 65 in the mass spectrum above. That pattern is due to fragment ions also containing one chlorine atom - which could either be ^{35}Cl or ^{37}Cl. The fragmentation that produced those ions was:



Two chlorine atoms in a compound



The lines in the molecular ion region (at m/z values of 98, 100 ands 102) arise because of the various combinations of chlorine isotopes that are possible. The carbons and hydrogens add up to 28 - so the various possible molecular ions could be:

$$28 + 35 + 35 = 98$$

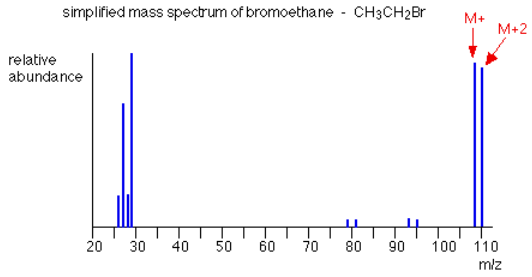
$$28 + 35 + 37 = 100$$

$$28 + 37 + 37 = 102$$

If you have the necessary math, you could show that the chances of these arrangements occurring are in the ratio of 9:6:1 - and this is the ratio of the peak heights. If you don't know the right bit of math, just learn this ratio! So . . . if you have 3 lines in the molecular ion region (M+, M+2 and M+4) with gaps of 2 m/z units between them, and with peak heights in the ratio of 9:6:1, the compound contains 2 chlorine atoms.

Compounds containing bromine atoms

Bromine has two isotopes, ^{79}Br and ^{81}Br in an approximately 1:1 ratio (50.5 : 49.5 if you want to be fussy!). That means that a compound containing 1 bromine atom will have two peaks in the molecular ion region, depending on which bromine isotope the molecular ion contains. Unlike compounds containing chlorine, though, the two peaks will be very similar in height.



The carbons and hydrogens add up to 29. The M+ and M+2 peaks are therefore at m/z values given by:

$$29 + 79 = 108$$

$$29 + 81 = 110$$

Hence, if two lines in the molecular ion region are observed with a gap of 2 m/z units between them and with almost equal heights, this suggests the presence of a bromine atom in the molecule.

Contributors and Attributions

- Jim Clark (Chemguide.co.uk)

This page titled Organic Compounds Containing Halogen Atoms is shared under a CC BY-NC 4.0 license and was authored, remixed, and/or curated by Jim Clark.

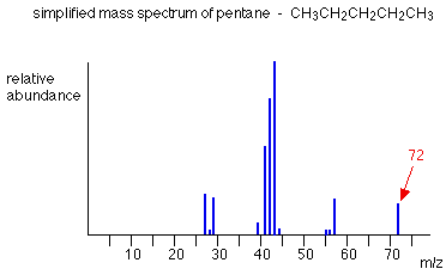
- **Organic Compounds Containing Halogen Atoms** by Jim Clark is licensed CC BY-NC 4.0.

The Molecular Ion (M^+) Peak

This page explains how to find the relative formula mass (relative molecular mass) of an organic compound from its mass spectrum. It also shows how high resolution mass spectra can be used to find the molecular formula for a compound.

When the vaporised organic sample passes into the ionization chamber of a mass spectrometer, it is bombarded by a stream of electrons. These electrons have a high enough energy to knock an electron off an organic molecule to form a positive ion. This ion is called the molecular ion. The molecular ion is often given the symbol M^+ or$M^{\cdot+}$ - the dot in this second version represents the fact that somewhere in the ion there will be a single unpaired electron. That's one half of what was originally a pair of electrons - the other half is the electron which was removed in the ionization process. The molecular ions tend to be unstable and some of them break into smaller fragments. These fragments produce the familiar stick diagram. Fragmentation is irrelevant to what we are talking about on this page - all we're interested in is the molecular ion.

In the mass spectrum, the heaviest ion (the one with the greatest m/z value) is likely to be the molecular ion. A few compounds have mass spectra which don't contain a molecular ion peak, because all the molecular ions break into fragments. For example, in the mass spectrum of pentane, the heaviest ion has an m/z value of 72.



Because the largest m/z value is 72, that represents the largest ion going through the mass spectrometer - and you can reasonably assume that this is the molecular ion. The relative formula mass of the compound is therefore 72.

Finding the relative formula mass (relative molecular mass) from a mass spectrum is therefore trivial. Look for the peak with the highest value for m/z, and that value is the relative formula mass of the compound. There are, however, complications which arise because of the possibility of different isotopes (either of carbon or of chlorine or bromine) in the molecular ion. These cases are dealt with on separate pages.

Using a mass spectrum to find a molecular formula

So far we've been looking at m/z values in a mass spectrum as whole numbers, but it's possible to get far more accurate results using a high resolution mass spectrometer. You can use that more accurate information about the mass of the molecular ion to work out the molecular formula of the compound.

For normal calculation purposes, you tend to use rounded-off relative isotopic masses. For example, you are familiar with the atomic mass numbers (Z). To 4 decimal places, however, these are the relative isotopic masses.

Isotope	Z	Mass
^{1}H	1	1.0078
^{12}C	12	12.0000
^{14}N	14	14.0031
^{16}O	16	15.9949

The carbon value is 12.0000, of course, because all the other masses are measured on the carbon-12 scale which is based on the carbon-12 isotope having a mass of exactly 12.

Using these accurate values to find a molecular formula

Two simple organic compounds have a relative formula mass of 44 - propane, C_3H_8, and ethanal, CH_3CHO. Using a high resolution mass spectrometer, you could easily decide which of these you had. On a high resolution mass spectrometer, the

molecular ion peaks for the two compounds give the following m/z values:

C_3H_8		44.0624
CH_3CHO		44.0261

You can easily check that by adding up numbers from the table of accurate relative isotopic masses above.

Example 1:

A gas was known to contain only elements from the following list:

^{1}H		1.0078
^{12}C		12.0000
^{14}N		14.0031
^{16}O		15.9949

The gas had a molecular ion peak at m/z = 28.0312 in a high resolution mass spectrometer. What was the gas?

Solution

After a bit of playing around, you might reasonably come up with 3 gases which had relative formula masses of approximately 28 and which contained the elements from the list. They are N_2, CO and C_2H_4. Working out their accurate relative formula masses gives:

N_2		28.0062
CO		27.9949
C_2H_4		28.0312

The gas is obviously C_2H_4.

Contributors and Attributions

- Jim Clark (Chemguide.co.uk)

This page titled The Molecular Ion (M^+) Peak is shared under a CC BY-NC 4.0 license and was authored, remixed, and/or curated by Jim Clark.

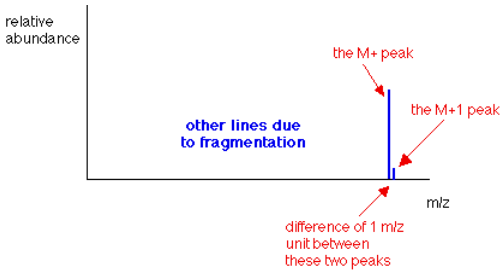
- **The Molecular Ion (M^+) Peak** by Jim Clark is licensed CC BY-NC 4.0.

The M 1 Peak

This page explains how the M+1 peak in a mass spectrum can be used to estimate the number of carbon atoms in an organic compound.

What causes the M+1 peak?

If you had a complete (rather than a simplified) mass spectrum, you will find a small line 1 m/z unit to the right of the main molecular ion peak. This small peak is called the M+1 peak.

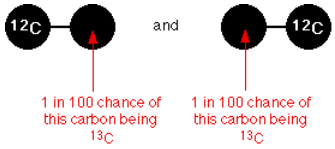


The carbon-13 isotope

The M+1 peak is caused by the presence of the ^{13}C isotope in the molecule. ^{13}C is a stable isotope of carbon - don't confuse it with the ^{14}C isotope which is radioactive. Carbon-13 makes up 1.11% of all carbon atoms. If you had a simple compound like methane, CH_4, approximately 1 in every 100 of these molecules will contain carbon-13 rather than the more common carbon-12. That means that 1 in every 100 of the molecules will have a mass of 17 (13 + 4) rather than 16 (12 + 4). The mass spectrum will therefore have a line corresponding to the molecular ion $[^{13}CH_4]^+$ as well as $[^{12}CH_4]^+$. The line at m/z = 17 will be much smaller than the line at m/z = 16 because the carbon-13 isotope is much less common. Statistically you will have a ratio of approximately 1 of the heavier ions to every 99 of the lighter ones. That's why the M+1 peak is much smaller than the M+ peak.

Using the M+1 peak

Imagine a compound containing 2 carbon atoms. Either of them has an approximately 1 in 100 chance of being ^{13}C.



There's therefore a 2 in 100 chance of the molecule as a whole containing one ^{13}C atom rather than a ^{12}C atom - which leaves a 98 in 100 chance of both atoms being ^{12}C. That means that the ratio of the height of the M+1 peak to the M+ peak will be approximately 2 : 98. That's pretty close to having an M+1 peak approximately 2% of the height of the M+ peak.

Using the relative peak heights to predict the number of carbon atoms

If you measure the peak height of the M+1 peak as a percentage of the peak height of the M+ peak, that gives you the number of carbon atoms in the compound. We've just seen that a compound with 2 carbons will have an M+1 peak approximately 2% of the height of the M+ peak. Similarly, you could show that a compound with 3 carbons will have the M+1 peak at about 3% of the height of the M+ peak. The approximations we are making won't hold with more than 2 or 3 carbons. The proportion of carbon atoms which are ^{13}C isn't 1% - it's 1.11%. And the approximation that a ratio of 2 : 98 is about 2% doesn't hold as the small number increases.

Consider a molecule with 5 carbons in it. You could work out that 5.55 (5 x 1.11) molecules will contain 1 ^{13}C to every 94.45 (100 - 5.55) which contain only ^{12}C atoms. If you convert that to how tall the M+1 peak is as a percentage of the M+ peak, you get an answer of 5.9% (5.55/94.45 x 100). That's close enough to 6% that you might assume wrongly that there are 6 carbon atoms. Above 3 carbon atoms, then, you shouldn't really be making the approximation that the height of the M+1 peak as a percentage of the height of the M+ peak tells you the number of carbons - you will need to do some fiddly sums!

Contributors and Attributions

Jim Clark (Chemguide.co.uk)

This page titled The M 1 Peak is shared under a CC BY-NC 4.0 license and was authored, remixed, and/or curated by Jim Clark.

- **The M+1 Peak** by Jim Clark is licensed CC BY-NC 4.0.

Welcome to the Chemistry Library. This Living Library is a principal hub of the LibreTexts project, which is a multi-institutional collaborative venture to develop the next generation of open-access texts to improve postsecondary education at all levels of higher learning. The LibreTexts approach is highly collaborative where an Open Access textbook environment is under constant revision by students, faculty, and outside experts to supplant conventional paper-based books.

LEGO Exercise

CHAPTER OVERVIEW

LEGO Exercise

This module introduces students to the relationship between chromatograms and mass spectra using hands-on group work with molecules built from LEGO™ bricks and environmental case studies involving the analysis of pesticides by GC-MS and oil spill dispersant chemicals by LC-MS/MS.

The first of three in-class exercises guides students through the process of creating total and extracted ion chromatograms and mass spectra using molecules built from LEGO™ bricks. The goals of this hands-on exercise are to build a solid conceptual understanding of mass spectral peak origin, interpretation, and connection to the chromatogram. Two environmental case studies, involving pesticides (GC-MS) and oil spill dispersants (LC-MS/MS), reinforce the relationships between chromatography and mass spectrometry, explore the mass spectrum of an isotopically-labeled internal standard, require recall of the factors influencing peak broadening, and introduce the idea of tandem mass spectrometry. The module assumes students have had prior exposure to chromatographic separations, the basic block diagram of a mass spectrometer, and common ionization mechanisms (e.g., EI and ESI).

Resources

- In-Class Exercises (Word, PDF)
  - Data Sheet (Excel, PDF)
  - Mass Spectra and Total Ion Chromatogram Simulation (Excel)
  - Mass Spectra Simulation (PDF)
  - Total Ion Chromatogram Simulation (PDF)
  - Key (Word, PDF)
- Instructor's Guide (Word, PDF)
  - TIC and MS Slides (PowerPoint, PDF)
  - Brick Sources and Costs (Excel, PDF)
- Assessment Questions: For Assessment questions that accompany this module, please contact **David Griffith** (dgriffit@willamette.edu)

Contributors

- Dr. David Griffith (Willamette University): dgriffit@willamette.edu

LEGO Exercise is shared under a CC BY-NC-SA 4.0 license and was authored, remixed, and/or curated by LibreTexts.

2.6: ESI-QTOF-MS Coupled to HPLC and its Application for Food Safety

ESI-QTOF-MS Coupled to HPLC and its Application for Food Safety

High-performance liquid chromatography (HPLC) is a very powerful separation method widely used in environmental science, pharmaceutical industry, biological and chemical research and other fields. Generally, it can be used to purify, identify and/or quantify one or several components in a mixture simultaneously.

Mass spectrometry (MS) is a detection technique by measuring mass-to-charge ratio of ionic species. The procedure consists of different steps. First, a sample is injected in the instrument and then evaporated. Second, species in the sample are charged by certain ionized methods, such as electron ionization (EI), electrospray ionization (ESI), chemical ionization (CI), matrix-assisted laser desorption/ionization (MALDI). Finally, the ionic species wil be analyzed depending on their mass-to-charge ratio (*m*/*z*) in the analyzer, such as quadrupole, time-of-flight (TOF), ion trap and fourier transform ion cyclotron resonance.

The mass spectrometric identification is widely used together with chromatographic separation. The most common ones are gas chromatography-mass spectrometry (GC-MS) and liquid chromatography-mass spectrometry (LC-MS). Because of the high sensitivity, selectivity and relatively low price of GC-MS, it has very wide applications in drug detection, environmental analysis and so forth. For those organic chemistry research groups, it is also a daily-used and convenient equipment. However, GC-MS is ineffective if the molecules have high boiling point and/or will be decomposed at high temperature.

In this module, we will mainly talk about liquid chromatography and electrospray ionization quadrupole time-of-flight mass spectrometry (LC/ESI-QTOF-MS). As mentioned above, the LC has an efficient capacity of separation and MS has a high sensitivity and strong ability of structural characterization. Furthermore, TOF-MS, has several distinctive properties on top of regular MS, including fast acquisition rates, high accuracy in mass measurements and a large mass range. The combination of LC and ESI-TOF-MS allow us to obtain a powerful in the quantitative and qualitative analysis of molecules in complex matrices by reducing the matrix interferences. It may play an important role in the area of food safety.

How it Works

Generally, LC-MS has four components, including an autosampler, HPLC, ionization source and mass spectrometer, as shown in Figure 2.6.1. Here we need to pay attention to the interface of HPLC and MS so that they can be suitable to each other and be connected. There are specified separation column for HPLC-MS, whose inner diameter (I.D.) is usually 2.0 mm. And the flow rate, which is 0.05 - 0.2 mL/min, is slower than typical HPLC. For the mobile phase, we use the combination of water and methanol and/acetonitrile. And because ions will inhibit the signals in MS, if we want to modify to mobile phase, the modifier should be volatile, such as HCO_2H, CH_3CO_2H, $[NH_4][HCO_2]$ and $[NH_4][CH_3CO_2]$.

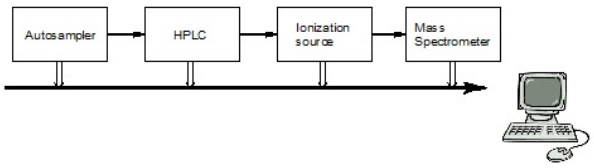


Figure 2.6.1 The component of a HPCL-MS system. Adapted from W. A . Korfmacher, *Drug Discov. Today*, 2005, **10**, 1357.

As the interface between HPLC and MS, the ionization source is also important. There are many types and ESI and atmospheric pressure chemical ionization (APCI) are the most common ones. Both of them are working at atmospheric pressure, high voltage and high temperature. In ESI, the column eluent as nebulized in high voltage field (3 - 5 kV). Then there will be very small charged droplet. Finally individual ions formed in this process and goes into mass spectrometer.

Comparison of ESI-QTOF-MS and Other Mass Spectrometer Methods

There are many types of mass spectrometers which can connect with the HPLC. One of the most widely-used MS systems is single quadrupole mass spectrometer, whichis not very expensive, shown in Figure 2.6.2. This system has two modes. One mode is *total ion monitoring* (TIM) mode which can provide the total ion chromatograph. The other is *selected ion monitoring* (SIM) mode, in which the user can choose to monitor some specific ions, and the latter's sensitivity is much higher than the former's. Further, the mass resolution of the single quadrupole mass spectrometer is 1 Da and its largest detection mass range is 30 - 3000 Da.

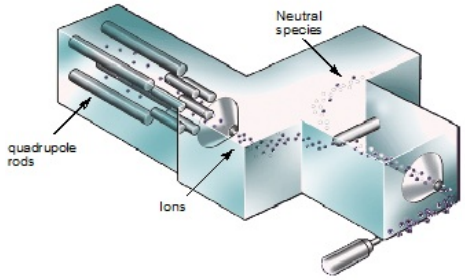


Figure 2.6.2 Single quadrupole mass spectrometer. Adapted from W. A. Korfmacher, *Using Mass Spectrometry for Drug Metabolism Studies*, 1st Edition, Taylor & Francis, Abingdon (2004).

The second MS system is the triple quadrupole MS-MS system, shown in Figure 2.6.3. Using this system, people can select the some ions, called parent ions, and use another electron beam to collide them again to get the fragment ions, called daughter ions. In other words, there are two steps to select the target molecules. So it reduces the matrix effect a lot. This system is very useful in the analysis of biological samples because biological samples always have very complex matrix; however, the mass resolution is still 1 Da.

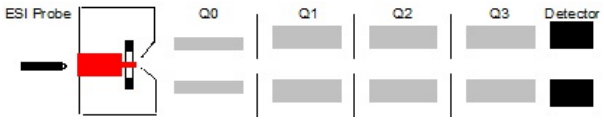


Figure 2.6.3 Triple quadrupole mass spectrometer. Adapted from W. A. Korfmacher, *Using Mass Spectrometry for Drug Metabolism Studies*, 1st Edition, Taylor & Francis, Abingdon (2004).

The third system is time-of-flight (TOF) MS, shown in Figure 2.6.4, which can provide a higher mass resolution spectrum, 3 to 4 decimals of Da. Furthermore, it can detect a very large range of mass at a very fast speed. The largest detection mass range is 20 - 10000 Da. But the price of this kind of MS is very high. The last technique is a hybrid mass spectrometer, Q-TOF MS, which combines a single quadrupole MS and a TOF MS. Using this MS, we can get high resolution chromatograph and we also can use the MS-MS system to identify the target molecules.

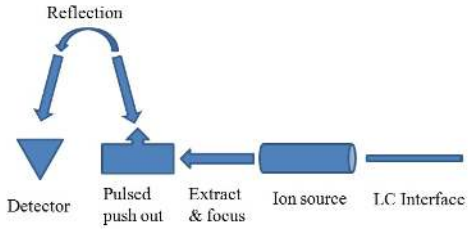


Figure 2.6.4 Time-of-flight mass spectrometer. Adapted from W. A. Korfmacher, *Using Mass Spectrometry for Drug Metabolism Studies*, 1st Edition, Taylor & Francis, 2004.

Application of LC/ESI-QTOF-MS in the Detection of Quinolones in Edible Animal Food

Quinolones are a family of common antibacterial veterinary medicine which can inhibit DNA-gyrase in bacterial cells. However, the residues of quinolone in edible animal products may be directly toxic or cause resistant pathogens in humans. Therefore, sensitive methods are required to monitor such residues possibly present in different animal-producing food, such as eggs, chicken, milk and fish. The molecular structures of eight quinolones, ciprofloxacin (CIP), anofloxacin methanesulphonate (DAN), enrofloxacin (ENR), difloxacin (DIF), sarafloxacin (SARA), oxolinic, acid (OXO), flumequine (FLU), ofloxacin (OFL), are shown in Figure 2.6.5.

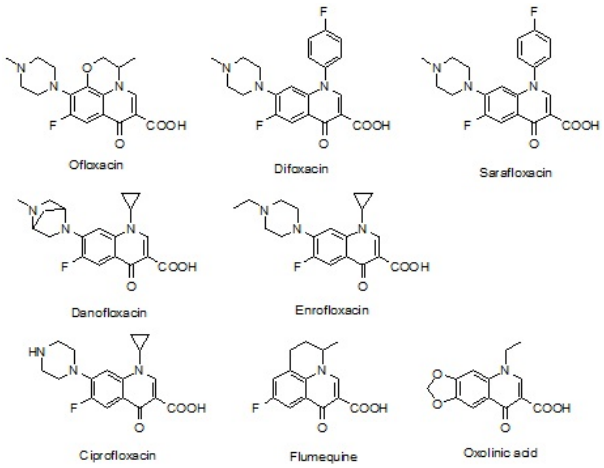


Figure 2.6.5 The molecular structure of eight quinolones. Adapted from M. M. Zheng, G. D. Ruan, and Y. Q. Feng, *J. Chromatogr. A*, 2009, **1216**, 7510.

LC-MS is a common detection approach in the field of food safety. But because of the complex matrix of the samples, it is always difficult to detect those target molecules of low concentration by using single quadrupole MS. The following gives an example of the application of LC/ESI-QTOF-MS.

Using a quaternary pump system, a Q-TOF-MS system, a C18 column (250 mm × 2.0 mm I.D., 5 µm) with a flow rate of 0.2 mL/min, and a mixture of solvents as the mobile phase comprising of 0.3% formic acid solution and acetonitrile. The gradient phofile for mobile phase is shown in Table 2.6.1. Since at acidic pH condition, the quinolones carried a positive charge, all mass spectra were acquired in the positive ion mode and summarizing 30,000 single spectra in the mass range of 100-500 Da.

Table 2.6.1 The gradient phofile for mobile phase

Time (min)	Volume % of Formic Acid Solution	Volume % of Acetonitrile
0	80	20
12	65	35
15	20	80
20	15	85
30	15	85
30.01	80	20

The optimal ionization source working parameters were as follows: capillary voltage 4.5 kV; ion energy of quadrupole 5 eV/z; dry temperature 200 °C; nebulizer 1.2 bar; dry gas 6.0 L/min. During the experiments, HCO_2Na (62 Da) was used to externally calibrate the instrument. Because of the high mass accuracy of the TOF mass spectrometer, it can extremely reduce the matrix effects. Three different chromatographs are shown in Figure 2.6.6. The top one is the total ion chromatograph at the window range of 400 Da. It's impossible to distinguish the target molecules in this chromatograph. The middle one is at one Da resolution, which is the resolution of single quadrupole mass spectrometer. In this chromatograph, some of the molecules can be identified. But noise intensity is still very high and there are several peaks of impurities with similar mass-to-charge ratios in the chromatograph. The bottom one is at 0.01 Da resolution. It clearly shows the peaks of eight quinolones with very high signal to noise ratio. In other words, due to the fast acquisition rates and high mass accuracy, LC/TOF-MS can significantly reduce the matrix effects.

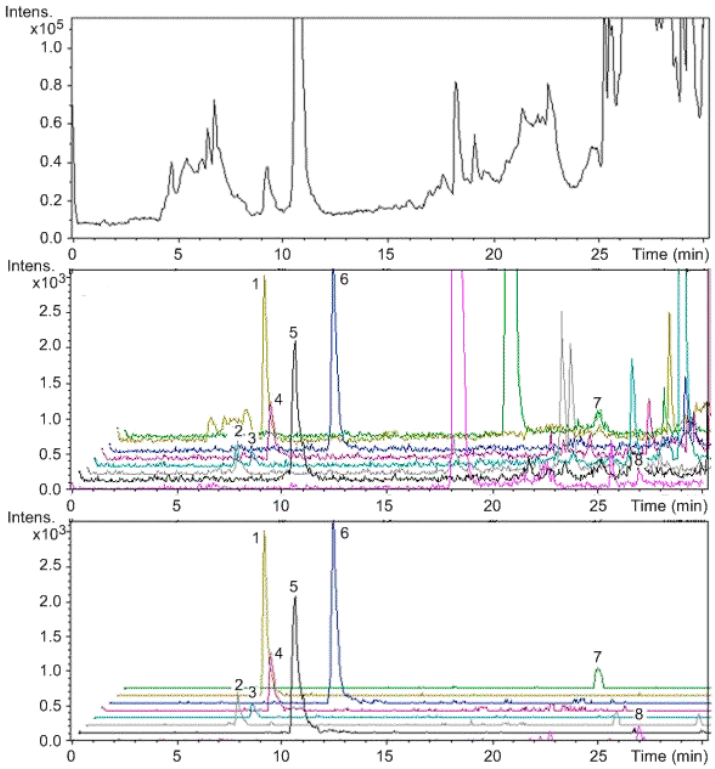


Figure 2.6.6 Different chromatographs of 4 ng/g eight quinolones spiked in fish samples at different mass resolutions. Peaks: 1 = OFL; 2 = CIP; 3 =DAN; 4 = ENR; 5 = SARA; 6 = DIF; 7 =OXO; 8 = FLU. Adapted from M. M. Zheng, G. D. Ruan, and Y. Q. Feng, *J. Chromatogr. A*, 2009, **1216**, 7510.

The quadrupole MS can be used to further confirm the target molecules. Figure 2.6.7 shows the chromatograms obtained in the confirmation of CIP (17.1 ng/g) in a positive milk sample and ENR (7.5 ng/g) in a positive fish sample. The chromatographs of parent ions are shown on the left side. On the right side, they are the characteristic daughter ion mass spectra of CIP and ENR.

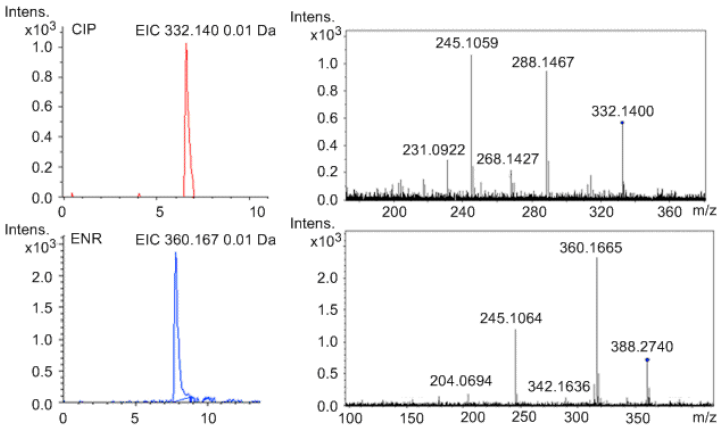


Figure 2.6.7 Chromatograms obtained in the confirmation of CIP (17.1 ng/g) in positive milk sample and ENR (7.5 ng/g) in positive fish sample. Adapted from M. M. Zheng, G. D. Ruan, and Y. Q. Feng, *J. Chromatogr. A*, 2009, **1216**, 7510.

Drawbacks of LC/Q-TOF-MS

Some of the drawbacks of LC/Q-TOF-MS are its high costs of purchase and maintenance. It is hard to apply this method in daily detection in the area of environmental protection and food safety.

In order to reduce the matrix effect and improve the detection sensitivity, people may use some sample preparation methods, such as liquid-liquid extraction (LLE), solid-phase extraction (SPE), distillation. But these methods would consume large amount of samples, organic solvent, time and efforts. Nowadays, there appear some new sample preparation methods. For example, people may use online microdialysis, supercritical fluid extraction (SFE) and pressurized liquid extraction. In the method mentioned in the

Application part, we use online in-tube solid-phase microextraction (SPME), which is an excellent sample preparation technique with the features of small sample volume, simplicity solventless extraction and easy automation.

This page titled 2.6: ESI-QTOF-MS Coupled to HPLC and its Application for Food Safety is shared under a CC BY license and was authored, remixed, and/or curated by Pavan M. V. Raja & Andrew R. Barron (OpenStax CNX) .

- **4.10: ESI-QTOF-MS Coupled to HPLC and its Application for Food Safety** by Pavan M. V. Raja & Andrew R. Barron is licensed CC BY 4.0. Original source: http://cnx.org/contents/ba27839d-5042-4a40-afcf-c0e6e39fb45425.2.

CHAPTER OVERVIEW

3: Infrared Spectroscopy

- 3.1: Infrared Spectroscopy
- 3.2: IR Spectroscopy
- 3.3: Theory
  - How an FTIR Spectrometer Operates
  - Theory
- 3.4: ATR-FTIR
- 3.5: Instrumentation
- 3.6: Sample Handling
- 3.7: Interpreting Infrared Spectra
- 3.8: Interpreting Infrared Spectra
  - Carbon Nitrogen Bonds
  - IR10. More Practice with IR Spectra
  - IR2. Hydrocarbon Spectra
  - IR3. Subtle Points of IR Spectroscopy
  - IR4. Carbon Carbon Multiple Bonds
  - IR5. Carbon Oxygen Single Bonds
  - IR6. Carbon Oxygen Double Bonds
  - IR8. More Complicated IR Spectra
  - IR9. Misleading Peaks
  - IR Table of Organic Compounds
  - What Does an IR Spectrum Look Like?
- 3.9: Interpretation
- 3.10: Identifying the Presence of Particular Groups
- 3.11: Infrared Spectra of Some Common Functional Groups
- 3.12: Application

3: Infrared Spectroscopy is shared under a CC BY-NC-SA 4.0 license and was authored, remixed, and/or curated by LibreTexts.

3.1: Infrared Spectroscopy

Objectives

After completing this section, you should be able to

1. identify (by wavelength, wavenumber, or both) the region of the electromagnetic spectrum which is used in infrared (IR) spectroscopy.
2. interconvert between wavelength and wavenumber.
3. discuss, in general terms, the effect that the absorption of infrared radiation can have on a molecule.

Key Terms

Make certain that you can define, and use in context, the key terms below.

- infrared spectrum
- wavenumber (reciprocal centimetres)

Study Notes

Notice that the scale at the bottom of the infrared spectrum for 2-hexanone shown is calibrated in wavenumbers (cm^{-1}). A wavenumber is the reciprocal of a wavelength (1/λ); thus, a wavenumber of 1600 cm^{-1} corresponds to a wavelength of

$$\frac{1}{1600\,\text{cm}^{-1}} = 6.25 \times 10^{-4}\text{cm or} 6.25\,\mu\text{m}$$

Organic chemists find it more convenient to deal with wavenumbers rather than wavelengths when discussing infrared spectra.

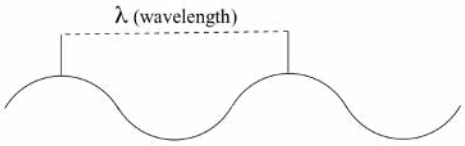
You will obtain infrared spectra for a number of the compounds you will synthesize in the laboratory component of this course.

The inverted peaks observed in the spectra correspond to molecular stretching and bending vibrations that only occur at certain quantized frequencies. When infrared radiation matching these frequencies falls on the molecule, the molecule absorbs energy and becomes excited. Eventually the molecule returns to its original (ground) state, and the energy which was absorbed is released as heat.

The electromagnetic spectrum

Electromagnetic radiation, as you may recall from a previous chemistry or physics class, is composed of electrical and magnetic waves which oscillate on perpendicular planes. Visible light is electromagnetic radiation. So are the gamma rays that are emitted by spent nuclear fuel, the x-rays that a doctor uses to visualize your bones, the ultraviolet light that causes a painful sunburn when you forget to apply sun block, the infrared light that the army uses in night-vision goggles, the microwaves that you use to heat up your frozen burritos, and the radio-frequency waves that bring music to anybody who is old-fashioned enough to still listen to FM or AM radio.

Just like ocean waves, electromagnetic waves travel in a defined direction. While the speed of ocean waves can vary, however, the speed of electromagnetic waves – commonly referred to as the speed of light – is essentially a constant, approximately 300 million meters per second. This is true whether we are talking about gamma radiation or visible light. Obviously, there is a big difference between these two types of waves – we are surrounded by the latter for more than half of our time on earth, whereas we hopefully never become exposed to the former to any significant degree. The different properties of the various types of electromagnetic radiation are due to differences in their wavelengths, and the corresponding differences in their energies: *shorter wavelengths correspond to higher energy.*



High-energy radiation (such as gamma- and x-rays) is composed of very short waves – as short as 10^{-16} meter from crest to crest. Longer waves are far less energetic, and thus are less dangerous to living things. Visible light waves are in the range of 400 – 700 nm (nanometers, or 10^{-9} m), while radio waves can be several hundred meters in length.

The notion that electromagnetic radiation contains a quantifiable amount of energy can perhaps be better understood if we talk about light as a stream of *particles*, called **photons**, rather than as a wave. (Recall the concept known as 'wave-particle duality': at the quantum level, wave behavior and particle behavior become indistinguishable, and very small particles have an observable 'wavelength'). If we describe light as a stream of photons, the energy of a particular wavelength can be expressed as:

$E = hc/\lambda$

where E is energy in kcal/mol, **λ** (the Greek letter *lambda*) is wavelength in meters, *c* is 3.00 x 10^{8} m/s (the speed of light), and *h* is 9.537 x 10^{-14} kcal·s·mol^{-1}, a number known as Planck's constant.

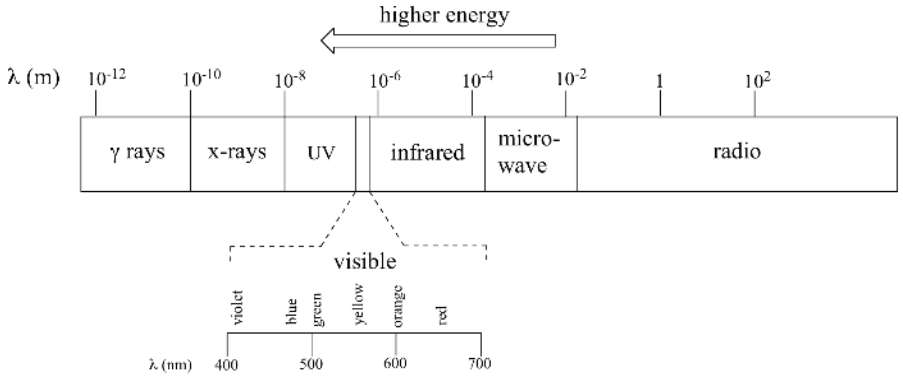
Because electromagnetic radiation travels at a constant speed, each wavelength corresponds to a given frequency, which is the number of times per second that a crest passes a given point. Longer waves have lower frequencies, and shorter waves have higher frequencies. Frequency is commonly reported in hertz (Hz), meaning 'cycles per second', or 'waves per second'. The standard unit for frequency is s^{-1}.

When talking about electromagnetic waves, we can refer either to wavelength or to frequency - the two values are interconverted using the simple expression:

$\lambda\nu = c$

where **ν** (the Greek letter '*nu*') is frequency in s^{-1}. Visible red light with a wavelength of 700 nm, for example, has a frequency of 4.29 x 10^{14} Hz, and an energy of 40.9 kcal per mole of photons.

The full range of electromagnetic radiation wavelengths is referred to as the **electromagnetic spectrum**.



Notice in the figure above that visible light takes up just a narrow band of the full spectrum. White light from the sun or a light bulb is a mixture of all of the visible wavelengths. You see the visible region of the electromagnetic spectrum divided into its different wavelengths every time you see a rainbow: violet light has the shortest wavelength, and red light has the longest.

? Exercise 3.1.1

Visible light has a wavelength range of about 400-700 nm. What is the corresponding frequency range? What is the corresponding energy range, in kcal/mol of photons?

Answer

Using $\lambda\nu = c$, we first rearrange to $\nu = c/\lambda$ to solve for frequency.

For light with a wavelength of 400 nm, the frequency is 7.50 × 10^{14} Hz:

$$\nu = \frac{3 \times 10^{8}\ \text{m s}^{-1}}{400 \times 10^{-9}\ \text{m}} = 7.50 \times 10^{14}\ \text{s}^{-1}$$

In the same way, we calculate that light with a wavelength of 700 nm has a frequency of 4.29 × 10^{14} Hz.

To calculate corresponding energies using hc/λ. We find for light at 400 nm:

$$E = \frac{(6.626 \times 10^{-34}\ \text{J s mol}^{-1})(3.00 \times 10^{8}\ \text{m s}^{-1})}{400 \times 10^{-9}\ \text{m}}$$

$$= 4.97 \times 10^{-19}\ \text{J per photon}$$

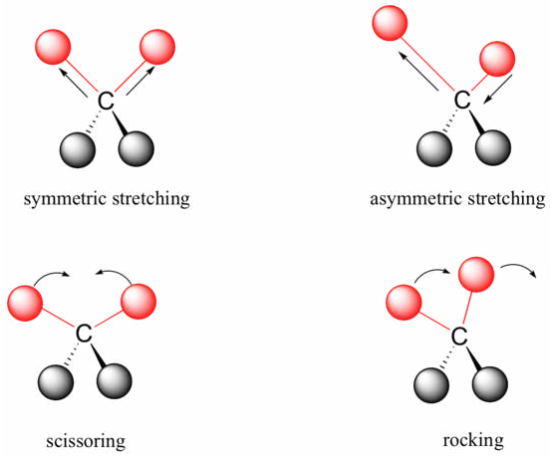
$$E\ (\text{one mole}) = E \times N$$

$$= (4.97 \times 10^{-19}\ \text{J})(6.02 \times 10^{23}\ \text{mol}^{-1})$$

$$= 299\ \text{kJ mol}^{-1}$$

Using the same equation, we find that light at 700 nm corresponds to 171 kJ mol^{-1}

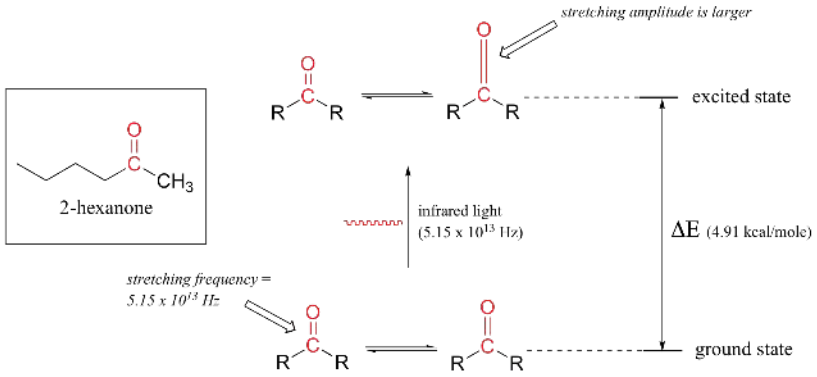
Covalent bonds in organic molecules are not rigid sticks – rather, they behave more like springs. At room temperature, organic molecules are always in motion, as their bonds stretch, bend, and twist. These complex vibrations can be broken down mathematically into individual **vibrational modes**, a few of which are illustrated below.



The energy of molecular vibration is *quantized* rather than continuous, meaning that a molecule can only stretch and bend at certain 'allowed' frequencies. If a molecule is exposed to electromagnetic radiation that matches the frequency of one of its vibrational modes, it will in most cases absorb energy from the radiation and jump to a higher vibrational energy state - what this means is that the *amplitude* of the vibration will increase, but the vibrational *frequency* will remain the same. The difference in energy between the two vibrational states is equal to the energy associated with the wavelength of radiation that was absorbed. It turns out that it is the *infrared* region of the electromagnetic spectrum which contains frequencies corresponding to the vibrational frequencies of organic bonds.

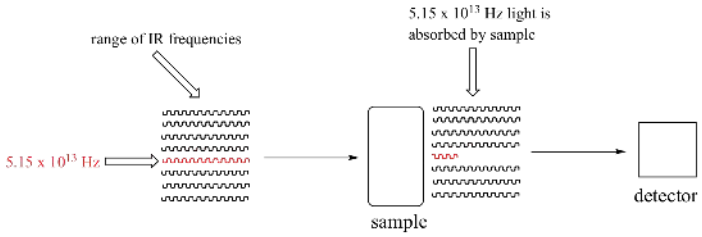
Let's take 2-hexanone as an example. Picture the carbonyl bond of the ketone group as a spring. This spring is constantly bouncing back and forth, stretching and compressing, pushing the carbon and oxygen atoms further apart and then pulling them together. This is the **stretching mode** of the carbonyl bond. In the space of one second, the spring 'bounces' back and forth 5.15 x 10^{13} times - in other words, the ground-state frequency of carbonyl stretching for a the ketone group is about 5.15 x 10^{13} Hz.

If our ketone sample is irradiated with infrared light, the carbonyl bond will specifically absorb light with this same frequency, which by equations 4.1 and 4.2 corresponds to a wavelength of 5.83 x 10^{-6} m and an energy of 4.91 kcal/mol. When the carbonyl bond absorbs this energy, it jumps up to an excited vibrational state.



The value of **ΔE** - the energy difference between the low energy (ground) and high energy (excited) vibrational states - is equal to 4.91 kcal/mol, the same as the energy associated with the absorbed light frequency. The molecule does not remain in its excited vibrational state for very long, but quickly releases energy to the surrounding environment in form of heat, and returns to the ground state.

With an instrument called an infrared spectrophotometer, we can 'see' this vibrational transition. In the spectrophotometer, infrared light with frequencies ranging from about 10^{13} to 10^{14} Hz is passed though our sample of cyclohexane. Most frequencies pass right through the sample and are recorded by a detector on the other side.



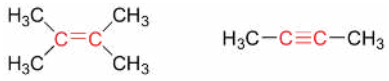
Our 5.15 x 10^{13} Hz carbonyl stretching frequency, however, is absorbed by the 2-hexanone sample, and so the detector records that the intensity of this frequency, after having passed through the sample, is something less than 100% of its initial intensity.

The vibrations of a 2-hexanone molecule are not, of course, limited to the simple stretching of the carbonyl bond. The various carbon-carbon bonds also stretch and bend, as do the carbon-hydrogen bonds, and all of these vibrational modes also absorb different frequencies of infrared light.

The power of infrared spectroscopy arises from the observation that *different functional groups have different characteristic absorption frequencies*. The carbonyl bond in a ketone, as we saw with our 2-hexanone example, typically absorbs in the range of 5.11 - 5.18 x 10^{13} Hz, depending on the molecule. The carbon-carbon triple bond of an alkyne, on the other hand, absorbs in the range 6.30 - 6.80 x 10^{13} Hz. The technique is therefore very useful as a means of identifying which functional groups are present in a molecule of interest. If we pass infrared light through an unknown sample and find that it absorbs in the carbonyl frequency range but not in the alkyne range, we can infer that the molecule contains a carbonyl group but not an alkyne.

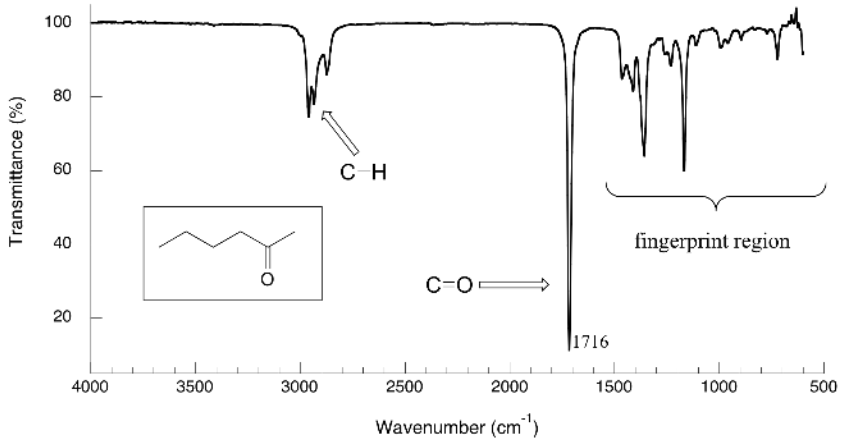
Some bonds absorb infrared light more strongly than others, and some bonds do not absorb at all. *In order for a vibrational mode to absorb infrared light, it must result in a periodic change in the dipole moment of the molecule*. Such vibrations are said to be **infrared active**. In general, the greater the polarity of the bond, the stronger its IR absorption. The carbonyl bond is very polar, and absorbs very strongly. The carbon-carbon triple bond in most alkynes, in contrast, is much less polar, and thus a stretching vibration does not result in a large change in the overall dipole moment of the molecule. Alkyne groups absorb rather weakly compared to carbonyls.

Some kinds of vibrations are **infrared inactive**. The stretching vibrations of completely symmetrical double and triple bonds, for example, do not result in a change in dipole moment, and therefore do not result in any absorption of light (but other bonds and vibrational modes in these molecules *do* absorb IR light).



infrared-inactive double and triple bonds

Now, let's look at some actual output from IR spectroscopy experiments. Below is the IR spectrum for 2-hexanone.



There are a number of things that need to be explained in order for you to understand what it is that we are looking at. On the horizontal axis we see IR wavelengths expressed in terms of a unit called **wavenumber** (cm^{-1}), which tells us how many waves fit into one centimeter. On the vertical axis we see '**% transmittance**', which tells us how strongly light was absorbed at each frequency (100% transmittance means no absorption occurred at that frequency). The solid line traces the values of % transmittance for every wavelength – the 'peaks' (which are actually pointing down) show regions of strong absorption. For some reason, it is typical in IR spectroscopy to report wavenumber values rather than wavelength (in meters) or frequency (in Hz). The 'upside down' vertical axis, with absorbance peaks pointing down rather than up, is also a curious convention in IR spectroscopy. We wouldn't want to make things too easy for you!

Contributors and Attributions

- Dr. Dietmar Kennepohl FCIC (Professor of Chemistry, Athabasca University)
- Prof. Steven Farmer (Sonoma State University)
- William Reusch, Professor Emeritus (Michigan State U.), Virtual Textbook of Organic Chemistry
- Organic Chemistry With a Biological Emphasis by Tim Soderberg (University of Minnesota, Morris)

3.1: Infrared Spectroscopy is shared under a CC BY-NC-SA 4.0 license and was authored, remixed, and/or curated by LibreTexts.

- **12.5: Spectroscopy and the Electromagnetic Spectrum** by Dietmar Kennepohl, Steven Farmer, William Reusch is licensed CC BY-SA 4.0.

3.2: IR Spectroscopy

IR Sample Preparation: A Practical Guide

Infrared spectroscopy is based on molecular vibrations caused by the oscillation of molecular dipoles. Bonds have characteristic vibrations depending on the atoms in the bond, the number of bonds and the orientation of those bonds with respect to the rest of the molecule. Thus, different molecules have specific spectra that can be collected for use in distinguishing products or identifying an unknown substance (to an extent.)

Collecting spectra through this method goes about one of three general ways. Nujol mulls and pressed pellets are typically used for collecting spectra of solids, while thin-film cells are used for solution-phase IR spectroscopy. Spectra of gases can also be obtained but will not be discussed in this guide.

Infrared Optical Materials and Handling

While it is all well and wonderful that substances can be characterized in this fashion one still has to be able to hold the substances inside of the instrument and properly prepare the samples. In an infrared spectrometer (Figure 3.2.1)

the sample to be analyzed is held in front of an infrared laser beam, in order to do this, the sample must be contained in something, consequently this means that the very container the sample is in will absorb some of the infrared beam.

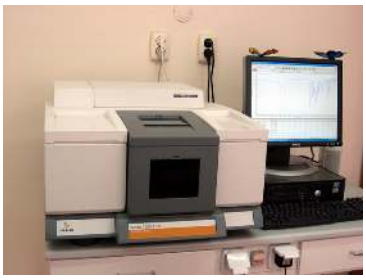


Figure 3.2.1 *An example of a modern benchtop FT-IR spectrometer (Varian Corp.)*

This is made somewhat complicated by the fact that all materials have some sort of vibration associated with them. Thus, if the sample holder has an optical window made of something that absorbs near where your sample does, the sample might not be distinguishable from the optical window of the sample holder. The range that is not blocked by a strong absorbance is known as a *window* (not to be confused with the optical materials of the cell.)

Windows are an important factor to consider when choosing the method to perform an analysis, as seen in Table 3.2.1 there are a number of different materials each with their own characteristic absorption spectra and chemical properties. Keep these factors in mind when performing analyses and precious sample will be saved. For most organic compounds NaCl works well though it is susceptible to attack from moisture. For metal coordination complexes KBr, or CsI typically work well due to their large windows. If money is not a problem then diamond or sapphire can be used for plates.

Table 3.2.1 Various IR-transparent materials and their solubilities and other notes. M. R. Derrick, D. Stulik, and J. M. Landry, in Scientific Tools in Conservation: Infrared Spectroscopy in Conservation Science. Getty Conservation Institute (1999).

Material	Transparent Ranges (cm^{-1})	Solubility	Notes
NaCl	40,000 - 625	H_{2O}	Easy to polish, hygroscopic
Silica glass	55,000-3,000	HF	Attacked by HF
Quartz	40,000-2,500	HF	Attacked by HF
Sapphire	20,000-1,780	-	Strong
Diamond	40,000-2,500 and 1,800-200	-	Very strong, expensive, hard, useless for pellets
CaF_2	70,000-1,110	Acids	Attacked by acids, avoid ammonium salts
BaF_2	65,000-700	-	Avoid ammonium salts

Material	Transparent Ranges (cm $^{-1}$)	Solubility	Notes
ZnSe	10,000 - 550	Acids	Brittle, attacked by acids
AgCl	25,000-400	-	Soft, sensitive to light.
KCl	40,000-500	H_2O, Et_2O, acetone	Hygroscopic, soft, easily polished, commonly used in making pellets.
KBr	40,000-400	H_2O, EtOH	Hygroscopic, soft, easily polished, commonly used in making pellets.
CsBr	10,000-250	H_2O, EtOH, acetone	Hygroscopic soft
CsI	10,000-200	H_2O, EtOH, MeOH, acetone	Hygroscopic, soft.
Teflon	5,000-1,200; 1,200-900	-	Inert, disposable
Polyethylene	4,000-3,000; 2,800-1,460; 1,380 - 730; 720- 30	-	Inert, disposable

Proper handling of these plates will ensure they have a long, useful life. Here follows a few simple pointers on how to handle plates:

- Avoid contact with solvents that the plates are soluble in.
- Keep the plates in a dessicator, the less water the better, even if the plates are insoluble to water.
- Handle with gloves, clean gloves.
- Avoid wiping the plates to prevent scratching.

That said, these simple guidelines will likely reduce most damage that can occur to a plate by simply holding it other faults such as dropping the plate from a sufficient height can result in more serious damage.

Preparation of Nujol Mulls

A common method of preparing solid samples for IR analysis is mulling. The principle here is by grinding the particles to below the wavelength of incident radiation that will be passing through there should be limited scattering. To suspend those tiny particles, an oil, often referred to as Nujol is used. IR-transparent salt plates are used to hold the sample in front of the beam in order to acquire data. To prepare a sample for IR analysis using a salt plate, first decide what segment of the frequency band should be studied, refer to Table 3.2.1 for the materials best suited for the sample. Figure 3.2.2 shows the materials needed for preparing a mull.



Figure 3.2.2 In this photograph, the sample, ferrocene, two clean and polished KBr plates, an agate mortar and pestle, a mounting card and a spatula are displayed as the base minimum requirements for preparing a sample though a Nujol mull. Of course, a small bottle of mineral oil is also necessary.

Preparing the mull is performed by taking a small portion of sample and adding approximately 10% of the sample volume worth of the oil and grinding this in an agate mortar and pestle as demonstrated in Figure 3.2.3. The resulting mull should be transparent

with no visible particles.



Figure 3.2.3 Mulling ferrocene into mineral oil with a mortar and pestle.

Another method involves dissolving the solid in a solvent and allowing it to dry in the agate pestle. If using this method ensure that all of the solvent has evaporated since the solvent bands will appear in the spectrum. Some gentle heating may assist this process. This method creates very fine particles that are of a relatively consistent size. After addition of the oil further mixing (or grinding) may be necessary.

Plates should be stored in a desiccator to prevent erosion by atmospheric moisture and should appear roughly transparent. Some materials such as silicon will not, however. Gently rinse the plates with hexanes to wash any residual material off of the plates. Removing the plates from the desiccator and cleaning them should follow the preparation of the mull in order to maintain the integrity of the salt plates. Of course, if the plate is not soluble in water then it is still a good idea just to prevent the threat of mechanical trauma or a stray jet of acetone from a wash bottle.

Once the mull has been prepared, add a drop to one IR plate (Figure 3.2.4), place the second plate on top of the drop and give it a quarter turn in order to evenly coat the plate surface as seen in Figure 3.2.5. Place it into the spectrometer and acquire the desired data.

Always handle with gloves and preferably away from any sinks, faucets, or other sources of running or spraying water.







Figure 3.2.4 The prepared mull from an agate mortar and pestle being applied to a polished KBr plate. Figure 3.2.5 Sandwiched KBr plates with a Nujol mull of ferrocene.

Spectra acquired by this method will have strong C-H absorption bands throughout several ranges 3,000 – 2,800 cm^{-1} and 1,500 – 1,300 cm^{-1} and may obscure signal.

Cleaning the plate is performed as previously mentioned with hexanes or chloroform can easily be performed by rinsing and leaving them to dry in the hood. Place the salt plates back into the desiccator as soon as reasonably possible to prevent damage. It is highly advisable to polish the plates after use, no scratches, fogging, or pits should be visible on the face of the plate. Chips, so long as they don't cross the center of the plate are survivable but not desired. The samples of damaged salt plates in Figure 3.2.6 show common problems associated with use or potentially mishandling. Clouding, and to an extent, scratches can be polished out with an iron rouge. Areas where the crystal lattice is disturbed below the surface are impossible to fix and chips cannot be reattached.

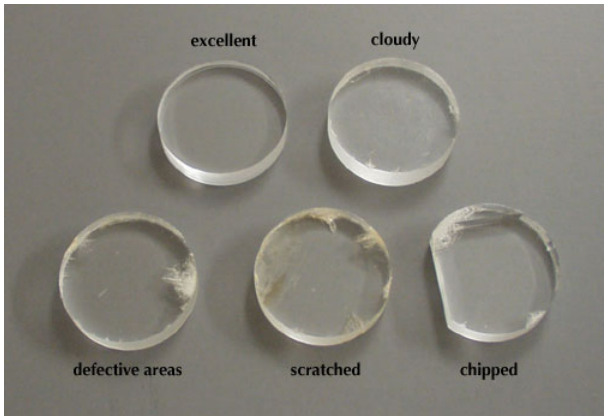


FIgure 3.2.6 A series of plates indicating various forms of physical damage with a comparison to a good plate (Copyright: Colorado University-Boulder).

Preparation of Pellets

In an alternate method, this technique is along the same lines of the nujol mull except instead of the suspending medium being mineral oil, the suspending medium is a salt. The solid is ground into a fine powder with an agate mortar and pestle with an amount of the suspending salt. Preparing pellets with diamond for the suspending agent is somewhat illadvised considering the great hardness of the substance. Generally speaking, an amount of KBr or CsI is used for this method since they are both soft salts. Two approaches can be used to prepare pellets, one is somewhat more expensive but both usually yield decent results.

The first method is the use of a press. The salt is placed into a cylindrical holder and pressed together with a ram such as the one seen in (Figure 3.2.7). Afterwards, the pellet, in the holder, is placed into the instrument and spectra acquired.



Figure 3.2.7 A large benchtop hydraulic press (Specac Inc.)

An alternate, and cheaper method requires the use of a large hex nut with a 0.5 inch inner diameter, two bolts, and two wrenches such as the kit seen in Figure 3.2.8. Step-by-step instructions for loading and using the press follows:

1. Screw one of the bolts into the nut about half way.

2. Place the salt pellet mixture into the other opening of the nut and level by tapping the assembly on a countertop.
3. Screw in the second bolt and place the assembly on its side with the bolts parallel to the countertop. Place one of the wrenches on the bolt on the right side with the handle aiming towards yourself.
4. Take the second wrench and place it on the other bolt so that it attaches with an angle from the table of about 45 degrees.
5. The second bolt is tightened with a body weight and left to rest for several minutes. Afterwards, the bolts are removed, and the sample placed into the instrument.



Figure 3.2.8 A simple pellet press with cell holder. (Cole-Parmer)

Some pellet presses also have a vacuum barb such as the one seen in (Figure 3.2.8. If your pellet press has one of these, consider using it as it will help remove air from the salt pellet as it is pressed. This ensures a more uniform pellet and removes absorbances in the collected spectrum due to air trapped in the pellet.

Preparation of Solution Cells

Solution cells (Figure 3.2.9) are a handy way of acquiring infrared spectra of compounds in solution and is particularly handy for monitoring reactions.



Figure 3.2.9 A sealed solution cell with two injection ports and a schematic of its construction (Perkin-Elmer Inc.)

A thin-film cell consists of two salt plates with a very thin space in between them (Figure 3.2.10). Two channels allow liquid to be injected and then subsequently removed. The windows on these cells can be made from a variety of IR optical materials. One particularly useful one for water-based solutions is CaF_2 as it is not soluble in water.

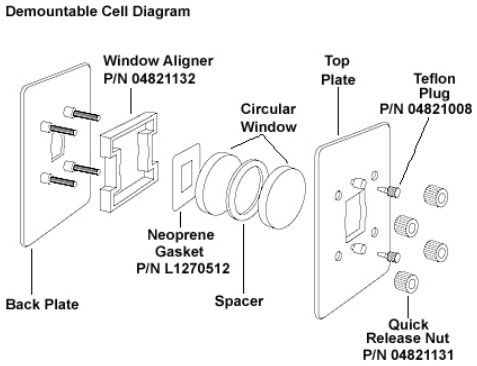


Figure 3.2.10 A sealed solution cell with two injection ports and a schematic of its construction (Perkin-Elmer Inc.).

Cleaning these cells can be performed by removing the solution, flushing with fresh solvent and gently removing the solvent by syringe. Do not blow air or nitrogen through the ports as this can cause mechanical deformation in the salt window if the pressure is high enough.

Deuterated Solvent Effects

One of the other aspects to solution-phase IR is that the solvent utilized in the cell has a characteristic absorption spectra. In some cases this can be alleviated by replacing the solvent with its deuterated sibling. The benefit here is that C-H bonds are now C-D bonds and have lower vibrational frequencies. Compiled in Figure 3.2.11 is a set of common solvents.

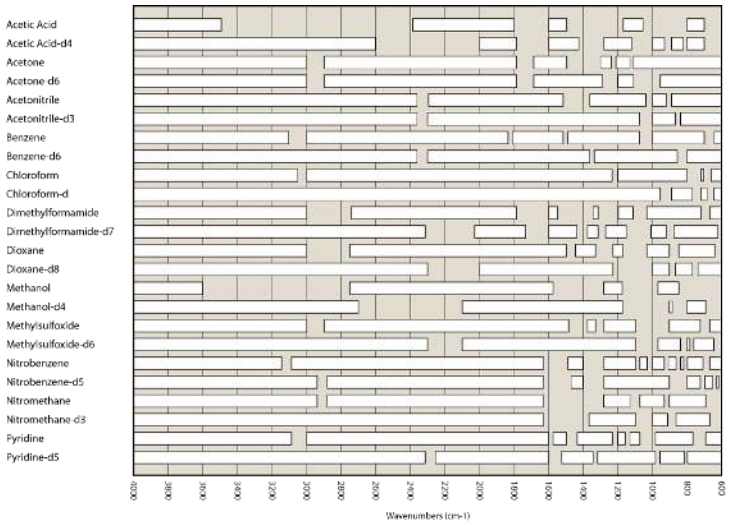


Figure 3.2.11 IR transparencies of various solvents and their heavy counterparts. Adapted from N. L. McNiven and R. Court, *Appl. Spectrosc.*, 1970, **24**, 296.

This effect has numerous benefits and is often applied to determining what vibrations correspond to what bond in a given molecular sample. This is often accomplished by using isotopically labeled "heavy" reagents such as ones that contain ^{2}H, ^{15}N, ^{18}O, or ^{13}C.

Basic Troubleshooting

There are numerous problems that can arise from improperly prepared samples, this section will go through some of the common problems and how to correct them. For this demonstration, spectra of ferrocene will be used. The molecular structure and a photograph of the brightly colored organometallic compound are shown in Figure 3.2.12 and Figure 3.2.13.

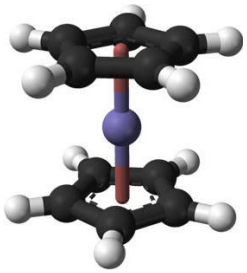


Figure 3.2.12 Structure of ferrocene ($Fe(C_5H_5)_2$).



Figure 3.2.13 Image of ferrocene powder ($Fe(C_5H_5)_2$).

Figure 3.2.14 illustrates what a good sample of ferrocene looks like prepared in a KBr pellet. The peaks are well defined and sharp. No peak is flattened at 0% transmittance and Christiansen scattering is not evident in the baseline.

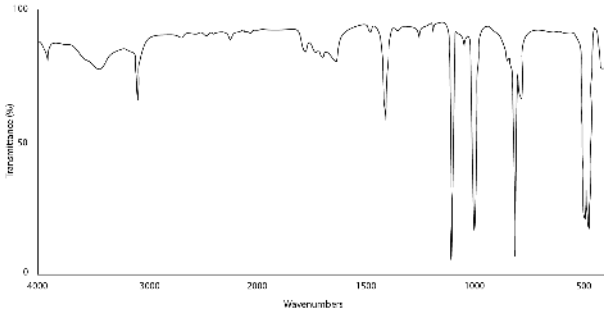


Figure 3.2.14 A good spectrum of ferrocene in a KBr Pellet. Adapted from NIST Chemistry WebBook.

Figure 3.2.15 illustrates a sample with some peaks with intensities that are saturated and lose resolution making peak-picking difficult. In order to correct for this problem, scrape some of the sample off of the salt plate with a rubber spatula and reseat the opposite plate. By applying a thinner layer of sample one can improve the resolution of strongly absorbing vibrations.

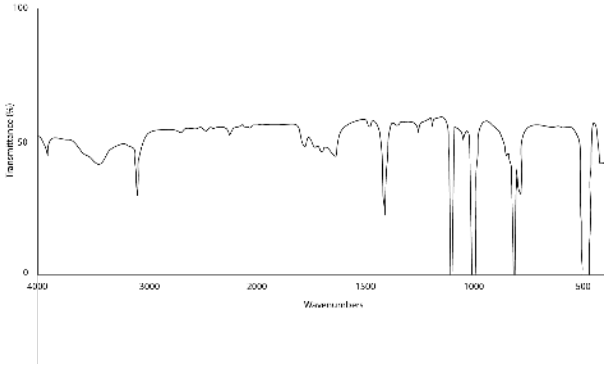


Figure 3.2.15 An overly concentrated sample of ferrocene in a KBr pellet. Adapted from NIST Chemistry WebBook.

Figure 3.2.16 illustrates a sample in which too much mineral oil was added to the mull so that the C-H bonds are far more intense than the actual sample. This can be remedied by removing the sample from the plate, grinding more sample and adding a smaller amount of the mull to the plate. Another possible way of doing this is if the sample is insoluble in hexanes, add a little to the mull and wick away the hexane-oil mixture to leave a dry solid sample. Apply a small portion of oil and replate.

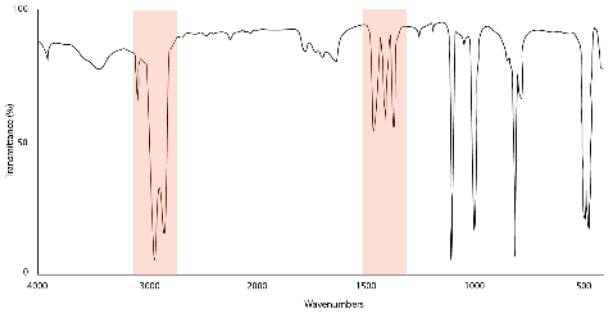


Figure 3.2.16 A spectrum illustrating the problems of using Nujol, areas highlighted in orange are absorbances related to the addition of Nujol to a sample. Notice how in the 1500 wavenumber region the addition of the Nujol has partially occulted the absorbance by the ferrocene. Adapted from NIST Chemistry WebBook.

Figure 3.2.17 illustrates the result of particles being too large and scattering light. To remedy this, remove the mull and grind further or else use the solvent deposition technique described earlier.

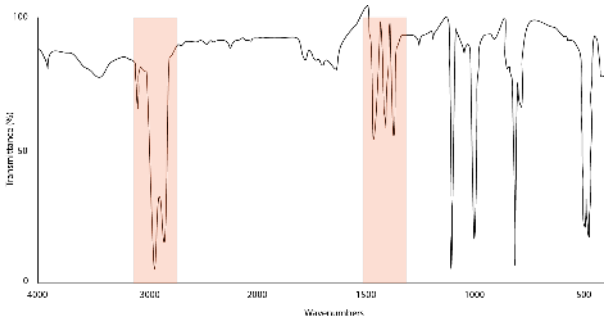


Figure 3.2.17 A sample exhibiting the Christiansen effect on ferrocene in a Nujol mull. Orange boxes indicate Nujol occult ranges. Adapted from NIST Chemistry WebBook.

Characteristic IR Vibrational Modes for Hydrocarbon Compounds

Table 3.2.2 Stretching and bending bands for alkanes.

Functional group	**Mode**	**Wavenumber range (cm^{-1})**
CH_3	Asymmetric stretch	2962±10
CH_3	Symmetric stretch	2872±10
CH_3	Asymmetric bend	1460±10
CH_3	Symmetric bend (umbrella mode)	1375±10
CH_2	Asymmetric stretch	2926±10
CH_2	Symmetric stretch	2855±10
CH_2	Scissors	1455±10
CH_2	Rock	720±10
CH	Stretch	~2900 (weak)
CH	Bend	~1350 (weak)

Table 3.2.3 The stretching bands for alkenes.

Substitution	C-H stretch (cm^{-1})	C=C stretch (cm^{-1})	Out of plane bend (cm^{-1})
Vinyl	3090-3075	1660-1630	900±5, 910±5
Vinylidine	3090-3075	1660-1630	890±5
Cis	3050-3000	1660-1630	690±10
Trans	3050-3000	1680-1665	965±5
Tri-substituted	3050-3000	1680-1665	815±25
Tetra-substituted	-	1680-1665	-

Table 3.2.4 The stretching bands for alkynes.

Substitution	**C-H stretch (cm^{-1})**	**C=C stretch (cm^{-1})**	**C-H wag (cm^{-1})**
Mono-substituted	3350-3250	2140-2100	700-600
Di-substituted	-	2260-2190	-

Table 3.2.5 Bands for mono- and di-substituted benzene rings.

Substitution	**Out of plane C-H bending**	**Ring bend (cm^{-1})**

Substitution	Out of plane C-H bending	Ring bend (cm^{-1})
Mono	770-710	690±10
Ortho	810-750	-
Meta	770-735	690±10
Para	860-790	-

Table 3.2.6 Bands for methyl groups bonded to benzene rings.

Vibration	Wavenumber (cm^{-1})
CH_3 symmetric stretch	2925±5
CH_3 bend overtone	2865±5

Fourier Transform Infrared Spectroscopy of Metal Ligand Complexes

The infrared (IR) range of the electromagnetic spectrum is usually divided into three regions:

- The far-infrared is always used for rotational spectroscopy, with wavenumber range 400 – 10 cm^{-1} and lower energy.
- The mid-infrared is suitable for a detection of the fundamental vibrations and associated rotational-vibrational structure with the frequency range approximately 4000 – 400 cm^{-1}.
- The near-Infrared with higher energy and wave number range 14000 – 4000 cm^{-1}, can excite overtone or higher harmonic vibrations.

For classical light material interaction theory, if a molecule can interact with an electromagnetic field and absorb a photon of certain frequency, the transient dipole of molecular functional group must oscillate at that frequency. Correspondingly, this transition dipole moment must be a non-zero value, however, some special vibration can be IR inactive for the stretching motion of a homonuclear diatomic molecule and vibrations do not affect the molecule's dipole moment (e.g., N_2).

Mechanistic Description of the Vibrations of Polyatomic Molecules

A molecule can vibrate in many ways, and each way is called a "vibrational mode". If a molecule has N atoms, linear molecules have 3N-5 degrees of vibrational modes whereas nonlinear molecules have 3N-6 degrees of vibrational modes. Take H_2O for example; a single molecule of H_2O has O-H bending mode (Figure 3.2.18a), antisymmetric stretching mode (Figure 3.2.18b), and symmetric stretching mode (Figure 3.2.18c).

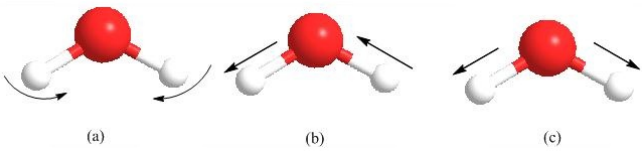


Figure 3.2.18 Three types of hydroxy vibration modes. (a) bending mode; (b) antisymmetric stretching mode; (c) symmetric stretching mode.

If a diatomic molecule has a harmonic vibration with the energy, 3.2.1, where $n+{}^1/_2$ with n = 0, 1, 2 ...). The motion of the atoms can be determined by the force equation, 3.2.2, where k is the force constant). The vibration frequency can be described by 3.2.3. In which *m* is actually the reduced mass (m_{red} or μ), which is determined from the mass m_1 and m_2 of the two atoms, 3.2.4.

$$E_n = -hv \tag{3.2.1}$$

$$F = -kx \tag{3.2.2}$$

$$\omega = (k/m)^{1/2} \tag{3.2.3}$$

$$m_{red} = \mu = \frac{m_1 m_2}{m_1 + m_2} \tag{3.2.4}$$

Principle of Absorption Bands

In IR spectrum, absorption information is generally presented in the form of both wavenumber and absorption intensity or percent transmittance. The spectrum is generally showing wavenumber (cm^{-1}) as the x-axis and absorption intensity or percent transmittance as the y-axis.

Transmittance, "T", is the ratio of radiant power transmitted by the sample (I) to the radiant power incident on the sample (I_0). Absorbance (A) is the logarithm to the base 10 of the reciprocal of the transmittance (T). The absorption intensity of molecule vibration can be determined by the Lambert-Beer Law, \label{5} . In this equation, the transmittance spectra ranges from 0 to 100%, and it can provide clear contrast between intensities of strong and weak bands. Absorbance ranges from infinity to zero. The absorption of molecules can be determined by several components. In the absorption equation, ε is called molar extinction coefficient, which is related to the molecule behavior itself, mainly the transition dipole moment, c is the concentration of the sample, and l is the sample length. Line width can be determined by the interaction with surroundings.

$$A = log(1/T) = -log(I/I_0) = \varepsilon cl \tag{3.2.5}$$

The Infrared Spectrometer

As shown in Figure 3.2.19, there are mainly four parts for fourier transform infrared spectrometer (FTIR):

- **Light source.** Infrared energy is emitted from a glowing black-body source as continuous radiations.
- **Interferometer.** It contains the interferometer, the beam splitter, the fixed mirror and the moving mirror. The beam splittertakes the incoming infrared beam and divides it into two optical beams. One beam reflects off the fixed mirror. The other beam reflects off of the moving mirror which moves a very short distance. After the divided beams are reflected from the two mirrors, they meet each other again at the beam splitter. Therefore, an interference pattern is generated by the changes in the relative position of the moving mirror to the fixed mirror. The resulting beam then passes through the sample and is eventually focused on the detector.
- **Sample compartment.** It is the place where the beam is transmitted through the sample. In the sample compartment, specific frequencies of energy are absorbed.
- **Detector.** The beam finally passes to the detector for final measurement. The two most popular detectors for a FTIR spectrometer are deuterated triglycine sulfate (pyroelectric detector) and mercury cadmium telluride (photon or quantum detector). The measured signal is sent to the computer where the Fourier transformation takes place.

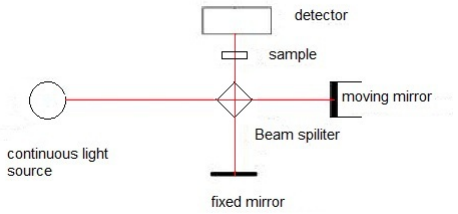


Figure 3.2.19 The main components of a fourier transform infrared (FTIR) spectrometer.

A Typical Application: the detection of metal ligand complexes

Some General Absorption peaks for common types of functional groups

It is well known that all molecules chemicals have distinct absorption regions in the IR spectrum. Table 3.2.7 shows the absorption frequencies of common types of functional groups. For systematic evaluation, the IR spectrum is commonly divided into some sub-regions.

- In the region of 4000 - 2000 cm^{-1}, the appearance of absorption bands usually comes from stretching vibrations between hydrogen and other atoms. The O-H and N-H stretching frequencies range from 3700 - 3000 cm^{-1}. If hydrogen bond forms between O-H and other group, it generally caused peak line shape broadening and shifting to lower frequencies. The C-H stretching bands occur in the region of 3300 - 2800 cm^{-1}. The acetylenic C-H exhibits strong absorption at around 3300 cm^{-1}. Alkene and aromatic C-H stretch vibrations absorb at 3200-3000 cm^{-1}. Generally, asymmetric vibrational stretch frequency of alkene C-H is around 3150 cm^{-1}, and symmetric vibrational stretch frequency is between 3100 cm^{-1} and 3000 cm^{-1}. The saturated aliphatic C-H stretching bands range from 3000 - 2850 cm^{-1}, with absorption intensities that are proportional to the number of C-H bonds. Aldehydes often show two sharp C-H stretching absorption bands at 2900 - 2700 cm^{-1}. However, in

water solution, C-H vibrational stretch is much lower than in non-polar solution. It means that the strong polarity solution can greatly reduce the transition dipole moment of C-H vibration.

- Furthermore, the stretching vibrations frequencies between hydrogen and other heteroatoms are between 2600 - 2000cm^{-1}, for example, S-H at 2600 - 2550 cm^{-1}, P-H at 2440 - 2275 cm^{-1}, Si-H at 2250 - 2100 cm^{-1}.
- The absorption bands at the 2300 - 1850 cm^{-1} region usually present only from triple bonds, such as C≡C at 2260 - 2100 cm^{-1}, C≡N at 2260 - 2000 cm^{-1}, diazonium salts –N≡N at approximately 2260 cm^{-1}, allenes C=C=C at 2000 - 1900 cm^{-1}. The peaks of these groups are all have strong absorption intensities. The 1950 - 1450 cm^{-1} region stands for double-bonded functional groups vibrational stretching.
- Most carbonyl C=O stretching bands range from 1870 - 1550 cm^{-1}, and the peak intensities are from mean to strong. Conjugation, ring size, hydrogen bonding, and steric and electronic effects can lead to significant shifts in absorption frequencies. Furthermore, if carbonyl links with electron-withdrawing group, such as acid chlorides and acid anhydrides, it would give rise to IR bands at 1850 - 1750 cm^{-1}. Ketones usually display stretching bands at 1715 cm^{-1}.
- None conjugated aliphatic C=C and C=N have absorption bands at 1690 - 1620 cm^{-1}. Besides, around 1430 and 1370cm^{-1}, there are two identical peaks presenting C-H bending.
- The region from 1300 - 910 cm^{-1} always includes the contributions from skeleton C-O and C-C vibrational stretches, giving additional molecular structural information correlated with higher frequency areas. For example, ethyl acetate not only shows its carbonyl stretch at 1750 - 1735 cm^{-1}, but also exhibits its identical absorption peaks at 1300 - 1000 cm^{-1} from the skeleton vibration of C-O and C-C stretches.

Table 3.2.7 The typical frequencies of functional groups.

Group	Frequency (cm^{-1})	Strength Appearance
C-H stretch	2850-3400	Strong in nonpolar solvent Weak in polar solvent
O-H stretch, N-H stretch	3200-3700	Broad in solvent
C≡N stretch, R-N=C=S stretch	2050-2300	Medium or strong
C≡O stretch (bound with metal)	around 2000	Medium or strong
C≡C stretch	2100-2260	Weak
C=O stretch	ca 1715 (ketone), ca 1650 (amides)	Strong
C=C stretch	1450-1700	Weak to strong
C-H bend	1260 - 1470	Strong
C-O stretch	1040-1300	Medium or strong

General Introduction of Metal Ligand Complex

The metal electrons fill into the molecular orbital of ligands (CN, CO, etc.) to form complex compound. As shown in Figure 3.2.20, a simple molecular orbital diagram for CO can be used to explain the binding mechanism.

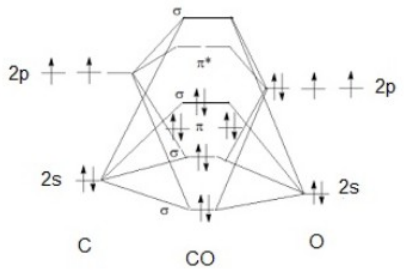
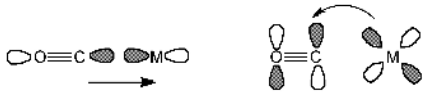


Figure 3.2.20 Molecular orbital diagram for carbon monoxide (CO).

The CO and metal can bind with three ways:

- Donation of a pair of electrons from the C-O σ* orbital into an empty metal orbital (Figure 3.2.21a).
- Donation from a metal d orbital into the C-O π* orbital to form a M-to-CO π-back bond (Figure 3.2.21b).
- Under some conditions a pair of carbon π electron can donate into an empty metal d-orbital.



(a) (b)

Figure 3.2.21 Main binding interaction types between metal and CO. (a) CO-to-metal σ bond; (b) M-to-CO π-back bond.

Some Factors to Include the Band Shifts and Strength

Herein, we mainly consider two properties: ligand stretch frequency and their absorption intensity. Take the ligand CO for example again. The frequency shift of the carbonyl peaks in the IR mainly depends on the bonding mode of the CO (terminal or bridging) and electron density on the metal. The intensity and peak numbers of the carbonyl bands depends on some factors: CO ligands numbers, geometry of the metal ligand complex and fermi resonance.

Effect on Electron Density on Metal

As shown in Table 3.2.8, a greater charge on the metal center result in the CO stretches vibration frequency decreasing. For example, [Ag(CO)]+show higher frequency of CO than free CO, which indicates a strengthening o

f the CO bond. σ donation removes electron density from the nonbonding HOMO of CO. From Figure, it is clear that the HOMO has a small amount of anti-bonding property, so removal of an electron actually increases (slightly) the CO bond strength. Therefore, the effect of charge and electronegativity depends on the amount of metal to CO π-back bonding and the CO IR stretching frequency.

Table 3.2.8 Different types of ligands frequencies of different electron density on a metal center.

d^x	Complex	CO stretch frequency (cm^{-1})
	free CO	2143
d^{10}	$[Ag(CO)]^+$	2204
d^{10}	$Ni(CO)_4$	2060
d^{10}	$[Co(CO)_4]^-$	1890
d^6	$[Mn(CO)_6]^+$	2090
d^6	$Cr(CO)_6$	2000
d^6	$[V(CO)_6]^-$	1860

If the electron density on a metal center is increasing, more π-back bonding to the CO ligand(s) will also increase, as shown in Table 3.2.9. It means more electron density would enter into the empty carbonyl π* orbital and weaken the C-O bond. Therefore, it makes the M-CO bond strength increasing and more double-bond-like (M=C=O).

Ligation Donation Effect

Some cases, as shown in Table 3.2.9, different ligands would bind with same metal at the same metal-ligand complex. For example, if different electron density groups bind with $Mo(CO)_3$ as the same form, as shown in Figure 3.2.22, the CO vibrational frequencies would depend on the ligand donation effect. Compared with the PPh_3 group, CO stretching frequency which the complex binds the PF_3 group (2090, 2055 cm^{-1}) is higher. It indicates that the absolute amount of electron density on that metal may have certain effect on the ability of the ligands on a metal to donate electron density to the metal center. Hence, it may be explained by the **Ligand donation effect**. Ligands that are *trans* to a carbonyl can have a large effect on the ability of the CO ligand to effectively π-backbond to the metal. For example, two *trans* π-backbonding ligands will partially compete for the same d-orbital electron density, weakening each other's net M-L π-backbonding. If the *trans* ligand is a π-donating ligand, the free metal to CO π-backbonding can increase the M-CO bond strength (more M=C=O character). It is well known that pyridine and amines are not those strong π-donors. However, they are even worse π-backbonding ligands. So the CO is actually easy for π-back donation

without any competition. Therefore, it naturally reduces the CO IR stretching frequencies in metal carbonyl complexes for the ligand donation effect.

Table 3.2.9 The effect of different types of ligands on the frequency of the carbonyl ligand

Metal Ligand Complex	CO Stretch Frequency (cm^{-1})
$Mo(CO)_3(PF_3)_3$	2090, 2055
$Mo(CO)_3[P(OMe)_3]_3$	1977, 1888
$Mo(CO)_3(PPh_3)_3$	1934, 1835
$Mo(CO)_3(NCCH_3)_3$	1915, 1783
$Mo(CO)_3(pyridine)_3$	1888, 1746



Figure 3.2.22 Schematic representation of competitive back-donation from a transition metal to multiple π-acceptor ligands

Geometry Effects

Some cases, metal-ligand complex can form not only terminal but also bridging geometry. As shown in Figure 3.2.23, in the compound $Fe_2(CO)_7$(dipy), CO can act as a bridging ligand. Evidence for a bridging mode of coordination can be easily obtained through IR spectroscopy. All the metal atoms bridged by a carbonyl can donate electron density into the π* orbital of the CO and weaken the CO bond, lowering vibration frequency of CO. In this example, the CO frequency in terminal is around 2080 cm^{-1}, and in bridge, it shifts to around 1850 cm^{-1}.

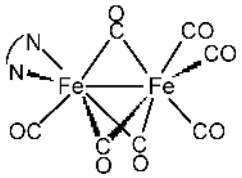


Figure 3.2.23 The structure of $Fe_2(CO)_7$(dipy)

Pump-probe Detection of Molecular Functional Group Vibrational Lifetime

The dynamics of molecular functional group plays an important role during a chemical process, chemical bond forming and breaking, energy transfer and other dynamics happens within picoseconds domain. It is very difficult to study such fast processes directly, for decades scientists can only learn from theoretical calculations, lacking experimental methods.

However, with the development of ultrashort pulsed laser enable experimental study of molecular functional group dynamics. With ultrafast laser technologies, people develop a series of measuring methods, among which, pump-probe technique is widely used to study the molecular functional group dynamics. Here we concentrate on how to use pump-probe experiment to measure functional group vibrational lifetime. The principle, experimental setup and data analysis will be introduced.

Principles of the Pump-probe Technique

For every function group within a molecule, such as the C≡N triple bond in phenyl selenocyanate (C_6H_5SeCN) or the C-D single bond in deuterated chloroform ($DCCl_3$), they have an individual infrared vibrational mode and associated energy levels. For a typical 3-level system (Figure 3.2.24, both the 0 to 1 and the 1 to 2 transition are near the probe pulse frequency (they don't necessarily need to have exactly the same frequency).

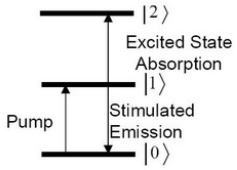


Figure 3.2.24 Schematic representation of a typical three level system

In a pump-probe experiment, we use the geometry as is shown in Figure 3.2.25. Two synchronized laser beams, one of which is called pump beam (E_{pu}) while the other probe beam (E_{pr}). There is a delay in time between each pulse. The laser pulses hit the sample, the intensity of ultrafast laser (fs or ps) is strong enough to generated 3rd order polarization and produce 3rd order optical response signal which is use to give dynamics information of molecular function groups. For the total response signals we have \label{6} , where μ_{10} μ_{21} are transition dipole moment and E_0, E_1, and E_2 are the energies of the three levels, and t_3 is the time delay between pump and probe beam. The delay t_3 is varied and the response signal intensity is measured. The functional group vibration life time is determined from the data.

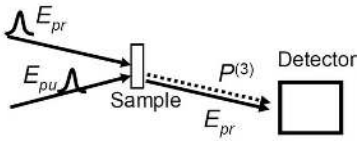


Figure 3.2.25

$$S = 4\mu_{10}^4 e^{-i(E_1-E_0)t3/h-\Gamma t3} \tag{3.2.6}$$

Typical Experimental Set-up

The optical layout of a typical pump-probe setup is schematically displayed in Figure 3.2.26. In the setup, the output of the oscillator (500 mW at 77 MHz repetition rate, 40 nm bandwidth centered at 800 nm) is split into two beams (1:4 power ratio). Of this, 20% of the power is to seed a femtosecond (fs) amplifier whose output is 40 fs pulses centered at 800 nm with power of ~3.4 W at 1 KHz repetition rate. The rest (80%) of the seed goes through a bandpass filter centered at 797.5nm with a width of 0.40 nm to seed a picosecond (ps) amplifier. The power of the stretched seed before entering the ps amplifier cavity is only ~3 mW. The output of the ps amplifier is 1ps pulses centered at 800 nm with a bandwidth ~0.6 nm. The power of the ps amplifier output is ~3 W. The fs amplifier is then to pump an optical parametric amplifier (OPA) which produces ~100 fs IR pulses with bandwidth of ~200 cm^{-1} that is tunable from 900 to 4000 cm^{-1}. The power of the fs IR pulses is 7~40 mW, depending on the frequencies. The ps amplifier is to pump a ps OPA which produces ~900 fs IR pulses with bandwidth of ~21 cm^{-1}, tunable from 900 - 4000 cm^{-1}. The power of the fs IR pulses is 10 ~ 40 mW, depending on frequencies.

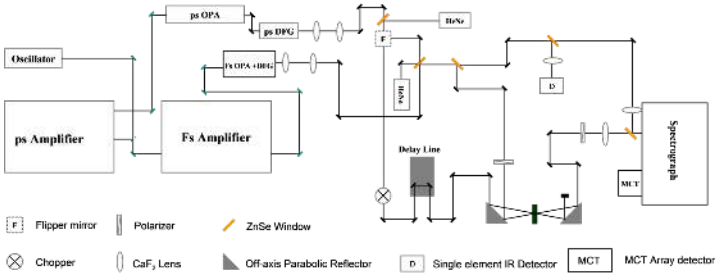


Figure 3.2.26 Schematic representation of the optical layout for a pump-probe experiment.

In a typical pump-probe setup, the ps IR beam is collimated and used as the pump beam. Approximately 1% of the fs IR OPA output is used as the probe beam whose intensity is further modified by a polarizer placed before the sample. Another polarizer is placed after the sample and before the spectrograph to select different polarizations of the signal. The signal is then sent into a spectrograph to resolve frequency, and detected with a mercury cadmium telluride (MCT) dual array detector. Use of a pump pulse (femtosecond, wide band) and a probe pulse (picoseconds, narrow band), scanning the delay time and reading the data from the spectrometer, will give the lifetime of the functional group. The wide band pump and spectrometer described here is for collecting multiple group of pump-probe combination.

Data Analysis

For a typical pump-probe curve shown in Figure 3.2.27life time *t* is defined as the corresponding time value to the half intensity as time zero.

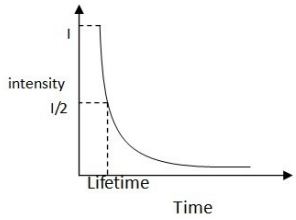


Figure 3.2.27 A Typical pump-probe curve.

Table 3.2.10 shows the pump-probe data of the C≡N triple bond in a series of aromatic cyano compounds: *n*-propyl cyanide (C_3H_7CN), ethyl thiocyanate (C_2H_5SCN), and ethyl selenocyanate (C_2H_5SeCN) for which the $\nu_{C\equiv N}$ for each compound (measured in CCl_4 solution) is 2252 cm^{-1}), 2156 cm^{-1}, and ~2155 cm^{-1}, respectively.

Table 3.2.10 Pump-probe intensity data for C≡N stretching frequency in *n*-propyl cyanide, ethyl thiocyanate, and ethyl selenocyanate as a function of delay (ps).

Delay (ps)	***C_3H_7CN***	***C_2H_5SCN***	***C_2H_5SeCN***
0	-0.00695	-0.10918	-0.06901
0.1	-0.0074	-0.10797	-0.07093
0.2	-0.00761	-0.1071	-0.07247
0.3	-0.00768	-0.10545	-0.07346
0.4	-0.0076	-0.10487	-0.07429
0.5	-0.00778	-0.10287	-0.07282
0.6	-0.00782	-0.10286	-0.07235
0.7	-0.00803	-0.10222	-0.07089
0.8	-0.00764	-0.10182	-0.07073
0.9	-0.00776	-0.10143	-0.06861
1	-0.00781	-0.10099	-0.06867
1.1	-0.00745	-0.10013	-0.06796
1.2	-0.00702	-0.10066	-0.06773
1.3	-0.00703	-0.0989	-0.0676
1.4	-0.00676	-0.0995	-0.06638
1.5	-0.00681	-0.09757	-0.06691
1.6	-0.00639	-0.09758	-0.06696
1.7	-0.00644	-0.09717	-0.06583
1.8	-0.00619	-0.09741	-0.06598
1.9	-0.00613	-0.09723	-0.06507
2	-0.0066	-0.0962	-0.06477
2.5	-0.00574	-0.09546	-0.0639
3	-0.0052	-0.09453	-0.06382

Delay (ps)	*C_3H_7CN*	*C_2H_5SCN*	*C_2H_5SeCN*
3.5	-0.0482	-0.09353	-0.06389
4	-0.0042	-0.09294	-0.06287
4.5	-0.00387	-0.09224	-0.06197
5	-0.00351	-0.09009	-0.06189
5.5	-0.00362	-0.09084	-0.06188
6	-0.00352	-0.08938	-0.06021
6.5	-0.00269	-0.08843	-0.06028
7	-0.00225	-0.08788	-0.05961
7.5	-0.00231	-0.08694	-0.06065
8	-0.00206	-0.08598	-0.05963
8.5	-0.00233	-0.08552	-0.05993
9	-0.00177	-0.08503	-0.05902
9.5	-0.00186	-0.08508	-0.05878
10	-0.00167	-0.0842	-0.0591
11	-0.00143	-0.08295	-0.05734

A plot of intensity versus time for the data from TABLE is shown Figure 3.2.28. From these curves the C≡N stretch lifetimes can be determined for C_3H_7CN, C_2H_5SCN, and C_2H_5SeCN as ~5.5 ps, ~84 ps, and ~282 ps, respectively.

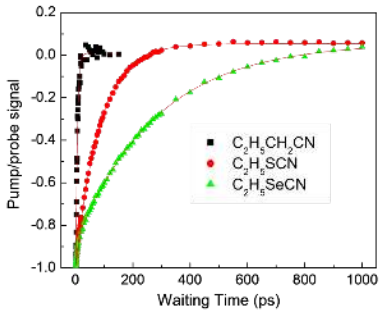


Figure 3.2.28 The C≡N stretch lifetimes for benzyl cyanide, phenyl thiocyanate, and phenyl selenocyanate.

From what is shown above, the pump-probe method is used in detecting C≡N vibrational lifetimes in different chemicals. One measurement only takes several second to get all the data and the lifetime, showing that pump-probe method is a powerful way to measure functional group vibrational lifetime.

Attenuated Total Reflectace- Fourier Transform Infrared Spectroscopy

Attenuated total reflectance-Fourier transform infrared spectroscopy (ATR-FTIR) is a physical method of compositional analysis that builds upon traditional transmission FTIR spectroscopy to minimize sample preparation and optimize reproducibility. Condensed phase samples of relatively low refractive index are placed in close contact with a crystal of high refractive index and the infrared (IR) absorption spectrum of the sample can be collected. Based on total internal reflection, the absorption spectra of ATR resemble those of transmission FTIR. To learn more about transmission IR spectroscopy (FTIR) please refer to the section further up this page titled Fourier Transform Infrared Spectroscopy of Metal Ligand Complexes.

First publicly proposed in 1959 by Jacques Fahrenfort from the Royal Dutch Shell laboratories in Amsterdam, ATR IR spectroscopy was described as a technique to effectively measure weakly absorbing condensed phase materials. In Fahrenfort's first

article describing the technique, published in 1961, he used a hemicylindrical ATR crystal (see Experimental Conditions) to produce single-reflection ATR (Figure 3.2.29). ATR IR spectroscopy was slow to become accepted as a method of characterization due to concerns about its quantitative effectiveness and reproducibility. The main concern being the sample and ATR crystal contact necessary to achieve decent spectral contrast. In the late 1980's FTIR spectrometers began improving due to an increased dynamic range, signal to noise ratio, and faster computers. As a result ATR-FTIR also started gaining traction as an efficient spectroscopic technique. These days ATR accessories are often manufactured to work in conjunction with most FTIR spectrometers, as can be seen in Figure 3.2.30

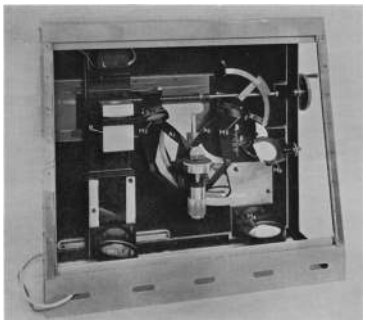


Figure 3.2.29 The first ATR Infrared Spectrometer designed by Jacques Fahrenfort featuring a hemicylindrical ATR crystal. Reproduced from J. Fahrenfort, *Spectrochim. Acta*, 1961, **17**, 698. Copyright: Elsevier (1961).



Figure 3.2.30 An ATR attachment on an FTIR spectrometer.

Total Internal Reflection

For additional information on light waves and their properties please refer to the module on Vertical Scanning Interferometry (VSI) in chapter 10.1.

When considering light propagating across an interface between two materials with different indices of refraction, the angle of refraction can be given by Snell's law, 3.2.7, where none of the incident light will be transmitted.

$$\varphi_c = \varphi_{max} \tag{3.2.7}$$

The reflectance of the interface is total and whenever light is incident from a higher refractive index medium onto a lower refractive index medium, the reflection is deemed internal (as opposed to external in the opposite scenario). Total internal reflectance experiences no losses, or no transmitted light (Figure 3.2.31

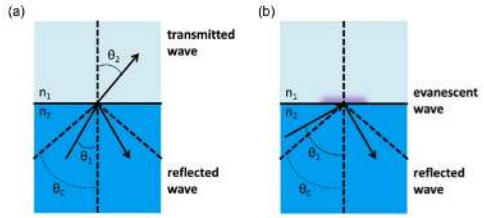


Figure 3.2.31 At the interface between two materials with different indices of refraction, (a) when the angle of incident light, θ_1, is below the critical angle, θ_c, both reflection and transmission occur, and (b) when the angle of incident light exceeds the critical angle, total internal reflection (TIR) occurs, spawning an evanescent wave at the interface. Adapted from M. Schnippering, S. R. T. Neil, S. R. Mackenzie, and P. R. Unwin, *Chem. Soc. Rev.*, 2011, **40**, 207. Copyright: Royal Society of Chemistry (2011).

Supercritical internal reflection refers to angles of incidence above the critical angle of incidence allowing total internal reflectance. It is in this angular regime where only incident and reflected waves will be present. The transmitted wave is confined to the interface where its amplitude is at a maximum and will damp exponentially into the lower refractive index medium as a function of distance. This wave is referred to as the evanescent wave and it extends only a very short distance beyond the interface.

To apply total internal reflection to the experimental setup in ATR, consider n_2 to be the internal reflectance element or ATR crystal (the blue trapezoid in Figure 3.2.32)

where n_2 is the material with the higher index of refraction. This should be a material that is fully transparent to the incident infrared radiation to give a real value for the refractive index. The ATR crystal must also have a high index of refraction to allow total internal reflection with many samples that have an index of refraction n_1, where $n_1<n_2$.

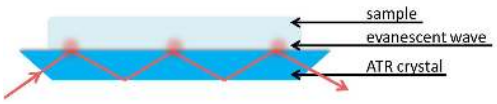


Figure 3.2.32 The ATR crystal shown in blue, within which the incident IR light shown in red is totally reflecting. Above the crystal the evanescent wave is emitted and penetrates the sample.

We can consider the sample to be absorbing in the infrared. Electromagnetic energy will pass through the crystal/sample interface and propagate into the sample via the evanescent wave. This energy loss must be compensated with the incident IR light. Thus, total reflectance is no longer occurring and the reflection inside the crystal is attenuated. If a sample does not absorb, the reflectance at the interface shows no attenuation. Therefore if the IR light at a particular frequency does not reach the detector, the sample must have absorbed it.

The penetration depth of the evanescent wave within the sample is on the order of 1µm. The expression of the penetration depth is given in 3.2.8 and is dependent upon the wavelength and angle of incident light as well as the refractive indices of the ATR crystal and sample. The effective path length is the product of the depth of penetration of the evanescent wave and the number of points that the IR light reflects at the interface between the crystal and sample. This path length is equivalent to the path length of a sample in a traditional transmission FTIR setup.

$$d_p = \frac{\lambda}{2\pi n_1}(sin\omega - (\frac{n_1}{n_2})^2)^{1/2} \tag{3.2.8}$$

Experimental Conditions

Refractive Indices of ATR Crystal and Sample

Typically an ATR attachment can be used with a traditional FTIR where the beam of incident IR light enters a horizontally positioned crystal with a high refractive index in the range of 1.5 to 4, as can be seen in Table 3.2.11 will consist of organic compounds, inorganic compounds, and polymers which have refractive indices below 2 and can readily be found on a database.

Table 3.2.11 A summary of popular ATR crystals. Data obtained from F. M. Mirabella, *Internal reflection spectroscopy: Theory and applications*, 15, Marcel Dekker, Inc., New York (1993).

Material	Refractive Index (RI)	Spectral Range (cm^{-1})
Zinc Selenide (ZnSe)	2.4	20,000 - 650
Germanium (Ge)	4	5,500 - 870
Sapphire (Al_2O_3)	1.74	50,000 - 2,000
Diamond (C)	2.4	45,000 - 2,500, 1650 - 200

Single and Multiple Reflection Crystals

Multiple reflection ATR was initially more popular than single reflection ATR because of the weak absorbances associated with single reflection ATR. More reflections increased the evanescent wave interaction with the sample, which was believed to increase the signal to noise ratio of the spectrum. When IR spectrometers developed better spectral contrast, single reflection ATR became more popular. The number of reflections and spectral contrast increases with the length of the crystal and decreases with the angle of incidence as well as thickness. Within multiple reflection crystals some of the light is transmitted and some is reflected as the

light exits the crystal, resulting in some of the light going back through the crystal for a round trip. Therefore, light exiting the ATR crystal contains components that experienced different number of reflections at the crystal-sample interface.

Angle of Incidence

It was more common in earlier instruments to allow selection of the incident angle, sometimes offering selection between 30°, 45°, and 60°. In all cases for total internal reflection to hold, the angle of incidence must exceed the critical angle and ideally complement the angle of the crystal edge so that the light enters at a normal angle of incidence. These days 45° is the standard angle on most ATR-FTIR setups.

ATR Crystal Shape

For the most part ATR crystals will have a trapezoidal shape as shown in Figure 3.2.31. This shape facilitates sample preparation and handling on the crystal surface by enabling the optical setup to be placed below the crystal. However, different crystal shapes (Figure 3.2.33) may be used for particular purposes, whether it is to achieve multiple reflections or reduce the spot size. For example, a hemispherical crystal may be used in a microsampling experiment in which the beam diameter can be reduced at no expense to the light intensity. This allows appropriate measurement of a small sample without compromising the quality of the resulting spectral features.

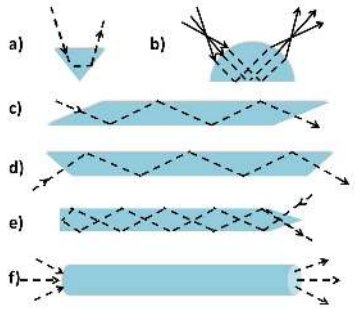


Figure 3.2.33 An assortment of ATR crystal shapes: a)triangular, b)hemispherical, c)parallelogram, d) trapezoidal, e) pentagonal, f)cylindrical. Adapted from F. M. Mirabella, *Internal reflection spectroscopy: Theory and applications*, 15, Marcel Dekker, Inc., New York (1993).

Crystal-sample contact

Because the path length of the evanescent wave is confined to the interface between the ATR crystal and sample, the sample should make firm contact with the ATR crystal (Figure 3.2.34). The sample sits atop the crystal and intimate contact can be ensured by applying pressure above the sample. However, one must be mindful of the ATR crystal hardness. Too much pressure may distort the crystal and affect the reproducibility of the resulting spectrum.



Figure 3.2.34 A close-up image of an ATR accessory attached to a Nexus 670 FTIR.

The wavelength effect expressed in \label{7} shows an increase in penetration depth at increased wavelength. In terms of wavenumbers the relationship becomes inverse. At 4000 cm^{-1} penetration of the sample is 10x less than penetration at 400 cm^{-1} meaning the intensity of the peaks may appear higher at lower wavenumbers in the absorbance spectrum compared to the spectral features in a transmission FTIR spectrum (if an automated correction to the ATR setup is not already in place).

Selecting an ATR Crystal

ATR functions effectively on the condition that the refractive index of the crystal is of a higher refractive index than the sample. Several crystals are available for use and it is important to select an appropriate option for any given experiment (Table 3.2.11).

When selecting a material, it is important to consider reactivity, temperature, toxicity, solubility, and hardness.

The first ATR crystals in use were KRS-5, a mixture of thallium bromide and iodide, and silver halides. These materials are not listed in the table because they are not in use any longer. While cost-effective, they are not practical due to their light sensitivity, softness, and relatively low refractive indices. In addition KRS-5 is terribly toxic and dissolves on contact with many solvents, including water.

At present diamond is a favorable option for its hardness, inertness and wide spectral range, but may not be a financially viable option for some experiments. ZnSe and germanium are the most common crystal materials. ZnSe is reasonably priced, has significant mechanical strength and a long endurance. However, the surface will become etched with exposure to chemicals on either extreme of the pH scale. With a strong acid ZnSe will react to form toxic hydrogen selenide gas. ZnSe is also prone to oxidation and care must be taken to avoid the formation of an IR absorbing layer of SeO_2. Germanium has a higher refractive index, which reduces the depth of penetration to 1 µm and may be preferable to ZnSe in applications involving intense sample absorptions or for use with samples that produce strong background absorptions. Sapphire is physically robust with a wide spectral range, but has a relatively low refractive index in terms of ATR crystals, meaning it may not be able to test as many samples as another crystal might.

Sample Versatility

Solids

The versatility of ATR is reflected in the various forms and phases that a sample can assume. Solid samples need not be compressed into a pellet, dispersed into a mull or dissolve in a solution. A ground solid sample is simply pressed to the surface of the ATR crystal. For hard samples that may present a challenge to grind into a fine solid, the total area in contact with the crystal may be compromised unless small ATR crystals with exceptional durability are used (e.g., 2 mm diamond). Loss of contact with the crystal would result in decreased signal intensity because the evanescent wave may not penetrate the sample effectively. The inherently short path length of ATR due to the short penetration depth (0.5-5 µm) enables surface-modified solid samples to be readily characterized with ATR.

Powdered samples are often tedious to prepare for analysis with transmission spectroscopy because they typically require being made into a KBr pellet to and ensuring the powdered sample is ground up sufficiently to reduce scattering. However, powdered samples require no sample preparation when taking the ATR spectra. This is advantageous in terms of time and effort, but also means the sample can easily be recovered after analysis.

Liquids

The advantage of using ATR to analyze liquid samples becomes apparent when short effective path lengths are required. The spectral reproducibility of liquid samples is certain as long as the entire length of the crystal is in contact with the liquid sample, ensuring the evanescent wave is interacting with the sample at the points of reflection, and the thickness of the liquid sample exceeds the penetration depth. A small path length may be necessary for aqueous solutions in order to reduce the absorbance of water.

Sample Preparation

ATR-FTIR has been used in fields spanning forensic analysis to pharmaceutical applications and even art preservation. Due to its ease of use and accessibility ATR can be used to determine the purity of a compound. With only a minimal amount of sample this researcher is able to collect a quick analysis of her sample and determine whether it has been adequately purified or requires further processing. As can be seen in Figure 3.2.35, the sample size is minute and requires no preparation. The sample is placed in close contact with the ATR crystal by turning a knob that will apply pressure to the sample (Figure 3.2.36).

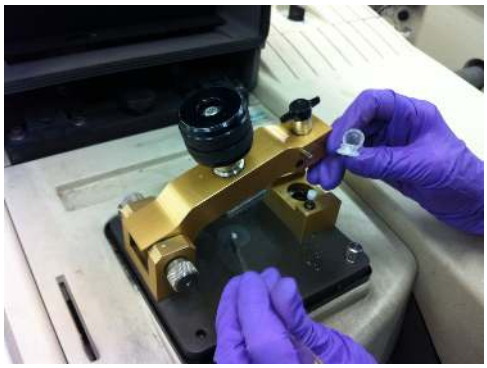


Figure 3.2.35 Photograph of a small sample size is being placed on the ATR crystal.

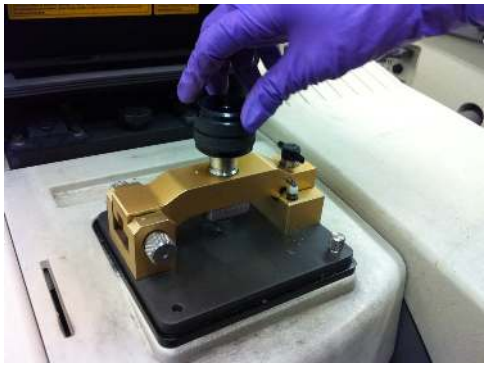


Figure 3.2.36 Turning the knob applies pressure to the sample, ensuring good contact with the ATR crystal.

ATR has an added advantage in that it inherently encloses the optical path of the IR beam. In a transmission FTIR, atmospheric compounds are constantly exposed to the IR beam and can present significant interference with the sample measurement. Of course the transmission FTIR can be purged in a dry environment, but sample measurement may become cumbersome. In an ATR measurement, however, light from the spectrometer is constantly in contact with the sample and exposure to the environment is reduced to a minimum.

Application to Inorganic Chemistry

One exciting application of ATR is in the study of classical works of art. In the study of fragments of a piece of artwork, where samples are scarce and one-of-a-kind, ATR is a suitable method of characterization because it requires only a small sample size. Determining the compounds present in art enables proper preservation and historical insight into the pieces.

In a study examining several paint samples from a various origins, a micro-ATR was employed for analysis. This study used a silicon crystal with a refractive index of 2.4 and a reduced beam size. Going beyond a simple surface analysis, this study explored the localization of various organic and inorganic compounds in the samples by performing a stratigraphic analysis. The researchers did so by embedding the samples in both KBr and a polyester resins. Two embedding techniques were compared to observe cross-sections of the samples. The mapping of the samples took approximately 1-3 hours which may seem quite laborious to some, but considering the precious nature of the sample, the wait time was acceptable to the researchers.

The optical microscope picture (Figure 3.2.37) shows a sample of a blue painted area from the robe of a 14th century Italian polychrome statue of a Madonna. The spectra shown in Figure 3.2.38 were acquired from the different layers pictured in the box marked in Figure 3.2.37. All spectra were collected from the cross-sectioned sample and the false-color map on each spectrum indicates the location of each of these compounds within the embedded sample. The spectra correspond to the inorganic compounds listed in Table 3.2.12, which also highlights characteristic vibrational bands.

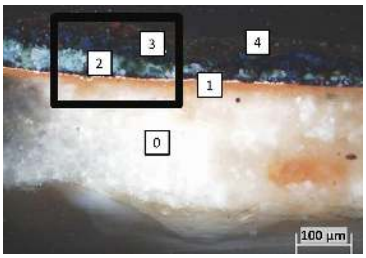


Figure 3.2.37 A paint sample from which four inorganic compounds were identified by ATR spectroscopy. The numbers indicate different layers in the sample, composed of different inorganic compounds. The boxed area shows the region within which ATR mapping occurred. Reproduced from R. Mazzeo, E. Joseph, S. Prati, and A. Millemaggi. Anal. Chim. Acta, 2007, 599, 107. Copyright: Elsevier (2007).

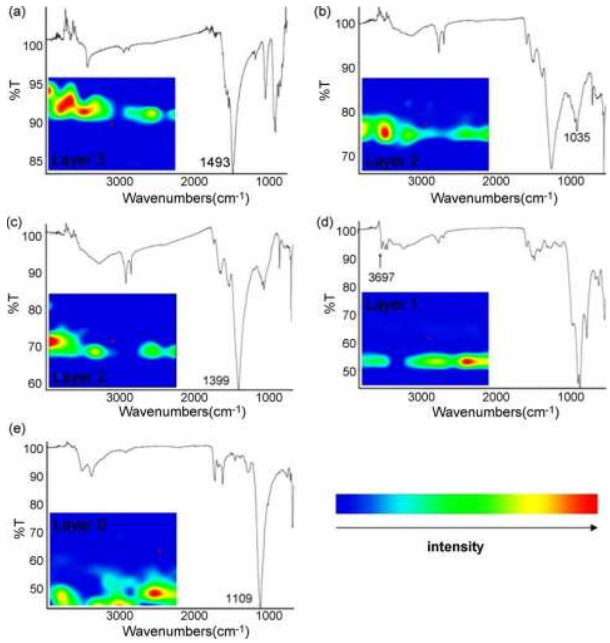


Figure 3.2.37. The images are labeled with the layer that corresponds to its location in the paint sample. Reproduced from R. Mazzeo, E. Joseph, S. Prati, and A. Millemaggi. *Anal. Chim. Acta*, 2007, **599**, 107. Copyright: Elsevier (2007)

Table 3.2.12 this table shows the inorganic compounds identified in the paint sample shown in 3.2.37. Data from R. Mazzeo, E. Joseph, S. Prati, and A. Millemaggi. *Anal. Chim. Acta*, 2007, **599**, 107.

Compound	Selected Spectral Bands	Assignment
$Cu_3(CO_3)_2(OH)_2$ (Azurite)	1493	CO_3^{2-} asymmetric stretch
Silicate based blue-pigments	1035	Si-O stretching
$2PbCO_3 \cdot Pb(OH)_2$ (White lead)	1399	CO_3^{2-} asymmetric stretch
A natural ferruginous aluminum silicate red pigment (Bole)	3697	OH stretching
$CaSO_4 \cdot$ (Gypsum)	1109	SO_4^{2-} asymmetric stretch

The deep blue layer 3 corresponds to azurite and the light blue paint layer 2 to a mixture of silicate based blue pigments and white lead. Although beyond the ATR crystal's spatial resolution limit of 20 µm, the absorption of bole was detected by the characteristic triple absorption bands of 3697, 3651, and 3619 cm^{-1} as seen in spectrum d of Figure 3.2.37. The white layer 0 was identified as gypsum.

To identify the binding material, the KBr embedded sample proved to be more effective than the polyester resin. This was due in part to the overwhelming IR absorbance of gypsum in the same spectral range (1700-1600 cm^{-1}) as a characteristic stretch of the binding as well as some contaminant absorption due to the polyester embedding resin.

To spatially locate specific pigments and binding media, ATR mapping was performed on the area highlighted with a box in Figure 3.2.37. The false color images alongside each spectrum in Figure 3.2.38 indicate the relative presence of the compound corresponding to each spectrum in the boxed area. ATR mapping was achieved by taking 108 spectra across the 220x160 µm area and selecting for each identified compound by its characteristic vibrational band.

This page titled 3.2: IR Spectroscopy is shared under a CC BY license and was authored, remixed, and/or curated by Pavan M. V. Raja & Andrew R. Barron (OpenStax CNX) .

- **4.2: IR Spectroscopy** by Pavan M. V. Raja & Andrew R. Barron is licensed CC BY 4.0. Original source: http://cnx.org/contents/ba27839d-5042-4a40-afcf-c0e6e39fb45425.2.

Welcome to the Chemistry Library. This Living Library is a principal hub of the LibreTexts project, which is a multi-institutional collaborative venture to develop the next generation of open-access texts to improve postsecondary education at all levels of higher learning. The LibreTexts approach is highly collaborative where an Open Access textbook environment is under constant revision by students, faculty, and outside experts to supplant conventional paper-based books.

How an FTIR Spectrometer Operates

Theory

How an FTIR Spectrometer Operates

FTIR spectrometers (Fourier Transform Infrared Spectrometer) are widely used in organic synthesis, polymer science, petrochemical engineering, pharmaceutical industry and food analysis. In addition, since FTIR spectrometers can be hyphenated to chromatography, the mechanism of chemical reactions and the detection of unstable substances can be investigated with such instruments.

Introduction

The range of Infrared region is 12800 ~ 10 cm^{-1} and can be divided into near-infrared region (12800 ~ 4000 cm^{-1}), mid-infrared region (4000 ~ 200 cm^{-1}) and far-infrared region (50 ~ 1000 cm^{-1}). The discovery of infrared light can be dated back to the 19th century. Since then, scientists have established various ways to utilize infrared light. Infrared absorption spectroscopy is the method which scientists use to determine the structures of molecules with the molecules' characteristic absorption of infrared radiation. Infrared spectrum is molecular vibrational spectrum. When exposed to infrared radiation, sample molecules selectively absorb radiation of specific wavelengths which causes the change of dipole moment of sample molecules. Consequently, the vibrational energy levels of sample molecules transfer from ground state to excited state. The frequency of the absorption peak is determined by the vibrational energy gap. The number of absorption peaks is related to the number of vibrational freedom of the molecule. The intensity of absorption peaks is related to the change of dipole moment and the possibility of the transition of energy levels. Therefore, by analyzing the infrared spectrum, one can readily obtain abundant structure information of a molecule. Most molecules are infrared active except for several homonuclear diatomic molecules such as O_2, N_2 and Cl_2 due to the zero dipole change in the vibration and rotation of these molecules. What makes infrared absorption spectroscopy even more useful is the fact that it is capable to analyze all gas, liquid and solid samples. The common used region for infrared absorption spectroscopy is 4000 ~ 400 cm^{-1} because the absorption radiation of most organic compounds and inorganic ions is within this region.

FTIR spectrometers are the third generation infrared spectrometer. FTIR spectrometers have several prominent advantages: (1) The signal-to-noise ratio of spectrum is significantly higher than the previous generation infrared spectrometers. (2) The accuracy of wavenumber is high. The error is within the range of ± 0.01 cm^{-1}. (3) The scan time of all frequencies is short (approximately 1 s). (4) The resolution is extremely high (0.1 ~ 0.005 cm^{-1}). (5) The scan range is wide (1000 ~ 10 cm^{-1}). (6) The interference from stray light is reduced. Due to these advantages, FTIR Spectrometers have replaced dispersive IR spectrometers.

Development of IR Spectrometers

Up till FTIR spectrometers, there have been three generations of IR spectrometers.

1. The first generation IR spectrometer was invented in late 1950s. It utilizes prism optical splitting system. The prisms are made of NaCl. The requirement of the sample's water content and particle size is extremely strict. Further more, the scan range is narrow. Additionally, the repeatability is fairly poor. As a result, the first generation IR spectrometer is no longer in use.
2. The second generation IR spectrometer was introduced to the world in 1960s. It utilizes gratings as the monochrometer. The performance of the second generation IR spectrometer is much better compared with IR spectrometers with prism monochrometer, But there are still several prominent weaknesses such as low sensitivity, low scan speed and poor wavelength accuracy which rendered it out of date after the invention of the third generation IR spectrometer.
3. The invention of the third generation IR spectrometer, Fourier transform infrared spectrometer, marked the abdication of monochrometer and the prosperity of interferometer. With this replacement, IR spectrometers became exceptionally powerful. Consequently, various applications of IR spectrometer have been realized.

Dispersive IR Spectrometers

To understand the powerfulness and usefulness of FTIR spectrometer, it is essential to have some background information of dispersive IR Spectrometer. The basic components of a dispersive IR spectrometer include a radiation source, monochromator, and detector. The common IR radiation sources are inert solids that are heated electrically to promote thermal emission of radiation in the infrared region of the electromagnetic spectrum. The monochromator is a device used to disperse or separate a broad spectrum of IR radiation into individual narrow IR frequencies.

Generally, dispersive spectrometers have a double-beam design with two equivalent beams from the same source passing through the sample and reference chambers as independent beams. These reference and sample beams are alternately focused on the detector by making use of an optical chopper, such as, a sector mirror. One beam will proceed, traveling through the sample, while the other beam will pass through a reference species for analytical comparison of transmitted photon wavefront information.

After the incident radiation travels through the sample species, the emitted wavefront of radiation is dispersed by a monochromator (gratings and slits) into its component frequencies. A combination of prisms or gratings with variable-slit mechanisms, mirrors, and filters comprise the dispersive system. Narrower slits gives better resolution by distinguishing more closely spaced frequencies of radiation and wider slits allow more light to reach the detector and provide better system sensitivity. The emitted wavefront beam (analog spectral output) hits the detector and generates an electrical signal as a response.

Detectors are devices that convert the analog spectral output into an electrical signal. These electrical signals are further processed by the computer using mathematical algorithm to arrive at the final spectrum. The detectors used in IR spectrometers can be classified as either photon/quantum detectors or thermal detectors.

It is the absorption of IR radiation by the sample, producing a change of IR radiation intensity, which gets detected as an off-null signal (e.g. different from reference signal). This change is translated into the recorder response through the actions of synchronous motors. Each frequency that passes through the sample is measured individually by the detector which consequently slows the process of scanning the entire IR region. A block diagram of a classic dispersive IR spectrometer is shown in Figure 1.

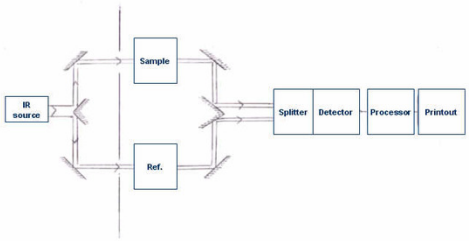


Figure 1. Simplified representation of a dispersive IR spectrometer.

FTIR Spectrometers

The Components of FTIR Spectrometers

A common FTIR spectrometer consists of a source, interferometer, sample compartment, detector, amplifier, A/D convertor, and a computer. The source generates radiation which passes the sample through the interferometer and reaches the detector. Then the signal is amplified and converted to digital signal by the amplifier and analog-to-digital converter, respectively. Eventually, the signal is transferred to a computer in which Fourier transform is carried out. Figure 2 is a block diagram of an FTIR spectrometer.

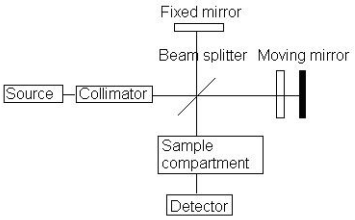


Figure 2. Block diagram of an FTIR spectrometer

The major difference between an FTIR spectrometer and a dispersive IR spectrometer is the Michelson interferometer.

Michelson Interferometer

The Michelson interferometer, which is the core of FTIR spectrometers, is used to split one beam of light into two so that the paths of the two beams are different. Then the Michelson interferometer recombines the two beams and conducts them into the detector where the difference of the intensity of these two beams are measured as a function of the difference of the paths. Figure 3 is a schematic of the Michelson Interferometer.

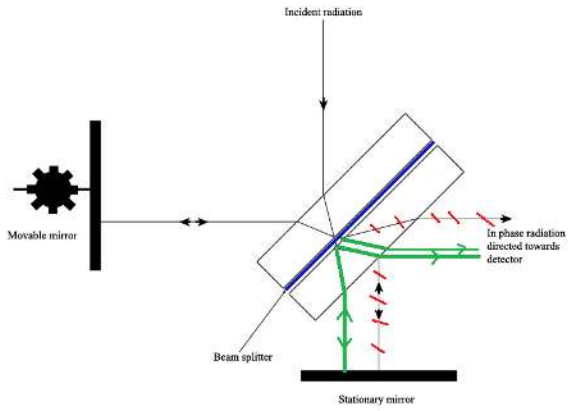


Figure 3. Schematic of the Michelson interferometer

A typical Michelson interferometer consists of two perpendicular mirrors and a beamsplitter. One of the mirror is a stationary mirror and another one is a movable mirror. The beamsplitter is designed to transmit half of the light and reflect half of the light. Subsequently, the transmitted light and the reflected light strike the stationary mirror and the movable mirror, respectively. When reflected back by the mirrors, two beams of light recombine with each other at the beamsplitter.

If the distances travelled by two beams are the same which means the distances between two mirrors and the beamsplitter are the same, the situation is defined as zero path difference (ZPD). But imagine if the movable mirror moves away from the beamsplitter, the light beam which strikes the movable mirror will travel a longer distance than the light beam which strikes the stationary mirror. The distance which the movable mirror is away from the ZPD is defined as the mirror displacement and is represented by Δ. It is obvious that the extra distance travelled by the light which strikes the movable mirror is 2Δ. The extra distance is defined as the optical path difference (OPD) and is represented by delta. Therefore,

$$\delta = 2\Delta \tag{1}$$

It is well established that when OPD is the multiples of the wavelength, constructive interference occurs because crests overlap with crests, troughs with troughs. As a result, a maximum intensity signal is observed by the detector. This situation can be described by the following equation:

$$\delta = n\lambda \tag{2}$$

with n = 0,1,2,3...

In contrast, when OPD is the half wavelength or half wavelength add multiples of wavelength, destructive interference occurs because crests overlap with troughs. Consequently, a minimum intensity signal is observed by the detector. This situation can be described by the following equation:

$$\delta = (n + \frac{1}{2})\lambda \tag{3}$$

with n = 0,1,2,3...

These two situations are two extreme situations. If the OPD is neither n-fold wavelengths nor (n+1/2)-fold wavelengths, the interference should be between constructive and destructive. So the intensity of the signal should be between maximum and minimum. Since the mirror moves back and forth, the intensity of the signal increases and decreases which gives rise to a cosine wave. The plot is defined as an interferogram. When detecting the radiation of a broad band source rather than a single-wavelength source, a peak at ZPD is found in the interferogram. At the other distance scanned, the signal decays quickly since the mirror moves back and forth. Figure 4(a) shows an interferogram of a broad band source.

Fourier Transform of Interferogram to Spectrum

The interferogram is a function of time and the values outputted by this function of time are said to make up the time domain. The time domain is Fourier transformed to get a frequency domain, which is deconvolved to product a spectrum. Figure 4 shows the Fast Fourier transform from an interferogram of polychromatic light to its spectrum.

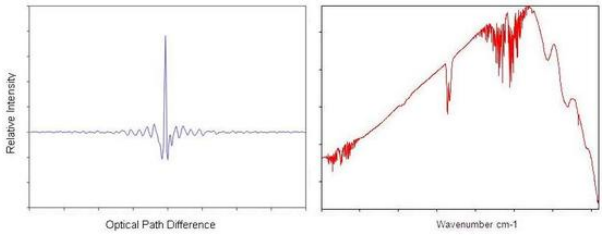


Figure 4. (a) Interferogram of a monochromatic light; (b) its spectrum

The Fourier Transform

The first one who found that a spectrum and its interferogram are related via a Fourier transform was Lord Rayleigh. He made the discover in 1892. But the first one who successfully converted an interferogram to its spectrum was Fellgett who made the accomplishment after more than half a century. Fast Fourier transform method on which the modern FTIR spectrometer based was introduced to the world by Cooley and Turkey in 1965. It has been applied widely to analytical methods such as infrared spectrometry, nuclear magnetic resonance and mass spectrometry due to several prominent advantages which are listed in **Table 1**.

feature	improvement factor	applicable to
speed	10,000	IR, NMR, MS
signal-to-noise	100	IR, NMR, MS
automation		IR, NMR, MS
double resonance	no. coupled spins or ions	NMR, MS
resolution	10,000	MS
upper mass limit	30	MS

Table 1. Advantages of Fourier Transform over Continuous-Wave Spectrometry

Fourier transform, named after the French mathematician and physicist Jean Baptiste Joseph Fourier, is a mathematical method to transform a function into a new function. The following equation is a common form of the Fourier transform with unitary normalization constants:

$$F(\omega) = \frac{1}{\sqrt{2\pi}} \int_{-\infty}^{\infty} f(t) e^{-i\omega t} dt \tag{4}$$

in which t is time, i is the square root of -1.

The following equation is another form of the Fourier transform(cosine transform) which applies to real, even functions:

$$F(\nu) = \frac{1}{\sqrt{2\pi}} \int_{-\infty}^{\infty} f(t) \cos(2\pi\nu t) dt \tag{5}$$

The following equation shows how f(t) is related to F(v) via a Fourier transform:

$$f(t) = \frac{1}{\sqrt{2\pi}} \int_{-\infty}^{\infty} F(\nu) \cos(2\pi\nu t) d\nu \tag{6}$$

An Alternative Explanation of the Fourier Transform in FTIR Spectrometers

The math description of the Fourier transform can be tedious and confusing. An alternative explanation of the Fourier transform in FTIR spectrometers is provided here before we jump into the math description to give you a rough impression which may help you understand the math description.

The interferogram obtained is a plot of the intensity of signal versus OPD. A Fourier transform can be viewed as the inversion of the independent variable of a function. Thus, Fourier transform of the interferogram can be viewed as the inversion of OPD. The unit of OPD is centimeter, so the inversion of OPD has a unit of inverse centimeters, cm^{-1}. Inverse centimeters are also known as wavenumbers. After the Fourier transform, a plot of intensity of signal versus wavenumber is produced. Such a plot is an IR spectrum. Although this explanation is easy to understand, it is not perfectly rigorous.

Simplified Math Description of the Fourier Transform in FTIR

The wave functions of the reflected and transmitted beams may be represented by the general form of:

$$E_1 = rtcE_m \times \cos(\nu t - 2\pi kx) \tag{7}$$

and

$$E_1 = rtcE_m \times \cos[\nu t - 2\pi k(\nu x + \Delta d)] \tag{8}$$

where

- Δd is the path difference,
- r is the reflectance (amplitude) of the beam splitter,
- t is the transmittance, and
- c is the polarization constant.

The resultant wave function of their superposition at the detector is represented as:

$$E = E_1 + E_2 = 2(r \times t \times c \times E_m) \times \cos(\nu t - 2\pi kx)\cos(\pi k\Delta d) \tag{9}$$

where E_m, ν, and k are the amplitude, frequency and wave number of the IR radiation source.

The intensity (I) detected is the time average of E_2 and is written as

$$I = 4r^2t^2c^2E_m^2 cos^2(\nu t - 2\pi kx)\cos^2(\pi k\Delta d) \tag{10}$$

Since the time average of the first cosine term is just ½, then

$$I = 2I(k)\cos^2(\pi k\Delta d) \tag{11}$$

and

$$I(\Delta d) = I(k)[1 + \cos(2\pi k\Delta d)] \tag{12}$$

where $I(k)$ is a constant that depends only upon k and $I(\Delta d)$ is the **interferogram**.

From $I(\Delta d)$ we can get $I(k)$ using Fourier transform as follows:

$$I(\Delta d) - I(\infty) = \int_0^{k_m} I(k)\cos(2\Pi k\Delta d)dk \tag{13}$$

Letting $K_m \rightarrow \infty$, we can write

$$I(k) = \int_0^{\infty} [I(\Delta d) - I(\infty)]\cos(2\Pi k\Delta d)d\Delta d \tag{14}$$

The physically measured information recorded at the detector produces an interferogram, which provides information about a response change over time within the mirror scan distance. Therefore, the interferogram obtained at the detector is a time domain spectrum. This procedure involves sampling each position, which can take a long time if the signal is small and the number of frequencies being sampled is large.

In terms of ordinary frequency, ν, the Fourier transform of this is given by (angular frequency $\omega = s\pi\nu$):

$$f(\nu) = \int_{-\infty}^{\infty} f(t)e^{-i2\Pi\nu t}dt \tag{15}$$

The inverse Fourier transform is given by:

$$f(\nu) = \int_{-\infty}^{\infty} f(t)e^{+i2\pi\nu t}dt \tag{16}$$

The interferogram is transformed into IR absorption spectrum (Figure 5) that is commonly recognizable with absorption intensity or % transmittance plotted against the wavelength or wavenumber. The ratio of radiant power transmitted by the sample (I) relative to the radiant power of incident light on the sample (I_0) results in quantity of Transmittance, (T). Absorbance (A) is the logarithm to the base 10 of the reciprocal of the transmittance (T):

$$A = log_{10}\frac{1}{T} = -log_{10}T = -log_{10}\frac{I}{I_0} \tag{17}$$

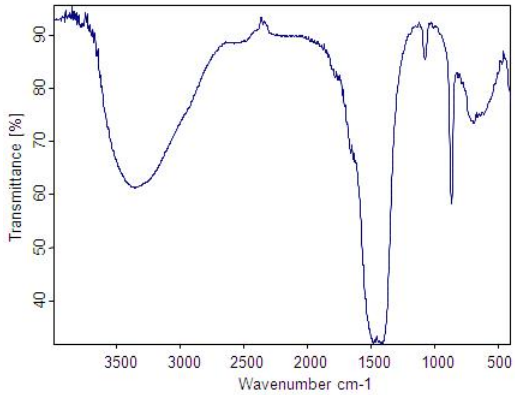


Figure 5. IR spectrum of a sample

Hands-on Operation of an FTIR Spectrometer

Step 1: The first step is sample preparation. The standard method to prepare solid sample for FTIR spectrometer is to use KBr. About 2 mg of sample and 200 mg KBr are dried and ground. The particle size should be unified and less than two micrometers. Then, the mixture is squeezed to form transparent pellets which can be measured directly. For liquids with high boiling point or viscous solution, it can be added in between two NaCl pellets. Then the sample is fixed in the cell by skews and measured. For volatile liquid sample, it is dissolved in CS_2 or CCl_4 to form 10% solution. Then the solution is injected into a liquid cell for measurement. Gas sample needs to be measured in a gas cell with two KBr windows on each side. The gas cell should first be vacuumed. Then the sample can be introduced to the gas cell for measurement.

Step 2: The second step is getting a background spectrum by collecting an interferogram and its subsequent conversion to frequency data by inverse Fourier transform. We obtain the background spectrum because the solvent in which we place our sample will have traces of dissolved gases as well as solvent molecules that contribute information that are not our sample. The background spectrum will contain information about the species of gases and solvent molecules, which may then be subtracted away from our sample spectrum in order to gain information about just the sample. Figure 6 shows an example of an FTIR background spectrum.

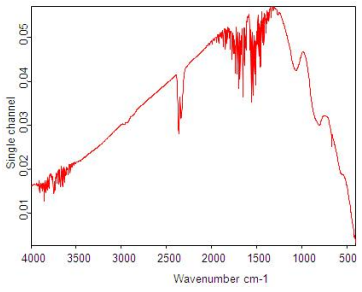


Figure 6. Background IR spectrum

The background spectrum also takes into account several other factors related to the instrument performance, which includes information about the source, interferometer, detector, and the contribution of ambient water (note the two irregular groups of lines at about 3600 cm^{-1} and about 1600 cm^{-1} in Figure 6) and carbon dioxide (note the doublet at 2360 cm^{-1} and sharp spike at 667 cm^{-1} in Figure 6) present in the optical bench.

Step 3: Next, we collect a single-beam spectrum of the sample, which will contain absorption bands from the sample as well as the background (gaseous or solvent).

Step 4: The ratio between the single-beam sample spectrum and the single beam background spectrum gives the spectrum of the sample (Figure 7).

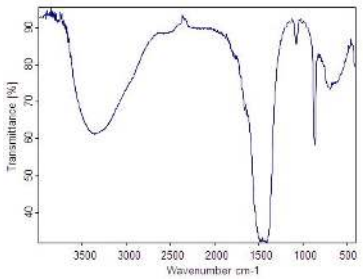


Figure 7. Sample IR spectrum

Step 5: Data analysis is done by assigning the observed absorption frequency bands in the sample spectrum to appropriate normal modes of vibrations in the molecules.

Portable FTIR Spectrometers

Despite of the powerfulness of traditional FTIR spectrometers, they are not suitable for real-time monitoring or field use. So various portable FTIR spectrometers have been developed. Below are two examples.

Ahonen *et al* developed a portable, real-time FTIR spectrometer as a gas analyzer for industrial hygiene use. The instrument consists of an operational keyboard, a control panel, signal and control processing electronics, an interferometer, a heatable sample cell and a detector. All the components were packed into a cart. To minimize the size of the instrument, the resolution of FTIR spectrometer was sacraficed. But it is good enough for the use of industrial hygiene. The correlation coefficient of hygienic effect between the analyzer and adsorption tubes is about 1 mg/m^3.

Korb *et al* developed a portable FTIR spectrometer which only weighs about 12.5 kg so that it can be held by hand. Moreover, the energy source of the instrument is battery so that the mobility is significantly enhanced. Besides, the instrument can function well within the temperature range of 0 to 45 ^oC and the humidity range of 0 to 100%. Additionally, this instrument resists vibration. It works well in an operating helicopter. Consequently, this instrument is excellent for the analysis of radiation from the surface and atmosphere of the Earth. The instrument is also very stable. After a three-year operation, it did not lose optical alignment. The reduction of size was implemented by a creative design of optical system and accessory components. Two KBr prisms were used to constitute the interferometer cavity. Optical coatings replaced the mirrors and beam splitter in the interferometer. The optical path is shortened with a much more compact packaging of components. A small, low energy consuming interferometer drive was designed. It is also mass balanced to resist vibration. The common He-Ne tube was replaced by a smaller laser diode.

References

1. P.R. Griffiths, *Science*, *21*, ***1983***, *297*
2. W.D. Perkins, "Fourier Transform-Infrared Spectroscopy". Part 1. Instrumentation. Topics in Chemical Instrumentation. Ed. Frank A. Settle, Jr. *Journal of Chemical Education*, **63**:1, January 1986: A5-A10.
3. D.A. Skoog and J.J. Leary. "Principles of Instrumental Analysis, 4th Ed.", Harcourt Brace Jovanovich. Philadelphia, PA, 1992. Chapter 12.
4. F. Daniels, J.W. Williams, P. Bender, R.A. Alberty, C.D. Cornwell, J. E. Harriman. "Experimental Physical Chemistry, 7th Ed.", McGraw-Hill, New York, NY, 1970.
5. J.W. Cooley and J.W. Turkey, *Math. Comp.*, **1965**, 19, 9
6. A.G. Marshall, *Acc. Chem. Res.*, **1985**, 18, 316
7. A. R. Korb, P. Dybwad, W. Wadsworth, J. W. Salisbury, *Applied Optics*, **1996**, 35, 1679
8. I. Ahonen, H. Riipinen, A. Roos, *Analyst*, **1996**, 121, 1253
9. D. W. Ball, *Field Guide to Spectroscopy*, SPIE Publication, Bellingham, 2006
10. V. Saptari, *Fourier-Transform Spectroscopy Instrumentation Engineering*, SPIE Publication, Bellingham, 2003
11. P. R. Griffiths, J. A. de Haseth, *Fourier Transform Infrared Spectrometry*, Wiley, New York, 1986
12. B. C. Smith, *Fundamentals of Fourier Transform Infrared Spectroscopy*, CRC press, 1996
13. B. Stuart, *Modern Infrared Spectroscopy*, Wiley, New York, 1996
14. A. L. Smith, *Applied Infrared Spectroscopy : Fundamentals, Techniques, and Analytical Problem-solving*, Wiley, New York, 1979
15. P. R. Griffiths, *Chemical Infrared Fourier Transform Spectroscopy*, Wiley, New York, 1975

How an FTIR Spectrometer Operates is shared under a CC BY-NC-SA 4.0 license and was authored, remixed, and/or curated by LibreTexts.

- **How an FTIR Spectrometer Operates** by Nancy Birkner, Qian Wang is licensed CC BY 4.0.

Theory

Infrared (IR) spectroscopy is one of the most common and widely used spectroscopic techniques employed mainly by inorganic and organic chemists due to its usefulness in determining structures of compounds and identifying them. Chemical compounds have different chemical properties due to the presence of different functional groups.

Introduction

Infrared (IR) spectroscopy is one of the most common and widely used spectroscopic techniques. Absorbing groups in the infrared region absorb within a certain wavelength region. The absorption peaks within this region are usually sharper when compared with absorption peaks from the ultraviolet and visible regions. In this way, IR spectroscopy can be very sensitive to determination of functional groups within a sample since different functional group absorbs different particular frequency of IR radiation. Also, each molecule has a characteristic spectrum often referred to as the fingerprint. A molecule can be identified by comparing its absorption peak to a data bank of spectra. IR spectroscopy is very useful in the identification and structure analysis of a variety of substances, including both organic and inorganic compounds. It can also be used for both qualitative and quantitative analysis of complex mixtures of similar compounds.

The use of infrared spectroscopy began in the 1950's by Wilbur Kaye. He had designed a machine that tested the near-infrared spectrum and provided the theory to describe the results. Karl Norris started using IR Spectroscopy in the analytical world in the 1960's and as a result IR Spectroscopy became an accepted technique. There have been many advances in the field of IR Spec, the most notable was the application of Fourier Transformations to this technique thus creating an IR method that had higher resolution and a decrease in noise. The year this method became accepted in the field was in the late 1960's.[4]

Absorption Spectroscopy

There are three main processes by which a molecule can absorb radiation. and each of these routes involves an increase of energy that is proportional to the light absorbed. The first route occurs when absorption of radiation leads to a higher rotational energy level in a rotational transition. The second route is a vibrational transition which occurs on absorption of quantized energy. This leads to an increased vibrational energy level. The third route involves electrons of molecules being raised to a higher electron energy, which is the electronic transition. It’s important to state that the energy is quantized and absorption of radiation causes a molecule to move to a higher internal energy level. This is achieved by the alternating electric field of the radiation interacting with the molecule and causing a change in the movement of the molecule. There are multiple possibilities for the different possible energy levels for the various types of transitions.

The energy levels can be rated in the following order: electronic > vibrational > rotational. Each of these transitions differs by an order of magnitude. Rotational transitions occur at lower energies (longer wavelengths) and this energy is insufficient and cannot cause vibrational and electronic transitions but vibrational (near infra-red) and electronic transitions (ultraviolet region of the electromagnetic spectrum) require higher energies.

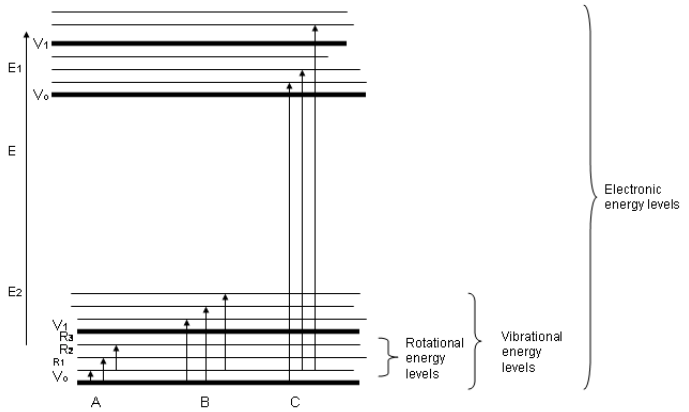


Figure 1: Energy levels for a molecule. Possible transitions that occur: (A): Pure rotational Transitions, (B) rotational-Vibrational Transitions, (C) Rotational-Vibrational-Electronic Transitions

The energy of IR radiation is weaker than that of visible and ultraviolet radiation, and so the type of radiation produced is different. Absorption of IR radiation is typical of molecular species that have a small energy difference between the rotational and vibrational

states. A criterion for IR absorption is a net change in dipole moment in a molecule as it vibrates or rotates. Using the molecule HBr as an example, the charge distribution between hydrogen and bromine is not evenly distributed since bromine is more electronegative than hydrogen and has a higher electron density. HBr thus has a large dipole moment and is thus polar. The dipole moment is determined by the magnitude of the charge difference and the distance between the two centers of charge. As the molecule vibrates, there is a fluctuation in its dipole moment; this causes a field that interacts with the electric field associated with radiation. If there is a match in frequency of the radiation and the natural vibration of the molecule, absorption occurs and this alters the amplitude of the molecular vibration. This also occurs when the rotation of asymmetric molecules around their centers results in a dipole moment change, which permits interaction with the radiation field.

> Molecules such as O_2, N_2, Br_2, do not have a changing dipole moment (amplitude nor orientation) when they undergo rotational and vibrational motions, as a result, they cannot cannot absorb IR radiation.

Diatomic Molecular Vibration

The absorption of IR radiation by a molecule can be likened to two atoms attached to each other by a massless spring. Considering simple diatomic molecules, only one vibration is possible. The Hook's law potential on the other hand is based on an ideal spring

$$F = -kx \tag{1}$$

$$= -\frac{dV(x)}{dx} \tag{2}$$

this results in one dimensional space

$$V(r) = \frac{1}{2}k(r - r_{eq})^2 \tag{3}$$

One thing that the Morse and Harmonic oscillator have in common is the small displacements ($x = r - r_{eq}$) from the equilibrium. Solving the Schrödinger equation for the harmonic oscillator potential results in the energy levels results in

$$E_v = \left(v + \frac{1}{2}\right) hv_e \tag{4}$$

with $v = 0, 1, 2, 3, \ldots, infinity$

$$v_e = \frac{1}{2\pi}\sqrt{\frac{k}{\mu}} \tag{5}$$

When calculating the energy of a diatomic molecule, factors such as anharmonicity (has a similar curve with the harmonic oscillator at low potential energies but deviates at higher energies) are considered. The energy spacing in the harmonic oscillator is equal but not so with the anharmonic oscillator. The anharmonic oscillator is a deviation from the harmonic oscillator. Other considered terms include; centrifugal stretching, vibrational and rotational interactions have to be taken into account. The energy can be expressed mathematically as

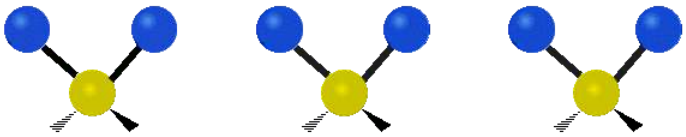
$$E_v = \underbrace{\left(v + \frac{1}{2}\right) hv_e}_{\text{Harmonic Oscillator}} - \underbrace{\left(v + \frac{1}{2}\right)^2 X_e hv_e}_{\text{anharmonicity}} + \underbrace{B_e J(J+1)}_{\text{Rigid Rotor}} - \underbrace{D_e J^2 (J+1)^2}_{\text{centrifugal stretching}} - \underbrace{\alpha_e \left(v + \frac{1}{2}\right) J(J+1)}_{\text{rovibrational coupling}} \tag{6}$$

The first and third terms represent the *harmonicity* and rigid rotor behavior of a diatomic molecule such as HCl. The second term represents anharmonicity and the fourth term represents centrifugal stretching. The fifth term represents the interaction between the vibration and rotational interaction of the molecule.

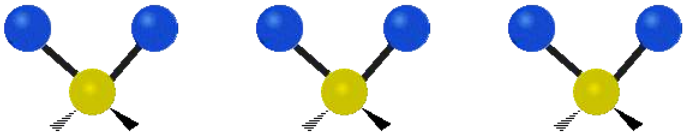
Polyatomic Molecular Vibration

The bond of a molecule experiences various types of vibrations and rotations. This causes the atom not to be stationary and to fluctuate continuously. Vibrational motions are defined by stretching and bending modes. These movements are easily defined for diatomic or triatomic molecules. This is not the case for large molecules due to several vibrational motions and interactions that will be experienced. When there is a continuous change in the interatomic distance along the axis of the bond between two atoms, this process is known as a stretching vibration. A change in the angle occurring between two bonds is known as a bending

vibration. Four bending vibrations exist namely, wagging, twisting, rocking and scissoring. A CH_2 group is used as an example to illustrate stretching and bending vibrations below.



Symmetric Stretch Asymmetric Stretch Twisting



Wagging Scissoring Rocking

Figure 3: Types of Vibrational Modes. To ensure that no center of mass motion occurs, the center atom (yellow ball) will also move. Figure from Wikipedia

As stated earlier, molecular vibrations consist of stretching and bending modes. A molecule consisting of (N) number of atoms has a total of 3N degrees of freedom, corresponding to the Cartesian coordinates of each atom in the molecule. In a non-linear molecule, 3 of these degrees of freedom are rotational, 3 are translational and the remainder is fundamental vibrations. In a linear molecule, there are 3 translational degrees of freedom and 2 are rotational. This is because in a linear molecule, all of the atoms lie on a single straight line and hence rotation about the bond axis is not possible. Mathematically the normal modes for a linear and non linear can be expressed as

Linear Molecules: (3N - 5) degrees of freedom

Non-Linear molecules: (3N - 6) degrees of freedom

Example 1: Vibrations of Water

Diagram of Stretching and Bending Modes for H_2O.

Solution

H_2O molecule is a non-linear molecule due to the uneven distribution of the electron density. O_2 is more electronegative than H_2 and carries a negative charge, while H has a partial positive charge. The total degrees of freedom for H_2O will be 3(3)-6 = 9-6 = 3 degrees of freedom which correspond to the following stretching and bending vibrations. The vibrational modes are illustrated below:

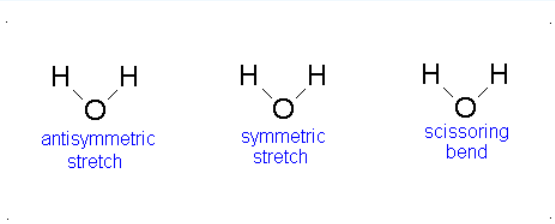


Figure 4 The vibrational modes of H_2O

Example Vibrations of CO_2

Diagram of Stretching and Bending Modes for CO_2.

Solution

CO_2 is a linear molecule and thus has the formula (3N-5). It has 4 modes of vibration (3(3)-5). CO_2 has 2 stretching modes, symmetric and asymmetric. The CO_2 symmetric stretch is not IR active because there is no change in dipole moment because

the net dipole moments are in opposite directions and as a result, they cancel each other. In the asymmetric stretch, O atom moves away from the C atom and generates a net change in dipole moments and hence absorbs IR radiation at 2350 cm^{-1}. The other IR absorption occurs at 666 cm^{-1}. CO_2 symmetry with $D_{\infty h}$ CO_2 has a total of four of stretching and bending modes but only two are seen. Two of its bands are degenerate and one of the vibration modes is symmetric hence it does not cause a dipole moment change because the polar directions cancel each other. The vibrational modes are illustrated below:

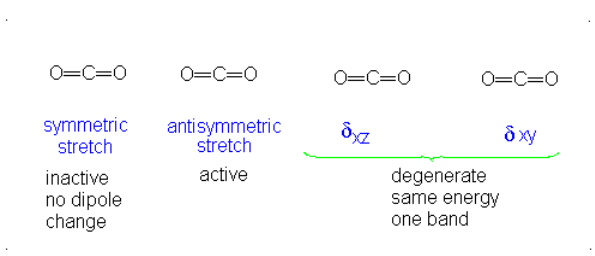


Figure 5 The vibrational modes of **CO_2**

The Deduction of Frequency

The second law of Newton states that

$$F = ma \tag{7}$$

where m is the mass and a is the acceleration, acceleration is a 2nd order differential equation of distance with respect to time. Thus "a" can be written as

$$a = \frac{d^2y}{dt} \tag{8}$$

Substituting this into Equation 1 gives

$$\frac{md^2y}{dt^2} = -ky \tag{9}$$

the 2nd order differential equation of this equation is equal to $\frac{-k}{m}$ displacement of mass and time can be stated as

$$y = A\cos 2\pi\nu_m t \tag{10}$$

where v_m is the natural vibrational frequency and A is the maximum amplitude of the motion. On differentiating a second time the equation becomes

$$\frac{d^2y}{dt^2} = -4\pi^2\nu_m^2 A\cos 2\pi\nu_m t$$

substituting the two equations above into Newton's second law for a harmonic oscillator,

$$m * \left(-4\pi^2\nu_m^2 A\cos 2\pi\nu_m t\right) = -k * \left(A\cos 2\pi\nu_m t\right) \tag{11}$$

If we cancel out the two functions y,

$$4m\pi^2\nu_m^2 = k \tag{12}$$

from above, we obtain the natural frequency of the oscillation.

$$\nu_m = \frac{1}{2\pi}\sqrt{\frac{k}{m}} \tag{13}$$

ν_m which is the natural frequency of the mechanical oscillator which depends on the force constant of the spring and the mass of the attached body and independent of energy imparted on the system. when there are two masses involved in the system then the mass used in the above equation becomes

$$\mu = \frac{m_1 m_2}{m_1 + m_2} \tag{14}$$

The vibrational frequency can be rewritten as

$$\nu_m = \frac{1}{2\pi}\sqrt{\frac{k}{\mu}} \tag{15}$$

The Deduction of Wave Number

Using the harmonic oscillator and wave equations of quantum mechanics, the energy can be written as

$$E = \left(v + \frac{1}{2}\right)\frac{h}{2\pi}\sqrt{\frac{k}{\mu}} \tag{16}$$

where h is Planck's constant and v is the vibrational quantum number and ranges from 0,1,2,3.... infinity.

$$E = \left(v + \frac{1}{2}\right)h\nu_m \tag{17}$$

where ν_m is the vibrational frequency. Transitions in vibrational energy levels can be brought about by absorption of radiation, provided the energy of the radiation exactly matches the difference in energy levels between the vibrational quantum states and provided the vibration causes a change in dipole moment. This can be expressed as

$$\triangle E = h\nu_m = \frac{h}{2\pi}\sqrt{\frac{k}{\mu}} \tag{18}$$

At room temperature, the majority of molecules are in the ground state v = 0, from the equation above

$$E_o = \frac{1}{2}h\nu_m \tag{19}$$

following the selection rule, when a molecule absorbs energy, there is a promotion to the first excited state

$$E_1 = \frac{3}{2}h\nu_m \tag{20}$$

$$\left(\frac{3}{2}h\nu_m - \frac{1}{2}h\nu_m\right) = h\nu_m \tag{21}$$

The frequency of radiation v that will bring about this change is identical to the classical vibrational frequency of the bond v_m and it can be expressed as

$$E_{radiation} = h\nu = \triangle E = h\nu_m = \frac{h}{2\pi}\sqrt{\frac{k}{\mu}} \tag{22}$$

The above equation can be modified so that the radiation can be expressed in wave numbers

$$\tilde{\nu} = \frac{h}{2\pi c}\sqrt{\frac{k}{\mu}} \tag{23}$$

where

- c is the velocity of light (cm s^{-1}) and
- $\tilde{\nu}$ is the wave number of an absorption maximum (cm^{-1})

Theory of IR

Molecular vibrational frequencies lie in the IR region of the electromagnetic spectrum, and they can be measured using the IR technique. In IR, polychromatic light (light having different frequencies) is passed through a sample and the intensity of the transmitted light is measured at each frequency. When molecules absorb IR radiation, transitions occur from a ground vibrational state to an excited vibrational state (Figure 1).

For a molecule to be IR active there must be a change in dipole moment as a result of the vibration that occurs when IR radiation is absorbed. Dipole moment is a vector quantity and depends on the orientation of the molecule and the photon electric vector. The dipole moment changes as the bond expands and contracts. When all molecules are aligned as in a crystal and the photon vector points along a molecular axis such as z. Absorption occurs for the vibrations that displace the dipole along z. Vibrations that are totally x or y polarized would be absent. Dipole moment in a heteronuclear diatomic molecule can be described as uneven distribution of electron density between the atoms. One atom is more electronegative than the other and has a net negative charge.

The dipole moment can be expressed mathematically as

$$\mu = er$$

The relationship between IR intensity and dipole moment is given as

$$I_{IR} \propto \left(\frac{d\mu}{dQ}\right)^2$$

relating this to intensity of the IR radiation, we have have the following equation below.

where μ is the dipole moment and Q is the vibrational coordinate. The *transition moment integral*, that gives information about the probability of a transition occurring, for IR can also be written as

$$\langle \psi_| \hat{M} | \psi_f \rangle$$

i and f represent are initial and final states. ψ_i is the wave function. Relating this to IR intensity we have

$$I_{IR} \propto \langle \psi_| \hat{M} | \psi_f \rangle$$

where $\hat{M}$ is the dipole moment and has the Cartesian coordinates, $\hat{M}_x$,$\hat{M}_y$, $\hat{M}_z$. In order for a transition to occur by dipole selection rules , at least one of the integrals must be non zero.

Region of IR

The IR region of the electromagnetic spectrum ranges in wavelength from 2 -15 µm. Conventionally the IR region is subdivided into three regions, near IR, mid IR and far IR. Most of the IR used originates from the mid IR region. The table below indicates the IR spectral regions

Region	Wavelength	Wavenumbers (V), cm^{-1}	Frequencies (v), HZ
Near	0.78 -2.5	12800 - 4000	3.8×10^{14} - 1.2×10^{14}
Middle	2.5 - 50	4000 - 200	3.8×10^{14} - 1.2×10^{14}
Far	50 -100	200 -10	3.8×10^{14} - 1.2×10^{14}
Most Used	2.5 -15	4000 -670	3.8×10^{14} - 1.2×10^{14}

IR deals with the interaction between a molecule and radiation from the electromagnetic region ranging (4000- 40 cm^{-1}). The cm^{-1} is the wave number scale and it can also be defined as 1/wavelength in cm. A linear wavenumber is often used due to its direct relationship with both frequency and energy. The frequency of the absorbed radiation causes the molecular vibrational frequency for the absorption process. The relationship is given below

$$\bar{v}(cm^{-1}) = \frac{1}{\lambda(\mu m)} \times 10^4 \left(\frac{\mu m}{cm}\right) = \frac{v(Hz)}{c(cm/s)} \tag{24}$$

- **Near InfraRed Spectroscopy:** Absorption bands in the near infrared (NIR) region (750 - 2500 nm) are weak because they arise from vibrational overtones and combination bands. Combination bands occur when two molecular vibrations are excited simultaneously. The intensity of overtone bands reduces by one order of overtone for each successive overtone. When a molecule is excited from the ground vibrational state to a higher vibrational state and the vibrational quantum number v is greater than or equal to 2 then an overtone absorption results. The first overtone results from v = 0 to v = 2. The second overtone occurs when v =0 transitions to v = 3. Transitions arising from the near ir absorption are weak, hence they are referred to as forbidden transitions but these transitions are relevant when non-destructive measurements are required such as a solid sample. Near IR spectra though have low absorption they have a high signal to noise ratio owing to intense radiation sources

and NIR is able to penetrate undiluted samples and use longer path lengths; it becomes very useful for rapid measurement of more representative samples.

- **Far InfraRed Spectroscopy:** The far IR region is particularly useful for inorganic studies due to stretching and bending vibrations of bonds between the metal atoms and ligands. The frequencies, which these vibrations are observed, are usually lower than 650 cm^{-1}. Pure rotational absorption of gases is observed in the far IR region when there is a permanent dipole moment present. Examples include H_2O, O_3, HCl.

IR Analysis

Qualitative Analysis

IR spectroscopy is a great method for identification of compounds, especially for identification of functional groups. Therefore, we can use group frequencies for structural analysis. Group frequencies are vibrations that are associated with certain functional groups. It is possible to identify a functional group of a molecule by comparing its vibrational frequency on an IR spectrum to an IR stored data bank.

Here, we take the IR spectrum of Formaldehyde for an example. Formaldehyde has a C=O functional group and C-H bond. The value obtained from the following graph can be compared to those in reference data banks stored for Formaldehyde. A molecule with a C=O stretch has an IR band which is usually found near 1700 cm^{-1} and around 1400 cm^{-1} for CH_2 bend. It's important to note that this value is dependent on other functional groups present on the molecule. The higher 1700 cm^{-1} indicates a large dipole moment change. It is easier to bend a molecule than stretch it, hence stretching vibrations have higher frequencies and require higher energies than bending modes. The finger print region is a region from 1400-650 cm^{-1}. Each molecule has it's own characteristic print and is often cumbersome to attach any values to this region.

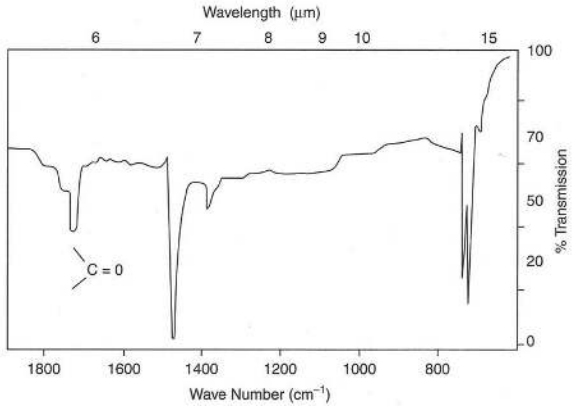


Figure 6 IR Spectrum of Formaldehyde

Quantitative Analysis

Infrared spectroscopy can also be applied in the field of quantitative analysis, although sometimes it's not as accurate as other analytical methods, like gas chromatography and liquid chromatography. The main theory of IR quantification is Beer's law or Beer-Lambert law, which is written as

$$A = \log\left(\frac{I_0}{I}\right) = \epsilon l c \tag{25}$$

Where A is the absorbance of the sample, I is the intensity of transmitted light, I_0 is the intensity of incident light, l is the path length, a is the molar absorptivity of the substance, and c is the concentration of the substance.

From the Beer's Law, we could figure out the relation between the absorbance and the concentration of the sample since the analytes have a particular molar absorptivity at a particular wavelength. Therefore, we could use IR spectroscopy and Beer's Law to find the concentration of substance or the components of mixture. This is how the IR quantification operated.

Selection Rules of IR

In order for vibrational transitions to occur, they are normally governed by some rules referred to as selection rules.

1. An interaction must occur between the oscillating field of the electromagnetic radiation and the vibrational molecule for a transition to occur. This can be expressed mathematically as

$$\left(\frac{d\mu}{dr}\right)_{r_{eq}} \neq 0$$

$$\triangle v = +1 \text{ and } \triangle J = +1$$

2. This holds for a harmonic oscillator because the vibrational levels are equally spaced and that accounts for the single peak observed in any given molecular vibration. For gases J changes +1 for the R branch and -1 for the P branch.$\triangle J = 0$ is a forbidden transition and hence a q branch for a diatomic will not be present. For any anharmonic oscillator, the selection rule is not followed and it follows that the change in energy becomes smaller. This results in weaker transitions called overtones, then $\triangle v = +2$ (first overtone) can occur, as well as the 2nd overtone $\triangle v = +3$. The frequencies of the 1st and 2nd overtones provides information about the potential surface and about two to three times that of the fundamental frequency.
3. For a diatomic, since μ is known, measurement of u_e provides a value for k, the force constant.

$$k = \left(\frac{d^2V(r)}{dr^2}\right)_{r_{eq}}$$

where k is the force constant and indicates the strength of a bond.

Influence Factors of IR

- **Isotope Effects:** It's been observed that the effect on k when an atom is replaced by an isotope is negligible but it does have an effect on ν due to changes in the new mass. This is because the reduced mass has an effect on the rotational and vibrational behavior.
- **Solvent Effects:** The polarity of solvent will have an influence on the IR spectra of organic compounds due to the interactions between solvent and compounds, which is called solvent effects. If we place a compound, which contains n, pi and pi* orbitals, into a polar solvent, the solvent will stabilizes these three orbitals in different extent. The stabilization effects of polar solvent on n orbital is the largest one, the next larger one is pi* orbital, and the effects on pi orbital is the smallest one. The spectra of n→pi* transition will shift to blue side, which means it will move to shorter wavelengths and higher energies since the polar solvent causes the energy difference between n orbital and pi* orbital to become bigger. The spectra of pi→pi* transition will shift to red side, which means it will move to longer wavelengths and lower energies since the polar solvent causes the energy difference between n orbital and pi* orbital to become smaller.

Advantages of IR

- **High Scan Speed**: Infrared spectroscopy can get information for the whole range of frequency simultaneously, within one second. Therefore, IR can be used to analyze a substance that is not very stable and finish the scan before it start to decompose.
- **High Resolution**: The resolution of general prism spectrometer is only about 3 cm^{-1}, but the resolution of infrared spectrometer is much higher. For example, the resolution of Grating infrared spectrometer could be 0.2 cm^{-1}, the resolution of FT infrared spectrometer could be 0.1-0.005 cm^{-1}.
- **High Sensitivity**: With Fourier Transform, the infrared spectrometer doesn't need to use the slit and monochromator. In this way, the reflection specularity will be increased and the loss of energy in the analysis process will be decreased. Therefore the energy that reaches the detector is large enough and even very small amount of analytes could be detected. Nowadays, the infrared spectroscopy could detect the sample as small as 1-10 grams.
- **Wide Range of Application**: Infrared spectroscopy could be used to analyze almost all organic compounds and some inorganic compounds. It has a wide range of application in both qualitative analysis and quantitative analysis. Also, the sample of Infrared spectroscopy doesn't have phase constraints. It could be gas, liquid or solid, which has enlarged the range of analytes a lot.
- **Large Amount of Information**: Infrared Spectra could give us lots of structural information of the analytes, such as the type of compound, the functional group of compound, the stereoscopic structure of compound, the number and position of substituent group and so on. Depending on the available information form the functional part and the fingerprint part, infrared spectroscopy has become a great method to identify different kinds of compounds.
- **Non-Destructive**: Infrared Spectroscopy is non-destructive to the sample.

Disadvantages of IR

- **Sample Constraint:** Infrared spectroscopy is not applicable to the sample that contains water since this solvent strongly absorb IR light.
- **Spectrum Complication**: The IR spectrum is very complicated and the interpretation depends on lots of experience. Sometimes, we cannot definitely clarify the structure of the compound just based on one single IR spectrum. Other spectroscopy methods, such as (Mass Spectrometry) MS and (Nuclear Magnetic Resonance) NMR, are still needed to further interpret the specific structure.
- **Quantification**: Infrared spectroscopy works well for the qualitative analysis of a large variety of samples, but quantitative analysis may be limited under certain conditions such as very high and low concentrations.

Symmetry & IR Spectroscopy

One of the most importance applications of IR spectroscopy is structural assignment of the molecule depending on the relationship between the molecule and observed IR absorption bands. Every molecule is corresponding to one particular symmetry point group. Then we can predict which point group the molecule is belonging to if we know its IR vibrational bands. Vice versa, we can also find out the IR active bands from the spectrum of the molecule if we know its symmetry. These are two main applications of group theory. We'll take the following problem as an example to illustrate how this works.

Question

How do you distinguish whether the structure of transition metal complex molecule $M(CO)_2L_4$ is *cis* or *trans* by inspection of the CO stretching region of the IR spectra?

Answer

For cis-$M(CO)_2L_4$, the symmetry point group of this molecule is C_{2v}.

C_{2v}	E	C_2	σ(xz)	σ(yz)
γ**co**	**2**	**0**	**2**	**0**

γ**co** = A1 + B1

Since A1 has a basis on z axis and B1 has a basis on x axis, there are two IR vibrational bands observed in the spectrum.

For trans-$M(CO)_2L_4$, the symmetry point group of this molecule is D_{4h}.

D_{4h}	E	C_4	C_2	C_2'	C_2''	i	S4	σ_h	σ_v	σ_d
γ**co**	**2**	**2**	**2**	**0**	**0**	**0**	**0**	**0**	**2**	**2**

γ**co** = $A_{1g} + A_{2u}$

Since A_{2u} has a basis on z axis, there is only one IR vibrational band observed in the spectrum.

Therefore, from what have been discussed above, we can distinguish these two structures based on the number of IR bands.

Problems

The frequency of C=O stretching is higher than that of C=C stretching. The Intensity of C=O stretching is stronger than that of C=C stretching. Explain it.

References

1. D. A. Skoog, F. J. Holler, S. R. Crouch. *Principles of Instrumental Analysis, 6th ed.* Belmont, CA. Thomson Higher Education. 2007
2. G. D. Christain. *Analytical Chemistry,* 5th ed. New York. John Wiley & Sons, INC. 1994
3. R. S. Drago. *Physical Methods,* 2nd ed. Mexico.Saunders College Publishing.1992
4. S.M. Blinder. Introduction to Quantum Mechanics. Academic Press. 2004
5. D. C. Harris, M. D. Bertolucci. *Symmetry and Spectroscopy: An Introduction to Vibrational and Electronic Spectroscopy.* New York. Dover Publications, INC

Contributors and Attributions

- Richard Osibanjo, Rachael Curtis, Zijuan Lai

Theory is shared under a CC BY-NC-SA 4.0 license and was authored, remixed, and/or curated by LibreTexts.

- **Infrared Spectroscopy** is licensed CC BY 4.0.

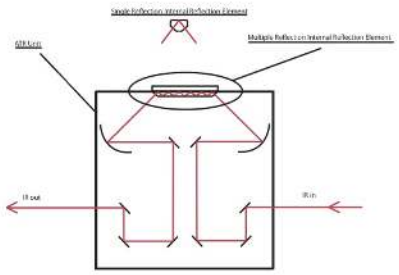
3.4: ATR-FTIR

This module will go over attenuated total reflectance Fourier transform infrared spectroscopy (ATR-FTIR). It will go over basic physics that describe and dictate the analytical technique. There will be a given example of how ATR-FTIR is used in biological studies. This example will be given in the format of real data and data analysis methods.

Introduction

ATR-FTIR is a tool that has been proven to be useful in various applications[1]. This technique is able to probe *in situ* single or multiple layers of adsorbed/deposited species at a solid/liquid interface[1,2]. It is for this reason that ATR-FTIR has been implemented in various different biological studies in order to probe chemical reactions/structure at the solid/liquid interface[2]. The reader should be aware that this module will not cover in depth about the physics that govern ATR-FTIR's ability to probe chemical species, but rather give the reader an introduction on the technique. This module will cover the basic experimental set-up that is currently being utilized in research, briefly go over essential equations that will help the reader better understand methods of experimentation, and finally provide an example of how ATR-FTIR can be utilized.

Experimental Setup



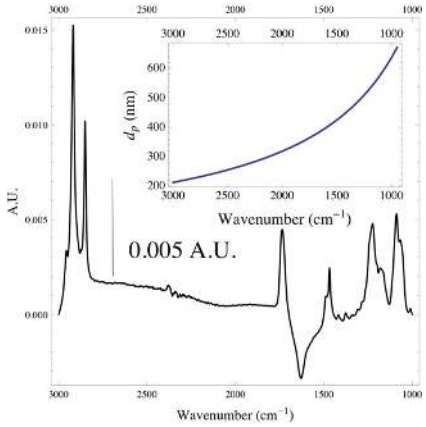
To the left is an image of what a typical ATR set-up includes. It shows the internal components found within a specific ATR setup which allows the infrared radiation to enter from the bottom of the ATR base and redirected by five different mirrors before the radiation enters then exits the internal reflection element (IRE) and continues towards the the detector. This setup allows for the infrared radiation to probe molecules at the interface of the IRE. The one shown above is an image of a multiple reflection internal reflection element. It is called a multiple reflection IRE because the radiation makes more than one reflection within the element prior to exiting towards the detector. There are advantages and disadvantages of using a multiple reflection element. One of the advantages is that the user is able to observe stronger absorbance by the sample due to the multiple points that the radiation is interacting, however the disadvantage of using a multiple reflection element is that the light absorbance is hard to quantify due to scattering that occurs with each reflection. One way for a user to overcome the disadvantage that multiple reflections brings is to use a single reflection IRE rather than a multiple reflection IRE.

ATR Basics

The infrared radiation that interacts with the adsorbed species is limited to a given depth, and is dependent on the wavelength and angle of the incoming radiation, refractive index of the IRE, and the refractive indices of the interacting layers at the IRE interface. This depth is known as the depth of penetration and the governing equation is shown below.

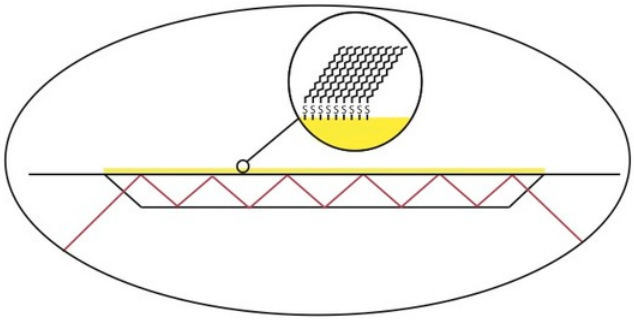
$$dp = \frac{\lambda}{2\pi\sqrt{n_1}}^{2} \sin[\theta]^2 - n_2^2 \tag{1}$$

It is good to keep in mind that the if working with systems that have more than one monolayer of adsorbed species that the depth of penetration is dependent on the wavelength of the incoming radiation. If this is the case the depth of penetration will be greater at higher wavelengths, and one will be probing deeper into the medium rather than at the interface of the IRE. Below is a spectrum of a monolayer of DPPC lipid vesicles adsorbed onto the surface of a ZnSe IRE. The inset plot shows the depth of penetration of the infrared radiation with respect to wavenumber.

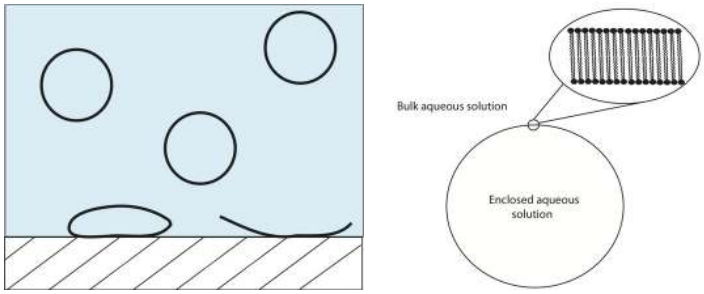


Vibrational Spectroscopy at the Solid/Liquid Interface

ATR-FTIR has been used to monitor and characterize organic thin film systems such as well formed self-assembled monolayers (SAM). This can be achieved forming a thin film of gold onto the IRE surface, exposing the gold surface to a thiol solution for a given amount of time. The figure below shows an example of an organic thin film formed on the surface of gold that was deposited on an IRE.

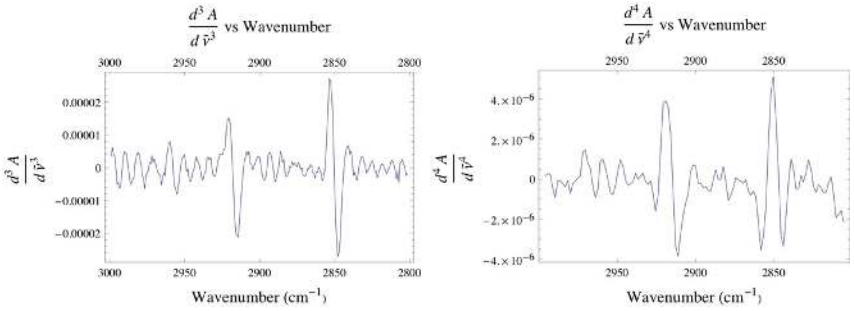


Lipid vesicles have received some attention over the years due to their ability to spontaneously form lipid aggregate spherical structures. These spherical structures have a wall made of lipids that separate the intracellular aqueous medium from the extracellular aqueous medium. They have been implemented in current forms of drug delivery systems, biological contrast agents, as well as serving as a model membrane. ATR-FTIR can be used to study these systems in a number of different ways. One such way to monitor the adsorption rate of these lipid vesicles from a bulk solution to a solid interface. Below is an example of one such experiment where 100 nm lipid vesicles were used to study the adsorption rate onto a ZnSe single reflection IRE.

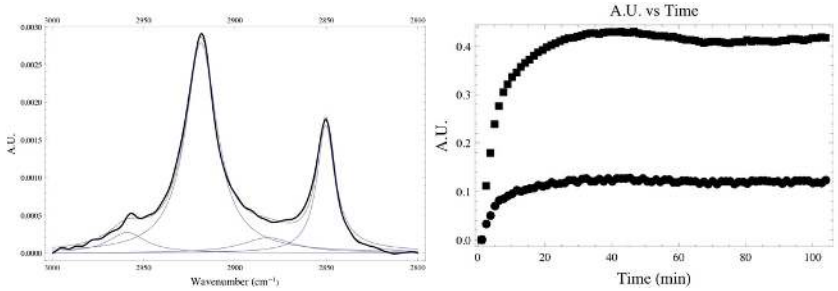


Below is the -C-H stretching region of DPPC found within the 2800 - 3000 cm^{-1}. The interval consists of the overlap of four different bands attributed to different $-CH_2$ and $-CH_3$ vibrational modes found within the acyl chain of DPPC. The bands found at 2850 and 2920 cm^{-1} are assigned to the $-CH_2$ symmetric and asymmetric vibrational modes, while the bands found at 2880 and 2960 cm^{-1} are assigned to the $-CH_3$ symmetric and asymmetric vibrational modes. Since the absorbance is proportional to the relative concentration of adsorbed lipid, it has been shown that if one monitors the absorbance under the $-CH_2$ bands one is able to attain precise adsorption rates of the lipid vesicles at the liquid/solid interface. Caution must be taken when finding the absorbance

of any absorption band, especially when dealing with overlapping absorption bands like the ones shown below. The proper way to analyze the data is to deconvolute the region of interest by identifying how many absorption bands are present by performing the proper 3rd and 4th derivative analysis on the spectrum, then fitting the data to the correct number of Gaussian/Lorentzian like bands.



Following the deconvolution and integration of the correct absorption bands one may create a time dependent absorbance plot similar to the one below. Where the top and bottom curve represent the time dependent absorbance of the asymmetric and symmetric -CH_2 bands.



References

1. What is the depth of penetration within water, if you are using a ZnSe internal reflection element, have an incident angle of 30°, and you are at 1000 cm^{-1}? (Hint: You will need the n_i for water and ZnSe.)

3.4: ATR-FTIR is shared under a CC BY-NC-SA 4.0 license and was authored, remixed, and/or curated by LibreTexts.

- **ATR-FTIR** is licensed CC BY-NC-SA 4.0.

3.5: Instrumentation

Your page has been created!

Remove this content and add your own.

- Edit page

  Click the Edit page button in your user bar. You will see a suggested structure for your content. Add your content and hit Save.

Tips:

- Drag and drop

  Drag one or more image files from your computer and drop them onto your browser window to add them to your page.

- Classifications

  Tags are used to link pages to one another along common themes. Tags are also used as markers for the dynamic organization of content in the CXone Expert framework.

- Working with templates

  CXone Expert templates help guide and organize your documentation, making it flow easier and more uniformly. Edit existing templates or create your own.

- Visit for all help topics.

3.5: Instrumentation is shared under a CC BY-NC-SA 4.0 license and was authored, remixed, and/or curated by LibreTexts.

3.6: Sample Handling

Your page has been created!

Remove this content and add your own.

Edit page

Click the Edit page button in your user bar. You will see a suggested structure for your content. Add your content and hit Save.

Tips:

Drag and drop

Drag one or more image files from your computer and drop them onto your browser window to add them to your page.

Classifications

Tags are used to link pages to one another along common themes. Tags are also used as markers for the dynamic organization of content in the CXone Expert framework.

Working with templates

CXone Expert templates help guide and organize your documentation, making it flow easier and more uniformly. Edit existing templates or create your own.

Visit for all help topics.

3.6: Sample Handling is shared under a CC BY-NC-SA 4.0 license and was authored, remixed, and/or curated by LibreTexts.

3.7: Interpreting Infrared Spectra

Objectives

After completing this section, you should be able to

1. describe how the so-called “fingerprint region” of an infrared spectrum can assist in the identification of an unknown compound.
2. identify the functional group or groups present in a compound, given a list of the most prominent absorptions in the infrared spectrum and a table of characteristic absorption frequencies.
3. identify the broad regions of the infrared spectrum in which occur absorptions caused by
   a. N–H, C–H, and O–H
   b. C≡C and C≡N
   c. C=O, C=N, and C=C

Key Terms

Make certain that you can define, and use in context, the key term below.

- fingerprint region

Study Notes

When answering assignment questions, you may use this IR table to find the characteristic infrared absorptions of the various functional groups. However, you should be able to indicate in broad terms where certain characteristic absorptions occur. You can achieve this objective by memorizing the following table.

Region of Spectrum (cm^{-1})	Absorption
2500-4000	N – H , O – H , C – H
2000-2500	C≡C , C≡N
1500-2000	C=O , C=N , C=C
below 1500	Fingerprint region

The Origin of Group Frequencies

An important observation made by early researchers is that many functional group absorb infrared radiation at about the same wavenumber, regardless of the structure of the rest of the molecule. For example, C-H stretching vibrations usually appear between 3200 and 2800cm^{-1} and carbonyl(C=O) stretching vibrations usually appear between 1800 and 1600cm^{-1}. This makes these bands diagnostic markers for the presence of a functional group in a sample. These types of infrared bands are called group frequencies because they tell us about the presence or absence of specific functional groups in a sample.

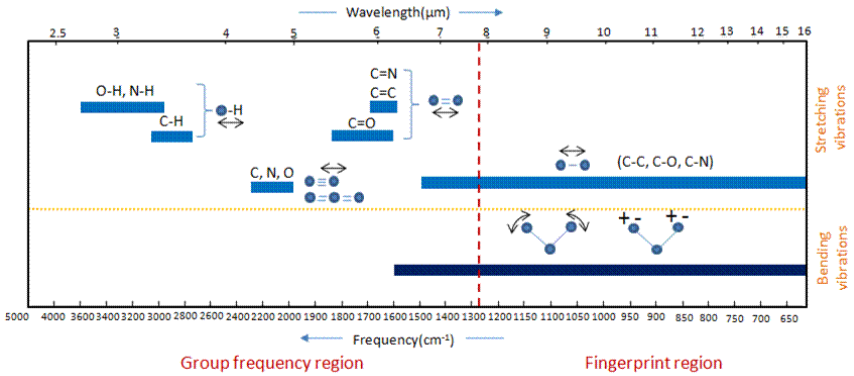
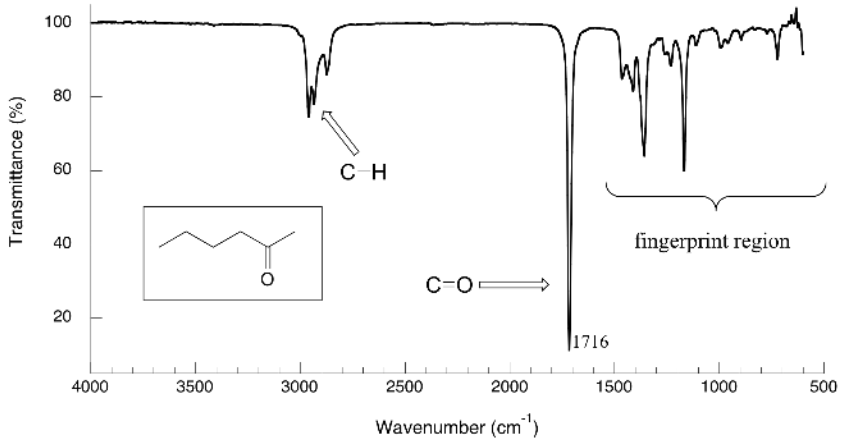


Figure 2. Group frequency and fingerprint regions of the mid-infrared spectrum

The region of the infrared spectrum from 1200 to 700 cm^{-1} is called the fingerprint region. This region is notable for the large number of infrared bands that are found there. Many different vibrations, including C-O, C-C and C-N single bond stretches, C-H bending vibrations, and some bands due to benzene rings are found in this region. The fingerprint region is often the most complex and confusing region to interpret, and is usually the last section of a spectrum to be interpreted. However, the utility of the fingerprint region is that the many bands there provide a fingerprint for a molecule.

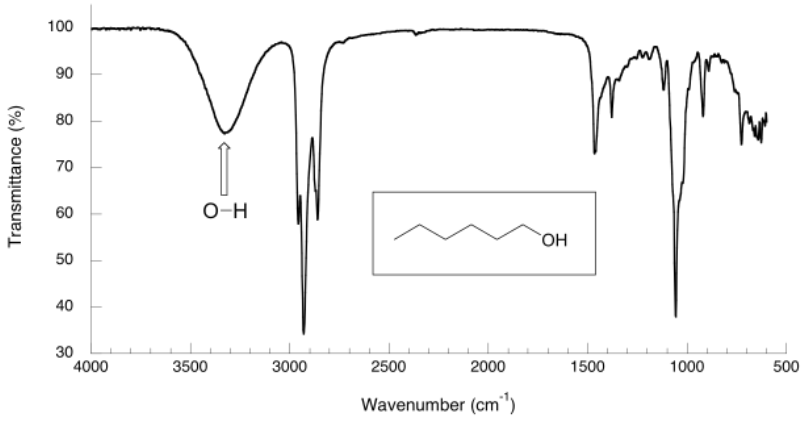


The key absorption peak in this spectrum is that from the carbonyl double bond, at 1716 cm^{-1} (corresponding to a wavelength of 5.86 mm, a frequency of 5.15 x 10^{13} Hz, and a **Δ**E value of 4.91 kcal/mol). Notice how strong this peak is, relative to the others on the spectrum: *a strong peak in the 1650-1750 cm^{-1} region is a dead giveaway for the presence of a carbonyl group*. Within that range, carboxylic acids, esters, ketones, and aldehydes tend to absorb in the shorter wavelength end (1700-1750 cm-1), while conjugated unsaturated ketones and amides tend to absorb on the longer wavelength end (1650-1700 cm^{-1}).

The jagged peak at approximately 2900-3000 cm^{-1} is characteristic of tetrahedral carbon-hydrogen bonds. This peak is not terribly useful, as just about every organic molecule that you will have occasion to analyze has these bonds. Nevertheless, it can serve as a familiar reference point to orient yourself in a spectrum.

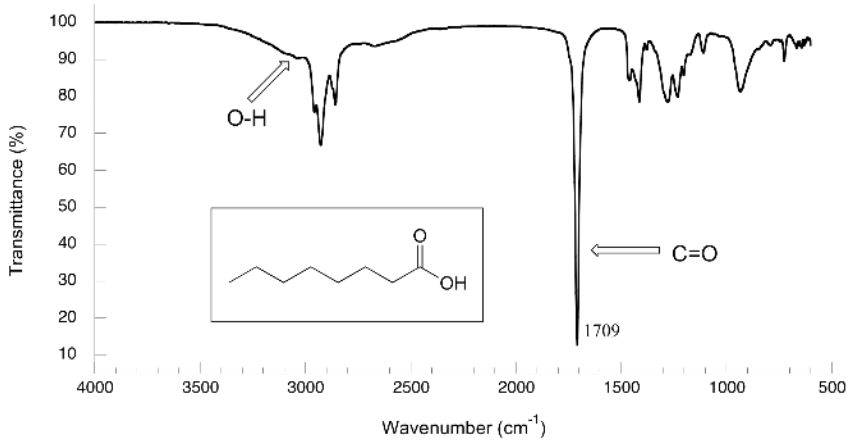
You will notice that there are many additional peaks in this spectrum in the longer-wavelength 400 -1400 cm^{-1} region. This part of the spectrum is called the **fingerprint region**. While it is usually very difficult to pick out any specific functional group identifications from this region, it does, nevertheless, contain valuable information. The reason for this is suggested by the name: just like a human fingerprint, the pattern of absorbance peaks in the fingerprint region is unique to every molecule, meaning that the data from an unknown sample can be compared to the IR spectra of known standards in order to make a positive identification. In the mid-1990's, for example, several paintings were identified as forgeries because scientists were able to identify the IR footprint region of red and yellow pigment compounds that would not have been available to the artist who supposedly created the painting (for more details see Chemical and Engineering News, Sept 10, 2007, p. 28).

Now, let's take a look at the IR spectrum for 1-hexanol.



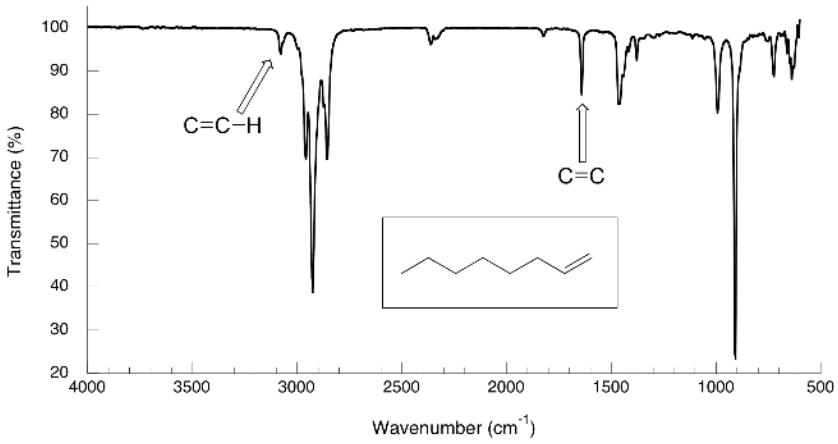
As you can see, the carbonyl peak is gone, and in its place is a very broad 'mountain' centered at about 3400 cm^{-1}. This signal is characteristic of the O-H stretching mode of alcohols, and is a dead giveaway for the presence of an alcohol group. The breadth of this signal is a consequence of hydrogen bonding between molecules.

In the spectrum of octanoic acid we see, as expected, the characteristic carbonyl peak, this time at 1709 cm^{-1}.



We also see a low, broad absorbance band that looks like an alcohol, except that it is displaced slightly to the right (long-wavelength) side of the spectrum, causing it to overlap to some degree with the C-H region. This is the characteristic carboxylic acid O-H single bond stretching absorbance.

The spectrum for 1-octene shows two peaks that are characteristic of alkenes: the one at 1642 cm^{-1} is due to stretching of the carbon-carbon double bond, and the one at 3079 cm-1 is due to stretching of the s bond between the alkene carbons and their attached hydrogens.



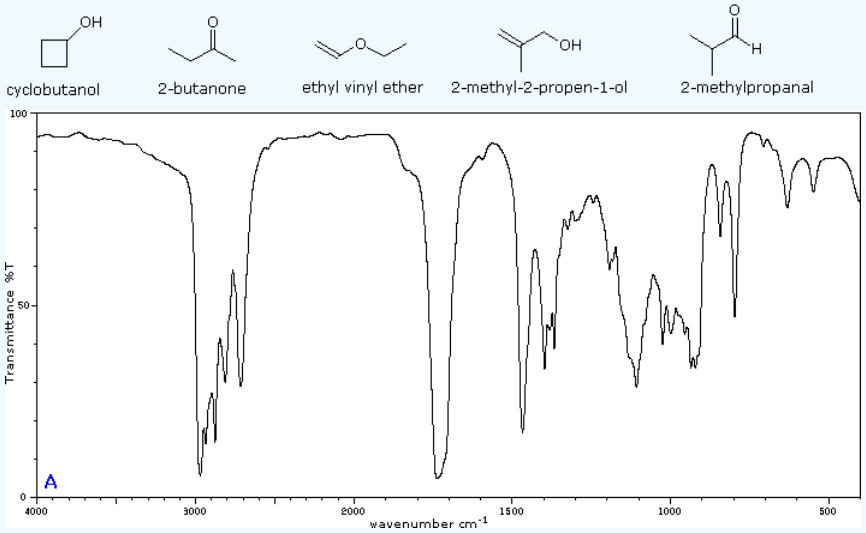
Alkynes have characteristic IR absorbance peaks in the range of 2100-2250 cm^{-1} due to stretching of the carbon-carbon triple bond, and terminal alkenes can be identified by their absorbance at about 3300 cm-1, due to stretching of the bond between the sp-hybridized carbon and the terminal hydrogen.

It is possible to identify other functional groups such as amines and ethers, but the characteristic peaks for these groups are considerably more subtle and/or variable, and often are overlapped with peaks from the fingerprint region. For this reason, we will limit our discussion here to the most easily recognized functional groups, which are summarized in this table.

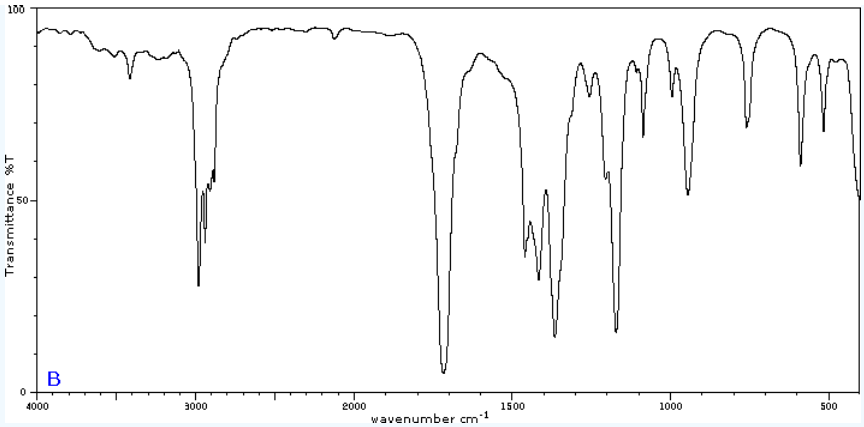
As you can imagine, obtaining an IR spectrum for a compound will not allow us to figure out the complete structure of even a simple molecule, unless we happen to have a reference spectrum for comparison. In conjunction with other analytical methods, however, IR spectroscopy can prove to be a very valuable tool, given the information it provides about the presence or absence of key functional groups. IR can also be a quick and convenient way for a chemist to check to see if a reaction has proceeded as planned. If we were to run a reaction in which we wished to convert cyclohexanone to cyclohexanol, for example, a quick comparison of the IR spectra of starting compound and product would tell us if we had successfully converted the ketone group to an alcohol.

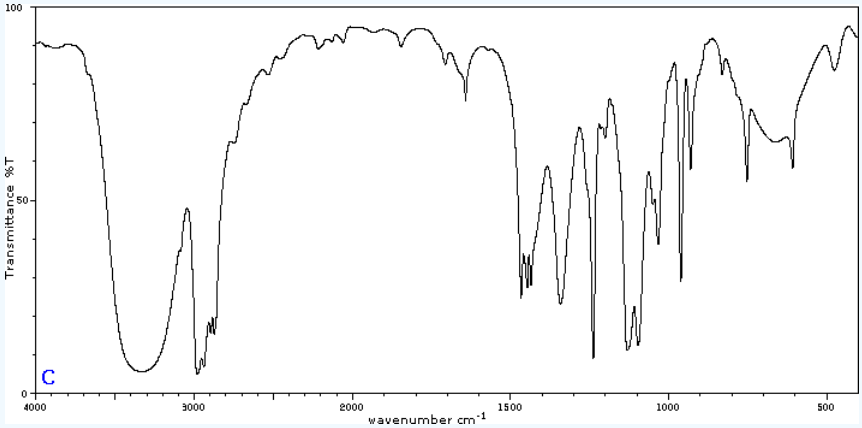
Example 3.7.1

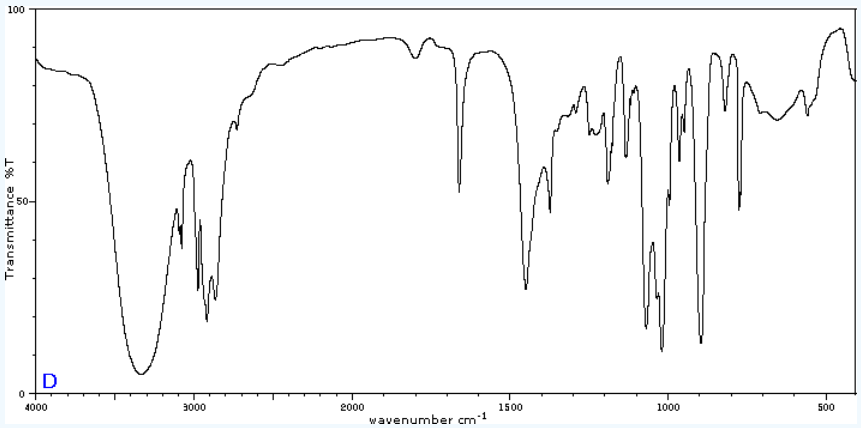
To illustrate the usefulness of infrared absorption spectra, examples for five C_4H_8O isomers are presented below their corresponding structural formulas. Try to associate each spectrum with one of the isomers in the row above it.

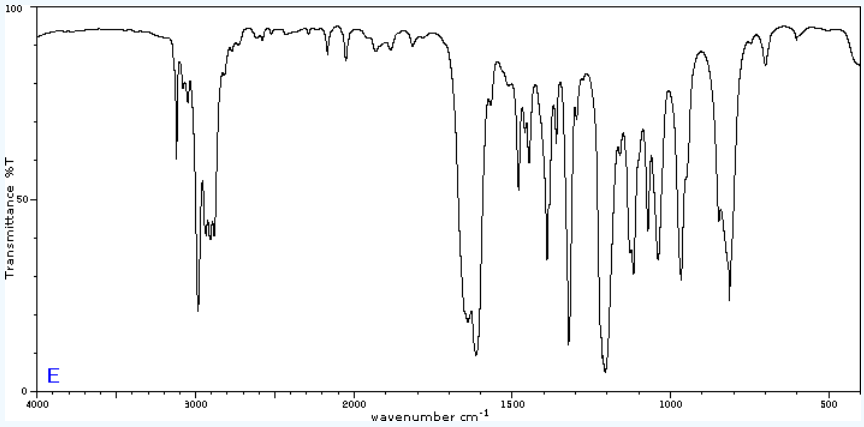


https://chem.libretexts.org/@go/page/167020



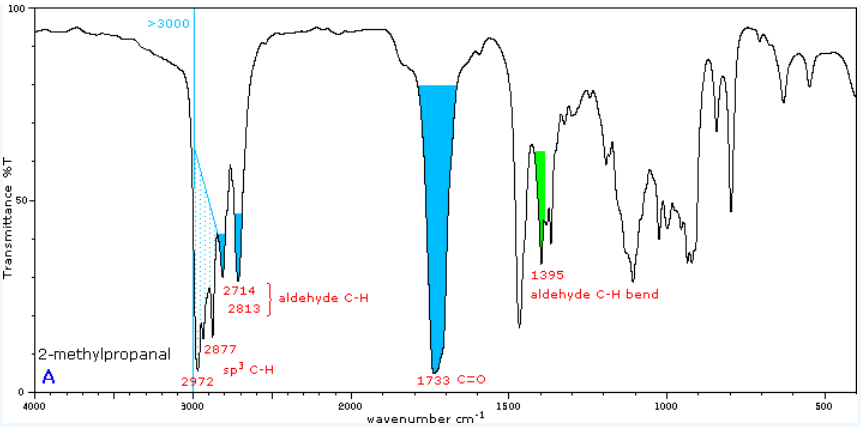


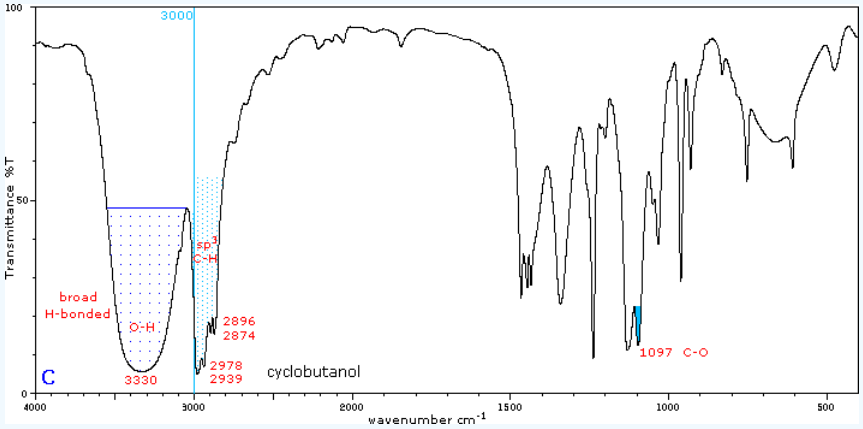


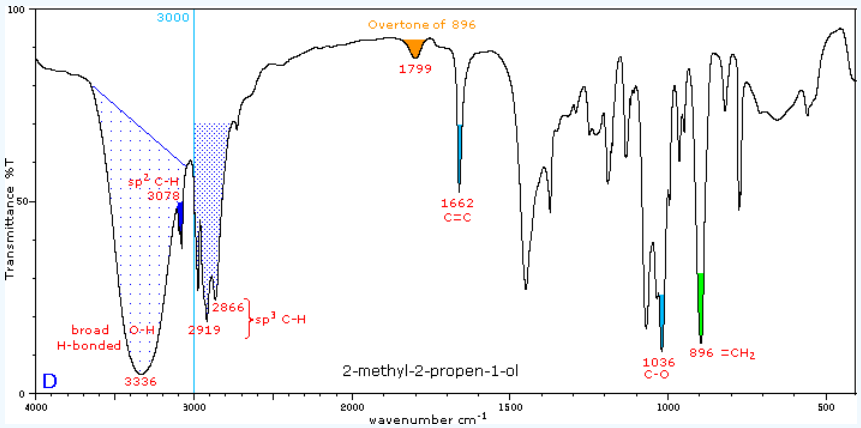


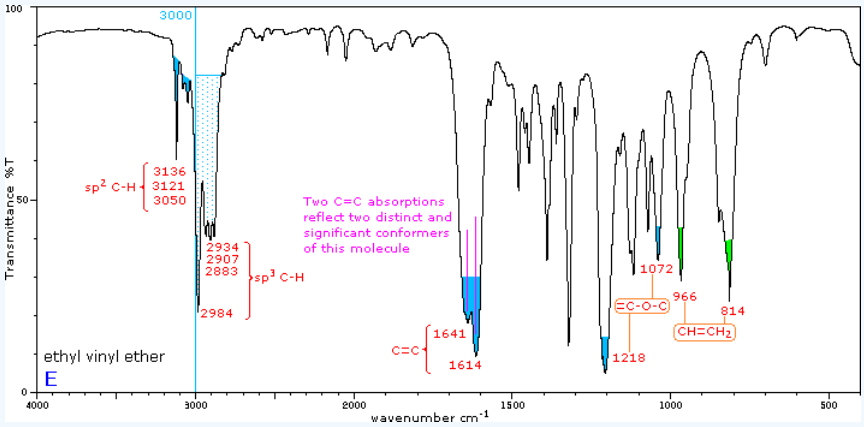
Solution

https://chem.libretexts.org/@go/page/167020









https://chem.libretexts.org/@go/page/167020

Exercises

Exercise 3.7.1

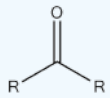
What functional groups give the following signals in an IR spectrum?

A – 1700 cm^{-1}

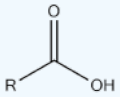
B – 1550 cm^{-1}

C – 1700 cm^{-1} and 2510-3000 cm^{-1}

Answer

A)  Carbonyl

B)  Nitro

C)  Carboxylic Acid

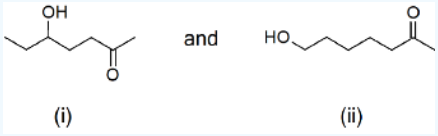
Exercise 3.7.2

How can you distinguish the following pairs of compounds through IR analysis?

A) CH_3OH (methanol) and $CH_3CH_2OCH_2CH_3$ (diethylether)

B) Cyclopentane and 1-pentene.

C)



Answer

A) A OH peak will be present around 3300 cm^{-1} for methanol and will be absent in the ether.

B) 1-pentene will have a alkene peak around 1650 cm^{-1} for the C=C and there will be another peak around 3100 cm^{-1} for the sp^2 C-H group on the alkene

C) Cannot distinguish these two isomers. They both have the same functional groups and therefore would have the same peaks on an IR spectra.

Questions

Q12.7.1

What functional groups give the following signals in an IR spectrum?

A) 1700 cm^{-1}

B) 1550 cm^{-1}

C) 1700 cm^{-1} and 2510-3000 cm^{-1}

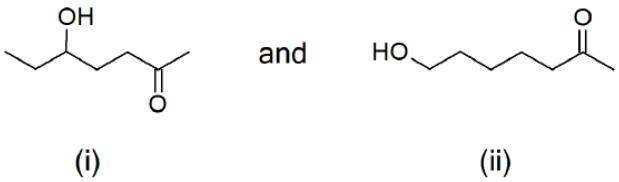
Q12.7.2

How can you distinguish the following pairs of compounds through IR analysis?

A) CH_3OH (Methanol) and $CH_3CH_2OCH_2CH_3$ (Diethylether)

B) Cyclopentane and 1-pentene.

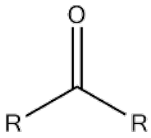
C)

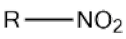


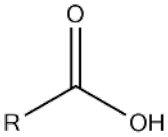
(i) (ii)

Solutions

S12.7.1

A)  Carbonyl

B)  Nitro

C)  Carboxylic Acid

S12.7.2

A) A OH peak will be present around 3300 cm^{-1} for methanol and will be absent in the ether.

B) 1-pentene will have a alkene peak around 1650 cm^{-1} for the C=C and there will be another peak around 3100 cm^{-1} for the sp^2 C-H group on the alkene

C) Cannot distinguish these two isomers. They both have the same functional groups and therefore would have the same peaks on an IR spectra.

Contributors and Attributions

- Dr. Dietmar Kennepohl FCIC (Professor of Chemistry, Athabasca University)
- Prof. Steven Farmer (Sonoma State University)
- William Reusch, Professor Emeritus (Michigan State U.), Virtual Textbook of Organic Chemistry
- **Organic Chemistry With a Biological Emphasis** by Tim Soderberg (University of Minnesota, Morris)

3.7: Interpreting Infrared Spectra is shared under a CC BY-NC-SA 4.0 license and was authored, remixed, and/or curated by LibreTexts.

SECTION OVERVIEW

3.8: Interpreting Infrared Spectra

This chapter will focus on infrared (IR) spectroscopy. The wavelengths found in infrared radiation are a little longer than those found in visible light. IR spectroscopy is useful for finding out what kinds of bonds are present in a molecule, and knowing what kinds of bonds are present is a good start towards knowing what the structure could be.

Topic hierarchy

Contributors

- Chris P Schaller, Ph.D., (College of Saint Benedict / Saint John's University)

This page titled 3.8: Interpreting Infrared Spectra is shared under a CC BY-NC 3.0 license and was authored, remixed, and/or curated by Chris Schaller.

Carbon Nitrogen Bonds

The IR spectra of nitrogen-containing compounds can be messier than the ones you have seen so far. N-H bends and C-N stretches tend to be broader and weaker than peaks involving oxygen atoms. However, some peaks in nitrogen compounds are useful. The problems in this section will guide you through some of these features.

Contributors and Attributions

Chris P Schaller, Ph.D., (College of Saint Benedict / Saint John's University)

This page titled Carbon Nitrogen Bonds is shared under a CC BY-NC 3.0 license and was authored, remixed, and/or curated by Chris Schaller.

- **Carbon Nitrogen Bonds** by Chris Schaller is licensed CC BY 3.0.

IR10. More Practice with IR Spectra

Contributors and Attributions

Chris P Schaller, Ph.D., (College of Saint Benedict / Saint John's University)

This page titled IR10. More Practice with IR Spectra is shared under a CC BY-NC 3.0 license and was authored, remixed, and/or curated by Chris Schaller.

- **IR10. More Practice with IR Spectra** by Chris Schaller is licensed CC BY 3.0.

IR2. Hydrocarbon Spectra

All organic and biological compounds contain carbon and hydrogen, usually with various other elements as well. Hydrocarbons are compounds containing only carbon and hydrogen, but no other types of atoms. Since all organic compounds contain carbon and hydrogen, looking at hydrocarbon spectra will tell us what peaks are due to the basic C&H part of these molecules. It is sometimes useful to think of the C&H part of a molecule as the basic skeleton or scaffolding used to construct the molecule. The other atoms often form more interesting and active features, like the doors, windows and lights on a building.

The simplest hydrocarbons contain only single bonds between their carbons, and no double or triple bonds. These hydrocarbons are variously referred to as saturated hydrocarbons, paraffins or alkanes. Examples of alkanes include hexane and nonane. (You can take a look at the Glossary to see what these names tell you about the structure.)



hexane

Look at the IR spectrum of hexane. You should see:

- Source: SDBSWeb : http://riodb01.ibase.aist.go.jp/sdbs/ (National Institute of Advanced Industrial Science and Technology of Japan, 14 July 2008)

  If you look at an IR spectrum of any other alkane, you will also see peaks at about 2900 and 1500 cm^{-1}. The IR spectra of many organic compounds will show these peaks because the compound may contain paraffinic parts in addition to parts with other elements in them.

  - Chris P Schaller, Ph.D., (College of Saint Benedict / Saint John's University)

This page titled IR2. Hydrocarbon Spectra is shared under a CC BY-NC 3.0 license and was authored, remixed, and/or curated by Chris Schaller.

- **IR2. Hydrocarbon Spectra** by Chris Schaller is licensed CC BY 3.0.

IR3. Subtle Points of IR Spectroscopy

Alkanes show two sets of peaks in the IR spectrum. Alkanes contain two kinds of bonds: C-C bonds and C-H bonds. However, these two facts are not related. The reasons are explained through bond polarity and molecular vibrations.

Bond polarity can play a role in IR spectroscopy.

- Molecular vibrations play a major role in IR spectroscopy.
  - The factors that govern what bonds (and what vibrations) show up at what frequencies are easily handled by computational chemistry software. In fact, prediction of absorption frequencies in IR spectra can be done using 17th century classical mechanics, specifically Hooke's Law (devised to explain the vibrational frequencies of springs). Computation is not the focus of this chapter but it may help you keep track of what kinds of vibrations absorb at what frequencies.

    Hooke's Law states:

    - IR light is absorbed if it is in resonance with a vibrating bond; that means the light's frequency is the same as the frequency of the bond vibration, or else an exact multiple of it (2x, 3x, 4x...). It's a little like pushing a child on a swing: unless you are pushing at the same frequency that the swing is swinging, you will not be able to transfer your energy to the swing.

      Hooke's Law in IR spectroscopy means:

      - Remember, there are two factors here, so you won't be able to make predictions knowing only one factor. Some strong bonds may not absorb at high frequency because they are between heavy atoms. The information is presented mostly to help you organize what bonds absorb at what general frequencies after you have learned about them.

        The reasons explaining why C-H bending vibrations are at lower frequency than C-H stretching vibrations are also related to Hooke's Law. An H-C-H bending vibration involves three atoms, not just two, so the mass involved is greater than in a C-H stretch. That means lower frequency. Also, it turns out that the "stiffness" of a bond angle (analogous to the strength of a spring) is less than the "stiffness" of a bond length; the angle has a little more latitude to change than does the length. Both factors lead to a lower bending frequency.

Contributors and Attributions

This page titled IR3. Subtle Points of IR Spectroscopy is shared under a CC BY-NC 3.0 license and was authored, remixed, and/or curated by Chris Schaller.

- **IR3. Subtle Points of IR Spectroscopy** by Chris Schaller is licensed CC BY 3.0.

IR4. Carbon Carbon Multiple Bonds

Unsaturated hydrocarbons contain only carbon and hydrogen, but also have some multiple bonds between carbons. One type of unsaturated hydrocarbon is an olefin, also known as an alkene. Alkenes contain double bonds between carbons. One example of an alkene is 1-heptene. It looks similar to hexane, except for the double bond from the first carbon to the second.

1-heptene

Look at the IR spectrum of 1-heptene. You should see:

- Source: SDBSWeb : http://riodb01.ibase.aist.go.jp/sdbs/ (National Institute of Advanced Industrial Science and Technology of Japan, 14 July 2008)

  So far, these peaks are the same as the ones seen for hexane. We can assign them as the C-H stretching and bending frequencies, respectively.

  Looking further, you will also see:

  - The peak at 3100 cm^{-1} hardly seems different from the C-H stretch seen before. It is also a C-H stretch, but from a different type of carbon. This stretch involves the sp^2 or trigonal planar carbon of the double bond, whereas the peak at 2900 involves an sp^3 or tetrahedral carbon.

    The peak at 1650 cm^{-1} can be identified via computational methods as arising from a carbon-carbon double bond stretch. It is a weak stretch because this bond is not very polar. Sometimes it is obscured by other, larger peaks.

Contributors and Attributions

Chris P Schaller, Ph.D., (College of Saint Benedict / Saint John's University)

This page titled IR4. Carbon Carbon Multiple Bonds is shared under a CC BY-NC 3.0 license and was authored, remixed, and/or curated by Chris Schaller.

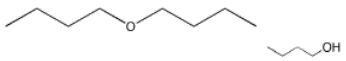
- **IR4. Carbon Carbon Multiple Bonds** by Chris Schaller is licensed CC BY 3.0.

IR5. Carbon Oxygen Single Bonds

These bonds are pretty polar, so they show up strongly in IR spectroscopy. IR spectroscopy is therefore a good way to determine what heteroatom-containing functional groups are present in a molecule.

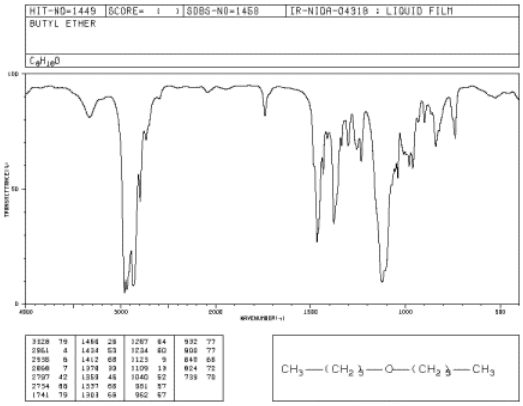
Compounds Containing C-O Single Bonds

Oxygen forms two bonds. An oxygen atom could be found in between two carbons, as in dibutyl ether, or between a carbon and a hydrogen as in 1-butanol. Dibutyl ether is an example of an ether and 1-butanol is an example of an alcohol.



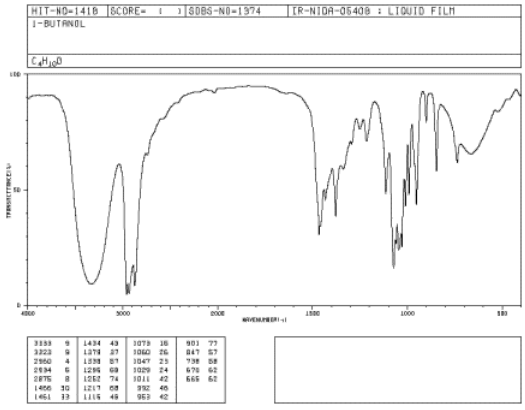
dibutyl ether or butyl ether 1-butanol

If you look at an IR spectrum of dibutyl ether, you will see:



- Source: SDBSWeb : http://riodb01.ibase.aist.go.jp/sdbs/ (National Institute of Advanced Industrial Science and Technology of Japan, 14 July 2008)

  If you look at an IR spectrum of 1-butanol, you will see:



  - Source: SDBSWeb : http://riodb01.ibase.aist.go.jp/sdbs/ (National Institute of Advanced Industrial Science and Technology of Japan, 14 July 2008)

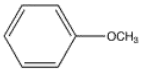
    Peak shapes are sometimes very useful in recognizing what kind of bond is present. The rounded shape of most O-H stretching modes occurs because of hydrogen bonding between different hydroxy groups. Because protons are shared to varying extent with neighboring oxygens, the covalent O-H bonds in a sample of alcohol all vibrate at slightly different frequencies and show up at slightly different positions in the IR spectrum. Instead of seeing one sharp peak, you see a whole lot of them all smeared out into one broad blob. Since C-H bonds don't hydrogen bond very well, you don't see that phenomenon in an ether, and an O-H peak is very easy to distinguish in the IR spectrum.

Problem IR.7.

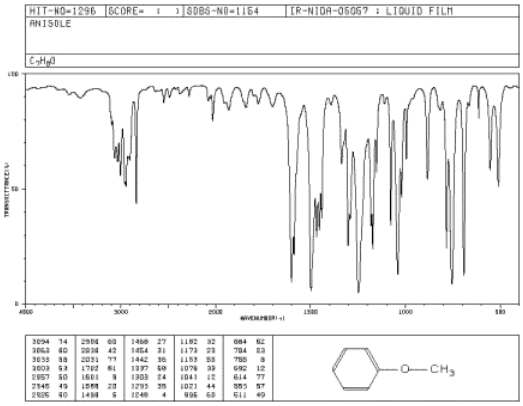
Even though there are only two C-O bonds in dibutyl ether, the C-O stretching mode is even stronger than the peak at 2900 cm^{-1} arising from 10 different C-H bonds. Explain why.

Problem IR.8.

The IR spectrum of methyl phenyl ether (aka anisole) has strong peaks at 1050 and 1250 cm^{-1}.



methoxybenzene

1. 

Source: SDBSWeb : http://riodb01.ibase.aist.go.jp/sdbs/ (National Institute of Advanced Industrial Science and Technology of Japan, 14 July 2008)

Contributors

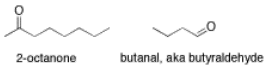
Chris P Schaller, Ph.D., (College of Saint Benedict / Saint John's University)

This page titled IR5. Carbon Oxygen Single Bonds is shared under a CC BY-NC 3.0 license and was authored, remixed, and/or curated by Chris Schaller.

- **IR5. Carbon Oxygen Single Bonds** by Chris Schaller is licensed CC BY 3.0.

IR6. Carbon Oxygen Double Bonds

The largest class of oxygen-containing molecules is carbonyl compounds, which contain C=O bonds. A C=O stretch is normally easy to find in an IR spectrum, because it is very strong and shows up in a part of the spectrum that is not cluttered with other peaks. Examples of carbonyl compounds include 2-octanone, a ketone, and butanal, an aldehyde. In an aldehyde, the carbonyl is at the end of a chain, with a hydrogen attached to the carbonyl carbon.



If you look at the IR spectrum of 2-octanone:

- Source: SDBSWeb : http://riodb01.ibase.aist.go.jp/sdbs/ (National Institute of Advanced Industrial Science and Technology of Japan, 14 July 2008)

  Even though there is just one C=O bond, the carbonyl stretch is often the strongest peak in the spectrum. That makes carbonyl compounds easy to identify by IR spectroscopy.

  If you look at the IR spectrum of butanal:

  - Source: SDBSWeb : http://riodb01.ibase.aist.go.jp/sdbs/ (National Institute of Advanced Industrial Science and Technology of Japan, 14 July 2008)

    The aldehyde C-H bond absorbs at two frequencies because it can vibrate in phase with the C=O bond (a symmetric stretch) and out of phase with the C=O bond (an asymmetric stretch), and these vibrations are of different energies. The probability of the symmetric stretch and the asymmetric stretch are about equal, so the two peaks are always about the same size. This unusual C-H peak can often be used to distinguish between an aldehyde and a ketone.

Contributors and Attributions

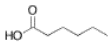
Chris P Schaller, Ph.D., (College of Saint Benedict / Saint John's University)

This page titled IR6. Carbon Oxygen Double Bonds is shared under a CC BY-NC 3.0 license and was authored, remixed, and/or curated by Chris Schaller.

- **IR6. Carbon Oxygen Double Bonds** by Chris Schaller is licensed CC BY 3.0.

IR8. More Complicated IR Spectra

Sometimes more complicated heteroatomic functional groups, containing bonds to more than one heteroatom, have slightly different spectra. Carboxylic acids feature a hydroxyl group bonded to a carbonyl. Hexanoic acid, a carboxylic acid in a six-atom chain, is one example.



hexanoic acid

If you look at the IR spectrum of hexanoic acid:

- Source: SDBSWeb : http://riodb01.ibase.aist.go.jp/sdbs/ (National Institute of Advanced Industrial Science and Technology of Japan, 14 July 2008)

  At first, the O-H peak appears to be absent. The C-H stretch appears to be very broad. The wide peak between 3000 and 2600 cm^{-1} is really the usual C-H stretch with a broad O-H stretch superimposed on it. The low frequency vibration of this O-H bond is related to the partial dissociation of protons due to strong hydrogen bonding.

Contributors and Attributions

Chris P Schaller, Ph.D., (College of Saint Benedict / Saint John's University)

This page titled IR8. More Complicated IR Spectra is shared under a CC BY-NC 3.0 license and was authored, remixed, and/or curated by Chris Schaller.

- **IR8. More Complicated IR Spectra** by Chris Schaller is licensed CC BY 3.0.

IR9. Misleading Peaks

There are some practical problems that can make IR interpretation in real life more difficult. Being aware of these problems may make you double-check your suspicions:

- In addition, there are complications that you may run into based on the instrument or technique used to obtain the spectrum.
  - Chris P Schaller, Ph.D., (College of Saint Benedict / Saint John's University)

This page titled IR9. Misleading Peaks is shared under a CC BY-NC 3.0 license and was authored, remixed, and/or curated by Chris Schaller.

- **IR9. Misleading Peaks** by Chris Schaller is licensed CC BY 3.0.

IR Table of Organic Compounds

Table of IR Absorptions Common. Note: strong, medium, weak refers to the length of the peak (in the y axis direction). Note: spectra taken by ATR method (used at CSB/SJU) have weaker peaks between 4000-2500 cm^{-1} compared to reference spectra taken by transmittance methods (typical on SDBS and other sites).

Approximate Frequency (cm^{-1})	Description	Bond Vibration	Notes
3500 - 3200	broad, round	O-H	much broader, lower frequency (3200-2500) if next to C=O
3400-3300	weak, triangular	N-H	stronger if next to C=O
3300	medium-strong	=C-H (sp C-H)	
3100-3000	weak-medium	=C-H (sp2 C-H)	can get bigger if lots of bonds present
3000-2900	weak-medium	-C-H (sp3 C-H)	can get bigger if lots of bonds present
2800 and 2700	medium	C-H in O=C-H	two peaks; "alligator jaws"
2250	medium	C=N	
2250-2100	weak-medium	C=C	stronger if near electronegative atoms
1800-1600	strong	C=O	lower frequency (1650-1550) if attached to O or N middle frequency if attached to C, H higher frequency (1800) if attached to Cl
1650-1450	weak-medium	C=C	lower frequency (1600-1450) if conjugated (i.e. C=C-C=C) often several if benzene present
1450	weak-medium	H-C-H bend	
1300 - 1000	medium-strong	C-O	higher frequency (1200-1300) if conjugated (i.e. O=C-O or C=C-O)
1250-1000	medium	C-N	
1000-650	strong	C=C-H bend	often several if benzene present

Contributors and Attributions

Chris P Schaller, Ph.D., (College of Saint Benedict / Saint John's University)

This page titled IR Table of Organic Compounds is shared under a CC BY-NC 3.0 license and was authored, remixed, and/or curated by Chris Schaller.

- **IR11. Appendix: IR Table of Organic Compounds** by Chris Schaller is licensed CC BY 3.0.

What Does an IR Spectrum Look Like?

A spectrum is a graph in which the amount of light absorbed is plotted on the y-axis and frequency is plotted on the x-axis. An example is shown below. You can run your finger along the graph and see whether any light of a particular frequency is absorbed; if so, you will see a "peak" at that frequency. If not, you will see "the baseline" at that frequency.

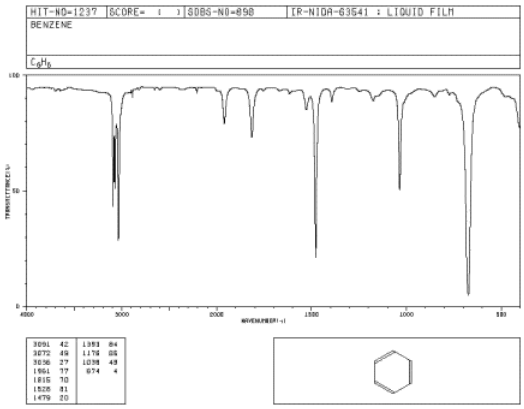


Figure IR1. IR spectrum of benzene. The x-axis labels are, from right to left, 500, 1000, 1500, 2000, 3000 and 4000 cm-1.

Source: SDBSWeb : http://riodb01.ibase.aist.go.jp/sdbs/ (National Institute of Advanced Industrial Science and Technology of Japan, 14 July 2008)

In IR spectra (spectra = plural of spectrum):

- As you run your finger from left to right across an IR spectrum, you can see whether or not light is absorbed at particular frequencies. When the curve dips down, less light is transmitted. That means light is absorbed. The dip in the graph is called a peak. Different bonds absorb different frequencies of light, so the peaks tell you what kinds of bonds are present.

Contributors and Attributions

This page titled What Does an IR Spectrum Look Like? is shared under a CC BY-NC 3.0 license and was authored, remixed, and/or curated by Chris Schaller.

- **What Does an IR Spectrum Look Like?** by Chris Schaller is licensed CC BY 3.0.

3.9: Interpretation

Infrared spectroscopy is the study of the interaction of infrared light with matter. The fundamental measurement obtained in infrared spectroscopy is an infrared spectrum, which is a plot of measured infrared intensity versus wavelength (or frequency) of light.

Introduction

In infrared spectroscopy, units called wavenumbers are normally used to denote different types of light. The frequency, wavelength, and wavenumber are related to each other via the following equation(1):

$$c = \nu\lambda$$

c = the speed of light (cm/sec)
ν = frequency in Hertz (sec^{-1})
λ = wavelength in cm

$$W = 1/\lambda$$

W = wavenumber in cm^{-1}
λ = wavelength in cm

(1)

These equations show that light waves may be described by their frequency, wavelength or wavenumber. Here, we typically refer to light waves by their wavenumber, however it will be more convenient to refer to a light wave's frequency or wavelength. The wavenumber of several different types of light are shown in table 1.

>14,000 cm^{-1} Visible UV & X-rays	14,000 to 4000cm^{-1} Near Infrared	4000 to 400cm^{-1} Mid Infrared	400 to 4cm^{-1} Far Infrared	<4cm^{-1} Microwaves Radio Waves
Higher Wavenumber				Lower Wavenumber
Higher Frequency				Lower Frequency
Higher Energy				Lower Energy
Shorter Wavelength				Longer Wavelength

Table 1. The Electromagnetic spectrum showing the wavenumber of several different types of light.

When a molecule absorbs infrared radiation, its chemical bonds vibrate. The bonds can stretch, contract, and bend. This is why infrared spectroscopy is a type of vibrational spectroscopy. Fortunately, the complex vibrational motion of a molecule can be broken down into a number of constituent vibrations called normal modes. For example, when a guitar string is plucked, the string vibrates at its normal mode frequency. Molecules, like guitar strings, vibrate at specfic frequencies so different molecules vibrate at different frequencies because their structures are different. This is why molecules can be distinguished using infrared spectroscopy. The first necessary condition for a molecule to absorb infrared light is that the molecule must have a vibration during which the change in dipole moment with respect to distance is non-zero. This condition can be summarized in equation(2) form as follows:

$$\frac{\partial \mu}{\partial x} \neq 0$$

∂μ = change in dipole moment
∂x = change in bond distance

(2)

Vibrations that satisfy this equation are said to be infrared active. The H-Cl stretch of hydrogen chloride and the asymmetric stretch of CO_2 are examples of infrared active vibrations. Infrared active vibrations cause the bands seen in an infrared spectrum.

The second necessary condition for infrared absorbance is that the energy of the light impinging on a molecule must equal a vibrational energy level difference within the molecule. This condition can be summarized in equation(3) form as follows:

$$\Delta E_{vib} = hcW$$

ΔE_{vib} = vibrational energy level difference in a molecule
h = Planck's Constant (Joule-sec)
c = the speed of light (cm/sec)
W = wavenumber in cm^{-1}

(3)

If the energy of a photon does not meet the criterion in this equation, it will be transmitted by the sample and if the photon energy satisfies this equation, that photon will be absorbed by the molecule.(See Infrared: Theory for more detail)

As any other analytical techniques, infrared spectroscopy works well on some samples, and poorly on others. It is important to know the strengths and weaknesses of infrared spectroscopy so it can be used in the proper way. Some advantages and disadvantages of infrared spectroscopy are listed in table 2.

Advantages	Disadvantages
Solids, Liquids, gases, semi-solids, powders and polymers are all analyzed The peak positions, intensities, widths, and shapes all provide useful information Fast and easy technique Sensitive technique (Micrograms of materials can be detected routinely) Inexpensive	Atoms or monatomic ions do not have infrared spectra Homonuclear diatomic molecules do not posses infrared spectra Complex mixture and aqueous solutions are difficult to analyze using infrared spectroscopy

Table 2. The Advantage and Disadvantage of Infrared Spectroscopy

Origin of Peak Positions, Intensities, and Widths

Peak Positions

The equation(4) gives the frequency of light that a molecule will absorb, and gives the frequency of vibration of the normal mode excited by that light.

$$\nu = \frac{1}{2\pi}\left(\frac{k}{\mu}\right)^{1/2} \quad (4)$$

ν = frequency in cm^{-1}

k = force constant in N/cm

μ = reduced mass in Kg

Only two variables in equation(4) are a chemical bond's force constant and reduced mass. Here, the reduced mass refers to $(M_1M_2)/(M_1+M_2)$ where M_1 and M_2 are the masses of the two atoms, respectively. These two molecular properties determine the wavenumber at which a molecule will absorb infrared light. No two chemical substances in the universe have the same force constants and atomic masses, which is why the infrared spectrum of each chemical substance is unique. To understand the effect of atomic masses and force constant on the positions of infrared bands, table 3 and 4 are shown as an example, respectively.

Table 3. An Example of an Mass Effect

Bond	C-H Stretch in cm^{-1}
C-^{1}H	~3000
C-^{2}D	~2120

The reduced masses of C-^{1}H and C-^{2}D are different, but their force constants are the same. By simply doubling the mass of the hydrogen atom, the carbon-hydrogen stretching vibration is reduced by over $800cm^{-1}$.

Table 4. An Example of an electronic Effect

Bond	C-H Stretch in cm^{-1}
C-H	~3000
H-C=O	~2750

When a hydrogen is attached to a carbon with a C=O bond, the C-H stretch band position decrease to $\sim 2750cm^{-1}$. These two C-H bonds have the same reduced mass but different force constants. The oxygen in the second molecule pulls electron density away from the C-H bond so it makes weaken and reduce the C-H force constant. This cause the C-H stretching vibration to be reduced by $\sim 250cm^{-1}$.

The Origin of Peak Intensities

The different vibrations of the different functional groups in the molecule give rise to bands of differing intensity. This is because $\frac{\partial \mu}{\partial x}$ is different for each of these vibrations. For example, the most intense band in the spectrum of octane shown in Figure 3 is at 2971, 2863 cm^{-1} and is due to stretching of the C-H bond. One of the weaker bands in the spectrum of octane is at 726cm^{-1}, and it is due to long-chain methyl rock of the carbon-carbon bonds in octane. The change in dipole moment with respect to distance for the C-H stretching is greater than that for the C-C rock vibration, which is why the C-H stretching band is the more intense than C-C rock vibration.

Another factor that determines the peak intensity in infrared spectra is the concentration of molecules in the sample. The equation(5) that relates concentration to absorbance is Beer's law,

$$A = \varepsilon l c \qquad (5)$$

A = absorbance

ε = absorptivity

l = pathlength

c = concentration

The absorptivity is the proportionality constant between concentration and absorbance, and is dependent on $(\partial\mu/\partial x)^2$. The absorptivity is an absolute measure of infrared absorbance intensity for a specific molecule at a specific wavenumber. For pure sample, concentration is at its maximum, and the peak intensities are true representations of the values of $\partial\mu/\partial x$ for different vibrations. However, in a mixture, two peaks may have different intensities because there are molecules present in different concentration.

The Orgins of Peak Widths

In general, the width of infrared bands for solid and liquid samples is determined by the number of chemical environments which is related to the strength of intermolecular interactions such as hydrogen bonding. Figure 1. shows hydrogen bond in water molecules and these water molecules are in different chemical environments. Because the number and strength of hydrogen bonds differs with chemical environment, the force constant varies and the wavenumber differs at which these molecules absorb infrared light.

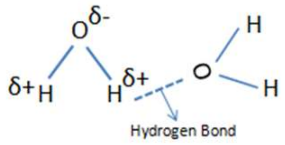


Figure 1. Hydrogen Bonding in water molecules

In any sample where hydrogen bonding occurs, the number and strength of intermolecular interactions varies greatly within the sample, causing the bands in these samples to be particularly broad. This is illustrated in the spectra of ethanol(Fig7) and hexanoic acid(Fig11). When intermolecular interactions are weak, the number of chemical environments is small, and narrow infrared bands are observed.

The Origin of Group Frequencies

An important observation made by early researchers is that many functional group absorb infrared radiation at about the same wavenumber, regardless of the structure of the rest of the molecule. For example, C-H stretching vibrations usually appear between 3200 and 2800cm^{-1} and carbonyl(C=O) stretching vibrations usually appear between 1800 and 1600cm^{-1}. This makes these bands diagnostic markers for the presence of a functional group in a sample. These types of infrared bands are called group frequencies because they tell us about the presence or absence of specific functional groups in a sample.

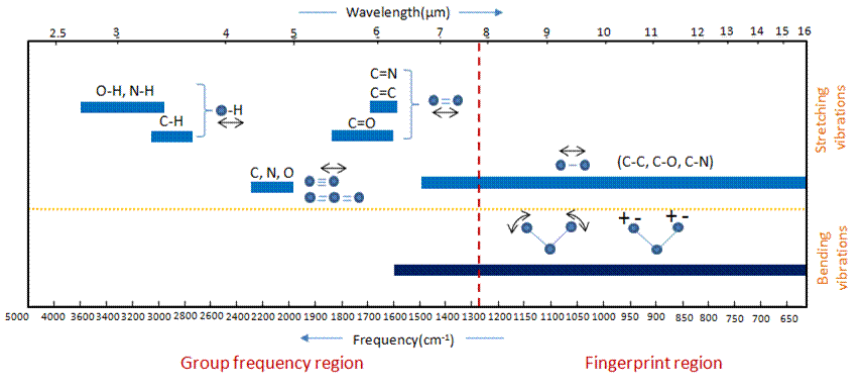


Figure 2. Group frequency and fingerprint regions of the mid-infrared spectrum

The region of the infrared spectrum from 1200 to 700 cm^{-1} is called the fingerprint region. This region is notable for the large number of infrared bands that are found there. Many different vibrations, including C-O, C-C and C-N single bond stretches, C-H bending vibrations, and some bands due to benzene rings are found in this region. The fingerprint region is often the most complex and confusing region to interpret, and is usually the last section of a spectrum to be interpreted. However, the utility of the fingerprint region is that the many bands there provide a fingerprint for a molecule.

Spectral Interpretation by Application of Group Frequencies

Organic Compounds

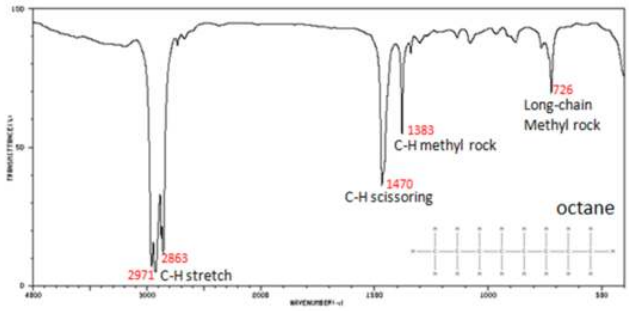
One of the most common application of infrared spectroscopy is to the identification of organic compounds. The major classes of organic molecules are shown in this category and also linked on the bottom page for the number of collections of spectral information regarding organic molecules.

Hydrocarbons

Hydrocarbons compounds contain only C-H and C-C bonds, but there is plenty of information to be obtained from the infrared spectra arising from C-H stretching and C-H bending.

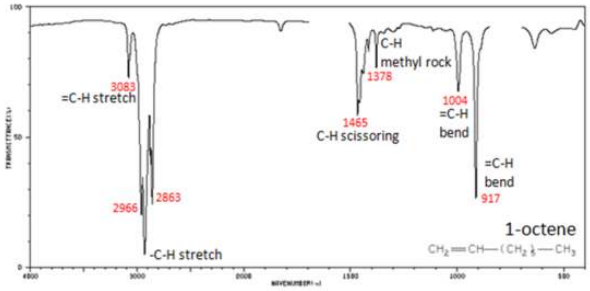
In alkanes, which have very few bands, each band in the spectrum can be assigned:

- Figure 3. shows the IR spectrum of octane. Since most organic compounds have these features, these C-H vibrations are usually not noted when interpreting a routine IR spectrum. Note that the change in dipole moment with respect to distance for the C-H stretching is greater than that for others shown, which is why the C-H stretch band is the more intense.



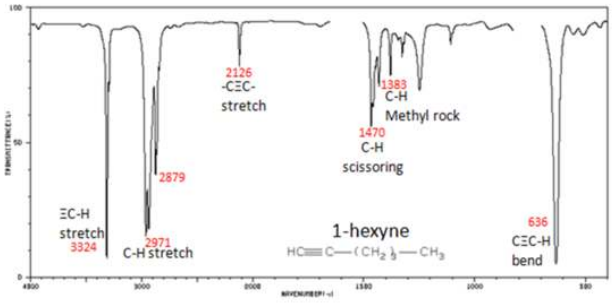
In alkenes compounds, each band in the spectrum can be assigned:

- Figure 4. shows the IR spectrum of 1-octene. As alkanes compounds, these bands are not specific and are generally not noted because they are present in almost all organic molecules.



In alkynes, each band in the spectrum can be assigned:

- The spectrum of 1-hexyne, a terminal alkyne, is shown below.



In aromatic compounds, each band in the spectrum can be assigned:

- Note that this is at slightly higher frequency than is the –C–H stretch in alkanes. This is a very useful tool for interpreting IR spectra. Only alkenes and aromatics show a C–H stretch slightly higher than 3000 cm^{-1}.

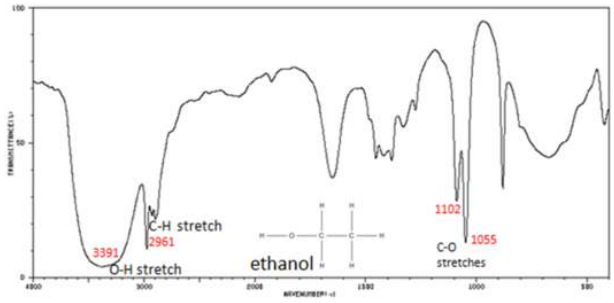
Figure 6. shows the spectrum of toluene.

Figure 6. Infrared Spectrum of Toluene

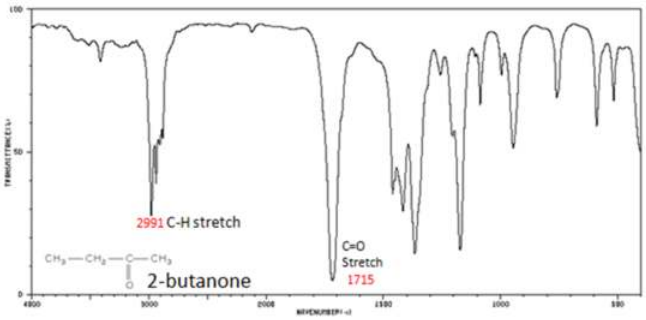
Functional Groups Containing the C-O Bond

Alcohols have IR absorptions associated with both the O-H and the C-O stretching vibrations.

- Figure 7. shows the spectrum of ethanol. Note the very broad, strong band of the O–H stretch.

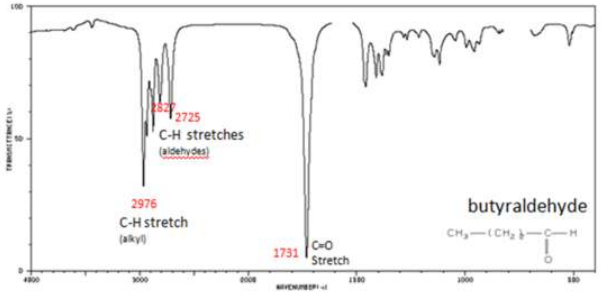


The carbonyl stretching vibration band C=O of saturated aliphatic ketones appears:



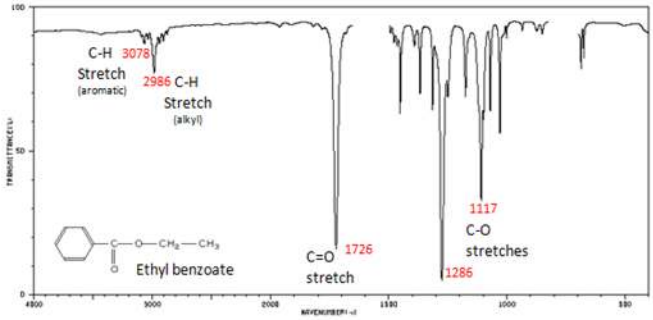
If a compound is suspected to be an aldehyde, a peak always appears around 2720 cm^{-1} which often appears as a shoulder-type peak just to the right of the alkyl C–H stretches.

- Figure 9. shows the spectrum of butyraldehyde.



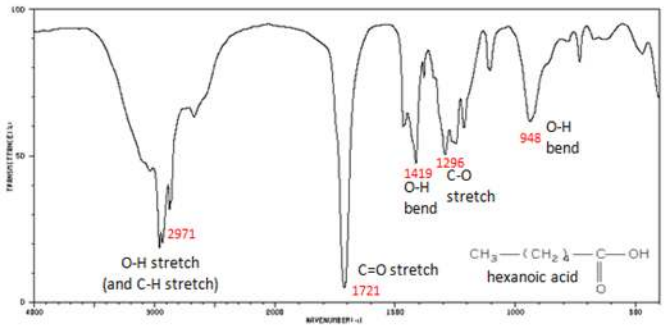
The carbonyl stretch C=O of esters appears:

- Figure 10. shows the spectrum of ethyl benzoate.

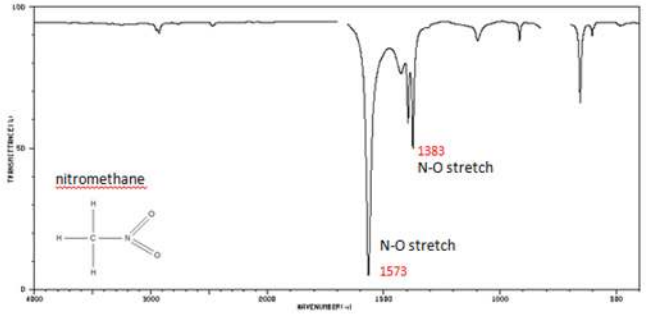


The carbonyl stretch C=O of a carboxylic acid appears as an intense band from 1760-1690 cm^{-1}. The exact position of this broad band depends on whether the carboxylic acid is saturated or unsaturated, dimerized, or has internal hydrogen bonding.

- Figure 11. shows the spectrum of hexanoic acid.



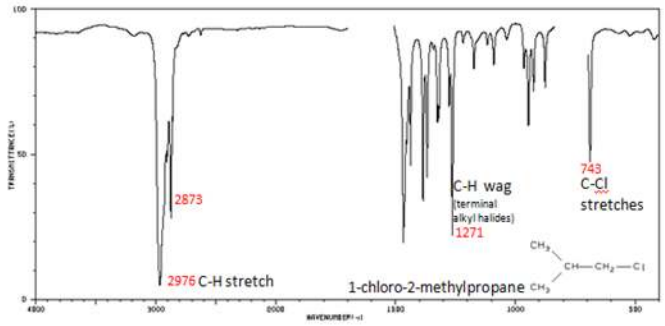
Organic Nitrogen Compounds



Organic Compounds Containing Halogens

Alkyl halides are compounds that have a C–X bond, where X is a halogen: bromine, chlorine, fluorene, or iodine.

- The spectrum of 1-chloro-2-methylpropane are shown below.



For more Infrared spectra Spectral database of organic molecules is introduced to use free database. Also, the infrared spectroscopy correlation tableis linked on bottom of page to find other assigned IR peaks.

Inorganic Compounds

Generally, the infrared bands for inorganic materials are broader, fewer in number and appear at lower wavenumbers than those observed for organic materials. If an inorganic compound forms covalent bonds within an ion, it can produce a characteristic infrared spectrum.

Main infrared bands of some common inorganic ions:

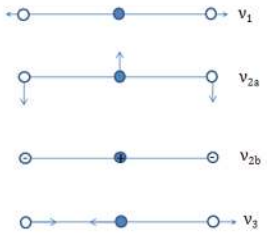
- Diatomic molecules produce one vibration along the chemical bond. Monatomic ligand, where metal s coordinate with atoms such as halogens, H, N or O, produce characteristic

bands. These bands are summarized in below.

Chracteristic infrared bands of diatomic inorganic molecules: M(metal), X(halogen)

- The normal modes of vibration of linear and bent triatomic molecules are illustrated and some common linear and bent triatomic molecules are shown below. Note that some molecules show two bands for $?_1$because of Fermi resonance.

  Characteristic infrared bands(cm^{-1}) of triatomic inorganic molecules:



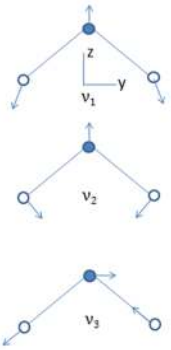
1388, 1286 3311 2053 714, 784 327

667 712 486, 471 380 249

2349 2049 748 2219 842

Bent Molecules H_2O O_3 $SnCl_2$

3675 1135 354



1595 716 120

3756 1089 334

Identification

There are a few general rules that can be used when using a mid-infrared spectrum for the determination of a molecular structure. The following is a suggested strategy for spectrum interpretation:[2]

1. Infrared spectroscopy is used to analyze a wide variety of samples, but it cannot solve every chemical analysis problem. When used in conjunction with other methods such as mass spectroscopy, nuclear magnetic resonance, and elemental analysis, infrared spectroscopy usually makes possible the positive identification of a sample.

References

1. Infrared Spectral Interpretation by Brian Smith, CRC Press, 1999
2. Infrared Spectroscopy: Fundamentals and Applications by Barbara Atuart, John Wiley&Sons, Ltd., 2004
3. Interpretation of Infrared Spectra, A Practical Approach by John Coates in Encyclopedia of Analytical Chemistry pp. 10815-10837, John Wiley&Sons Ltd, Chichester, 2000

Outside Links

- Spectral Database for Organic Compounds SDBS: http://riodb01.ibase.aist.go.jp/sdbs/ (National Institute of Advanced Industrial Science and Technology, date of access)
- Infrared Spectroscopy Correlation Table: en.Wikipedia.org/wiki/Infrared_spectroscopy_correlation_table
- FDM Reference Spectra Databases: http://www.fdmspectra.com/index.html
- Other Usuful Web Pages:
  - www.cem.msu.edu/~reusch/Virtu...d/infrared.htm
  - Fermi resonance : en.Wikipedia.org/wiki/Fermi_resonance

3.9: Interpretation is shared under a CC BY-NC-SA 4.0 license and was authored, remixed, and/or curated by LibreTexts.

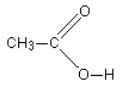
- **Infrared: Interpretation** is licensed CC BY 4.0.

3.10: Identifying the Presence of Particular Groups

This page explains how to use an infra-red spectrum to identify the presence of a few simple bonds in organic compounds.

The infrared spectrum for a simple carboxylic acid: Ethanoic acid

Ethanoic acid has the structure:



You will see that it contains the following bonds:

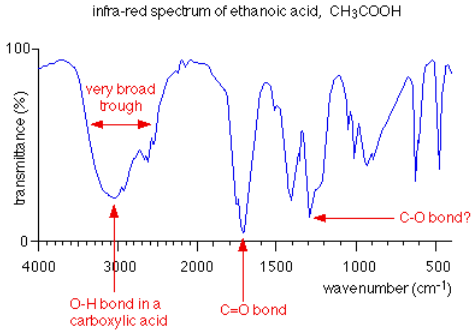
- carbon-oxygen double, C=O
- carbon-oxygen single, C-O
- oxygen-hydrogen, O-H
- carbon-hydrogen, C-H
- carbon-carbon single, C-C

The carbon-carbon bond has absorptions which occur over a wide range of wavenumbers in the fingerprint region - that makes it very difficult to pick out on an infra-red spectrum. The carbon-oxygen single bond also has an absorbtion in the fingerprint region, varying between 1000 and 1300 cm^{-1} depending on the molecule it is in. You have to be very wary about picking out a particular trough as being due to a C-O bond.

The other bonds in ethanoic acid have easily recognized absorptions outside the fingerprint region.

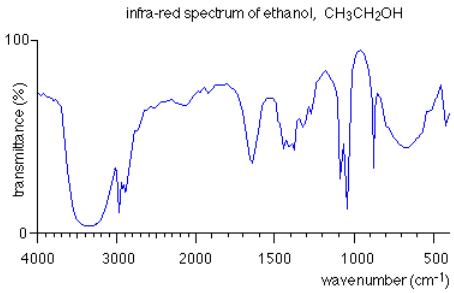
- The C-H bond (where the hydrogen is attached to a carbon which is singly-bonded to everything else) absorbs somewhere in the range from 2853 - 2962 cm^{-1}. Because that bond is present in most organic compounds, that's not terribly useful! What it means is that you can ignore a trough just under 3000 cm^{-1}, because that is probably just due to C-H bonds.
- The carbon-oxygen double bond, C=O, is one of the really useful absorptions, found in the range 1680 - 1750 cm^{-1}. Its position varies slightly depending on what sort of compound it is in.
- The other really useful bond is the O-H bond. This absorbs differently depending on its environment. It is easily recognised in an acid because it produces a very broad trough in the range 2500 - 3300 cm^{-1}.

The infrared spectrum for ethanoic acid looks like this:



The possible absorption due to the C-O single bond is queried because it lies in the fingerprint region. You couldn't be sure that this trough wasn't caused by something else.

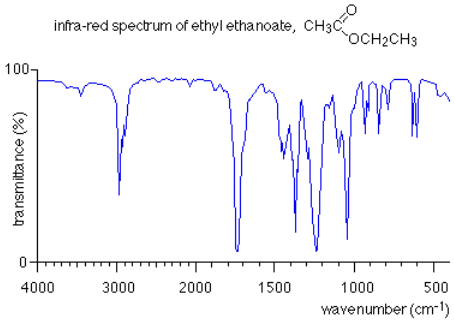
The infrared spectrum for an alcohol: Ethanol



The O-H bond in an alcohol absorbs at a higher wavenumber than it does in an acid - somewhere between 3230 - 3550 cm^{-1}. In fact this absorption would be at a higher number still if the alcohol isn't hydrogen bonded - for example, in the gas state. All the infra-red spectra on this page are from liquids - so that possibility will never apply.

> *Notice the absorption due to the C-H bonds just under 3000 cm^{-1}, and also the troughs between 1000 and 1100 cm^{-1} - one of which will be due to the C-O bond.*

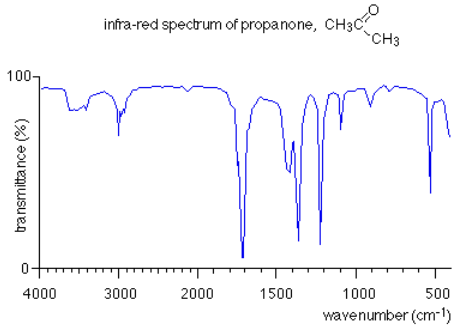
The infrared spectrum for an ester: Ethyl ethanoate



This time the O-H absorption is missing completely. Don't confuse it with the C-H trough fractionally less than 3000 cm^{-1}. The presence of the C=O double bond is seen at about 1740 cm^{-1}.

The C-O single bond is the absorption at about 1240 cm^{-1}. Whether or not you could pick that out would depend on the detail given by the table of data which you get in your exam, because C-O single bonds vary anywhere between 1000 and 1300 cm^{-1} depending on what sort of compound they are in. Some tables of data fine it down, so that they will tell you that an absorption from 1230 - 1250 is the C-O bond in an ethanoate.

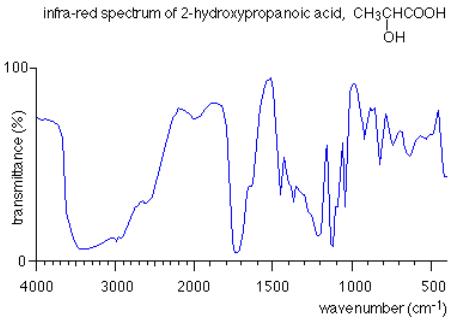
The infrared spectrum for a ketone: Propanone



You will find that this is very similar to the infra-red spectrum for ethyl ethanoate, an ester. Again, there is no trough due to the O-H bond, and again there is a marked absorption at about 1700 cm^{-1} due to the C=O.

Confusingly, there are also absorptions which look as if they might be due to C-O single bonds - which, of course, aren't present in propanone. This reinforces the care you have to take in trying to identify any absorptions in the fingerprint region. Aldehydes will have similar infra-red spectra to ketones.

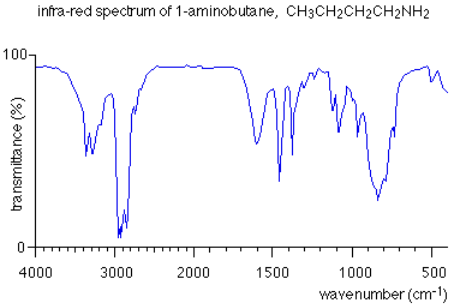
The infrared spectrum for a hydroxy-acid: 2-hydroxypropanoic acid (lactic acid)



This is interesting because it contains two different sorts of O-H bond - the one in the acid and the simple "alcohol" type in the chain attached to the -COOH group.

The O-H bond in the acid group absorbs between 2500 and 3300, the one in the chain between 3230 and 3550 cm^{-1}. Taken together, that gives this immense trough covering the whole range from 2500 to 3550 cm^{-1}. Lost in that trough as well will be absorptions due to the C-H bonds. Notice also the presence of the strong C=O absorption at about 1730 cm^{-1}.

The infrared spectrum for a primary amine: 1-aminobutane



Primary amines contain the $-NH_2$ group, and so have N-H bonds. These absorb somewhere between 3100 and 3500 cm^{-1}. That double trough (typical of primary amines) can be seen clearly on the spectrum to the left of the C-H absorptions.

Contributors and Attributions

- Jim Clark (Chemguide.co.uk)

This page titled 3.10: Identifying the Presence of Particular Groups is shared under a CC BY-NC 4.0 license and was authored, remixed, and/or curated by Jim Clark.

- **Identifying the Presence of Particular Groups** by Jim Clark is licensed CC BY-NC 4.0.

3.11: Infrared Spectra of Some Common Functional Groups

Objective

After completing this section, you should be able to use an infrared spectrum to determine the presence of functional groups, such as alcohols, amines and carbonyl groups, in an unknown compound, given a list of infrared absorption frequencies.

Study Notes

In Chapter 12.7, you should have learned, in broad terms, where a few key absorptions occur. Otherwise, to find the characteristic infrared absorptions of the various functional groups, refer to this IR table.

Spectral Interpretation by Application of Group Frequencies

One of the most common application of infrared spectroscopy is to the identification of organic compounds. The major classes of organic molecules are shown in this category and also linked on the bottom page for the number of collections of spectral information regarding organic molecules.

Hydrocarbons

Hydrocarbons compounds contain only C-H and C-C bonds, but there is plenty of information to be obtained from the infrared spectra arising from C-H stretching and C-H bending.

In alkanes, which have very few bands, each band in the spectrum can be assigned:

- C–H stretch from 3000–2850 cm^{-1}
- C–H bend or scissoring from 1470-1450 cm^{-1}
- C–H rock, methyl from 1370-1350 cm^{-1}
- C–H rock, methyl, seen only in long chain alkanes, from 725-720 cm^{-1}

Figure 3. shows the IR spectrum of octane. Since most organic compounds have these features, these C-H vibrations are usually not noted when interpreting a routine IR spectrum. Note that the change in dipole moment with respect to distance for the C-H stretching is greater than that for others shown, which is why the C-H stretch band is the more intense.

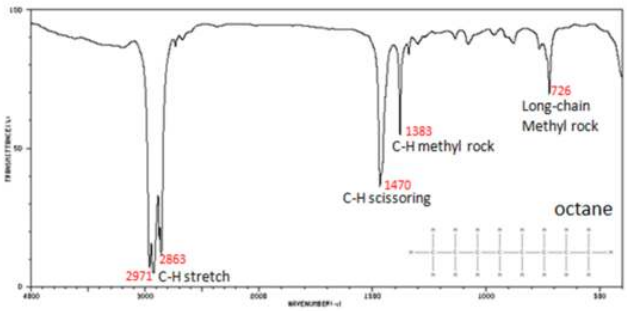


Figure 3. Infrared Spectrum of Octane

In alkenes compounds, each band in the spectrum can be assigned:

- C=C stretch from 1680-1640 cm^{-1}
- =C–H stretch from 3100-3000 cm^{-1}
- =C–H bend from 1000-650 cm^{-1}

Figure 4. shows the IR spectrum of 1-octene. As alkanes compounds, these bands are not specific and are generally not noted because they are present in almost all organic molecules.

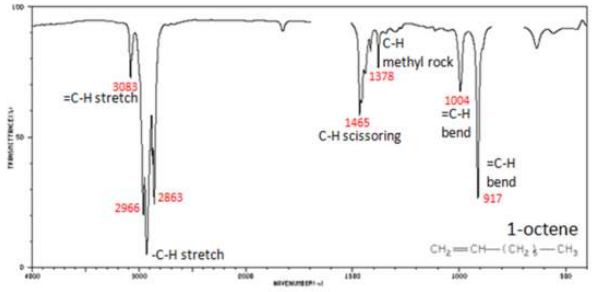


Figure 4. Infrared Spectrum of 1-Octene

In alkynes, each band in the spectrum can be assigned:

- –C≡C– stretch from 2260-2100 cm^{-1}
- –C≡C–H: C–H stretch from 3330-3270 cm^{-1}
- –C≡C–H: C–H bend from 700-610 cm^{-1}

The spectrum of 1-hexyne, a terminal alkyne, is shown below.

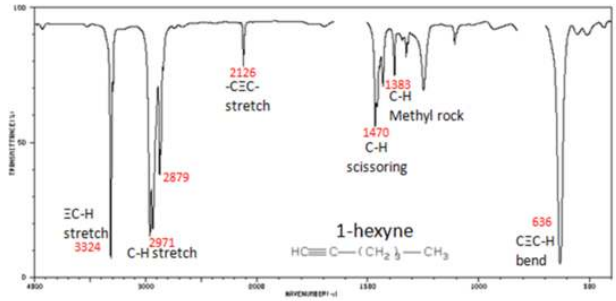


Figure 5. Infrared Spectrum of 1-Hexyne

In aromatic compounds, each band in the spectrum can be assigned:

- C–H stretch from 3100-3000 cm^{-1}
- overtones, weak, from 2000-1665 cm^{-1}
- C–C stretch (in-ring) from 1600-1585 cm^{-1}
- C–C stretch (in-ring) from 1500-1400 cm^{-1}
- C–H "oop" from 900-675 cm^{-1}

Note that this is at slightly higher frequency than is the –C–H stretch in alkanes. This is a very useful tool for interpreting IR spectra. Only alkenes and aromatics show a C–H stretch slightly higher than 3000 cm^{-1}.

Figure 6. shows the spectrum of toluene.

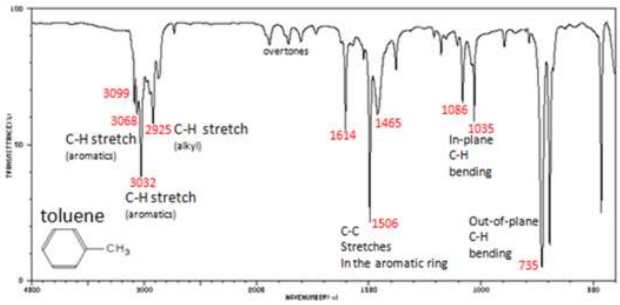


Figure 6. Infrared Spectrum of Toluene

Functional Groups Containing the C-O Bond

Alcohols have IR absorptions associated with both the O-H and the C-O stretching vibrations.

- O–H stretch, hydrogen bonded 3500-3200 cm^{-1}
- C–O stretch 1260-1050 cm^{-1} (s)

Figure 7. shows the spectrum of ethanol. Note the very broad, strong band of the O–H stretch.

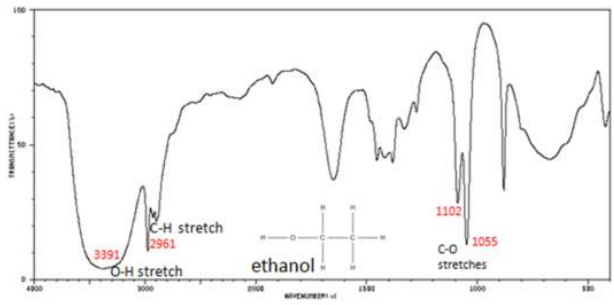


Figure 7. Infrared Spectrum of Ethanol

The carbonyl stretching vibration band C=O of saturated aliphatic ketones appears:

- C=O stretch - aliphatic ketones 1715 cm^{-1}
- α, β -unsaturated ketones 1685-1666 cm^{-1}

Figure 8. shows the spectrum of 2-butanone. This is a saturated ketone, and the C=O band appears at 1715.

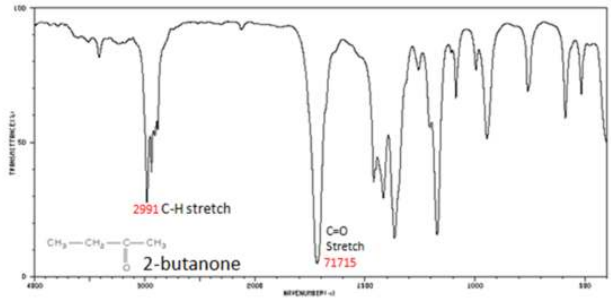


Figure 8. Infrared Spectrum of 2-Butanone

If a compound is suspected to be an aldehyde, a peak always appears around 2720 cm^{-1} which often appears as a shoulder-type peak just to the right of the alkyl C–H stretches.

- H–C=O stretch 2830-2695 cm^{-1}
- C=O stretch:
  - aliphatic aldehydes 1740-1720 cm^{-1}
  - α, β-unsaturated aldehydes 1710-1685 cm^{-1}

Figure 9. shows the spectrum of butyraldehyde.

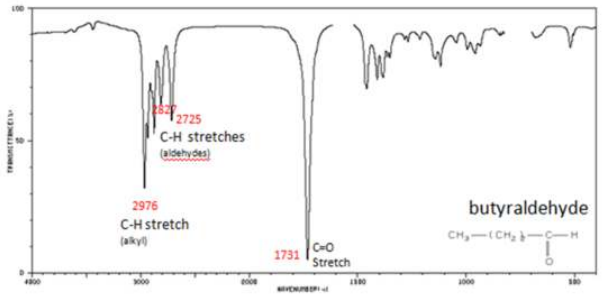


Figure 9. Infrared Spectrum of Butyraldehyde

The carbonyl stretch C=O of esters appears:

- C=O stretch
  - aliphatic from 1750-1735 cm^{-1}
  - α, β -unsaturated from 1730-1715 cm^{-1}
- C–O stretch from 1300-1000 cm^{-1}

Figure 10. shows the spectrum of ethyl benzoate.

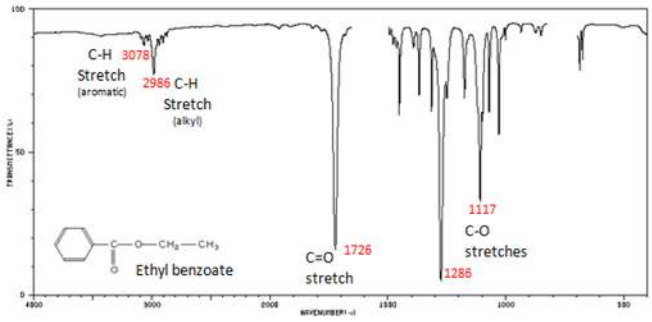


Figure 10. Infrared Spectrum of Ethyl benzoate

The carbonyl stretch C=O of a carboxylic acid appears as an intense band from 1760-1690 cm^{-1}. The exact position of this broad band depends on whether the carboxylic acid is saturated or unsaturated, dimerized, or has internal hydrogen bonding.

- O–H stretch from 3300-2500 cm^{-1}
- C=O stretch from 1760-1690 cm^{-1}
- C–O stretch from 1320-1210 cm^{-1}
- O–H bend from 1440-1395 and 950-910 cm^{-1}

Figure 11. shows the spectrum of hexanoic acid.

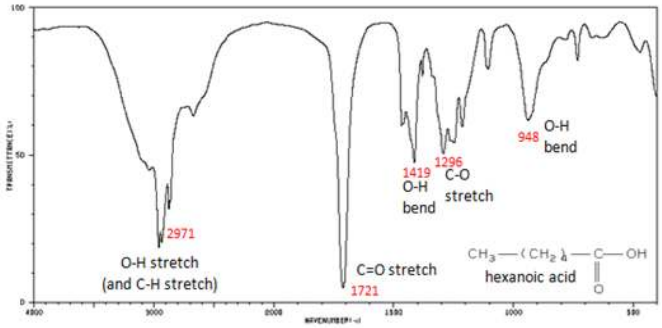


Figure 11. Infrared Spectrum of Hexanoic acid

Organic Nitrogen Compounds

- N–O asymmetric stretch from 1550-1475 cm^{-1}
- N–O symmetric stretch from 1360-1290 cm^{-1}

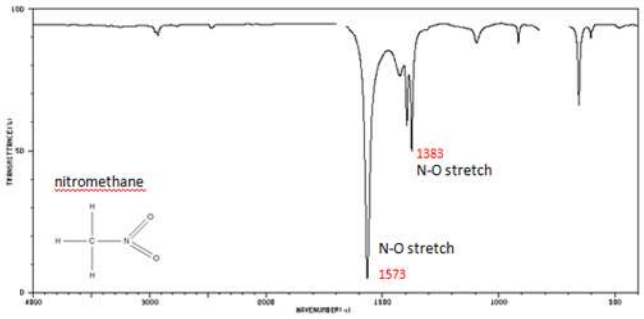


Figure 12. Infrared Spectrum of Nitomethane

Organic Compounds Containing Halogens

Alkyl halides are compounds that have a C–X bond, where X is a halogen: bromine, chlorine, fluorene, or iodine.

- C–H wag (-CH_2X) from 1300-1150 cm^{-1}
- C–X stretches (general) from 850-515 cm^{-1}
  - C–Cl stretch 850-550 cm^{-1}
  - C–Br stretch 690-515 cm^{-1}

The spectrum of 1-chloro-2-methylpropane are shown below.

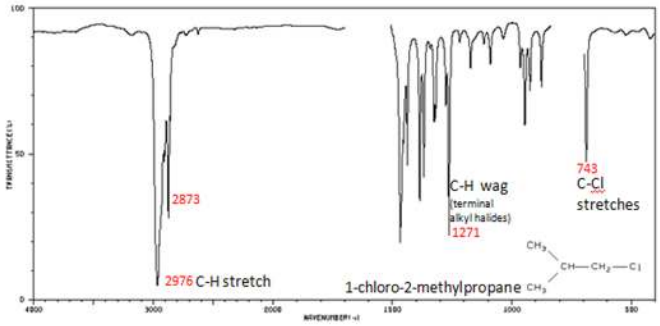


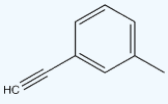
Figure 13. Infrared Spectrum of 1-chloro-2-methylpropane

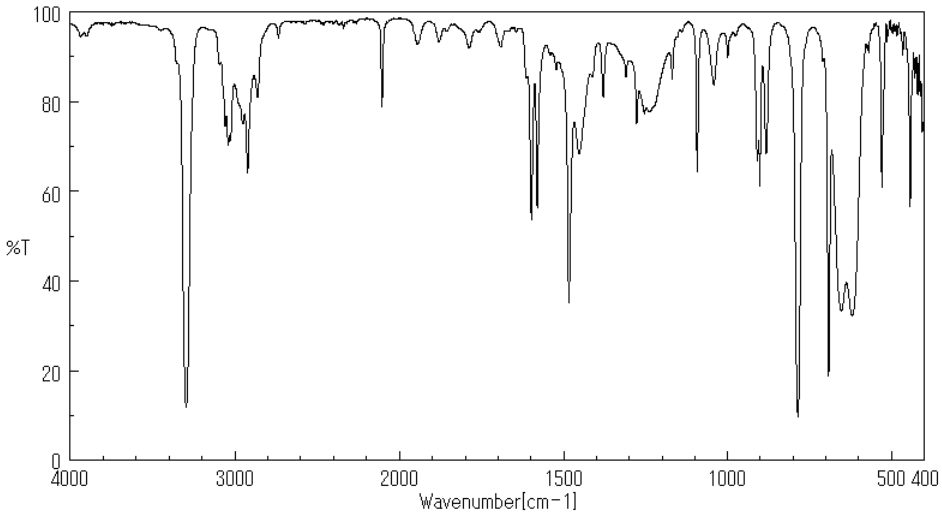
For more Infrared spectra Spectral database of organic molecules is introduced to use free database. Also, the infrared spectroscopy correlation table is linked on bottom of page to find other assigned IR peaks.

Exercises

? Exercise 3.11.1

The following spectrum is for the accompanying compound. What are the peaks that you can identify?





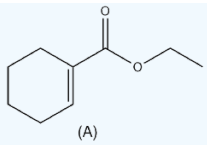
Answer

Frequency (cm^{-1})	Functional Group
3200	C≡C-H
2900-3000	C-C-H, C=C-H
2100	C≡C
1610	C=C

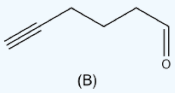
(There is also an aromatic undertone region between 2000-1600 which describes the substitution on the phenyl ring.)

? Exercise 3.11.2

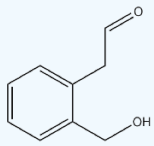
What absorptions would the following compounds have in an IR spectra?



(A)



(B)



(C)

Answer

A

Frequency (cm^{-1})	**Functional Group**
2900-3000	C-C-H, C=C-H
1710	C=O
1610	C=C
1100	C-O

B

Frequency (cm^{-1})	**Functional Group**
3200	C≡C-H

2900-3000	C-C-H, C=C-H
2100	C≡C
1710	C=O

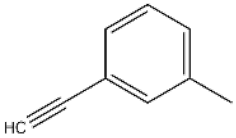
C

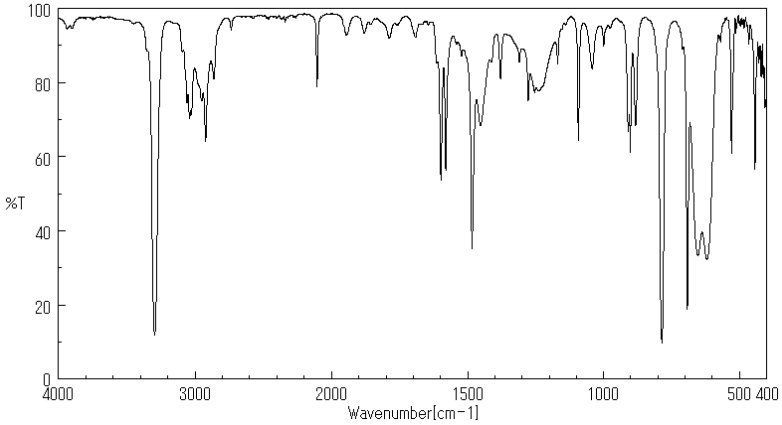
Frequency (cm^{-1})	**Functional Group**
3300 (broad)	O-H
2900-3000	C-C-H, C=C-H
2000-1800	Aromatic Overtones
1710	C=O
1610	C=C

Questions

Q12.8.1

The following spectra is for the accompanying compound. What are the peaks that you can I identify in the spectrum?

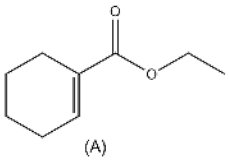




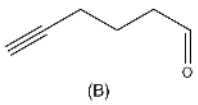
Source: SDBSWeb : http://sdbs.db.aist.go.jp (National Institute of Advanced Industrial Science and Technology, 2 December 2016)

Q12.8.2

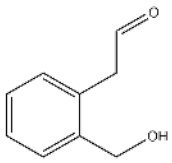
What absorptions would the following compounds have in an IR spectra?



(A)



(B)



(C)

Solutions

S12.8.1

Frequency (cm-1) Functional Group

3200 C≡C-H

2900-3000 C-C-H, C=C-H

2100 C≡C

1610 C=C

(There is also an aromatic undertone region between 2000-1600 which describes the substitution on the phenyl ring.)

S12.8.2

A)

Frequency (cm-1) Functional Group

2900-3000 C-C-H, C=C-H

1710 C=O

1610 C=C

1100 C-O

B)

Frequency (cm-1) Functional Group

3200 C≡C-H

2900-3000 C-C-H, C=C-H

2100 C≡C

1710 C=O

C)

Frequency (cm-1) Functional Group

3300 (broad) O-H

2900-3000 C-C-H, C=C-H

2000-1800 Aromatic Overtones

1710 C=O

1610 C=C

Contributors and Attributions

- Dr. Dietmar Kennepohl FCIC (Professor of Chemistry, Athabasca University)
- Prof. Steven Farmer (Sonoma State University)
- William Reusch, Professor Emeritus (Michigan State U.), Virtual Textbook of Organic Chemistry

3.11: Infrared Spectra of Some Common Functional Groups is shared under a CC BY-NC-SA 4.0 license and was authored, remixed, and/or curated by LibreTexts.

3.12: Application

Infrared spectroscopy, an analytical technique that takes advantage of the vibrational transitions of a molecule, has been of great significance to scientific researchers in many fields such as protein characterization, nanoscale semiconductor analysis and space exploration.

Introduction

Infrared spectroscopy is the study of interaction of infrared light with matter, which can be used to identify unknown materials, examine the quality of a sample or determine the amount of components in a mixture. Infrared light refers to electromagnetic radiation with wavenumber ranging from 13000 – 10 cm^{-1} (corresponding wavelength from 0.78 – 1000 μm). Infrared region is further divided into three subregions: near-infrared (13000 – 4000 cm^{-1} or 0.78 – 2.5 μm), mid-infrared (4000 – 400 cm^{-1} or 2.5 – 25 μm) and far-infrared (400 – 10 cm^{-1} or 25 – 1000 μm). The most commonly used is the middle infrared region, since molecules can absorb radiations in this region to induce the vibrational excitation of functional groups. Recently, applications of near infrared spectroscopy have also been developed.

By passing infrared light through a sample and measuring the absorption or transmittance of light at each frequency, an infrared spectrum is obtained, with peaks corresponding to the frequency of absorbed radiation. Since all groups have their characteristic vibrational frequencies, information regarding molecular structure can be gained from the spectrum. Infrared spectroscopy is capable of analyzing samples in almost any phase (liquid, solid, or gas), and can be used alone or in combination with other instruments following different sampling procedures. Besides fundamental vibrational modes, other factors such as overtone and combination bands, Fermi resonance, coupling and vibration-rotational bands also appear in the spectrum. Due to the high information content of its spectrum, infrared spectroscopy has been a very common and useful tool for structure elucidation and substance identification.

Instrumentation

Most commonly used instruments in infrared spectroscopy are dispersive infrared spectrometer and Fourier transform infrared spectrometer.

Dispersive infrared spectrometer

Dispersive infrared spectrometer is mainly composed of radiation source, monochromator and detector. For mid-infrared region, Globar (silicon carbide), Nernst glower (oxides of zirconium, yttrium and erbium) and metallic helices (chromium-nickel alloy or tungsten) are frequently used as radiation sources. Tungsten-halogen lamps and metallic conductors coated with ceramic are utilized as sources for near-infrared region. A mercury high-pressure lamp is suitable for far-infrared region.

Monochromator in conjunction with slits, mirrors and filters separates the wavelengths of light emitted. The dispersive elements within monochromator are prisms or gratings. Gratings have gradually replaced prisms due to their comparatively low cost and good quality. As shown in **Figure 1**, radiation passes through both a sample and a reference path. Then the beams are directed to a diffraction grating (splitter), which disperses the light into component frequencies and directs each wavelength through a slit to the detector. The detector produces an electrical signal and results in a recorder response.

Figure 1. Schematic illustration of dispersive infrared spectrometer. Figure from Wikipedia.

Two types of detectors are employed in dispersive infrared spectrometer, namely, thermal detectors and photon detectors. Thermal detectors include thermocouples, thermistors, and pneumatic devices, which measure the heating effect generated by infrared radiation. Photon detectors are semiconductor-based. Radiation is able to promote electrons in photon detectors from valence band to conduction band, generating a small current. Photon detectors have faster response and higher sensitivity than do thermal detectors but are more susceptible to thermal noise.

Fourier transform infrared spectrometer

Dispersive infrared spectrometer has many limitations because it examines component frequencies individually, resulting in slow speed and low sensitivity. Fourier transform infrared (FTIR) spectrometer is preferred over dispersive spectrometer, since it is capable of handling all frequencies simultaneously with high throughput, reducing the time required for analysis. The radiation sources used in dispersive infrared spectrometer can also be used in FTIR spectrometer.

In contrast with the monochromator in dispersive spectrometer, FTIR spectrometer as shown in **Figure 2** employs an interferometer. The beamsplitter within the interferometer splits the incoming infrared beam into two beams, one of which is reflected by a fixed mirror, while the other one reflected by a moving mirror perpendicular to the fixed one. The length of path one beam travels is fixed and that of the other one is changing as the mirror moves, generating an optical path difference between the two beams. After meeting back at the beamsplitter, the two beams recombine, interfere with each other, and yield an interferogram. The interferogram produces inference signal as a function of optical path difference. It is converted to a spectrum of absorbance or transmittance versus wavenumber or frequency by Fourier transform.

Figure 2. Schematic representation of Fourier transform infrared spectrometer. Figure from Wikipedia.

Detectors used in FTIR spectrometers are mainly pyroelectric and photoconductive detectors. The former are constructed of crystalline materials (such as deuterated triglycine sulfate) whose electric polarization rely on temperature. The change in temperature leads to change in charge distribution of the detector and electric signal is produced. The latter (such as mercury cadmium telluride) provide better sensitivity and faster speed than do pyroelectric detectors over a broad spectral range. However, liquid nitrogen is needed for cooling of photoconductive detectors.

Application

Since different molecules with different combination of atoms produce their unique spectra, infrared spectroscopy can be used to qualitatively identify substances. In addition, the intensity of the peaks in the spectrum is proportional to the amount of substance present, enabling its application for quantitative analysis.

Qualitative analysis

For qualitative identification purposes, the spectrum is commonly presented as transmittance versus wavenumber. Functional groups have their characteristic fundamental vibrations which give rise to absorption at certain frequency range in the spectrum (**Figure 3**).

Figure 3.Infrared spectrum of 1-hexanol.

Each band in a spectrum can be attributed to stretching or bending mode of a bond. Almost all the fundamental vibrations appear in the mid-infrared region. For instance, 4000 – 2500 cm^{-1} region usually can be assigned to stretching modes of O-H, N-H or C-H. Triple-bond stretching modes appear in the region of 2500 – 2000 cm^{-1}. C=C and C=O stretching bands fall in the 2000 – 1500 cm^{-1} region. Hence, characterization of functional groups in substances according to the frequencies and intensities of absorption peaks is feasible, and also structures of molecules can be proposed. This method is applicable to organic molecules, inorganic molecules, polymers, etc. A detailed frequency list of functional groups is shown in **Figure 4**. Note that several functional groups may absorb at the same frequency range, and a functional group may have multiple-characteristic absorption peaks, especially for 1500 – 650 cm^{-1}, which is called the fingerprint region.

Figure 4. Characteristic infrared absorption frequencies.

Bands in the near-infrared region are overtones or combination bands. They are weak in intensity and overlapped, making them not as useful for qualitative analysis as those in mid-infrared region. However, absorptions in this region are helpful in exploiting information related to vibrations of molecules containing heavy atoms, molecular skeleton vibrations, molecular torsions and crystal lattice vibrations.

Besides structural elucidation, another qualitative application of infrared spectroscopy is the identification of a compound with a reference infrared spectrum. If all the peaks of the unknown match those of the reference, the compound can be identified. Additional reference spectra are available online at databases such as NIST Chemistry WebBook.

Quantitative analysis

Absorbance is used for quantitative analysis due to its linear dependence on concentration. Given by Beer-Lambert law, absorbance is directly proportional to the concentration and pathlength of sample:

$$A = \epsilon c l \tag{3.12.1}$$

where A is absorbance, ε the molar extinction coefficient or molar absorptivity which is characteristic for a specific substance, c the concentration and l the pathlength (or the thickness) of sample. The conversion from transmittance to absorbance is given by

$$A = -\log T \tag{3.12.2}$$

where T is transmittance.

For quantitative analysis of liquid samples, usually an isolated peak with high molar absorptivity that appears in the spectrum of the compound is chosen. A calibration curve of absorbance at the chosen frequency against concentration of the compound is acquired by measuring the absorbance of a series of standard compound solution with known concentrations. These data are then graphed to get a linear plot, from which the concentration of the unknown can be calculated after measuring its absorbance at the same frequency. The number of functional groups can also be calculated in this way, since the molar absorptivity of the band is proportional to the number of functional groups that are present in the compound.

For solid samples, an internal standard with a constant known amount is added to the unknown sample and the standards. Then similar procedures as those with liquid samples are carried out except that the calibration curve is a graph of the ratio of absorbance of analyte to that of the internal standard versus concentration of the analyte.

A multi-component analysis of the mixture is also feasible since different components have different values of molar absorptivity at the same frequency.

However, infrared spectroscopy may be more susceptible to deviation from Beer's law than is UV-Vis spectroscopy because of its narrow bands, complex spectra, weak incident beam, low transducer sensitivity and solvent absorption.

Reference

1. Settle, F. A. *Handbook of instrumental techniques for analytical chemistry*; Prentice Hall PTR: Upper Saddle River, NJ, **1997**.
2. Heigl, J. J.; Bell, M.; White, J. U. *Anal. Chem.*1947, *19*, 293.
3. Baker, A. W. *J. Phys. Chem.* **1957**, *61*, 450.
4. Kamariotis, A.; Boyarkin, O. V.; Mercier, S. R.; Beck, R. D.; Bush, M. F.; Williams, E. R.; Rizzo, T. R. *J. Am. Chem. Soc.* **2006**, *128*, 905.
5. Stuart, B. *Infrared spectroscopy fundamentals and applications*; J. Wiley: Chichester, Eng.; Hoboken, N.J., **2004**.
6. Günzler, H.; Heise, H. M. *IR spectroscopy: an introduction*; Wiley-VCH: Weinheim, **2002**.
7. Wartewig, S. *IR and Raman spectroscopy: fundamental processin;* Wiley-VCH: Weinheim, **2003**.

Outside Links

- NIST Chemistry WebBook: http://webbook.nist.gov/
- Wikipedia: http://en.Wikipedia.org/wiki/Infrared_spectroscopy

Contributor

- Xixuan Li (UC Davis)

3.12: Application is shared under a CC BY-NC-SA 4.0 license and was authored, remixed, and/or curated by LibreTexts.

- **Infrared: Application** is licensed CC BY 4.0.

CHAPTER OVERVIEW

4: Conjugated Compounds and Ultraviolet Spectroscopy

You have already studied the chemistry of compounds that contain one carbon-carbon double bond. In this chapter, you will focus your attention on compounds that contain two or more such bonds. In particular you will study the properties of those compounds that contain two carbon-carbon double bonds which are separated by one carbon-carbon single bond. These compounds are called “conjugated dienes.”

To understand the properties exhibited by conjugated dienes, you must first examine their bonding in terms of the molecular orbital theory introduced in Section 1.5. Then, you must learn how the products of a reaction are dependent on both thermodynamic and kinetic considerations. Which of these two factors is the most important can sometimes determine which of two possible products will predominate when a reaction is carried out under specific conditions. Although we shall not make extensive use of ultraviolet spectroscopy, this technique can often provide important information when conjugated compounds are being investigated. In general, ultraviolet spectroscopy is less useful than the other spectroscopic techniques introduced earlier.

Topic hierarchy

4.1: Chapter Objectives
4.2: 14.0 Introduction
4.3: Molecular Orbital Theory
4.4: Allylic Carbocations
4.5: 14.3 Kinetic vs. Thermodynamic Control of Reactions
4.6: 14.4 The Diels-Alder Cycloaddition Reaction
4.7: 14.5 Characteristics of the Diels-Alder Reaction
4.8: Natural and Synthetic Rubbers
4.9: Ultraviolet Spectroscopy
4.10: The Effect of Conjugation
4.11: 14.9 Conjugation, Color, and the Chemistry of Vision
4.12: UV-Visible Spectroscopy
Index

4: Conjugated Compounds and Ultraviolet Spectroscopy is shared under a CC BY-NC-SA 4.0 license and was authored, remixed, and/or curated by LibreTexts.

4.1: Chapter Objectives

4.1: Chapter Objectives is shared under a CC BY-NC-SA 4.0 license and was authored, remixed, and/or curated by LibreTexts.

4.2: 14.0 Introduction

Objective

After completing this section, you should be able to determine whether or not a molecule contains a conjugated system, given its Kekulé, condensed or shorthand formula.

Key Terms

Make certain that you can define, and use in context, the key terms below.

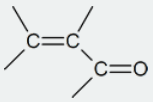
- conjugated diene
- conjugated double bonds
- diene
- enone
- polyene

Study Notes

Conjugated double bonds are double bonds which are separated by one carbon-carbon single bond. Thus the double bonds in butadiene, $CH_2{=}CH{-}CH{=}CH_2$, are conjugated, and this compound is an example of a *conjugated diene*.

Just as the term *diene*indicates the presence of two carbon-carbon double bonds in a compound, so the term *polyene* is used to describe compounds containing many carbon-carbon double bonds.

An *enone* is a compound containing a carbon-carbon double bond (ene) and a carbonyl group (one). A conjugated enone contains the structural unit:



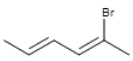
Conjugated **Dienes**

A diene is a hydrocarbon chain that has two double bonds that may or may not be adjacent to each other. This section focuses on the delocalization of pi systems by comparing two neighboring double bonds. The arrangements of these double bonds can have varying affects on the compounds reactivity and stability.

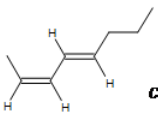
Naming Dienes

First identify the longest chain containing both carbons with double bonds in the compound. Then give the lowest possible number for the location of the carbons with double bonds and any other functional groups present (remember when naming alkenes that some groups take priority such as alcohols). Do not forget stereochemistry or any other orientation of the double bond such as (E/Z,cis or trans).

Examples:



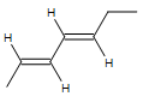
2-Bromo-2,4-hexadiene



cis-2-*trans*-4-octadiene



1,3-cyclopentadiene

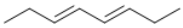


trans-2,4-heptadiene

https://chem.libretexts.org/@go/page/167039

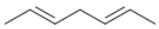
Conjugated vs. Nonconjugated vs. Cumulated Dienes

Conjugated dienes are two double bonds separated by a single bond



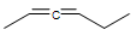
3,5-octadiene

Nonconjugated (Isolated) Dienes are two double bonds are separated by more than one single bond.



2,5-heptadiene

Cumulated Dienes are two double bond connected to a similar atom.



2,3-hexadiene

Contributors and Attributions

- Dr. Dietmar Kennepohl FCIC (Professor of Chemistry, Athabasca University)
- Shravan Rao

4.2: 14.0 Introduction is shared under a CC BY-NC-SA 4.0 license and was authored, remixed, and/or curated by LibreTexts.

4.3: Molecular Orbital Theory

Objectives

After completing this section, you should be able to

1. write a reaction sequence to show a convenient method for preparing a given conjugated diene from an alkene, allyl halide, alkyl dihalide or alcohol (diol).
2. identify the reagents needed to prepare a given diene from one of the starting materials listed in Objective 1, above.
3. compare the stabilities of conjugated and nonconjugated dienes, using evidence obtained from hydrogenation experiments.
4. discuss the bonding in a conjugated diene, such as 1,3-butadiene, in terms of the hybridization of the carbon atoms involved.
5. discuss the bonding in 1,3-butadiene in terms of the molecular orbital theory, and draw a molecular orbital for this and similar compounds.

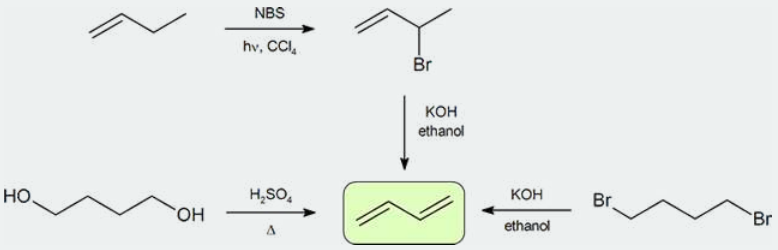
Key Terms

Make certain that you can define, and use in context, the key terms below.

- delocalized electrons
- node

Study Notes

The two most frequent ways to synthesize conjugated dienes are dehydration of alcohols and dehydrohalogenation of organohalides, which were introduced in the preparation of alkenes (Section 8.1). The following scheme illustrates some of the routes to preparing a conjugated diene.



The formation of synthetic polymers from dienes such as 1,3-butadiene and isoprene is discussed in Section 14.6. Synthetic polymers are large molecules made up of smaller repeating units. You are probably somewhat familiar with a number of these polymers; for example, polyethylene, polypropylene, polystyrene and poly(vinyl chloride).

As the hydrogenation of 1,3-butadiene releases less than the predicted amount of energy, the energy content of 1,3-butadiene must be lower than we might have expected. In other words, 1,3-butadiene is more stable than its formula suggests.

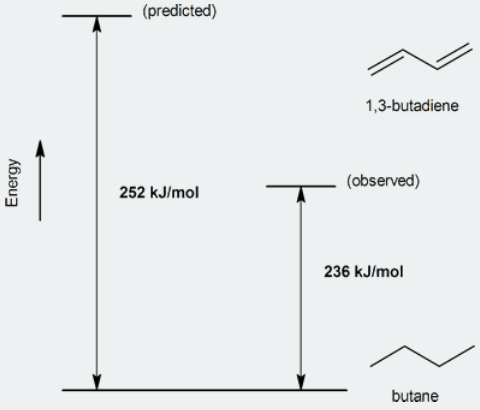
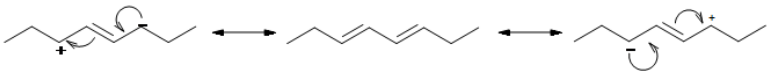


Figure 14.1: Energy diagram for the hydrogenation of 1,3-butadiene (not to scale).

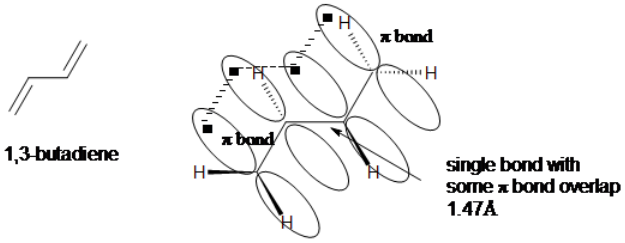
Some university-level general chemistry courses do not introduce the subject of molecular orbitals. If you have taken such a course, or forgotten what is meant by the term “molecular orbital,” combine a review of Section 1.11 with your study of this section.

Conjugated dienes are more stable than non conjugated dienes (both isolated and cumulated) due to factors such as delocalization of charge through resonance and hybridization energy. This can also explain why allylic radicals are much more stable than secondary or even tertiary carbocations. This is all due to the positioning of the pi orbitals and ability for overlap to occur to strengthen the single bond between the two double bonds.

The resonance structure shown below gives a good understanding of how the charge is delocalized across the four carbons in this conjugated diene. This delocalization of charges stablizes the conjugated diene:

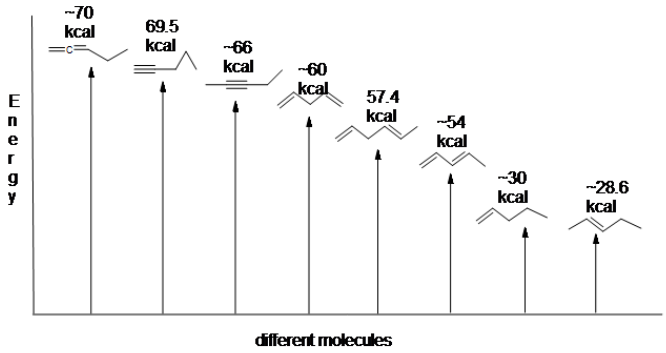


Along with resonance, hybridization energy effect the stability of the compound. For example in 1,3-butadiene the carbons with the single bond are sp2 hybridized unlike in nonconjugated dienes where the carbons with single bonds are sp3 hybridized. This difference in hybridization shows that the conjugated dienes have more 's' character and draw in more of the pi electrons, thus making the single bond stronger and shorter than an ordinary alkane C-C bond (1.54Å).



Another useful resource to consider are the heats of hydrogenation of different arrangements of double bonds. Since the higher the heat of hydrogenation the less stable the compound, it is shown below that conjugated dienes (~54 kcal) have a lower heat of hydrogenation than their isolated (~60 kcal) and cumulated diene (~70 kcal) counterparts.

Here is an energy diagram comparing different types of bonds with their heats of hydrogenation to show relative stability of each molecule:

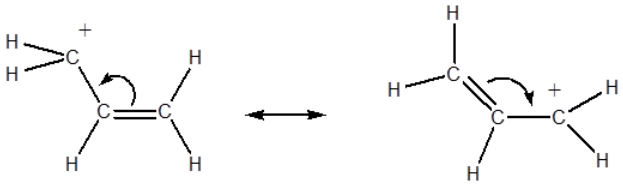


The stabilization of dienes by conjugation is less dramatic than the aromatic stabilization of benzene. Nevertheless, similar resonance and molecular orbital descriptions of conjugation may be written.

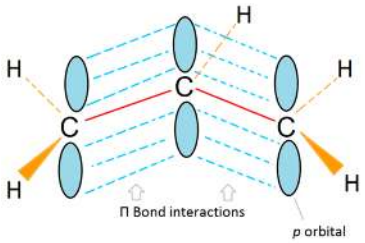
Allylic Carbocation

Conjugation occurs when p orbital on three or more adjacent atoms can overlap Conjugation tends to stabilize molecules

Allylic carbocations are a common conjugated system.



The positive charge of a carbocation is contained in a P orbital of a sp^2 hybrizied carbon. This allows for overlap with double bonds. The positive charge is more stable because it is spread over 2 carbons.



Molecular Orbitals of an Allylic Carbocation

The stability of the carbocation of propene is due to a conjugated π electron system. A "double bond" doesn't really exist. Instead, it is a group of 3 adjacent, overlapping, non-hybridized *p* orbitals we call a **conjugated π electron system**. You can clearly see the interactions between all three of the *p* orbitals from the three carbons resulting in a really stable cation. It all comes down to where the location of the electron-deficient carbon is.

Molecular orbital descriptions can explain allylic stability in yet another way using 2-propenyl. Fig.6

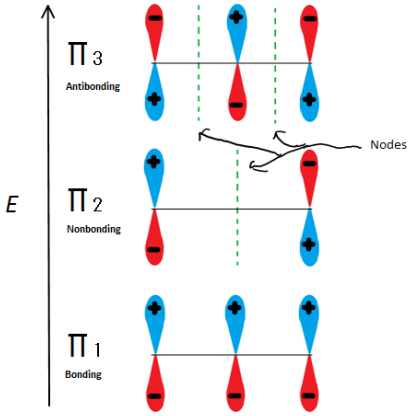


Fig.6 Shows the 3 possible Molecular orbitals of 2-propenyl

If we just take the π molecular orbital and not any of the s, we get three of them. π_1 is bonding with no nodes, π_2 is nonbonding (In other words, the same energy as a regular *p*-orbital) with a node, and π_3 is antibonding with 2 nodes (none of the orbitals are interacting). The first two electrons will go into the π_1 molecular orbital, regardless of whether it is a cation, radical, or anion. If it is a radical or anion, the next electron goes into the π_2 molecular orbital. The last anion electron goes into the nonbonding orbital also. So no matter what kind of carbon center exists, no electron will ever go into the antibonding orbital.

The Bonding orbitals are the lowest energy orbitals and are favorable, which is why they are filled first. Even though the nonbonding orbitals can be filled, the overall energy of the system is still lower and more stable due to the filled bonding molecular orbitals.

This figure also shows that π_2 is the only molecular orbital where the electron differs, and it is also where a single node passes through the middle. Because of this, the charges of the molecule are mainly on the two terminal carbons and not the middle carbon.

This molecular orbital description can also illustrate the stability of allylic carbon centers in figure 7.

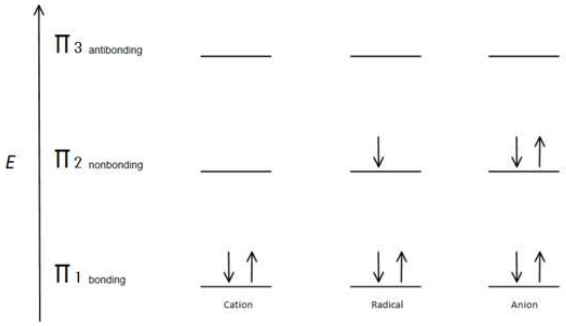
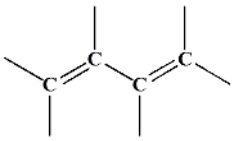


***Fig. 7:** diagram showing how the electrons fill based on the Aufbau principle.*

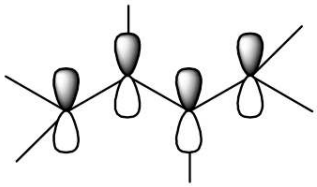
The π bonding orbital is lower in energy than the nonbonding *p* orbital. Since every carbon center shown has two electrons in the lower energy, bonding π orbitals, the energy of each system is lowered overall (and thus more stable), regardless of cation, radical, or anion.

1,3-Dienes

Conjugated double bonds are separated by a single bond. 1,3-dienes are an excellent example of a conjugated system. Each carbon in 1,3 dienes are sp^2 hybridized and therefore have one *p* orbital. The four *p* orbitals in 1,3-butadiene overlap to form a conjugated system.

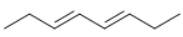


1,3-Diene



Conjugated vs. Nonconjugated Dienes

Conjugated dienes are two double bonds separated by a single bond



3,5-octadiene

Nonconjugated (Isolated) Dienes are two double bonds are separated by more than one single bond.



2,5-heptadiene

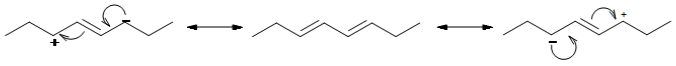
When using electrostatic potential maps, it is observed that the pi electron density overlap is closer together and delocalized in conjugated dienes, while in non conjugated dienes the pi electron density is located differently across the molecule. Since having more electron density delocalized makes the molecule more stable conjugated dienes are more stable than non conjugated

For example in 1,3-butadiene the carbons with the single bond are sp2 hybridized unlike in nonconjugated dienes where the carbons with single bonds are sp3 hybridized. This difference in hybridization shows that the conjugated dienes have more 's' character and draw in more of the pi electrons, thus making the single bond stronger and shorter than an ordinary alkane C-C bond (1.54Å).

Stability of Conjugated Dienes

Conjugated dienes are more stable than non conjugated dienes (both isolated and cumulated) due to factors such as delocalization of charge through resonance and hybridization energy. This can also explain why allylic radicals are much more stable than secondary or even tertiary carbocations. This is all due to the positioning of the pi orbitals and ability for overlap to occur to strengthen the single bond between the two double bonds.

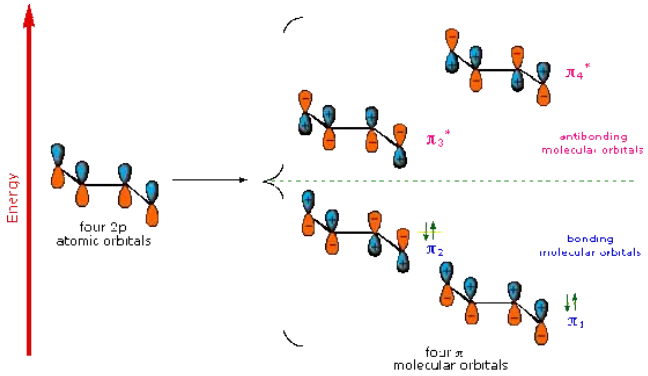
The resonance structure shown below gives a good understanding of how the charge is delocalized across the four carbons in this conjugated diene. This delocalization of charges stabilizes the conjugated diene:



Along with resonance, hybridization energy effect the stability of the compound. For example in 1,3-butadiene the carbons with the single bond are sp2 hybridized unlike in nonconjugated dienes where the carbons with single bonds are sp3 hybridized. This difference in hybridization shows that the conjugated dienes have more 's' character and draw in more of the pi electrons, thus making the single bond stronger and shorter than an ordinary alkane C-C bond (1.54Å).

Molecular Orbitals of 1,3 Dienes

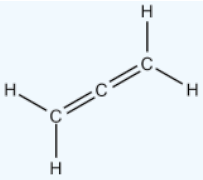
A molecular orbital model for 1,3-butadiene is shown below. Note that the lobes of the four p-orbital components in each pi-orbital are colored differently and carry a plus or minus sign. This distinction refers to different phases, defined by the mathematical wave equations for such orbitals. Regions in which adjacent orbital lobes undergo a phase change are called **nodes**. Orbital electron density is zero in such regions. Thus a single p-orbital has a node at the nucleus, and all the pi-orbitals shown here have a nodal plane that is defined by the atoms of the diene. This is the only nodal surface in the lowest energy pi-orbital, π_1. Higher energy pi-orbitals have an increasing number of nodes.



Exercise

? Exercise 4.3.1

The heat of hydrogenation for allene is about 300 kJ/mol. Order a conjugated diene, a non-conjugated diene, and allene in increasing stability.



Allene

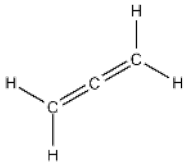
Answer

allene < non-conjugated diene < conjugated diene (most stable)

Questions

Q14.1.1

The heat of hydrogenation for allene is about 300 kJ/mol. Order a conjugated diene, a non-conjugated diene, and allene in increasing stability.



Allene

Solutions

S14.1.1

allene < non-conjugated diene < conjugated diene (most stable)

Contributors and Attributions

- Dr. Dietmar Kennepohl FCIC (Professor of Chemistry, Athabasca University)
- Prof. Steven Farmer (Sonoma State University)
- William Reusch, Professor Emeritus (Michigan State U.), Virtual Textbook of Organic Chemistry
- Organic Chemistry With a Biological Emphasis by Tim Soderberg (University of Minnesota, Morris)

4.3: Molecular Orbital Theory is shared under a CC BY-NC-SA 4.0 license and was authored, remixed, and/or curated by LibreTexts.

4.4: Allylic Carbocations

Objectives

After completing this section, you should be able to

1. write an equation for the addition of one or two mole equivalents of a halogen or a hydrogen halide to a nonconjugated diene.
2. write an equation for the addition of one or two mole equivalents of a halogen or a hydrogen halide to a conjugated diene.
3. write the mechanism for the addition of one mole equivalent of hydrogen halide to a conjugated diene, and hence account for the formation of 1,2- and 1,4-addition products.
4. explain the stability of allylic carbocations in terms of resonance.
5. draw the resonance contributors for a given allylic carbocation.
6. predict the products formed from the reaction of a given conjugated diene with one mole equivalent of halogen or hydrogen halide.
7. predict which of the possible 1,2- and 1,4-addition products is likely to predominate when one mole equivalent of a hydrogen halide is reacted with a given conjugated diene.
8. use the concept of carbocation stability to explain the ratio of the products obtained when a given conjugated diene is reacted with one mole equivalent of hydrogen halide.

Key Terms

Make certain that you can define, and use in context, the key terms below.

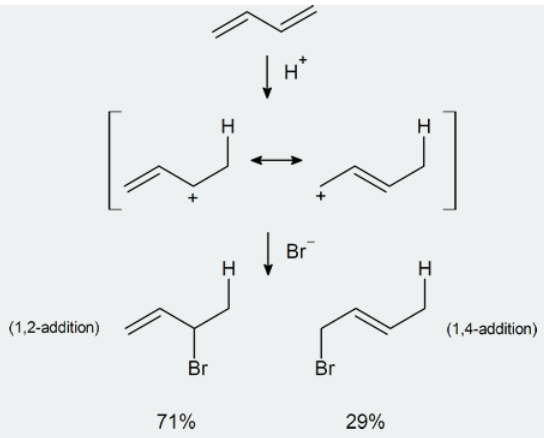
- 1,2-addition
- 1,4-addition

Study Notes

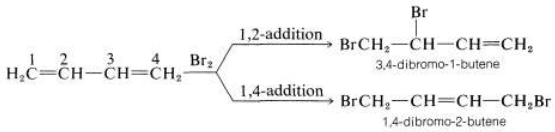
Notice that the numbers used in the expressions 1,2-addition and 1,4-addition do *not* refer to the positions of the carbon atoms in the diene molecule. Here, 1,2 indicates two neighbouring carbon atoms, while 1,4 indicates two carbon atoms which are separated in the carbon chain by two additional carbon atoms. Thus in 1,2- and 1,4-additions to 2,4-hexadiene, the additions actually occur at carbons 2 and 3, and 2 and 5, respectively.

The term “monoadduct” should be interpreted as meaning the product or products formed when one mole of reagent adds to one mole of substrate. In the objectives above, this process is referred to as the addition of one mole equivalent (or one mol equiv).

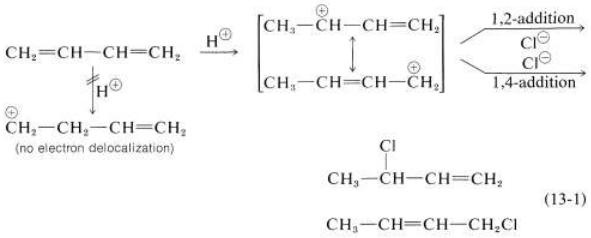
In Section 7.9 we saw that electrophilic addition to a simple alkene would follow Markovnikov’s rule, where the stability of the carbocation intermediate would increase: primary < secondary < tertiary. With conjugated dienes the allylic carbocation intermediately generated has different resonance forms. The following scheme represents the mechanism for the addition of HBr to 1,3-butadiene (at 0°C). Note the resonance contributors for the allylic carbocation intermediate and that the product resulting from the secondary cation is generated in higher yield than from the primary cation as you might expect from our discussions until now. However, in the next section you will see that the resulting product ratio can be drastically affected by a number of reaction conditions, including temperature.



The reactions of 1,3-butadiene are reasonably typical of conjugated dienes. The compound undergoes the usual reactions of alkenes, such as catalytic hydrogenation or radical and polar additions, but it does so *more readily* than most alkenes or dienes that have isolated double bonds. Furthermore, the products frequently are those of 1,2 *and* **1,4 addition:**



Formation of both 1,2- and 1,4-addition products occurs not only with halogens, but also with other electrophiles such as the hydrogen halides. The mechanistic course of the reaction of 1,3-butadiene with hydrogen chloride is shown in Equation 13-1. The first step, as with alkenes, is formation of a carbocation. However, with 1,3-butadiene, if the proton is added to C_1 (but not C_2), the resulting cation has a substantial delocalization energy, with the charge distributed over two carbons (review Sections 6-5 and 6-5C if this is not clear to you). Attack of $Cl^{\ominus}$ as a nucleophile at one or the other of the positive carbons yields the 1,2- or the 1,4-addition product:



An important feature of reactions in which 1,2 and 1,4 additions occur in competition with one another is that the ratio of the products can depend on the temperature, the solvent, and also on the *total time of reaction*.

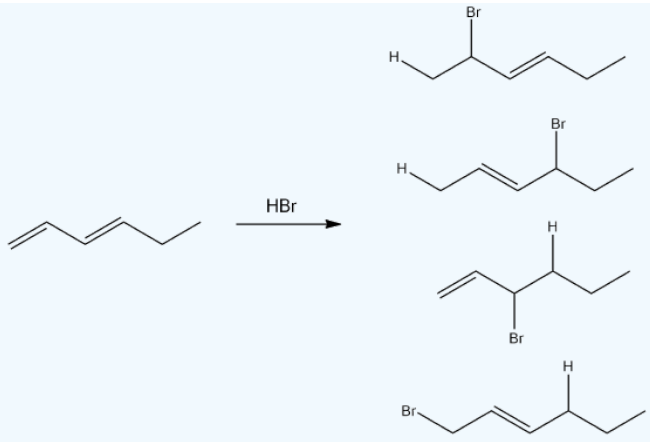
Exercise

? Exercise 4.4.1

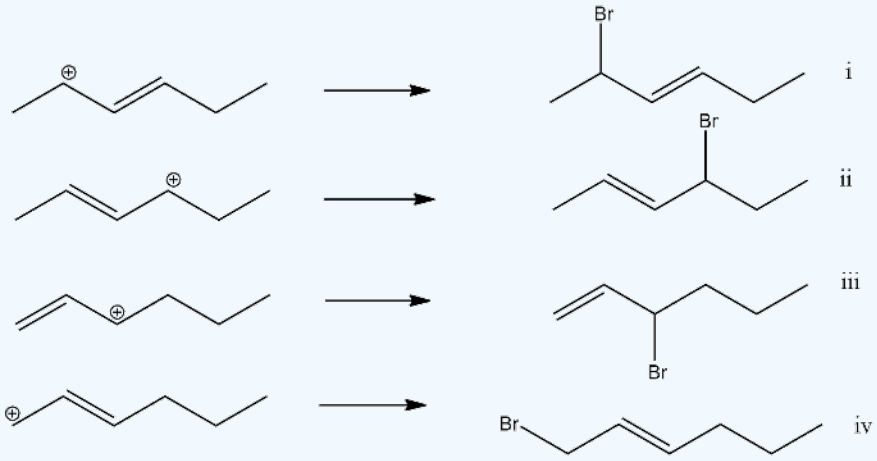
1. Give the 1,2 and the 1,4 products of the addition of one equivalent of HBr to 1,3-hexa-diene.
2. Look at the previous addition reaction of HBr with a diene. Consider the transition states, predict which of them would be the major products and which will be the minor.
3. Write out the products of 1,2 addition and 1,4- addition of HBr to 1,3-cyclohexadiene.
4. What is unusual about the products of 1,2- and 1,4- addition of HX to an unsubstituted cyclic 1,3-diene?
5. Write out the products of 1,2 addition and 1,4- addition of Br2 to 1,3-cyclohexadiene.

Answer

1)



2) The products i-iii all show a secondary cation intermediate which is more stable than primary. Therefore those would be major products and the iv product would be the minor product.

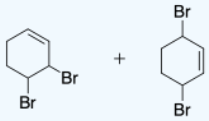


3) The same product will result from 1,2 and 1,4 addition.



4) Addition of the HX to unsubstituted cycloalka-1,3-dienes in either 1,2- or 1,4- manner gives the same product because of symmetry.

5) Both 1,2 and 1,4 products will form.



Questions

Q14.2.1

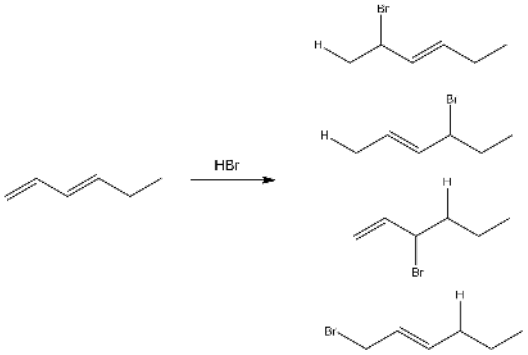
Give the 1,2 and the 1,4 products of the addition of one equivalent of HBr to 1,3-hexa-diene.

Q14.2.2

Look at the previous addition reaction of HBr with a diene. Consider the transition states, predict which of them would be the major products and which will be the minor.

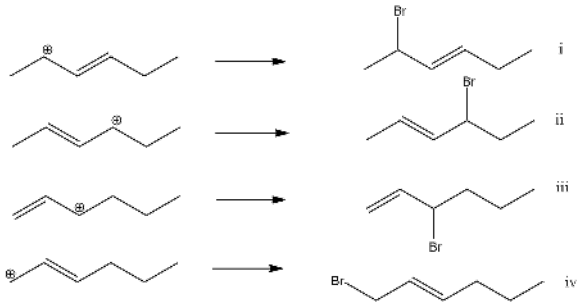
Solutions

S14.2.1



S14.2.2

The products i-iii all show a secondary cation intermediate which is more stable than primary. Therefore those would be major products and the iv product would be the minor product.



Contributors and Attributions

- Dr. Dietmar Kennepohl FCIC (Professor of Chemistry, Athabasca University)
- Prof. Steven Farmer (Sonoma State University)
- John D. Robert and Marjorie C. Caserio (1977) *Basic Principles of Organic Chemistry, second edition.* W. A. Benjamin, Inc. , Menlo Park, CA. ISBN 0-8053-8329-8. This content is copyrighted under the following conditions, "You are granted permission for individual, educational, research and non-commercial reproduction, distribution, display and performance of this work in any format."

4.4: Allylic Carbocations is shared under a CC BY-NC-SA 4.0 license and was authored, remixed, and/or curated by LibreTexts.

4.5: 14.3 Kinetic vs. Thermodynamic Control of Reactions

Objectives

After completing this section, you should be able to

1. explain the difference between thermodynamic and kinetic control of a chemical reaction; for example, the reaction of a conjugated diene with one equivalent of hydrogen halide.
2. draw a reaction energy diagram for a reaction which can result in both a thermodynamically controlled product and a kinetically controlled product.
3. explain how reaction conditions can determine the product ratio in a reaction in which there is competition between thermodynamic and kinetic control.

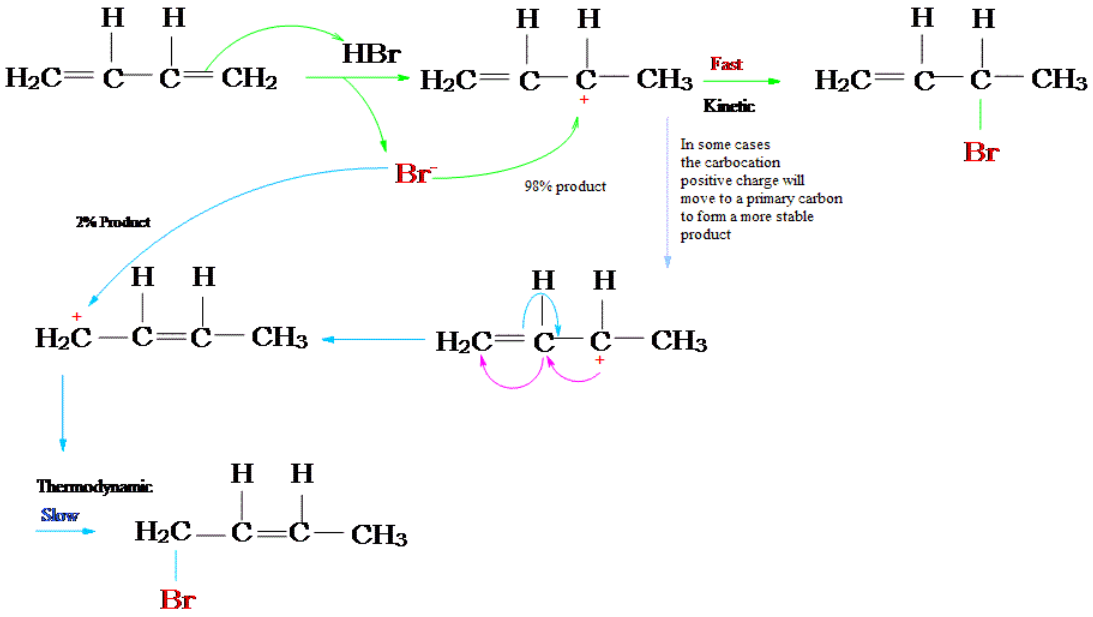
Key Terms

Make certain that you can define, and use in context, the key terms below.

- kinetic control
- thermodynamic control

Like nonconjugated dienes, conjugated dienes are subject to attack by electrophiles. In fact, conjugated electrophiles experience relatively greater kinetic reactivity when reacted with electrophiles than nonconjugated dienes do. Upon electrophilic addition, the conjugated diene forms a mixture of two products—the kinetic product and the thermodynamic product—whose ratio is determined by the conditions of reaction. A reaction yielding more thermodynamic product is under thermodynamic control, and likewise, a reaction that yields more kinetic product is under kinetic control.

The reaction of one equivalent of hydrogen bromide with 1,3-butadiene gives different products at under different conditions and is a classic example of the concept of *thermodynamic* versus *kinetic* control of a reaction



Take a look at this energy profile diagram in Figure 4.5.1. In this scenario, the starting material A can react to form either B (to the left) or C (to the right). The formation of the product B involves overcoming barriers with *lower* *activation energies*, which means that it will form faster (ignoring the pre-exponential constant effects).

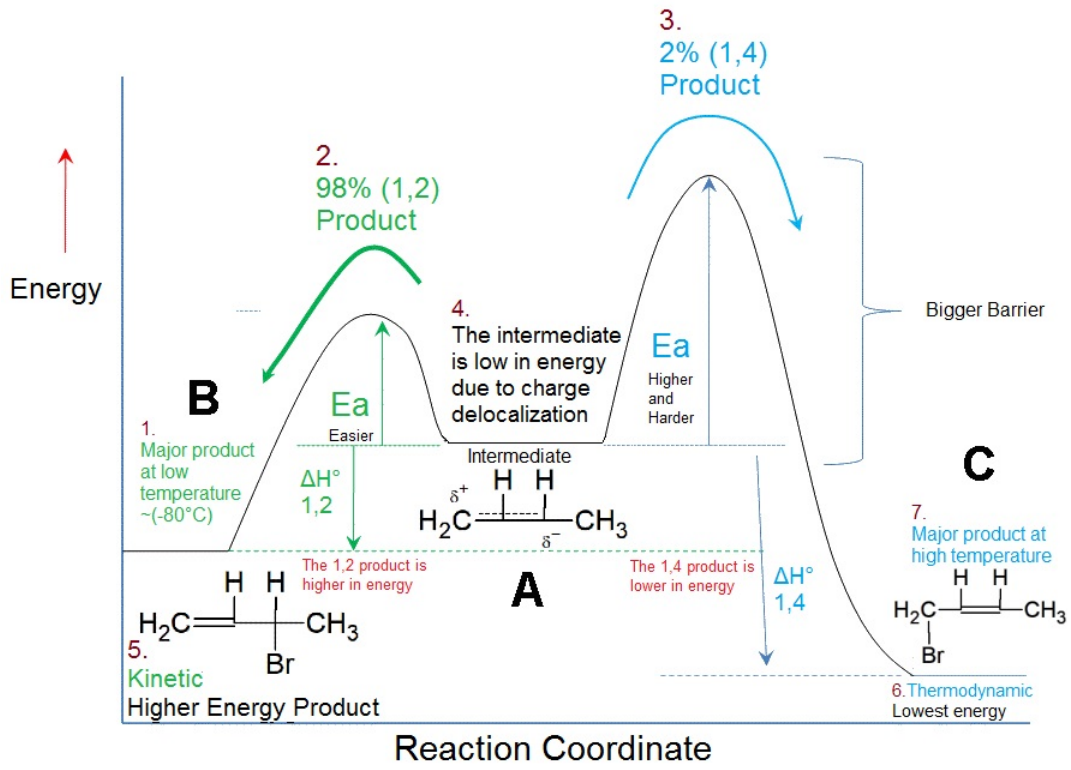


***Figure* 4.5.1:** *Energy profile diagram for A → B (left) and A → C (right). The horizontal axis is a reaction coordinate, and the vertical axis represents Gibbs energy. The delocalized carbocation intermediate (A) is the protonated form of 1,3-butadiene (first step of the reaction of 1,3-butadiene with HBr).*

If we keep the temperature sufficiently *low*, the molecules of B, which are inevitably formed faster, will probably not have enough energy to overcome the reverse activation barrier (i.e., B → A) to regenerate A (Table 4.5.1). The forward reactions A ⟶ B and A ⟶ C are, under such conditions, effectively irreversible. Since the formation of B is faster, it will predominate, and the major product formed will be B. This is known as *kinetic control* and B is the *kinetic product*.

At elevated temperatures, B is still going to be the product that is formed *faster*. However, it also means that all the reactions will be reversible. This means that molecules of B can revert back to A. Since the system is no longer limited by temperature, the system will minimize its Gibbs free energy, which is the thermodynamic criterion for chemical equilibrium. This means that, as the most thermodynamically stable molecule, C will be predominantly formed.[2] The reaction is said to be under *thermodynamic control* and C is the *thermodynamic product*.

Table 4.5.1: Conjugated Dienese: Kinetic vs. Thermodynamic Conditions

Temperature	Kinetic or Thermodynamically Controlled	Speed of Reaction	1,2-adduct (B) : 1,4-adduct (C) Ratio
-15 °C	Kinetic	Fast	70:30
0 °C	Kinetic	Fast	60:40
40 °C	Thermodynamic	Slow	15:85
60 °C	Thermodynamic	Slow	10:90

> *A simple definition is that the kinetic product is the product that is formed faster, and the thermodynamic product is the product that is more stable. This is precisely what is*

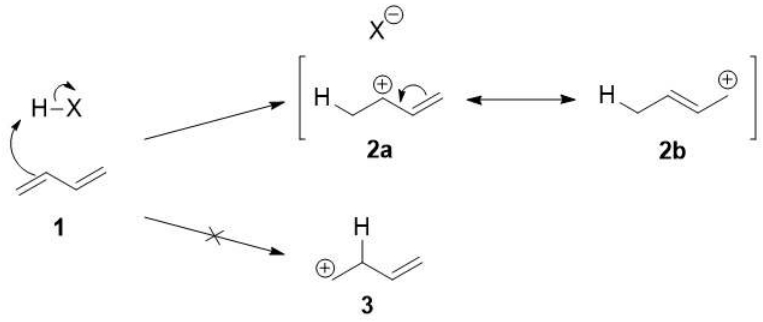
> *happening here. The kinetic product is 3-bromobut-1-ene, and the thermodynamic product is 1-bromobut-2-ene (specifically, the trans isomer).*

A Warning: Not every reaction has different thermodynamic and kinetic products!

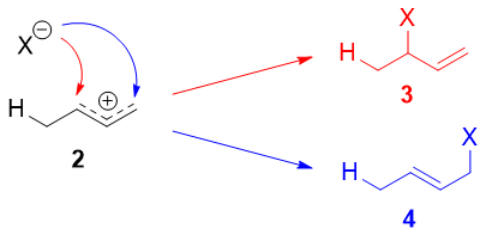
Note that not every reaction has an energy profile diagram like Figure 4.5.1, and not every reaction has different thermodynamic and kinetic products! If the transition states leading to the formation of **B** were to be higher in energy than that leading to **C**, then **C** would simultaneously be both the thermodynamic and kinetic product. There are plenty of reactions in which the more stable product (*thermodynamic*) is also formed faster (*kinetic*).

The Reaction Mechanism

The first step is the protonation of one of the C=C double bonds. In butadiene (**1**), both double bonds are the same, so it does not matter which one is protonated. The protonation occurs regioselectively to give the more stable carbocation (i.e., I_B=I_C in Figure 4.5.11):



The more stable cation is not only secondary, but also *allylic*, and therefore enjoys stabilization via resonance (or conjugation). This is depicted in the resonance forms **2a** and **2b** above. This allylic carbocation, more properly denoted as the resonance hybrid **2**, has two carbons which have significant positive charge, and the bromide ion (here denoted as X^-) can attack either carbon. Attacking the central carbon, adjacent to the site of protonation, leads to the kinetic product **3** (called the 1,2-adduct); attacking the terminal carbon, distant from the site of protonation, leads to the thermodynamic product **4** (called the 1,4-adduct).



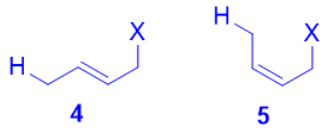
A Common Mistake: Resonance Structures do not Independently Exist

There are some people who write that **3** results from attack of X^- on resonance form **2a**, and **4** from attack of X^- on resonance form **2b**. ***This is not correct!*** Resonance forms do not separately exist, and they are not distinct species that rapidly interconvert. As such, one cannot speak of *one single resonance form* undergoing a reaction.

Now, why **4** is the thermodynamic product, and why **3** is the kinetic product for this reaction?

The thermodynamic product: *trans*-1-bromobut-2-ene

It is perhaps simple enough to see why **4** is more stable than **3**. It has an internal, disubstituted double bond, and we know that as a general rule of thumb, the thermodynamic stability of an alkene increases with increasing substitution. So, compared to the terminal, monosubstituted alkene **3**, **4** is more stable.



Both the *trans* isomer **4** as well as the *cis* isomer **5** can be formed via attack of the nucleophile at the terminal carbon, and both are disubstituted alkenes. However, the *trans* isomer **4** is more stable than the *cis* isomer **5**, because there is less steric repulsion between the two substituents on the double bond. As such, **4** is the thermodynamic product.

The kinetic product: 3-bromobut-1-ene

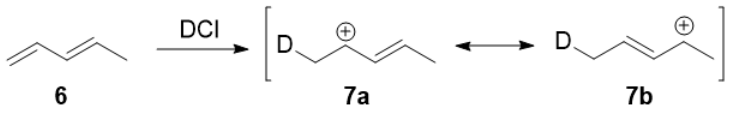
Several explanations may be proposed to explain the nature of the kinetic product.

The worst possible argument argues that the resonance form **2a**, being an allylic *secondary* carbocation, is more stable than resonance form **2b**, which is an allylic *primary* carbocation. Therefore, resonance form **2a** exists in greater relative proportion (i.e., more molecules will look like **2a** than **2b**), and the nucleophile preferentially reacts with this specific carbocation, leading to the formation of **3**. However, this is incorrect, since individual resonance forms do not exist. Moreover, such an argument suggests that we are looking for the more stable *intermediate* (I_B or I_C in Figure 4.5.1). In fact, we should be looking for the more stable *transition states* (T_{B1}, T_{B2}, T_{C1}, *and* T_{C2} in Figure 4.5.1). The carbocation is an *intermediate*, and not a *transition state*.

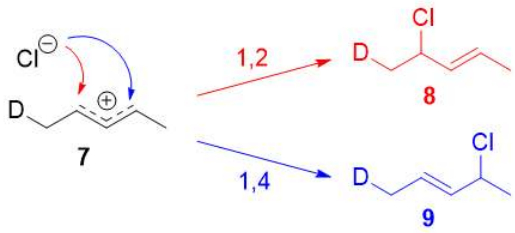
The most common argument is since resonance form **2a** is more stable than **2b**, is that it contributes more towards the *resonance hybrid* **2**. As such, the positive charge on the internal carbon is greater than the positive charge on the terminal carbon. The nucleophile, being negatively charged, is more strongly attracted to the more positively charged or more electrophilic carbon, and therefore attack there occurs faster (the transition state being stabilized by greater electrostatic interactions). That's actually a very sensible explanation; with only the data that has been presented so far, we would not be able to disprove it, and it was indeed the accepted answer for quite a while.

Experimental Results

In 1979, Nordlander *et al.* carried out a similar investigation on the addition of \(\ce{DCl}\) to a different substrate, 1,3-pentadiene.[7] This experiment was ingenious, because it was designed to proceed via an almost symmetrical intermediate:



Resonance forms **7a** and **7b** are both allylic and secondary. There is a very minor difference in their stabilities arising from the different hyperconjugative ability of $C-D$ *vs* $C-H$ bonds, but in any case, it is not very large. Therefore, if we adopt the explanation in the previous section, one would expect there not to be any major *kinetic* pathway, and both 1,2- and 1,4-addition products (**8** and **9**) would theoretically be formed roughly equally.



Instead, it was found that the 1,2-addition product was favored over the 1,4-addition product. For example, at $-78\,^{\circ}C$ in the absence of solvent, there was a roughly $75:25$ ratio of 1,2- to 1,4-addition products. Clearly, there is a factor that favors 1,2-addition that does not depend on the electrophilicity of the carbon being attacked! The authors attributed this effect to an *ion pair* mechanism. This means that, after the double bond is protonated (deuterated in this case), the chloride counterion remains in close proximity to the carbocation generated. Immediately following dissociation of DCl, the chloride ion is going to be much closer to

C−2 than it is to C−4, and therefore attack at C−2 is much faster. In fact, normal electrophilic addition of HX to conjugated alkenes in polar solvents can also proceed via similar ion pair mechanisms. This is reflected by the greater proportion of *syn* addition products to such substrates.[11]

> *The mechanism that favors 1,2-addition clearly does not depend on the electrophilicity of the carbon being attacked.*

This ion pair mechanism is a pre-exponential constant effects that is attributed to the proximity and frequency of collision rather than a activation barrier effect.

Conclusion

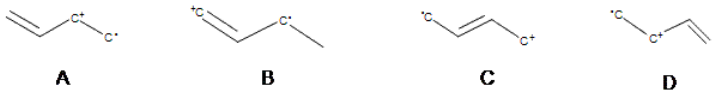
The reactivity of conjugated dienes (hydrocarbons that contain two double bonds) varies depending on the location of double bonds and temperature of the reaction.These reactions can produce both thermodynamic and kinetic products. Isolated double bonds provide dienes with less stability thermodynamically than conjugated dienes. However, they are more reactive kinetically in the presence of electrophiles and other reagents. This is a result of Markovnikov addition to one of the double bonds. A carbocation is formed after a double bond is opened. This carbocation has two resonance structures and addition can occur at either of the positive carbons.

References

1. Smith, M. B. *March's Advanced Organic Chemistry*, 7th ed., p 272
2. This does not mean that *all* of A will be converted to B; the reaction is still an *equilibrium*, and equilibria always go forward and backward. In general, the minimum system Gibbs free energy (G_{syst}) will occur at a certain proportion of A, B, and C. However, since B has the lowest Gibbs free energy, it will be formed in a greater proportion than C.
3. http://www.ochempal.org/index.php/alphabetical/a-b/14-addition/
4. *J. Am. Chem. Soc.* **1979,** *101* (5), 1288–1289
5. Because of the larger reduced mass and lower zero-point energy, a $\ce{C-D}$ bond is stronger and therefore less willing to donate electron density into an adjacent empty p orbital. This is the origin of some secondary kinetic isotope effects; in our case, it means that **7a** is marginally less stable than **7b**.
6. *J. Am. Chem. Soc.* **1969,** *91* (14), 3865–3869
7. Addition of HX to butadiene in the gas phase gives approximately a 1 : 1 ratio of 1,2- to 1,4-addition product, suggesting that an ion pair mechanism (which would favor the 1,2-addition product) does not operate: *J. Org. Chem.*, **1991,** *56* (2), 595–601

Practice Problems

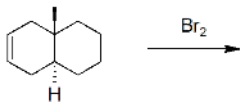
1. Write out the products of 1,2 addition and 1,4- addition of a) HBr and b) DBr to 1,3-cyclo-hexadiene. What is unusual about the products of 1,2- and 1,4- addition of HX to unsubstituted cyclic 1,3-dienes?
2. Is the 1,2-addition product formed more rapidly at higher temperatures, even though it is the 1,4-addition product that predominates under these conditions?
3. Why is the 1,4-addition product the thermodynamically more stable product?
4. Out of the following radical cations which one is not a reasonable resonance structure?

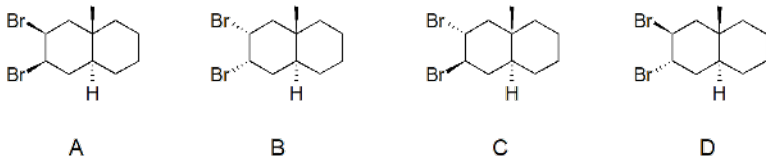


5. Addition of 1 equivalent of Bromine to 2,4-hexadiene at 0 degrees C gives 4,5-dibromo-2-hexene plus an isomer. Which of the following is that isomer:

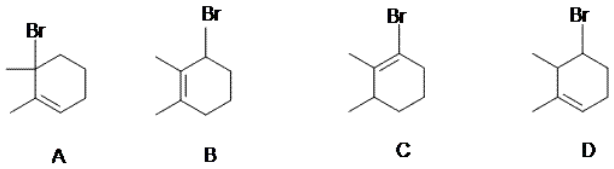
a. 5,5-dibromo-2-hexene
b. 2,5-dibromo-3-hexene
c. 2,2-dibromo-3-hexene
d. 2,3-dibromo-4-hexene

6. Which of the following will be the kinetically favored product from the depicted reaction?

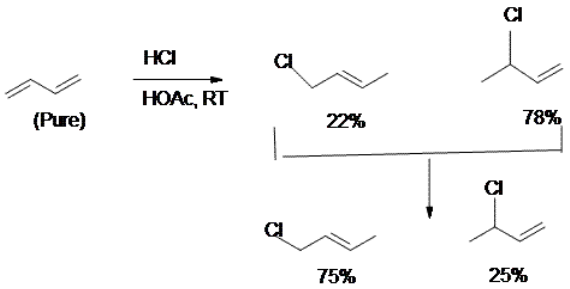




7. Addition of HBr to 2,3-dimethyl-1,3-cyclohexadiene may occur in the absence or presence of peroxides. In each case two isomeric $C_8H_{13}Br$ products are obtained. Which of the following is a common product from both reactions?



8. and 9.



8. The kinetically controlled product in the above reaction is:

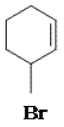
a. 3-Chloro-1-Butene
b. 1-Chloro-2-Butene

9. For the reaction in question 8, which one is the result of 1,4-addition?

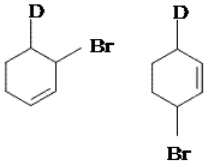
a. 3-Chloro-1-Butene
b. 1-Chloro-2-Butene

Answers to Problems

1. A) Same product for both modes of addition.



B) Both cis and trans isomers will form.



Addition of the HX to unsubstituted cycloalka-1,3-dienes in either 1,2- or 1,4- manner gives the same product becasuse of symmetry.

2. Yes. the Kinetic Product will still form faster but in this case there will be enough energy to form the thermodynamic product because the thermodynamic product is still more stable.

3. The 1,4- product is more thermodynamically stable because there are two alkyl groups on each side of the double bond. This form offers stability to the overall structure.

4. All of these isomers are viable.

5. B

6. C

7. D

8. A

9. B

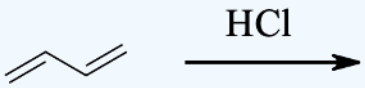
Exercise

? Exercise 4.5.1

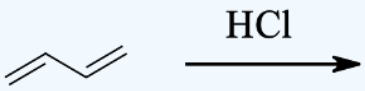
1) Why is the 1,4-addition product the thermodynamically more stable product?

2) Addition of 1 equivalent of bromine to 2,4-hexadiene at 0 degrees C gives 4,5-dibromo-2-hexene plus an isomer. What is the structure of that isomer?

3) The kinetically controlled product in the below reaction is:



4) For the reaction above, which product is the result of 1,4-addition?



5) What would be the major product of the addition of HBr to 2,3-dimethyl-1,3-cyclohexadiene under thermodynamic conditions?

6) Consider the reaction with 1,3-buta-diene reacting with HCl. Propose a mechanism for the reaction. Also, Predict why the 1,4 adduct is the major product in this reaction compared to the 1,2.

Answer

1) The 1,4- product is more thermodynamically stable because there are two alkyl groups on each side of the double bond and more substituted alkenes are more stable.

2) 2,5-Dibromo-3-hexene

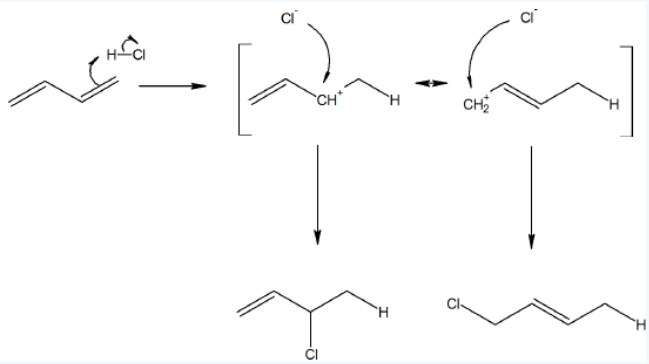
3) 3-Chloro-1-butene

4) 1-Chloro-2-butene

5)



6)



Even though the cation would prefer to be in a secondary position in the transition state, the final product is less stable with a terminal alkene. Therefore the major product will be the 1,4 adduct.

Questions

Q14.3.1

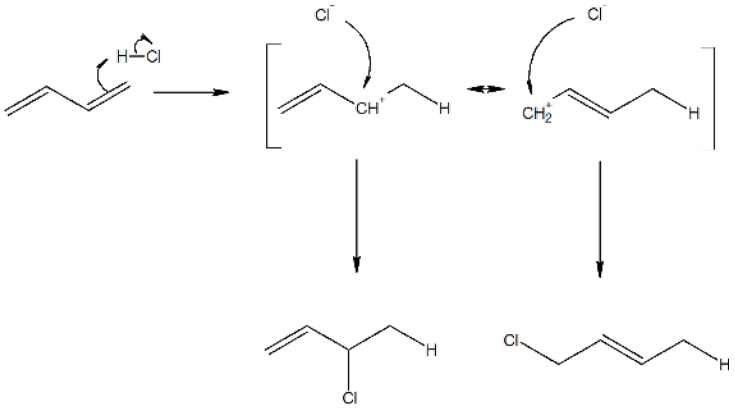
Consider the reaction with 1,3-buta-diene reacting with HCl. Propose a mechanism for the reaction.

Q14.3.2

Predict why the 1,4 adduct is the major product in this reaction compared to the 1,2.

Solutions

S14.3.1



S14.3.2

Even though the cation would prefer to be in a secondary position in the transition state, the final product is less stable with a terminal alkene. Therefore the major product will be the 1,4 adduct.

Contributors and Attributions

- Orthocresol (@chemistry StackExchange)
- Dr. Dietmar Kennepohl FCIC (Professor of Chemistry, Athabasca University)
- Natasha Singh

4.5: 14.3 Kinetic vs. Thermodynamic Control of Reactions is shared under a CC BY-NC-SA 4.0 license and was authored, remixed, and/or curated by LibreTexts.

4.6: 14.4 The Diels-Alder Cycloaddition Reaction

Objectives

After completing this section, you should be able to

1. write an equation to represent a typical Diels-Alder reaction.
2. draw the structure of the product formed when a given conjugated diene reacts with a given dienophile in a Diels-Alder reaction.
3. identify the diene and dienophile that must be used to prepare a given compound by a Diels-Alder reaction.
4. explain the general mechanism of the Diels-Alder reaction, without necessarily being able to describe it in detail.

Key Terms

Make certain that you can define, and use in context, the key terms below.

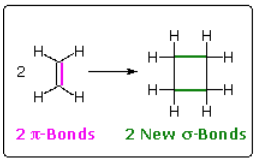
- Diels-Alder cycloaddition
- pericyclic reaction

Study Notes

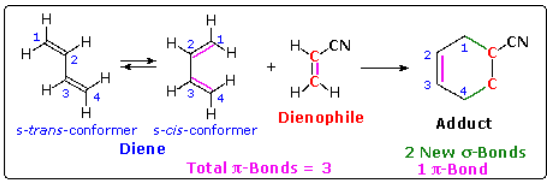
The Diels-Alder reaction is an example of an organic chemical reaction which does not proceed by either a polar or a free radical pathway, but rather a pericyclic reaction.

Although we do not expect you to be able to provide a detailed account of the mechanism of this reaction, you should learn enough about the Diels-Alder reaction to fulfil the objectives stated above. You will find it useful to contrast the mechanism of the Diels-Alder reaction with the polar and radical mechanisms studied earlier.

The unique character of conjugated dienes manifests itself dramatically in the **Diels-Alder Cycloaddition Reaction**. A cycloaddition reaction is the concerted bonding together of two independent pi-electron systems to form a new ring of atoms. When this occurs, two pi-bonds are converted to two sigma-bonds, the simplest example being the hypothetical combination of two ethene molecules to give cyclobutane. This does not occur under normal conditions, but the cycloaddition of 1,3-butadiene to cyanoethene (acrylonitrile) does, and this is an example of the Diels-Alder reaction. The following diagram illustrates two cycloadditions, and introduces several terms that are useful in discussing reactions of this kind.



A [2+2] Cycloaddition



A [4+2] Cycloaddition

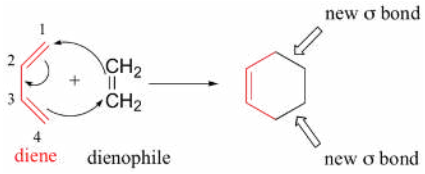
In the hypothetical ethylene dimerization on the left, each reactant molecule has a pi-bond (colored orange) occupied by two electrons. The cycloaddition converts these pi-bonds into new sigma-bonds (colored green), and this transformation is then designated a [2+2] cycloaddition, to enumerate the reactant pi-electrons that change their bonding location.
The Diels-Alder reaction is an important and widely used method for making six-membered rings, as shown on the right. The reactants used in such reactions are a conjugated diene, simply referred to as the **diene**, and a double or triple bond coreactant called the **dienophile**, because it combines with (has an affinity for) the diene. The Diels-Alder cycloaddition is classified as a [4+2] process because the diene has four pi-electrons that shift position in the reaction and the dienophile has two.

The Diels-Alder reaction is a single step process, so the diene component must adopt an s-cisconformation in order for the end carbon atoms (#1 & #4) to bond simultaneously to the dienophile. For many acyclic dienes the s-trans conformer is more stable than the s-cis conformer (due to steric crowding of the end groups), but the two are generally in rapid equilibrium, permitting the use of all but the most hindered dienes as reactants in Diels-Alder reactions. In its usual form, the diene component is electron rich, and the best dienophiles are electron poor due to electron withdrawing substituents such as CN, C=O & NO_2. The initial bonding

interaction reflects this electron imbalance, with the two new sigma-bonds being formed simultaneously, but not necessarily at equal rates.

Mechanism

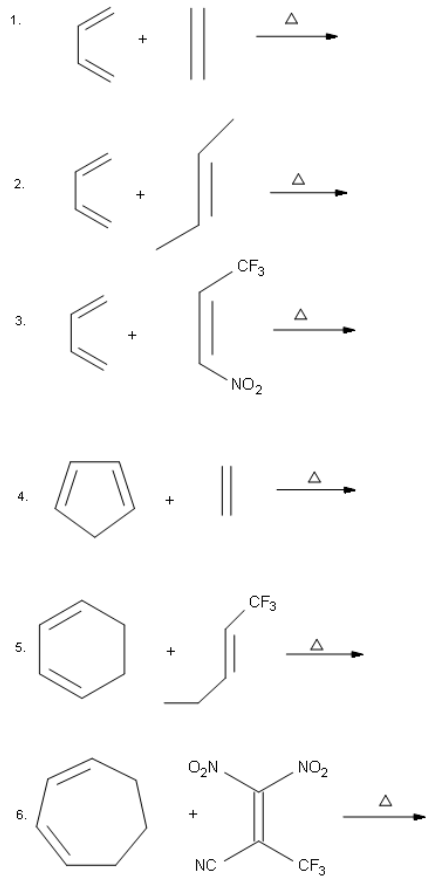
We end this chapter with a discussion of a type of reaction that is different from anything we have seen before. In the Diels-Alder cycloaddition reaction, a conjugated diene reacts with an alkene to form a ring structure.



In a Diels-Alder reaction, the alkene reacting partner is referred to as the **dienophile**. Essentially, this process involves overlap of the 2p orbitals on carbons 1 and 4 of the diene with 2p orbitals on the two sp^2-hybridized carbons of the dienophile. Both of these new overlaps end up forming new sigma bonds, and a new pi bond is formed between carbon 2 and 3 of the diene.

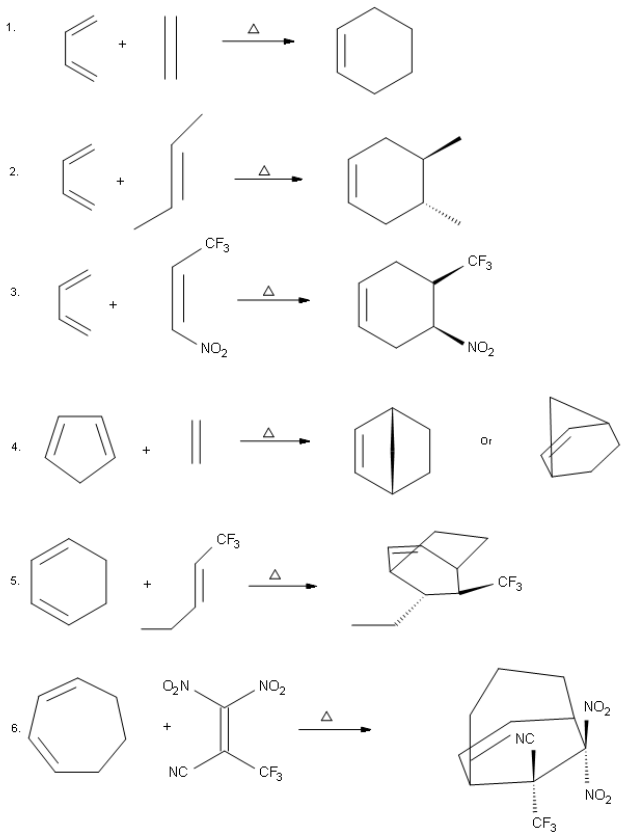
One of the most important things to understand about this process is that it is *concerted* – all of the electron rearrangement takes place at once, with no carbocation intermediates.

Problems



https://chem.libretexts.org/@go/page/167043

Answers



Contributors and Attributions

- Dr. Dietmar Kennepohl FCIC (Professor of Chemistry, Athabasca University)
- Prof. Steven Farmer (Sonoma State University)
- William Reusch, Professor Emeritus (Michigan State U.), Virtual Textbook of Organic Chemistry
- Organic Chemistry With a Biological Emphasis by Tim Soderberg (University of Minnesota, Morris)
- Amar Patel (UCD)

4.6: 14.4 The Diels-Alder Cycloaddition Reaction is shared under a CC BY-NC-SA 4.0 license and was authored, remixed, and/or curated by LibreTexts.

4.7: 14.5 Characteristics of the Diels-Alder Reaction

Objectives

After completing this section, you should be able to

1. determine whether or not a given compound would behave as a reactive dienophile in a Diels-Alder reaction.
2. predict the stereochemistry of the product obtained from the reaction of a given diene with a given dienophile.
3. recognize that in order to undergo a Diels-Alder reaction, a diene must be able to assume ans-cis geometry, and determine whether or not a given diene can assume this geometry.

Key Terms

Make certain that you can define, and use in context, the key terms below.

- dienophile
- dimerization

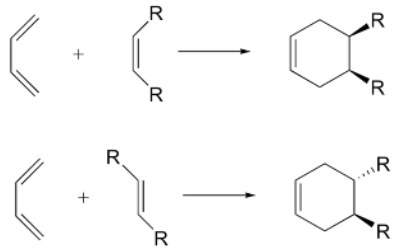
Study Notes

Make sure that you understand that the *s*-cis and *s*-trans forms of a diene such as 1,3-butadiene are conformers, not isomers. Note that some textbooks can confuse the issue further by referring to a compound such as (2Z, 4Z)-hexadiene as cis, cis-2,4-hexadiene, and saying that the most stable form of this compound is its *s*-trans conformer!

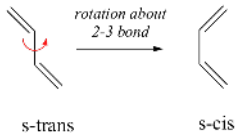
In fulfilling Objective 2, above, you must recognize that the Diels-Alder reaction is stereospecific.

Finally, note reaction **B** in the reading shows 1,3-cyclopentadiene reacting with another molecule of 1,3-cyclopentadiene. When the same compound acts as both diene and dienophile in a Diels-Alder reaction to couple it is a dimerization.

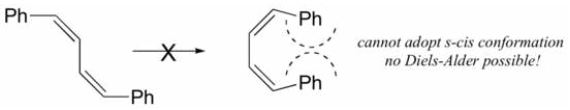
The Diels-Alder reaction is enormously useful for synthetic organic chemists, not only because ring-forming reactions are useful in general but also because in many cases two new stereocenters are formed, and the reaction is inherently stereospecific. A *cis* dienophile will generate a ring with *cis* substitution, while a *trans* dienophile will generate a ring with *trans* substitution:



In order for a Diels-Alder reaction to occur, the diene molecule must adopt what is called the **s-cis conformation**:



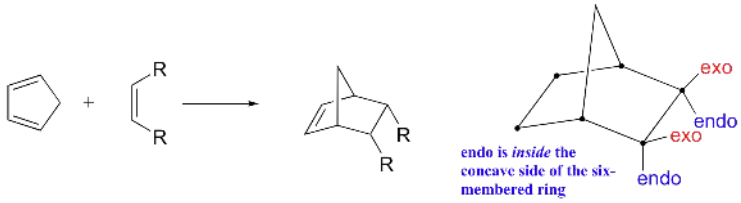
The s-cis conformation is higher in energy than the s-trans conformation, due to steric hindrance. For some dienes, extreme steric hindrance causes the s-cis conformation to be highly strained, and for this reason such dienes do not readily undergo Diels-Alder reactions.



Cyclic dienes, on the other hand, are 'locked' in the s-cis conformation, and are especially reactive. The result of a Diels-Alder reaction involving a cyclic diene is a **bicyclic** structure:

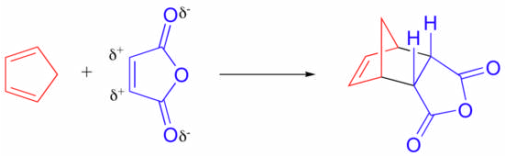


Here, we see another element of stereopecificity: Diels-Alder reactions with cyclic dienes favor the formation of bicyclic structures in which substituents are in the **endo position**.



The endo position on a bicyclic structure refers to the position that is *inside* the concave shape of the larger (six-membered) ring. As you might predict, the **exo position** refers to the *outside* position.

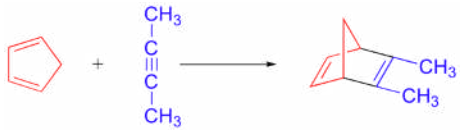
The rate at which a Diels-Alder reaction takes place depends on electronic as well as steric factors. A particularly rapid Diels-Alder reaction takes place between cyclopentadiene and maleic anhydride.



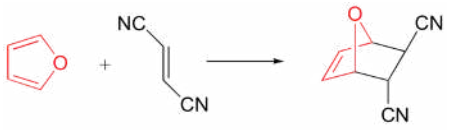
We already know that cyclopentadiene is a good diene because of its inherent s-cis conformation. Maleic anhydride is also a very good dienophile, because the electron-withdrawing effect of the carbonyl groups causes the two alkene carbons to be electron-poor, and thus a good target for attack by the pi electrons in the diene.

In general, Diels-Alder reactions proceed fastest with electron-donating groups on the diene (eg. alkyl groups) and electron-withdrawing groups on the dienophile.

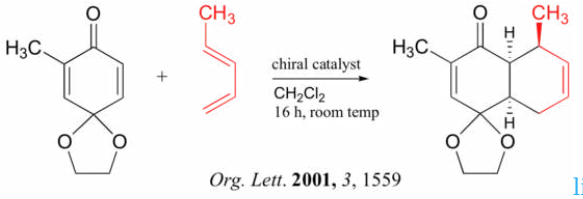
Alkynes can also serve as dienophiles in Diels-Alder reactions:



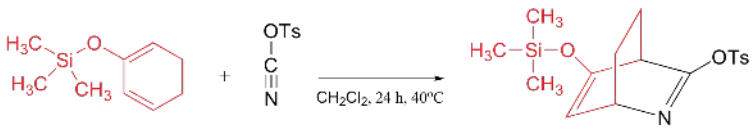
Below are just three examples of Diels-Alder reactions that have been reported in recent years:



J. Med. Chem. **2008,** *51*, 424 link



Org. Lett. **2001,** *3*, 1559 link



J. Org. Chem. **2003,** *68,* 8256 link

The Diels-Alder reaction is just one example of a **pericyclic** reaction: this is a general term that refers to concerted rearrangements that proceed though cyclic transition states. Two well-studied intramolecular pericyclic reactions are known as the Cope rearrangement . . .

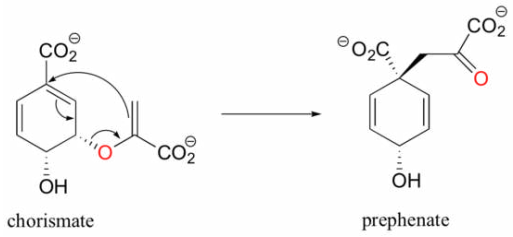


. . .and the Claisen rearrangement (when an oxygen is involved):



Notice that the both of these reactions require compounds in which two double bonds are separated by three single bonds.

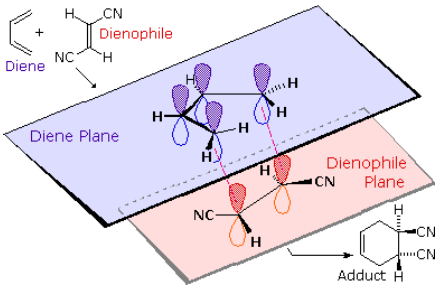
Pericyclic reactions are rare in biological chemistry, but here is one example: the Claisen rearrangement catalyzed by chorismate mutase in the aromatic amino acid biosynthetic pathway.



The study of pericyclic reactions is an area of physical organic chemistry that blossomed in the mid-1960s, due mainly to the work of R.B. Woodward, Roald Hoffman, and Kenichi Fukui. The **Woodward-Hoffman rules** for pericyclic reactions (and a simplified version introduced by Fukui) use molecular orbital theory to explain why some pericyclic processes take place and others do not. A full discussion is beyond the scope of this text, but if you go on to study organic chemistry at the advanced undergraduate or graduate level you are sure to be introduced to this fascinating area of inquiry.

Stereochemistry of the Diels-Alder reaction

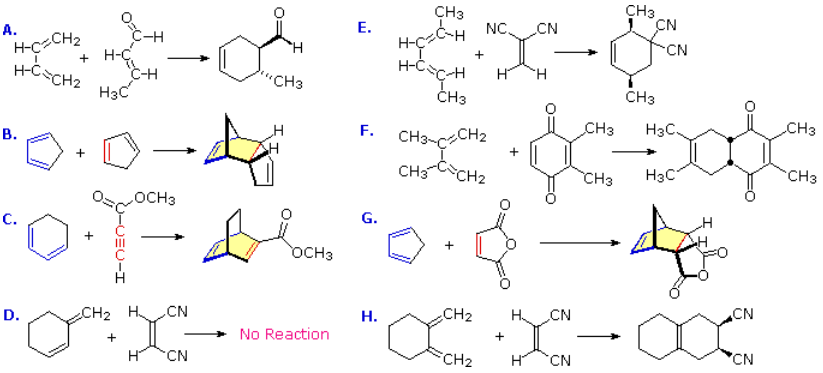
We noted earlier that addition reactions of alkenes often exhibited stereoselectivity, in that the reagent elements in some cases added syn and in other cases anti to the the plane of the double bond. Both reactants in the Diels-Alder reaction may demonstrate stereoisomerism, and when they do it is found that the relative configurations of the reactants are preserved in the product (the adduct). The following drawing illustrates this fact for the reaction of 1,3-butadiene with (E)-dicyanoethene. The trans relationship of the cyano groups in the dienophile is preserved in the six-membered ring of the adduct. Likewise, if the terminal carbons of the diene bear substituents, their relative configuration will be retained in the adduct. Using the earlier terminology, we could say that bonding to both the diene and the dienophile is syn. An alternative description, however, refers to the planar nature of both reactants and terms the bonding in each case to be **suprafacial** (i.e. to or from the same face of each plane). This stereospecificity also confirms the synchronous nature of the 1,4-bonding that takes place.



The essential characteristics of the Diels-Alder cycloaddition reaction may be summarized as follows:

i. The reaction always creates a new six-membered ring. When intramolecular, another ring may also be formed.
ii. The diene component must be able to assume a s-cis conformation.
iii. Electron withdrawing groups on the dienophile facilitate reaction.
iv. Electron donating groups on the diene facilitate reaction.
v. Steric hindrance at the bonding sites may inhibit or prevent reaction.
vi. The reaction is stereospecific with respect to substituent configuration in both the dienophile and the diene.

These features are illustrated by the following eight examples, one of which does not give a Diels-Alder cycloaddition.

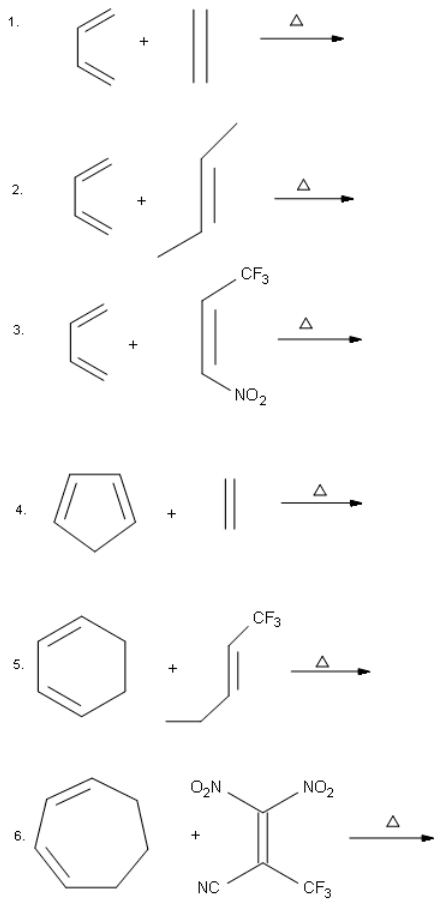


There is no reaction in example **D** because this diene cannot adopt an s-cis orientation. In examples **B, C, F, G & H** at least one of the reactants is cyclic so that the product has more than one ring, but the newly formed ring is always six-membered. In example **B** the the same cyclic compound acts as both the diene colored blue) and the dienophile (colored red). The adduct has three rings, two of which are the five-membered rings present in the reactant, and the third is the new six-membered ring (shaded light yellow). Example **C** has an alkyne as a dienophile (colored red), so the adduct retains a double bond at that location. This double bond could still serve as a dienophile, but in the present case the diene is sufficiently hindered to retard a second cycloaddition. The quinone dienophile in reaction **F** has two dienophilic double bonds. However, the double bond with two methyl substituents is less reactive than the unsubstituted dienophile due in part to the electron donating properties of the methyl groups and in part to steric hindrance. The stereospecificity of the Diels-Alder reaction is demonstrated by examples **A, E & H**. In **A & H** the stereogenic centers lie on the dienophile, whereas in **E** these centers are on the diene. In all cases the configuration of the reactant is preserved in the adduct.

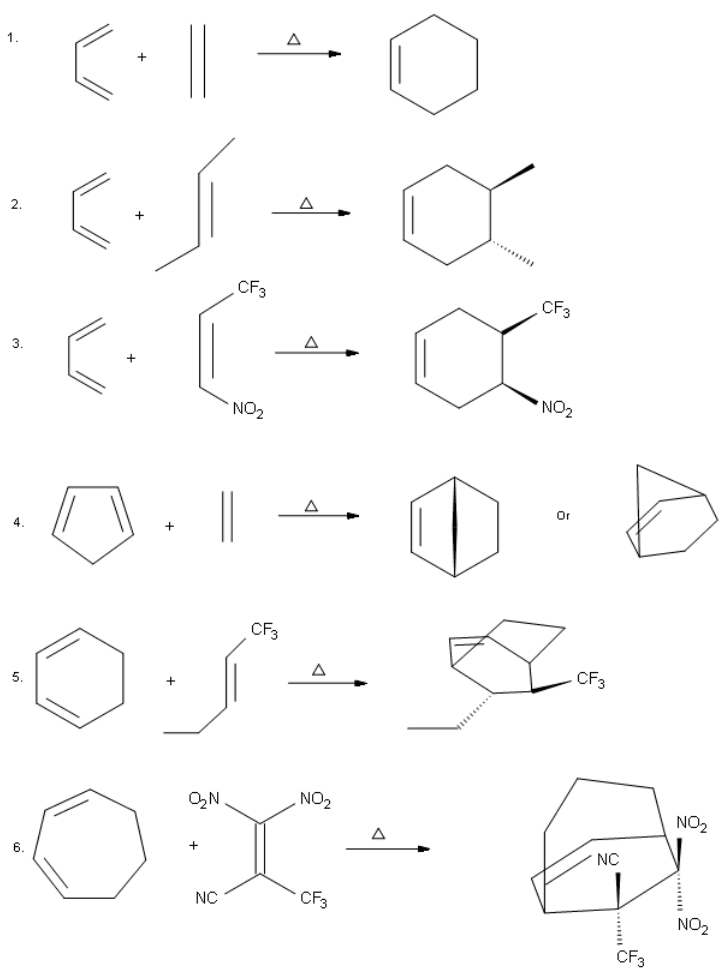
Exercises

? Exercise 4.7.1

https://chem.libretexts.org/@go/page/167044

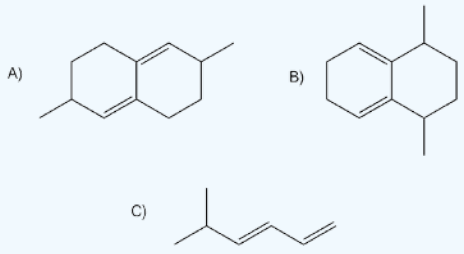


Answer



Exercise 4.7.2

Of the following dienes, which are *s*-trans and which are *s*-cis? Of those that are *s*-trans, are they able to rotate to become *s*-cis?



Answer

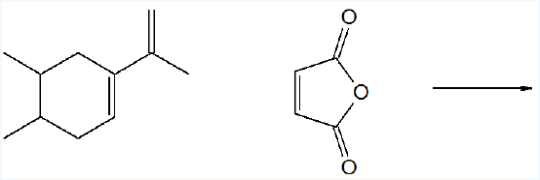
A) s-trans, unable to rotate to become s-cis

B) s-cis

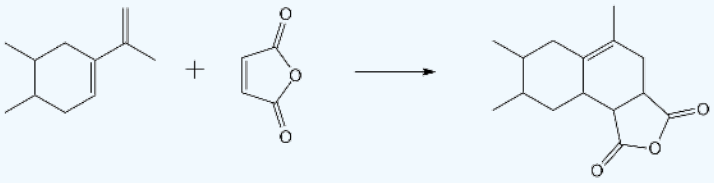
C) s-trans, can rotate to become s-cis.

Exercise 4.7.3

Predict the product of the following reaction.



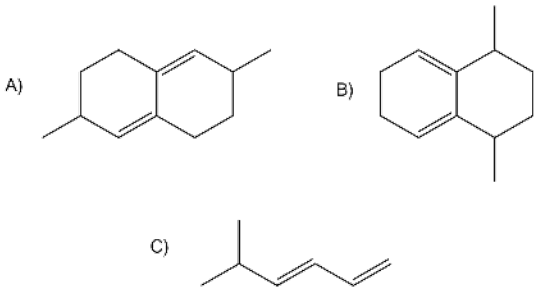
Answer



Questions

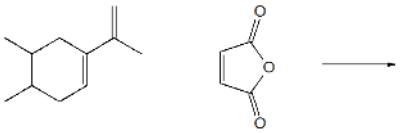
Q14.5.1

Of the following dienes, which are S-trans and which are s-cis? Of those that are s-trans, are they able to rotate to become s-cis?



Q14.5.2

Predict the product of the following reaction.



Solutions

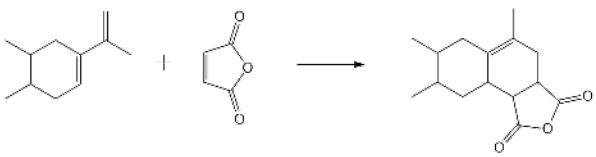
S14.5.1

A) s-trans, unable to rotate to become s-cis

B) s-cis

C) s-trans, can rotate to become s-cis.

S14.5.2



Contributors and Attributions

- Dr. Dietmar Kennepohl FCIC (Professor of Chemistry, Athabasca University)
- Prof. Steven Farmer (Sonoma State University)
- William Reusch, Professor Emeritus (Michigan State U.), Virtual Textbook of Organic Chemistry
- Organic Chemistry With a Biological Emphasis by Tim Soderberg (University of Minnesota, Morris)

4.7: 14.5 Characteristics of the Diels-Alder Reaction is shared under a CC BY-NC-SA 4.0 license and was authored, remixed, and/or curated by LibreTexts.

4.8: Natural and Synthetic Rubbers

Objectives

After completing this section, you should be able to

1. show that the polymerization of a diene, such as 1,3-butadiene or isoprene (2-methyl-1,3-butadiene), can result in the formation of either a cis or trans polymer.
2. draw the structure of natural rubber.
3. explain, briefly, the process of vulcanization.

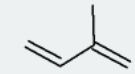
Key Terms

Make certain that you can define, and use in context, the key terms below.

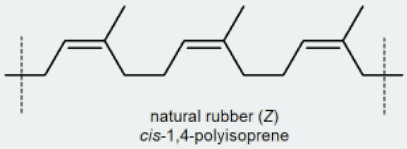
- cross-link
- vulcanization

Study Notes

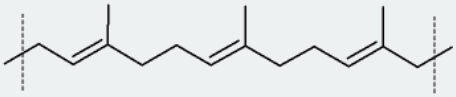
Natural rubber is formed from the isoprene monomer and has *Z* stereochemistry. The *E* polymer gutta-percha also occurs naturally, but is more brittle than rubber. Uses of this thermoplastic include dentistry, electrical insulators and the covering on golf balls.



isoprene
2-methyl-1,3-butadiene



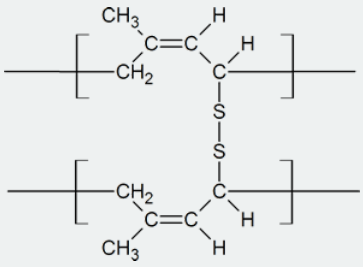
natural rubber (*Z*)
cis-1,4-polyisoprene



gutta-percha (*E*)
trans-1,4-polyisoprene

Before 1839, the uses of natural rubber were somewhat limited. It became sticky in summer, hardened and cracked in winter, and was susceptible to attack by a variety of solvents. Charles Goodyear became interested in rubber in 1831, and bought the Eagle India Rubber Company of Woburn, Massachusetts, in 1838. In January of 1839, Goodyear accidentally placed a sample of rubber that had been mixed with sulfur and lead(II) oxide on a hot stove; the result was a product similar to charred leather, which did not melt below 138°C. Goodyear was granted a U.S. patent for his process (called vulcanization) in June of 1844. The story of vulcanization is an example of how major scientific and technological advances are often brought about as a result of an accidental discovery.

Notice that in the vulcanization process, the sulfur bridges are attached to allylic carbon atoms which connect the long *Z* polymer chains of rubber.



Vulcanized rubber

https://chem.libretexts.org/@go/page/167045

The amount of sulfur used in the vulcanization process will depend on the rigidity required in the product. For example, about 5% sulfur is used when producing rubber for rubber bands; about 30% sulfur is used when making rubber for use in battery casings. There are several characteristics of dienes and rubbers that you should recognize. First, be aware of the similarity between the polymerization of a diene and the 1,4-addition reactions of dienes. Second, recognize the similarity between a vulcanized rubber and a peptide containing cysteine cross-links. Third, be aware that as natural rubber contains double bonds, it will display some of the properties of simple alkenes.

The 1,4 polymerization of 1,3-butadiene shown in the reading produces the *trans* form of polybutadiene. However, it should be noted that the *cis* form shown here can also be formed.

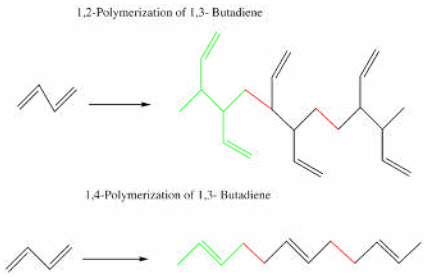


cis- polbutadiene

Conjugated dienes (alkenes with two double bonds and a single bond in between) can be polymerized to form important compounds like rubber. This takes place, in different forms, both in nature and in the laboratory. Interactions between double bonds on multiple chains leads to cross-linkage which creates elasticity within the compound.

Polymerization of 1,3-Butadiene

For rubber compounds to be synthesized, 1,3-butadiene must be polymerized. Below is a simple illustration of how this compound is formed into a chain. The 1,4 polymerization is much more useful to polymerization reactions.



Above, the green structures represent the base units of the polymers that are synthesized and the red represents the bonds between these units which form these polymers. Whether the 1,3 product or the 1,4 product is formed depends on whether the reaction is thermally or kinetically controlled.

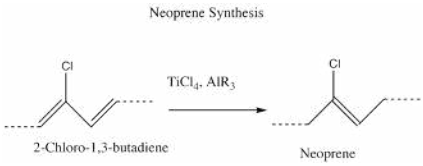
Natural Rubber

Natural rubber is an addition polymer that is obtained as a milky white fluid known as latex from a tropical rubber tree. Natural rubber is from the monomer isoprene (2-methyl-1,3-butadiene), which is a conjugated diene hydrocarbon as mentioned above. In natural rubber, most of the double fonds formed in the polymer chain have the Z configuration, resulting in natural rubber's elastomer qualities.

Charles Goodyear accidentally discovered that by mixing sulfur and rubber, the properties of the rubber improved in being tougher, resistant to heat and cold, and increased in elasticity. This process was later called vulcanization after the Roman god of fire. Vulcanization causes shorter chains to cross link through the sulfur to longer chains. The development of vulcanized rubber for automobile tires greatly aided this industry.

Synthetic Rubber

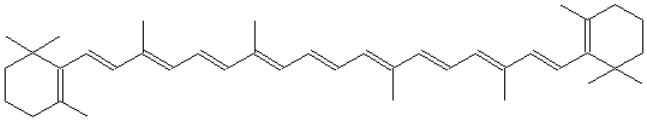
The most important synthetic rubber is Neoprene which is produced by the polymerization of 2-chloro-1,3-butadiene.



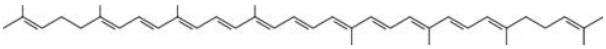
In this illustration, the dashed lines represent repetition of the same base units, so both the products and reactants are polymers. The reaction proceeds with a mechanism similar to the Friedel-Crafts mechanism. Cross-linkage between the chlorine atom of one chain and the double bond of another contributes to the overall elasticity of neoprene. This cross-linkage occurs as the chains lie next to each other at random angles, and the attractions between double bonds prevent them from sliding back and forth.

Colored molecules

The counjugated double bonds in beta-carotene produce the orange color in carrots. The conjugated double bons in lycopene produce the red color in tomatoes.



ß carotene



lycopene

Outside links

- "Dienes," http://en.Wikipedia.org/wiki/Diene
- "Rubber," http://en.Wikipedia.org/wiki/Rubber
- "Neoprene," http://en.Wikipedia.org/wiki/Neoprene

References

1. Vollhardt, Peter, and Neil E. Schore. Organic Chemistry: Structure and Function. New York: W. H. Freeman & Company, 2007.
2. Buehr, Walter. Rubber: Natural and Synthetic. Morrow, 1964.

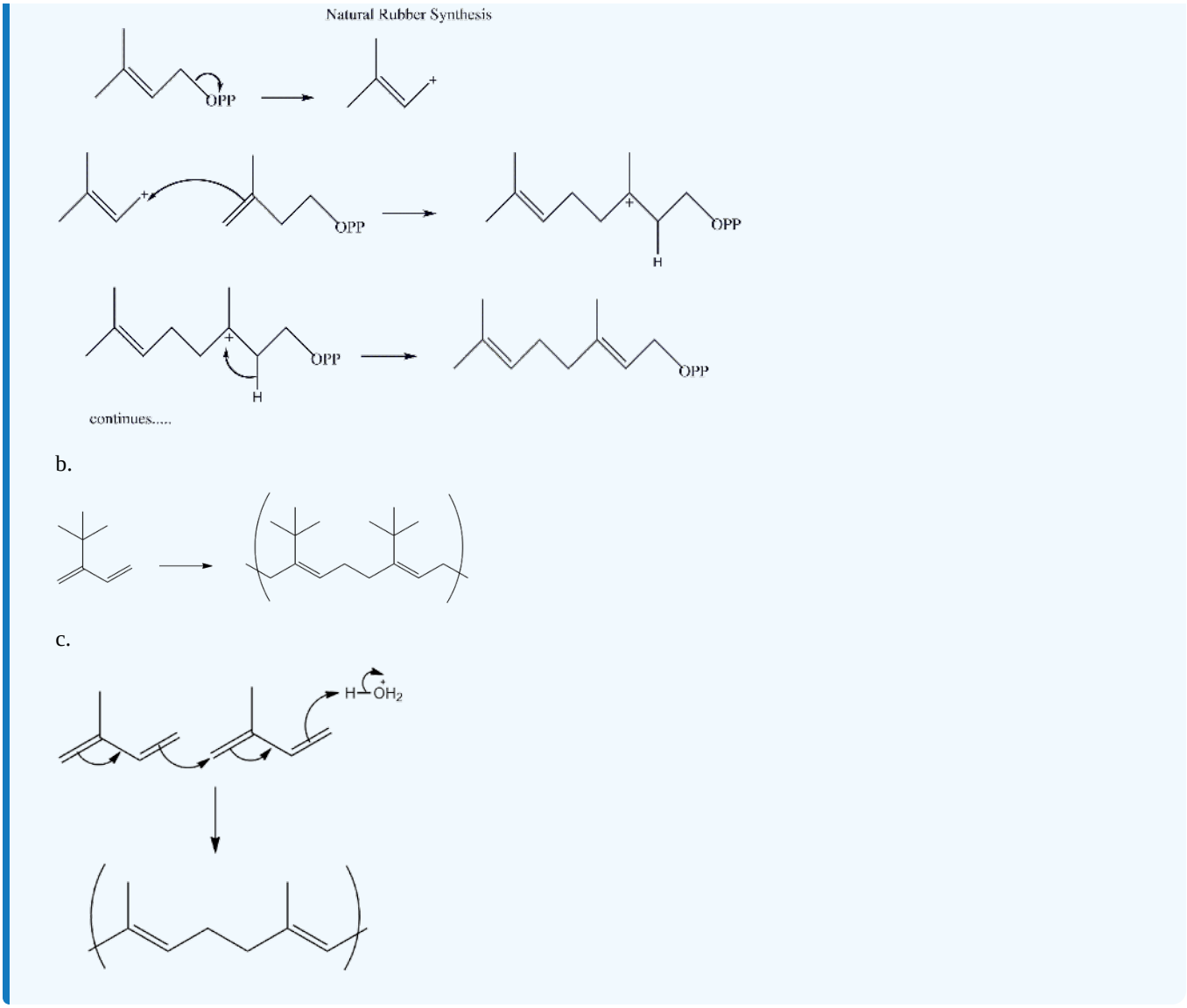
Exercise

? Exercise 4.8.1

a. Draw out the mechanism for the natural synthesis of rubber from 3-methyl-3-butenyl pyrophosphate and 2-methyl-1,3-butadiene. Show the movement of electrons with arrows
b. Draw a segment for the polymer that may be made from 2-*tert*-butyl-1,3-butadiene.
c. Propose the mechanism for the acid catalyzed polymerization of 2-methyl-1,3-butadiene.

Answer

a.



Contributors and Attributions

- Dr. Dietmar Kennepohl FCIC (Professor of Chemistry, Athabasca University)
- Prof. Steven Farmer (Sonoma State University)
- William Reusch, Professor Emeritus (Michigan State U.), Virtual Textbook of Organic Chemistry
- Organic Chemistry With a Biological Emphasis by Tim Soderberg (University of Minnesota, Morris)

4.8: Natural and Synthetic Rubbers is shared under a CC BY-NC-SA 4.0 license and was authored, remixed, and/or curated by LibreTexts.

4.9: Ultraviolet Spectroscopy

Objectives

After completing this section, you should be able to

1. identify the ultraviolet region of the electromagnetic spectrum which is of most use to organic chemists.
2. interpret the ultraviolet spectrum of 1,3-butadiene in terms of the molecular orbitals involved.
3. describe in general terms how the ultraviolet spectrum of a compound differs from its infrared and NMR spectra.

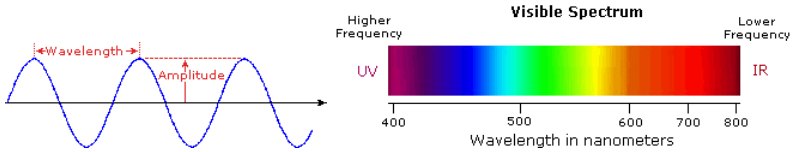
Key Terms

Make certain that you can define, and use in context, the key term below.

- ultraviolet (UV) spectroscopy

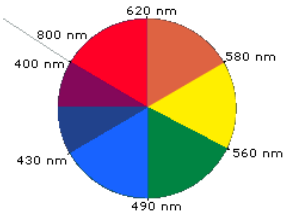
Study Notes

Ultraviolet spectroscopy provides much less information about the structure of molecules than do the spectroscopic techniques studied earlier (infrared spectroscopy, mass spectroscopy, and NMR spectroscopy). Thus, your study of this technique will be restricted to a brief overview. You should, however, note that for an organic chemist, the most useful ultraviolet region of the electromagnetic spectrum is that in which the radiation has a wavelength of between 200 and 400 nm.



- **Violet:** 400 - 420 nm
- **Indigo:** 420 - 440 nm
- **Blue:** 440 - 490 nm
- **Green:** 490 - 570 nm
- **Yellow:** 570 - 585 nm
- **Orange:** 585 - 620 nm
- **Red:** 620 - 780 nm

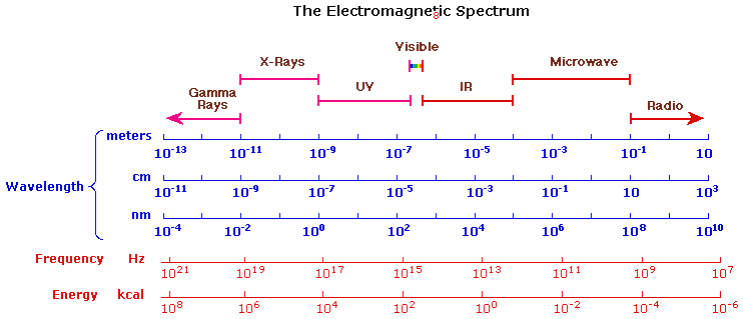
When white light passes through or is reflected by a colored substance, a characteristic portion of the mixed wavelengths is absorbed. The remaining light will then assume the complementary color to the wavelength(s) absorbed. This relationship is demonstrated by the color wheel shown below. Here, complementary colors are diametrically opposite each other. Thus, absorption of 420-430 nm light renders a substance yellow, and absorption of 500-520 nm light makes it red. Green is unique in that it can be created by absoption close to 400 nm as well as absorption near 800 nm.



Early humans valued colored pigments, and used them for decorative purposes. Many of these were inorganic minerals, but several important organic dyes were also known. These included the crimson pigment, kermesic acid, the blue dye, indigo, and the yellow saffron pigment, crocetin. A rare dibromo-indigo derivative, punicin, was used to color the robes of the royal and wealthy. The deep orange hydrocarbon carotene is widely distributed in plants, but is not sufficiently stable to be used as permanent pigment, other than for food coloring. A common feature of all these colored compounds, displayed below, is a system of **extensively conjugated π-electrons**.

The Electromagnetic Spectrum

The visible spectrum constitutes but a small part of the total radiation spectrum. Most of the radiation that surrounds us cannot be seen, but can be detected by dedicated sensing instruments. This **electromagnetic spectrum** ranges from very short wavelengths (including gamma and x-rays) to very long wavelengths (including microwaves and broadcast radio waves). The following chart displays many of the important regions of this spectrum, and demonstrates the inverse relationship between wavelength and frequency (shown in the top equation below the chart).



The energy associated with a given segment of the spectrum is proportional to its frequency. The bottom equation describes this relationship, which provides the energy carried by a photon of a given wavelength of radiation.

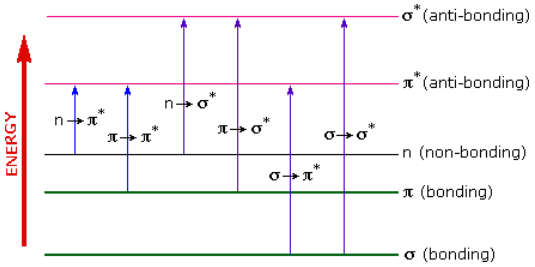
$\upsilon = c/\lambda$ υ=frequency, λ=wavelength, c=velocity of light ($c = 3 \cdot 10^{10}$ cm/sec)
$\Delta E = h\upsilon$ E=energy, υ=frequency, h=Planck's constant ($h = 6.6 \cdot 10^{-27}$ erg sec)

To obtain specific frequency, wavelength and energy values use this calculator.

UV-Visible Absorption Spectra

To understand why some compounds are colored and others are not, and to determine the relationship of conjugation to color, we must make accurate measurements of light absorption at different wavelengths in and near the visible part of the spectrum. Commercial optical spectrometers enable such experiments to be conducted with ease, and usually survey both the near ultraviolet and visible portions of the spectrum.

The visible region of the spectrum comprises photon energies of 36 to 72 kcal/mole, and the near ultraviolet region, out to 200 nm, extends this energy range to 143 kcal/mole. Ultraviolet radiation having wavelengths less than 200 nm is difficult to handle, and is seldom used as a routine tool for structural analysis.



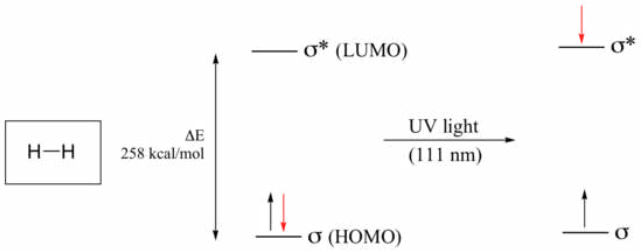
The energies noted above are sufficient to promote or excite a molecular electron to a higher energy orbital. Consequently, absorption spectroscopy carried out in this region is sometimes called "electronic spectroscopy". A diagram showing the various kinds of electronic excitation that may occur in organic molecules is shown on the left. Of the six transitions outlined, only the two lowest energy ones (left-most, colored blue) are achieved by the energies available in the 200 to 800 nm spectrum. As a rule, energetically favored electron promotion will be from the highest occupied molecular orbital (HOMO) to the lowest unoccupied molecular orbital (LUMO), and the resulting species is called an **excited state**.

When sample molecules are exposed to light having an energy that matches a possible electronic transition within the molecule, some of the light energy will be absorbed as the electron is promoted to a higher energy orbital. An optical spectrometer records the wavelengths at which absorption occurs, together with the degree of absorption at each wavelength. The resulting spectrum is presented as a graph of absorbance (A) versus wavelength, as in the isoprene spectrum shown below. Since isoprene is colorless, it

does not absorb in the visible part of the spectrum and this region is not displayed on the graph. **Absorbance** usually ranges from 0 (no absorption) to 2 (99% absorption), and is precisely defined in context with spectrometer operation.

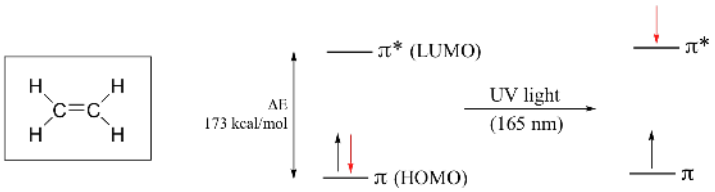
Electronic transitions

Let's take as our first example the simple case of molecular hydrogen, H_2. As you may recall from section 2.1A, the molecular orbital picture for the hydrogen molecule consists of one bonding σ MO, and a higher energy antibonding σ* MO. When the molecule is in the ground state, both electrons are paired in the lower-energy bonding orbital – this is the Highest Occupied Molecular Orbital (HOMO). The antibonding σ* orbital, in turn, is the Lowest Unoccupied Molecular Orbital (LUMO).



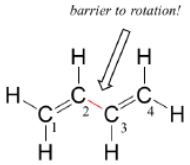
If the molecule is exposed to light of a wavelength with energy equal to **ΔE**, the HOMO-LUMO energy gap, this wavelength will be absorbed and the energy used to bump one of the electrons from the HOMO to the LUMO – in other words, from the σ to the σ* orbital. This is referred to as a **σ - σ* transition**. **ΔE** for this electronic transition is 258 kcal/mol, corresponding to light with a wavelength of 111 nm.

When a double-bonded molecule such as ethene (common name ethylene) absorbs light, it undergoes a **π - π* transition.** Because π- π* energy gaps are narrower than σ - σ* gaps, ethene absorbs light at 165 nm - a longer wavelength than molecular hydrogen.



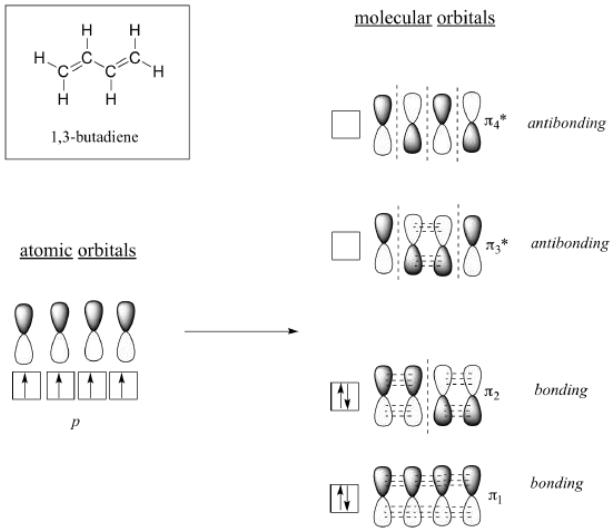
The electronic transitions of both molecular hydrogen and ethene are too energetic to be accurately recorded by standard UV spectrophotometers, which generally have a range of 220 – 700 nm. Where UV-vis spectroscopy becomes useful to most organic and biological chemists is in the study of molecules with conjugated pi systems. In these groups, the energy gap for π -π* transitions is smaller than for isolated double bonds, and thus the wavelength absorbed is longer. Molecules or parts of molecules that absorb light strongly in the UV-vis region are called **chromophores**.

Next, we'll consider the 1,3-butadiene molecule. From valence orbital theory alone we might expect that the C_2-C_3 bond in this molecule, because it is a sigma bond, would be able to rotate freely.



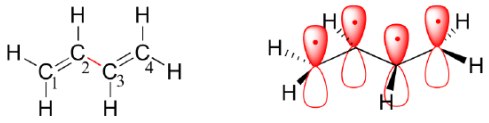
Experimentally, however, it is observed that there is a significant barrier to rotation about the C_2-C_3 bond, and that the entire molecule is planar. In addition, the C_2-C_3 bond is 148 pm long, shorter than a typical carbon-carbon single bond (about 154 pm), though longer than a typical double bond (about 134 pm).

Molecular orbital theory accounts for these observations with the concept of **delocalized π bonds**. In this picture, the four *p* atomic orbitals combine mathematically to form four pi molecular orbitals of increasing energy. Two of these - the bonding pi orbitals - are lower in energy than the *p* atomic orbitals from which they are formed, while two - the antibonding pi orbitals - are higher in energy.



The lowest energy molecular orbital, pi_1, has only constructive interaction and zero nodes. Higher in energy, but still lower than the isolated *p* orbitals, the pi_2 orbital has one node but two constructive interactions - thus it is still a bonding orbital overall. Looking at the two antibonding orbitals, pi_3* has two nodes and one constructive interaction, while pi_4* has three nodes and zero constructive interactions.

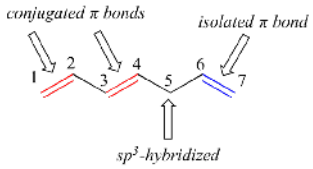
By the *aufbau* principle, the four electrons from the isolated $2p_z$ atomic orbitals are placed in the bonding pi_1 and pi_2 MO's. Because pi_1 includes constructive interaction between C_2 and C_3, there is a degree, in the 1,3-butadiene molecule, of pi-bonding interaction between these two carbons, which accounts for its shorter length and the barrier to rotation. The valence bond picture of 1,3-butadiene shows the two pi bonds as being isolated from one another, with each pair of pi electrons 'stuck' in its own pi bond. However, molecular orbital theory predicts (accurately) that the four pi electrons are to some extent delocalized, or 'spread out', over the whole pi system.



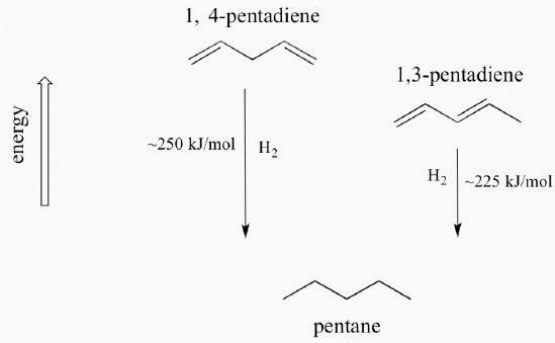
1,3-butadiene

space-filling view

1,3-butadiene is the simplest example of a system of **conjugated pi bonds**. To be considered conjugated, two or more pi bonds must be separated by only one single bond – in other words, there cannot be an intervening sp^3-hybridized carbon, because this would break up the overlapping system of parallel *p* orbitals. In the compound below, for example, the C_1-C_2 and C_3-C_4 double bonds are conjugated, while the C_6-C_7 double bond is **isolated** from the other two pi bonds by sp^3-hybridized C_5.

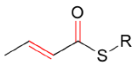


A very important concept to keep in mind is that *there is an inherent thermodynamic stability associated with conjugation.* This stability can be measured experimentally by comparing the **heat of hydrogenation** of two different dienes. (Hydrogenation is a reaction type that we will learn much more about in chapter 15: essentially, it is the process of adding a hydrogen molecule - two protons and two electrons - to a p bond). When the two *conjugated* double bonds of 1,3-pentadiene are 'hydrogenated' to produce pentane, about 225 kJ is released per mole of pentane formed. Compare that to the approximately 250 kJ/mol released when the two *isolated* double bonds in 1,4-pentadiene are hydrogenated, also forming pentane.

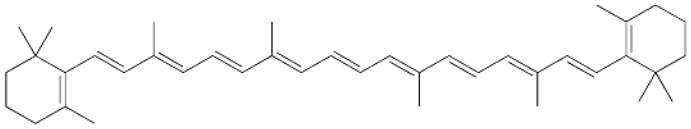


The conjugated diene is lower in energy: in other words, it is more stable. In general, conjugated pi bonds are more stable than isolated pi bonds.

Conjugated pi systems can involve oxygen and nitrogen atoms as well as carbon. In the metabolism of fat molecules, some of the key reactions involve alkenes that are conjugated to carbonyl groups.



In molecules with extended pi systems, the HOMO-LUMO energy gap becomes so small that absorption occurs in the visible rather then the UV region of the electromagnetic spectrum. Beta-carotene, with its system of 11 conjugated double bonds, absorbs light with wavelengths in the blue region of the visible spectrum while allowing other visible wavelengths – mainly those in the red-yellow region - to be transmitted. This is why carrots are orange.

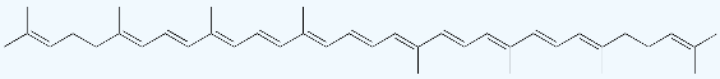


β-carotene

Exercise

? Exercise 4.9.1

1. 50 microliters of an aqueous sample of double stranded DNA is dissolved in 950 microliters of water. This diluted solution has a maximal absorbance of 0.326 at 260 nm. What is the concentration of the original (more concentrated) DNA sample, expressed in micrograms per microliter?
2. What is the energy range for 300 nm to 500 nm in the ultraviolet spectrum? How does this compare to energy values from NMR and IR spectroscopy?
3. Identify all isolated and conjugated pi bonds in lycopene, the red-colored compound in tomatoes. How many pi electrons are contained in the conjugated pi system?



lycopene

Answer

1) Using ε = A/c, we plug in our values for ε and A and find that c = 3.27 x 10^{-5}M, or 32.7 mM.

2)

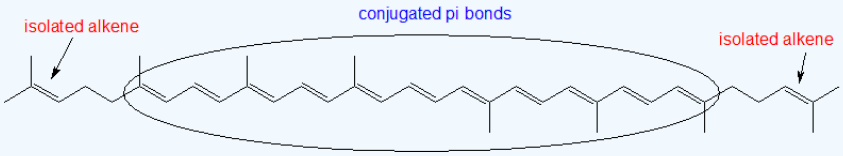
$E = hc/\lambda$

$E = (6.62 \times 10^{-34}\ \text{Js})(3.00 \times 10^{8}\ \text{m/s})/(3.00 \times 10^{-7}\ \text{m})$

$E = 6.62 \times 10^{-19}\ \text{J}$

The range of 3.972×10^{-19} to 6.62×10^{-19} joules. This energy range is greater in energy than the in NMR and IR.

3)



Questions

Q14.7.1

What is the energy range for 300 nm to 500 nm in the ultraviolet spectrum? How does this compare to energy values from NMR and IR spectroscopy?

Solutions

S14.7.1

$E = hc/\lambda$

$E = (6.62 \times 10^{-34}\ \text{Js})(3.00 \times 10^{8}\ \text{m/s})/(3.00 \times 10^{-7}\ \text{m})$

$E = 6.62 \times 10^{-19}\ \text{J}$

The range of 3.972×10^{-19} to 6.62×10^{-19} joules. This energy range is greater in energy than the in NMR and IR.

Contributors and Attributions

- Dr. Dietmar Kennepohl FCIC (Professor of Chemistry, Athabasca University)
- Prof. Steven Farmer (Sonoma State University)
- Organic Chemistry With a Biological Emphasis by Tim Soderberg (University of Minnesota, Morris)

4.9: Ultraviolet Spectroscopy is shared under a CC BY-NC-SA 4.0 license and was authored, remixed, and/or curated by LibreTexts.

4.10: The Effect of Conjugation

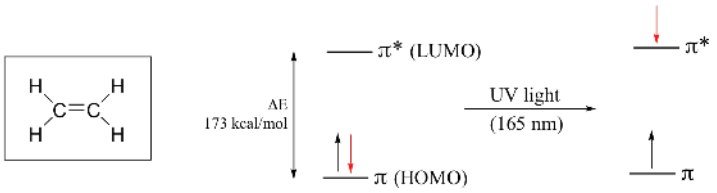
Objective

After completing this section, you should be able to use data from ultraviolet spectra to assist in the elucidation of unknown molecular structures.

Study Notes

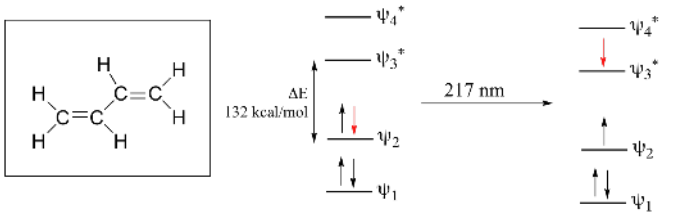
It is important that you recognize that the ultraviolet absorption maximum of a conjugated molecule is dependent upon the extent of conjugation in the molecule.

When a double-bonded molecule such as ethene (common name ethylene) absorbs light, it undergoes a **π - π* transition.** Because π- π* energy gaps are narrower than σ - σ***** gaps, ethene absorbs light at 165 nm - a longer wavelength than molecular hydrogen.



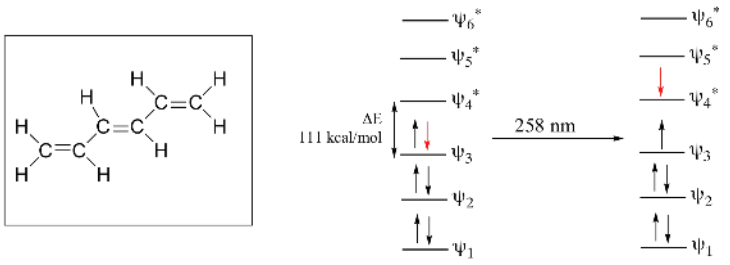
The electronic transitions of both molecular hydrogen and ethene are too energetic to be accurately recorded by standard UV spectrophotometers, which generally have a range of 220 – 700 nm. Where UV-vis spectroscopy becomes useful to most organic and biological chemists is in the study of molecules with conjugated pi systems. In these groups, the energy gap for π -π* transitions is smaller than for isolated double bonds, and thus the wavelength absorbed is longer. Molecules or parts of molecules that absorb light strongly in the UV-vis region are called **chromophores**.

Let's revisit the MO picture for 1,3-butadiene, the simplest conjugated system (see section 2.1B). Recall that we can draw a diagram showing the four pi MO's that result from combining the four $2p_z$ atomic orbitals. The lower two orbitals are bonding, while the upper two are antibonding.



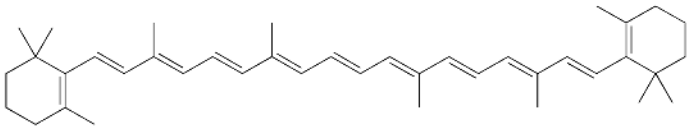
Comparing this MO picture to that of ethene, our isolated pi-bond example, we see that the HOMO-LUMO energy gap is indeed smaller for the conjugated system. 1,3-butadiene absorbs UV light with a wavelength of 217 nm.

As conjugated pi systems become larger, the energy gap for a π - π* transition becomes increasingly narrow, and the wavelength of light absorbed correspondingly becomes longer. The absorbance due to the π - π* transition in 1,3,5-hexatriene, for example, occurs at 258 nm, corresponding to a **Δ**E of 111 kcal/mol.



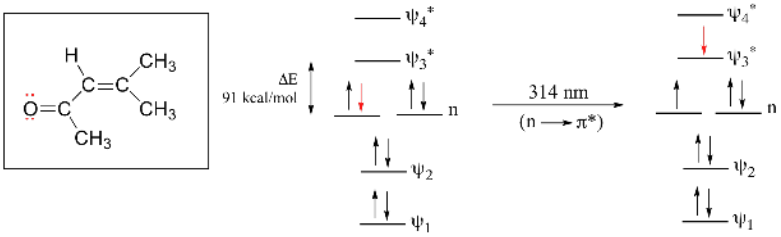
In molecules with extended pi systems, the HOMO-LUMO energy gap becomes so small that absorption occurs in the visible rather then the UV region of the electromagnetic spectrum. Beta-carotene, with its system of 11 conjugated double bonds, absorbs

light with wavelengths in the blue region of the visible spectrum while allowing other visible wavelengths – mainly those in the red-yellow region - to be transmitted. This is why carrots are orange.



β-carotene

The conjugated pi system in 4-methyl-3-penten-2-one gives rise to a strong UV absorbance at 236 nm due to a π - π* transition. However, this molecule also absorbs at 314 nm. This second absorbance is due to the transition of a non-bonding (lone pair) electron on the oxygen up to a π* antibonding MO:

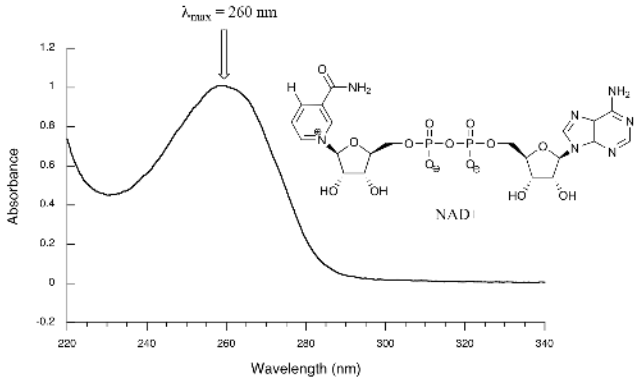


This is referred to as an **n - π* transition**. The nonbonding (n) MO's are higher in energy than the highest bonding p orbitals, so the energy gap for an n - π* transition is smaller that that of a π - π* transition – and thus the n - π* peak is at a longer wavelength. In general, n - π* transitions are weaker (less light absorbed) than those due to π - π* transitions.

Looking at UV-vis spectra

Edit section

We have been talking in general terms about how molecules absorb UV and visible light – now let's look at some actual examples of data from a UV-vis absorbance spectrophotometer. The basic setup is the same as for IR spectroscopy: radiation with a range of wavelengths is directed through a sample of interest, and a detector records which wavelengths were absorbed and to what extent the absorption occurred. Below is the absorbance spectrum of an important biological molecule called nicotinamide adenine dinucleotide, abbreviated NAD^+ (we'll learn what it does in section 16.4) This compound absorbs light in the UV range due to the presence of conjugated pi-bonding systems.



You'll notice that this UV spectrum is much simpler than the IR spectra we saw earlier: this one has only one peak, although many molecules have more than one. Notice also that the convention in UV-vis spectroscopy is to show the baseline at the bottom of the graph with the peaks pointing up. Wavelength values on the x-axis are generally measured in nanometers (nm) rather than in cm^{-1} as is the convention in IR spectroscopy.

Peaks in UV spectra tend to be quite broad, often spanning well over 20 nm at half-maximal height. Typically, there are two things that we look for and record from a UV-Vis spectrum.. The first is $\lambda_{max,}$ which is the wavelength at maximal light absorbance. As you can see, NAD^+ has $\lambda_{max,}$ = 260 nm. We also want to record how much light is absorbed at $\lambda_{max.}$ Here we use a unitless number called **absorbance**, abbreviated 'A'. This contains the same information as the 'percent transmittance' number used in IR spectroscopy, just expressed in slightly different terms. To calculate absorbance at a given wavelength, the computer in the

spectrophotometer simply takes the intensity of light at that wavelength *before* it passes through the sample (I_0), divides this value by the intensity of the same wavelength *after* it passes through the sample (I), then takes the $\log_{10}$ of that number:

$A = \log I_0/I$

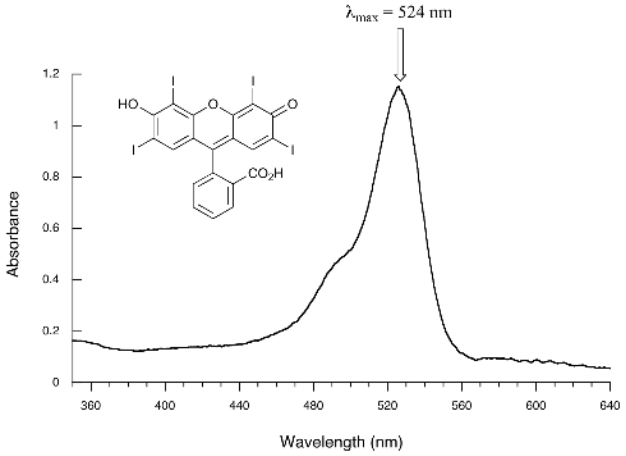
You can see that the absorbance value at 260 nm (A_{260}) is about 1.0 in this spectrum.

Example 14.8.1

Express A = 1.0 in terms of percent transmittance (%T, the unit usually used in IR spectroscopy (and sometimes in UV-vis as well).

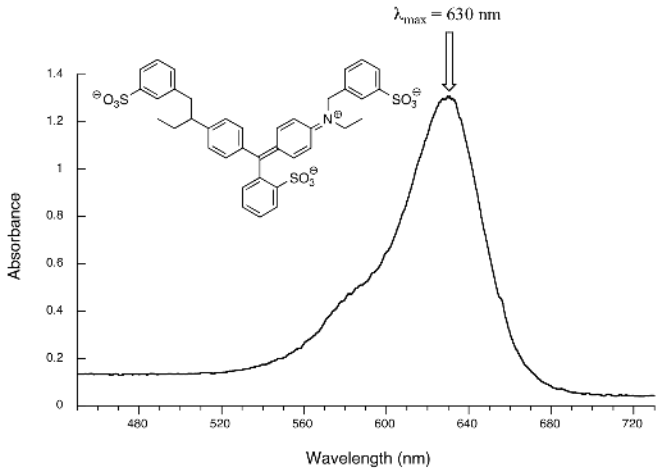
Solution

Here is the absorbance spectrum of the common food coloring Red #3:



Here, we see that the extended system of conjugated pi bonds causes the molecule to absorb light in the visible range. Because the λ_{max} of 524 nm falls within the green region of the spectrum, the compound appears red to our eyes.

Now, take a look at the spectrum of another food coloring, Blue #1:

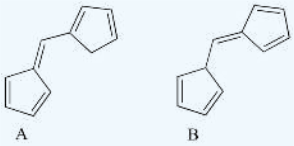


Here, maximum absorbance is at 630 nm, in the orange range of the visible spectrum, and the compound appears blue.

Exercises

Exercise 4.10.1

Which of the following molecules would you expect absorb at a longer wavelength in the UV region of the electromagnetic spectrum? Explain your answer.

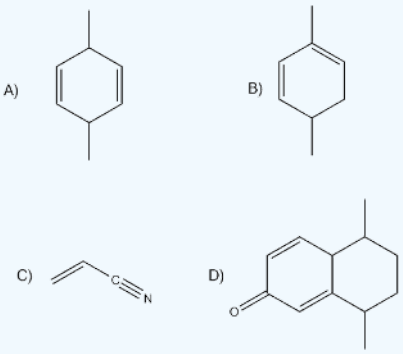


Answer

Compound A would have the longer wavelength as all 5 allylic fragments are conjugated, whereas Compound B has a group of 3 and a group of 2 allyic fragments congugated.

Exercise 4.10.2

Which of the following would show UV absorptions in the 200-300 nm range?



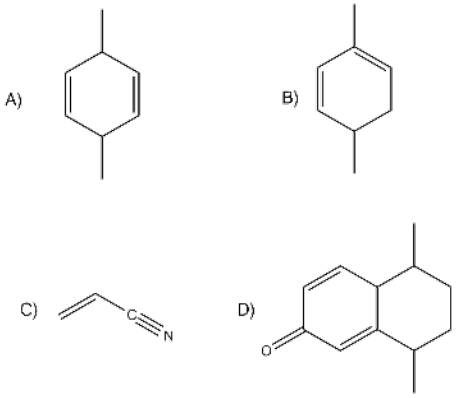
Answer

B and D would be in that range.

Questions

Q14.8.1

Which of the following would show UV absorptions in the 200-300 nm range?



Solutions

S14.8.1

B and D would be in that range.

Contributors and Attributions

- Dr. Dietmar Kennepohl FCIC (Professor of Chemistry, Athabasca University)
- Prof. Steven Farmer (Sonoma State University)
- William Reusch, Professor Emeritus (Michigan State U.), Virtual Textbook of Organic Chemistry
- Organic Chemistry With a Biological Emphasis by Tim Soderberg (University of Minnesota, Morris)

4.10: The Effect of Conjugation is shared under a CC BY-NC-SA 4.0 license and was authored, remixed, and/or curated by LibreTexts.

4.11: 14.9 Conjugation, Color, and the Chemistry of Vision

Objectives

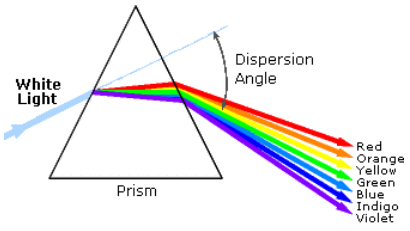
After completing this section, you should be able to

1. explain why some organic compounds have different colours based on compound structure and our perception of light.
2. state the relationship between frequency of light absorbed and the extent of conjugation in an extended pi electron system.

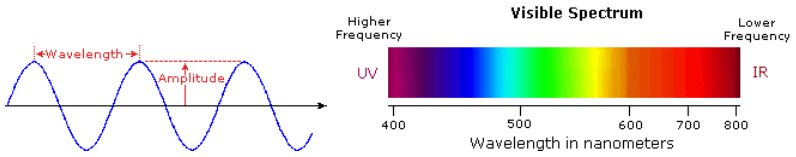
Eyes receive light energy then transfer and passing the energy into neural impulses to brain. This page will show the role of light plays in vision.

Introduction

An obvious difference between certain compounds is their color. Thus, quinone is yellow; chlorophyll is green; and aspirin is colorless. In this respect the human eye is functioning as a spectrometer analyzing the light reflected from the surface of a solid or passing through a liquid. Although we see sunlight (or white light) as uniform or homogeneous in color, it is actually composed of a broad range of radiation wavelengths in the ultraviolet (UV), visible and infrared (IR) portions of the spectrum. As shown on the image below, the component colors of the visible portion can be separated by passing sunlight through a prism, which acts to bend the light in differing degrees according to wavelength.

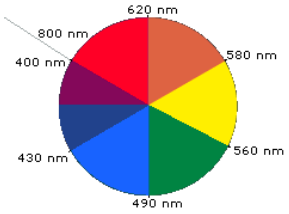


Visible wavelengths cover a range from approximately 400 to 800 nm. The longest visible wavelength is red and the shortest is violet. The wavelengths of what we perceive as particular colors in the visible portion of the spectrum are displayed and listed below.

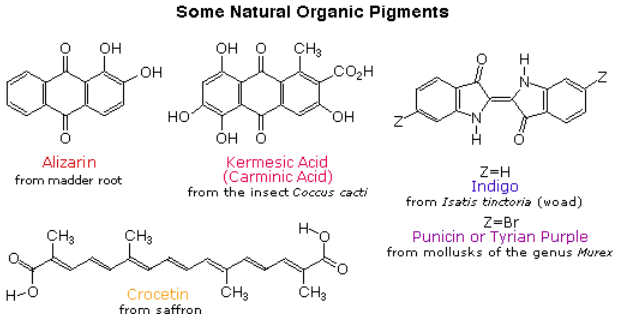


- **Violet:** 400 - 420 nm
- **Indigo:** 420 - 440 nm
- **Blue:** 440 - 490 nm
- **Green:** 490 - 570 nm
- **Yellow:** 570 - 585 nm
- **Orange:** 585 - 620 nm
- **Red:** 620 - 780 nm

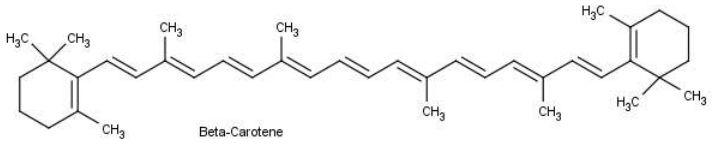
When white light passes through or is reflected by a colored substance, a characteristic portion of the mixed wavelengths is absorbed. The remaining light will then assume the complementary color to the wavelength(s) absorbed. This relationship is demonstrated by the color wheel shown below. Here, complementary colors are diametrically opposite each other. Thus, absorption of violet (400-440 nm) light renders a substance yellow, and absorption of 490-560 nm (green) light makes it red. Green is unique in that it can be created by absorption close to 400 nm as well as absorption near 800 nm.

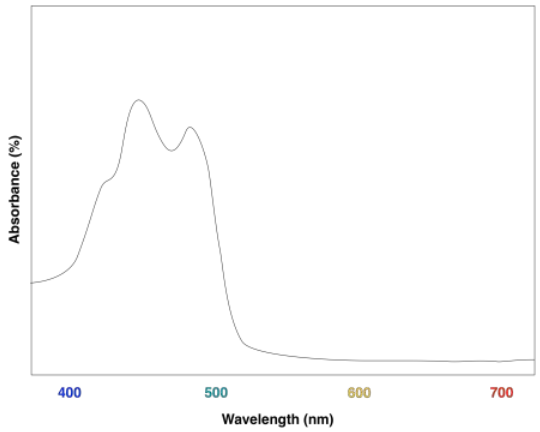


Early humans valued colored pigments, and used them for decorative purposes. Many of these were inorganic minerals, but several important organic dyes were also known. These included the crimson pigment, kermesic acid, the blue dye, indigo, and the yellow saffron pigment, crocetin. A rare dibromo-indigo derivative, punicin, was used to color the robes of the royal and wealthy. A common feature of all these colored compounds, displayed below, is a system of **extensively conjugated π-electrons**.

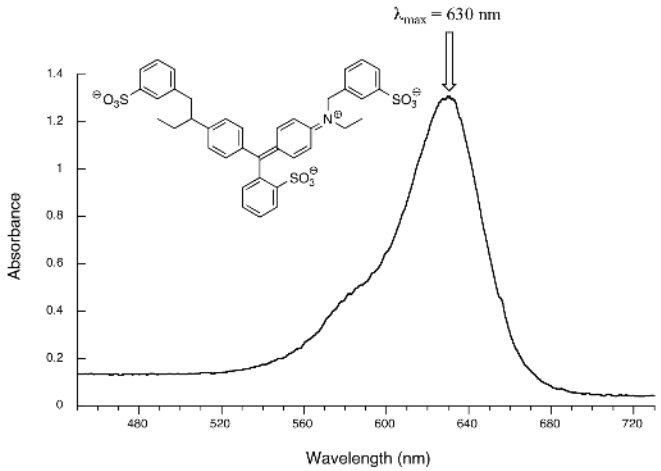


By understanding visible light, complementary colors, and adsorption the color of organic compounds can be understood. Beta-carotene, a compound found in carrots, is a deep orange color. Beta-carotene has 11 conjugated double bonds which places its λ_{max} at 455 nm which is within the blue region of the visible spectrum. The Beta-carotene compound absorbs blue from white light so it appears orange which is the the complementary color of blue.





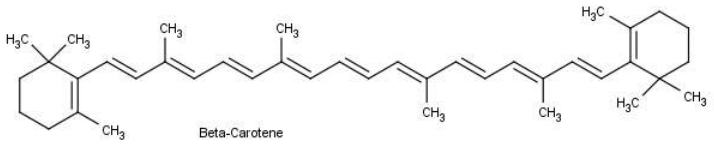
Another example is seen in the absorption spectrum of another food coloring, Blue #1:

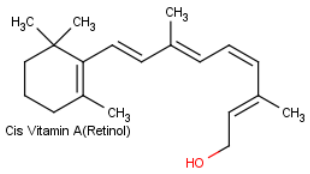


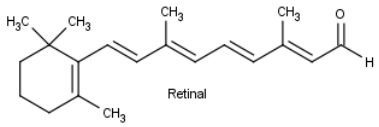
Blue #1 absorbs at a λ_{max} at 630 nm which is the color red in the visible spectrum. Blue is the complementary color of red.

Mechanism of Vision

Conjugation is also important in light sensitive compounds used for vision. Beta carotene, found in carrots and other natural products is cleaved into the liver and converted into Vitamin A, also known as retinol. Vitamin A is critical for vision because it is needed by the retina of eye. Retinol can be oxidized to an aldehyde called retinal which is also important for vision.



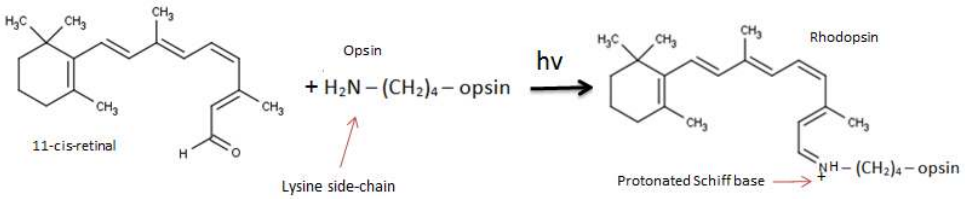




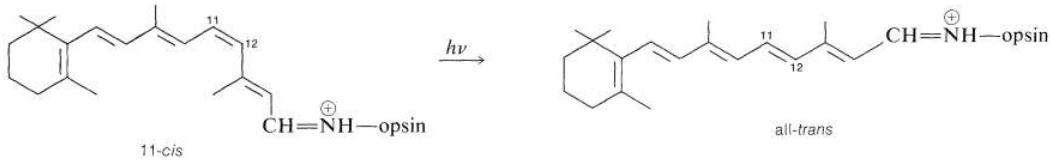
The eye is an extraordinarily sensitive instrument. Although its wavelength response is restricted to 400-800 nm, but its degree of sensitivity is such that a fully dark-adapted eye can clearly detect objects in light so dim as to correspond to a light input over the retina of only about 10,000 quanta per second - one light quantum per three minutes per receptor cell in the retina!

The retina is made up of two kinds of light-sensitive (photoreceptor) cells, known as rods and cones. The rods are the more sensitive and are responsible for vision in dim light. The cones are much fewer in number than the rods and provide detail and color vision in good light. The part of the retina that corresponds to the center of the visual field contains only cones. A red pigment called **rhodopsin** is the photosensitive substance in the rod cells of the retina. It absorbs most strongly in the blue-green region of the visible spectrum (λ_{max} = 500nm) and is essentially unaffected by the far-red end of the spectrum. Cone vision appears to involve a different pigment called **iodopsin**, which absorbs farther toward the red than does rhodopsin.

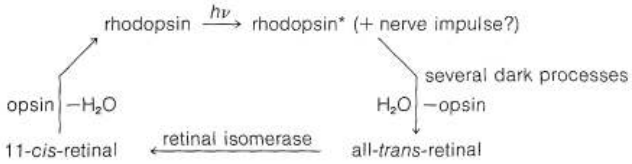
Rhodopsin, is made up of a protein (opsin) and retinal. Opsin does not absorb visible light, but when it is bonded with 11-cis-retinal to from rhodopsin, the new molecule has a very broad absorption band in the visible region of the spectrum. Rhodopsin is formed by an an imine (Schiff base) functional group formed between the aldehyde group of the retinal and the side-chain amino function of a lysine unit of opsin.



Opsin itself is colorless, whereas 11-cis-retinal absorbs strongly at 370 nm. The combination of opsin with 11-cis-retinal produces a remarkable shift of λ_{max} to longer wavelengths (430 nm to 620 nm, depending on the species). Light striking the retina changes the color of rhodopsin from red to yellow. The primary photochemical event in this process was established by G. Wald (Nobel Laureate in Physiology and Medicine, 1967), who showed that light absorption led to a change of configuration about the C_{11}-C_{12} double bond of the retinal moiety fo rhodopsin from *cis* to *trans* to form a compound called metarhodopsin II. The new form of trans-retinal does not fit as well into the opsin protein, and so a series of geometry changes in the protein begins. As the protein changes its geometry, it initiates a cascade of biochemical reactions that result in changes in charge so that a large potential difference builds up across the neuron membranes. This potential difference is passed along to an adjoining nerve cell as an electrical impulse. The nerve cell carries this impulse to the brain, where the visual information is interpreted.



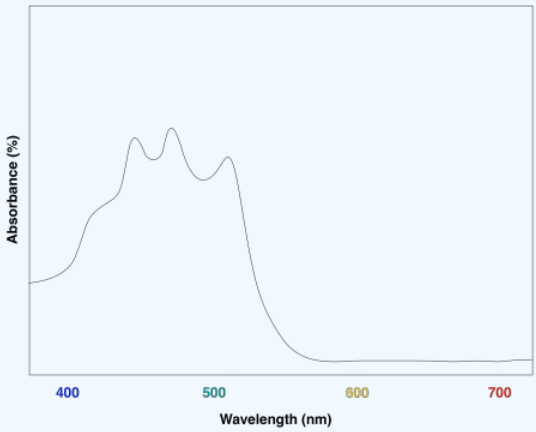
Metarhodopsin II can then be recycled back to rhodopsin by first cleaving to form all-*trans*-retinal and the isomerization back to 11-*cis*-retinal by the enzyme retinal isomerase. Finally, 11-*cis*-retinal is once again coupled with opsin to form rhodopsin.



Exercises

? Exercise 4.11.1

Lycopene is conjugated compound found in tomatoes. What colors correspond to the UV-Vis absorption maxima of lycopene? What color do we see when we look at lycopene?



Answer

The absorption maxima of lycopene are regions of blue and green in the visible spectrum. Lycopene would be expected to appears orange and red.

? Exercise 4.11.2

Asprin has a λ_{max} of 220 nm. Briefly explain why Asprin appears white.

Answer

Asprin absorbs in the ultraviolet portion of the electromagnetic spectrum. Asprin cannot remove any colors from white light by absorption so the compound itself appears white. Many compounds with a relatively small amount of conjugation appear white because they only absorb in the ultraviolet and not the visible region.

References

1. Biochemistry, L. Stryer (W.H. Freeman and Co, San Francisco, 1975).
2. *The Cambridge Guide to the Material World*, Rodney Cotterill (Cambridge University Press, Cambridge, 1985)

4.11: 14.9 Conjugation, Color, and the Chemistry of Vision is shared under a CC BY-NC-SA 4.0 license and was authored, remixed, and/or curated by LibreTexts.

- **14.9: Conjugation, Color, and the Chemistry of Vision** by Dietmar Kennepohl, Steven Farmer, Tim Soderberg, William Reusch is licensed CC BY-SA 4.0.
- **14.7: Structure Determination in Conjugated Systems - Ultraviolet Spectroscopy** by Dietmar Kennepohl, Steven Farmer, Tim Soderberg is licensed CC BY-SA 4.0.
- **14.8: Interpreting Ultraviolet Spectra- The Effect of Conjugation** by Dietmar Kennepohl, Steven Farmer, Tim Soderberg, William Reusch is licensed CC BY-SA 4.0.
- **28.8: Chemistry of Vision** by John D. Roberts and Marjorie C. Caserio is licensed CC BY-NC-SA 4.0.

4.12: UV-Visible Spectroscopy

Ultraviolet-visible (UV-vis) spectroscopy is used to obtain the absorbance spectra of a compound in solution or as a solid. What is actually being observed spectroscopically is the absorbance of light energy or electromagnetic radiation, which excites electrons from the ground state to the first singlet excited state of the compound or material. The UV-vis region of energy for the electromagnetic spectrum covers 1.5 - 6.2 eV which relates to a wavelength range of 800 - 200 nm. The Beer-Lambert Law, Equation 4.12.1, is the principle behind absorbance spectroscopy. For a single wavelength, A is absorbance (unitless, usually seen as arb. units or arbitrary units), ε is the molar absorptivity of the compound or molecule in solution ($M^{-1}cm^{-1}$), *b* is the path length of the cuvette or sample holder (usually 1 cm), and *c* is the concentration of the solution (M).

$$A = \varepsilon bc \tag{4.12.1}$$

All of these instruments have a light source (usually a deuterium or tungsten lamp), a sample holder and a detector, but some have a filter for selecting one wavelength at a time. The single beam instrument (Figure 4.12.1) has a filter or a monochromator between the source and the sample to analyze one wavelength at a time. The double beam instrument (Figure 4.12.2) has a single source and a monochromator and then there is a splitter and a series of mirrors to get the beam to a reference sample and the sample to be analyzed, this allows for more accurate readings. In contrast, the simultaneous instrument (Figure 4.12.3) does not have a monochromator between the sample and the source; instead, it has a diode array detector that allows the instrument to simultaneously detect the absorbance at all wavelengths. The simultaneous instrument is usually much faster and more efficient, but all of these types of spectrometers work well.

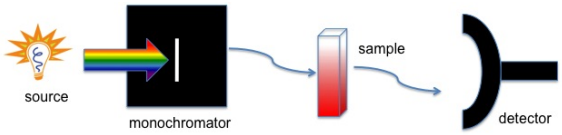


Figure 4.12.1 Illustration of a single beam UV-vis instrument.

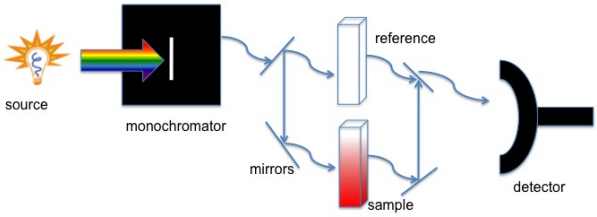


Figure 4.12.2 Illustration of a double beam UV-vis instrument.

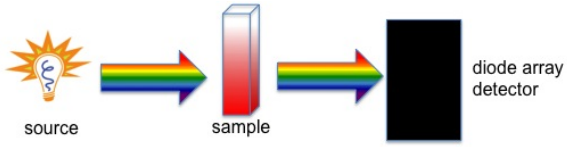


Figure 4.12.3 Illustration of a simultaneous UV-vis instrument.

What Information can be Obtained from UV-vis Spectra?

UV-vis spectroscopic data can give qualitative and quantitative information of a given compound or molecule. Irrespective of whether quantitative or qualitative information is required it is important to use a reference cell to zero the instrument for the solvent the compound is in. For quantitative information on the compound, calibrating the instrument using known concentrations of the compound in question in a solution with the same solvent as the unknown sample would be required. If the information needed is just proof that a compound is in the sample being analyzed, a calibration curve will not be necessary; however, if a degradation study or reaction is being performed, and concentration of the compound in solution is required, thus a calibration curve is needed.

To make a calibration curve, at least three concentrations of the compound will be needed, but five concentrations would be most ideal for a more accurate curve. The concentrations should start at just above the estimated concentration of the unknown sample and should go down to about an order of magnitude lower than the highest concentration. The calibration solutions should be spaced relatively equally apart, and they should be made as accurately as possible using digital pipettes and volumetric flasks instead of graduated cylinders and beakers. An example of absorbance spectra of calibration solutions of Rose Bengal (4,5,6,7-

tetrachloro-2',4',5',7'-tetraiodofluorescein, Figure 4.12.4, can be seen in Figure 4.12.5. To make a calibration curve, the value for the absorbances of each of the spectral curves at the highest absorbing wavelength, is plotted in a graph similar to that in Figure 4.12.6 of absorbance versus concentration. The correlation coefficient of an acceptable calibration is 0.9 or better. If the correlation coefficient is lower than that, try making the solutions again as the problem may be human error. However, if after making the solutions a few times the calibration is still poor, something may be wrong with the instrument; for example, the lamps may be going bad.

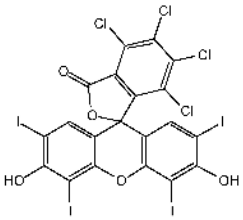


Figure 4.12.4 The molecular structure of Rose Bengal (4,5,6,7-tetrachloro-2',4',5',7'-tetraiodofluorescein).

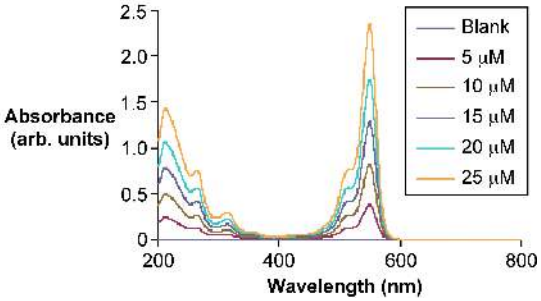


Figure 4.12.5 UV-vis spectra of different concentrations of Rose Bengal.

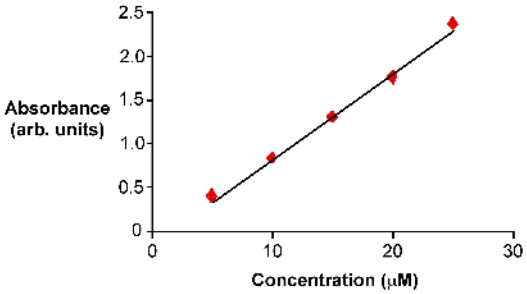


Figure 4.12.6 Calibration curve of Rose Bengal. Equation of line: y = 0.0977x – 0.1492 (R^2 = 0.996)

Limitations of UV-vis Spectroscopy

Sample

UV-vis spectroscopy works well on liquids and solutions, but if the sample is more of a suspension of solid particles in liquid, the sample will scatter the light more than absorb the light and the data will be very skewed. Most UV-vis instruments can analyze solid samples or suspensions with a diffraction apparatus (Figure 4.12.7), but this is not common. UV-vis instruments generally analyze liquids and solutions most efficiently.

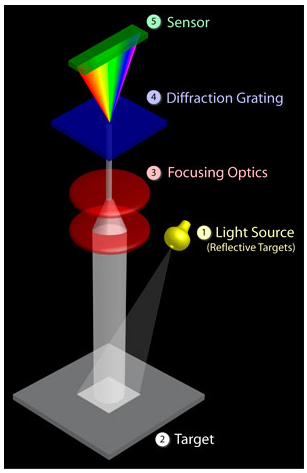


Figure 4.12.7 Schematic representation of the apparatus for collecting UV-vis spectra from solid materials.

Calibration and Reference

A blank reference will be needed at the very beginning of the analysis of the solvent to be used (water, hexanes, etc), and if concentration analysis needs to be performed, calibration solutions need to be made accurately. If the solutions are not made accurately enough, the actual concentration of the sample in question will not be accurately determined.

Choice of Solvent or Container

Every solvent has a UV-vis absorbance cutoff wavelength. The solvent cutoff is the wavelength below which the solvent itself absorbs all of the light. So when choosing a solvent be aware of its absorbance cutoff and where the compound under investigation is thought to absorb. If they are close, chose a different solvent. Table 4.12.1 provides an example of solvent cutoffs.

Table 4.12.1: UV absorbance cutoffs of various common solvents

Solvent	UV Absorbance Cutoff (nm)
Acetone	329
Benzene	278
Dimethylformamide	267
Ethanol	205
Toluene	285
Water	180

The material the cuvette (the sample holder) is made from will also have a UV-vis absorbance cutoff. Glass will absorb all of the light higher in energy starting at about 300 nm, so if the sample absorbs in the UV, a quartz cuvette will be more practical as the absorbance cutoff is around 160 nm for quartz (Table 4.12.2).

Table 4.12.2: Three different types of cuvettes commonly used, with different usable wavelengths.

Material	Wavelength Range (nm)
Glass	380-780
Plastic	380-780
Fused Quartz	< 380

Concentration of Solution

To obtain reliable data, the peak of absorbance of a given compound needs to be at least three times higher in intensity than the background noise of the instrument. Obviously using higher concentrations of the compound in solution can combat this. Also, if the sample is very small and diluting it would not give an acceptable signal, there are cuvettes that hold smaller sample sizes than

the 2.5 mL of a standard cuvettes. Some cuvettes are made to hold only 100 µL, which would allow for a small sample to be analyzed without having to dilute it to a larger volume, lowering the signal to noise ratio.

This page titled 4.12: UV-Visible Spectroscopy is shared under a CC BY license and was authored, remixed, and/or curated by Pavan M. V. Raja & Andrew R. Barron (OpenStax CNX) .

- **4.4: UV-Visible Spectroscopy** by Pavan M. V. Raja & Andrew R. Barron is licensed CC BY 4.0. Original source: http://cnx.org/contents/ba27839d-5042-4a40-afcf-c0e6e39fb45425.2.

CHAPTER OVERVIEW

5: Proton Nuclear Magnetic Resonance Spectroscopy (NMR)

- 5.1: Nuclear Magnetic Resonance Spectroscopy
- 5.2: Introduction
- 5.3: NMR Spectroscopy
- 5.4: Theory
  - Bloch Equations
  - Larmor Precession
  - NMR Interactions
  - Quantum Mechanic Treatment
  - Relaxation
  - Rotations and Irreducible Tensor Operators
- 5.5: The Nature of NMR Absorptions
- 5.6: Interpretation
- 5.7: Interpretation
  - Integration in NMR
  - Pascal’s Triangle
- 5.8: Structural Assignment
  - (n 1) Rule
  - Background to C-13 NMR
  - Determine Structure with Combined Spectra
  - High Resolution Proton NMR Spectra
  - Integration in Proton NMR
  - Interpreting C-13 NMR Spectra
  - Introduction to Proton NMR
  - Low Resolution Proton NMR Spectra
  - More About Electronics
  - Multiplicity in Proton NMR
  - NMR11. More About Multiplicity
  - NMR14. More Practice with NMR Spectroscopy
  - NMR2. Carbon-13 NMR
  - NMR3. Symmetry in NMR
  - NMR4. 13C NMR and Geometry
  - NMR5. 13C NMR and Electronics
  - NMR8. Chemical Shift in 1H NMR
  - NMR Appendix. Useful Charts for NMR identification
- 5.9: Active Learning with NMR
  - In-Class Questions
    - Set 1 – Basic Concepts
    - Set 2 – Energy Transition and Population
    - Set 3 – Electron Shielding
    - Set 4 – Nuclear Coupling
    - Set 5 – Exchange Effects
    - Set 6 – Classical Description

Instructor’s Manual
Learning Objectives
Text
5.10: Chemical Shifts
5.11: \(^1H\) NMR Spectroscopy and Proton Equivalence
5.12: Chemical Shifts in \(^1H\) NMR Spectroscopy
5.13: Integration of Proton Spectra
5.14: Spin-Spin Splitting in \(^1H\) NMR Spectra
5.15: Chemical Equivalence
5.16: More Complex Spin-Spin Splitting Patterns
5.17: Uses of \(^1H\) NMR Spectroscopy

5: Proton Nuclear Magnetic Resonance Spectroscopy (NMR) is shared under a CC BY-NC-SA 4.0 license and was authored, remixed, and/or curated by LibreTexts.

5.1: Nuclear Magnetic Resonance Spectroscopy

Objectives

After completing this section, you should be able to

1. discuss the principles of NMR spectroscopy.
2. identify the two magnetic nuclei that are most important to an organic chemist.

Key Terms

Make certain that you can define, and use in context, the key term below.

- resonance

Study Notes

Notice that the word “resonance” has a different meaning when we are discussing nuclear magnetic resonance spectroscopy than it does when discussing molecular structures.

Introduction

Some types of atomic nuclei act as though they spin on their axis similar to the Earth. Since they are positively charged they generate an electromagnetic field just as the Earth does. So, in effect, they will act as tiny bar magnetics. Not all nuclei act this way, but fortunately both ^{1}H and ^{13}C do have nuclear spins and will respond to this technique.



NMR Spectrometer

In the absence of an external magnetic field the direction of the spin of the nuclei will be randomly oriented (see figure below left). However, when a sample of these nuclei is place in an external magnetic field, the nuclear spins will adopt specific orientations much as a compass needle responses to the Earth’s magnetic field and aligns with it. Two possible orientations are possible, with the external field (*i.e.* parallel to and in the same direction as the external field) or against the field (*i.e.* antiparallel to the external field). See figure below right.

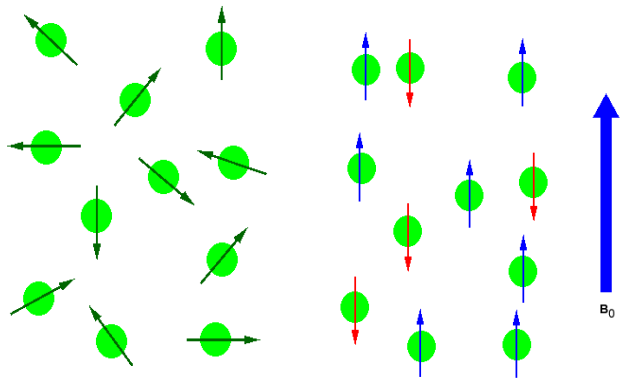
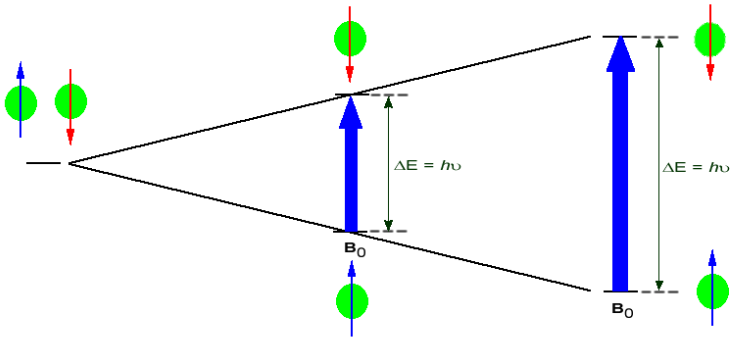


Figure 1: (Left) Random nuclear spin without an external magnetic field. (Right) Ordered nuclear spin in an external magnetic field

If the ordered nuclei are now subjected to EM radiation of the proper frequency the nuclei aligned with the field will absorb energy and "spin-flip" to align themselves against the field, a higher energy state. When this spin-flip occurs the nuclei are said to be in "resonance" with the field, hence the name for the technique, **N**uclear **M**agentic **R**esonance or NMR.

The amount of energy, and hence the exact frequency of EM radiation required for resonance to occur is dependent on both the strength of the magnetic field applied and the type of the nuclei being studied. As the strength of the magnetic field increases the energy difference between the two spin states increases and a higher frequency (more energy) EM radiation needs to be applied to achieve a spin-flip (see image below).



Superconducting magnets can be used to produce very strong magnetic field, on the order of 21 tesla (T). Lower field strengths can also be used, in the range of 4 - 7 T. At these levels the energy required to bring the nuclei into resonance is in the MHz range and corresponds to radio wavelength energies, *i.e.* at a field strength of 4.7 T 200 MHz bring ^{1}H nuclei into resonance and 50 MHz bring ^{13}C into resonance. This is considerably less energy then is required for IR spectroscopy, ~10^{-4} kJ/mol versus ~5 - ~50 kJ/mol.

^{1}H and ^{13}C are not unique in their ability to undergo NMR. All nuclei with an odd number of protons (^{1}H, ^{2}H, ^{14}N, ^{19}F, ^{31}P ...) or nuclei with an odd number of neutrons (*i.e.* ^{13}C) show the magnetic properties required for NMR. Only nuclei with even number of both protons and neutrons (^{12}C and ^{16}O) do not have the required magnetic properties.

Exercises

? Exercise 5.1.1

If in a field strength of 4.7 T, H^{1} requires 200 MHz of energy to maintain resonance. If atom X requires 150 MHz, calculate the amount of energy required to spin flip atom X's nucleus. Is this amount greater than the energy required for hydrogen?

Answer

Add

$E = h\upsilon$

$E = (6.62 \times 10^{-34})(150\ MHz)$

$E = 9.93 \times 10^{-26}\ J$

The energy is equal to 9.93 x 10^{-26} J. This value is smaller than the energy required for hydrogen (1.324×10^{-25} J).

? Exercise 5.1.2

Calculate the energy required to spin flip at 400 MHz. Does changing the frequency to 500 MHz decrease or increase the energy required? What about 300 MHz.

Answer

Add

$E = h\upsilon$

$E = (6.62 \times 10^{-34})(400\ MHz)$

$E = 2.648 \times 10^{-25}\ J$

The energy would increase if the frequency would increase to 500 MHz, and decrease if the frequency would decrease to 300 MHz.

Questions

Q13.1.1

If in a field strength of 4.7 T, H^1 requires 200 MHz of energy to maintain resonance. If atom X requires 150 MHz, calculate the amount of energy required to spin flip atom X's nucleus. Is this amount greater than the energy required for hydrogen?

Q13.1.2

Calculate the energy required to spin flip at 400 MHz. Does changing the frequency to 500 MHz decrease or increase the energy required? What about 300 MHz.

Solutions

S13.1.1

$E = h\upsilon$

$E = (6.62 \times 10^{-34})(150\ MHz)$

$E = 9.93 \times 10^{-26}\ J$

The energy is equal to 9.93x10^{-26} J. This value is smaller than the energy required for hydrogen (1.324×10^{-25} J).

S13.1.2

$E = h\upsilon$

$E = (6.62 \times 10^{-34})(400\ MHz)$

$E = 2.648 \times 10^{-25}\ J$

The energy would increase if the frequency would increase to 500 MHz, and decrease if the frequency would decrease to 300 MHz.

Contributors and Attributions

- Dr. Dietmar Kennepohl FCIC (Professor of Chemistry, Athabasca University)
- Prof. Steven Farmer (Sonoma State University)

Dr. Richard Spinney (The Ohio State University)

5.1: Nuclear Magnetic Resonance Spectroscopy is shared under a CC BY-NC-SA 4.0 license and was authored, remixed, and/or curated by LibreTexts.

5.2: Introduction

Nuclear Magnetic Resonance (NMR) is a nuclei (Nuclear) specific spectroscopy that has far reaching applications throughout the physical sciences and industry. NMR uses a large magnet (Magnetic) to probe the intrinsic spin properties of atomic nuclei. Like all spectroscopies, NMR uses a component of electromagnetic radiation (radio frequency waves) to promote transitions between nuclear energy levels (Resonance). Most chemists use NMR for structure determination of small molecules.

Introduction

In 1946, NMR was co-discovered by Purcell, Pound and Torrey of Harvard University and Bloch, Hansen and Packard of Stanford University. The discovery first came about when it was noticed that magnetic nuclei, such as ^{1}H and ^{31}P (read: proton and Phosphorus 31) were able to absorb radio frequency energy when placed in a magnetic field of a strength that was specific to the nucleus. Upon absorption, the nuclei begin to resonate and different atoms within a molecule resonated at different frequencies. This observation allowed a detailed analysis of the structure of a molecule. Since then, NMR has been applied to solids, liquids and gasses, kinetic and structural studies, resulting in 6 Nobel prizes being awarded in the field of NMR.

Spin and Magnetic Properties

The nucleus consists of elementary particles called neutrons and protons, which contain an intrinsic property called spin. Like electrons, the spin of a nucleus can be described using quantum numbers of I for the spin and m for the spin in a magnetic field. Atomic nuclei with even numbers of protons and neutrons have zero spin and all the other atoms with odd numbers have a non-zero spin. Furthermore, all molecules with a non-zero spin have a magnetic moment, μ, given by

$$\mu = \gamma I \tag{5.2.1}$$

where γ is the gyromagnetic ratio, a proportionality constant between the magnetic dipole moment and the angular momentum, specific to each nucleus (Table 1).

Table 5.2.1: The gyromagnetic ratios for several common nuclei

Nuclei	Spin	Gyromagetic Ratio (MHz/T)	Natural Abundance (%)
^{1}H	1/2	42.576	99.9985
^{13}C	1/2	10.705	1.07
^{31}P	1/2	17.235	100
^{27}Al	5/2	11.103	100
^{23}Na	3/2	11.262	100
^{7}Li	3/2	16.546	92.41
^{29}Si	1/2	-8.465	4.68
^{17}O	5/2	5.772	0.038
^{15}N	1/2	-4.361	0.368

The magnetic moment of the nucleus forces the nucleus to behave as a tiny bar magnet. In the absence of an external magnetic field, each magnet is randomly oriented. During the NMR experiment the sample is placed in an external magnetic field, B_0, which forces the bar magnets to align with (low energy) or against (high energy) the B_0. During the NMR experiment, a spin flip of the magnets occurs, requiring an exact quanta of energy. To understand this rather abstract concept it is useful to consider the NMR experiment using the nuclear energy levels.

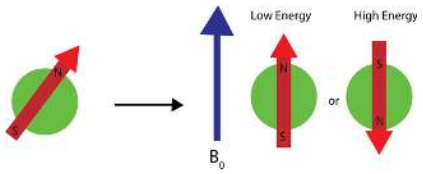


Figure 5.2.1: Application of a magnetic field to a randomly oriented bar magnet. The red arrow denotes magnetic moment of the nucleus. The application of the external magnetic field aligns the nuclear magnetic moments with or against the field.

Nuclear Energy Levels

As mentioned above, an exact quanta of energy must be used to induce the spin flip or transition. For any m, there are 2m+1 energy levels. For a spin 1/2 nucleus, there are only two energy levels, the low energy level occupied by the spins which aligned with B_0 and the high energy level occupied by spins aligned against B_0. Each energy level is given by

$$E = -m\hbar\gamma B_0 \tag{5.2.2}$$

where m is the magnetic quantum number, in this case +/- 1/2. The energy levels for $m > 1/2$, known as *quadrupolar nuclei*, are more complex and information regarding them can be found here.

The energy difference between the energy levels is then

$$\Delta E = \hbar\gamma B_0 \tag{5.2.3}$$

where $\hbar$ is Planks constant.

A schematic showing how the energy levels are arranged for a spin=1/2 nucleus is shown below. Note how the strength of the magnetic field plays a large role in the energy level difference. In the absence of an applied field the nuclear energy levels are degenerate. The splitting of the degenerate energy level due to the presence of a magnetic field in known as Zeeman Splitting.

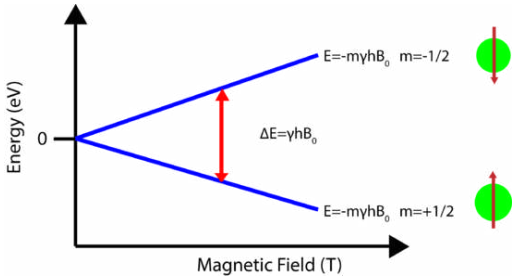


Figure 5.2.2: The splitting of the degenerate nuclear energy levels under an applied magnetic field. The green spheres represent atomic nuclei which are either aligned with (low energy) or against (high energy) the magnetic field.

Energy Transitions (Spin Flip)

In order for the NMR experiment to work, a spin flip between the energy levels must occur. The energy difference between the two states corresponds to the energy of the electromagnetic radiation that causes the nuclei to change their energy levels. For most NMR spectrometers, B_0 is on the order of Tesla (T) while γ is on the order of 10^7. Consequently, the electromagnetic radiation required is on the order of 100's of MHz and even GHz. The energy of a photon is represented by

$$E = h\nu \tag{5.2.4}$$

and thus the frequency necessary for absorption to occur is represented as:

$$\nu = \frac{\gamma B_0}{2\pi} \tag{5.2.5}$$

For the beginner, the NMR experiment measures the resonant frequency that causes a spin flip. For the more advanced NMR users, the sections on NMR detection and Larmor frequency should be consulted.

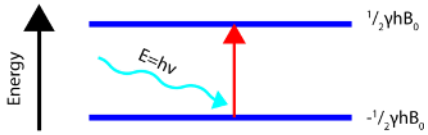


Figure 5.2.3: Absorption of radio frequency radiation to promote a transition between nuclear energy levels, called a spin flip.

Nuclear Shielding

The power of NMR is based on the concept of nuclear shielding, which allows for structural assignments. Every atom is surrounded by electrons, which orbit the nucleus. Charged particles moving in a loop will create a magnetic field which is felt by the nucleus. Therefore the local electronic environment surrounding the nucleus will slightly change the magnetic field experienced by the nucleus, which in turn will cause slight changes in the energy levels! This is known as shielding. Nuclei that experience different magnetic fields due to the local electronic interactions are known as inequivalent nuclei. The change in the energy levels requires a different frequency to excite the spin flip, which as will be seen below, creates a new peak in the NMR spectrum. The shielding allows for structural determination of molecules.

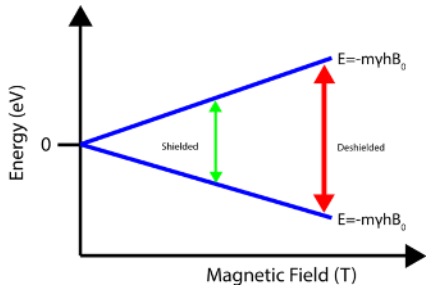


Figure 5.2.4: The effect that shielding from electrons has on the splitting of the nuclear energy levels. Electrons impart their own magnetic field which shields the nucleus from the externally applied magnetic field. This effect is greatly exaggerated in this illustration.

The shielding of the nucleus allows for chemically inequivalent environments to be determined by Fourier Transforming the NMR signal. The result is a spectrum, shown below, that consists of a set of peaks in which each peak corresponds to a distinct chemical environment. The area underneath the peak is directly proportional to the number of nuclei in that chemical environment. Additional details about the structure manifest themselves in the form of different NMR interactions, each altering the NMR spectrum in a distinct manner. The x-axis of an NMR spectrum is given in parts per million (ppm) and the relation to shielding is explained here.

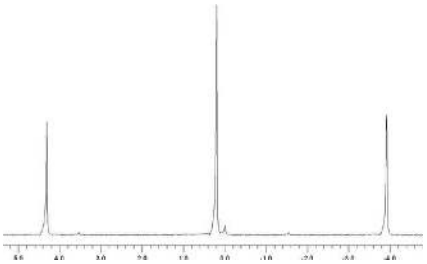


Figure 5.2.5: ^{31}P spectrum of phosphinic acid. Each peak corresponds to a distinct chemical environment while the area under the peak is proportional to the number of nuclei in a given environment.

Relaxation

Relaxation refers to the phenomenon of nuclei returning to their thermodynamically stable states after being excited to higher energy levels. The energy absorbed when a transition from a lower energy level to a high energy level occurs is released when the opposite happens. This can be a fairly complex process based on different timescales of the relaxation. The two most common types of relaxation are spin lattice relaxation (T_1) and spin spin relaxation (T_2). A more complex treatment of relaxation is given elsewhere.

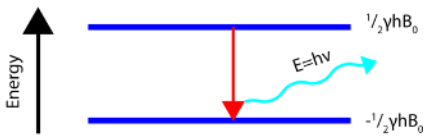


Figure 5.2.6: The process of relaxation

To understand relaxation, the entire sample must be considered. By placing the nuclei in an external magnetic field, the nuclei create a bulk magnetization along the z-axis. The spins of the nuclei are also coherent. The NMR signal may be detected as long as the spins are coherent with one another. The NMR experiment moves the bulk magnetization from the z-axis to the x-y plane, where it is detected.

- **Spin-Lattice Relaxation** (T_1): T_1 is the time it takes for the 37% of bulk magnetization to recovery along Z-axis from the x-y plane. The more efficient the relaxation process, the smaller relaxation time (T_1) value you will get. In solids, since motions between molecules are limited, the relaxation time (T_1) values are large. Spin-lattice relaxation measurements are usually carried out by pulse methods.
- **Spin-Spin Relaxation** (T_2): T_2 is the time it takes for the spins to lose coherence with one another. T_2 can either be shorter or equal to T_1.

Applications

The two major areas where NMR has proven to be of critical importance is in the fields of medicine and chemistry, with new applications being developed daily

Nuclear magnetic resonance imaging, better known as magnetic resonance imaging (MRI) is an important medical diagnostic tool used to study the function and structure of the human body. It provides detailed images of any part of the body, especially soft tissue, in all possible planes and has been used in the areas of cardiovascular, neurological, musculoskeletal and oncological imaging. Unlike other alternatives, such as computed tomography (CT), it does not used ionized radiation and hence is very safe to administer.

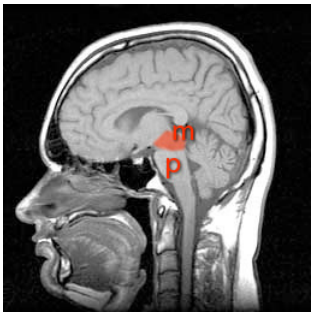


Figure 5.2.7: ^{1}H MRI of a human head showing the soft tissue such as the brain and sinuses. The MRI also clearly shows the spinal column and skull.

In many laboratories today, chemists use nuclear magnetic resonance to determine structures of important chemical and biological compounds. In NMR spectra, different peaks give information about different atoms in a molecule according specific chemical environments and bonding between atoms. The most common isotopes used to detect NMR signals are ^{1}H and ^{13}C but there are many others, such as ^{2}H, ^{3}He, ^{15}N, ^{19}F, etc., that are also in use.

NMR has also proven to be very useful in other area such as environmental testing, petroleum industry, process control, earth's field NMR and magnetometers. Non-destructive testing saves a lot of money for expensive biological samples and can be used again if more trials need to be run. The petroleum industry uses NMR equipment to measure porosity of different rocks and permeability of different underground fluids. Magnetometers are used to measure the various magnetic fields that are relevant to one's study.

Problems

1. Calculate the magnetic field, B_0 that corresponds to a precession frequency of 600 MHz for ^{1}H.
2. What is the field strength (in tesla) needed to generate a ^{1}H frequency of 500 MHz?
3. How do spin-spin relaxation and spin-lattice relaxation differ from each other?
4. The ^{1}H NMR spectrum of toluene shows that it has two peaks because of methyl and aromatic protons recorded at 60 MHz and 1.41 T. Given this information, what would be the magnetic field at 400 MHz?
5. What is the difference between ^{13}C and ^{1}H NMR?

Solutions

1. B_0= 14.1 T.
2. Using the equation used in problem 1 and solving it for B_0we get a field strength of 11.74 T.
3. Look under relaxation.
4. Since we know that the NMR frequency is directly proportional to the magnetic strength, we calculate the magnetic field at 400 MHz: B_0 = (400 MHz/60MHz) x 1.41 T = 9.40 T
5. Look under applications.

References

- Atta-ur-Rahman. Nuclear Magnetic Resonance. New York: Springer-Verlag, 1986.
- Freeman, Ray. Magnetic Resonance in Chemistry and Medicine. New York: Oxford University Press, 2003.
- Lambert, Joseph B and Eugene P Mazzola. Nuclear Magnetic Resonance Spectroscopy: An Introduction to Princliples, Applications, and Experimental Methods. Upper Saddle River: Pearson Education, 2004.
- Chang, Raymond. Physical Chemistry for the Biosciences. University Science Books, 2005

5.2: Introduction is shared under a CC BY-NC-SA 4.0 license and was authored, remixed, and/or curated by LibreTexts.

- **Introduction to NMR** by Derrick Kaseman, Revathi Srinivasan Ganesh Iyer is licensed CC BY 4.0.

5.3: NMR Spectroscopy

Nuclear magnetic resonance spectroscopy (NMR) is a widely used and powerful method that takes advantage of the magnetic properties of certain nuclei. The basic principle behind NMR is that some nuclei exist in specific nuclear spin states when exposed to an external magnetic field. NMR observes transitions between these spin states that are specific to the particular nuclei in question, as well as that nuclei's chemical environment. However, this only applies to nuclei whose spin, I, is not equal to 0, so nuclei where I = 0 are 'invisible' to NMR spectroscopy. These properties have led to NMR being used to identify molecular structures, monitor reactions, study metabolism in cells, and is used in medicine, biochemistry, physics, industry, and almost every imaginable branch of science.

Theory

The chemical theory that underlies NMR spectroscopy depends on the intrinsic spin of the nucleus involved, described by the quantum number S. Nuclei with a non-zero spin are always associated with a non-zero magnetic moment, as described by Equation 5.3.1, where μ is the magnetic moment, S is the spin, and γ is always non-zero. It is this magnetic moment that allows for NMR to be used; therefore nuclei whose quantum spin is zero cannot be measured using NMR. Almost all isotopes that have both an even number of protons and neutrons have no magnetic moment, and cannot be measured using NMR.

$$\mu = \gamma \cdot S \tag{5.3.1}$$

In the presence of an external magnetic field (B) for a nuclei with a spin I = $^1/_2$, there are two spin states present of $+^1/_2$ and $-^1/_2$. The difference in energy between these two states at a specific external magnetic field (B_x) are given by Equation 5.3.2, and are shown in Figure 5.3.1 where E is energy, I is the spin of the nuclei, and μ is the magnetic moment of the specific nuclei being analyzed. The difference in energy shown is always extremely small, so for NMR strong magnetic fields are required to further separate the two energy states. At the applied magnetic fields used for NMR, most magnetic resonance frequencies tend to fall in the radio frequency range.

$$E = \mu \cdot B_x / I \tag{5.3.2}$$

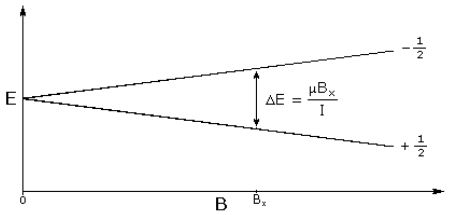


Figure 5.3.1 The difference in energy between two spin states over a varying magnetic field B.

The reason NMR can differentiate between different elements and isotopes is due to the fact that each specific nuclide will only absorb at a very specific frequency. This specificity means that NMR can generally detect one isotope at a time, and this results in different types of NMR: such as ^{1}H NMR, ^{13}C NMR, and ^{31}P NMR, to name only a few.

The subsequent absorbed frequency of any type of nuclei is not always constant, since electrons surrounding a nucleus can result in an effect called nuclear shielding, where the magnetic field at the nucleus is changed (usually lowered) because of the surrounding electron environment. This differentiation of a particular nucleus based upon its electronic (chemical) environment allows NMR be used to identify structure. Since nuclei of the same type in different electron environments will be more or less shielded than another, the difference in their environment (as observed by a difference in the surrounding magnetic field) is defined as the chemical shift.

Instrumentation

An example of an NMR spectrometer is given in Figure 5.3.2. NMR spectroscopy works by varying the machine's emitted frequency over a small range while the sample is inside a constant magnetic field. Most of the magnets used in NMR machines to create the magnetic field range from 6 to 24 T. The sample is placed within the magnet and surrounded by superconducting coils, and is then subjected to a frequency from the radio wave source. A detector then interprets the results and sends it to the main console.

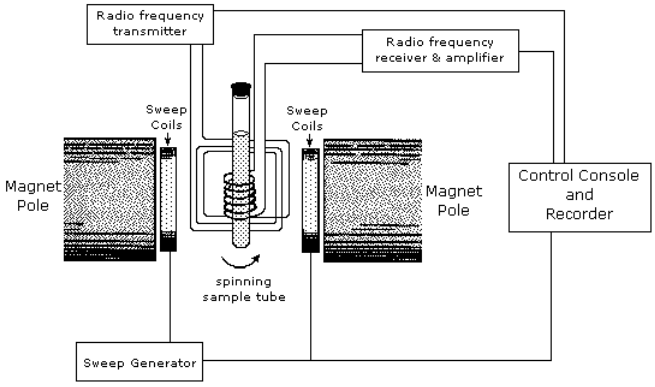


Figure 5.3.2 Diagram of NMR spectrometer.

Interpreting NMR spectra

Chemical Shift

The different local chemical environments surrounding any particular nuclei causes them to resonate at slightly different frequencies. This is a result of a nucleus being more or less shielded than another. This is called the chemical shift (δ). One factor that affects chemical shift is the changing of electron density from around a nucleus, such as a bond to an electronegative group. Hydrogen bonding also changes the electron density in ^{1}H NMR, causing a larger shift. These frequency shifts are miniscule in comparison to the fundamental NMR frequency differences, on a scale of Hz as compared to MHz. For this reason chemical shifts (δ) are described by the unit ppm on an NMR spectra, 5.3.3, where H_{ref} = the resonance frequency of the reference, H_{sub} = resonance frequency of the substance, and $H_{machine}$ = operating frequency of the spectrometer.

$$\delta = \left(\frac{H_{ref} - H_{sub}}{H_{machine}}\right) \times 10^6 \tag{5.3.3}$$

Since the chemical shift (δ in ppm) is reported as a relative difference from some reference frequency, so a reference is required. In ^{1}H and ^{13}C NMR, for example, tetramethylsilane (TMS, $Si(CH_3)_4$) is used as the reference. Chemical shifts can be used to identify structural properties in a molecule based on our understanding of different chemical environments. Some examples of where different chemical environments fall on a ^{1}H NMR spectra are given in Table 5.3.1.

Table 5.3.1 Representative chemical shifts for organic groups in the ^{1}H NMR.

Functional Group	Chemical Shift Range (ppm)
Alkyl (e.g. methyl-CH_3)	~ 1
Alkyl adjacent to oxygen (-CH_2-O)	3 - 4
Alkene (=CH_2)	~ 6
Alkyne (C-H)	~ 3
Aromatic	7 - 8

In Figure 5.3.3, an ^{1}H NMR spectra of ethanol, we can see a clear example of chemical shift. There are three sets of peaks that represent the six hydrogens of ethanol (C_2H_6O). The presence of three sets of peaks means that there are three different chemical environments that the hydrogens can be found in: the terminal methyl (CH_3) carbon's three hydrogens, the two hydrogens on the methylene (CH_2) carbon adjacent to the oxygen, and the single hydrogen on the oxygen of the alcohol group (OH). Once we cover spin-spin coupling, we will have the tools available to match these groups of hydrogens to their respective peaks.

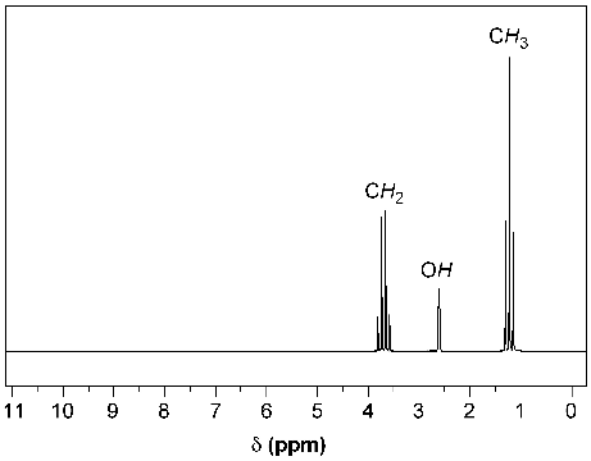


Figure 5.3.3: A ^{1}H NMR spectra of ethanol (CH_3CH_2OH).

Spin-spin Coupling

Another useful property that allows NMR spectra to give structural information is called spin-spin coupling, which is caused by spin coupling between NMR active nuclei that are not chemically identical. Different spin states interact through chemical bonds in a molecule to give rise to this coupling, which occurs when a nuclei being examined is disturbed or influenced by a nearby nuclear spin. In NMR spectra, this effect is shown through peak splitting that can give direct information concerning the connectivity of atoms in a molecule. Nuclei which share the same chemical shift do not form splitting peaks in an NMR spectra.

In general, neighboring NMR active nuclei three or fewer bonds away lead to this splitting. The splitting is described by the relationship where n neighboring nuclei result in n+1 peaks, and the area distribution can be seen in Pascal's triangle (Figure 5.3.4). However, being adjacent to a strongly electronegative group such as oxygen can prevent spin-spin coupling. For example a doublet would have two peaks with intensity ratios of 1:1, while a quartet would have four peaks of relative intensities 1:3:3:1. The magnitude of the observed spin splitting depends on many factors and is given by the coupling constant J, which is in units of Hz.

1
1 1
1 2 1
1 3 3 1
1 4 6 4 1
1 5 10 10 5 1
1 6 15 20 15 6 1
1 7 21 35 35 21 7 1
1 8 28 56 70 56 28 8 1

Figure 5.3.4: Pascal's triangle.

Referring again to Figure 5.3.4, we have a good example of how spin-spin coupling manifests itself in an NMR spectra. In the spectra we have three sets of peaks: a quartet, triplet, and a singlet. If we start with the terminal carbon's hydrogens in ethanol, using the n+1 rule we see that they have two hydrogens within three bonds (i.e., H-C-C-H), leading us to identify the triplet as the peaks for the terminal carbon's hydrogens. Looking next at the two central hydrogens, they have four NMR active nuclei within three bonds (i.e., H-C-C-H), but there is no quintet on the spectra as might be expected. This can be explained by the fact that the single hydrogen bonded to the oxygen is shielded from spin-spin coupling, so it must be a singlet and the two central hydrogens form the quartet. We have now interpreted the NMR spectra of ethanol by identifying which nuclei correspond to each peak.

Peak Intensity

Mainly useful for proton NMR, the size of the peaks in the NMR spectra can give information concerning the number of nuclei that gave rise to that peak. This is done by measuring the peak's area using integration. Yet even without using integration the size of different peaks can still give relative information about the number of nuclei. For example a singlet associated with three hydrogen atoms would be about 3 times larger than a singlet associated with a single hydrogen atom.

This can also be seen in the example in Figure 5.3.3. If we integrated the area under each peak, we would find that the ratios of the areas of the quartet, singlet, and triplet are approximately 2:1:3, respectively.

Limitations of NMR

Despite all of its upsides, there are several limitations that can make NMR analysis difficult or impossible in certain situations. One such issue is that the desired isotope of an element that is needed for NMR analysis may have little or no natural abundance. For example the natural abundance of ^{13}C, the active isotope for carbon NMR, is about 11%, which works well for analysis. However, in the case of oxygen the active isotope for NMR is ^{17}O, which is only 0.035% naturally abundant. This means that there are certain elements that can essentially never be measured through NMR.

Another problem is that some elements have an extremely low magnetic moment, μ. The sensitivity of NMR machines is based on the magnetic moment of the specific element, but if the magnetic moment is too low it can be very difficult to obtain an NMR spectra with enough peak intensity to properly analyze.

NMR Properties of the Element

Table 5.3.1 NMR properties of selected spin $^1/_2$ nuclei. [a] Other spin $^1/_2$ also exist.

Isotope	Natural Abundance (%)	Relative NMR Frequency (MHz)	Relative Receptivity as Compared to 1H
^{1}H	99.985	100	1.00
^{3}H	-	106.7	-
^{3}He	0.00013	76.2	5.8×10^{-7}
^{13}C	1.11	25.1	1.8×10^{-4}
^{15}N	0.37	10.1	3.9×10^{-6}
^{19}F	100	94.1	8.3×10^{-1}
^{29}Si	4.7	19.9	3.7×10^{-4}
^{31}P	100	40.5	6.6×10^{-2}
^{57}Fe	2.2	3.2	7.4×10^{-7}
^{77}Se	7.6	19.1	5.3×10^{-4}
^{89}Y	100	4.9	1.2×10^{-4}
^{103}Rh	100	3.2	3.2×10^{-5}
^{107}Ag	51.8	4.0	3.5×10^{-5}
^{109}Ag	48.2	4.7	4.9×10^{-5}
^{111}Cd	12.8	21.2	1.2×10^{-3}
^{113}Cd	12.3	22.2	1.3×10^{-3}
$^{117}Sn^{a}$	7.6	35.6	3.5×10^{-3}
^{119}Sn	8.6	37.3	4.5×10^{-3}
$^{125}Te^{a}$	7.0	31.5	2.2×10^{-3}
^{129}Xe	26.4	27.8	5.7×10^{-3}
^{169}Tm	100	8.3	5.7×10^{-4}
^{171}Yb	14.3	17.6	7.8×10^{-4}
^{183}W	14.4	4.2	1.1×10^{-5}
^{187}Os	1.6	2.3	2.0×10^{-7}
^{195}Pt	33.8	21.4	3.4×10^{-3}

Isotope	Natural Abundance (%)	Relative NMR Frequency (MHz)	Relative Receptivity as Compared to 1H
^{199}Hg	16.8	17.9	9.8×10^{-4}
^{203}Ti	29.5	57.1	5.7×10^{-2}
^{205}Ti	70.5	57.6	1.4×10^{-1}
^{207}Pb	22.6	20.9	2.0×10^{-1}

Table 5.3.2 NMR properties of selected quadrupolar nuclei. [a] A spin $^1/_2$ isotope also exists. [b] Other quadrupolar nuclei exist.

Isotope	**Spin**	**Natural Abundance (%)**	**Relative NMR Frequency (%)**	**Relative Receptivity as Compared to ^{1}H**	**Quadropole moment (10^{-28} m^2)**
^{2}H	1	0.015	15.4	1.5×10^{-6}	2.8×10^{-3}
^{6}Li	1	7.4	14.7	6.3×10^{-4}	-8×10^{-4}
^{7}Li	$^3/_2$	92.6	38.9	2.7×10^{-1}	-4×10^{-2}
^{9}Be	$^3/_2$	100	14.1	1.4×10^{-2}	5×10^{-2}
^{10}B	3	19.6	10.7	3.9×10^{-3}	8.5×10^{-2}
^{11}B	$^3/_2$	80.4	32.1	1.3×10^{-1}	4.1×10^{-2}
^{14}Na	1	99.6	7.2	1.0×10^{-3}	1×10^{-2}
^{17}O	$^5/_2$	0.037	13.6	1.1×10^{-5}	-2.6×10^{-2}
^{23}Na	$^5/_2$	100	26.5	9.3×10^{-2}	1×10^{-1}
^{25}Mg	$^5/_2$	10.1	6.1	2.7×10^{-4}	2.2×10^{-1}
^{27}Al	$^5/_2$	100	26.1	2.1×10^{-1}	1.5×10^{-1}
^{33}S	$^3/_2$	0.76	7.7	1.7×10^{-5}	-5.5×10^{-2}
^{35}Cl	$^3/_2$	75.5	9.8	3.6×10^{-3}	-1×10^{-1}
^{37}Cl	$^3/_2$	24.5	8.2	6.7×10^{-4}	-7.9×10^{-2}
^{39}K[b]	$^3/_2$	93.1	4.7	4.8×10^{-4}	4.9×10^{-2}
^{43}Ca	$^7/_2$	0.15	6.7	8.7×10^{-6}	2×10^{-1}
^{45}Sc	$^7/_2$	100	24.3	3×10^{-1}	-2.2×10^{-1}
^{47}Ti	$^5/_2$	7.3	5.6	1.5×10^{-4}	2.9×10^{-1}
^{49}Ti	$^7/_2$	5.5	5.6	2.1×10^{-4}	2.4×10^{-1}
^{51}V[b]	$^7/_2$	99.8	26.3	3.8×10^{-1}	-5×10^{-2}
^{53}Cr	$^3/_2$	9.6	5.7	8.6×10^{-5}	3×10^{-2}
^{55}Mn	$^5/_2$	100	24.7	1.8×10^{-1}	4×10^{-1}
^{59}Co	$^7/_2$	100	23.6	2.8×10^{-1}	3.8×10^{-1}
^{61}Ni	$^3/_2$	1.2	8.9	4.1×10^{-1}	1.6×10^{-1}
^{63}Cu	$^3/_2$	69.1	26.5	6.5×10^{-2}	-2.1×10^{-1}
^{65}Cu	$^3/_2$	30.9	28.4	3.6×10^{-2}	-2.0×10^{-1}

Isotope	Spin	Natural Abundance (%)	Relative NMR Frequency (%)	Relative Receptivity as Compared to ^{1}H	Quadropole moment (10^{-28} m^2)
^{67}Zn	$^{5}/_{2}$	4.1	6.3	1.2×10^{-4}	1.6×10^{-1}
^{69}Ga	$^{3}/_{2}$	60.4	24.0	4.2×10^{-2}	1.9×10^{-1}
^{71}Ga	$^{3}/_{2}$	39.6	30.6	5.7×10^{-2}	1.2×10^{-1}
^{73}Ge	$^{9}/_{2}$	7.8	3.5	1.1×10^{-4}	-1.8×10^{-1}
^{75}As	$^{3}/_{2}$	100	17.2	2.5×10^{-2}	2.9×10^{-1}
^{79}Br	$^{3}/_{2}$	50.5	25.1	4.0×10^{-2}	3.7×10^{-1}
^{81}Br	$^{3}/_{2}$	49.5	27.1	4.9×10^{-2}	3.1×10^{-1}
$^{87}Rb^{b}$	$^{3}/_{2}$	27.9	32.8	4.9×10^{-2}	1.3×10^{-1}
^{87}Sr	$^{9}/_{2}$	7.0	4.3	1.9×10^{-4}	3×10^{-1}
^{91}Zr	$^{5}/_{2}$	11.2	9.3	1.1×10^{-3}	-2.1×10^{-1}
^{93}Nb	$^{9}/_{2}$	100	24.5	4.9×10^{-1}	-2.2×10^{-1}
^{95}Mo	$^{5}/_{2}$	15.7	6.5	5.1×10^{-4}	$\pm 1.2 \times 10^{-1}$
^{97}Mo	$^{5}/_{2}$	9.5	6.7	3.3×10^{-4}	± 1.1
^{99}Ru	$^{5}/_{2}$	12.7	4.6	1.5×10^{-4}	7.6×10^{-2}
^{101}Ru	$^{5}/_{2}$	17.1	5.2	2.8×10^{-4}	4.4×10^{-1}
^{105}Pd	$^{5}/_{2}$	22.2	4.6	2.5×10^{-4}	8×10^{-1}
$^{115}In^{b}$	$^{9}/_{2}$	95.7	22.0	3.4×10^{-1}	8.3×10^{-1}
^{121}Sb	$^{5}/_{2}$	57.3	24.0	9.3×10^{-2}	-2.8×10^{-1}
^{123}Sb	$^{7}/_{2}$	42.7	13.0	2.0×10^{-2}	3.6×10^{-1}
^{127}I	$^{5}/_{2}$	100	20.1	9.5×10^{-2}	-7.9×10^{-1}
$^{131}Xe^{a}$	$^{3}/_{2}$	21.3	8.2	5.9×10^{-4}	-1.2×10^{-1}
^{133}Cs	$^{7}/_{2}$	100	13.2	4.8×10^{-2}	-3×10^{-3}
$^{137}Ba^{b}$	$^{3}/_{2}$	11.3	11.1	7.9×10^{-4}	2.8×10^{-1}
^{139}La	$^{7}/_{2}$	99.9	14.2	6.0×10^{-2}	2.2×10^{-1}
^{177}Hf	$^{7}/_{2}$	18.5	4.0	2.6×10^{-4}	4.5
^{179}Hf	$^{9}/_{2}$	13.8	2.5	7.4×10^{-5}	5.1
^{181}Ta	$^{7}/_{2}$	99.99	12.0	3.7×10^{-2}	3
^{185}Re	$^{5}/_{2}$	37.1	22.7	5.1×10^{-2}	2.3
^{187}Re	$^{5}/_{2}$	62.9	22.9	8.8×10^{-2}	2.2
$^{189}Os^{a}$	$^{3}/_{2}$	16.1	7.8	3.9×10^{-4}	8×10^{-1}
^{191}Ir	$^{3}/_{2}$	37.3	1.7	9.8×10^{-6}	1.1
^{193}Ir	$^{3}/_{2}$	62.7	1.9	2.1×10^{-5}	1.0
^{197}Au	$^{3}/_{2}$	100	1.7	2.6×10^{-5}	5.9×10^{-1}

Isotope	Spin	Natural Abundance (%)	Relative NMR Frequency (%)	Relative Receptivity as Compared to ^{1}H	Quadropole moment (10^{-28} m^2)
^{201}Hg	$^{3}/_{2}$	13.2	6.6	1.9×10^{-4}	4.4×10^{-1}
^{209}Bi	$^{9}/_{2}$	100	16.2	1.4×10^{-1}	-3.8×10^{-1}

NMR Spin Coupling

The Basis of Spin Coupling

Nuclear magnetic resonance (NMR) signals arise when nuclei absorb a certain radio frequency and are excited from one spin state to another. The exact frequency of electromagnetic radiation that the nucleus absorbs depends on the magnetic environment around the nucleus. This magnetic environment is controlled mostly by the applied field, but is also affected by the magnetic moments of nearby nuclei. Nuclei can be in one of many spin states Figure 5.3.5, giving rise to several possible magnetic environments for the observed nucleus to resonate in. This causes the NMR signal for a nucleus to show up as a multiplet rather than a single peak.

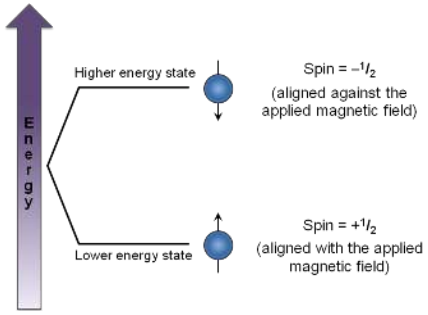


Figure 5.3.5 The different spin states of a nucleus (I = $^{1}/_{2}$) in a magnetic field. These different states increase or decrease the effective magnetic field experienced by a nearby nucleus, allowing for two distinct signals.

When nuclei have a spin of I = $^{1}/_{2}$ (as with protons), they can have two possible magnetic moments and thus split a single expected NMR signal into two signals. When more than one nucleus affects the magnetic environment of the nucleus being examined, complex multiplets form as each nucleus splits the signal into two additional peaks. If those nuclei are magnetically equivalent to each other, then some of the signals overlap to form peaks with different relative intensities. The multiplet pattern can be predicted by Pascal's triangle (Figure 5.3.6), looking at the nth row, where n = number of nuclei equivalent to each other but *not* equivalent to the one being examined. In this case, the number of peaks in the multiplet is equal to n + 1

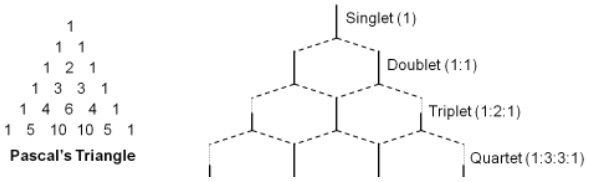


Figure 5.3.6 Pascal's triangle predicts the number of peaks in a multiplet and their relative intensities.

When there is more than one type of nucleus splitting an NMR signal, then the signal changes from a multiplet to a group of multiplets (Figure 5.3.7). This is caused by the different coupling constants associated with different types of nuclei. Each nucleus splits the NMR signal by a different width, so the peaks no longer overlap to form peaks with different relative intensities.

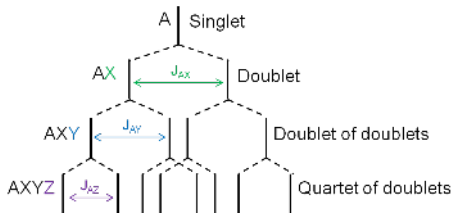


Figure 5.3.7 The splitting tree of different types of multiplets.

When nuclei have I > $^{1}/_{2}$, they have more than two possible magnetic moments and thus split NMR signals into more than two peaks. The number of peaks expected is 2I + 1, corresponding to the number of possible orientations of the magnetic moment. In

reality however, some of these peaks may be obscured due to quadrupolar relaxation. As a result, most NMR focuses on I = $^1/_2$ nuclei such as ^{1}H, ^{13}C, and ^{31}P.

Multiplets are centered around the chemical shift expected for a nucleus had its signal not been split. The total area of a multiplet corresponds to the number of nuclei resonating at the given frequency.

Spin Coupling in molecules

Looking at actual molecules raises questions about which nuclei can cause splitting to occur. First of all, it is important to realize that only nuclei with I ≠ 0 will show up in an NMR spectrum. When I = 0, there is only one possible spin state and obviously the nucleus cannot flip between states. Since the NMR signal is based on the absorption of radio frequency as a nucleus transitions from one spin state to another, I = 0 nuclei do not show up on NMR. In addition, they do not cause splitting of other NMR signals because they only have one possible magnetic moment. This simplifies NMR spectra, in particular of organic and organometallic compounds, greatly, since the majority of carbon atoms are ^{12}C, which have I = 0.

For a nucleus to cause splitting, it must be close enough to the nucleus being observed to affect its magnetic environment. The splitting technically occurs through bonds, not through space, so as a general rule, only nuclei separated by three or fewer bonds can split each other. However, even if a nucleus is close enough to another, it may not cause splitting. For splitting to occur, the nuclei must also be non-equivalent. To see how these factors affect real NMR spectra, consider the spectrum for chloroethane (Figure 5.3.8).

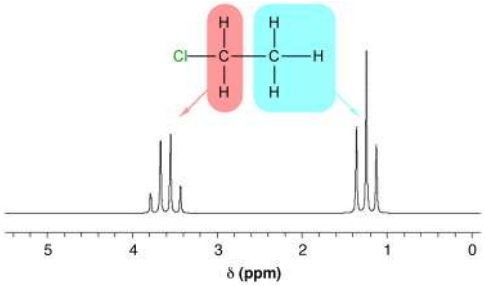


Figure 5.3.8 The NMR spectrum for chloroethane. Adapted from A. M. Castillo, L. Patiny, and J. Wist. *J. Magn. Reson.*, 2010, **209**, 123.

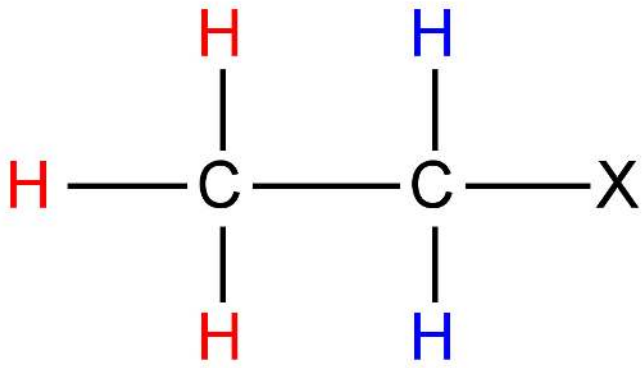
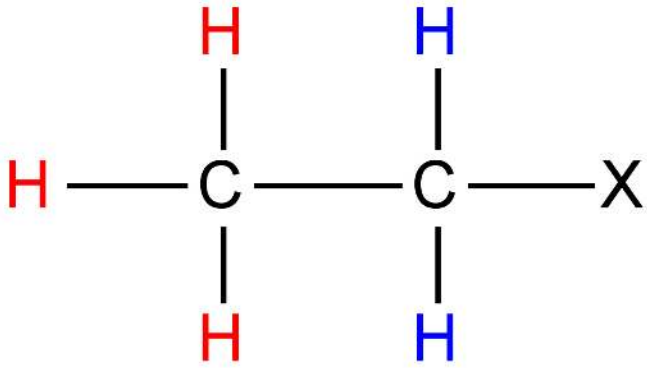
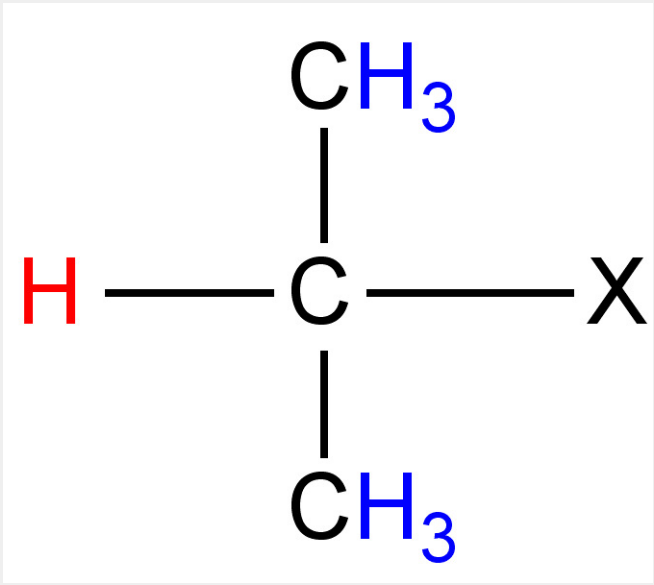
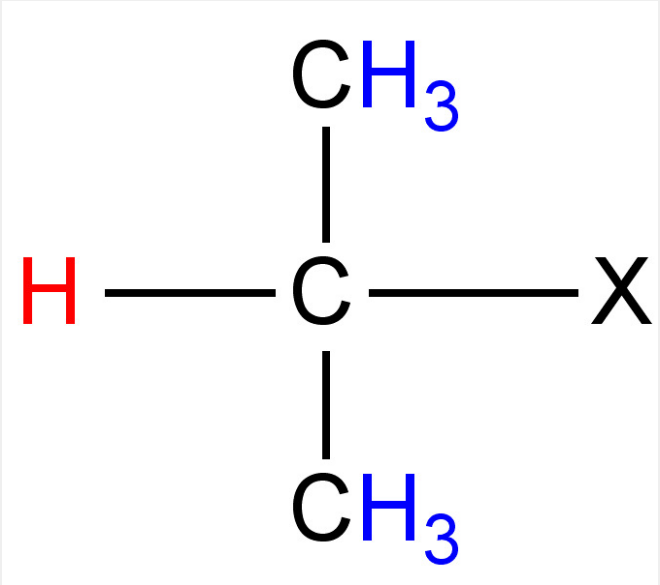
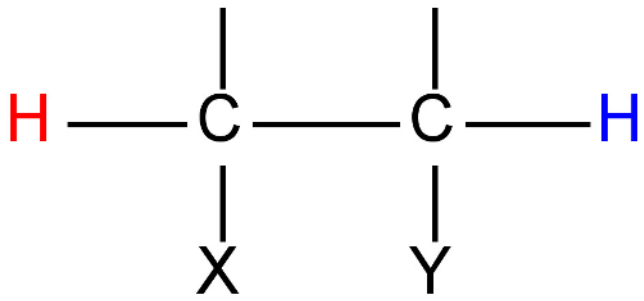
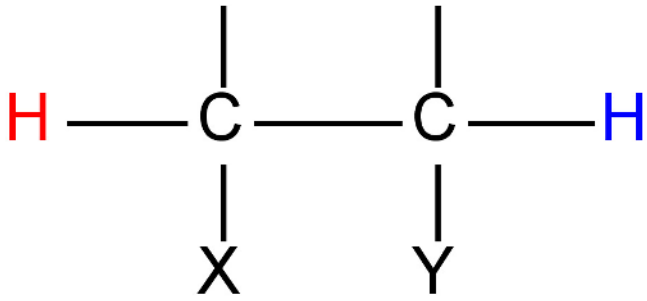
Notice that in Figure 5.3.8 there are two groups of peaks in the spectrum for chloroethane, a triplet and a quartet. These arise from the two different types of I ≠ 0 nuclei in the molecule, the protons on the methyl and methylene groups. The multiplet corresponding to the CH_3 protons has a relative integration (peak area) of three (one for each proton) and is split by the two methylene protons (n = 2), which results in n + 1 peaks, i.e., 3 which is a triplet. The multiplet corresponding to the CH_2 protons has an integration of two (one for each proton) and is split by the three methyl protons ((n = 3) which results in n + 1 peaks, i.e., 4 which is a quartet. Each group of nuclei splits the other, so in this way, they are *coupled*.

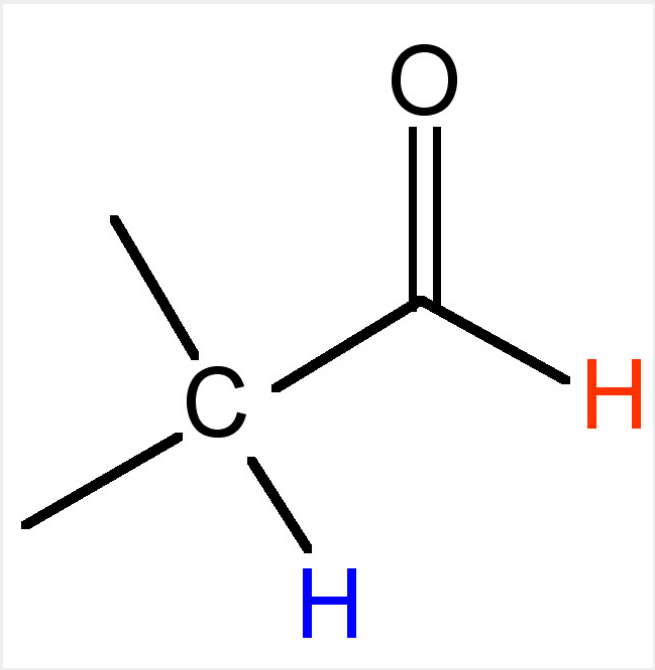
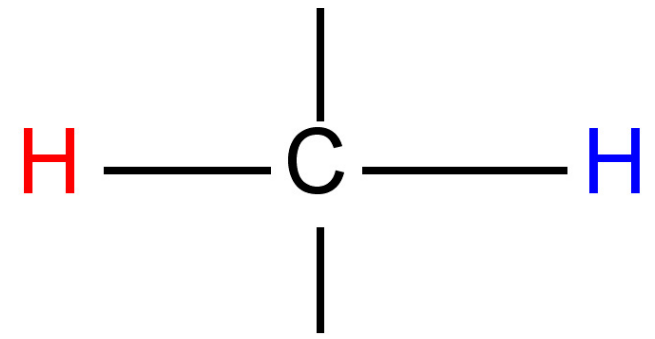
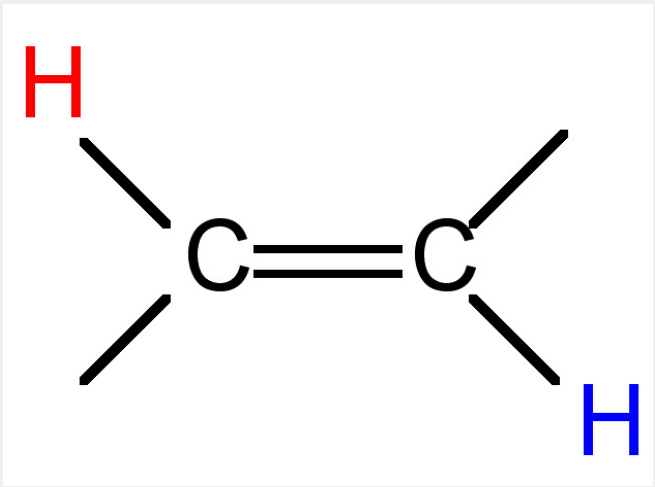
Coupling Constants

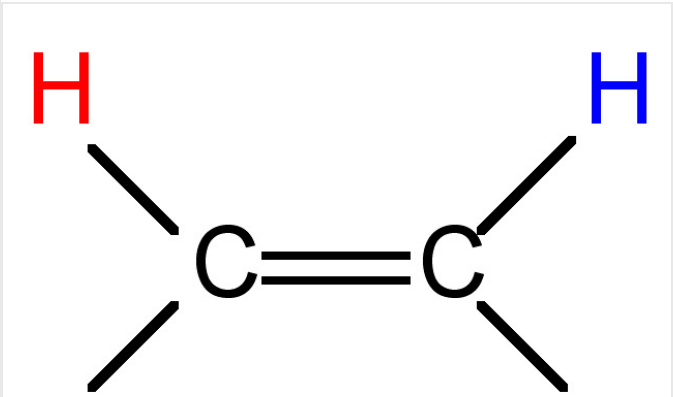
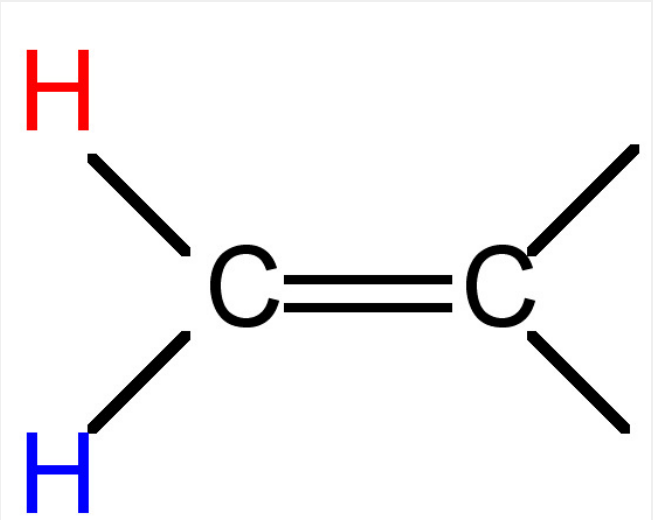
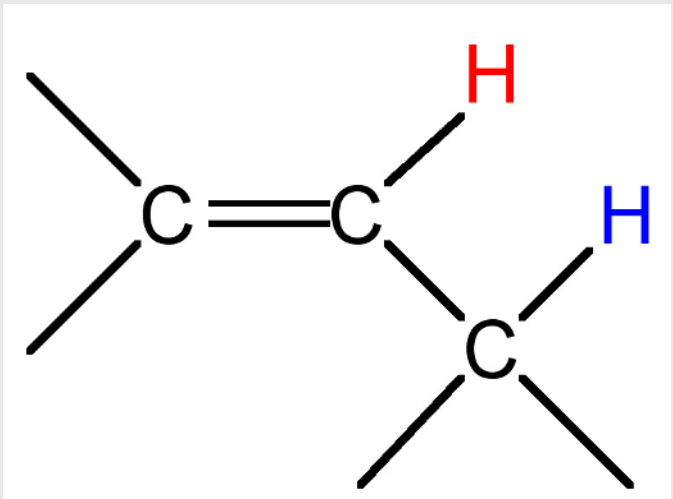
The difference (in Hz) between the peaks of a mulitplet is called the *coupling constant*. It is particular to the types of nuclei that give rise to the multiplet, and is independent of the field strength of the NMR instrument used. For this reason, the coupling constant is given in Hz, not ppm. The coupling constant for many common pairs of nuclei are known (Table 5.3.3), and this can help when interpreting spectra.

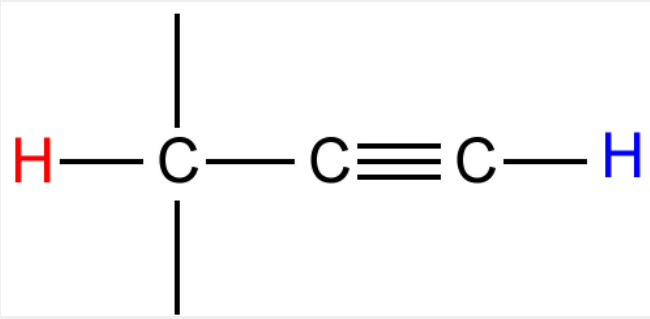
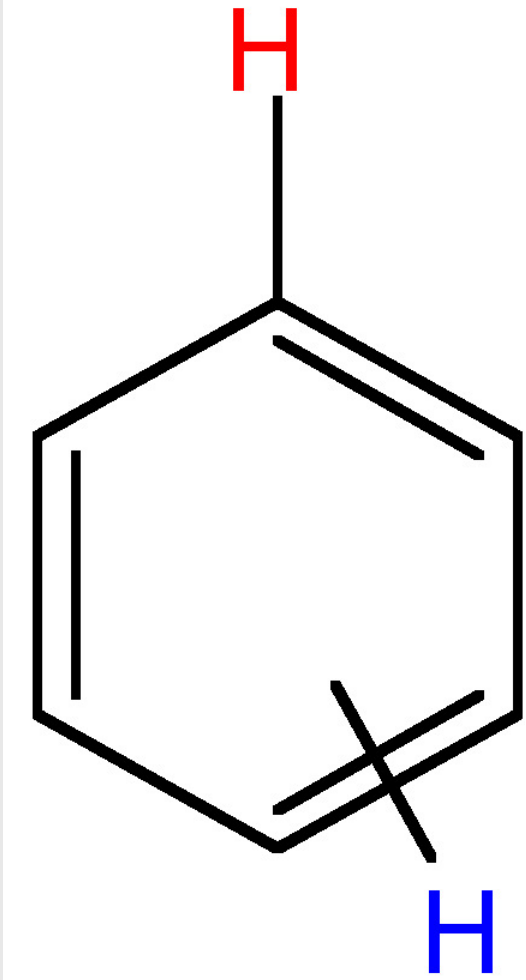
Table 5.3.3 Typical coupling constants for various organic structural types.

Structural Type

Structural Type	
	
	
	

	Structural Type
	0.5 - 3
	12 - 15
	12 - 18

	Structural Type
	7 - 12
	0.5 - 3
	3 - 11

	Structural Type
	2 - 3
	ortho = 6 - 9; meta = 1 - 3; para = 0 - 1

Coupling constants are sometimes written ^{n}J to denote the number of bonds (n) between the coupled nuclei. Alternatively, they are written as J(H-H) or J_{HH} to indicate the coupling is between two hydrogen atoms. Thus, a coupling constant between a phosphorous atom and a hydrogen would be written as J(P-H) or J_{PH}. Coupling constants are calculated empirically by measuring the distance between the peaks of a multiplet, and are expressed in Hz.

Coupling constants may be calculated from spectra using frequency or chemical shift data. Consider the spectrum of chloroethane shown in Figure 5.3.5 and the frequency of the peaks (collected on a 60 MHz spectrometer) give in Table 5.3.4.

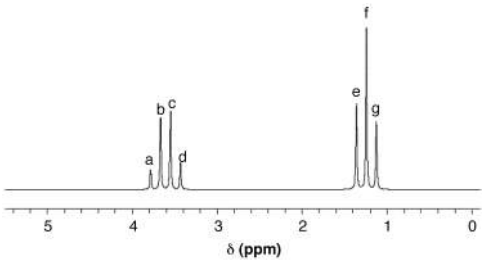


Figure 5.3.5 ^{1}H NMR spectrum of chloroethane. Peak positions for labeled peaks are given in Table 5.3.4.

Table 5.3.4 Chemical shift in ppm and Hz for all peaks in the 1H NMR spectrum of chloroethane. Peak labels are given in Figure 5.3.5.

Peak Label	δ (ppm)	v (Hz)
a	3.7805	226.83
b	3.6628	219.77
c	3.5452	212.71
d	3.4275	205.65
e	1.3646	81.88
f	1.2470	74.82
g	1.1293	67.76

To determine the coupling constant for a multiplet (in this case, the quartet in Figure 5.3.3, the difference in frequency (v) between each peak is calculated and the average of this value provides the coupling constant in Hz. For example using the data from Table 5.3.4:

Frequency of peak c - frequency of peak d = 212.71 Hz - 205.65 Hz = 7.06 Hz

Frequency of peak b - frequency of peak c = 219.77 Hz – 212.71 Hz = 7.06 Hz

Frequency of peak a - frequency of peak b = 226.83 Hz – 219.77 Hz = 7.06 Hz

Average: 7.06 Hz

$\therefore J$(H-H) = 7.06 Hz

In this case the difference in frequency between each set of peaks is the same and therefore an average determination is not strictly necessary. In fact for 1st order spectra they should be the same. However, in some cases the peak picking programs used will result in small variations, and thus it is necessary to take the trouble to calculate a true average.

To determine the coupling constant of the same multiplet using chemical shift data (δ), calculate the difference in ppm between each peak and average the values. Then multiply the chemical shift by the spectrometer field strength (in this case 60 MHz), in order to convert the value from ppm to Hz:

Chemical shift of peak c - chemical shift of peak d = 3.5452 ppm – 3.4275 ppm = 0.1177 ppm

Chemical shift of peak b - chemical shift of peak c = 3.6628 ppm – 3.5452 ppm = 0.1176 ppm

Chemical shift of peak a - chemical shift of peak b = 3.7805 ppm – 3.6628 ppm = 0.1177 ppm

Average: 0.1176 ppm

Average difference in ppm x frequency of the NMR spectrometer = 0.1176 ppm x 60 MHz = 7.056 Hz

$\therefore J$(H-H) = 7.06 Hz

Calculate the coupling constant for triplet in the spectrum for chloroethane (Figure 5.3.6) using the data from Table 5.3.5.

Using frequency data:
Frequency of peak f - frequency of peak g = 74.82 Hz – 67.76 Hz = 7.06 Hz
Frequency of peak e - frequency of peak f = 81.88 Hz – 74.82 Hz = 7.06 Hz

Average = 7.06 Hz
∴ J(H-H) = 7.06 Hz

Alternatively, using chemical shift data:
Chemical shift of peak f - chemical shift of peak g = 1.2470 ppm – 1.1293 ppm = 0.1177 ppm
Chemical shift of peak e - chemical shift of peak f = 1.3646 ppm – 1.2470 ppm = 0.1176 ppm
Average = 0.11765 ppm
0.11765 ppm x 60 MHz = 7.059 Hz
∴ J(H-H) = 7.06 Hz

Notice the coupling constant for this multiplet is the same as that in the example. This is to be expected since the two multiplets are coupled with each other.

Second-Order Coupling

When coupled nuclei have similar chemical shifts (more specifically, when Δν is similar in magnitude to J), *second-order coupling* or *strong coupling* can occur. In its most basic form, second-order coupling results in "roofing" (Figure 5.3.6). The coupled multiplets point to or lean toward each other, and the effect becomes more noticeable as Δν decreases. The multiplets also become off-centered with second-order coupling. The midpoint between the peaks no longer corresponds exactly to the chemical shift.

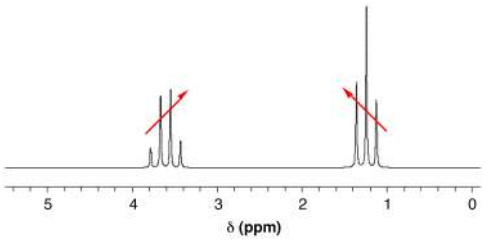


Figure 5.3.6 Roofing can be seen in the NMR spectrum of chloroethane. Adapted from A. M. Castillo, L. Patiny, and J. Wist, *J. Magn. Reson.*, 2010, **209**, 123.

In more drastic cases of strong coupling (when Δν ≈ J), multiplets can merge to create deceptively simple patterns. Or, if more than two spins are involved, entirely new peaks can appear, making it difficult to interpret the spectrum manually. Second-order coupling can often be converted into first-order coupling by using a spectrometer with a higher field strength. This works by altering the Δν (which is dependent on the field strength), while J (which is independent of the field strength) stays the same.

P-31 NMR Spectroscopy

Phosphorus-31 nuclear magnetic resonance (^{31}P NMR) is conceptually the same as proton (^{1}H) NMR. The ^{31}P nucleus is useful in NMR spectroscopy due to its relatively high gyromagnetic ratio (17.235 MHzT^{-1}). For comparison, the gyromagnetic ratios of ^{1}H and ^{13}C are (42.576 MHz T^{-1}) and (10.705 MHz T^{-1}), respectively. Furthermore, ^{31}P has a 100% natural isotopic abundance. Like the ^{1}H nucleus, the ^{31}P nucleus has a nuclear spin of $^{1}/_{2}$ which makes spectra relatively easy to interpret. ^{31}P NMR is an excellent technique for studying phosphorus containing compounds, such as organic compounds and metal coordination complexes.

Differences Between ^{1}H and ^{31}P NMR

There are certain significant differences between ^{1}H and ^{31}P NMR. While ^{1}H NMR spectra is referenced to tetramethylsilane [Si(C$\underline{H}_3$)$_4$], the chemical shifts in ^{31}P NMR are typically reported relative to 85% phosphoric acid (δ = 0 ppm), which is used as an external standard due to its reactivity. However, trimethyl phosphite, $\underline{P}(OCH_3)_3$, is also used since unlike phosphoric acid its shift (δ = 140 ppm) is not dependent on concentration or pH. As in ^{1}H NMR, positive chemical shifts correspond to a downfield shift from the standard. However, prior to the mid-1970s, the convention was the opposite. As a result, older texts and papers report shifts using the opposite sign. Chemical shifts in ^{31}P NMR commonly depend on the concentration of the sample, the solvent used, and the presence of other compounds. This is because the external standard does not take into account the bulk properties of the sample. As a result, reported chemical shifts for the same compound could vary by 1 ppm or more, especially for phosphate groups (P=O). ^{31}P NMR spectra are often recorded with all proton signals decoupled, i.e., ^{31}P-{^{1}H}, as is done with ^{13}C NMR. This gives rise to single, sharp signals per unique ^{31}P nucleus. Herein, we will consider both coupled and decoupled spectra.

Interpreting Spectra

As in ^{1}H NMR, phosphorus signals occur at different frequencies depending on the electron environment of each phosphorus nucleus Figure 5.3.7. In this section we will study a few examples of phosphorus compounds with varying chemical shifts and coupling to other nuclei.

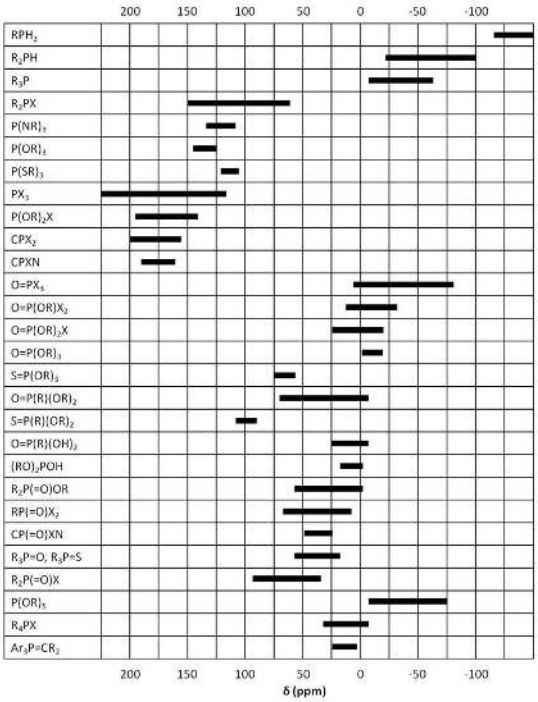


Figure 5.3.7 Chemical shift ranges for different types of phosphorus compounds.

Different Phosphorus Environments and their Coupling to ^{1}H

Consider the structure of 2,6,7-trioxa-1,4-diphosphabicyclo[2.2.2]octane [$P_\alpha(OCH_2)_3P_\beta$] shown in Figure 5.3.8. The subscripts α and β are simply used to differentiate the two phosphorus nuclei. According to Table 1, we expect the shift of P_α to be downfield of the phosphoric acid standard, roughly around 125 ppm to 140 ppm and the shift of P_β to be upfield of the standard, between -5 ppm and -70 ppm. In the decoupled spectrum shown in Figure 5.3.8, we can assign the phosphorus shift at 90.0 ppm to P_α and the shift at -67.0 ppm to P_β.

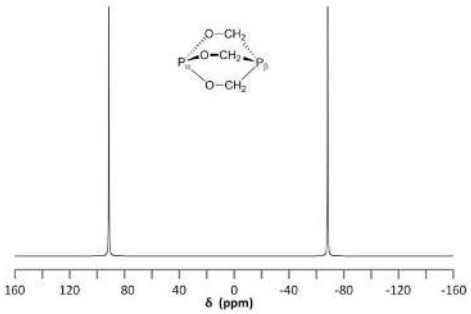


Figure 5.3.8 Structure and decoupled ^{31}P spectrum (^{31}P-{^{1}H}) of $P_\alpha(OCH_2)_3P_\beta$.

Figure 5.3.9 shows the coupling of the phosphorus signals to the protons in the compound. We expect a stronger coupling for P_β because there are only two bonds separating P_β from H, whereas three bonds separate $P_\alpha$from H ($J_{PCH} > J_{POCH}$). Indeed, J_{PCH} = 8.9 Hz and J_{POCH} = 2.6 Hz, corroborating our peak assignments above.

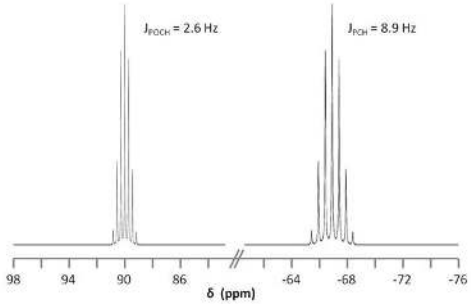


Figure 5.3.9 The ^{31}P spin coupled spectrum of $P_\alpha(OCH_2)_3P_\beta$.

Finally, Figure 5.3.10 shows the ^{1}H spectrum of $P_\alpha(OCH_2)_3P_\beta$ (Figure 5.3.11), which shows a doublet of doublets for the proton signal due to coupling to the two phosphorus nuclei.

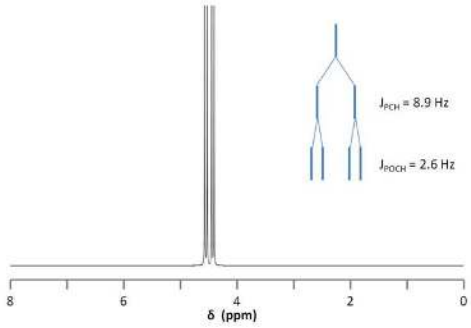


Figure 5.3.10 ^{1}H spectrum of $P_\alpha(OCH_2)_3P_\beta$ and proton splitting pattern due to phosphorus.

As suggested by the data in Figure 5.3.7 we can predict and observe changes in phosphorus chemical shift by changing the coordination of P. Thus for the series of compounds with the structure shown in Figure 5.3.11 the different chemical shifts corresponding to different phosphorus compounds are shown in Table 5.3.3.

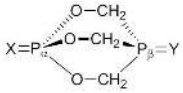


Figure 5.3.11 Structure of $[XP_\alpha(OCH_2)_3P_\beta Y]$.

Table 5.3.5 ^{31}P chemical shifts for variable coordination of $[XP_\alpha(OCH_2)_3P_\beta Y]$ (Figure 5.3.11). Data from K. J. Coskran and J. G. Verkade, *Inorg. Chem.*, 1965, **4**, 1655.

X	Y	P_α chemical shift (ppm)	P_β chemical shift (ppm)
-	-	90.0	-67.0
O	O	-18.1	6.4
S	-	51.8	-70.6

Coupling to Fluorine

^{19}F NMR is very similar to ^{31}P NMR in that ^{19}F has spin $^{1}/_{2}$ and is a 100% abundant isotope. As a result, ^{19}F NMR is a great technique for fluorine-containing compounds and allows observance of P-F coupling. The coupled ^{31}P and ^{19}F NMR spectra of ethoxy*bis*(trifluoromethyl)phosphine, $P(CF_3)_2(OCH_2CH_3)$, are shown in Figure 5.3.11. It is worth noting the splitting due to J_{PCF} = 86.6 Hz.

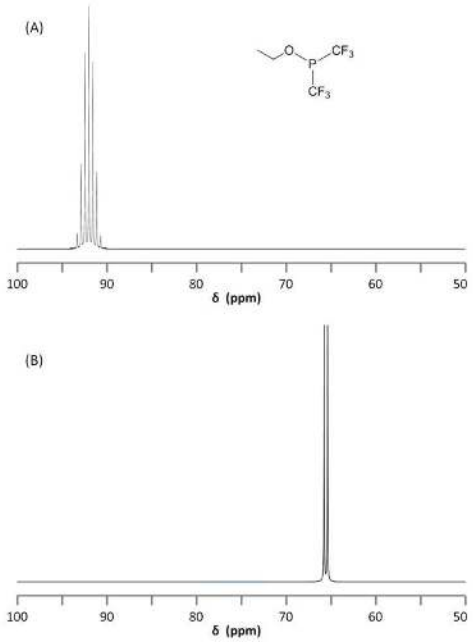


Figure 5.3.11 Structure, ^{31}P-{^{1}H} spectrum (A), and ^{19}F-{^{1}H} spectrum (B) for $P(CF_3)_2(OCH_2CH_3)$. Data from K. J. Packer, *J. Chem. Soc.*, 1963, 960.

^{31}P - ^{1}H Coupling

Consider the structure of dimethyl phosphonate, $OPH(OCH_3)_2$, shown in Figure 5.3.12 As the phosphorus nucleus is coupled to a hydrogen nucleus bound directly to it, that is, a coupling separated by a single bond, we expect J_{PH} to be very high. Indeed, the separation is so large (715 Hz) that one could easily mistake the split peak for two peaks corresponding to two different phosphorus nuclei.

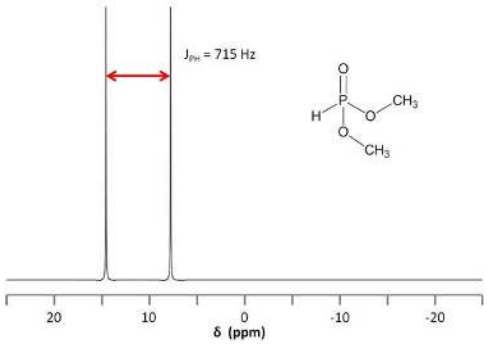


Figure 5.3.12 Structure and ^{31}P NMR spectrum of $OPH(OCH_3)_2$ with only the $OC\underline{H}_3$ protons decoupled.

This strong coupling could also lead us astray when we consider the ^{1}H NMR spectrum of dimethyl phosphonate (Figure 5.3.13). Here we observe two very small peaks corresponding to the phosphine proton. The peaks are separated by such a large distance and are so small relative to the methoxy doublet (ratio of 1:1:12), that it would be easy to confuse them for an impurity. To assign the small doublet, we could decouple the phosphorus signal at 11 ppm, which will cause this peak to collapse into a singlet.

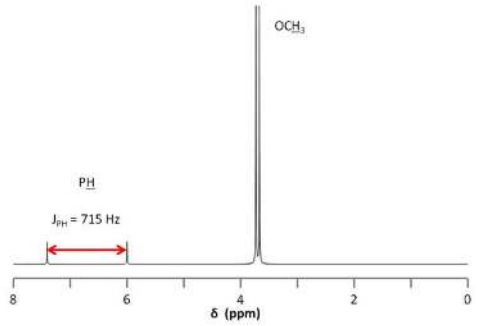


Figure 5.3.13 ^{1}H spectrum of $OPH(OCH_3)_2$. Data from K. Moedritzer, *J. Inorg. Nucl. Chem.*, 1961, **22**, 19.

Obtaining ^{31}P Spectra

Sample Preparation

Unlike ^{13}C NMR, which requires high sample concentrations due to the low isotopic abundance of ^{13}C, ^{31}P sample preparation is very similar to ^{1}H sample preparation. As in other NMR experiments, a ^{31}P NMR sample must be free of particulate matter. A reasonable concentration is 2-10 mg of sample dissolved in 0.6-1.0 mL of solvent. If needed, the solution can be filtered through a small glass fiber. Note that the solid will not be analyzed in the NMR experiment. Unlike ^{1}H NMR, however, the sample does **not** to be dissolved in a deuterated solvent since common solvents do not have ^{31}P nuclei to contribute to spectra. This is true, of course, only if a ^{1}H NMR spectrum is not to be obtained from this sample. Being able to use non-deuterated solvents offers many advantages to ^{31}P NMR, such as the simplicity of assaying purity and monitoring reactions, which will be discussed later.

Instrument Operation

Instrument operation will vary according to instrumentation and software available. However, there are a few important aspects to instrument operation relevant to ^{31}P NMR. The instrument probe, which excites nuclear spins and detects chemical shifts, must be set up appropriately for a ^{31}P NMR experiment. For an instrument with a multinuclear probe, it is a simple matter to access the NMR software and make the switch to a ^{31}P experiment. This will select the appropriate frequency for ^{31}P. For an instrument which has separate probes for different nuclei, it is imperative that one be trained by an expert user in changing the probes on the spectrometer.

Before running the NMR experiment, consider whether the ^{31}P spectrum should include coupling to protons. Note that ^{31}P spectra are typically reported with all protons decoupled, i.e., ^{31}1P-{^{1}H}. This is usually the default setting for a ^{31}P NMR experiment. To change the coupling setting, follow the instructions specific to your NMR instrument software.

As mentioned previously, chemical shifts in ^{31}P NMR are reported relative to 85% phosphoric acid. This must be an external standard due to the high reactivity of phosphoric acid. One method for standardizing an experiment uses a coaxial tube inserted into the sample NMR tube (Figure 5.3.14). The 85% H_3PO_4 signal will appear as part of the sample NMR spectrum and can thus be set to 0 ppm.

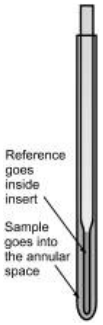


Figure 5.3.14 Diagram of NMR tube with inserted coaxial reference insert. Image Courtesy of Wilmad-LabGlass; All Rights Reserved.

Another way to reference an NMR spectrum is to use a 85% H_3PO_4 standard sample. These can be prepared in the laboratory or purchased commercially. To allow for long term use, these samples are typically vacuum sealed, as opposed to capped the way NMR samples typically are. The procedure for using a separate reference is as follows.

1. Insert NMR sample tube into spectrometer.

2. Tune the ^{31}P probe and shim the magnetic field according to your individual instrument procedure.
3. Remove NMR sample tube and insert H_3PO_4 reference tube into spectrometer.
4. Begin NMR experiment. As scans proceed, perform a fourier transform and set the phosphorus signal to 0 ppm. Continue to reference spectrum until the shift stops changing.
5. Stop experiment.
6. Remove H_3PO_4 reference tube and insert NMR sample into spectrometer.
7. Run NMR experiment without changing the referencing of the spectrum.

^{31}P NMR Applications

Assaying Sample Purity

^{31}P NMR spectroscopy gives rise to single sharp peaks that facilitate differentiating phosphorus-containing species, such as starting materials from products. For this reason, ^{31}P NMR is a quick and simple technique for assaying sample purity. Beware, however, that a "clean" ^{31}P spectrum does not necessarily suggest a pure compound, only a mixture free of phosphorus-containing contaminants.

^{31}P NMR can also be used to determine the optical purity of a chiral sample. Adding an enantiomer to the chiral mixture to form two different diastereomers will give rise to two unique chemical shifts in the ^{31}P spectrum. The ratio of these peaks can then be compared to determine optical purity.

Monitoring Reactions

As suggested in the previous section, ^{31}P NMR can be used to monitor a reaction involving phosphorus compounds. Consider the reaction between a slight excess of organic diphosphine ligand and a nickel(0) *bis*-cyclooctadiene, Figure 5.3.15.

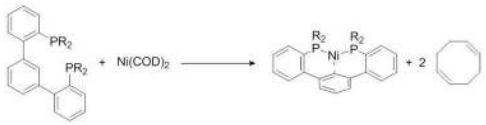


Figure 5.3.15 Reaction between diphosphine ligand and nickel

The reaction can be followed by ^{31}P NMR by simply taking a small aliquot from the reaction mixture and adding it to an NMR tube, filtering as needed. The sample is then used to acquire a ^{31}P NMR spectrum and the procedure can be repeated at different reaction times. The data acquired for these experiments is found in Figure 5.3.16. The changing in ^{31}P peak intensity can be used to monitor the reaction, which begins with a single signal at -4.40 ppm, corresponding to the free diphosphine ligand. After an hour, a new signal appears at 41.05 ppm, corresponding the the diphosphine nickel complex. The downfield peak grows as the reaction proceeds relative to the upfield peak. No change is observed between four and five hours, suggesting the conclusion of the reaction.

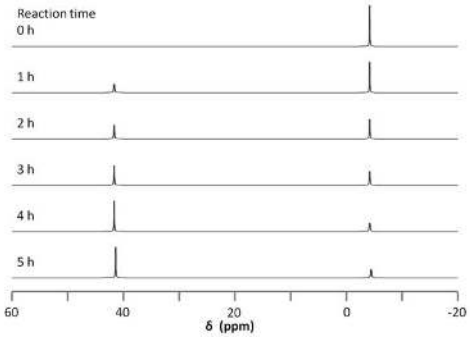


Figure 5.3.16 ^{31}P-{^{1}H} NMR spectra of the reaction of diphosphine ligand with nickel(0) *bis*-cyclooctadiene to make a diphosphine nickel complex over time.

There are a number of advantages for using ^{31}P for reaction monitoring when available as compared to ^{1}H NMR:

- There is no need for a deuterated solvent, which simplifies sample preparation and saves time and resources.
- The ^{31}P spectrum is simple and can be analyzed quickly. The corresponding ^{1}H NMR spectra for the above reaction would include a number of overlapping peaks for the two phosphorus species as well as peaks for both free and bound cyclooctadiene ligand.
- Purification of product is also easy assayed.

^{31}P NMR does not eliminate the need for ^{1}H NMR chacterization, as impurities lacking phosphorus will not appear in a ^{31}P experiment. However, at the completion of the reaction, both the crude and purified products can be easily analyzed by both ^{1}H and ^{31}P NMR spectroscopy.

Measuring Epoxide Content of Carbon Nanomaterials

One can measure the amount of epoxide on nanomaterials such as carbon nanotubes and fullerenes by monitoring a reaction involving phosphorus compounds in a similar manner to that described above. This technique uses the catalytic reaction of methyltrioxorhenium (Figure 5.3.17). An epoxide reacts with methyltrioxorhenium to form a five membered ring. In the presence of triphenylphosphine (PPH_3), the catalyst is regenerated, forming an alkene and triphenylphosphine oxide ($OPPh_3$). The same reaction can be applied to carbon nanostructures and used to quantify the amount of epoxide on the nanomaterial. Figure 5.3.18 illustrates the quantification of epoxide on a carbon nanotube.

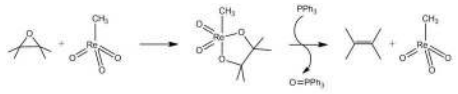


Figure 5.3.17

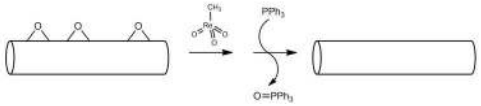


Figure 5.3.18

Because the amount of initial PPh_3 used in the reaction is known, the relative amounts of PPh_3 and $OPPh_3$can be used to stoichiometrically determine the amount of epoxide on the nanotube. ^{31}P NMR spectroscopy is used to determine the relative amounts of PPh_3 and $OPPh_3$ (Figure 5.3.19).

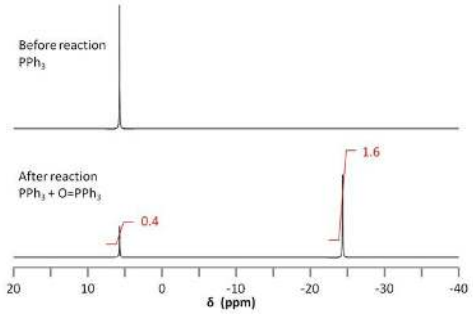


Figure 5.3.19 ^{31}P spectrum of experiment before addition of Re complex (top) and at the completion of experiment (bottom).

The integration of the two ^{31}P signals is used to quantify the amount of epoxide on the nanotube according to 5.3.4.

$$Moles\ of\ Epoxide\ =\ \frac{area\ of\ OPPH_3\ peak}{area\ of\ PPh_3\ peak}\times\ moles\ PPh_3 \tag{5.3.4}$$

Thus, from a known quantity of PPh_3, one can find the amount of $OPPh_3$ formed and relate it stoichiometrically to the amount of epoxide on the nanotube. Not only does this experiment allow for such quantification, it is also unaffected by the presence of the many different species present in the experiment. This is because the compounds of interest, PPh_3 and $OPPh_3$, are the only ones that are characterized by ^{31}P NMR spectroscopy.

Conclusion

^{31}P NMR spectroscopy is a simple technique that can be used alongside ^{1}H NMR to characterize phosphorus-containing compounds. When used on its own, the biggest difference from ^{1}H NMR is that there is no need to utilize deuterated solvents. This advantage leads to many different applications of ^{31}P NMR, such as assaying purity and monitoring reactions.

NMR Spectroscopy of Stereoisomers

Nuclear magnetic resonance (NMR) spectroscopy is a very useful tool used widely in modern organic chemistry. It exploits the differences in the magnetic properties of different nuclei in a molecule to yield information about the chemical environment of the nuclei, and subsequently the molecule, in question. NMR analysis lends itself to scientists more easily than say the more cryptic data achieved form ultraviolet or infared spectra because the differences in magnetic properties lend themselves to scientists very

well. The chemical shifts that are characteristic of different chemical environments and the multiplicity of the peaks fit well with our conception of the way molecules are structured.

Using NMR spectroscopy, we can differentiate between constitutional isomers, stereoisomers, and enantiomers. The later two of these three classifications require close examination of the differences in NMR spectra associated with changes in chemical environment due to symmetry differences; however, the differentiation of constitutional isomers can be easily obtained.

Constitutional Isomerism

Nuclei both posses charge and spin, or angular momentum, and from basic physics we know that a spinning charge generates a magnetic moment. The specific nature of this magnetic moment is the main concern of NMR spectroscopy.

For proton NMR, the local chemical environment makes different protons in a molecule resonate at different frequencies. This difference in resonance frequencies can be converted into a chemical shift (δ) for each nucleus being studied. Because each chemical environment results in a different chemical shift, one can easily assign peaks in the NMR data to specific functional groups based upon president. Presidents for chemical shifts can be found in any number of basic NMR text. For example, Figure 5.3.20 shows the spectra of ethyl formate and benzyl acetate. In the lower spectra, benzyl acetate, notice peaks at δ = 1.3, 4.2, and 8.0 ppm characteristic of the primary, secondary, and aromatic protons, respectively, present in the molecule. In the spectra of ethyl formate (Figure 5.3.20 b), notice that the number of peaks is is the same as that of benzyl acetate (Figure 5.3.20 a); however, the multiplicity of peaks and their shifts is very different.

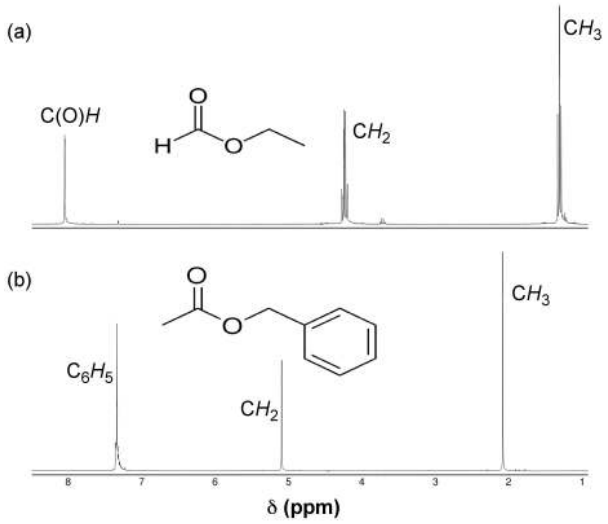


Figure 5.3.20 ^{1}H NMR spectra of (a) ethyl formate and (b) benzyl acetate.

The difference between these two spectra is due to geminal spin-spin coupling. Spin-spin coupling is the result of magnetic interaction between individual protons transmitted by the bonding electrons between the protons. This spin-spin coupling results in the speak splitting we see in the NMR data. One of the benefits of NMR spectroscopy is the sensitivity to very slight changes in chemical environment.

Stereoisomerism

Diastereomers

Based on their definition, diastereomers are stereoisomers that are not mirror images of each other and are not superimposable. In general, diastereomers have differing reactivity and physical properties. One common example is the difference between threose and erythrose (Figure 5.3.21.

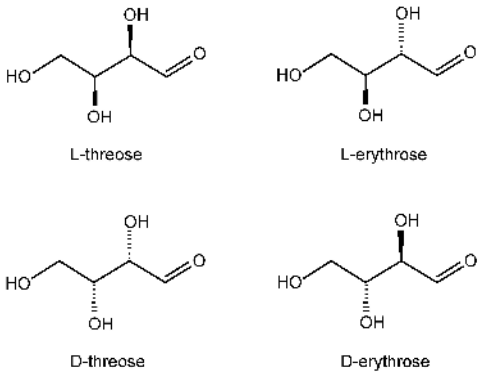


Figure 5.3.21 The structures of threose and erythrose.

As one can see from Figure 5.3.22, these chemicals are very similar each having the empirical formula of $C_4H_7O_4$. One may wonder: how are these slight differences in chemical structure represented in NMR? To answer this question, we must look at the Newman projections for a molecule of the general structure Figure 5.3.22

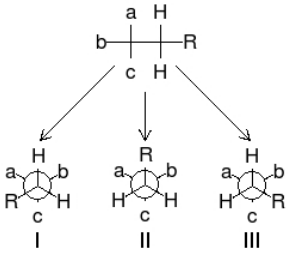


Figure 5.3.22 Newman projections of a general diastereomer.

One can easily notice that the two protons represented are always located in different chemical environments. This is true because the R group makes the proton resonance frequencies $v_1(I) \neq v_2(III)$, $v_2(I) \neq v_1(II)$, and $v_2(II) \neq v_1(III)$. Thus, diastereomers have different vicinal proton-proton couplings and the resulting chemical shifts can be used to identify the isomeric makeup of the sample.

Enantiomers

Enantiomers are compounds with a chiral center. In other words, they are non-superimposable mirror images. Unlike diastereomers, the only difference between enantiomers is their interaction with polarized light. Unfortunately, this indistinguishability of racemates includes NMR spectra. Thus, in order to differentiate between enantiomers, we must make use of an optically active solvent also called a chiral derivatizing agent (CDA). The first CDA was (α-methoxy-α-(trifluoromethyl)phenylacetic acid) (MTPA also known as Mosher's acid) (Figure 5.3.23).

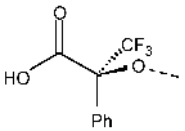


Figure 5.3.23 The structure of the S-isomer of Mosher's Acid (S-MTPA)

Now, many CDAs exist and are readily available. It should also be noted that CDA development is a current area of active research. In simple terms, one can think of the CDA turning an enantiomeric mixture into a mixture of diastereomeric complexes, producing doublets where each half of the doublet corresponds to each diastereomer, which we already know how to analyze. The resultant peak splitting in the NMR spectra due to diastereomeric interaction can easily determine optical purity. In order to do this, one may simply integrate the peaks corresponding to the different enantiomers thus yielding optical purity of incompletely resolved racemates. One thing of note when performing this experiment is that this interaction between the enantiomeric compounds and the solvent, and thus the magnitude of the splitting, depends upon the asymmetry or chirality of the solvent, the intermolecular interaction between the compound and the solvent, and thus the temperature. Thus, it is helpful to compare the spectra of the enantiomer-CDA mixture with that of the pure enantiomer so that changes in chemical shift can be easily noted.

Basics of Solid-State NMR

NMR stands for nuclear magnetic resonance and functions as a powerful tool for chemical characterization. Even though NMR is used mainly for liquids and solutions, technology has progressed to where NMR of solids can be obtained with ease. Aptly named as solid state NMR, the expansion of usable phases has invariably increased our ability to identify chemical compounds. The reason behind difficulties using the solid state lie in the fact that solids are never uniform. When put through a standard NMR, line broadening interactions cannot be removed by rapid molecular motions, which results in unwieldy wide lines which provide little to no useful information. The difference is so staggering that lines broaden by hundreds to thousands of hertz as opposed to less than 0.1 Hz in solution when using an $I = {}^{1}/_{2}$ spin nucleus.

A process known as magic angle spinning (MAS), where the sample is tilted at a specific angle, is used in order to overcome line broadening interactions and achieve usable peak resolutions. In order to understand solid state NMR, its history, operating chemical and mathematical principles, and distinctions from gas phase/solution NMR will be explained.

History

The first notable contribution to what we know today as NMR was Wolfgang Pauli's (Figure 5.3.24) prediction of nuclear spin in 1926. In 1932 Otto Stern (Figure 5.3.25) used molecular beams and detected nuclear magnetic moments.



Figure 5.3.26 German physicist Otto Stern (1888 - 1969)

Four years later, Gorter performed the first NMR experiment with lithium fluoride (LiF) and hydrated potassium alum ($K[Al(SO_4)_2]\cdot 12H_2O$) at low temperatures. Unfortunately, he was unable to characterize the molecules and the first successful NMR for a solution of water was taken in 1945 by Felix Bloch (Figure 5.3.27). In the same year, Edward Mills Purcell (Figure 5.3.27) managed the first successful NMR for the solid paraffin. Continuing their research, Bloch obtained the ^{1}H NMR of ethanol

and Purcell obtained that of paraffin in 1949. In the same year, the chemical significance of chemical shifts was discovered. Finally, high resolution solid state NMR was made possible in 1958 by the discovery of magic angle spinning.



Figure 5.3.28 American physicist Edward Mills Purcell (1912-1997).

How it Works: From Machine to Graph

NMR spectroscopy works by measuring the nuclear shielding, which can also be seen as the electron density, of a particular element. Nuclear shielding is affected by the chemical environment, as different neighboring atoms will have different effects on nuclear shielding, as electronegative atoms will tend to decrease shielding and vice versa. NMR requires the elements analyzed to have a spin state greater than zero. Commonly used elements are ^{1}H, ^{13}C, and ^{29}Si. Once inside the NMR machine, the presence of a magnetic field splits the spin states (Figure 5.3.29).

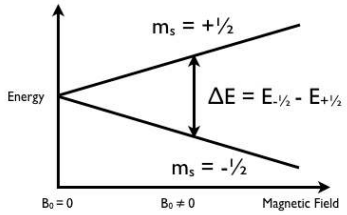


Figure 5.3.29 Spin state splitting as a function of applied magnetic field.

From (Figure 5.3.29 we see that a spin state of $^{1}/_{2}$ is split into two spin states. As spin state value increases, so does the number of spin states. A spin of 1 will have three spin states, $^{3}/_{2}$ will have four spin states, and so on. However, higher spin states increases the difficulty to accurately read NMR results due to confounding peaks and decreased resolution, so spin states of ½ are generally preferred. The E, or radiofrequency shown in (Figure 5.3.29 can be described by 5.3.5, where μ is the magnetic moment, a

property intrinsic to each particular element. This constant can be derived from 5.3.6, where ϒ is the gyromagnetic ratio, another element dependent quantity, h is Planck's constant, and I is the spin.

$$E = \mu B_0 H_0 \tag{5.3.5}$$

$$\mu = \gamma h(I(I+1))^{1/2} \tag{5.3.6}$$

In 5.3.5 can have E substituted for hν, leading to 5.3.7, which can solve for the NMR resonance frequency (ν).

$$h\nu = \mu B_0 H_0 \tag{5.3.7}$$

Using the frequency (ν), the δ, or expected chemical shift may be computed using 5.3.8.

$$\delta = \frac{(\nu_{observed} - \nu_{reference})}{\nu_{spectrometer}} \tag{5.3.8}$$

Delta (δ) is observed in ppm and gives the distance from a set reference. Delta is directly related to the chemical environment of the particular atom. For a low field, or high delta, an atom is in an environment which produces induces less shielding than in a high field, or low delta.

NMR Instrument

An NMR can be divided into three main components: the workstation computer where one operates the NMR instrument, the NMR spectrometer console, and the NMR magnet. A standard sample is inserted through the bore tube and pneumatically lowered into the magnet and NMR probe (Figure 5.3.30).

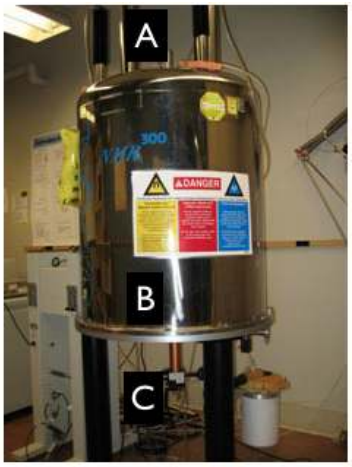


Figure 5.3.30 Standard NMR instrument, with main components labeled: (A) bore tube, (B) outer magnet shell, (C) NMR probe.

The first layer inside the NMR (Figure 5.3.31 is the liquid nitrogen jacket. Normally, this space is filled with liquid nitrogen at 77 K. The liquid nitrogen reservoir space is mostly above the magnet so that it can act as a less expensive refrigerant to block infrared radiation from reaching the liquid helium jacket.

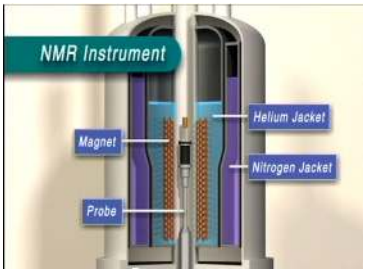


Figure 5.3.31 Diagram of the main layers inside an NMR machine.

The layer following the liquid nitrogen jacket is a 20 K radiation shield made of aluminum wrapped with alternating layers of aluminum foil and open weave gauze. Its purpose is to block infrared radiation which the 77 K liquid nitrogen vessel was unable to eliminate, which increases the ability for liquid helium to remain in the liquid phase due to its very low boiling point. The liquid

helium vessel itself, the next layer, is made of stainless steel wrapped in a single layer of aluminum foil, acting once again as an infrared radiation shield. It is about 1.6 mm thick and kept at 4.2 K.

Inside the vessel and around the magnet is the aluminum baffle, which acts as another degree of infrared radiation protection as well as a layer of protection for the superconducting magnet from liquid helium reservoir fluctuations, especially during liquid helium refills. The significance is that superconducting magnets at low fields are not fully submerged in liquid helium, but higher field superconducting magnets must maintain the superconducting solenoid fully immersed in liquid helium The vapor above the liquid itself is actually enough to maintain superconductivity of most magnets, but if it reaches a temperature above 10 K, the magnet quenches. During a quench, the solenoid exceeds its critical temperature for superconductivity and becomes resistive, generating heat. This heat, in turn, boils off the liquid helium. Therefore, a small opening at the very base of the baffle exists as a path for the liquid helium to reach the magnet surface so that during refills the magnet is protected from accidental quenching.

Problems with Solid State NMR

The most notable difference between solid samples and solution/gas in terms of NMR spectroscopy is that molecules in solution rotate rapidly while those in a solid are fixed in a lattice. Different peak readings will be produced depending on how the molecules are oriented in the magnetic field because chemical shielding depends upon the orientation of a molecule, causing chemical shift anisotropy. Therefore, the effect of chemical shielding also depends upon the orientation of the molecule with respect to the spectrometer. These counteracting forces are balanced out in gases and solutions because of their randomized molecular movement, but become a serious issue with fixed molecules observed in solid samples. If the chemical shielding isn't determined accurately, neither will the chemical shifts (δ).

Another issue with solid samples are dipolar interactions which can be very large in solid samples causing linewidths of tens to hundreds of kilohertz to be generated. Dipolar interactions are tensor quantities, which demonstrate values dependent on the orientation and placement of a molecule in reference to its surroundings. Once again the issue goes back to the lattice structure of solids, which are in a fixed location. Even though the molecules are fixed, this does not mean that nuclei are evenly spread apart. Closer nuclei display greater dipolar interactions and vice versa, creating the noise seen in spectra of NMR not adapted for solid samples. Dipolar interactions are averaged out in solution states because of randomized movement. Spin state repulsions are averaged out by molecular motion of solutions and gases. However, in solid state, these interactions are not averaged and become a third source of line broadening.

Magic Angle Spinning

In order to counteract chemical shift anisotropy and dipolar interactions, magic angle spinning was developed. As discussed above, describing dipolar splitting and chemical shift aniostoropy interactions respectively, it becomes evident that both depend on the geometric factor ($3\cos^2\theta$-1).

$$Dipolar\ splitting\ =\ C(\mu_0/8\pi)(\gamma_a\gamma_x/r_{ax}^2)(3cos^2\theta_{iz}-1) \tag{5.3.9}$$

$$\sigma_{zz}\ =\ \bar{\sigma}+1/3\Sigma\sigma_{ii}(3cos^2\theta_{iz}-1) \tag{5.3.10}$$

If this factor is decreased to 0, then line broadening due to chemical shift anisotropy and dipolar interactions will disappear. Therefore, solid samples are rotated at an angle of 54.74˚, effectively allowing solid samples to behave similarly to solutions/gases in NMR spectroscopy. Standard spinning rates range from 12 kHz to an upper limit of 35 kHz, where higher spin rates are necessary to remove higher intermolecular interactions.

Application of Solid State NMR

The development of solid state NMR is a technique necessary to understand and classify compounds that would not work well in solutions, such as powders and complex proteins, or study crystals too small for a different characterization method.

Solid state NMR gives information about local environment of silicon, aluminum, phosphorus, etc. in the structures, and is therefore an important tool in determining structure of molecular sieves. The main issue frequently encountered is that crystals large enough for X-Ray crystallography cannot be grown, so NMR is used since it determines the local environments of these elements. Additionally, by using ^{13}C and ^{15}N, solid state NMR helps study amyloid fibrils, filamentous insoluble protein aggregates related to neurodegenerative diseases such as Alzheimer's disease, type II diabetes, Huntington's disease, and prion diseases.

Using 13-C NMR to Study Carbon Nanomaterials

Carbon Nanomaterial

There are several types of carbon nanomaterial. Members of this family are graphene, single-walled carbon nanotubes (SWNT), multi-walled carbon nanotubes (MWNT), and fullerenes such as C_{60}. Nano materials have been subject to various modification and functionalizations, and it has been of interest to develop methods that could observe these changes. Herein we discuss selected applications of ^{13}C NMR in studying graphene and SWNTs. In addition, a discussion of how ^{13}C NMR could be used to analyze a thin film of amorphous carbon during a low-temperature annealing process will be presented.

^{13}C NMR vs. ^{1}H NMR

Since carbon is found in any organic molecule NMR that can analyze carbon could be very helpful, unfortunately the major isotope, ^{12}C, is not NMR active. Fortunately, ^{13}C with a natural abundance of 1.1% is NMR active. This low natural abundance along with lower gyromagnetic ratio for ^{13}C causes sensitivity to decrease. Due to this lower sensitivity, obtaining a ^{13}C NMR spectrum with a specific signal-to-noise ratio requires averaging more spectra than the number of spectra that would be required to average in order to get the same signal to noise ratio for a ^{1}H NMR spectrum. Although it has a lower sensitivity, it is still highly used as it discloses valuable information.

Peaks in a ^{1}H NMR spectrum are split to $n + 1$ peak, where n is the number of hydrogen atoms on the adjacent carbon atom. The splitting pattern in ^{13}C NMR is different. First of all, C-C splitting is not observed, because the probability of having two adjacent ^{13}C is about 0.01%. Observed splitting patterns, which is due to the hydrogen atoms on the same carbon atom not on the adjacent carbon atom, is governed by the same $n + 1$ rule.

In ^{1}H NMR, the integral of the peaks are used for quantitative analysis, whereas this is problematic in ^{13}C NMR. The long relaxation process for carbon atoms takes longer comparing to that of hydrogen atoms, which also depends on the order of carbon (i.e., 1°, 2°, etc.). This causes the peak heights to not be related to the quantity of the corresponding carbon atoms.

Another difference between ^{13}C NMR and ^{1}H NMR is the chemical shift range. The range of the chemical shifts in a typical NMR represents the different between the minimum and maximum amount of electron density around that specific nucleus. Since hydrogen is surrounded by fewer electrons in comparison to carbon, the maximum change in the electron density for hydrogen is less than that for carbon. Thus, the range of chemical shift in ^{1}H NMR is narrower than that of ^{13}C NMR.

Solid State NMR

^{13}C NMR spectra could also be recorded for solid samples. The peaks for solid samples are very broad because the sample, being solid, cannot have all anisotropic, or orientation-dependent, interactions canceled due to *rapid random tumbling*. However, it is still possible to do high resolution solid state NMR by spinning the sample at 54.74° with respect to the applied magnetic field, which is called the *magic angle*. In other words, the sample can be spun to artificially cancel the orientation-dependent interaction. In general, the spinning frequency has a considerable effect on the spectrum.

^{13}C NMR of Carbon Nanotubes

Single-walled carbon nanotubes contain sp^2 carbons. Derivatives of SWNTs contain sp^3 carbons in addition. There are several factors that affect the ^{13}C NMR spectrum of a SWNT sample, three of which will be reviewed in this module: ^{13}C percentage, diameter of the nanotube, and functionalization.

^{13}C Percentage

For sp^2 carbons, there is a slight dependence of ^{13}C NMR peaks on the percentage of ^{13}C in the sample. Samples with lower ^{13}C percentage are slighted shifted downfield (higher ppm). Data are shown in Table 5.3.4. Please note that these peaks are for the sp^2 carbons.

Table 5.3.4 Effects of ^{13}C percentage on the sp^2 peak. Data from S. Hayashi, F. Hoshi, T. Ishikura, M. Yumura, and S. Ohshima, *Carbon*, 2003, **41**, 3047.

Sample	**δ (ppm)**
SWNTs(100%)	116±1
SWNTs(1%)	118±1

Diameter of the Nanotubes

The peak position for SWNTs also depends on the diameter of the nanotubes. It has been reported that the chemical shift for sp^2 carbons decreases as the diameter of the nanotubes increases. Figure 5.3.32 shows this correlation. Since the peak position depends on the diameter of nanotubes, the peak broadening can be related to the diameter distribution. In other words, the narrower the peak is, the smaller the diameter distribution of SWNTs is. This correlation is shown in Figure 5.3.33.

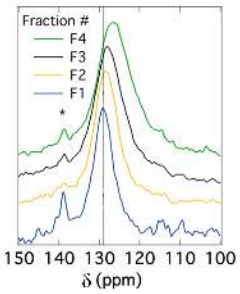


Figure 5.3.32 Correlation between the chemical shift of the sp^2 carbon and the diameter of the nanotubes. The diameter of the nanotubes increases from F1 to F4. Image from C. Engtrakul, V. M. Irurzun, E. L. Gjersing, J. M. Holt, B. A. Larsen, D. E. Resasco, and J. L. Blackburn, *J. Am. Chem. Soc.*, 2012, **134**, 4850. Copyright: American Chemical Society (2012).

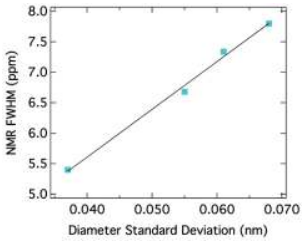


Figure 5.3.33 Correlation between FWHM and the standard deviation of the diameter of nanotubes. Image from C. Engtrakul, V. M. Irurzun, E. L. Gjersing, J. M. Holt, B. A. Larsen, D. E. Resasco, and J. L. Blackburn, *J. Am. Chem. Soc.*, 2012, **134**, 4850. Copyright: American Chemical Society (2012).

Functionalization

Solid stated ^{13}C NMR can also be used to analyze functionalized nanotubes. As a result of functionalizing SWNTs with groups containing a carbonyl group, a slight shift toward higher fields (lower ppm) for the sp^2carbons is observed. This shift is explained by the perturbation applied to the electronic structure of the whole nanotube as a result of the modifications on only a fraction of the nanotube. At the same time, a new peak emerges at around 172 ppm, which is assigned to the carboxyl group of the substituent. The peak intensities could also be used to quantify the level of functionalization. Figure 5.3.34 shows these changes, in which the substituents are $–(CH_2)_3COOH$, $–(CH_2)_2COOH$, and $–(CH_2)_2CONH(CH_2)_2NH_2$ for the spectra Figure 5.3.34 b, Figure 5.3.34 c, and Figure 5.3.34 d, respectively. Note that the bond between the nanotube and the substituent is a C-C bond. Due to low sensitivity, the peak for the sp^3 carbons of the nanotube, which does not have a high quantity, is not detected. There is a small peak around 35 ppm in Figure 5.3.34, can be assigned to the aliphatic carbons of the substituent.

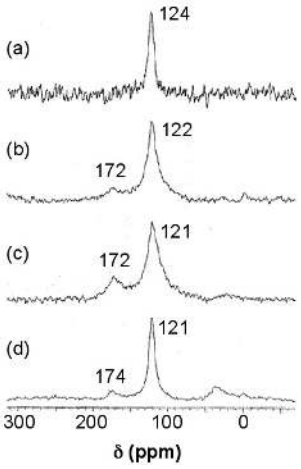


Figure 5.3.34 ^{13}C NMR spectra for (a) pristine SWNT, (b) SWNT functionalized with $–(CH_2)_3COOH$, (c) SWNT functionalized with $–(CH_2)_2COOH$, and (d) SWNT functionalized with $–(CH_2)_2CONH(CH_2)_2NH_2$. Image from H. Peng, L. B. Alemany, J. L. Margrave, and V. N. Khabashesku, *J. Am. Chem. Soc.*, 2003, **125**, 15174. Copyright: American Chemical Society (2003).

For substituents containing aliphatic carbons, a new peak around 35 ppm emerges, as was shown in Figure 5.3.34, which is due to the aliphatic carbons. Since the quantity for the substituent carbons is low, the peak cannot be detected. Small substituents on the sidewall of SWNTs can be chemically modified to contain more carbons, so the signal due to those carbons could be detected. This idea, as a strategy for enhancing the signal from the substituents, can be used to analyze certain types of sidewall modifications. For example, when Gly ($–NH_2CH_2CO_2H$) was added to F-SWNTs (fluorinated SWNTs) to substitute the fluorine atoms, the ^{13}C NMR spectrum for the Gly-SWNTs was showing one peak for the sp^2 carbons. When the aliphatic substituent was changed to 6-aminohexanoic acid with five aliphatic carbons, the peak was detectable, and using 11-aminoundecanoic acid (ten aliphatic carbons) the peak intensity was in the order of the size of the peak for sp^2 carbons. In order to use ^{13}C NMR to enhance the substituent peak (for modification quantification purposes as an example), Gly-SWNTs was treated with 1-dodecanol to modify Gly to an amino ester. This modification resulted in enhancing the aliphatic carbon peak at around 30 ppm. Similar to the results in Figure 5.3.34, a peak at around 170 emerged which was assigned to the carbonyl carbon. The sp^3 carbon of the SWNTs, which was attached to nitrogen, produced a small peak at around 80 ppm, which is detected in a cross-polarization magic angle spinning (CP-MAS) experiment.

F-SWNTs (fluorinated SWNTs) are reported to have a peak at around 90 ppm for the sp^3 carbon of nanotube that is attached to the fluorine. The results of this part are summarized in Figure 5.3.34 (approximate values).

Table 5.3.5 Chemical shift for different types of carbons in modified SWNTs. Note that the peak for the aliphatic carbons gets stronger if the amino acid is esterified. Data are obtained from: H. Peng, L. B. Alemany, J. L. Margrave, and V. N. Khabashesku, *J. Am. Chem. Soc.*, 2003, **125**, 15174; L. Zeng, L. Alemany, C. Edwards, and A. Barron, *Nano. Res.*, 2008, **1**, 72; L. B. Alemany, L. Zhang, L. Zeng, C. L. Edwards, and A. R. Barron, *Chem. Mater.*, 2007, **19**, 735.

Group	**δ(ppm)**	**Intensity**
sp^2 carbons of SWNTs	120	Strong
$–NH_2(CH_2)_nCO_2H$ (aliphatic carbon, n=1,5, 10)	20-40	Depends on ‘n’
$–NH_2(CH_2)_nCO_2H$ (carboxyl carbon, n=1,5, 10)	170	Weak
sp^3 carbon attached to nitrogen	80	Weak
sp^3 carbon attached to fluorine	90	Weak

The peak intensities that are weak in Figure 5.3.34 depend on the level of functionalization and for highly functionalized SWNTs, those peaks are not weak. The peak intensity for aliphatic carbons can be enhanced as the substituents get modified by attaching to other molecules with aliphatic carbons. Thus, the peak intensities can be used to quantify the level of functionalization.

^{13}C NMR of Functionalized Graphene

Graphene is a single layer of sp^2 carbons, which exhibits a benzene-like structure. Functionalization of graphene sheets results in converting some of the sp^2 carbons to sp^3. The peak for the sp^2 carbons of graphene shows a peak at around 140 ppm. It has been reported that fluorinated graphene produces an sp^3peak at around 82 ppm. It has also been reported for graphite oxide (GO), which contains –OH and epoxy substituents, to have peaks at around 60 and 70 ppm for the epoxy and the –OH substituents, respectively. There are chances for similar peaks to appear for graphene oxide. Table 5.3.6 summarizes these results.

Table 5.3.6 Chemical shifts for functionalized graphene. Data are obtained from: M. Dubois, K. Guérin, J. P. Pinheiro, Z. Fawal, F. Masin, and A. Hamwi, *Carbon*, 2004, **42**, 1931; L. B. Casabianca, M. A. Shaibat, W. W. Cai, S. Park, R. Piner, R. S. Ruoff, and Y. Ishii, *J. Am. Chem. Soc.*, 2010, **132**, 5672.

Type of Carbon	**δ(ppm)**
sp^2	140
sp^3 attached to fluorine	80
sp^3 attached to -OH (for GO)	70
sp^3 attached to epoxide (for GO)	60

Analyzing Annealing Process Using ^{13}C NMR

^{13}C NMR spectroscopy has been used to study the effects of low-temperature annealing (at 650 °C) on thin films of amorphous carbon. The thin films were synthesized from a ^{13}C enriched carbon source (99%). There were two peaks in the ^{13}C NMR spectrum at about 69 and 142 ppm which were assigned to sp^3 and sp^2carbons, respectively Figure 5.3.35. The intensity of each peak was used to find the percentage of each type of hybridization in the whole sample, and the broadening of the peaks was used to estimate the distribution of different types of carbons in the sample. It was found that while the composition of the sample didn't change during the annealing process (peak intensities didn't change, see Figure 5.3.35b), the full width at half maximum (FWHM) did change (Figure 5.3.35a). The latter suggested that the structure became more ordered, i.e., the distribution of sp^2 and sp^3carbons within the sample became more homogeneous. Thus, it was concluded that the sample turned into a more homogenous one in terms of the distribution of carbons with different hybridization, while the fraction of sp^2 and sp^3 carbons remained unchanged.

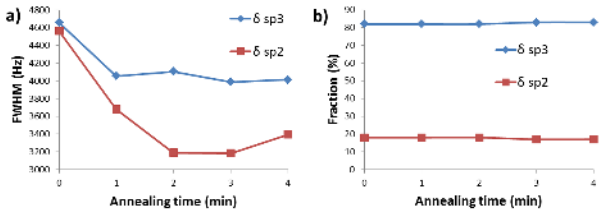


Figure 5.3.35 a) Effect of the annealing process on the FWHM, which represents the change in the distribution of sp^2 and sp^3 carbons. b) Fractions of sp^2 and sp^3 carbon during the annealing process. Data are obtained from T. M. Alam, T. A. Friedmann, P. A. Schultz, and D. Sebastiani, *Phys. Rev. B.*, 2003, **67**, 245309.

Aside from the reported results from the paper, it can be concluded that ^{13}C NMR is a good technique to study annealing, and possibly other similar processes, in real time, if the kinetics of the process is slow enough. For these purposes, the peak intensity and FWHM can be used to find or estimate the fraction and distribution of each type of carbon respectively.

Summary

^{13}C NMR can reveal important information about the structure of SWNTs and graphene. ^{13}C NMR chemical shifts and FWHM can be used to estimate the diameter size and diameter distribution. Though there are some limitations, it can be used to contain some information about the substituent type, as well as be used to quantify the level of functionalization. Modifications on the substituent can result in enhancing the substituent signal. Similar type of information can be achieved for graphene. It can also be employed to track changes during annealing and possibly during other modifications with similar time scales. Due to low natural abundance of ^{13}C it might be necessary to synthesize ^{13}C-enhanced samples in order to obtain suitable spectra with a sufficient signal-to-noise ratio. Similar principles could be used to follow the annealing process of carbon nano materials. C_{60}will not be discussed herein.

Lanthanide Shift Reagents

Nuclear magnetic resonance spectroscopy (NMR) is the most powerful tool for organic and organometallic compound determination. Even structures can be determined just using this technique. In general NMR gives information about the number of magnetically distinct atoms of the specific nuclei under study, as well as information regarding the nature of the immediate environment surrounding each nuclei. Because hydrogen and carbon are the major components of organic and organometallic compounds, proton (^1H) NMR and carbon-13 (^{13}C) NMR are the most useful nuclei to observe.

Not all the protons experience resonance at the same frequency in a ^1H NMR, and thus it is possible to differentiate between them. The diversity is due to the existence of a different electronic environment around chemically different nuclei. Under an external magnetic field (B_0), the electrons in the valence shell are affected; they start to circulate generating a magnetic field, which is apposite to the applied magnetic field. This effect is called diamagnetic shielding or diamagnetic anisotropy Figure 5.3.36.

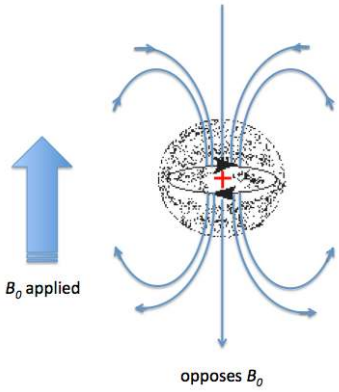


Figure 5.3.36 Schematic representation of diamagnetic anisotropy. Adapted from D. L. Pavia, G. M. Lampman, and G. S. Kriz, *Introduction to Spectroscopy*, 3th Ed., Thomson Learning, Tampa, FL, (2011).

The greater the electron density around one specific nucleus, the greater will be the induced field that opposes the applied field, and this will result in a different resonance frequency. The identification of protons sounds simple, however, the NMR technique has a relatively low sensitivity of proton chemical shifts to changes in the chemical and stereochemical environment; as a consequence the resonance of chemically similar proton overlap. There are several methods that have been used to resolve this problem, such as: the use of higher frequency spectrometers or by the use of shift reagents as aromatic solvents or lanthanide complexes. The main issue with high frequency spectrometers is that they are very expensive, which reduces the number of institutions that can have access to them. In contrast, shift reagents work by reducing the equivalence of nuclei by altering their magnetic environment, and can be used on any NMR instrument. The simplest shift reagent is the one of different solvents, however problems with some solvents is that they can react with the compound under study, and also that these solvents usually just alter the magnetic environment of a small part of the molecule. Consequently, although there are several methods, most of the work has been done with lanthanide complexes.

The History of Lanthanide Shift Reagents

The first significant induced chemical shift using paramagnetic ions was reported in 1969 by Conrad Hinckley (Figure 5.3.37), where he used bispyridine adduct of tris(2,2,6,6-tetramethylhepta-3,5-dionato)europium(III) ($Eu(tmhd)_3$), better known as $Eu(dpm)_3$, where dpm is the abbreviation of dipivaloyl- methanato, the chemical structure is shown in Figure 5.3.38. Hinckley used $Eu(tmhd)_3$ on the ^1H NMR spectrum of cholesterol from 347 – 2 Hz. The development of this new chemical method to improve the resolution of the NMR spectrum was the stepping-stone for the work of Jeremy Sanders and Dudley Williams, Figure 5.3.39 and Figure 5.3.40 respectively. They observed a significant increase in the magnitude of the induced shift after using just the lanthanide chelate without the pyridine complex. Sugesting that the pyridine donor ligands are in competition for the active sides of the lanthanide complex. The efficiency of $Eu(tmhd)_3$ as a shift reagent was published by Sanders and Williams in 1970, where they showed a significant difference in the ^1H NMR spectrum of n-pentanol using the shift reagent, see Figure 5.3.41.



Figure 5.3.40 British chemist Dudley Williams (1937-2010).

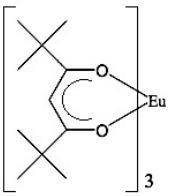


Figure 5.3.38 Chemical Structure of $Eu(tmhd)_3$.

https://chem.libretexts.org/@go/page/167053

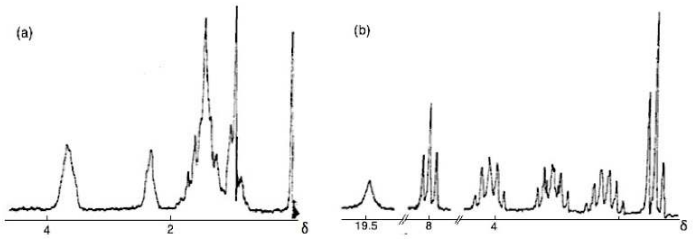


Figure 5.3.41 ^{1}H NMR spectra of n-pentanol, (a) without the present of lanthanide reagents and (b) in the present of the lanthanide reagent Eu(tmhd)$_3$. Adapted from *Chem Reviews*, 1973, **73**, 553. Copyright: American Chemical Society 1973.

Analyzing the spectra in Figure 5.3.41 it is easy to see that with the use of Eu(tmhd)$_3$ there is any overlap between peaks. Instead, the multiplets of each proton are perfectly clear. After these two publications the potential of lanthanide as shift reagents for NMR studies became a popular topic. Other example is the fluorinate version of Eu(dpm)$_3$; (*tris*(7,7,-dimethyl-1,1,2,2,2,3,3-heptafluoroocta-7,7-dimethyl-4,6-dionato)europium(III), best known as Eu(fod)$_3$, which was synthesized in 1971 by Rondeau and Sievers. This LSR presents better solubility and greater Lewis acid character, the chemical structure is show in Figure 5.3.42

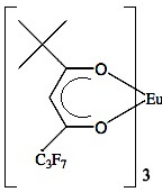


Figure 5.3.42 Chemical structure of (*tris*(7,7,-dimethyl-1,1,2,2,2,3,3-heptafluoroocta-7,7-dimethyl-4,6-dionato)europium(III).

Mechanism of Inducement of Chemical Shift

Lanthanide atoms are Lewis acids, and because of that, they have the ability to cause chemical shift by the interaction with the basic sites in the molecules. Lanthanide metals are especially effective over other metals because there is a significant delocalization of the unpaired *f* electrons onto the substrate as a consequence of unpaired electrons in the *f* shell of the lanthanide. The lanthanide metal in the complexes interacts with the relatively basic lone pair of electrons of aldehydes, alcohols, ketones, amines and other functional groups within the molecule that have a relative basic lone pair of electrons, resulting in a NMR spectral simplification.

There are two possible mechanisms by which a shift can occur: shifts by contact and shifts by pseudocontact. The first one is a result of the transfer of electron spin density via covalent bond formation from the lanthanide metal ion to the associated nuclei. While the magnetic effects of the unpaired electron magnetic moment causes the pseudocontact shift. Lanthanide complexes give shifts primarily by the pseudocontact mechanism. Under this mechanism, there are several factors that influence the shift of a specific NMR peak. The principal factor is the distance between the metal ion and the proton; the shorter the distance, the greater the shift obtained. On the other hand, the direction of the shift depends on the lanthanide complex used. The complexes that produce a shift to a lower field (downfield) are the ones containing erbium, europium, thulium and ytterbium, while complexes with cerium, neodymium, holmium, praseodymium, samarium and terbium, shift resonances to higher field. Figure 6 shows the difference betwen an NMR spectrum without the use of shift reagent versus the same spectrum in the present of a europium complex (downfield shift) and a praseodymium complex (high-field shift).

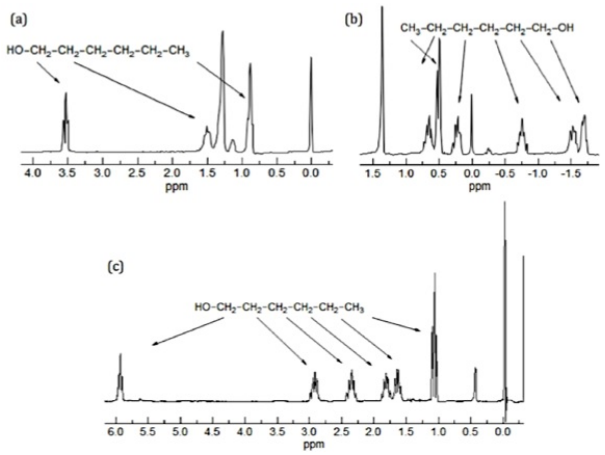


Figure 5.3.43 (a) ^{1}H NMR spectrum of n-hexanol without the presence of shift reagents. (b) ^{1}H NMR spectrum of n-hexanol in present of 14% Pr(fod)$_3$ and the thirt spectrum (c) is the ^{1}H NMR spectrum of n-hexanol in the present of 6.5% Eu(fod)$_3$. Adapted from http://www.chem.wisc.edu/areas/reich...ech-07-lis.htm

Linewidth broadening is not desired because of loss of resolution, and lanthanide complexes unfortunately contribute extremely to this effect when they are used in high concentrations due to their mechanism that shortens the relaxation times (T_2), which in turn increases the bandwidth. However europium and praseodymium are an extraordinary exception giving a very low shift broadening, 0.003 and 0.005 Hz/Hz respectively. Europium specially is the most used lanthanide as shift reagent because of its inefficient nuclear spin-lattice ratio properties. It has low angular momentum quantum numbers and a diamagnetic 7F0 ground state. These two properties contribute to a very small separation of the highest and lowest occupied metal orbitals leading to an inefficient relaxation and a very little broadening in the NMR spectra. The excited 7F1 state will then contribute to the pseudocontact shift.

We have mentioned above that lanthanide complexes have a mechanism that influences relaxation times, and this is certainly because paramagnetic ions have an influence in both: chemical shifts and relaxation rates. The relaxation times are of great significant because they depend on the width of a specific resonance (peak). Changes in relaxation time could also be related with the geometry of the complex.

Measuring the Shift

The easiest and more practical way to measure the lanthanide-induced shift (LIS) is to add aliquots of the lanthanide shift reagent (LSR or Δvi) to the sample that has the compound of interest (substrate), and take an NMR spectra after each addition. Because the shift of each proton will change after each addition of the LSR to lower or upper field, the LIS can me measured. With the data collected, a plot of the LIS against the ratio of LSR: substrate will generate a straight line where the slope is representative of the compound that is being studied. The identification of the compound by the use of chiral lanthanide shift reagents can be so precise that it is possible to estimate the composition of enantiomers in the solution under study, see Figure 5.3.44

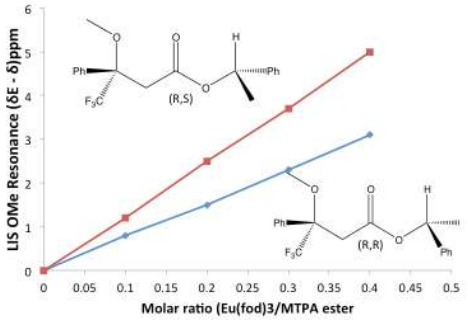


Figure 5.3.45 Lanthanide induced shift of methoxyl proton resonance versus molar ratio of Eu(fod)$_3$, for the diastereomeric MTPA esters. δ is the normal chemical shift and δ_E is the chemical shift in ppm for the OMe signal in the presence of a specified molar ratio of Eu(fod)$_3$, in CCl_4 as solvent. Adapted from S. Yamaguchi, F. Yasuhara and K. Kabuto, *Tetrahedron*, 1976, **32**, 1363.

Now, what is the mechanism that is actually happening between the LSR and the compound under study? The LSR is a metal complex of six coordinate sides. The LSR, in presence of substrate that contains heteroatoms with Lewis basicity character, expands its coordination sides in solution in order to accept additional ligands. An equilibrium mixture is formed between the

substrate and the LSR. 5.3.11 and 5.3.12 show the equilibrium, where L is LSR, S is the substrate, and LS is the concentration of the complex formed is solution.

$$L + S \overset{K_1}{\rightleftarrows} [LS] \tag{5.3.11}$$

$$[LS] + S \overset{K_2}{\rightleftarrows} [LS_2] \tag{5.3.12}$$

The abundance of these species depends on K_1 and K_2, which are the binding constant. The binding constant is a special case of equilibrium constant, but it refers with the binding and unbinding mechanism of two species. In most of the cases like, K_2 is assumed to be negligible and therefore just the first complex [LS] is assumed to be formed. The equilibrium between L + S and LS in solution is faster than the NMR timescale, consequently a single average signal will be recorded for each nucleus.

Determination of Enantiomeric Purity

Besides the great potential of lanthanide shift reagents to improve the resolution of NMR spectrums, these complexes also have been used to identify enantiomeric mixtures in solution. To make this possible the substrate must meet certain properties. The fist one is that the organic compounds in the enantiomeric composition must to have a hard organic base as functional group. The shift reagents are not effective with most of the soft bases. Though hundreds of chelates have been synthesized after $Eu(dcm)_3$, this one is the LSR that resulted in the most effective reagent for the resolution of enantiotopic resonances. Basically if you take an NMR of an enantiomeric mixture sample, a big variety of peaks will appear and the hard part is to identify which of those peaks correspond to which specific enantiomer. The differences in chemical shifts observed for enantiomeric mixtures in solution containing LSR might arise from at least two sources: the equilibrium constants of the formation of the possible diastereometic complexes between the substrate and the LSR, and the geometries of these complexes, which might be distinct. The enantiomeric shift differences sometimes are defined as ΔΔδ.

In solution the exchange between substrate coordinated to the europium ion and the free substrate in solution is very fast. To be sure that the europium complexes are binding with one or two substrate molecules, an excess of substrate is usually added.

Determination of Relaxation Parameters of Contrast Agents

Magnetic resonance imaging (MRI) (also known as nuclear magnetic resonance imaging (NMRI) or magnetic resonance tomography (MRT)) is a powerful noninvasive diagnostic technique, which is used to generate magnetic field (B_0) and interacts with spin angular momentum of the nucleus in the tissue. Spin angular momentum depends on number of protons and neutrons of nucleus. Nuclei with even number of protons plus neutrons are insensitive to magnetic field, so cannot be viewed by MRI.

Each nucleus can be considered as an arrow with arbitrary direction in absence of external magnetic field (Figure 5.3.46). And we consider them to get oriented in the same direction once magnetic field applied (Figure 5.3.47). In order to get nuclei orient in specific direction, energy is supplied, and to bring it to original position energy is emitted. All this transitions eventually lead to changes in angular velocity, which is defined as Larmor frequency and the expression 5.3.13, where ω is the Larmor frequency, γ is the gyromagnetic ratio, and B_0 is the magnetic field. It is not easy to detect energy, which is involved in such a transition, that's why use of high resolution spectrometers required, those which are developed by nowadays as a most powerful MRI are close to 9 Tesla with mass approaching forty five tons. Unfortunately it is expensive tool to purchase and to operate. That's why new techniques should be developed, so most of the MRI spectrometers can be involved in imaging. Fortunately presence of huge amount of nuclei in analyzed sample or body can provide with some information.

$$\omega = \gamma B_0 \tag{5.3.13}$$



Figure 5.3.46 Representation of nuclei in absence of magnetic field.

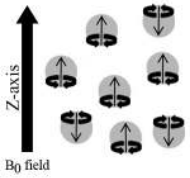


Figure 5.3.47 Representation of nuclei in presence of magnetic field.

Nuclear Magnetic Resonance Relaxometer

Each nucleus possesses microscopic magnetic spins of *x*, *y* and *z*. Presence of randomly distributed atoms with varying *x* and *y* spins will lead to zero upon summation of *x* and *y* planes. But in case of *z*, summation of magnetic spins will not lead to cancellation. According to Currie's law, 5.3.14, ($M_z$is the resulting magnetization of *z* axis, C is a material specific Curie constant, B_0 is the magnetic field, and T is absolute temperature), magnetization of *z* axis proportional to magnetic field applied from outside. Basically, excitation happens by passing current through coil which leads to magnetization of *x*, *y* and *z* axis. It is the way of changing magnetism from *z* axis to *x* and *y* axis. Once external current supply is turned off, magnetization will eventually quench. This means a change of magnetization from x and y axis to *z* axis, were it eventually become equilibrated and device no more can detect the signals. Energy which is emitted from excited spin leads to development of new current inside of the same coil recorded by detector; hence same coil can be used as detector and source of magnetic field. This process called as a relaxation and that's why, return of magnetization to *z* axis called as spin-lattice relaxation or T_1 relaxation (time required for magnetization to align on *z* axis). Eventual result of zero magnetization on *x* and *y* axis called as spin-spin relaxation or T_2 relaxation (Figure 5.3.48).

$$M_z = CB_0/T \tag{5.3.14}$$

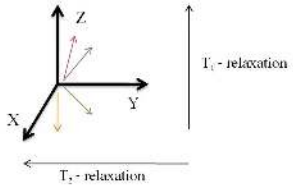


Figure 5.3.48 Magnetic spins relaxation mechanism

Contrast Agents for MRI

In MRI imaging contrast is determined according to T_1, T_2 or the proton density parameter. Therefor we can obtain three different images. By changing intervals between radio frequency (RF) 90° pulses and RF 180° pulses, the desired type of image can be obtained. There are few computational techniques available to improve contrast of image; those are repetitive scans and different mathematical computations. Repetitive scans take a long time, therefore cannot be applied in MRI. Mathematical computation on their own, do not provide with desired results. For that reason, in order to obtain high resolution images, contrast agents (CA) are important part of medical imaging.

Types of Contrast Agents

There are different types of contrast agents available in markets which reduce the supremacy of T_1or T_2, and differentiate according to relaxivity$_1$ (r_1) and relaxivity$_2$ (r_2) values. The relaxivity (r_i) can be described as $1/T_i$ (s^{-1}) of water molecules per mM concentration of CA. Contrast agents are paramagnetic and can interact with dipole moments of water molecules, causing fluctuations in molecules. This theory is known as Solomon-Bloembergen-Morgan (SBM) theory. Those which are efficient were derivatives of gadolinium (e.g., gadobenic acid (Figure 5.3.49 a) and gadoxetic acid (Figure 5.3.49 b), iron (e.g., superparamagnetic iron oxide and ultrasmall superparamagnetic iron oxide) and manganese (e.g., manganese dipyridoxal diphosphate). Fundamentally the role of contrast agents can be played by any paramagnetic species.

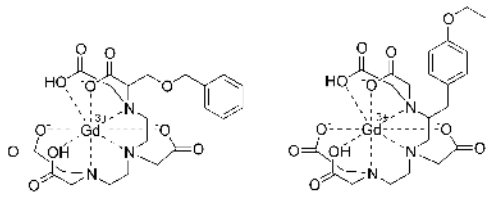


Figure 5.3.49 The structures of two representative commercial gadolinium MRI contrast agents; (a) gadobenic acid and (b) gadoxetic acid.

Principal of Interactions of CA with Surrounding Media

There are two main principles of interactions of contrast agents with water molecules. One is direct interaction, which is called inner sphere relaxation, and the other mechanism that happens in the absence of direct interaction with water molecule which is outer sphere relaxation. If we have water molecules in the first coordination sphere of metal ion, we can consider them as the inner sphere, and if diffusion of protons from outside happens randomly we define them as outer sphere relaxation. Another type of relaxivity comes from already affected water molecules, which transfers their relaxivity to protons of close proximity, this type of relaxivity called second sphere and is usually neglected or contributed as outer sphere. In inner sphere proton relaxivity there are two main mechanisms involved in relaxation. One is dipole-dipole interactions between metal and proton and another is scalar mechanism. Dipole-dipole interaction affects electron spin vectors and scalar mechanism usually controls water exchange. Effect of contrast agents on T_1 relaxation is much larger than on T_2, since T_1 is much larger for tissues than T_2.

Determination of Relaxivity

Determination of relaxivity became very easy with the advancements of NMR and computer technology, where you need just to load your sample and read values from the screen. But let's consider in more detail what are the precautions should be taken during sample preparation and data acquisition.

Sample Preparation

The sample to be analyzed is dissolved in water or another solvent. Generally water is used since contrast agents for medical MRI are used in aqueous media. The amount of solution used is determined according to the internal standard volume, which is used for calibration purposes of device and is usually provided by company producing device. A suitable sample holder is a NMR tube. It is important to degas solvent prior measurements by bubbling gas through it (nitrogen or argon works well), so no any traces of oxygen remains in solution, since oxygen is paramagnetic.

Data Acquisition

Before collecting data it is better to keep the sample in the device compartment for few minutes, so temperature of magnet and your solution equilibrates. The relaxivity (r_i) calculated according to (5.3.15), where T_i is the relaxation time in the presence of CAs, T_{id} is the relaxation time in the absence of CAs, and CA is the concentration of paramagnetic CAs (mM). Having the relaxivity values allows for a comparison of a particular compound to other known contrast agents.

$$r_i = (1/T_i - 1/T_{id})/[CA] \tag{5.3.15}$$

Two-Dimensional NMR

General Principles of Two-Dimensional Nuclear Magnetic Resonance Spectroscopy

History

Jean Jeener (Figure 5.3.50 from the Université Libre de Bruxelles first proposed 2D NMR in 1971. In 1975 Walter P. Aue, Enrico Bartholdi, and Richard R. Ernst (Figure 5.3.51 first used Jeener's ideas of 2D NMR to produce 2D spectra, which they published in their paper "Two-dimensional spectroscopy, application to nuclear magnetic resonance". Since this first publication, 2D NMR has increasing been utilized for structure determination and elucidation of natural products, protein structure, polymers, and inorganic compounds. With the improvement of computer hardware and stronger magnets, newly developed 2D NMR techniques can easily become routine procedures. In 1991 Richard R. Ernst won the Nobel Prize in Chemistry for his contributions to Fourier Transform NMR. Looking back on the development of NMR techniques, it is amazing that 2D NMR took so long to be developed considering the large number of similarities that it has with the simpler 1D experiments.

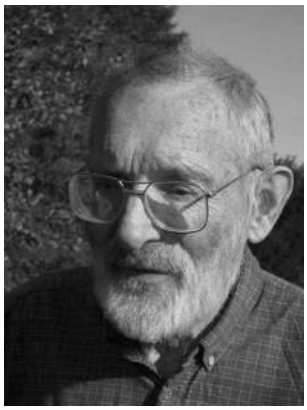


Figure 5.3.50 Belgian physical chemist and physicist Jean L. C. Jeener (1931-).



Figure 5.3.51 Swiss physical chemist and Nobel Laureate Richard R. Ernst (1933-).

Why do We Need 2D NMR?

2D NMR was developed in order to address two major issues with 1D NMR. The first issue is the limited scope of a 1D spectrum. A 2D NMR spectrum can be used to resolve peaks in a 1D spectrum and remove any overlap present. With a 1D spectrum, this is typically performed using an NMR with higher field strength, but there is a limit to the resolution of peaks that can be obtained. This is especially important for large molecules that result in numerous peaks as well as for molecules that have similar structural motifs in the same molecule. The second major issue addressed is the need for more information. This could include structural or stereochemical information. Usually to overcome this problem, 1D NMR spectra are obtained studying specific nuclei present in the molecule (for example, this could include fluorine or phosphorus). Of course this task is limited to only nuclei that have active spin states/spin states other than zero and it requires the use of specialized NMR probes.

2D NMR can address both of these issues in several different ways. The following four techniques are just few of the methods that can be used for this task. The use of J-resolved spectroscopy is used to resolve highly overlapping resonances, usually seen as complex multiplicative splitting patterns. Homonuclear correlation spectroscopy can identify spin-coupled pairs of nuclei that overlap in 1D spectra. Heteronuclear shift-correlation spectroscopy can identify all directly bonded carbon-proton pairs, or other combinations of nuclei pairs. Lastly, **N**uclear **O**verhauser **E**ffect (NOE) interactions can be used to obtain information about through-space interactions (rather than through-bond). This technique is often used to determine stereochemistry or protein/peptide interactions.

One-dimensional vs. Two-dimensional NMR

Similarities

The concept of 2D NMR can be considered as an extension of the concept of 1D NMR. As such there are many similarities between the two. Since the acquisition of a 2D spectrum is almost always preceded by the acquisition of a 1D spectrum, the standard used for reference Since 2D NMR is a more complicated experiment than 1D NMR, there are also some differences between the two. One of the differences is in the complexity of the data obtained. A 2D spectrum often results from a change in pulse time; therefore, it is important to set up the experiment correctly in order to obtain meaningful information. Another difference arises from the fact that one spectrum is 1D while the other is 2D. As such interpreting a 2D spectrum requires a much greater understanding of the experiment parameters. For example, one 2D experiment might investigate the specific coupling of two protons or carbons, rather than focusing on the molecule as a whole (which is generally the target of a 1D experiment). The specific pulse sequence used is often very helpful in interpreting the information obtained. The software used for 1D spectra is not always compatible with 2D spectra. This is due to the fact that a 2D spectrum requires more complex processing, and the 2D

spectra generated often look quite different than 1D spectra. Some software that is commonly used to interpret 2D spectra is either Sparky or Bruker's TopSpin. Lastly the NMR instrument used to obtain a 2D spectrum typically generates a much larger magnetic field (700-1000 MHz). Due to the increased cost of buying and maintaining such an instrument, 2D NMR is usually reserved for rather complex molecules.(TMS) and the solvent used (typically $CDCl_3$ or other deuterated solvent) are the same for both experiments. Furthermore, 2D NMR is most often used to reveal any obscurity in a 1D spectrum (whether that is peak overlap, splitting overlap, or something else), so the nuclei studied are the same. Most often these are ^{1}H and ^{13}C, but other nuclei could also be studied.

Differences

Since 2D NMR is a more complicated experiment than 1D NMR, there are also some differences between the two. One of the differences is in the complexity of the data obtained. A 2D spectrum often results from a change in pulse time; therefore, it is important to set up the experiment correctly in order to obtain meaningful information. Another difference arises from the fact that one spectrum is 1D while the other is 2D. As such interpreting a 2D spectrum requires a much greater understanding of the experiment parameters. For example, one 2D experiment might investigate the specific coupling of two protons or carbons, rather than focusing on the molecule as a whole (which is generally the target of a 1D experiment). The specific pulse sequence used is often very helpful in interpreting the information obtained. The software used for 1D spectra is not always compatible with 2D spectra. This is due to the fact that a 2D spectrum requires more complex processing, and the 2D spectra generated often look quite different than 1D spectra. Some software that is commonly used to interpret 2D spectra is either Sparky or Bruker's TopSpin. Lastly the NMR instrument used to obtain a 2D spectrum typically generates a much larger magnetic field (700-1000 MHz). Due to the increased cost of buying and maintaining such an instrument, 2D NMR is usually reserved for rather complex molecules.

The Rotating Frame and Fourier Transform

One of the central ideas that is associated with 2D NMR is the rotating frame, because it helps to visualize the changes that take place in dimensions. Our ordinary "laboratory" frame consists of three axes (the Cartesian *x*, *y*, and *z*). This frame can be visualized if one pictures the corner of a room. The intersections of the floor and the walls are the *x* and the *y* dimensions, while the intersection of the walls is the *z* axis. This is usually considered the "fixed frame." When an NMR experiment is carried out, the frame still consists of the Cartesian coordinate system, but the *x* and *y*coordinates rotate around the *z* axis. The speed with which the *x*-*y* coordinate system rotates is directly dependent on the frequency of the NMR instrument.

When any NMR experiment is carried out, a majority of the spin states of the nucleus of interest line up with one of these three coordinates (which we can pick to be *z*). Once an equilibrium of this alignment is achieved, a magnetic pulse can be exerted at a certain angle to the *z* axis (usually 90° or 180°) which temporarily disrupts the equilibrium alignment of the nuclei. As the pulse is removed, the nuclei are allowed to relax back to this equilibrium alignment with the magnetic field of the instrument. When this relaxation takes place, the progression of the nuclei back to the equilibrium orientation is detected by a computer as a **f**ree **i**nduction **d**ecay (FID). When a sample has different nuclei or the same nucleus in different environments, different FID can be recorded for each individual relaxation to the equilibrium position. The FIDs of all of the individual nuclei can be recorded and superimposed. The complex FID signal obtained can be converted to a recording of the NMR spectrum obtained by a **F**ourier **t**ransform(FT). The FT is a complex mathematical concept that can be described by 5.3.16, where ω is the angular frequency.

$$z(t) = \sum_{k\to\infty}^{\infty} c_i e^{ik\omega t} \tag{5.3.16}$$

This concept of the FT is similar for both 1D and 2D NMR. In 2D NMR a FID is obtained in one dimension first, then through the application of a pulse a FID can be obtained in a second dimension. Both FIDs can be converted to a series of NMR spectra through a Fourier transform, resulting in a spectrum that can be interpreted. The coupling of the two FID's in 2D NMR usually reveals a lot more information about the specific connectivity between two atoms.

Four Phases and Pulse Sequence of 2D NMR

There are four general stages or time periods that are present for any 2D NMR experiment. These are preparation, evolution, mixing, and detection. A general schematic representation is seen in Figure 5.3.53. The preparation period defines the system at the first time phase. The evolution period allows the nuclei to precess (or move relative to the magnetic field). The mixing period introduces a change in the way the spectra is obtained. The detection period records the FID. In obtaining a spectrum, the pulse sequence is the most important factor that determines what data will be obtained. In general 2D experiments are a combination of 1D experiments collected by varying the timing and pulsing.



Figure 5.3.53 Visual representation of the general pulse scheme of any 2D NMR Experiment

Preparation

This is the first step in any 2D NMR experiment. It is a way to start all experiments from the same state. This state is typically either thermal equilibrium, obeying Boltzmann statistics, or it could be a state where the spins of one nucleus are randomized in orientation and the spins of another nucleus are in thermal equilibrium. At the end of the preparation period, the magnetizations are usually placed perpendicular, or at a specific angle, to the magnetic field axis. This phase creates magnetizations in the *x*-*y* plane.

Evolution

The nuclei are then allowed to precess around the direction of the magnetic field. This concept is very similar to the precession of a top in the gravitational field of the Earth. In this phase of the experiment, the rates at which different nuclei precess, as shown in Figure 5.3.54 determine how the nuclei are reacting based on their environment. The magnetizations that are created at the end of the preparation step are allowed to evolve or change for a certain amount of time (t_1) in the environment defined by the magnetic and **r**adio **f**requency (RF) fields. In this phase, the chemical shifts of the nuclei are measured similarly to a 1D experiment, by letting the nucleus magnetization rotate in the *x*-*y* plane. This experiment is carried out a large number of times, and then the recorded FID is used to determine the chemical shifts.

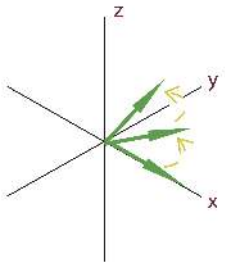


Figure 5.3.54 Visual representation of the precession of an object.

Mixing

Once the evolution period is over, the nuclear magnetization is distributed among the spins. The spins are allowed to communicate for a fixed period of time. This typically occurs using either magnetic pulses and/or variation in the time periods. The magnetic pulses typically consist of a change in the rotating frame of reference relative to the original "fixed frame" that was introduced in the preparation period, as seen in Figure 5.3.55. Experiments that only use time periods are often tailored to look at the effect of the RF field intensity. Using either the bonds connecting the different nuclei (J-coupling) or using the small space between them (NOE interaction), the magnetization is allowed to move from one nucleus to another. Depending on the exact experiment performed, these changes in magnetizations are going to differ based on what information is desired. This is the step in the experiment that determines exactly what new information would be obtained by the experiment. Depending on which chemical interactions require suppression and which need to be intensified to reveal new information, the specific "mixing technique" can be adjusted for the experiment.

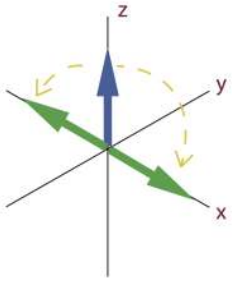


Figure \PgeIndex55 Demonstration of a specific (90°) change in the frame of reference during mixing.

Detection

This is always the last period of the experiment, and it is the recording of the FID of the second nucleus studied. This phase records the second acquisition time (t_2) resulting in a spectrum, similar to the first spectrum, but typically with differences in intensity and phase. These differences can give us information about the exact chemical and magnetic environment of the nuclei that are present. The two different Fourier transforms are used to generate the 2D spectrum, which consists of two frequency dimensions. These two frequencies are independent of each other, but when plotted on a single spectrum the frequency of the signal obtained in time t_1 has been converted in another coherence affected by the frequency in time t_2. While the first dimension represents the chemical shifts of the nucleus in question, the second dimension reveals new information. The overall spectrum, Figure 5.3.56, is the result of a matrix in the two frequency domains obtained during the experiment.

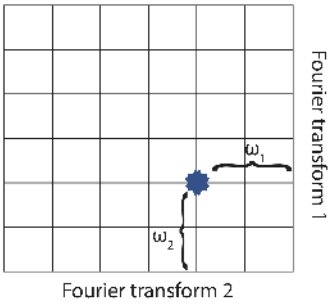


Figure 5.3.56 Simple representation of a 2D spectrum, reflecting the result of two Fourier transforms.

Pulse Variation

As mentioned earlier, the pulse sequence and the mixing period are some of the most important factors that determine the type of spectrum that will be identified. Depending on whether the magnetization is transferred through a J-coupling or NOE interaction, different information and spectra can be obtained. Furthermore, depending on the experimental setup, the mixing period could transfer magnetization either through a single J-coupling or through several J-couplings for nuclei that are connected together. Similarly NOE interactions can also be controlled to specific distances. Two types of NOE interactions can be observed, positive and negative. When the rate at which fluctuation occurs in the transverse plane of a fluctuating magnetic field matches the frequency of double quantum transition, a positive NOE is observed. When the fluctuation is slower, a negative NOE is produced.

Obtaining a Spectrum

Sample Preparation

Sample preparation for 2D NMR is essentially the same as that for 1D NMR. Particular caution should be exercised to use clean and dry sample tubes and use only deuterated solvents. The amount of sample used should be anywhere between 15 and 25 mg although with sufficient time even smaller quantities may be used. The filling height of the solvent should be about 4 cm. The solution must be clear and homogenous. Any participate needs to be filtered off prior to obtaining the spectra.

The Actual Experiment and Important Acquisition Parameters

The acquisition of a 2D spectrum will vary from instrument to instrument, but the process is virtually identical to obtaining a ^{13}C spectrum. It is important to obtain a 1D spectrum (especially ^{1}H) before proceeding to obtain a 2D spectrum. The acquisition range should be adjusted based on the 1D spectrum to minimize instrument time. Depending on the specific type of 2D experiment (such as COSY or NOESY) several parameters need to be adjusted. The following 6 steps can followed to obtain almost any 2D NMR spectrum.

1. Login to the computer system.
2. Change the sample.
3. Lock and shim the magnet.
4. Setup parameters and run the experiment. Use the 1D spectra already obtained to adjust experiment settings, paying special attention to important acquisition parameters.
5. Process the obtained data and print the spectrum.
6. Exit and logout.

The parameters listed in Table 5.3.7 should be given special attention, as they can significantly affect the quality of the spectra obtained.

Table 5.3.7 Some of the most important parameters for obtaining a 2D spectrum and their meaning.

Parameter	Description
Acquisition Time (AQ)	Data points (TD) x dwell time (DW)
Dwell Time	1/spectral width (SW)
Digital Resolution	1/AQ
Number of Scans	Multiples of 8/16
TD1	Number of data points in the first time domain (~128-512)
SW1	Spectral Width in the first (direct) dimension
TD2	Number of data points in the second time domain (~2048-4096)
SW2	Spectral Width in the second (indirect) dimension

After Obtaining a Spectrum and Analysis

After a 2D spectrum has successfully been obtained, depending on the type of spectrum (COSY, NOESY, INEPT), it might need to be phased. Phasing is the adjustment of the spectrum so that all of the peaks across the spectrum are in the absorptive mode (pointing either up or down). With 2D spectra, phasing is done in both frequency dimensions. This can either be done automatically by a software program (for simple 2D spectra with no cluster signals) or manually by the user (for more complex 2D spectra). Sometimes, phasing can be done with the program that is used to obtain the spectrum. Afterwards the spectrum could either be printed out or further analyzed. One example of further analysis is integrating parts of the spectrum. This could give the user meaningful information about the relative ratio of different types of nuclei (and even quantify the ratios between two diasteriomeric molecules).

Conclusion

Two-dimensional NMR is increasingly becoming a routine method for analyzing complex molecules, whether they are inorganic compounds, organic natural products, proteins, or polymers. A basic understanding of 2D NMR can make it significantly easier to analyze complex molecules and provide further confirmation for results obtained by other methods. The variation in pulse sequences provides chemists the opportunity to analyze a large diversity of compounds. The increase in the magnetic strength of NMR machines has allowed 2D NMR to be more often used even for simpler molecules. Furthermore, higher dimension techniques have also been introduced, and they are slowly being integrated into the repertoire of chemists. These are essentially simple extensions of the ideas of 2D NMR.

Two-Dimensional NMR Experiments

Since the advent of NMR, synthetic chemists have had an excellent way to characterize their synthetic products. With the arrival of multidimensional NMR into the realm of analytical techniques, scientists have been able to study larger and more complicated molecules much easier than before, due to the great amount of information 2D and 3D NMR experiments can offer. With 2D NMR, overlapping multiplets and other complex splitting patterns seen in 1D NMR can be easily deciphered, since instead of one frequency domain, two frequency domains are plotted and the couplings are plotted with respect to each other, which makes it easier to determine molecular connectivity.

Spectra are obtained using a specific sequence of radiofrequency (RF) pulses that are administered to the sample, which can vary in the angle at which the pulse is given and/or the number of pulses. Figure 5.3.57 shows a schematic diagram for a generic pulse sequence in a 2D NMR experiment. First, a pulse is administered to the sample in what is referred to as the preparation period. This period could be anything from a single pulse to a complex pattern of pulses. The preparation period is followed by a “wait” time (also known as the evolution time), t_1, during which no data is observed. The evolution time also can be varied to suit the needs of the specific experiment. A second pulse is administered next during what is known as the mixing period, where the coherence at the end of t_1 is converted into an observable signal, which is recorded during the observation time, t_2. Figure 5.3.58 shows a schematic diagram of how data is converted from the time domain (depicted in the free induction decay, or FID) to a frequency domain. The process of this transformation using Fourier Transform (FT) is the same as it is in 1D NMR, except here, it is done twice (or three times when conducting a 3D NMR experiment).

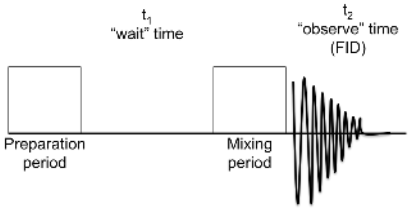


Figure adapted from J. Keeler, *Understanding NMR Spectroscopy*, 2nd, Wiley, West Sussex (2010).

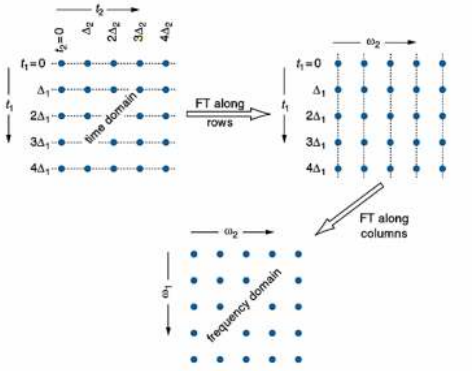


Figure from J. Keeler, *Understanding NMR Spectroscopy*, 2nd, Wiley, West Sussex (2010).

In 1D NMR, spectra are plotted with frequency (in ppm or Hz, although most commonly ppm) on the horizontal axis and with intensity on the vertical axis. However, in 2D NMR spectra, there are two frequency domains being plotted, each on the vertical and horizontal axes. Intensity, therefore, can be shown as a 3D plot or topographically, much like a contour map, with more contour lines representing greater intensities, as shown in Figure 5.3.59a. Since it is difficult to read a spectrum in a 3D plot, all spectra are plotted as contour plots. Furthermore, since resolution in a 2D NMR spectrum is not needed as much as in a 1D spectrum, data acquisition times are often short.

2D NMR is very advantageous for many different applications, though it is mainly used for determining structure and stereochemistry of large molecules such as polymers and biological macromolecules, that usually exhibit higher order splitting effects and have small, overlapping coupling constants between nuclei. Further, some 2D NMR experiments can be used to elucidate the components of a complex mixture. This module aims to describe some of the common two-dimensional NMR experiments used to determine qualitative information about molecular structure.

2D Experiments

COSY

COSY (COrrelation SpectroscopY) was one of the first and most popular 2D NMR experiments to be developed. It is a homonuclear experiment that allows one to correlate different signals in the spectrum to each other. In a COSY spectrum (see Figure 5.3.59b), the chemical shift values of the sample's 1D NMR spectrum are plotted along both the vertical and horizontal axes (some 2D spectra will actually reproduce the 1D spectra along the axes, along with the frequency scale in ppm, while others may simply show the scale). This allows for a collection of peaks to appear down the diagonal of the spectrum known as diagonal peaks (shown in Figure 5.3.59b, highlighted by the red dotted line). These diagonal peaks are simply the peaks that appear in the normal 1D spectrum, because they show nuclei that couple to themselves. The other type of peaks appears symmetric across the diagonal and is known as cross peaks. These peaks show which groups in the molecule that have different chemical shifts are coupled to each other by producing a signal at the intersection of the two frequency values.

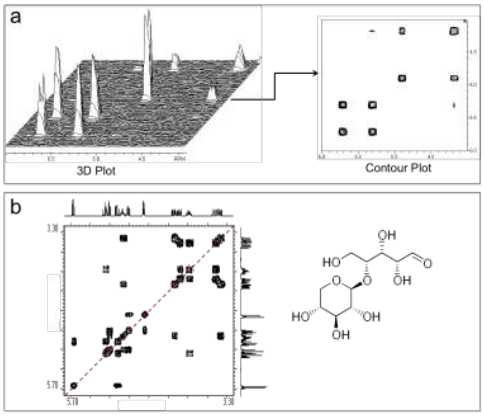


Figure 5.3.59 Example of correlation spectroscopy: (a) On the left is shown a portion of a 3D or "stacked" plot of a 2D NMR COSY spectrum in which two frequency domains are plotted in two dimensions and intensity is plotted in the third. On the right is shown a contour plot, where the intensities have been depicted topographically. Spectra from Acorn NMR, Inc. (b) A spectrum of the disaccharide xylobiose (structure shown), taken from a COSY 2D NMR experiment. The red dotted line highlights the diagonal peaks. Spectrum adapted from F. Sauriol, *NMR Webcourse*, Department of Chemistry, Queen's University, Ontario, www.chem.queensu.ca/facilities/nmr/nmr/webcourse/.

One can then determine the structure of a sample by examining what chemical shift values the cross peaks occur at in a spectrum. Since the cross peaks are symmetric across the diagonal peaks, one can easily identify which cross peaks are real (if a certain peak has a counterpart on the other side of the diagonal) and which are digital artifacts of the experiment. The smallest coupling that can be detected using COSY is dependent on the linewidth of the spectrum and the signal-to-noise ratio; a maximum signal-to-noise ratio and a minimum linewidth will allow for very small coupling constants to be detected.

Variations of COSY

Although COSY is very useful, it does have its disadvantages. First of all, because the anti-phase structure of the cross peaks, which causes the spectral lines to cancel one another out, and the in-phase structure of the diagonal peaks, which causes reinforcement among the peaks, there is a significant difference in intensity between the diagonal and cross peaks. This difference in intensity makes identifying small cross peaks difficult, especially if they lie near the diagonal. Another problem is that when processing the data for a COSY spectrum, the broad lineshapes associated with the experiment can make high-resolution work difficult.

In one of the more popular COSY variations known as DQF COSY (Double-Quantum Filtered COSY), the pulse sequence is altered so that all of the signals are passed through a double-quantum coherence filter, which suppresses signals with no coupling (i.e. singlets) and allows cross peaks close to the diagonal to be clearly visible by making the spectral lines much sharper. Since most singlet peaks are due to the solvent, DQF COSY is useful to suppress those unwanted peaks.

ECOSY (Exclusive COrrelation SpectroscopY) is another derivative of COSY that was made to detect small J-couplings, predominantly among multiplets, usually when $J \leq 3$ Hz. Also referred to as long-range COSY, this technique involves adding a delay of about 100-400 ms to the pulse sequence. However, there is more relaxation that is occurring during this delay, which causes a loss of magnetization, and therefore a loss of signal intensity. This experiment would be advantageous for one who would like to further investigate whether or not a certain coupling exists that did not appear in the regular COSY spectrum.

GS-COSY (Gradient Selective COSY) is a very applied offshoot of COSY since it eliminates the need for what is known as phase cycling. Phase cycling is a method in which the phase of the pulses is varied in such a way to eliminate unwanted signals in the spectrum, due to the multiple ways which magnetization can be aligned or transferred, or even due to instrument hardware. In practical terms, this means that by eliminating phase cycling, GS-COSY can produce a cleaner spectrum (less digital artifacts) in much less time than can normal COSY.

Another variation of COSY is COSY-45, which administers a pulse at 45° to the sample, unlike DQF COSY which administers a pulse perpendicular to the sample. This technique is useful because one can elucidate the sign of the coupling constant by looking at the shape of the peak and in which direction it is oriented. Knowing the sign of the coupling constant can be useful in discriminating between vicinal and geminal couplings. However, COSY-45 is less sensitive than other COSY experiments that use a 90° RF pulse.

TOCSY

TOCSY (TOtal Correlation SpectroscopY) is very similar to COSY in that it is a homonuclear correlation technique. It differs from COSY in that it not only shows nuclei that are directly coupled to each other, but also signals that are due to nuclei that are in the same spin system, as shown in Figure 5.3.60 below. This technique is useful for interpreting large, interconnected networks of spin couplings. The pulse sequence is arranged in such a way to allow for isotropic mixing during the sequence that transfers magnetization across a network of atoms coupled to each other. An alternative technique to 2D TOCSY is selective 1D TOCSY, which can excite certain regions of the spectrum by using shaped pulses. By specifying particular chemical shift values and setting a desired excitation width, one can greatly simplify the 1D experiment. Selective 1D TOCSY is particularly useful for analyzing polysaccharides, since each sugar subunit is an isolated spin system, which can produce its own subspectrum, as long as there is at least one resolved multiplet. Furthermore, each 2D spectrum can be acquired with the same resolution as a normal 1D spectrum, which allows for an accurate measurement of multiplet splittings, especially when signals from different coupled networks overlap with one another.

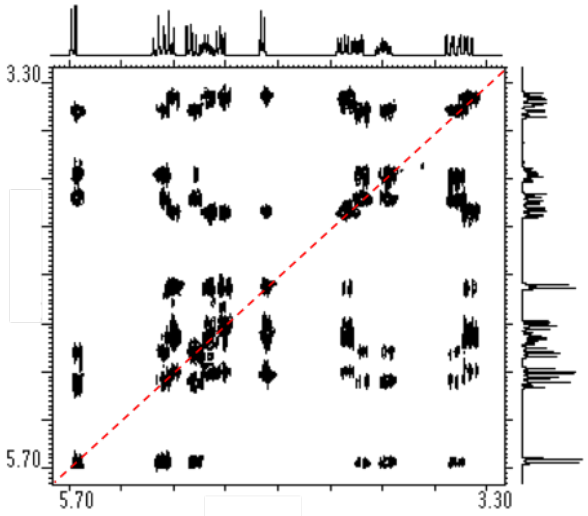


Figure from F. Sauriol, *NMR Webcourse*, Department of Chemistry, Queen's University, Ontario, www.chem.queensu.ca/facilities/nmr/nmr/webcourse/.

Heteronuclear Experiments

HETCOR (Heteronuclear Correlation) refers to a 2D NMR experiment that correlates couplings between different nuclei (usually ^{1}H and a heteroatom, such as ^{13}C or ^{15}N). Heteronuclear experiments can easily be extended into three or more dimensions, which can be thought of as experiments that correlate couplings between three or more different nuclei. Because there are two different frequency domains, there are no diagonal peaks like there are in COSY or TOCSY. Recently, inverse-detected HETCOR experiments have become extremely useful and commonplace, and it will be those experiments that will be covered here. Inverse-detection refers to detecting the nucleus with the higher gyromagnetic ratio, which offers higher sensitivity. It is ideal to determine which nucleus has the highest gyromagnetic ratio for detection and set the probe to be the most sensitive to this nucleus. In HETCOR, the nucleus that was detected first in a ^{1}H -^{13}C experiment was ^{13}C, whereas now ^{1}H is detected first in inverse-detection experiments, since protons are inherently more sensitive. Today, regular HETCOR experiments are not usually in common laboratory practice.

The HMQC (Heteronuclear Multiple-Quantum Coherence) experiment acquires a spectrum (see Figure 5.3.61 a) by transferring the proton magnetization by way of $^{1}J_{CH}$ to a heteronucleus, for example, ^{13}C. The ^{13}C atom then experiences its chemical shift in the t_1 time period of the pulse sequence. The magnetization then returns to the ^{1}H for detection. HMQC detects $^{1}J_{CH}$ coupling and can also be used to differentiate between geminal and vicinal proton couplings just as in COSY-45. HMQC is very widely used and offers very good sensitivity at much shorter acquisition times than HETCOR (about 30 min as opposed to several hours with HETCOR).

However, because it shows the ^{1}H -^{1}H couplings in addition to ^{1}H -^{13}C couplings and because the cross peaks appear as multiplets, HMQC suffers when it comes to resolution in the ^{13}C peaks. The HSQC (Heteronuclear Single-Quantum Coherence) experiment can assist, as it can suppress the ^{1}H -^{1}H couplings and collapse the multiplets seen in the cross peaks into singlets, which greatly enhances resolution (an example of an HSQC is shown in Figure 5.3.61 b). Figure 5.3.61 shows a side-by-side comparison of

spectra from HMQC and HSQC experiments, in which some of the peaks in the HMQC spectrum are more resolved in the HSQC spectrum. However, HSQC administers more pulses than HMQC, which causes miss-settings and inhomogeneity between the RF pulses, which in turn leads to loss of sensitivity. In HMBC (Heteronuclear Multiple Bond Coherence) experiments, two and three bond couplings can be detected. This technique is particularly useful for putting smaller proposed fragments of a molecule together to elucidate the larger overall structure. HMBC, on the other hand, cannot distinguish between $^{2}J_{CH}$ and $^{3}J_{CH}$ coupling constants. An example spectrum is shown in Figure 5.3.61d.

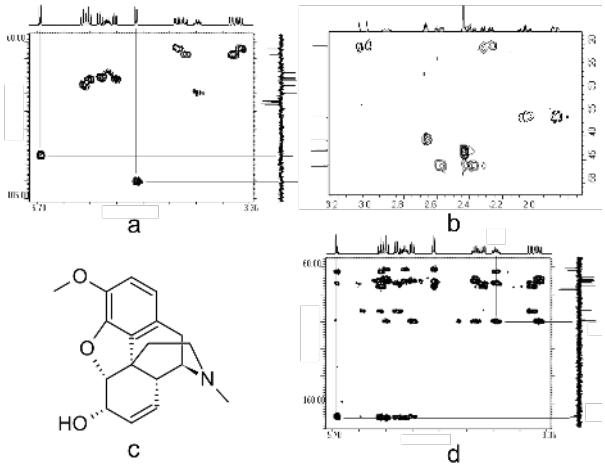


Figure 5.3.59 b) taken from a ^{1}H-^{13}C HMQC 2D NMR experiment. (b) A spectrum of codeine taken from an HSQC ^{1}H-^{13}C 2D NMR experiment. Spectrum from Acorn NMR, Inc. c) The chemical structure of codeine. d) Another spectrum of xylobiose taken from a ^{1}H-^{13}C HMBC 2D NMR experiment. Panels (a) and (d) from F. Sauriol, *NMR Webcourse*, Department of Chemistry, Queen's University, Ontario, www.chem.queensu.ca/facilities/nmr/nmr/webcourse/.

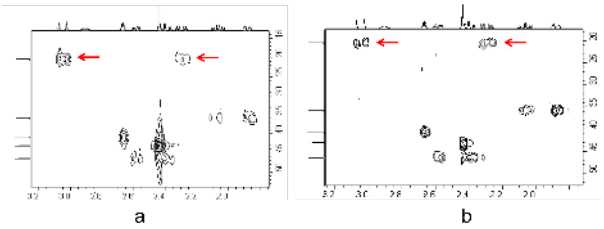
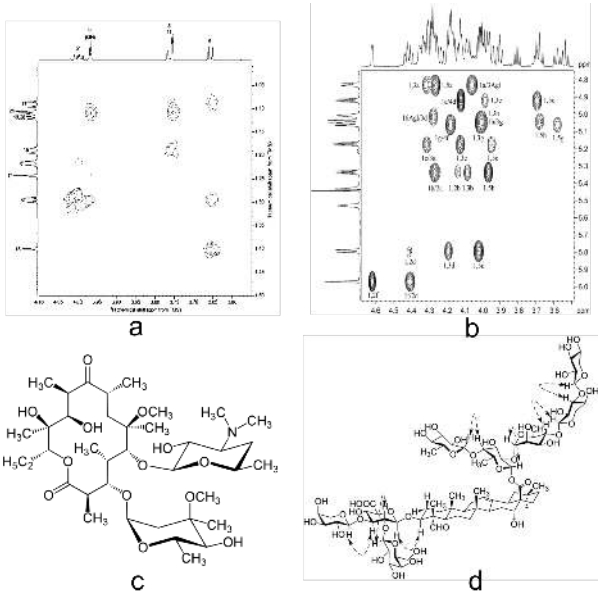


Figure 5.3.62 Side-by-side comparison of an HMQC spectrum (a) and an HSQC spectrum (b). The HSQC experiment offers better resolution than the HMQC as well as sharper peaks. HSQC helps solve the problem of overlapping peaks, which is often seen in NMR experiments. The sample in both spectra is codeine. Spectra from Acorn NMR, Inc.

NOESY and ROESY

NOESY (Nuclear Overhauser Effect SpectroscopY) is an NMR experiment that can detect couplings between nuclei through spatial proximity (< 5 Å apart) rather than coupling through covalent bonds. The Nuclear Overhauser Effect (NOE) is the change in the intensity of the resonance of a nucleus upon irradiation of a nearby nucleus (about 2.5-3.5 Å apart). For example, when an RF pulse specifically irradiates a proton, its spin population is equalized and it can transfer its spin polarization to another proton and alter its spin population. The overall effect is dependent on a distance of r^{-6}. NOESY uses a mixing time without pulses to accumulate NOEs and its counterpart ROESY (Rotating frame nuclear Overhauser Effect SpectroscopY) uses a series of pulses to accumulate NOEs. In NOESY, NOEs are positive when generated from small molecules, are negative when generated from large molecules (or molecules dissolved in a viscous solvent to restrict molecular tumbling), and are quite small (near zero) for medium-sized molecules. On the contrary, ROESY peaks are always positive, regardless of molecular weight. Both experiments are useful for determine proximity of nuclei in large biomolecules, especially proteins, where two atoms may be nearby in space, but not necessarily through covalent connectivity. Isomers, such as ortho-, meta-, and para-substituted aromatic rings, as well as stereochemistry, can also be distinguished through the use of an NOE experiment. Although NOESY and ROESY can generate COSY and TOCSY artifacts, respectively, those unwanted signals could be minimized by variations in the pulse sequences. Example NOESY and ROESY spectra are shown in Figure 5.3.63



Figures (b) and (d) from E. A. Khatuntseva, V.M. Men'shov, A.S. Shashkov, Y.E. Tsvetkov, R.N. Stepanenko, R.Y. Vlasenko, E.E. Shults, G.A. Tolstikov, T.G. Tolstikova, D.S. Baev, V.A. Kaledin, N.A. Popova, V.P. Nikolin, P.P. Laktionov, A.V. Cherepanova, T.V. Kulakovskaya, E.V. Kulakovskaya, and N.E. Nifantiev, *Beilstein J. Org. Chem.* 2012, **8**, 763.

How to Interpret 2D NMR Spectra

Much of the interpretation one needs to do with 2D NMR begins with focusing on the cross peaks and matching them according to frequency, much like playing a game of Battleship®. The 1D spectrum usually will be plotted along the axes, so one can match which couplings in one spectrum correlate to which splitting patterns in the other spectrum using the cross peaks on the 2D spectrum (see Figure 5.3.64).

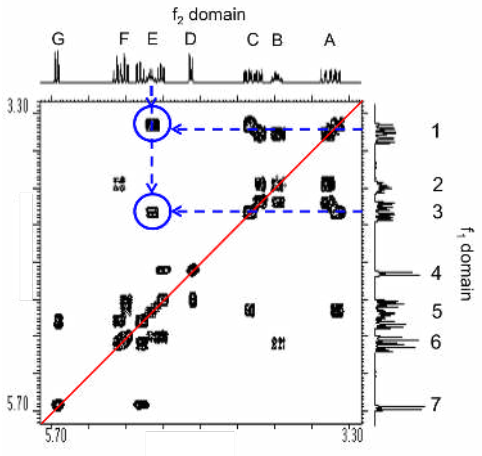


Figure 5.3.59 b). By matching up the two couplings that intersect at the cross peaks, one can easily determine which atoms are connected to which (shown by the blue dashed lines). The diagonal peaks are highlighted by the red line for clarity – the real COSY information is within the cross peaks.

Also, multiple 2D NMR experiments are used to elucidate the structure of a single molecule, combining different information from the various sources. For example, one can combine homonuclear and heteronuclear experiments and piece together the information from the two techniques, with a process known as Parallel Acquisition NMR Spectroscopy or PANSY. In the 1990s, co-variance processing came onto the scene, which allowed scientists to process information from two separate experiments, without having to run both experiments at the same time, which made for shorter data acquisition time. Currently, the software for co-variance processing is available from various NMR manufacturers. There are many possible ways to interpret 2D NMR spectra, though one common method is to label the cross peaks and make connections between the signals as they become apparent. Prof. James Nowick at UC Irvine describes his method of choice for putting the pieces together when determining the structure of a sample; the lecture in which he describes this method is posted in the links above. In this video, he provides a stepwise method to deciphering a spectrum.

Conclusion

Within NMR spectroscopy, there are a vast variety of different methods to acquire data on molecular structure. In 1D and 2D experiments, one can simply adjust the appearance of the spectrum by changing any one of the many parameters that are set when running a sample, such as number of scans, relaxation delay times, the amount of pulses at various angles, etc. Many 3D and 4D NMR experiments are actually simply multiple 2D NMR pulse sequences run in sequence, which generates more correlation between different nuclei in a spin system. With 3D NMR experiments, three nuclei, for example ^{1}H, ^{13}C, and ^{15}N can be studied together and their connectivity can be elucidated. These techniques become invaluable when working with biological molecules with complex 3D structures, such as proteins and polysaccharides, to analyze their structures in solution. These techniques, coupled with ultra-fast data acquisition, leads to monitoring complex chemical reactions and/or non-covalent interactions in real time. Through the use of these and other techniques, one can begin to supplement a characterization “toolbox” in order to continue solving complex chemical problems.

Chemical Exchange Saturation Transfer (CEST)

Paramagnetic chemical exchange saturation transfer (PARACEST) is a powerful analytical tool that can elucidate many physical properties of molecules and systems of interest both in vivo and in vitro through specific paramagnetic agents. Although a relatively new imaging technique, applications for PARACEST imaging are growing as new imaging agents are being developed with enhanced exchange properties. Current applications revolve around using these PARACEST agents for MRI imaging to enhance contrast. However, the fundamentals of PARACEST can be used to measure properties such as temperature, pH, and concentration of molecules and systems as we will discuss. PARACEST was developed in response to several imaging limitations presented by diamagnetic agents. PARACEST spectral data can be easily obtained using NMR Spectroscopy while imaging can be typically achieved with widely available clinical 1.5/4 T MRI scanners.

History

Chemical exchange saturation transfer (CEST) is a phenomenon that has been around since the 1960s. It was first discovered by Forsén, pictured below in Figure 5.3.65, and Hoffman in 1963 and was termed magnetization transfer NMR. This technique was limited in its applications to studying rapid chemical exchange reactions. However in 2000, Balaban, pictured below in Figure 5.3.66, revisited this topic and discovered the application of this phenomenon for imaging purposes. He termed the phenomenon chemical exchange saturation transfer. From this seminal finding, Balaban elucidated techniques to modulate MRI contrasts to reflect the exchange for imaging purposes.

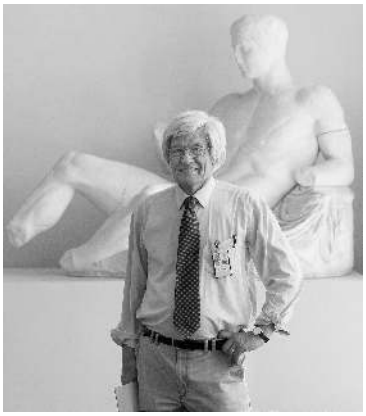


Figure 5.3.65 Swedish physical chemist Sture Forsén (1932-).



Figure 5.3.66 American chemist and biologist Robert S Balaban

CEST imaging focuses on N-H, O-H, or S-H exchangeable protons. Observing these exchanges in diamagnetic molecules can be very challenging. Several models have been developed to overcome the challenges associated with imaging with clinical scanners. The focus of recent research has been to develop paramagnetic chemical exchange saturation transfer (PARACEST) agents. Typical PARACEST complexes are based on lanthanide atoms. Historically, these molecules were thought to be useless for chemical exchange due to their very fast water exchanges rates. However, recent works by Silvio Aime and Dean Sherry have shown modified lanthanide complexes that have very slow exchange rates that make it ideal for CEST imaging. In addition to slow exchange rates, these molecules have vastly different resonance frequencies which contributes to their enhanced contrast.

Chemical Exchange Saturation Transfer

Saturation Transfer

Chemical exchange is defined as the process of proton exchange with surrounding bulk water. Exchange can occur with non-water exchange sites but it has been shown that its' contribution is negligible. As stated before, CEST imaging focuses on N-H, O-H, or S-H exchangeable protons. Molecularly every exchange proton has a very specific saturation frequency. Applying a radio-frequency pulse that is the same as the proton's saturation frequency results in a net loss of longitudinal magnetization. Longitudinal magnetization exists by virtue of being in a magnet. All protons in a solution line up with the magnetic field either in a parallel or antiparallel manner. There is a net longitudinal magnetization at equilibrium as the antiparallel state is higher in energy. A 90° RF pulse sequence causes many of the parallel protons to move to the higher energy antiparallel state causing zero longitudinal magnetization. This nonequilibrium state is termed as saturation, where the same amount of nuclear spins is aligned against and with the magnetic field. These saturated protons are exchangeable and the surrounding bulk water participates in this exchange called chemical exchange saturation transfer.

This exchange can be visualized through spectral data. The saturated proton exchange with the surrounding bulk water causes the spectral signal from the bulk water to decrease due to decreased net longitudinal magnetization. This decrease can then be quantified and used to measure a wide variety of properties of a molecule or a solution. In the next sub-section, we will explore the quantification in more detail to provide a stronger conceptual understanding.

Two-system Model

Derivations of the chemical exchange saturation transfer mathematical models arise fundamentally from an understanding of the Boltzmann equation, 5.3.17. The Boltzmann equation mathematically defines the distribution of spins of a molecule placed in a magnetic field. There are many complex models that are used to provide a better understanding of the phenomenon. However, we will stick with a two-system model to simplify the mathematics to focus on conceptual understanding. In this model, there are two systems: bulk water (alpha) and an agent pool (beta). When the agent pool is saturated with a radiofrequency pulse, we make two important assumptions. The first is that all the exchangeable protons are fully saturated and the second is that the saturation process does not affect the bulk water protons, which retain their characteristic longitudinal magnetization.

$$\frac{N_{high\ energy}}{N_{low\ energy}} = exp(\frac{-\Delta E}{kT}) \tag{5.3.17}$$

To quantify the following proton exchange we shall define the equilibrium proton concentration. The Boltzmann equation gives us the distribution of the spin states at equilibrium which is proportional to the proton concentration. As such, we shall label the two system's equilibrium states as M_α^0 and M_β^0. Following saturation, the saturated protons of the bulk pool exchange with the agent pool at a rate k_α. As such the decrease in longitudinal (Z) magnetization is given by $k_\alpha M_\alpha^Z$. Furthermore, another effect that needs to be considered is the inherent relaxation of the protons which increase the Z magnetization back to equilibrium levels, M_α^0. This can be estimated with the following 5.3.18 where $T_{1\alpha}$ is the longitudinal relaxation time for bulk water. Setting the two systems equal to represent equilibrium we get the following relationship 5.3.19 that can be manipulated mathematically to yield the generalized chemical exchange Equation 5.3.20 where $\tau_\alpha = k_\alpha^{-1}$ and defined as lifetime of a proton in the system and c being the concentrations of protons in their respective system. [n] represents the number of exchangeable protons per CEST molecule. In terms of CEST calculations, the lower the ratio of Z the more prominent the CEST effect. A plot of this equation over a range of pulse frequencies results in what is called a Z-spectra also known as a CEST spectra, shown in Figure 5.3.67. This spectrum is then used to create CEST Images.

$$\frac{M_\alpha^0 - M_\alpha^Z}{T_{1\alpha}} \tag{5.3.18}$$

$$k_\alpha M_\alpha^Z = \frac{M_\alpha^0 - M_\alpha^Z}{T_{1\alpha}} \tag{5.3.19}$$

$$Z = \frac{M_\alpha^Z}{M_\alpha^0} = \frac{1}{1 + \frac{C_\beta[n]}{C_\alpha}\frac{T_{1\alpha}}{\tau_\alpha}} \tag{5.3.20}$$

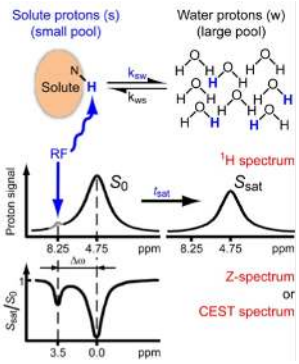


Figure 5.3.67 Solute protons are saturated with a specific resonance frequency shown here as 8.25 ppm. This saturation is transferred to water at an exchange rate with unsaturated protons. After a brief period, this saturation effect becomes visible on the water signal as a decrease in proton signal. Z-spectrum is generated by measuring the normalized water saturation (S_{sat}/S_0) as a function of irradiation frequency. Adapted from P. C. M. Van Zijl and N. N. Yadav, *Magn. Reson. Med.*, 2011, **65**, 927.

Limitations of Diamagnetic CEST Imaging and Two-system Model

A CEST agent must have several properties to maximize the CEST effect. Maximum CEST effect is observed when the residence lifetime of bulk water (τ_α) is as short as possible. This indirectly means that an effective CEST agent has a high exchange rate, k_α. Furthermore, maximum effect is noted when the CEST agent concentration is high.

In addition to these two properties, we need to consider the fact that the two-system model's assumptions are almost never true. There is often a less than saturated system resulting in a decrease in the observed CEST effect. As a result, we need to consider the power of the saturation pulses, B_1. The relationship between the τ_α and B_1 is shown in the below 5.3.21. As such, an increase in saturation pulse power results in increase CEST effect. However, we cannot apply too much B1 due to in vivo limitations. Furthermore, the ideal τ_α can be calculated using the above relationship.

$$\tau = \frac{1}{2\pi B_1} \tag{5.3.21}$$

Finally, another limitation that needs to be considered is the inherent only to diamagnetic CEST and provides an important distinction between CEST and PARACEST as we will soon discuss. We assumed with the two-system model that saturation with a radiofrequency pulse did not affect the surrounded bulk water Z-magnetization. However, this is large generalization that can only be made for PARACEST agents as we shall soon see. Diamagnetic species, whether endogenous or exogenous, have a chemical shift difference (Δω) between the exchangeable –NH or –OH groups and the bulk water of less than 5 ppm. This small shift difference is a major limitation. Selective saturation often lead to partial saturation of bulk water protons. This is a more important consideration where in-vivo water peak is very broad. As such, we need to maximize the shift difference between bulk water and the contrast agent.

Paramagnetic Chemical Exchange Saturation Transfer

Strengths of PARACEST

PARACEST addresses the two complications that arise with CEST. Application of a radio frequency pulse close to the bulk water signal will result in some off-resonance saturation of the wa

ter. This essentially limits power which enhances CEST effect. Furthermore, a slow exchange condition less than the saturation frequency difference (Δω) means that a very slow exchange rate is required for diamagnetic CEST agents of this sort. Both problems can be alleviated by using an agent that has a larger chemical shift separation such as paramagnetic species. Figure 5.3.68 shows the broad Δω of Eu^{3+}complex.

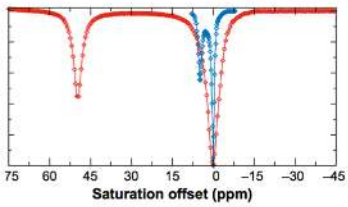


Figure 5.3.68 Eu^{3+} complex broadens the chemical shift leading to a larger saturation frequency difference that can easily be detected. Red spectral line represents EuDOTA-(glycine ethyl ester)$_4$. Blue spectral line represents barbituric acid. Adapted from A. D. Sherry and M. Woods, *Annu. Rev. Biomed. Eng.*, 2008, **10**, 391.

Selection of Lanthanide Species

Based on the criteri a established in 5.3.22, we see that only Eu^{3+}, Tb^{3+}, Dy^{3+}, and Ho^{3+} are effective lanthanide CEST agents at the most common MRI power level (1.5 T). However, given stronger field strengths the Table 5.3.8 suggests more CEST efficiency. With exception of Sm^{3+}, all other lanthanide molecules have shifts far from water peak providing a large Δω that is desired of CEST agents. This table should be considered before design of a PARACEST experiment. Furthermore, this table eludes the relationship between power of the saturation pulse and the observed CEST effect. Referring to the following 5.3.23, we see that for increased saturation pulse we notice increased CEST effect. In fact, varying B_1 levels changes saturation offset. The higher the B_1frequency the higher the signal intensity of the saturation offset As such, it is important to select a proper saturation pulse before experimentation.

Table 5.3.8 The chemical shifts and proton lifetime values for various lanthanide metals in a lanthanide DOTA-4AmCE complex (Figure 5.3.68).

Complex	T_m at 298 K (μ s)	δ ^{1}H (ppm)	$\Delta\omega.\tau_\alpha$ at 1.5 T	$\Delta\omega.\tau_\alpha$ at 4.7 T	$\Delta\omega.\tau_\alpha$ at 11.75 T
Pr^{3+}	20	-60	0.5	1.5	3.8
Nd^{3+}	80	-32	1.0	3.2	8.0
Sm^{3+}	320	-4	0.5	1.6	4.0
Eu^{3+}	382	50	7.7	24.0	60.0
Tb^{3+}	31	-600	7.5	23.4	58.5
Dy^{3+}	17	-720	4.9	15.4	38.5
Ho^{3+}	19	-360	2.8	8.6	21.5
Er^{3+}	9	200	0.7	2.3	5.7
Tm^{3+}	3	500	0.6	1.9	4.7
Yb^{3+}	3	200	0.2	0.5	1.9

Based on the criteria established in 5.3.22, we see that only Eu^{3+}, Tb^{3+}, Dy^{3+}, and Ho^{3+} are effective lanthanide CEST agents at the most common MRI power level (1.5 T). However, given stronger field strengths the Table 5.3.9 suggests more CEST efficiency. With exception of Sm^{3+}, all other lanthanide molecules have shifts far from water peak providing a large Δω that is desired of CEST agents. This table should be considered before design of a PARACEST experiment. Furthermore, this table eludes the relationship between power of the saturation pulse and the observed CEST effect. Referring to the following 5.3.23, we see that for increased saturation pulse we notice increased CEST effect. In fact, varying B_1 levels changes saturation offset. The higher the B_1frequency the higher the signal intensity of the saturation offset As such, it is important to select a proper saturation pulse before experimentation.

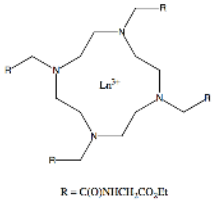


Figure 5.3.69 Structure of lanthanide DOTA-4AmCE complex.

$$\Delta\omega \cdot \tau_\alpha = \frac{1}{2\pi B_1} \tag{5.3.22}$$

$$\tau_\alpha = \frac{1}{2\pi B_1} \tag{5.3.23}$$

Running a PARACEST Experiment

Two types of experiments can be run to quantify PARACEST. The first produces quantifiable Z-spectral data and is typically run on 400 MHz spectrometers with a B1 power between 200-1000 KHz and an irradiation time between 2 and 6 seconds based on the lanthanide complex. Imaging experiments are typically performed on either clinical scanners are small bore MRI scanner at room temperature using a custom surface coil. Imaging experiments usually require the followings sequence of steps:

1. Bulk water spectra are collected from PARACEST using a 2 second presaturation pulse at a desired power level based on lanthanide complex.
2. Following base scan, the saturation frequency is stepped between ±100 ppm (relative to the bulk water frequency at 0 ppm) in 1 ppm increments. The scanning frequency can be altered to include a wider scan if lanthanide complex has a larger chemical shift difference.
3. Following collection of data, the bulk water signal is integrated using a Matlab program. The difference between the integrated signals measured at equivalent positive and negative saturation frequencies are plotted and subtracted using the following 5.3.24 and mapped to produce gradient images.
4. To create a CEST Image the data set is first filtered to improve signal-to-noise ratio and normalized with phantom data by subtraction and color-coded.
5. For data tools to perform CEST Imaging analysis. Please refer to the following links for free access to open source software tools: https://github.com/cest-sources/CEST_EVAL/ or http://www.med.upenn.edu/cmroi/software-overview.html.

$$\frac{S_{sat(-\Delta\omega)} - S_{sat(\Delta\omega)}}{S_0} \tag{5.3.24}$$

Applications of PARACEST

Temperature Mapping

PARACEST imaging has shown to be a promising area of research in developing a noninvasive technique for temperature mapping. Sherry et. al shows a variable-temperature dependence of a lanthanide bound water molecule resonance frequency. They establish a linear correspondence over the range of 20-50 °C. Furthermore, they show a feasible analysis technique to locate the chemical shift (δ) of a lanthanide in images with high spatial resolution. By developing a plot of pixel intensity versus frequency offset they can individually identify temperature at each pixel and hence create a temperature map as shown in the Figure 5.3.70

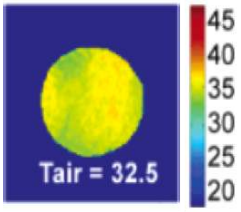


Figure 5.3.70 Temperature map of a phantom containing 1 mL of 10 mM Eu in water at pH 7.0 in degrees Celsius. Adapted from S. Zhang, C. R. Malloy, and A. D. Sherry, *J. Am. Chem. Soc.*, 2005, **127**, 17572.

Zinc Ion Detection

Divalent zinc is an integral transition-metal that is prominent in many aqueous solutions and plays an important role in physiological systems. The ability to detect changes in sample concentrations of Zinc ions provides valuable information regarding a system's. Developing specific ligands that coordinate with specific ions to enhance wate-rexchange characteristics can amplify CEST profile. In this paper, the authors develop a Eu(dotampy) sensor shown in Figure 5.3.71 for Zn ions. This authors theorize that the sensor coordinates with Zinc using its four pyridine donors in a square anti-prism manner as determined by NMR Spectroscopy by observing water exchange rates and by base catalysis by observing CEST sensitivity. Authors were unable to analyze coordination by X-ray crystallography. Following, determination of successful CEST profiles, the authors mapped in-vitro samples of varying concentrations of Zn and were successfully able to correlate image voxel intensity with Zn concentrations as shown in Figure 5.3.72 Furthermore, they were able to successfully demonstrate specificity of the sensor to Zn over Magnesium and Calcium. This application proves promising as a potential detection method for Zn ions in solutions with a range of concentrations between 5 nm to 0.12 µm.

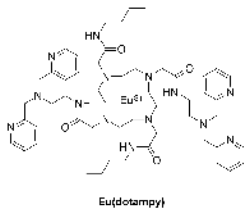


Figure 5.3.71 Structure of Eu(dotampy) where dotampy = 1,7-bis(N,N-bis(2-pyridylmethyl) aminoethylcarbamoylmethyl)-4,10-bis(butylcarbamoylmethyl)-1,4,7,10-tetraazacyclododecane. The four Pyridine rings are hypothesized to serve as coordinators with Zn leading to its CEST sensitivity and specificity.

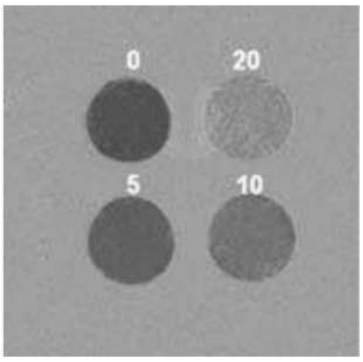


Figure 5.3.72 CEST images of phantoms with varying concentrations of Zn in mM containing 20 mM of Eu(dotampy). The CEST images represent the intensity difference between saturation at 50 ppm and 25 ppm from bulk water. Adapted from R. Trokowski, J. Ren, F. K. Kálmán, and A. D. Sherry, *Angew. Chemie., Int. Ed.*, 2005, **44**, 6920.

This page titled 5.3: NMR Spectroscopy is shared under a CC BY license and was authored, remixed, and/or curated by Pavan M. V. Raja & Andrew R. Barron (OpenStax CNX) .

- **4.7: NMR Spectroscopy** by Pavan M. V. Raja & Andrew R. Barron is licensed CC BY 4.0. Original source: http://cnx.org/contents/ba27839d-5042-4a40-afcf-c0e6e39fb45425.2.

5.4: Theory

Nuclear magnetic resonance plays an important role in the fields chemistry, materials science, physics and engineering. It is becoming a more and more useful method to probe the structure of molecules. The primary object of this module is to understand the fundamental concepts of NMR. It is assumed that the reader already understands the quantum numbers associated with electrons. For a more basic understanding of how NMR works, the reader is directed to the NMR introduction page.

Introduction

Nuclear magnetic resonance, NMR, is a physical phenomenon of resonance transition between magnetic energy levels, happening when atomic nuclei are immersed in an external magnetic field and applied an electromagnetic radiation with specific frequency. By detecting the absorption signals, one can acquire NMR spectrum. According to the positions, intensities and fine structure of resonance peaks, people can study the structures of molecules quantitatively. The size of molecules of interest varies from small organic molecules, to biological molecules of middle size, and even to some macromolecules such as nucleic acids and proteins. Apart from these commonly utilized applications in organic compound, NMR also play an important role in analyzing inorganic molecules, which makes NMR spectroscopy a powerful technique.

But the a major question still remains- Why does NMR work? This module will begin by developing the concept of nuclear spin then moving into a discussion about energy levels and the relative populations and the interactions of a nucleus with the magnetic field.

Nuclear Spin Origins

The concept of spin is regularly addressed in subatomic particle physics. However, to most people spin seems like an abstract concept. This is due to the fact there is no macroscopic equivalent of what spin is. However, for those people who have taken an introduction to chemistry course have seen the concept of spin in electrons. Electrons are subatomic particles which have spin intrinsic to them. The nucleus is not much different. Spin is just another form of angular momentum. The nucleus consists of protons and neutrons and neutrons and protons are comprised of subatomic particles known as quarks and gluons. The neutron has 2 quarks with a -e/3 charge and one quark with a +2e/3 charge resulting in a total charge of 0. The proton however, has 2 quarks with +2e/3 charge and only one quark with a -e/3 charge giving it a net positive charge. Both protons and neutrons are spin=1/2.

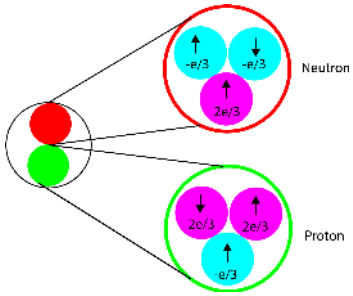


Figure 5.4.1: The atomic nucleus (black) of ^{2}H. The proton (green) and neutron (red) are composed of quarks (purple and teal) which have a charge and spin (arrow).

For any system consisting of n multiple parts, each with an angular momentum the total angular momentum can be described by J where

$$J = |J_1 + J_2 + \ldots + J_n|, |J_1 + J_2 + \ldots + J_n| - 1, \ldots |J_1 - J_2 - \ldots - J_n| \tag{5.4.1}$$

Here are some examples using the isotopes of hydrogen

- ^1H = 1 proton so J=1/2
- ^2H= 1 proton and 1 neutron so $J = 1$ or 0.

For larger nuclei, it is not immediately evident what the spin should be as there are a multitude of possible values. For the remainder of the discussion we will attribute the spin of the nucleus, I, to be an intrinsic value. There are some rules that the nuclei do follow with respect to nuclear spin. They are summarized in the table below.

Table 1. General rules for determination of nuclear spin quantum numbers

Mass Number	Number of Protons	Number of Neutrons	Spin (I)	Example
Even	Even	Even	0	^{16}O
	Odd	Odd	Integer (1,2,...)	^2H

Mass Number	Number of Protons	Number of Neutrons	Spin (I)	Example
Odd	Even	Odd	Half-Integer (1/2, 3/2,...)	^{13}C
	Odd	Even	Half-Integer (1/2, 3/2,...)	^{15}N

Nuclear Spin Angular Momentum and Quantum Numbers

As mentioned above, spin is a type of angular momentum. Nuclear spin angular momentum was first reported by Pauli in 1924 and will be described here. Analogous to the angular momentum commonly encountered in electron, the angular momentum is a vector which can be described by a magnitude L and a direction, m. The magnitude is given by

$$L = \hbar\sqrt{I(I+1)} \tag{5.4.2}$$

The projection of the vector on the z axis (arbitrarily chosen), takes on discretized values according to m, where

$$m = -I, -I+1, -I+2, \ldots +I \tag{5.4.3}$$

The angular momentum along the z-axis is now

$$I_z = m\hbar \tag{5.4.4}$$

Pictorially, this is represented in the figure below for three values of I.

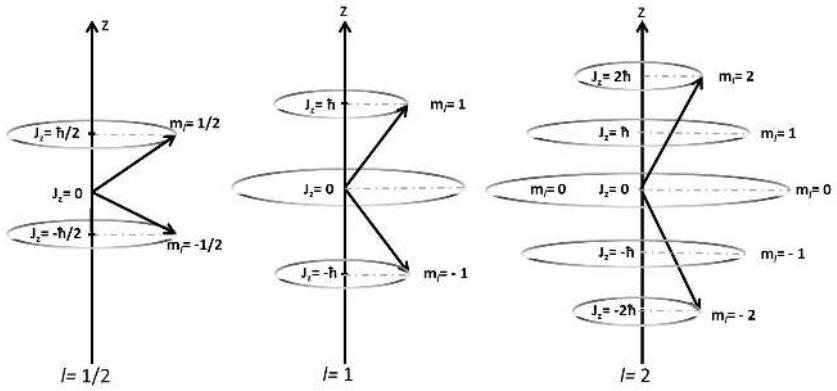


Figure 5.4.2: The quantized angular momentum values for a I=1/2 (left) I=1(middle) and I=2 (right). The magnitude is denoted by the arrow while the projection along the z-axis is denoted by the circle.

The quantum numbers of the nucleus are denoted below.

Interaction	Symbol	Quantum Numbers
Nuclear Spin Angular Momentum	I	0<I<9/2 by 1/2
Spin Angular Momentum Magnitude	L	$L = \hbar\sqrt{I(I+1)}$ (5.4.5)
Spin Angular Momentum Direction	m	$m = -I, -I+1, -I+2, \ldots +I$ (5.

Magnetic Moment of a Nucleus

We have now established that the nucleus has spin which can be denoted using specific quantum numbers. As with all charged particles, if the nucleus is moved in a loop it will generate a magnetic field. The magnetic moment μ is related to the angular momentum of the nucleus by

$$\mu = \gamma I \tag{5.4.7}$$

where γ is the gyromagnetic ratio, a proportionality constant unique to each nucleus. The table below shows some of the gyromagnetic ratios for some commonly studies nuclei.

Nuclei	Unpaired Protons	Unpaired Neutrons	Net Spin

Nuclei	Unpaired Protons	Unpaired Neutrons	Net Spin
^{1}H	1	0	1/2
^{2}H	1	1	1
^{31}P	1	0	1/2
^{23}Na	1	2	3/2
^{14}N	1	1	1
^{13}C	0	1	1/2
^{19}F	1	0	1/2

The net or bulk magnetization of the sample is given by M and is the sum of each individual magnetic vector, or

$$M = \sum \mu \tag{5.4.8}$$

since these magnetic moments are vectors and are randomly aligned, the bulk magnetization arising from the nucleus is zero. There may be unpaired electrons which give rise to paramagnetic, anti ferromagnetic, or ferromagnetic properties. However, if an external magnetic field is applied, the nuclei will align either with or against the field and result in a non-zero bulk magnetization.

Nuclear Energy Levels in a Magnetic Field

We now understand why the nucleus has a magnetic moment associated with it. Now we are getting to the crux of NMR, the use of an external magnetic field. Initially, the nucleus is in the nuclear ground state which is degenerate. The degeneracy of the ground state is $2I+1$. The application of a magnetic field splits the degenerate 2I+1 nuclear energy levels. The energy of a particular level is

$$E = -\mu \cdot B_0 \tag{5.4.9}$$

where B_0 is the external magnetic field. Along the z-direction, which we assume the magnetic field is applied,

$$E = -\mu B_0 \tag{5.4.10}$$

by substitution,

$$E = -m\hbar\gamma B_0 \tag{5.4.11}$$

The magnitude of the splitting therefore depends on the size of the magnetic field. In most labs this magnetic field is somewhere between 1 and 21T. Those spins which align with the magnetic field are lower in energy, while those that align against the field are higher in energy.

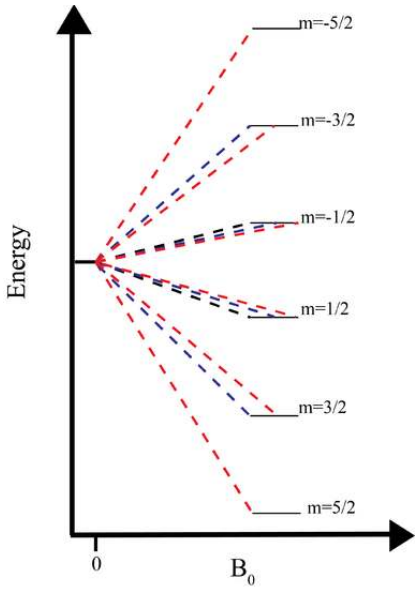


Figure 5.4.3: Splitting of the energy levels for a I=1/2 (black dashed lines), I= 3/2 (blue dashed lines), and I=5/2 (red dashed lines). Note how the energy level is dependent on the applied magnetic field. The offset of the red and blue lines is for illustrative purposes only.

Energy Level Spin Distribution

In the absence of a magnetic field the magnetic dipoles are oriented randomly and there is no net magnetization (vector sum of μ is zero). Application of an external magnetic field, as was shown above, creates distinct energy levels based on the spin angular momentum of the nucleus. Each energy level is populated by the spins which have the same angular momentum. To illustrate this, consider a I=1/2 system. There are two energy levels, +1/2 and -1/2, which are populated by spins that have aligned against or with the external magnetic field, respectively.

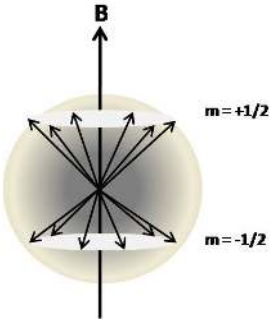


Figure 5.4.4: Spins configurations according to applied magnetic field

The energy separation between these states is relatively small and the energy from thermal collisions is sufficient to place many nuclei into higher energy spin states. The number of nuclei in each spin state can be described by the Boltzmann distribution. The Boltzmann equation expresses the relationship between temperature and the related energy as shown below.

$$\frac{N_{upper}}{N_{lower}} = e^{\frac{-\Delta E}{kT}} = e^{\frac{-h\nu}{kT}} \tag{5.4.12}$$

Where N_{upper} and N_{lower} represent the population of nuclei in upper and lower energy states, E is the energy difference between the spin states, k is the Boltzmann constant (1.3805x10-23 J/Kelvin) and T is the temperature in K. At room temperature, the number of spins in the lower energy level, N_{lower}, slightly outnumbers the number in the upper level, N_{upper}.

Selection Rules

The selection rule in NMR is

$$\Delta m = \pm 1 \tag{5.4.13}$$

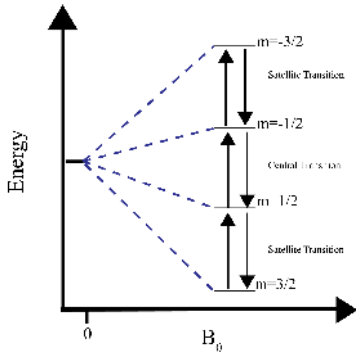
For a nucleus with I=1/2 there is only one allowed transition. For nuclei with $I > 1/2$, there are multiple transitions which can take place. Consider the case of I=3/2. The following transitions can take place

$$-\frac{3}{2} \leftrightarrow -\frac{1}{2} \tag{5.4.14}$$

$$-\frac{1}{2} \leftrightarrow \frac{1}{2} \tag{5.4.15}$$

$$\frac{1}{2} \leftrightarrow \frac{3}{2} \tag{5.4.16}$$

which is illustrated below.



The transition from

$$-\frac{3}{2} \leftrightarrow -\frac{1}{2} \tag{5.4.17}$$

$$\frac{1}{2} \leftrightarrow \frac{3}{2} \tag{5.4.18}$$

are known as satellite transitions, while the

$$-\frac{1}{2} \leftrightarrow \frac{1}{2} \tag{5.4.19}$$

transition is known as the central transition. The central transition is primarily observed in an NMR experiment. For more information about satellite transitions please look at quarupole interactions.

The NMR Experiment

During the NMR experiment several things happen to the nucleus, the bulk magnetization is rotated from the z axis into the xy plane and then allowed to relax back along the z-axis. A full theoretical explanation for a single atom was developed by Bloch into a set of equations known as the Bloch equations. From the NMR experiment chosen a variety of information can be gleaned by studying different interactions.

References

1. Claude H. Yoder, Charles D. Schaeffer,Introduction to multinuclear NMR : theory and application, Benjamin/Cummings Pub. Co., Menlo Park, Calif., 1987.
2. Robin K. Harris, Nuclear magnetic resonance spectroscopy : a physicochemical view, Pitman, Marshfield, Mass., 1983.
3. Jeremy K.M. Sanders and Brian K. Hunter, Modern NMR spectroscopy : a guide for chemists, Oxford University Press, New York, 1993.
4. David A.R. Williams ; editor, David J. Mowthorpe, Nuclear magnetic resonance spectroscopy, Published on behalf of ACOL, London, by J. Wiley, New York, 1986.
5. Frank A. Bovey, Lynn Jelinski, Peter A. Mirau, Nuclear magnetic resonance spectroscopy, Academic Press, San Diego, 1988.
6. R.J. Abraham, J. Fisher and P. Loftus, Introduction to NMR spectroscopy, Wiley, New York, 1988.
7. J.W. Akitt, NMR and chemistry : an introduction to modern NMR spectroscopy, Chapman & Hall, London; New York, 1992.

Contributors

- Derrick Kaseman (UC Davis), Sureyya OZCAN, Siyi Du

5.4: Theory is shared under a CC BY-NC-SA 4.0 license and was authored, remixed, and/or curated by LibreTexts.

- **NMR - Theory** by Derrick Kaseman, Siyi Du, Sureyya Ozcan is licensed CC BY 4.0.

Bloch Equations

In 1946 Felix Bloch, co-discoverer of NMR, proposed a set of equations to described the time dependence of the net magnetization during the course of the NMR experiment. These equations are known as the Bloch equations and give insights into many processes in NMR. The Bloch equations follow first order kinetics and the derivations are first-order differentials.

Bloch Equations in the Lab Frame

It has been shown that nuclei in placed in a magnetic field precess with a characteristic Larmor frequency, ω.

$$\omega_0 = -\gamma(1-\sigma)B_0 \tag{1}$$

which can be made time-dependent by considering a time-dependent magnetic field B(t).

In addition we have also seen that there is a bulk magnetization, based on Boltzmann statistics, which lies along the direction of the applied magnetic field, B_0. This bulk magnetization can then be thought of preces\sing at the Larmor frequency. Assuming that the B_0 is along the Z-axis, we can describe the time dependence of the magnetization M, by

$$\frac{dM}{dt} = \omega(t)xM(t) - [R][M(t) - M_eq] \tag{2}$$

where R is a rotation matrix, and M_{eq} is the magnetization at equilibrium along the z-axis. The rotation matrix accounts for relaxation processes and is given by

$$R = \begin{pmatrix} \frac{1}{T_2} & 0 & 0 \\ 0 & \frac{1}{T_2} & 0 \\ 0 & 0 & \frac{1}{T_1} \end{pmatrix} \tag{3}$$

The $[R][M(t) - M_{eq}]$ term then describes the decay of the magnetization in the x-y plane and the growth of the equilibrium magnetization, due to T_2 and T_1 effects, repectively.

Expansion of the equation yeilds the magnetization in each direction

$$\begin{pmatrix} \frac{dM_x^*(t)}{dt} \\ \frac{dM_y^*(t)}{dt} \\ \frac{dM_z^*(t)}{dt} \end{pmatrix} = \begin{pmatrix} [M_x(t)\omega_y(t) - M_y\omega_z(t)] - \frac{M_x(t)}{T_2} \\ [M_x(t)\omega_z(t) - M_z\omega_x(t)] - \frac{M_y(t)}{T_2} \\ [M_y(t)\omega_x(t) - M_x\omega_y(t)] - \frac{[M_z(t) - M_{eq}]}{T_1} \end{pmatrix} \tag{4}$$

Assuming that we have a static magnetic field these equations simplify to

$$\begin{pmatrix} \frac{dM_x^*(t)}{dt} \\ \frac{dM_y^*(t)}{dt} \\ \frac{dM_z^*(t)}{dt} \end{pmatrix} = \begin{pmatrix} -\omega_0 M_y(t) - \frac{M_x(t)}{T_2} \\ \omega_0 M_x(t) - \frac{M_y(t)}{T_2} \\ -\frac{[M_z(t) - M_{eq}]}{T_1} \end{pmatrix} \tag{5}$$

As the magnetization is preces\sing about the Z axis as it recovers from the x-y plane it is realized that the time dependance will follow an oscillatory pattern which can be described u\sing trigonometric functions. Therefore at a given time the magnetization in any direction will be

$$\begin{pmatrix} M_x(t) \\ M_y(t) \\ M_z(t) \end{pmatrix} = \begin{pmatrix} [M_x(0)\cos\omega_0 t - M_y(0)\sin\omega_0 t]e^{\frac{-t}{T_2}} \\ [M_y(0)\cos\omega_0 t - M_x(0)\sin\omega_0 t]e^{\frac{-t}{T_2}} \\ M_z(0)e^{\frac{-t}{T_1}} + M_{eq}(1-e^{\frac{-t}{T_1}}) \end{pmatrix} \tag{6}$$

Where $M_{x,y,z}(0)$ is the magnetization at t=0.

What Do The Equations Describe?

From this derivation we are able to describe the motion of the bulk magnetization of the nuclei after a pulse as a function of time accounting for relaxation.

Bloch Equations in the Rotating Frame

One can imagine that application of a $\frac{\pi}{2}$ pulse in which the B- field now becomes time dependent would be challenging to calculate u\sing the Bloch equations in the lab frame. Therefore we now shift our discussion to the rotating frame. It should be stated here that the insertion of the * to denote the magnetization projection on the rotating frame.

The frequency of rotation ω_{rot}, is equivalent to spins precession frequency, which will be the Larmor frequency. From this we can describe the change of the magnetization as

$$\frac{d^*M}{dt} = \frac{dM}{dt} - \omega_{rot} x M \tag{7}$$

We know that $\frac{dM}{dt}$ is given by the bloch equations we derived for the lab frame that is:

$$\frac{dM}{dt} = \omega(t) x M(t) - [R][M(t) - M_e q] \tag{8}$$

Substituting this into our equation, we obtain

$$\frac{d^*M}{dt} = \omega(t) X M - \omega_{rot} x M - [R][M - M_{eq}] \tag{9}$$

which simplifies (u\sing cross product relations) to

$$\frac{d^*M}{dt} = \omega_{eff}(t) x M - [R][M - M_{eq}] \tag{10}$$

where

$$\omega_{eff}(t) = \omega - \omega_{rot} \tag{11}$$

Noting that the relation between the lab frame frame and the rotating frame is the common z-axis, we can define the Bloch equations in the rotating frame

$$\begin{pmatrix} \frac{dM_x^*(t)}{dt} \\ \frac{dM_y^*(t)}{dt} \\ \frac{dM_z^*(t)}{dt} \end{pmatrix} = \begin{pmatrix} \gamma[M_y^*(t)B_z(t) - M_z^*(t)B_y(t)] - \frac{M_x^*(t)}{T_2} \\ \gamma[M_z^*(t)B_x(t) - M_x^*(t)B_z(t)] - \frac{M_y^*(t)}{T_2} \\ \gamma[M_x^*(t)B_y(t) - M_y^*(t)B_x(t)] - \frac{[M_z^*(t) - M_{eq}^*]}{T_2} \end{pmatrix} \tag{12}$$

Which can be simplified to give

$$\begin{pmatrix} \frac{dM_x^*(t)}{dt} \\ \frac{dM_y^*(t)}{dt} \\ \frac{dM_z^*(t)}{dt} \end{pmatrix} = \begin{pmatrix} -\Omega M_y^*(t) - \gamma M_z^*(t) B_y^*(t)] - \frac{M_x^*(t)}{T_2} \\ -\gamma [M_x^*(t) + \gamma M_z^*(t) B_x^*(t)] - \frac{M_y^*(t)}{T_2} \\ \gamma [M_x^*(t) B_y^*(t) - M_y^*(t) B_x^*(t)] - \frac{[M_z^*(t) - M_{eq}^*]}{T_2} \end{pmatrix} \tag{13}$$

where

$$\Omega = \omega_0 - \omega_{rot} \tag{14}$$

Effects of RF pulses

During the NMR experiment, we can choose which direction we can apply our magnetic field during the pulse. For simplicity we assume that we apply the pulse along the +x axis. The nutation frequency is then defined as

$$\omega_1 = \mid \gamma B_1(t) \mid \tag{15}$$

where B_1 is the magnetic field applied along rhe x-axis. Application of this to the Bloch equations in the rotating frame we obtain

$$\begin{pmatrix} M_x^*(t) \\ M_y^*(t) \\ M_z^*(t) \end{pmatrix} = \begin{pmatrix} \omega_1 M_z^* \sin\phi - \frac{-M_x^*}{T_2} \\ -\omega_1 M_z^* \cos\phi - \frac{-M_y^*}{T_2} \\ -\omega_1 M_z^* \sin\phi + \omega_1 M_z^* \cos\phi - \frac{(M_z^* - M_e^* q)}{T_1} \end{pmatrix} \tag{16}$$

where ϕ is the phase of the pulse (0=x axis and 270=-y axis). The RF pulse is much shorter than T_1, T_2, or ω_0. Therefore we can neglect any terms containing these values.THe equations then simplify to

$$\begin{pmatrix} M_x^*(t) \\ M_y^*(t) \\ M_z^*(t) \end{pmatrix} = \begin{pmatrix} \omega_1 M_z^* \sin\phi \\ -\omega_1 M_z^* \cos\phi \\ -\omega_1 M_z^* \sin\phi + \omega_1 M_z^* \cos\phi \end{pmatrix} \tag{17}$$

Thereby application of a pulse of phase zero will result in the following result for the magnetization as a function of time

$$\begin{pmatrix} \frac{dM_x^*(t)}{dt} \\ \frac{dM_y^*(t)}{dt} \\ \frac{dM_z^*(t)}{dt} \end{pmatrix} = \begin{pmatrix} 0 \\ \gamma B_1(t) M_z^* \\ -\gamma B_1(t) M_z^* \end{pmatrix} \tag{18}$$

Or more generally as

$$\begin{pmatrix} M_x^*(t) \\ M_y^*(t) \\ M_z^*(t) \end{pmatrix} = \begin{pmatrix} M_x^* \\ M_y^* \cos\omega_1 t - M_z^* \sin\omega_1 t \\ M_z^* \cos\omega_1 t - M_y^* \sin\omega_1 t \end{pmatrix} \tag{19}$$

We can also describe the effect of a pulse of any phase on a Cartesian basis

$$\begin{pmatrix} M_x^*(t) \\ M_y^*(t) \\ M_z^*(t) \end{pmatrix} = \begin{pmatrix} \frac{1}{2} M_x^*(1 + \cos\omega_1 t) + \frac{1}{2}(M_x^* \cos 2\phi + M_y^* \sin 2\phi)(1 - \cos\omega_1 t) + M_z^* \sin\phi \sin\omega_1 t \\ \frac{1}{2} M_y^*(1 + \cos\omega_1 t) - \frac{1}{2}(M_y^* \cos 2\phi + M_x^* \sin 2\phi)(1 - \cos\omega_1 t) + M_z^* \cos\phi \sin\omega_1 t \\ M_z^* \cos\omega_1 t - (M_x^* \sin\phi - M_y^* cps\phi) \sin\omega_1 t \end{pmatrix} \tag{20}$$

Steady State Approximation

If the movement of the magnetization is slow, then

$$\frac{dM_x^*}{dt} = \frac{dM_y^*}{dt} = \frac{dM_z}{dt} = 0 \tag{21}$$

When can then solve for the magnetizations in each direction

$$M_x^* = -\frac{2\pi\gamma\, B_1 M_0 T_2^2 \Omega}{1 + 4\pi^2 T_2^2 \Omega^2 + \gamma^2 B_1^2 T_1 T_2} \tag{22}$$

$$M_y^* = -\frac{\gamma\, B_1 M_0 T_2}{1 + 4\pi^2 T_2^2 \Omega^2 + \gamma^2 B_1^2 T_1 T_2} \tag{23}$$

$$M_z = \frac{M_0[1 + 4\pi^2 T_2^2 \Omega^2]}{1 + 4\pi^2 T_2^2 \Omega^2 + \gamma^2 B_1^2 T_1 T_2} \tag{24}$$

Free Precession

In the absences of any magnetization applied in the x-y plane, the change in the magnetization is due to relaxation effects of T_1 and T_2 processes.
The Bloch equations in the rotating fram then reduce to

$$\begin{pmatrix} \frac{dM_x^*(t)}{dt} \\ \frac{dM_y^*(t)}{dt} \\ \frac{dM_z^*(t)}{dt} \end{pmatrix} = \begin{pmatrix} -(\omega_{rot} - \omega_0) M_y^*(t) - \frac{M_x^*(t)}{T_2} \\ (\omega_{rot} - \omega_0) M_x^*(t) - \frac{M_y^*(t)}{T_2} \\ \frac{-[M_z^*(t) - M_{eq}^*]}{T_1} \end{pmatrix} \tag{25}$$

which can be solved to give

$$\begin{pmatrix} M_x^*(t) \\ M_y^*(t) \\ M_z^*(t) \end{pmatrix} = \begin{pmatrix} [M_x^*(0)\cos\Omega t - M_y^* \sin\Omega t] e^{\frac{-t}{T_2}} \\ [M_y^*(0)\cos\Omega t + M_x^* \sin\Omega t] e^{\frac{-t}{T_2}} \\ M_z^*(0) e^{\frac{-t}{T_1}} + M_{eq}(1 - e^{\frac{-t}{T_1}}) \end{pmatrix} \tag{26}$$

Bloch Equations in the Spherical Reference Frame

The effect of an RF pulse on the bulk magnetization using a spherical basis set is important concept. Assuming we have an arbitrary phase of the pulse ϕ then the effect of the pulse is

$$M^{+1*} = \frac{M^{+1*}(1 + cos\omega_1 t)}{2} - \frac{M_0^* e^{i\phi}(isin\omega_1 t)}{\sqrt{2}} + \frac{M^{-1*} e^{2i\phi}(1 - cos\omega_1 t)}{2} \tag{27}$$

$$M^{0*} = \frac{M^{+1*} e^{-i\phi}(isin\omega_1 t)}{\sqrt{2}} + M_0^* cos\omega_1 t - \frac{M^{-1*} e^{i\phi}(isin\omega_1 t)}{\sqrt{2}} \tag{28}$$

$$M^{-1*} = \frac{M^{+1*} e^{-i2\phi}(1 - cos\omega_1 t)}{2} + \frac{M_0^* e^{-i\phi}(isin\omega_1 t)}{\sqrt{2}} + \frac{M^{+1*}(1 + cos\omega_1 t)}{2} \tag{29}$$

or more simply

$$M^{p_i *} = \sum_{p_f=-1}^{1} x_{p_i,p_f}(t) M^{p_f *} e^{-i\Delta p\phi} \tag{30}$$

where $x_{p_0,p_1}(t)$ is the efficiency of the transfer of magnetization of from pi to pf and $\Delta p = p_f - p_i$

The evolution of the magnetization when we consider the effects of relaxation then

$$M^{p*} = y(t) M^{p*} e^{ip\Omega t} \tag{31}$$

where y(t) is the decay of the coherence.

References

- http://bouman.chem.georgetown.edu/nmr/bloch/bloch.htm
- http://mrsrl.stanford.edu/~brian/bloch/
- www.chm.davidson.edu/vce/NMR/...Equations.html
- comp.uark.edu/~jgeabana/blochapps/index.html

Bloch Equations is shared under a CC BY-NC-SA 4.0 license and was authored, remixed, and/or curated by LibreTexts.

- **Bloch Equations** by Derrick Kaseman is licensed CC BY 4.0.

Larmor Precession

When placed in a magnetic field, charged particles will precess about the magnetic field. In NMR, the charged nucleus, will then exhibit precessional motion at a characteristic frequency known as the Larmor Frequency. The Larmor frequency is specific to each nucleus. The Larmor frequency is measured during the NMR experiment, as it is dependent on the magnetic field that the nucleus experiences.

Spinning Top Analogy

Often it is difficult in NMR to understand the microscopic processes that are occurring. However, precession is easily observed on the macroscopic scale, as toy tops. When a top is spun, it rotates about a central axis (Figure 1). The angular momentum of the top (L) is aligned along this central axis. If the top is set at an angle, the central axis will move in a circle. The top now spinning along its own central axis precesses around in a circle around earths gravitational field.

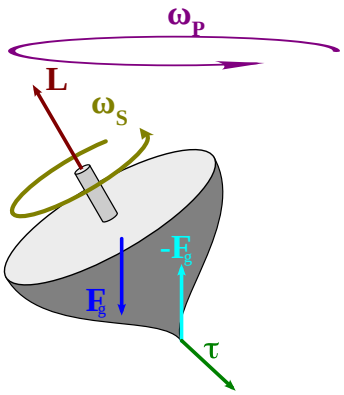


Figure 1: This diagram explains the precession of a top. The torque created by the force of gravity applied at the center of gravity and the reactive force applied where the top touches the table causes the top to precess. (CC BY-SA 2.5 Generic; Xavier Snelgrove via Wikipedia).

Atomic nuclei contain intrinsic spin. The nucleus, like a top, will spin along an axis, which is the direction of the angular momentum for the nucleus. The spin of the nucleus can be related to the magnetic moment of the nucleus through the relation

$$\mu = \gamma I \tag{1}$$

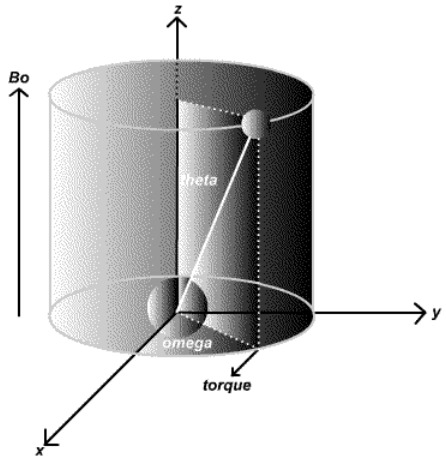
where

- μ is the magnetic moment and
- γ is a proportionality constant known as the gyromagnetic moment.

This constant may be positive of negative, depending on if the nucleus precesses clockwise or counterclockwise, respectively. The nuclear magnetic moment will couple to the external magnetic field, which produces a torque on the nucleus and causes the precession around the magnetic field. This is analogous to the macroscopic tops in that the gravitational force couples with the mass of the top. In the absence of friction, the top would precess forever! The frequency of precession is known as the **Larmor frequency**, ν_0 where

$$\nu_0 = \gamma B_0 \tag{2}$$

The effect is illustrated below:



Ensemble Effects

The net magnetization for a sample is the sum of the individual magnetic moments in the sample

$$M = \sum_i \mu_i \tag{3}$$

we have already defined the magnetic moment for a nucleus with spin I. The magnetization can then be written as

$$M = \gamma J \tag{4}$$

where J is the net spin angular momentum.

The torque, T, of the sample will then be

$$T = \frac{dJ}{dt} \tag{5}$$

Subsituting M for J we obtain

$$T = M \times B \tag{6}$$

and finally

$$\frac{dM}{dt} = \gamma M \times B \tag{7}$$

then

$$\frac{dM}{dt} = \gamma M B sin\theta \tag{8}$$

since M and B are parallel the sin term drops out. We want to know the rate at which the magnetization is changing with respect to time so we take the second derivative and the result is the Larmor frequency

$$\omega_0 = \gamma B \tag{9}$$

since M and B are both vector quantities, the cross product with B in only the Z direction i.e. (B=(0, 0, B_0)) then we obtain the Larmor frequency

$$\omega_0 = \gamma B_0 \tag{10}$$

References

1. Duer, M.J., *Solid State NMR Spectroscopy: Principles and Applications*. Blackwell Science Ltd. USA. 2002
2. Fukushima, E., Roeder, S.B.W., *Experimental Pulse NMR A Nuts and Bolts Approach*. Perseus Books Publishing, USA. 1981

Larmor Precession is shared under a CC BY-NC-SA 4.0 license and was authored, remixed, and/or curated by LibreTexts.

- **Larmor Precession** by Derrick Kaseman is licensed CC BY 4.0.

NMR Interactions

When an atomic nucleus is placed in a magnetic field, the ground state will split into different energy levels proportional to the strength of the magnetic field. This effect is known as Zeeman splitting. While the Zeeman interaction is useful for identifying different types of nuclei placed in magnetic fields, structural and dynamic information may be obtained by considering other magnetic and electronic interactions coupling with the nucleus. These interactions are perturbations to the Zeeman interaction. The full NMR Hamiltonian may therefore be expressed as

$$\hat{H} = \hat{H}_{Zeeman} + \hat{H}_J + \hat{H}_{CS} + \hat{H}_{DD} + \hat{H}_Q \tag{1}$$

where H_{Zeeman} is the Zeeman interaction, H_J is the J coupling, H_{CS} is the chemical shift coupling, H_{DD} is the dipolar coupling, and H_Q is the quadrupolar coupling. The relative magnitude of these interactions is shown in the table below. The Zeeman interaction is the largest, followed by the quadrupolar interactions which are on the order of MHz. The chemical shift and the dipolar coupling are on the order of kHz while the scalar coupling is the smallest which is only tens of Hz. Clearly, some of these interactions are more pronounced than others.

Interaction	Magnitude (Hz)
Zeeman	10^8
Quadrupolar	10^6
Chemical Shift	10^3
Dipole	10^3
J	10

Table 1. *Magnitude of different NMR interactions*

In the liquid state, the dipolar and anisotropic contribution to the chemical shift are averaged due to the molecular reorientation occurring in liquids. The averaging of these interactions gives the characteristically narrow isotropic peaks. Additionally, liquid state NMR primarily looks at spin $^1/_2$ nuclei (^{13}C , ^{1}H) which eliminates any quadrupole interactions. Only the J coupling and isotropic part of the chemical shift remains. In the solid state, molecular reorientation does not occur and the solids may have a variety of bond lengths and angles of a given chemical site. These factors broaden in the NMR spectrum with the broadest peaks over 1MHz wide!

NMR Interactions is shared under a CC BY-NC-SA 4.0 license and was authored, remixed, and/or curated by LibreTexts.

- **NMR Interactions** by Derrick Kaseman is licensed CC BY 4.0.

Quantum Mechanic Treatment

Introduction

NMR employs strong magnetic field which interact with the intrinsic spin of the nucleus to form degenerate energy levels. Treating this phenomenon classically is mathematically tedious and/or impossible. Here we outline the fundamentals of NMR in quantum mechanical terms.

Zeeman Interaction

If we begin with the historical Schrödinger equation

$$H|\psi\rangle = E|\psi\rangle \tag{1}$$

we can immediately realize that by defining the Hamiltonian of the system will result with an corresponding energy level of the wave function.

The Hamiltonian for a magnetic vector ($\vec{\mu}$ in J/T)in a magnetic field (also a vector), ($\vec{B}$ in T) is given by the expression

$$H = -\vec{\mu} \cdot \vec{B} \tag{2}$$

We then see that the Hamiltonian has units of energy (J). Therefore operating the Hamiltonian on a wavefinction will result in an energy eigenvalue! We can further refine the Hamiltonian by relating the magnetic moment of a nucleus to the particles angular momentum ari\sing from the intrinsic spin, I, of the nucleus thus

$$\vec{\mu} = -\gamma \vec{I} \tag{3}$$

where gamma is the ratio of the angular momentum to the magnetic moment. Then the Hamiltonian may be rewritten as

$$H = -\gamma \vec{I} \cdot \vec{B} \tag{4}$$

Assuming that the magnetic field lies along the Z-axis, then

$$H_z = -\gamma(I_x \hat{i} + I_y \hat{j} + I_z \hat{k}) \cdot (B_0 \hat{k}) = -\gamma B_0 I_z = -\omega_0 I_z \tag{5}$$

where ω_0 is the Larmor frequency. Therefore if the $|\psi\rangle$ is an eigenfunction of H then the $|\pm\rangle$ spin states are eigenfunctions of the total and z-component of angular momentum. We can describe this is three ways in a DC magnetic field:

Operator:

$$H_z|+\rangle = -\omega_0 I_z|+\rangle = -\frac{\omega_0}{2}|+\rangle \tag{6}$$

$$H_z|-\rangle = -\omega_0 I_z|-\rangle = -\frac{\omega_0}{2}|-\rangle \tag{7}$$

Matrix:

$$H_z = \tag{8}$$

Energy Level

Insert picture

These representations rely on the fact that spin states are eigenfunctions of the angular momentum and therefore have the following properties, with I and m defining the state of the system.

$$I^2|I,m\rangle = I(I+1)|I,m\rangle \tag{9}$$

$$I_z|I,m\rangle = m|I,m\rangle \tag{10}$$

$$I_{+1}|I,m\rangle = -\sqrt{\frac{1}{2}(I(I+1) - m(m+1))}\,|I,m_{+1}\rangle \tag{11}$$

$$I_{-1}|I,m\rangle = \sqrt{\frac{1}{2}(I(I+1) - m(m-1))}\,|I,m_{-1}\rangle \tag{12}$$

where

$$I_x = \frac{1}{\sqrt{2}}(I_{+1} - I_{-1}) \tag{13}$$

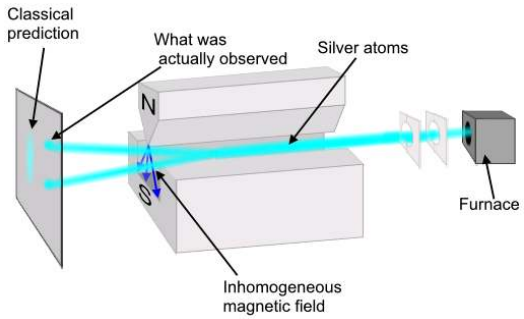
$$I_y = \frac{i}{\sqrt{2}}(I_{+1} + I_{-1}) \tag{14}$$

Note that in contrast to the harmonic oscillator, the $|I, m\rangle$ spin basis is orthogonal and complete. This means for the spin I, there are only $2I+1$ spin states and the the overlap integral $\langle I, m|I', m'\rangle = \delta_{mm'}\delta_{II'}$ holds. This formalism holds equally well for $I > 1/2$ particles as well.

Effects of Radio Frequency

While it is relatively straightforward to understand the Zeeman interaction, understanding the effects of radio frequency pulses on the Hamiltonian needs careful consideration. To examine this we will look at a modification to the Stern-Gerlach experiment made by Rabi in the 1930's.

\since no one has bothered to discuss the Stern Gerlach experiment in any detail on the chemwiki a brief glimpse into the initial experiment is necessary. Essentially a beam of silver atoms was shot through a magnetic field and instead of a \single line of atoms or \single spot, depending on the dispersion of the atoms, two spots were observed. This of course was due to the the fact that Zeeman splitting had occurred due to silvers spin=1/2 nature. A figure is provided below for reference.



Rabi modified this experiment by adding a coil of wire which generated a magnetic field perpendicular to the applied magnetic field from the stern gerlach experiment. By selecting only 1 of the nuclei either +/- 1/2 and running these particles through the radio frequency coil Rabi noted a characteristic nutation of the magnetization shown below.

insert figure

We can see then that the number of particles appearing on the screen is characterisitc of the frequency. This behavior is denoted as the Rabi or nutation frequency. This experiment serves as a good bridge into the NMR experiment. First, we must calculate the appropriate Hamiltonian for the sitation. We have two magnetic fields, one is the large external magnetic field which splits the degenerate ground states into energy levels, and the second is the osciallting magnetic field from the coil. As such the magnetic field experienced by the spins is

$$\vec{B} = B_0\hat{k} + 2B_1\cos(\omega_0 t)\hat{i} \tag{15}$$

Here we define the coil to be along the x direction and the external magnetic field about the z direction. \since the field is oscillating in time, a \co\sine function is the appropriate choice to model the behavior of this magnetic field.

We may now express the Hamiltonian in eith operator or matrix form as

$$H = -\gamma\vec{I}\cdot\vec{B} = -\gamma B_0 I_z - 2\gamma B_1\cos(\omega_o t)I_x = -\omega_0 I_z - 2\omega_1\cos(\omega_0 t)I_x \tag{16}$$

insert matrix here.

We now see that our Hamiltonian become time dependent. In order to solve the observation made by Rabi we must use the time depedent Schrödinger equation.

$$\frac{d}{dt}|\psi(t)\rangle = -iH(t)|\psi(t)\rangle \tag{17}$$

where H(t) is in frequency units and |ψ(t=0)>=|+>. Assuming that the Hamiltonian is time independent we can use a time dependent unity operator $\hat{U}$ defined as

$$|\psi(t)\rangle = \hat{U}(t)|\psi(0) > \tag{18}$$

$$\hat{U}(t) = e^{-iHt} \tag{19}$$

that transforms the initial wavefunction |ψ (0)>to a wavefunction at a given time |ψ (t) \rangle.

insert figure

This issue with the case above is that we assumed the Hamiltonian is time-independent, which is clearly not the our case. Therefore, we need to solve this problem by transforming the time-dependent Schrödinger equation into a reference frame that renders the Hamiltonian time independent.

Consider the development of the time evolution of |Q(t) \rangle under the following conditions

$$|\psi(t)\rangle = R(t)|Q(t)\rangle \tag{20}$$

$$Q(t)\rangle = R^{+}(t)|\psi(t)\rangle \tag{21}$$

$$R(t)R^{+}(t) = R^{+}(t)R(t) = 1 \tag{22}$$

As you can see R commutes and the adjoint give the unity operator. We can then rewrite the Schrödinger equation as

$$\frac{d}{dt}|\psi(t)\rangle = \frac{d}{dt}R(t)|Q(t)\rangle = [\frac{d}{dt}R(t)]|Q(t)\rangle + R(t)\frac{d}{Dt}|Q(t)\rangle \tag{23}$$

$$= -iH(t)|\psi(t)\rangle = -iH(t)R(t)|Q(t)\rangle \tag{24}$$

Mow if we multiple both sides of the equation by the adjoint then we can rearrange to obtain a new form of the Schrödinger equations

$$[R^{+}(t)\frac{d}{dt}R(t)]|Q(t)\rangle + \frac{d}{dt}|Q(t)\rangle = -iR^{+}(t)H(t)R(t)|Q(t)\rangle \tag{25}$$

$$\frac{d}{dt}|Q(t)\rangle = -iH_{int}(t)|Q(t)\rangle \tag{26}$$

where

$$H_{int} = R^{+}(t)H(t)R(t) - iR^{+}(t)\frac{d}{dt}R(t) \tag{27}$$

To apply this to our situation consider the case where

$$R(t) = e^{-iH_{z}t} = e^{i\omega_{0}I_{z}t} \tag{28}$$

$$R^{+} = e^{-i\omega_{0}I_{z}t} \tag{29}$$

Then we can develop the following Identities

$$R(t) = \begin{bmatrix} e^{\frac{i\omega_{0}t}{2}} & 0 \\ 0 & e^{\frac{-i\omega_{0}t}{2}} \end{bmatrix} \tag{30}$$

$$R^{\dagger}(t) = \begin{bmatrix} e^{\frac{-i\omega_{0}t}{2}} & 0 \\ 0 & e^{\frac{i\omega_{0}t}{2}} \end{bmatrix} \tag{31}$$

in which we can easily take derivitives of leading to

$$\frac{d}{dt}R(t) = \begin{bmatrix} \frac{d}{dt}e^{\frac{i\omega_0 t}{2}} & 0 \\ 0 & \frac{d}{dt}e^{\frac{-i\omega_0 t}{2}} \end{bmatrix} \tag{32}$$

$$\frac{d}{dt}R(t) = \begin{bmatrix} \frac{i\omega_0}{2}e^{\frac{i\omega_0 t}{2}} & 0 \\ 0 & \frac{-i\omega_0}{2}e^{\frac{-i\omega_0 t}{2}} \end{bmatrix} \tag{33}$$

$$\frac{d}{dt}R(t) = i\omega_0 \begin{bmatrix} \frac{1}{2} & 0 \\ 0 & \frac{1}{2} \end{bmatrix} \cdot \begin{bmatrix} e^{\frac{i\omega_0 t}{2}} & 0 \\ 0 & e^{\frac{-i\omega_0 t}{2}} \end{bmatrix} \tag{34}$$

$$\frac{d}{dt}R(t) = i\omega_0 I_z \cdot e^{i\omega_0 t I_z} \tag{35}$$

We can also calculate

$$R^\dagger(t) I_x R(t) = \begin{bmatrix} e^{\frac{-i\omega_0 t}{2}} & 0 \\ 0 & e^{\frac{i\omega_0 t}{2}} \end{bmatrix} \cdot \begin{bmatrix} 0 & \frac{1}{2} \\ \frac{1}{2} & 0 \end{bmatrix} \cdot \begin{bmatrix} e^{\frac{i\omega_0 t}{2}} & 0 \\ 0 & e^{\frac{-i\omega_0 t}{2}} \end{bmatrix} \tag{36}$$

$$R^\dagger(t) I_x R(t) = \begin{bmatrix} 0 & \frac{1}{2}e^{\frac{-i\omega_0 t}{2}} \\ \frac{1}{2}e^{\frac{i\omega_0 t}{2}} & 0 \end{bmatrix} \tag{37}$$

$$R^\dagger(t) I_x R(t) = \cos\omega t \begin{bmatrix} 0 & \frac{1}{2} \\ \frac{1}{2} & 0 \end{bmatrix} + \sin\omega t \begin{bmatrix} 0 & \frac{-i}{2} \\ \frac{i}{2} & 0 \end{bmatrix} = \cos\omega_0 t I_x + \sin\omega_0 t I_y \tag{38}$$

Similarly we can show (left as an exercise for the reader)

$$R^\dagger(t) I_x R(t) = \cos\omega_0 t I_y - \sin\omega_0 t I_x \tag{39}$$

We now have all the pieces we need to solve the Hamiltonian. We will show this in multiple ways

Matrix Approach

$$R^\dagger(t)\frac{d}{dt}R(t) = \begin{bmatrix} e^{\frac{-i\omega_0 t}{2}} & 0 \\ 0 & e^{\frac{i\omega_0 t}{2}} \end{bmatrix} \cdot \begin{bmatrix} \frac{i\omega_0}{2}e^{\frac{i\omega_0 t}{2}} & 0 \\ 0 & \frac{-i\omega_0}{2}e^{\frac{-i\omega_0 t}{2}} \end{bmatrix} = \begin{bmatrix} \frac{i\omega_0}{2} & 0 \\ 0 & \frac{-i\omega_0}{2} \end{bmatrix} \tag{40}$$

$$\begin{aligned} R^\dagger(t)H(t)R(t) &= \begin{bmatrix} e^{\frac{-i\omega_0 t}{2}} & 0 \\ 0 & e^{\frac{i\omega_0 t}{2}} \end{bmatrix} \cdot \begin{bmatrix} \frac{-\omega_0}{2} & -\omega_1\cos\omega_0 t \\ -\omega_1\cos\omega_0 t & \frac{\omega_0}{2} \end{bmatrix} \cdot \begin{bmatrix} e^{\frac{i\omega_0 t}{2}} & 0 \\ 0 & e^{\frac{-i\omega_0 t}{2}} \end{bmatrix} \\ &= \begin{bmatrix} \frac{-\omega_0}{2} & -\omega_1\cos\omega_0 t e^{-i\omega_0 t} \\ -\omega_1\cos\omega_0 t e^{i\omega_0 t} & \frac{\omega_0}{2} \end{bmatrix} \end{aligned} \tag{41}$$

Then

$$H_{int} = -\omega_1 \begin{bmatrix} 0 & 1/2 \\ 1/2 & 0 \end{bmatrix} - \omega_1 \cos 2\omega_0 t \begin{bmatrix} 0 & 1/2 \\ 1/2 & 0 \end{bmatrix} - \omega_1 \sin 2\omega_0 t \begin{bmatrix} 0 & -i/2 \\ i/2 & 0 \end{bmatrix} \tag{42}$$

$$H_{int} = \omega_1 I_x - \omega_1 \cos 2\omega_0 t I_x - \omega_1 \sin 2\omega_0 t I_y \tag{43}$$

Operator Approach

We now wish to solve the Hamiltonian u\sing the I operators we have defined previously.

$$R^{\dagger}(d)\frac{d}{dt}R(t) = e^{-i\omega_0 I_z} \cdot i\omega_0 I_z \cdot e^{i\omega_0 I_z} = i\omega_0 I_z \tag{44}$$

$$R^{\dagger}(t)H(t)R(t) = e^{-i\omega_0 I_z}(-\omega_0 I_z - 2\omega_1 I_x)e^{i\omega_0 I_z} \tag{45}$$

$$= -\omega_0 I_z - 2\omega_1 \cos\omega_0 t I_x E^{i\omega_0 t I_z} I_x e^{-i\omega_o t I_z} \tag{46}$$

$$= -\omega_0 I_z - 2\omega_1 \cos^2 \omega_0 t I_x - 2\omega_1 \cos\omega_0 t \sin\omega_0 t I_y \tag{47}$$

$$= -\omega_0 I_z - \omega_1 I_x - \omega_1 \cos 2\omega_0 t I_x - \omega_1 \sin 2\omega_0 t I_y \tag{48}$$

$$H_{int}(t) = -\omega_1 I_x - \omega_1 \cos 2\omega_0 t I_x - \omega_1 \sin 2\omega_0 t I_y \tag{49}$$

This is the exact expression we obtained u\sing the matrix approach!

Rotating Wave Approximation

It can be shown that the time dependent part of the Hamiltonian modifies the first term in the above equation by $\frac{\omega_1^2}{\omega_0}$ (Need to prove this). Standard NMR spectrometers typically output ω_1 on the order of kHz, whereas the larmor frequency is on the order of MHz and we can neglect the time department part of the Hamiltonian. This is known as the Rotating Wave Approximation. The Hamiltonian becomes

$$H_{int} = -\omega_1 I_x = -\omega_1 \begin{bmatrix} 0 & \frac{1}{2} \\ \frac{1}{2} & 0 \end{bmatrix} \tag{50}$$

We now need to find the describe the initial state of the system

$$|Q(0)> = R^{\dagger}(t=0) > = \begin{bmatrix} 1 & 0 \\ 0 & 1 \end{bmatrix} \begin{pmatrix} 0 \\ 1 \end{pmatrix} = \begin{pmatrix} 0 \\ 1 \end{pmatrix} \tag{51}$$

Now we if we diagonalize the matrix then we can find the state of the system at any time t. The diagonalized Hamiltonian is then

$$U(t) = \begin{bmatrix} \cos\frac{\omega_1 t}{2} & i\sin\frac{\omega_1 t}{2} \\ i\sin\frac{\omega_1 t}{2} & \cos\frac{\omega_1 t}{2} \end{bmatrix} \tag{52}$$

We can now evaluate |Q(t) \rangle as \Q(t) \rangle=U(t)|Q(0)

$$|Q(t)\rangle = \begin{bmatrix} \cos\frac{\omega_1 t}{2} & i\sin\frac{\omega_1 t}{2} \\ i\sin\frac{\omega_1 t}{2} & \cos\frac{\omega_1 t}{2} \end{bmatrix} \begin{pmatrix} 0 \\ 1 \end{pmatrix} = \begin{bmatrix} i\sin\frac{\omega_1 t}{2} \\ \cos\frac{\omega_1 t}{2} \end{bmatrix} \tag{53}$$

Finally recognizing that $|\Psi(t)\rangle$=R(t)|Q(t). There for

$$|\Psi(t)\rangle = \begin{bmatrix} e^{\frac{i\omega_0 t}{2}} & 0 \\ 0 & e^{\frac{-i\omega_0 t}{2}} \end{bmatrix} \begin{bmatrix} i\sin\frac{\omega_1 t}{2}/ \\ cos\frac{\omega_1 t}{2} \end{bmatrix} = \begin{bmatrix} i\sin\frac{\omega_1 t}{2} e^{\frac{i\omega_0 t}{2}} \\ \cos\frac{\omega_1 t}{2} e^{\frac{-i\omega_0 t}{2}} \end{bmatrix} \tag{54}$$

$$= i\sin\frac{\omega_1 t}{2} e^{\frac{i\omega_0 t}{2}} |-\rangle + \cos\frac{\omega_1 t}{2} e^{\frac{-i\omega_0 t}{2}} |+> \tag{55}$$

$$= c_-(t)|-\rangle + c_+(t)|+> \tag{56}$$

The probability that Rabi obsereved is given by multiplying the complex congugates which are calculated as

$$P_{|-\rangle} = \frac{1}{2} - \frac{1}{2}\cos\omega_1 t \tag{57}$$

$$P_{|+>} = \frac{1}{2} + \frac{1}{2}\cos\omega_1 t \tag{58}$$

The Hamiltonian we found to govern Rabi's experiment is the exact Hamiltonian used in the NMR experiment, with two slight modifications. First, Rabi was able to select an initial state, while in NMR we have a thermal equilibrium population. Secondly we measure a transverse magnetization instead of |+> and |-\rangle.

Liouville Von Neumann Equation

\since we are dealing with a system that can be described by both a statistical and quantum mechanical aspects, we need a way to unify these descriptions. The solution is the Liouville-von Neumann equation, which describes how the density operator evolves in time. More specifically, it describes the time evolution of a mixed state, which is directly applicable to NMR, as we want to know how the off-diagonal elements of the density matrix evolve after an applied RF. The density matrix is evolving in time, thus we must derive a differential equation to describe this behavior then integrate it with each step of the NMR experiment. As usual we begin with the time-dependent Schroedinger Equation.

$$i\bar{h}\frac{d}{dt}\Psi(t) = H(t)\Psi(t) \tag{59}$$

Lets also look at the thermal equilibrium of the spins. U\sing Boltzmann statistics the initial condition of our spins is described by

$$c_+(0)c_+^*(0) = \frac{Ne^{-\frac{E_+}{kT}}}{Z} \tag{60}$$

$$c_-(0)c_-^*(0) = \frac{Ne^{-\frac{E_-}{kT}}}{Z} \tag{61}$$

where

$$Z = [e^{-\frac{E_-}{kT}} + e^{-\frac{E_+}{kT}} \tag{62}$$

and

$$c_+(0)c_-^*(0) = 0 \tag{63}$$

$$c_-(0)c_+^*(0) = 0 \tag{64}$$

Defining

$$|\Psi(t)\rangle = c_+(t)\backslash + > + c_-(t)|-\rangle \tag{65}$$

\[\langle \Psi(t)|=c^*_+(t)\langle+| +c^*_-(t)<-|\

we immediately realize that we have a density operator!

$$\rho(t) = |\Psi(t)\rangle < \Psi(t)| = c_+(t)c_+^*(t)\backslash + > \langle +| + c_-(t)c_-^*(t)|-\rangle < -| + c_+(t)c_-^*(t)|+ >< -| + c_-(t)c_+^*(t)|-\rangle\langle +| \tag{66}$$

Then the time evolution is

$$\frac{d}{dt}\rho(t) = \frac{d}{dt}|\Psi(t)\rangle < \Psi(t)| + |\Psi(t)\rangle\frac{d}{dt} < \Psi(t)| = -iH(t)|\Psi(t)\rangle < \Psi(t)| + i|\Psi(t)\rangle < \Psi(t)|H(t) \tag{67}$$

which gives the Liouville-von Neumann Equation as

$$\frac{d}{dt}\rho(t) = i[H(t), \rho(t)] \tag{68}$$

Lets now look at how this evolves in a simples NMR experiment.

Initially we can define the density matrix at thermal equilibrium as

$$\rho(0) = \begin{bmatrix} c_+(0)c_+^*(0) & c_+(0)c_-^*(0) \\ c_-(0)c_+^*(0) & c_-(0)c_-^*(0) \end{bmatrix} = \frac{1}{Z}\begin{bmatrix} e^{-\frac{E_+}{kT}} & 0 \\ 0 & e^{-\frac{E_-}{kT}} \end{bmatrix} \tag{69}$$

High Temperature Approximation

We can further refine the inital density operator by substituting in the equations for the energy levels E_+ and E_-.

$$E_(\pm) = \mp\frac{\bar{h}\omega_0}{2} \tag{70}$$

but \since we know the kT>>ω_0 then we can use a high temperature approximation of

$$e^{\pm\frac{\bar{h}\omega_0}{2kT}} = 1 \pm \frac{\bar{h}\omega_0}{2kT} \tag{71}$$

ans

$$Z = 2 \tag{72}$$

resulting in a new density operator as

$$\rho(0)\begin{bmatrix} \frac{1}{2} + \frac{\bar{h}\omega_0}{2kT} & 0 \\ 0 & \frac{1}{2} - \frac{\bar{h}\omega_0}{2kT} \end{bmatrix} = \frac{N}{2}1 + \frac{N\bar{h}\omega_0}{2kT}I_z \tag{73}$$

Normally the magnetization constant is taken to be a scaling factor and the unity operator is invariant to applied fields which firther reduces the density matrix to

$$\rho(0) = I_z \tag{74}$$

NMR Observables

In a simple NMR experiment, the magnetization along the externally applied magnetix field is knocked into the x-y plane u\sing a rf pulse. As the spins recover along the external field direction (z direction) they precess near their Larmor frequencies through a coil which in turn produces an EMF. In order for an EMF to be generated the preces\sing magnetization must be perpendicular to the coil. According the Kirchoff

$$EMF = -\mu_0\eta A\frac{d}{dt}M_x \tag{75}$$

as is immediatley evident the magnetizaion is time dependent and our problem is essentially reduced to

$$M_x(t) =< T_x >=< \Psi(t)|I_x|\Psi(t)\rangle \tag{76}$$

which is the expectation value of I_x. If instead we consider a generic operator <O> then

$$|\Psi(t)\rangle = \sum_n c_n(t)|n> \tag{77}$$

$$< \Psi(t)| = \sum_n c_n^*(t) < n| \tag{78}$$

$$< O >=< \Psi(t)|O|\Psi(t)\rangle = \sum_{n,m} c_n(t)c_m^*(t) < m|O|n > \tag{79}$$

and recalling that

$$< n|\rho(t)|m >= c_n(t)c_m^*(t) \tag{80}$$

results in

$$< O > \sum_{n,m} < n|\rho(t)|m >< m|O|n >= Tr[\rho(t)O] \tag{81}$$

Now for M_x

$$M_x =< I_x >= TR[I_x\rho(t) \tag{82}$$

$$\rho(t) = I_z \tag{83}$$

$$H(t) = -\omega_0 I_z - 2\omega_1 \cos\omega_0 t I_x \tag{84}$$

Then all we need to do is calculate $\rho(t)$ and <I_x>!

Matrix Approach

Like we did in the above treatment for the roatating wave, we need to move $\rho(t)$ into a different representation.

$$\sigma(t) = R^\dagger(t)\rho(t)R(t) \tag{85}$$

$$\rho(t) = R(t)\sigma(t)R^\dagger(t) \tag{86}$$

$$\frac{d}{dt}\sigma(t) = -iH[H_{int}, \sigma(t)] \tag{87}$$

and remembering that

$$R(t) = e^{i\omega_0 t I_z} \tag{88}$$

$$\sigma(0) = \rho(0) \tag{89}$$

We get

$$U(t) = \begin{bmatrix} \cos\frac{\omega_1 t}{2} & i\sin\frac{\omega_1 t}{2} \\ i\sin\frac{\omega_1 t}{2} & \cos\frac{\omega_1 t}{2} \end{bmatrix} \tag{90}$$

$$U^\dagger(t) = \begin{bmatrix} \cos\frac{\omega_1 t}{2} & -i\sin\frac{\omega_1 t}{2} \\ -i\sin\frac{\omega_1 t}{2} & \cos\frac{\omega_1 t}{2} \end{bmatrix} \tag{91}$$

which gives

$$\sigma(t) = U(t)\sigma(0)U^\dagger(t) \tag{92}$$

$$= \begin{bmatrix} \cos\frac{\omega_1 t}{2} & i\sin\frac{\omega_1 t}{2} \\ i\sin\frac{\omega_1 t}{2} & \cos\frac{\omega_1 t}{2} \end{bmatrix} \begin{bmatrix} \frac{1}{2} & 0 \\ 0 & \frac{1}{2} \end{bmatrix} \begin{bmatrix} \cos\frac{\omega_1 t}{2} & -i\sin\frac{\omega_1 t}{2} \\ -i\sin\frac{\omega_1 t}{2} & \cos\frac{\omega_1 t}{2} \end{bmatrix} = \frac{1}{2}\begin{bmatrix} \cos\omega_1 t & -i\sin\omega_1 t \\ -i\sin\omega_1 t & \cos\omega_1 t \end{bmatrix} \tag{93}$$

Now we can use $\sigma(t)$ to find $\rho(t)$.

$$\rho(t) = R(t)\sigma(t)R^\dagger(t) = \frac{1}{2}\begin{bmatrix} e^{\frac{i\omega_0 t}{2}} & 0 \\ 0 & e^{\frac{-i\omega_0 t}{2}} \end{bmatrix} \begin{bmatrix} \cos\omega_1 t & -i\sin\omega_1 t \\ -i\sin\omega_1 t & \cos\omega_1 t \end{bmatrix} \begin{bmatrix} e^{\frac{-i\omega_0 t}{2}} & 0 \\ 0 & e^{\frac{i\omega_0 t}{2}} \end{bmatrix} \tag{94}$$

$$= \begin{bmatrix} \cos\omega_1 t & -i\sin\omega_1 t e^{i\omega_0 t} \\ -i\sin\omega_1 t e^{-i\omega_0 t} & \cos\omega_0 t \end{bmatrix}$$

Now lets look at the observables I_x and I_y.

$$< I_x >= TrI_x\rho(t) = Tr\begin{bmatrix} 0 & 1/2 \\ 1/2 & 0 \end{bmatrix} \begin{bmatrix} \cos\omega_1 t & -i\sin\omega_1 t e^{i\omega_0 t} \\ -i\sin\omega_1 t e^{-i\omega_0 t} & \cos\omega_1 t \end{bmatrix} \tag{95}$$

$$= \frac{sin\omega_1 t sin\omega_0 t}{2} \tag{96}$$

Then <I_y> is

$$< I_y >= \frac{sin\omega_1 t cos\omega_0 t}{2} \tag{97}$$

And <I_z> is

$$< I_z >= \frac{cos\omega_1 t}{2} \tag{98}$$

Operator Approach

Alternatively we can use the operator approach, which is much less mathemtically intensive.

$$\sigma(0) = \rho(0) = I_z \tag{99}$$

$$H_{int} = -\omega_1 I_x \tag{100}$$

$$\sigma(t) = e^{-iH_{int}t}\sigma(0)e^{iH_{int}t} = cos\omega_1 t I_z + sin\omega_1 t I_y \tag{101}$$

$$\rho(t) = R(t)\sigma(t)R^{\dagger}(t) = cos\omega_1 t I_z + sin\omega_1 t cos\omega_0 t I_y + sin\omega_1 t sin\omega_0 t I_x \tag{102}$$

Using

$$Tr[I_n I_m] = \frac{1}{2}\delta_{nm} \tag{103}$$

we obtain the same expectation values as before.

Quantum Mechanic Treatment is shared under a CC BY-NC-SA 4.0 license and was authored, remixed, and/or curated by LibreTexts.

- **Quantum Mechanic Treatment** by Derrick Kaseman is licensed CC BY-NC-SA 4.0.

Relaxation

Relaxation in NMR is a fundamental concept which describes the coherence loss of the magnetization in the x-y plane and the recovery of relaxation along the z-axis. One can easily imagine that in the absence of any other effects, the magnetization in the x-y plane will recover along the z-axis as the external magnetic field forces the spins to align with it. This is known as T_1 relaxation. The loss of coherence of the magnetization in the x-y plane is due to spins "forgetting" their orientation with respect to the bulk magnetization. This is known as T_2 relaxation. There are many factors that contribute to the relaxation processes. This page will examine the different types of relaxation at a basic level. For those interested in a deeper discussion please see article on T_1 and T_2 relaxation.

T_1 Relaxation

T_1 relaxation, also known as spin lattice or longitudinal relaxation is the time constant used to describe when ~63% of the magnetization has recovered to equilibrium. The T_1 of a given spin is dictated by field fluctuations (both magnetic and electric) that occur in the sample. Consequently, T_1 measurements can tell us important information regarding inter and intra molecular dynamics of the system. Several factor may cause this alternating field: molecular motion, J-Coupling, Dipolar Coupling, Chemical Shift Anisotropy, and quadrupole-phonon interactions.

We can also look at relaxation from the energy level standpoint. Initially, we have a Boltzmann distribution of spins in the (For I=1/2) in two energy levels, with the lower energy level slightly more populated than the higher energy level. After a pulse these spin populations are inverted and now the higher energy level has more spins in it. Eventually, these spins will go back to their lower energy state due to relaxation. The timescale on which this occurs is T_1.

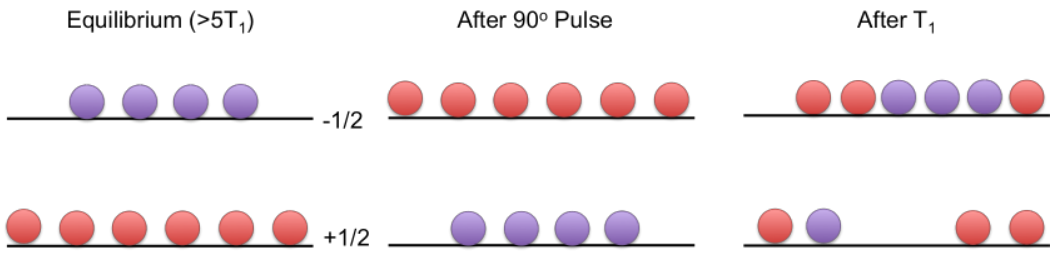


Figure 1: Energy level diagram of T_1 relaxation. Initially, the spins are at equilibrium with the red spins in the +1/2 energy level and the purple spins in the -1/2 energy level. Note that the energy level distribution is grossly exaggerated. After a 90° pulse (center figure), the energy level spin populations switch, where red spins are now in the -1/2 state. After some time T_1, ~60% of the spins have relaxed back to their equilibrium energy levels. After $5T_1$ (left figure) all of the spins have relaxed back to their equilibrium levels.

From the Bloch Equations, we know that magnetization is along the Z-axis is

$$M_z = M_0(1 - \exp\frac{-t}{T_1}) \quad (1)$$

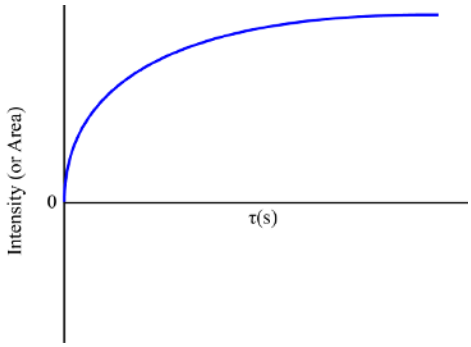


Figure 2: magnetization is along the Z-axis

$T_{1\rho}$ Relaxation

$T_{1\rho}$ is the relaxation of the magnetization during a spin lock. This becomes particularly important in the cross-polarization.

T_2 Relaxation

T_2 relaxation is also known as spin-spin or transverse relaxation. T_2 relaxation involves energy transfer between interacting spins via dipole and exchange interactions. Spin-spin relaxation energy is transferred to a neighboring nucleus. The time constant for this process is called the ***spin-spin relaxation time (T_2)***. The relaxation rate is proportional to the concentration of paramagnetic ions in the sample. This mechanism is largely temperature independent. T_2 values are generally much less dependent on field strength, B, than T_1 values.

In the process of relaxation, the component of magnetization in xy-plane will become zero as M_0 returns to z-axis. Time constant T_2 is used here to describe spin-spin relaxation with the following function. This process involves energy changing between the spin-active and their adjacent nuclei.

$$M_{xy} = M_{xy0} exp \frac{-t}{T_2} \tag{2}$$

T_2* Relaxation

In an ideal NMR spectrometer, the external magnetic field is completely homogeneous. However, all magnets have small inhomegneities in them. Consequently, nuclei experience different magnetic fields which changes the precessional frequency of each nucleus. The change in Larmor frequency results in dphasing in the transverse plane and is known as T_2*

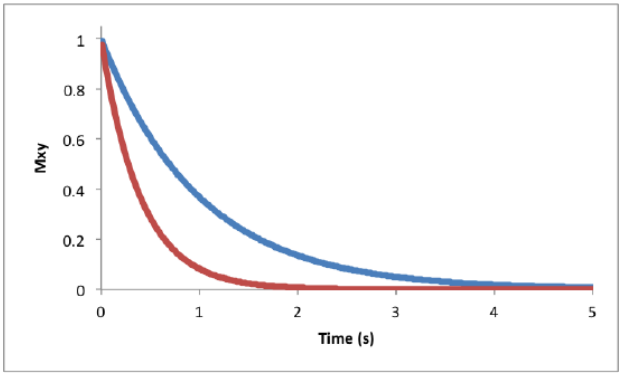


Figure 3: Effect of magnetic field inhomogeneity on the observed T_2. When there is no inhomogeneity, M_{xy} decays at a slower rate T_2 (blue). Usually there is inhomogeneity in the field, which causes the decay of M_{xy} to be faster with the apparent time constant T_2* (red).

Magnetic Field Dependence

So far, we have only described what the relaxation parameters are, but have largely omitted the equations that give us the results. All elaxation measurements are based on the idea of a correlation time, tc. The correlation time is based on the environment that the spin is in. For T_1 relaxation, the correlation time must be on the order of the larmor frequency of the nucleus, while the correlation time for the for T_2 must be on the order of the inverse of the linewidth to make effects. The correlation time are random fluctuations in the magnetic field that couple to the nucleus. The equations that govern T_1 and T_2 are given below with no additional proof..

$$\frac{1}{T_1} = C\left(\frac{t_c}{1+w^2t_c^2} + \frac{2t_c}{1+4w^2t_c^2}\right)$$

$$\frac{1}{T_2} = 3Ct_c\left(\frac{2}{\pi}\right)^{\frac{3}{2}} + \frac{1}{2}$$

where w is the Larmor frequency, and C is a constant that contains temperature and frequency independent terms and defined as....

References

1. Levitt, M. H., Spin Dynamics, Wiley
2. Bloembergen, E.M. Purcell, R.V. Pound "Relaxation Effects in Nuclear Magnetic Resonance Absorption" Physical Review 1948, 73, 679-746
3. www.uthgsbsmedphys.org/GS02-0032/documents/RelaxationMechanisms.pdf

4. http://chem.ch.huji.ac.il/nmr/techniques/other/t1t2/t1t2.html

Problems

1. Derive why only 63% of spins have recovered to equilibrium after T_1

2. Explain the differences between T_1, $T_{1/(rho/)}$,T_2, and T_2*.

Relaxation is shared under a CC BY-NC-SA 4.0 license and was authored, remixed, and/or curated by LibreTexts.

- **Relaxation** by Derrick Kaseman is licensed CC BY 4.0.

Rotations and Irreducible Tensor Operators

Page under construction!

Irreducible Tensor Operators are extremely valuable to help reduce complex mathematical problems commonly found in NMR. This page will be devoted to deriving the tensors and showing how to use the tensors in calculations.

Cartesian Rotations

Irreducible Tensor Operators operate on angular momenta, which is a fairly abstract concept to understand. We begin this discussion by investigating rotations in 2 and 3 dimensions so the reader understands a physical picture before moving into a complex quantum mechanical treatment.

2D Rotations

Let's begin with the simple example of the hand of a clock. The clock hand is a vector which has a magnitude (the length of the hand) and a direction (the direction the arrow is pointing). The vector is rotating in a 2D plane (the clock face). We define our cartesian axes that the y axis lies along 12 and the x axis is along 3 on the clock. Initally, lets say it is 3:00 (t=0) and the vector lies along the x-axis and rotates counter-clockwise, then a some time, (t=2.2hrs) later the vector points along some arbitrary angle theta from the inital x-axis. Taking a snapshot of the vector at this time, we can see that vector a can now be described by

$$\vec{r} = a\hat{i} + b\hat{j} = r\hat{i}\cos(\theta)\hat{j} + r\sin(\theta)\hat{j} \tag{1}$$

insert picture

We can actually describe this vectors position using any arbitrary axis (time) for x and y as long as x and y remain orthogonal. If for example the axes are rotated by ϕ then the vector a time=2.2hrs is

$$\vec{r} = c\hat{i} + d\hat{j} = r\hat{i}\cos(\theta-\phi)\hat{j} + r\sin(\theta-\phi)\hat{j} \tag{2}$$

insert picture

Using the following triognometric identities, we can solve for a ,b, c, and d.

$$\cos(\theta-\phi) = \cos\theta\cos\phi + \sin\theta\sin\phi \tag{3}$$

$$\sin(\theta-\phi) = \sin\theta\cos\phi - \cos\theta\sin\phi \tag{4}$$

the it follows that

$$a = r\cos\theta \tag{5}$$

$$b = r\sin\theta \tag{6}$$

$$c = r\cos(\theta-\phi) = r\cos\theta\cos\phi + r\sin\theta\sin\phi = a\cos\phi + b\sin\phi \tag{7}$$

$$d = r\sin(\theta-\phi) = r\sin\theta\cos\phi - r\cos\theta\sin\phi = b\cos\phi - a\sin\phi \tag{8}$$

From inspection we can see that this can be readily transformed into a matrix

$$\begin{pmatrix} c \\ d \end{pmatrix} = \begin{pmatrix} \cos\phi & \sin\phi \\ -\sin\phi & \cos\phi \end{pmatrix} \begin{pmatrix} a \\ b \end{pmatrix} \tag{9}$$

In other word we can rotate r into r' by applying a rotation trnasformation R or

$$r' = Rr \tag{10}$$

where R has the property

$$RR^{\dagger} = 1 \tag{11}$$

leading to

$$\begin{pmatrix} a \\ b \end{pmatrix} = \begin{pmatrix} \cos\phi & -\sin\phi \\ \sin\phi & \cos\phi \end{pmatrix} \begin{pmatrix} c \\ d \end{pmatrix} \tag{12}$$

3D Rotations

In 3 dimensions rotations are slightly more complex. We need to specify another dimension in which the object can be rotated. In order to do this we need to employ three angles α, β, γ, commonly referred to as the euler angles. α is rotation about the original z-axis, $beta$ is rotation about y' and γ is rotation about z'. How the angle correspond to rotations are shown below.

insert figure

Our vector, r, may now be described as

$$\vec{r} = a\hat{i} + b\hat{j} + c\hat{k} \tag{13}$$

We can now describe rotations R when one of the 3 axes is fixed If Z axis is fixed,

$$R_z = \begin{pmatrix} \cos\alpha & \sin\alpha & 0 \\ -\sin\alpha & \cos\alpha & 0 \\ 0 & 0 & 1 \end{pmatrix} \tag{14}$$

When Y axis is fixed

$$R_y = \begin{pmatrix} \cos\beta & 0 & -\sin\beta \\ 0 & 1 & 0 \\ \sin\beta & 0 & \cos\beta \end{pmatrix} \tag{15}$$

When X axis is fixed

$$R_z = \begin{pmatrix} \cos\gamma & \sin\gamma & 0 \\ -\sin\gamma & \cos\gamma & 0 \\ 0 & 0 & 1 \end{pmatrix} \tag{16}$$

Then rotation of the original axis system to the new axis system is then

$$R = R_x R_y R_z = \begin{pmatrix} \cos\alpha & \sin\alpha & 0 \\ -\sin\alpha & \cos\alpha & 0 \\ 0 & 0 & 1 \end{pmatrix} \begin{pmatrix} \cos\beta & 0 & -\sin\beta \\ 0 & 1 & 0 \\ \sin\beta & 0 & \cos\beta \end{pmatrix} \begin{pmatrix} \cos\gamma & \sin\gamma & 0 \\ -\sin\gamma & \cos\gamma & 0 \\ 0 & 0 & 1 \end{pmatrix} \tag{17}$$

Angular Momentum Rotations

J=1/2

In a similar manner we can rotated angular momentum states. Like we developed a rotation operator, R for Cartesian space, we can define a new rotation operators which operates on angular momentum states using the Euler relations we made for 3D rotations.

$$D(\alpha, \beta, \gamma) = e^{i\gamma J_z} e^{i\beta J_y} e^{i\alpha J_x} \tag{18}$$

Lets examine what happens when D operates on |J,m>

$$D(\alpha, \beta, \gamma) = \sum_{J', m'} |J', m' >< J', m'| D(\alpha, \beta, \gamma) |J, m > \tag{19}$$

The operator can only operate on a \single J value reducing the above equation to

$$D(\alpha, \beta, \gamma) = \sum_{m'} < J, m'| D(\alpha, \beta, \gamma) |J, m > |J, m' = \sum_{m'} D^{(J)}_{m', m}(\alpha, \beta, \gamma) |J, m' > \tag{20}$$

where

$$D^{(J)}_{m', m}(\alpha, \beta, \gamma) =< J, m'| D(\alpha, \beta, \gamma) |J, m > \tag{21}$$

which can be simplified to

$$D^{(J)}_{m', m}(\alpha, \beta, \gamma) = \sum_{n', n'} < J, m'| e^{i\gamma J_z} |J, n >< J, n| e^{i\beta J_y} |J, n' >< J, n'| e^{i\alpha J_z} |J, m > \tag{22}$$

It is then realized that

$$e^{i\alpha J_z}|J,m>=[1+i\alpha J_z+\frac{(i\alpha J_z)^2}{2!}+\ldots]|J,m>=[1+i\alpha m+\frac{(i\alpha m)^2}{2!}+\ldots]|J,m=e^{1\alpha m}|J,m \tag{23}$$

Then

$$D^J_{m',m}(\alpha,\beta,\gamma)=e^{im'\gamma}<J,m'|e^{i\beta J_y}|J,m>e^{im\alpha}=e^{im'\gamma}d^J_{m',m}(\beta)e^{im\alpha} \tag{24}$$

where

$$d^J_{m',m}(\beta)=<J,m'|e^{i\beta J_y}|J,m> \tag{25}$$

We now must calculate $d^J_{m',m}(\beta)$ for a arbitrary J. Lets examine the case where J=1/2 for rotation operator $d^{1/2}(\beta)$

$$d^{1/2}(\beta)=e^{i\beta J_y} \tag{26}$$

Taking a Taylor expansion gives

$$e^{i\beta J_y}=1+i\beta J_y-\frac{1}{2!}\beta^2J_y^2-\frac{1}{3!}\beta^3j_Y^3 \tag{27}$$

$$=\begin{pmatrix}1&0\\0&1\end{pmatrix}(1-\frac{\frac{\beta}{2}^2}{2!}+\ldots)+\begin{pmatrix}0&1\\-1&0\end{pmatrix}(\frac{\beta}{2}-\frac{\frac{\beta}{2}^3}{3!}+\ldots) \tag{28}$$

We then see that multiplying the Taylor expansion of $e^{i\beta J_y}$ by the respective matrices, we obtain the Taylor expansions of \cos and \sin which can be rewritten as:

$$=\begin{pmatrix}\cos(\beta/2)&\sin(\beta/2)\\-\sin(\beta/2)&\cos(\beta/2)\end{pmatrix} \tag{29}$$

Then we have obtained the values for d

$$d^{(1/2)}_{1/2,1/2}=\cos(\beta/2) \tag{30}$$

$$d^{(1/2)}_{1/2,-1/2}=\sin(\beta/2) \tag{31}$$

J>1/2

Now we must calculate $d^J_{m',m}(\beta)$ for J>1/2. To do this we must first uncouple J and m'

$$D^J_{m',m}(\alpha,\beta,\gamma)|J,m>=\sum_{m'}D^J_{m',m}(\alpha,\beta,\gamma)|J,m'> \tag{32}$$

$$=(-1)^{j_2-j_1-m}\sqrt{2J+1}\sum m_1,m_2D(\alpha,\beta,\gamma)|j_1,m_1>D(\alpha,\beta,\gamma)|j_2,m_2>\begin{pmatrix}j_1&j_2&J\\m_1&m_2&-m\end{pmatrix} \tag{33}$$

$$=(-1)^{j_2-j_1-m}\sqrt{2J+1}\sum m_1,m_2,m_1',m_2'D(\alpha,\beta,\gamma)^{(j_1)}_{m_1'm_1}D(\alpha,\beta,\gamma)^{(j_2)}_{m_2'm_2}\begin{pmatrix}j_1&j_2&J\\m_1&m_2&-m\end{pmatrix}|j_1m_1';j_2,m_2'> \tag{34}$$

Taking this result and left multiplying by <Jm'| and uncoupling J and m' to the other j and m states results in the expression for $D(\alpha,\beta,\gamma)^{(J)}_{m',m}$

$$D(\alpha,\beta,\gamma)^{(J)}_{m',m}=(-1)^{j_2-j_1-m}\sqrt{2J+1}\sum m_1,m_2,m_1',m_2'D(\alpha,\beta,\gamma)^{(j_1)}_{m_1'm_1}D(\alpha,\beta,\gamma)^{(j_2)}_{m_2'm_2}\begin{pmatrix}j_1&j_2&J\\m_1&m_2&-m\end{pmatrix}<J, \tag{35}$$

$$m'||j_1m_1';j_2,m_2'>$$

$$=(2J+1)\sum_{m_1,m_2}\begin{pmatrix}j_1&j_2&J\\m_1&m_2&-m\end{pmatrix}\begin{pmatrix}j_1&j_2&J\\m_1'&m_2'&-m'\end{pmatrix}D(\alpha,\beta,\gamma)^{(j_1)}_{m_1'm_1}D(\alpha,\beta,\gamma)^{(j_2)}_{m_2'm_2} \tag{36}$$

From this result we can calculate any $D(\alpha,\beta,\gamma)^{(J)}_{m',m}$ for any J value. This is important since the observables we wish to calculate in NMR are simply rotations of the angular momentum. Looking at the time-dependant Schrödinger equation

$$\frac{d}{dt}|\psi(t)>=-iH|\psi(t)> \tag{37}$$

$$|\psi(t) = e^{iHt}|\psi(t) > \tag{38}$$

Lets now examine what we can do by rotating the angular momentum vector J,m to J m'. Looking at the z component of J we know

$$< J, m'|J_z|J, m >= m\delta_{m',m} \tag{39}$$

which results in a diagonal matriz for J_z with the digonal elements being the m quantum numbers.

Then J_z may be written as

$$J_z = \sum_m m|J, m >< J, m| \tag{40}$$

which has the complex conjugate

need to figure this out!

Now we have created the operatore for J_z.. In principle we can create an operator for any combination of |J'm'><J,m|. Now lets see what happens weh nwe rotate the operator in which the states are weighted by the angular momentum characteristics. We choose to label the new operator $T^{(1)}_{(2)}(3,4)$ by the following indicie.

$$k = J + J' \tag{41}$$

The Total Angular Momentum

$$Q = m' - m \tag{42}$$

The difference in M values

$$J \tag{43}$$

The initial and

$$J' \tag{44}$$

the final angular momentum.

$$T^{(k)}_{(Q)}(J, J') = \sqrt{2k+1}\sum_{m,m'}(-1)^{J'-m'}\begin{pmatrix} J' & J & k \\ m' & -m & -Q \end{pmatrix}|J', m' >< J, m| \tag{45}$$

To rotate this operator we must left multiply by $D(\alpha, \beta, \gamma)$ and right multiple by $D(\alpha, \beta, \gamma)^\dagger$. This corresponds the rotation of the final and initial states.

$$D(\alpha, \beta, \gamma)T^{(k)}_{(Q)}(J, J')(D(\alpha, \beta, \gamma)^\dagger = \sqrt{2k+1}\sum_{m,m',n,n'}(-1)^{J'-m'}\begin{pmatrix} J' & J & k \\ m' & -m & -Q \end{pmatrix}D(\alpha, \beta, \gamma)^{(J)}_{n',m}D(\alpha, \beta, \gamma)^{(J)\dagger}_{m,n}|J', \tag{46}$$
$$m' >< J, m|$$

where

$$D^{J_1}(\alpha, \beta, \gamma)D^{J_2}(\alpha, \beta, \gamma)^\dagger = \sum_{J,m,m'}(2J+1)\begin{pmatrix} j_1 & j_2 & J \\ m'_1 & M'_2 & -m' \end{pmatrix}\begin{pmatrix} j_1 & j_2 & J \\ m_1 & M_2 & -m \end{pmatrix}(-1)^{m'-m}D(\alpha, \beta, \gamma)^{(J)}_{-m',m} \tag{47}$$

which simplifies the previous equation to

$$D(\alpha, \beta, \gamma)T^{(k)}_{(Q)}(J, J')(D(\alpha, \beta, \gamma)^\dagger = \sqrt{2k+1}\sum_{n',n,q}(-1)^{J'-n'}\begin{pmatrix} J' & J & k \\ n' & -n & -q \end{pmatrix}D^{(k)}_{qQ}(\alpha, \beta, \gamma)|J', n' >< J, n| \tag{48}$$

which is really $T^{(k)}_{(Q)}(J, J')$ with Q replaced by q and m',m with n',n or

$$D(\alpha, \beta, \gamma)T^{(k)}_{(Q)}(J, J')(D(\alpha, \beta, \gamma)^\dagger = \sum_q D^{(k)}_{qQ}(\alpha, \beta, \gamma)T^{(k)}_{(q)}(J, J') \tag{49}$$

This is a very unique property of these operators! Rotation of one operator produces another operator that is weighted by $D^{(k)}_{qQ}(\alpha, \beta, \gamma)$. It is now trivial to create analytical solutions as $D^{(J)}_{mm'}(\alpha, \beta, \gamma)$ are known.

Rotations and Irreducible Tensor Operators is shared under a CC BY-NC-SA 4.0 license and was authored, remixed, and/or curated by LibreTexts.

- **Rotations and Irreducible Tensor Operators** by Derrick Kaseman is licensed CC BY 4.0.

5.5: The Nature of NMR Absorptions

Objectives

After completing this section, you should be able to

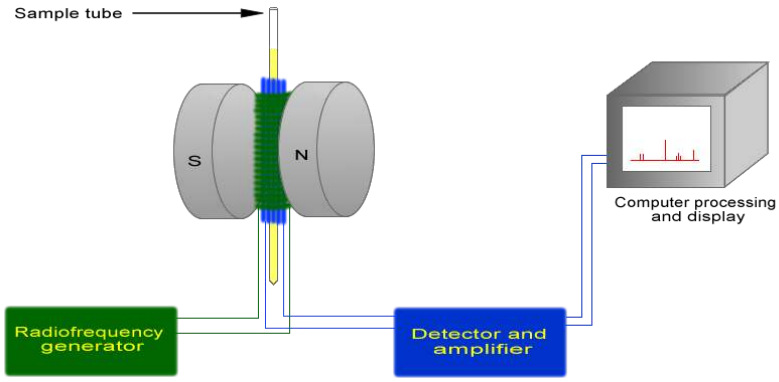
1. explain, in general terms, the origin of shielding effects in NMR spectroscopy.
2. explain the number of peaks occurring in the ^{1}H or ^{13}C NMR spectrum of a simple compound, such as methyl acetate.
3. describe, and sketch a diagram of, a simple NMR spectrometer.
4. explain the difference in time scales of NMR and infrared spectroscopy.
5. predict the number of peaks expected in the ^{1}H or ^{13}C NMR spectrum of a given compound.

Study Notes

Before you go on, make sure that you understand that each signal in the ^{1}H NMR spectrum shown for methyl acetate is due to a different proton environment. The three protons on the same methyl group are equivalent and appear in the spectrum as one signal. However, the two methyl groups are in two different environments (one is more deshielded) and so we see two signals in the whole spectrum (aside from the TMS reference peak).

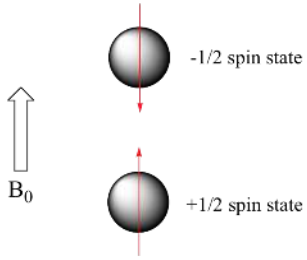
Methyl acetate has a very simple ^{1}H NMR spectrum, because there is no proton-proton coupling, and therefore no splitting of the signals. In later sections, we discuss splitting patterns in ^{1}H NMR spectra and how they help a chemist determine the structure of organic compounds.

The basic arrangement of an NMR spectrometer is displayed below. A sample (in a small glass tube) is placed between the poles of a strong magnetic. A radio frequency generator pulses the sample and excites the nuclei causing a spin-flip. The spin flip is detected by the detector and the signal sent to a computer where it is processed.



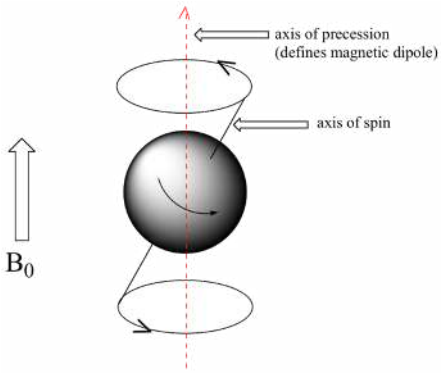
Nuclear precession, spin states, and the resonance condition

When a sample of an organic compound is sitting in a flask on a laboratory benchtop, the magnetic moments of its hydrogen atoms are randomly oriented. When the same sample is placed within the field of a very strong magnet in an NMR instrument (this field is referred to by NMR spectroscopists as the **applied field**, abbreviated $\mathbf{B_0}$) each hydrogen will assume one of two possible **spin states**. In what is referred to as the +½ spin state, the hydrogen's magnetic moment is aligned *with* the direction of B_0, while in the -½ spin state it is aligned *opposed to* the direction of B_0.



Because the +½ spin state is slightly lower in energy, in a large population of organic molecules slightly more than half of the hydrogen atoms will occupy this state, while slightly less than half will occupy the –½ state. *The difference in energy between the two spin states increases with increasing strength of B_0.*This last statement is in italics because it is one of the key ideas in NMR spectroscopy, as we shall soon see.

At this point, we need to look a little more closely at how a proton spins in an applied magnetic field. You may recall playing with spinning tops as a child. When a top slows down a little and the spin axis is no longer completely vertical, it begins to exhibit **precessional motion**, as the spin axis rotates slowly around the vertical. In the same way, hydrogen atoms spinning in an applied magnetic field also exhibit precessional motion about a vertical axis. It is this axis (which is either parallel or antiparallel to B_0) that defines the proton's magnetic moment. In the figure below, the proton is in the +1/2 spin state.

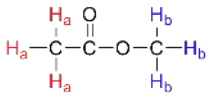


The **frequency of precession** (also called the **Larmour frequency,** abbreviated $\boldsymbol{\omega_L}$) is simply the number of times per second that the proton precesses in a complete circle. A proton`s precessional frequency increases with the strength of B_0.

If a proton that is precessing in an applied magnetic field is exposed to electromagnetic radiation of a frequency ν that matches its precessional frequency ω_L, we have a condition called **resonance**. *In the resonance condition, a proton in the lower-energy +½ spin state (aligned with B_0) will transition (flip) to the higher energy –½ spin state (opposed to B_0). In doing so, it will absorb radiation at this resonance frequency* $\boldsymbol{\nu = \omega_L}$. This frequency, as you might have already guessed, corresponds to the energy difference between the proton's two spin states. With the strong magnetic fields generated by the superconducting magnets used in modern NMR instruments, the resonance frequency for protons falls within the radio-wave range, anywhere from 100 MHz to 800 MHz depending on the strength of the magnet.

The basics of an NMR experiment

Given that chemically nonequivalent protons have different resonance frequencies in the same applied magnetic field, we can see how NMR spectroscopy can provide us with useful information about the structure of an organic molecule. A full explanation of how a modern NMR instrument functions is beyond the scope of this text, but in very simple terms, here is what happens. First, a sample compound (we'll use methyl acetate) is placed inside a very strong applied magnetic field (B_0).

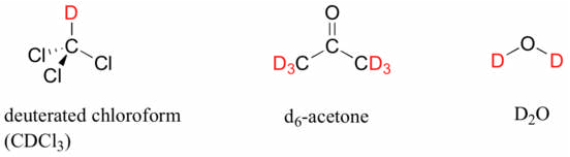


methyl acetate

All of the protons begin to precess: the H_a protons at precessional frequency ω_a, the H_b protons at ω_b.At first, the magnetic moments of (slightly more than) half of the protons are aligned with B_0, and half are aligned against B_0. Then, the sample is hit with electromagnetic radiation in the radio frequency range. The two specific frequencies which match $\omega_a$andω_b(i.e. the resonance frequencies) cause those H_a and H_b protons which are aligned *with* B_0 to 'flip' so that they are now aligned *against* B_0. In doing so, the protons absorb radiation at the two resonance frequencies. The NMR instrument records which frequencies were absorbed, as well as the intensity of each absorbance.

In most cases, a sample being analyzed by NMR is in solution. If we use a common laboratory solvent (diethyl ether, acetone, dichloromethane, ethanol, water, etc.) to dissolve our NMR sample, however, we run into a problem – there many more solvent protons in solution than there are sample protons, so the signals from the sample protons will be overwhelmed. To get around this problem, we use special NMR solvents in which all protons have been replaced by deuterium. Recall that deuterium is NMR-

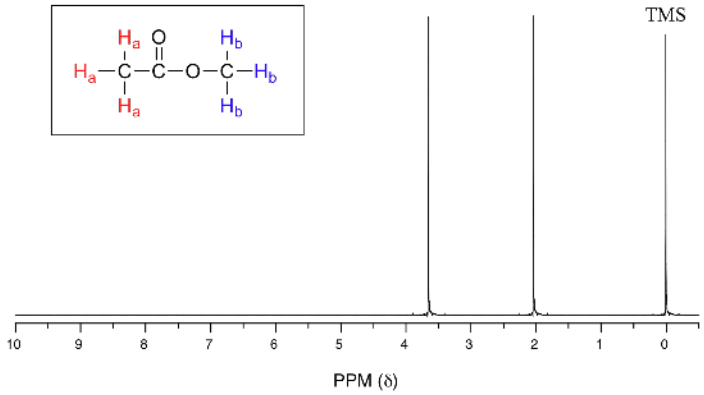
active, but its resonance frequency is very different from that of protons, and thus it is `invisible` in ^{1}H-NMR. Some common NMR solvents are shown below.



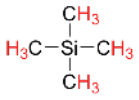
deuterated chloroform ($CDCl_3$) | d_6-acetone | D_2O

The Chemical Shift

Let's look at an actual ^{1}H-NMR plot for methyl acetate. Just as in IR and UV-vis spectroscopy, the vertical axis corresponds to intensity of absorbance, the horizontal axis to frequency (typically the vertical axis is not shown in an NMR spectrum).



We see three absorbance signals: two of these correspond to H_a and H_b, while the peak at the far right of the spectrum corresponds to the 12 chemically equivalent protons in tetramethylsilane (TMS), a standard reference compound that was added to our sample.



tetramethylsilane (TMS)

You may be wondering about a few things at this point - why is TMS necessary, and what is the meaning of the `ppm (δ)` label on the horizontal axis? Shouldn't the frequency units be in Hz? Keep in mind that NMR instruments of many different applied field strengths are used in organic chemistry laboratories, and that the proton's resonance frequency range depends on the strength of the applied field. The spectrum above was generated on an instrument with an applied field of approximately 7.1 Tesla, at which strength protons resonate in the neighborhood of 300 million Hz (chemists refer to this as a 300 MHz instrument). If our colleague in another lab takes the NMR spectrum of the same molecule using an instrument with a 2.4 Tesla magnet, the protons will resonate at around 100 million Hz (so we'd call this a 100 MHz instrument). It would be inconvenient and confusing to always have to convert NMR data according to the field strength of the instrument used. Therefore, chemists report resonance frequencies not as absolute values in Hz, but rather as values *relative to a common standard*, generally the signal generated by the protons in TMS. This is where the ppm – parts per million – term comes in. Regardless of the magnetic field strength of the instrument being used, the resonance frequency of the 12 equivalent protons in TMS is defined as a zero point. The resonance frequencies of protons in the sample molecule are then reported in terms of how much higher they are, in ppm, relative to the TMS signal (almost all protons in organic molecules have a higher resonance frequency than those in TMS, for reasons we shall explore quite soon).

The two proton groups in our methyl acetate sample are recorded as resonating at frequencies 2.05 and 3.67 ppm higher than TMS. One-millionth (1.0 ppm) of 300 MHz is 300 Hz. Thus 2.05 ppm, on this instrument, corresponds to 615 Hz, and 3.67 ppm corresponds to 1101 Hz. If the TMS protons observed by our 7.1 Tesla instrument resonate at exactly 300,000,000 Hz, this means that the protons in our ethyl acetate samples are resonating at 300,000,615 and 300,001,101 Hz, respectively. Likewise, if the TMS protons in our colleague's 2.4 Tesla instrument resonate at exactly 100 MHz, the methyl acetate protons in her sample resonate at 100,000,205 and 100,000,367 Hz (on the 100 MHz instrument, 1.0 ppm corresponds to 100 Hz). The absolute frequency values in

each case are not very useful – they will vary according to the instrument used – but the *difference* in resonance frequency from the TMS standard, expressed in parts per million, should be the same regardless of the instrument.

Expressed this way, the resonance frequency for a given proton in a molecule is called its **chemical shift**. A frequently used symbolic designation for chemical shift in ppm is the lower-case Greek letter *delta* (δ). Most protons in organic compounds have chemical shift values between 0 and 12 ppm from TMS, although values below zero and above 12 are occasionally observed. By convention, the left-hand side of an NMR spectrum (higher chemical shift) is called **downfield**, and the right-hand direction is called **upfield**.

In our methyl acetate example we included for illustrative purposes a small amount of TMS standard directly in the sample, as was the common procedure for determining the zero point with older NMR instruments . That practice is generally no longer necessary, as modern NMR instruments are designed to use the deuterium signal from the solvent as a standard reference point, then to extrapolate the 0 ppm baseline that corresponds to the TMS proton signal (in an applied field of 7.1 Tesla, the deuterium atom in $CDCl_3$ resonates at 32 MHz, compared to 300 MHz for the protons in TMS). In the remaining NMR spectra that we will see in this text we will not see an actual TMS signal, but we can always assume that the 0 ppm point corresponds to where the TMS protons *would* resonate if they were present.

Example

A proton has a chemical shift (relative to TMS) of 4.56 ppm.

a. a) What is its chemical shift, expressed in Hz, in a 300 MHz instrument? On a 200 MHz instrument?
b. b) What is its resonance frequency, expressed in Hz, in a 300 MHz instrument? On a 200 MHz instrument?

(Assume that in these instruments, the TMS protons resonate at exactly 300 or 200 MHz, respectively)

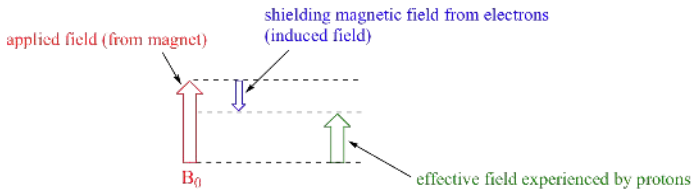
Answer

a) 1 ppm = 300 Hz, so 4.56 ppm corresponds to 1368 Hz on the 300 MHz instrument. On the 200 MHz instrument, the chemical shift is 912 Hz.

b) 300 MHz instrument: 300,001,368 Hz. 200 MHz instrument: 200,000,912 Hz.

Diamagnetic shielding and deshielding

We come now to the question of *why* nonequivalent protons have different chemical shifts. The chemical shift of a given proton is determined primarily by its immediate electronic environment. Consider the methane molecule (CH_4), in which the protons have a chemical shift of 0.23 ppm. The valence electrons around the methyl carbon, when subjected to B_0, are induced to circulate and thus generate their own very small magnetic field that *opposes* B_0. This **induced field**, to a small but significant degree, *shields* the nearby protons from experiencing the full force of B_0, an effect known as **local diamagnetic shielding**. The methane protons therefore do not experience the full force of B_0 - what they experience is called B_{eff}, or the **effective field**, which is slightly *weaker* than B_0.



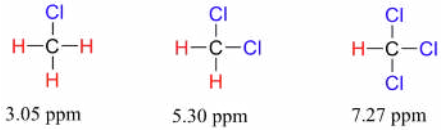
Therefore, their resonance frequency is slightly lower than what it would be if they did not have electrons nearby to shield them.

Now consider methyl fluoride, CH_3F, in which the protons have a chemical shift of 4.26 ppm, significantly higher than that of methane. This is caused by something called the **deshielding effect**. Because fluorine is more electronegative than carbon, it pulls valence electrons away from the carbon, effectively *decreasing* the electron density around each of the protons. For the protons, lower electron density means less diamagnetic shielding, which in turn means a greater overall exposure to B_0, a stronger B_{eff}, and a higher resonance frequency. Put another way, the fluorine, by pulling electron density away from the protons, is *deshielding* them, leaving them more exposed to B_0. As the electronegativity of the substituent increases, so does the extent of deshielding, and so

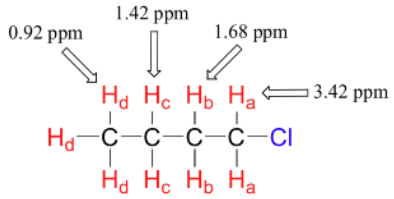
does the chemical shift. This is evident when we look at the chemical shifts of methane and three halomethane compounds (remember that electronegativity increases as we move up a column in the periodic table).



To a large extent, then, we can predict trends in chemical shift by considering how much deshielding is taking place near a proton. The chemical shift of trichloromethane is, as expected, higher than that of dichloromethane, which is in turn higher than that of chloromethane.



The deshielding effect of an electronegative substituent diminishes sharply with increasing distance:



The presence of an electronegative oxygen, nitrogen, sulfur, or sp^2-hybridized carbon also tends to shift the NMR signals of nearby protons slightly downfield:

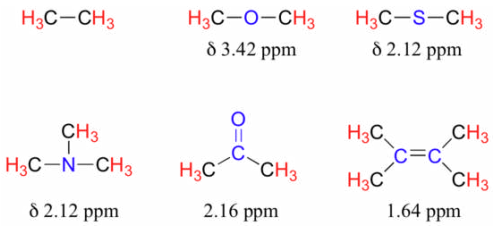
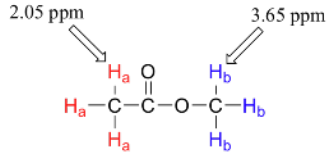
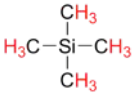


Table 2 lists typical chemical shift values for protons in different chemical environments.

Armed with this information, we can finally assign the two peaks in the the ^{1}H-NMR spectrum of methyl acetate that we saw a few pages back. The signal at 3.65 ppm corresponds to the methyl ester protons (H_b), which are deshielded by the adjacent oxygen atom. The upfield signal at 2.05 ppm corresponds to the acetate protons (H_a), which is deshielded - but to a lesser extent - by the adjacent carbonyl group.



Finally, a note on the use of TMS as a standard in NMR spectroscopy: one of the main reasons why the TMS proton signal was chosen as a zero-point is that the TMS protons are highly shielded: silicon is slightly *less* electronegative than carbon, and therefore *donates* some additional shielding electron density. Very few organic molecules contain protons with chemical shifts that are negative relative to TMS.

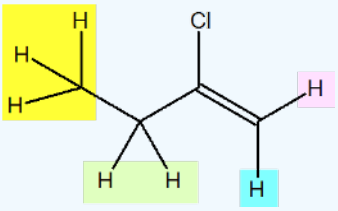


Exercise

Exercise 5.5.1

2-cholorobutene shows 4 different hydrogen signals. Explain why this is.

Answer



The same colors represent the same signal. 4 different colors for 4 different signals of hydrogens in 4 different magnetic environments. The hydrogen on the alkene would give two different signals.

13.2 Exercises

Questions

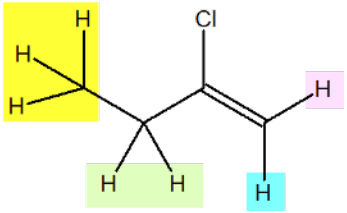
Q13.2.1

2-cholorobutene shows 4 different hydrogen signals. Explain why this is.

Solutions

S13.2.1

The same colors represent the same signal. 4 different colors for 4 different signals. The hydrogen on the alkene would give two different signals.



Contributors and Attributions

- Dr. Dietmar Kennepohl FCIC (Professor of Chemistry, Athabasca University)
- Prof. Steven Farmer (Sonoma State University)
- Organic Chemistry With a Biological Emphasis by Tim Soderberg (University of Minnesota, Morris)

5.5: The Nature of NMR Absorptions is shared under a CC BY-NC-SA 4.0 license and was authored, remixed, and/or curated by LibreTexts.

5.6: Interpretation

Nuclear Magnetic Resonance (NMR) interpretation plays a pivotal role in molecular identifications. As interpreting NMR spectra, the structure of an unknown compound, as well as known structures, can be assigned by several factors such as chemical shift, spin multiplicity, coupling constants, and integration. This Module focuses on the most important ^{1}H and ^{13}C NMR spectra to find out structure even though there are various kinds of NMR spectra such as ^{14}N, ^{19}F, and ^{31}P. NMR spectrum shows that x- axis is chemical shift in ppm. It also contains integral areas, splitting pattern, and coupling constant.

Strategy for Solving Structure

Here is the general strategy for solving structure with NMR:

1. Molecular formula is determined by chemical analysis such as elementary analysis
2. **Double-bond equivalent** (also known as Degree of Unsaturation) is calculated by a simple equation to estimate the number of the multiple bonds and rings. It assumes that oxygen (O) and sulfur (S) are ignored and halogen (Cl, Br) and nitrogen is replaced by CH. The resulting empirical formula is C_aH_b

$$\text{Double bond equivalent(DBE)} = \frac{(2a+2)-b}{2} \qquad at\ [C_aH_b]$$

3. Structure fragmentation is determined by chemical shift, spin multiplicity, integral (peak area), and coupling constants (^{1}J, ^{2}J)
4. Molecular skeleton is built up using 2-dimensional NMR spectroscopy.
5. Relative configuration is predicted by coupling constant (^{3}J).

^{1}H NMR

Chemical Shift

Chemical shift is associated with the Larmor frequency of a nuclear spin to its chemical environment. Tetramethylsilane (TMS, $(CH_3)_4Si$) is generally used as an internal standard to determine chemical shift of compounds: δ_{TMS}=0 ppm. In other words, frequencies for chemicals are measured for a ^{1}H or ^{13}C nucleus of a sample from the ^{1}H or ^{13}C resonance of TMS. It is important to understand trend of chemical shift in terms of NMR interpretation. The proton NMR chemical shift is affect by nearness to electronegative atoms (O, N, halogen.) and unsaturated groups (C=C,C=O, aromatic). Electronegative groups move to the down field (left; increase in ppm). Unsaturated groups shift to downfield (left) when affecting nucleus is in the plane of the unsaturation, but reverse shift takes place in the regions above and below this plane. ^{1}H chemical shift play a role in identifying many functional groups. Figure 5.6.1. indicates important example to figure out the functional groups.

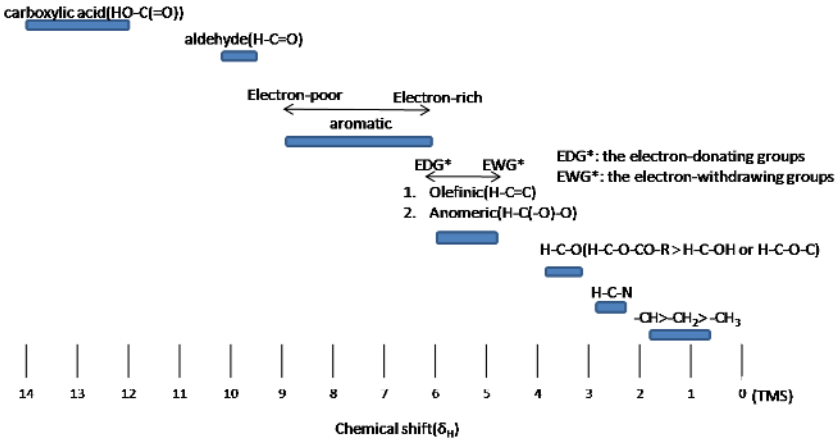


Figure 5.6.1: 1H chemical shift ranges for organic compound

Chemical equivalence

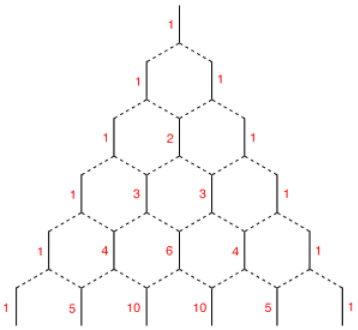
Protons with Chemical equivalence has the same chemical shift due to symmetry within molecule (CH_3COCH_3) or fast rotation around single bond (-CH_3; methyl groups).

Spin-Spin Splitting

Spin-Spin splitting means that an absorbing peak is split by more than one “neighbor” proton. Splitting signals are separated to J Hz, where is called the coupling constant. The spitting is a very essential part to obtain exact information about the number of the neighboring protons. The maximum of distance for splitting is three bonds. Chemical equivalent protons do not result in spin-spin splitting. When a proton splits, the proton’s chemical shift is determined in the center of the splitting lines.

Spin Multiplicity (Splitting pattern)

Spin Multiplicity plays a role in determining the number of neighboring protons. Here is a multiplicity rules: In case of A_mB_n system, the multiplicity rule is that Nuclei of B element produce a splitting the A signal into $nB+1$ lines. The general formula which applies to all nuclei is 2_nI+1, where I is the spin quantum number of the coupled element. The relative intensities of the each lines are given by the coefficients of the Pascal’s triangle (Figure 5.6.2).



splitting pattern	the ratio of heights of lines in the peak
singlet	1
doublet	1:1
triplet	1:2:1
quartet	1:3:3:1
quintet	1:4:6:4:1
sextet	1:5:10:10:5:1

Figure 5.6.2: Pascal's triangle

First-order splitting pattern

The chemical shift difference in Hertz between coupled protons in Hertz is much larger than the J coupling constant:

$$\frac{\Delta\nu}{J} \geq 8 \tag{5.6.1}$$

Where $\Delta\nu$ is the difference of chemical shift. In other word, the proton is only coupled to other protons that are far away in chemical shift. The spectrum is called *first-order spectrum*. The splitting pattern depends on the magnetic field. The second-order splitting at the lower field can be resolved into first-order splitting pattern at the high field. The first-order splitting pattern is allowed to multiplicity rule (N+1) and Pascal’s triangle to determine splitting pattern and intensity distribution.

Example 5.6.1

The note is that structure system is $A_3M_2X_2$. H_a and H_x has the triplet pattern by Hm because of N+1 rule. The signal of Hm is split into six peaks by H_x and H_a (Figure3) The First order pattern easily is predicted due to separation with equal splitting pattern.

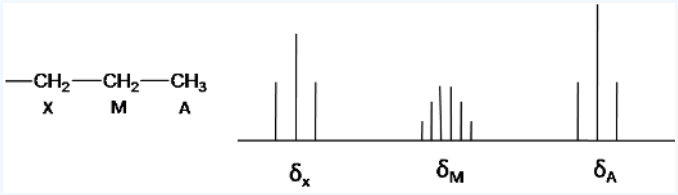


Figure 5.6.3: An example of splitting pattern

High-order splitting pattern

High-order splitting pattern takes place when chemical shift difference in Hertz is much less or the same that order of magnitude as the j coupling.

$$\frac{\Delta v}{J} \leq 10 \tag{5.6.2}$$

The second order pattern is observed as leaning of a classical pattern: the inner peaks are taller and the outer peaks are shorter in case of AB system (Figure 5.6.4). This is called the **roof effect**.

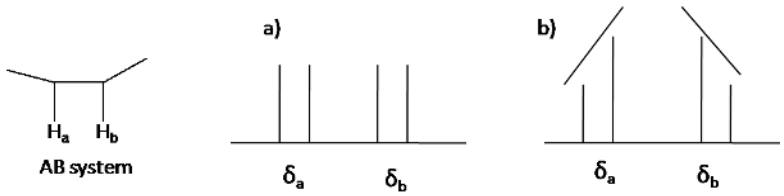


Figure 5.6.4: a) first-order pattern and b) second-order pattern of AB system

Here is other system as an example: A_2B_2 (Figure 5.6.5). The two triplet incline toward each other. Outer lines of the triplet are less than 1 in relative area and the inner lines are more than 1. The center lines have relative area 2.

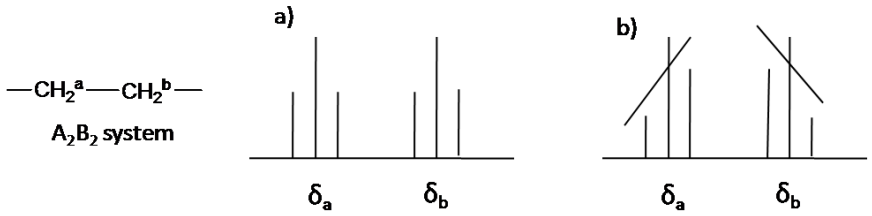


Figure 5.6.5: a) first-order pattern and b) second-order pattern of A_2B_2 system

Coupling constant (J Value)

Coupling constant is the strength of the spin-spin splitting interaction and the distance between the split lines. The value of distance is equal or different depending on the coupled nuclei. The coupling constants reflect the bonding environments of the coupled nuclei. Coupling constant is classified by the number of bonds:

Geminal proton-proton coupling ($^2J_{HH}$)

Germinal coupling generates through two bonds (Figure 5.6.6). Two proton having geminal coupling are not chemically equivalent. This coupling ranges from -20 to 40 Hz. $^2J_{HH}$depends on hybridization of carbon atom and the bond angle and the substituent such as electronegative atoms. When S-character is increased, Geminal coupling constant is increased: $^2J_{sp1}>^2J_{sp2}>^2J_{sp3}$ The bond angle(HCH) gives rise to change $^2J_{HH}$ value and depend on the strain of the ring in the cyclic systems. Geminal coupling constant determines ring size. When bond angle is decreased, ring size is decreased so that geminal coupling constant is more positive. If a atom is replace to an electronegative atom, Geminal coupling constant move to positive value.

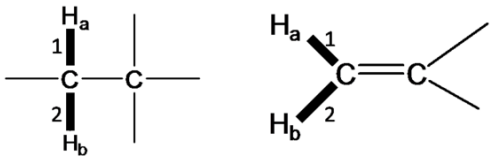


Figure 5.6.6: Geminal coupling

Vicinal proton-proton coupling ($^3J_{HH}$)

Vicinal coupling occurs though three bonds (Figure 5.6.7.). The Vicinal coupling is the most useful information of dihedral angle, leading to stereochemistry and conformation of molecules. Vicinal coupling constant always has the positive value and is affected by the dihedral angle (?;HCCH), the valence angle (?; HCC), the bond length of carbon-carbon, and the effects of electronegative atoms. Vicinal coupling constant depending on the dihedral angle (Figure 5.6.8) is given by the Karplus equation.

$$^3J = 7.0 - 0.5\cos\phi + 4.5\cos^2\phi \tag{5.6.3}$$

When ? is the 90°, vicinal coupling constant is zero. In addition, vicinal coupling constant ranges from 8 to 10 Hz at the and ? =180°, where ?=0° and ?=180° means that the coupled protons have cis and trans configuration, respectively.

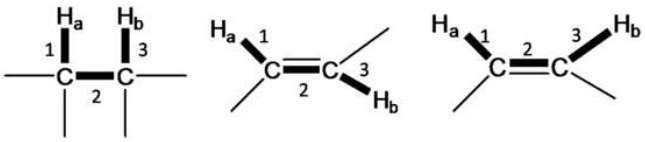


Figure 5.6.7: Vicinal coupling

The valence angle(?;Figure 5.6.8) also causes change of $^{3}J_{HH}$ value. Valence angle is related with ring size. Typically, when the valence angle decreases, the coupling constant reduces. The distance between the carbons atoms gives influences to vicinal coupling constant

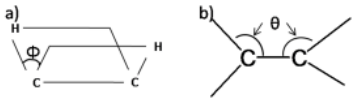


Figure 5.6.8: a) Dihedral angle and b) valence angle

The coupling constant increases with the decrease of bond length. Electronegative atoms affect vicinal coupling constants so that electronegative atoms decrease the vicinal coupling constants.

Integral

Integral is referred to integrated peak area of 1H signals. The intensity is directly proportionally to the number of hydrogen.

^{13}C NMR

Chemical Shift

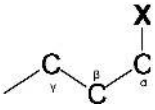


Figure 5.6.9 shows typical ^{13}C chemical shift regions of the major chemical class.

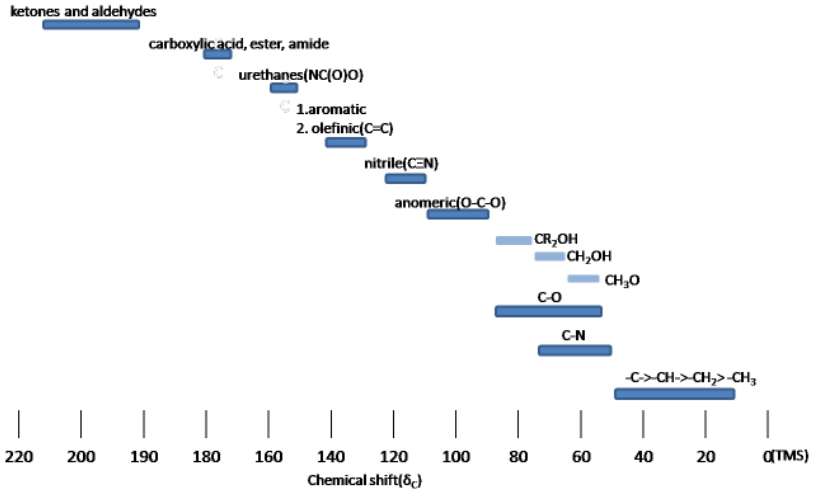


Figure 5.6.9: ^{13}C Chemical shift range for organic compound

Spin-Spin splitting

Comparing the ^{1}H NMR, there is a big difference thing in the ^{13}C NMR. The ^{13}C- ^{13} C spin-spin splitting rarely exit between adjacent carbons because ^{13}C is naturally lower abundant (1.1%)

- **^{13}C-^{1}H Spin coupling**: ^{13}C-^{1}H Spin coupling provides useful information about the number of protons attached a carbon atom. In case of one bond coupling ($^{1}J_{CH}$), -CH, -CH_2, and CH_3 have respectively doublet, triplet, quartets for the ^{13}C resonances in the spectrum. However, ^{13}C-^{1}H Spin coupling has an disadvantage for ^{13}C spectrum interpretation. ^{13}C-^{1}H Spin coupling is hard to analyze and reveal structure due to a forest of overlapping peaks that result from 100% abundance of ^{1}H.
- **Decoupling**: Decoupling is the process of removing ^{13}C-^{1}H coupling interaction to simplify a spectrum and identify which pair of nuclei is involved in the J coupling. The decoupling ^{13}C spectra shows only one peak(singlet) for each unique carbon in the

molecule(Figure 5.6.10). Decoupling is performed by irradiating at the frequency of one proton with continuous low-power RF.

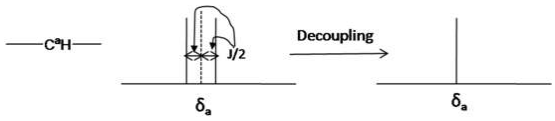


Figure 5.6.10. Decoupling in the ^{13}C NMR

- **Distortionless enhancement by polarization transfer (DEPT):** DEPT is used for distinguishing between a CH_3 group, a CH_2 group, and a CH group. The proton pulse is set at 45º, 90º, or 135º in the three separate experiments. The different pulses depend on the number of protons attached to a carbon atom. Figure 5.6.11. is an example about DEPT spectrum.

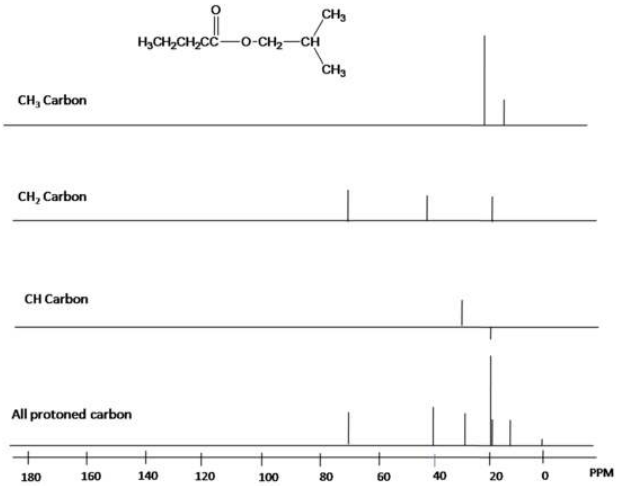


Figure 5.6.11. DEPT spectrum of n-isobutlybutrate

2-dimensional NMR spectroscopy (COSY)

COSY stands for COrrelation SpectroscopY. COSY spectrum is more useful information about what is being correlated.

^1H-^1H COSY (COrrelation SpectroscopY)

^1H-^1H COSY is used for clearly indicate correlation with coupled protons. A point of entry into a COSY spectrum is one of the keys to predict information from it successfully. Relation of Coupling protons is determined by cross peaks(correlation peaks) and in the COSY spectrum. In other words, Diagonal peaks by lines ar e coupled to each other. Figure 5.6.12 indicates that there are correlation peaks between proton H_1 and H_2 as well as between H_2 and H_4. This means the H_2 coupled to H_1 and H_4.

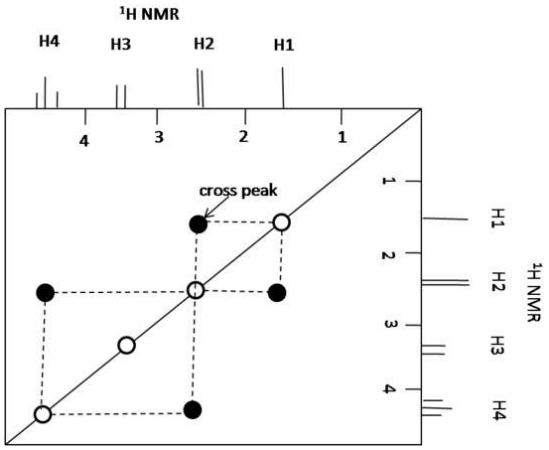


Figure 5.6.12. ^1H-^1H COSY spectrum

^{1}H-^{13}C COSY (HETCOR)

^{1}H-^{13}C COSY is the heteronuclear correlation spectroscopy. The HETCOR spectrum is correlated ^{13}C nuclei with directly attached protons. ^{1}H-^{13}C coupling is one bond. The cross peaks mean correlation between a proton and a carbon (Figure 5.6.13). If a line does not have cross peak, this means that this carbon atoms has no attached proton (e.g. a quaternary carbon atom)

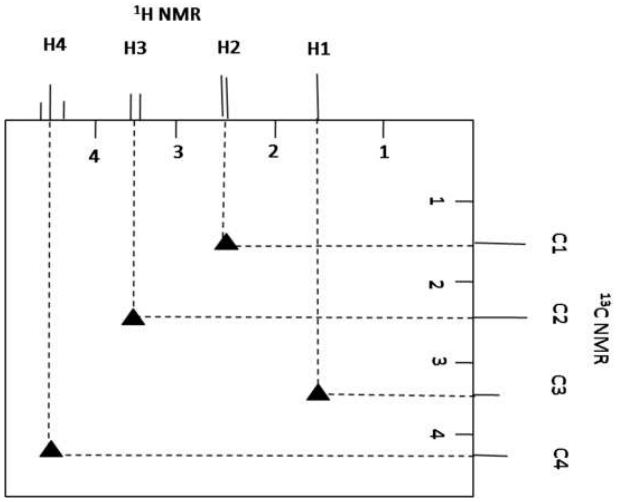


Figure 5.6.13. ^{1}H-^{13}C COSY spectrum

References

1. Balc*, M., Basic p1 sH- and p13 sC-NMR spectroscopy. 1st ed.; Elsevier: Amsterdam ; Boston, 2005; p xii, 427.
2. Breitmaier, E., Structure elucidation by NMR in organic chemistry : a practical guide. 3rd rev. ed.; Wiley: Chichester, West Sussex, England, 2002; p xii, 258.
3. Jacobsen, N. E., NMR spectroscopy explained : simplified theory, applications and examples for organic chemistry and structural biology. Wiley-Interscience: Hoboken, N.J., 2007; p xv, 668.
4. Silverstein, R. M.; Webster, F. X., Spectrometric identification of organic compounds. 6th ed.; Wiley: New York, 1998; p xiv, 482.

Outside Links

- NMRShiftDB: a Free web database for NMR data : nmrshiftdb.chemie.uni-mainz.de/nmrshiftdb
- NMR database from ACD/LAbs : www.acdlabs.com/products/spec_lab/exp_spectra/spec_libraries/aldrich.html
- NMR database from John Crerar Library : http://crerar.typepad.com/crerar_lib...h_ir_nmr_.html

Problems

Draw the 1H NMR spectrum for 2-Hydroxypropane in CDCl3. Assume sufficient resolution to provide a first-order spectrum and ignore vicinal proton-proton coupling(3JHH)

Solution

1) the structure of 2-hydoroxyporpane is drawn

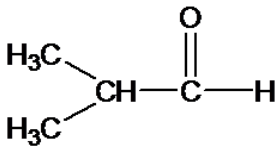


Figure out which protons are chemically equivalent, i.e., two methyl (-CH_3) groups are chemical equivalent.

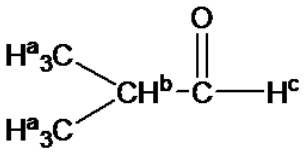
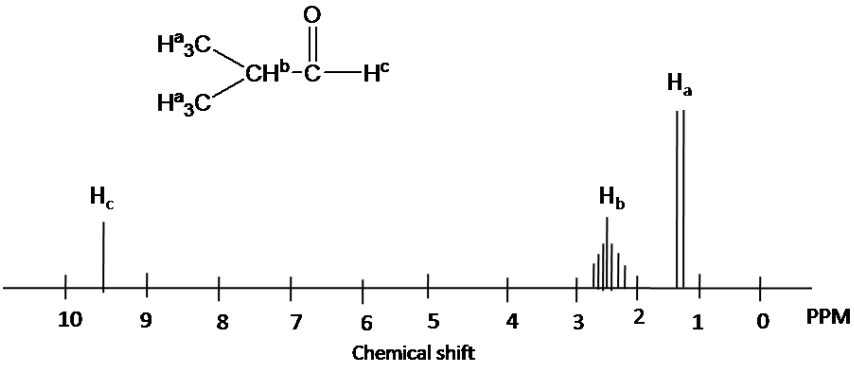


Figure1): chemical shift of methyl groups (H_a) : 1-2 ppm (?H_a=1.1 ppm); chemical shift of -CH- groups (H_b) moves to downfield due to effect on aldehyde groups:2-3ppm (?H_b=2.4 ppm); chemical shift of aldehyde groups (H_c):9-10 ppm (?H_c=9.6 ppm)

4) Splitting pattern is determined by (N+1) rule: Ha is split into two peaks by H_b(#of proton=1). H_b has the septet pattern by H_a (#of proton=6). H_c has one peak.(Note that H_c has doublet pattern by H_b due to vicinal proton-proton coupling.)



Contributors and Attributions

- You Jin Seo

5.6: Interpretation is shared under a CC BY-NC-SA 4.0 license and was authored, remixed, and/or curated by LibreTexts.

- **NMR - Interpretation** is licensed CC BY 4.0.

5.7: Interpretation

Nuclear Magnetic Resonance (NMR) interpretation plays a pivotal role in molecular identifications. As interpreting NMR spectra, the structure of an unknown compound, as well as known structures, can be assigned by several factors such as chemical shift, spin multiplicity, coupling constants, and integration. This Module focuses on the most important ^{1}H and ^{13}C NMR spectra to find out structure even though there are various kinds of NMR spectra such as ^{14}N, ^{19}F, and ^{31}P. NMR spectrum shows that x- axis is chemical shift in ppm. It also contains integral areas, splitting pattern, and coupling constant.

Strategy for Solving Structure

Here is the general strategy for solving structure with NMR:

1. Molecular formula is determined by chemical analysis such as elementary analysis
2. **Double-bond equivalent** (also known as Degree of Unsaturation) is calculated by a simple equation to estimate the number of the multiple bonds and rings. It assumes that oxygen (O) and sulfur (S) are ignored and halogen (Cl, Br) and nitrogen is replaced by CH. The resulting empirical formula is C_aH_b

$$\text{Double bond equivalent(DBE)} = \frac{(2a+2)-b}{2} \qquad at\ [C_aH_b]$$

3. Structure fragmentation is determined by chemical shift, spin multiplicity, integral (peak area), and coupling constants (^{1}J, ^{2}J)
4. Molecular skeleton is built up using 2-dimensional NMR spectroscopy.
5. Relative configuration is predicted by coupling constant (^{3}J).

^{1}H NMR

Chemical Shift

Chemical shift is associated with the Larmor frequency of a nuclear spin to its chemical environment. Tetramethylsilane (TMS, $(CH_3)_4Si$) is generally used as an internal standard to determine chemical shift of compounds: δ_{TMS}=0 ppm. In other words, frequencies for chemicals are measured for a ^{1}H or ^{13}C nucleus of a sample from the ^{1}H or ^{13}C resonance of TMS. It is important to understand trend of chemical shift in terms of NMR interpretation. The proton NMR chemical shift is affect by nearness to electronegative atoms (O, N, halogen.) and unsaturated groups (C=C,C=O, aromatic). Electronegative groups move to the down field (left; increase in ppm). Unsaturated groups shift to downfield (left) when affecting nucleus is in the plane of the unsaturation, but reverse shift takes place in the regions above and below this plane. ^{1}H chemical shift play a role in identifying many functional groups. Figure 5.7.1. indicates important example to figure out the functional groups.

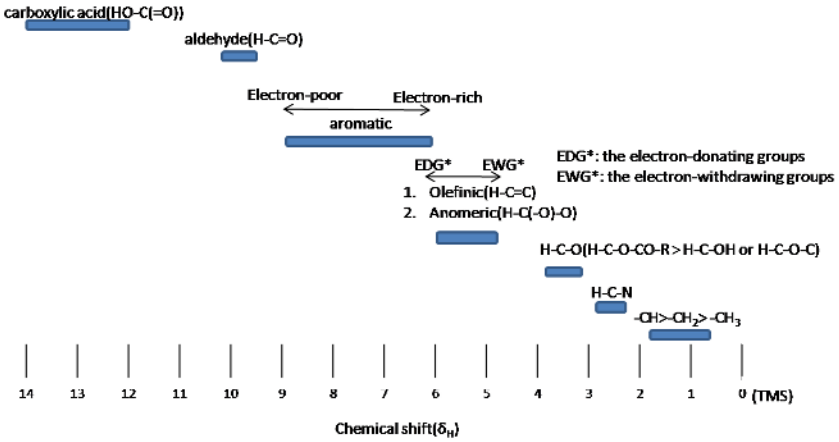


Figure 5.7.1: 1H chemical shift ranges for organic compound

Chemical equivalence

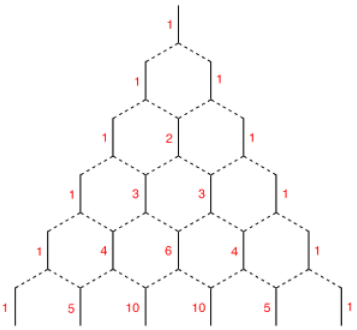
Protons with Chemical equivalence has the same chemical shift due to symmetry within molecule (CH_3COCH_3) or fast rotation around single bond (-CH_3; methyl groups).

Spin-Spin Splitting

Spin-Spin splitting means that an absorbing peak is split by more than one “neighbor” proton. Splitting signals are separated to J Hz, where is called the coupling constant. The spitting is a very essential part to obtain exact information about the number of the neighboring protons. The maximum of distance for splitting is three bonds. Chemical equivalent protons do not result in spin-spin splitting. When a proton splits, the proton’s chemical shift is determined in the center of the splitting lines.

Spin Multiplicity (Splitting pattern)

Spin Multiplicity plays a role in determining the number of neighboring protons. Here is a multiplicity rules: In case of A_mB_n system, the multiplicity rule is that Nuclei of B element produce a splitting the A signal into $nB+1$ lines. The general formula which applies to all nuclei is 2_nI+1, where I is the spin quantum number of the coupled element. The relative intensities of the each lines are given by the coefficients of the Pascal’s triangle (Figure 5.7.2).



splitting pattern	the ratio of heights of lines in the peak
singlet	1
doublet	1:1
triplet	1:2:1
quartet	1:3:3:1
quintet	1:4:6:4:1
sextet	1:5:10:10:5:1

Figure 5.7.2: Pascal's triangle

First-order splitting pattern

The chemical shift difference in Hertz between coupled protons in Hertz is much larger than the J coupling constant:

$$\frac{\Delta\nu}{J} \geq 8 \tag{5.7.1}$$

Where $\Delta\nu$ is the difference of chemical shift. In other word, the proton is only coupled to other protons that are far away in chemical shift. The spectrum is called *first-order spectrum*. The splitting pattern depends on the magnetic field. The second-order splitting at the lower field can be resolved into first-order splitting pattern at the high field. The first-order splitting pattern is allowed to multiplicity rule (N+1) and Pascal’s triangle to determine splitting pattern and intensity distribution.

Example 5.7.1

The note is that structure system is $A_3M_2X_2$. H_a and H_x has the triplet pattern by Hm because of N+1 rule. The signal of Hm is split into six peaks by H_x and H_a (Figure3) The First order pattern easily is predicted due to separation with equal splitting pattern.

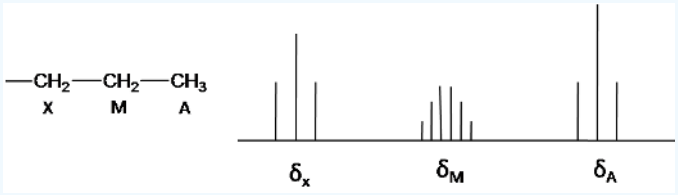


Figure 5.7.3: An example of splitting pattern

High-order splitting pattern

High-order splitting pattern takes place when chemical shift difference in Hertz is much less or the same that order of magnitude as the j coupling.

$$\frac{\Delta v}{J} \leq 10 \tag{5.7.2}$$

The second order pattern is observed as leaning of a classical pattern: the inner peaks are taller and the outer peaks are shorter in case of AB system (Figure 5.7.4). This is called the **roof effect**.

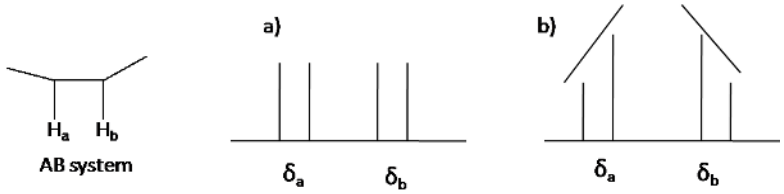


Figure 5.7.4: a) first-order pattern and b) second-order pattern of AB system

Here is other system as an example: A_2B_2 (Figure 5.7.5). The two triplet incline toward each other. Outer lines of the triplet are less than 1 in relative area and the inner lines are more than 1. The center lines have relative area 2.

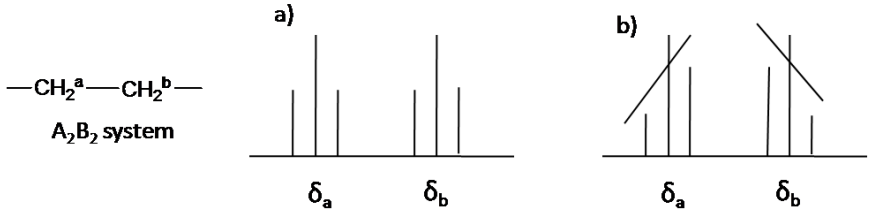


Figure 5.7.5: a) first-order pattern and b) second-order pattern of A_2B_2 system

Coupling constant (J Value)

Coupling constant is the strength of the spin-spin splitting interaction and the distance between the split lines. The value of distance is equal or different depending on the coupled nuclei. The coupling constants reflect the bonding environments of the coupled nuclei. Coupling constant is classified by the number of bonds:

Geminal proton-proton coupling ($^2J_{HH}$)

Germinal coupling generates through two bonds (Figure 5.7.6). Two proton having geminal coupling are not chemically equivalent. This coupling ranges from -20 to 40 Hz. $^2J_{HH}$depends on hybridization of carbon atom and the bond angle and the substituent such as electronegative atoms. When S-character is increased, Geminal coupling constant is increased: $^2J_{sp1}>^2J_{sp2}>^2J_{sp3}$ The bond angle(HCH) gives rise to change $^2J_{HH}$ value and depend on the strain of the ring in the cyclic systems. Geminal coupling constant determines ring size. When bond angle is decreased, ring size is decreased so that geminal coupling constant is more positive. If a atom is replace to an electronegative atom, Geminal coupling constant move to positive value.

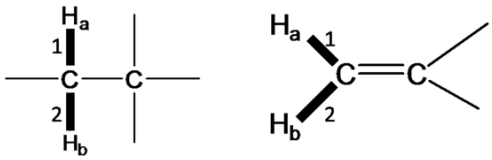


Figure 5.7.6: Geminal coupling

Vicinal proton-proton coupling ($^3J_{HH}$)

Vicinal coupling occurs though three bonds (Figure 5.7.7.). The Vicinal coupling is the most useful information of dihedral angle, leading to stereochemistry and conformation of molecules. Vicinal coupling constant always has the positive value and is affected by the dihedral angle (?;HCCH), the valence angle (?; HCC), the bond length of carbon-carbon, and the effects of electronegative atoms. Vicinal coupling constant depending on the dihedral angle (Figure 5.7.8) is given by the Karplus equation.

$$^3J = 7.0 - 0.5\cos\phi + 4.5\cos^2\phi \tag{5.7.3}$$

When ? is the 90°, vicinal coupling constant is zero. In addition, vicinal coupling constant ranges from 8 to 10 Hz at the and ? =180°, where ?=0° and ?=180° means that the coupled protons have cis and trans configuration, respectively.

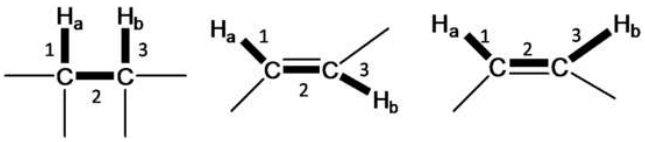


Figure 5.7.7: Vicinal coupling

The valence angle(?;Figure 5.7.8) also causes change of $^{3}J_{HH}$ value. Valence angle is related with ring size. Typically, when the valence angle decreases, the coupling constant reduces. The distance between the carbons atoms gives influences to vicinal coupling constant

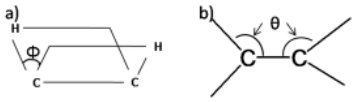


Figure 5.7.8: a) Dihedral angle and b) valence angle

The coupling constant increases with the decrease of bond length. Electronegative atoms affect vicinal coupling constants so that electronegative atoms decrease the vicinal coupling constants.

Integral

Integral is referred to integrated peak area of 1H signals. The intensity is directly proportionally to the number of hydrogen.

^{13}C NMR

Chemical Shift

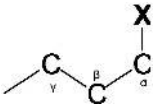


Figure 5.7.9 shows typical ^{13}C chemical shift regions of the major chemical class.

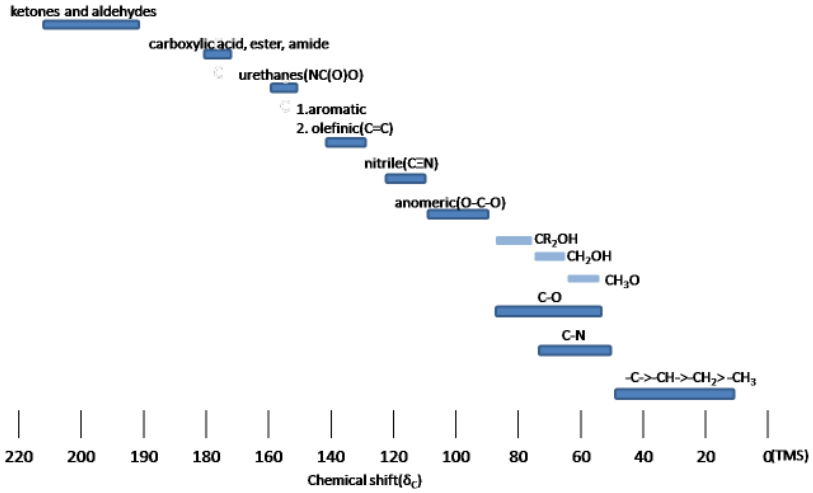


Figure 5.7.9: ^{13}C Chemical shift range for organic compound

Spin-Spin splitting

Comparing the ^{1}H NMR, there is a big difference thing in the ^{13}C NMR. The ^{13}C- ^{13} C spin-spin splitting rarely exit between adjacent carbons because ^{13}C is naturally lower abundant (1.1%)

- **^{13}C-^{1}H Spin coupling**: ^{13}C-^{1}H Spin coupling provides useful information about the number of protons attached a carbon atom. In case of one bond coupling ($^{1}J_{CH}$), -CH, -CH_2, and CH_3 have respectively doublet, triplet, quartets for the ^{13}C resonances in the spectrum. However, ^{13}C-^{1}H Spin coupling has an disadvantage for ^{13}C spectrum interpretation. ^{13}C-^{1}H Spin coupling is hard to analyze and reveal structure due to a forest of overlapping peaks that result from 100% abundance of ^{1}H.
- **Decoupling**: Decoupling is the process of removing ^{13}C-^{1}H coupling interaction to simplify a spectrum and identify which pair of nuclei is involved in the J coupling. The decoupling ^{13}C spectra shows only one peak(singlet) for each unique carbon in the

molecule(Figure 5.7.10). Decoupling is performed by irradiating at the frequency of one proton with continuous low-power RF.

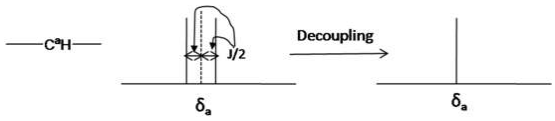


Figure 5.7.10. Decoupling in the ^{13}C NMR

- **Distortionless enhancement by polarization transfer (DEPT):** DEPT is used for distinguishing between a CH_3 group, a CH_2 group, and a CH group. The proton pulse is set at 45º, 90º, or 135º in the three separate experiments. The different pulses depend on the number of protons attached to a carbon atom. Figure 5.7.11. is an example about DEPT spectrum.

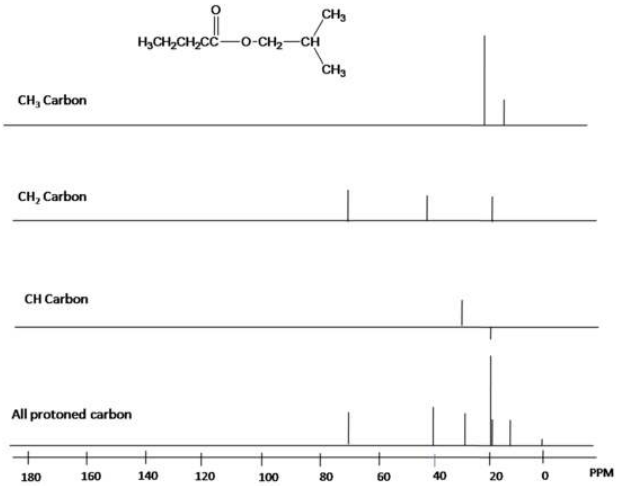


Figure 5.7.11. DEPT spectrum of n-isobutlybutrate

2-dimensional NMR spectroscopy (COSY)

COSY stands for COrrelation SpectroscopY. COSY spectrum is more useful information about what is being correlated.

^1H-^1H COSY (COrrelation SpectroscopY)

^1H-^1H COSY is used for clearly indicate correlation with coupled protons. A point of entry into a COSY spectrum is one of the keys to predict information from it successfully. Relation of Coupling protons is determined by cross peaks(correlation peaks) and in the COSY spectrum. In other words, Diagonal peaks by lines ar e coupled to each other. Figure 5.7.12 indicates that there are correlation peaks between proton H_1 and H_2 as well as between H_2 and H_4. This means the H_2 coupled to H_1 and H_4.

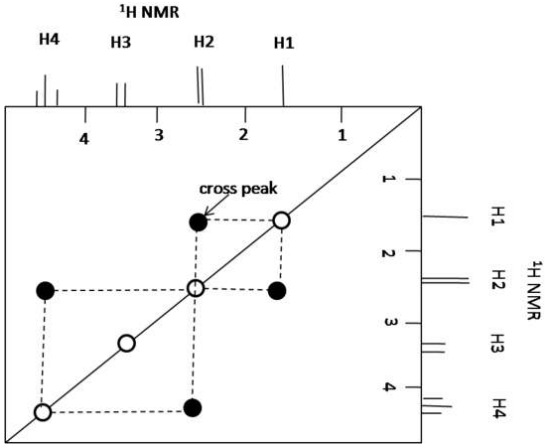


Figure 5.7.12. ^1H-^1H COSY spectrum

^{1}H-^{13}C COSY (HETCOR)

^{1}H-^{13}C COSY is the heteronuclear correlation spectroscopy. The HETCOR spectrum is correlated ^{13}C nuclei with directly attached protons. ^{1}H-^{13}C coupling is one bond. The cross peaks mean correlation between a proton and a carbon (Figure 5.7.13). If a line does not have cross peak, this means that this carbon atoms has no attached proton (e.g. a quaternary carbon atom)

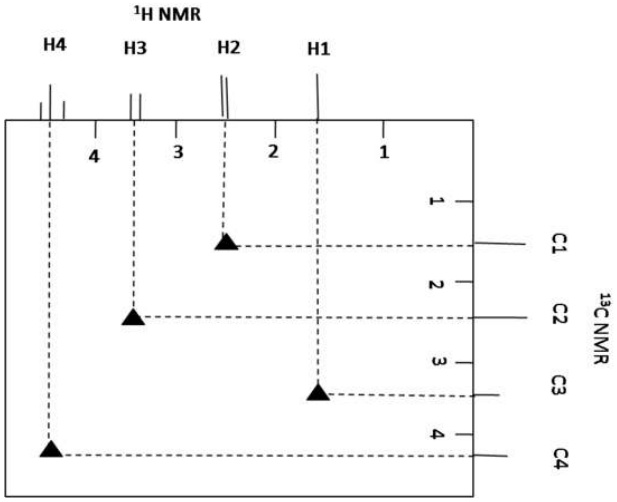


Figure 5.7.13. ^{1}H-^{13}C COSY spectrum

References

1. Balc*, M., Basic p1 sH- and p13 sC-NMR spectroscopy. 1st ed.; Elsevier: Amsterdam ; Boston, 2005; p xii, 427.
2. Breitmaier, E., Structure elucidation by NMR in organic chemistry : a practical guide. 3rd rev. ed.; Wiley: Chichester, West Sussex, England, 2002; p xii, 258.
3. Jacobsen, N. E., NMR spectroscopy explained : simplified theory, applications and examples for organic chemistry and structural biology. Wiley-Interscience: Hoboken, N.J., 2007; p xv, 668.
4. Silverstein, R. M.; Webster, F. X., Spectrometric identification of organic compounds. 6th ed.; Wiley: New York, 1998; p xiv, 482.

Outside Links

- NMRShiftDB: a Free web database for NMR data : nmrshiftdb.chemie.uni-mainz.de/nmrshiftdb
- NMR database from ACD/LAbs : www.acdlabs.com/products/spec_lab/exp_spectra/spec_libraries/aldrich.html
- NMR database from John Crerar Library : http://crerar.typepad.com/crerar_lib...h_ir_nmr_.html

Problems

Draw the 1H NMR spectrum for 2-Hydroxypropane in CDCl3. Assume sufficient resolution to provide a first-order spectrum and ignore vicinal proton-proton coupling(3JHH)

Solution

1) the structure of 2-hydoroxyporpane is drawn

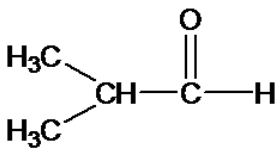


Figure out which protons are chemically equivalent, i.e., two methyl (-CH_3) groups are chemical equivalent.

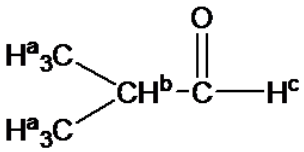
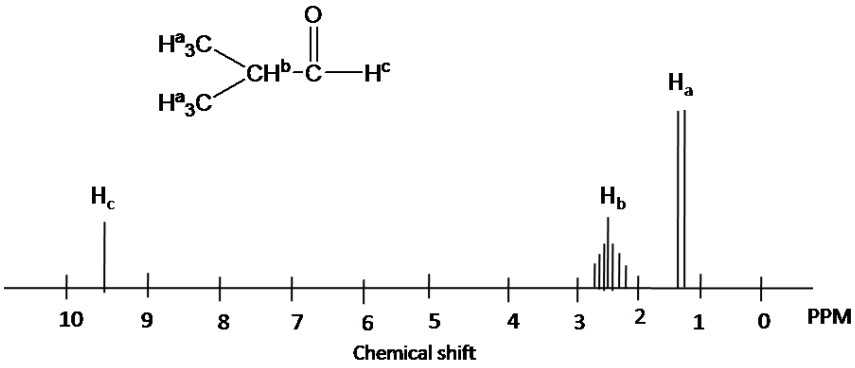


Figure1): chemical shift of methyl groups (H_a) : 1-2 ppm (?H_a=1.1 ppm); chemical shift of -CH- groups (H_b) moves to downfield due to effect on aldehyde groups:2-3ppm (?H_b=2.4 ppm); chemical shift of aldehyde groups (H_c):9-10 ppm (?H_c=9.6 ppm)

4) Splitting pattern is determined by (N+1) rule: Ha is split into two peaks by H_b(#of proton=1). H_b has the septet pattern by H_a (#of proton=6). H_c has one peak.(Note that H_c has doublet pattern by H_b due to vicinal proton-proton coupling.)



Contributors and Attributions

- You Jin Seo

5.7: Interpretation is shared under a CC BY-NC-SA 4.0 license and was authored, remixed, and/or curated by LibreTexts.

- **NMR - Interpretation** is licensed CC BY 4.0.

Integration in NMR

The intensity of the signal is proportional to the number of hydrogens that make the signal. Sometimes, NMR machines display signal intensity as an automatic display above the regular spectrum. (The exact number of hydrogens giving rise to each signal is sometimes also explicitly written above each peak, making our job a lot easier.) The intensity of the signal allows us to conclude that the more hydrogens there are in the same chemical environment, the more intense the signal will be.

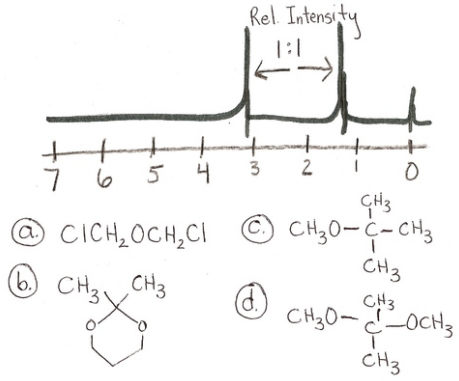
Introduction

We can get the following information from a ^{1}H Nuclear Magnetic Resonance (NMR) structure:

1. The integrated intensity of a signal in a ^{1}H NMR spectrum (does not apply to ^{13}C NMR) gives a ratio for the number of hydrogens that give rise to the signal, thereby helping calculate the total number of hydrogens present in a sample.NMR machines can be used to measure signal intensity, a plot of which is sometimes automatically displayed above the regular spectrum. To show these integrations, a recorder pen marks a vertical line with a length that is proportional to the integrated area under a signal (sometimes referred to as a peak)-- a value that is proportional to the number of hydrogens that are accountable for the signal. The pen then moves horizontally until another signal is reached, at which point, another vertical marking is made. We can manually measure the lengths by which the horizontal line is displaced at each peak to attain a ratio of hydrogens from the various signals. We can use this technique to figure out the hydrogen ratio when the number of hydrogens responsible for each signal is not written directly above the peak (look in the links section for an animation on how to manually find the ratio of hydrogens as described here).

   Now that we've seen how the signal intensity is directly proportionate to the number of hydrogens that give rise to that signal, it makes sense to conclude that the more hydrogens of one kind there are in a molecule (equivalent hydrogens, so in the same chemical environment), the more intense the corresponding NMR signal will be. **Here's a model that may help clear up some of the uncertainties.** NMR model

Study tips



1. 3.)

Answers

1. False. The *relative* number of hydrogens determines the intensity of a signal. The signal given by the three hydrogens in $C\mathbf{H_3}CH_2CHCl_2$ will not have the same intensity as the three hydrogens in $ClCH_2OC\mathbf{H_3}$.
2. There are 2 signals. One is at 3.3 ppm (6 hydrogens); the other at 3.5 ppm (4 hydrogens).
3. a and d
4. c
5. d

Integration in NMR is shared under a CC BY-NC-SA 4.0 license and was authored, remixed, and/or curated by LibreTexts.

- **Integration in NMR** is licensed CC BY 4.0.

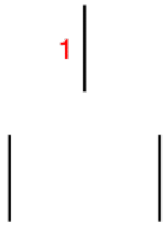
Pascal's Triangle

The Pascal's triangle is a graphical device used to predict the ratio of heights of lines in a split NMR peak. To construct the Pascal's triangle, use the following procedure.

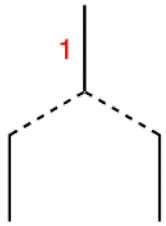
Step 1: Draw a short, vertical line and write number one next to it.



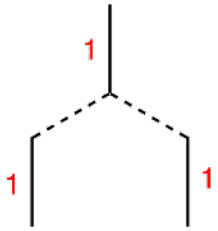
Step 2: Draw two vertical lines underneath it symmetrically.



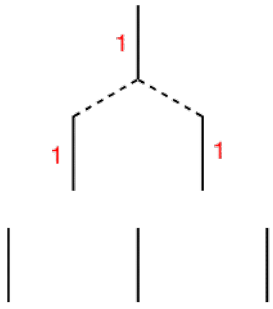
Step 3: Connect each of them to the line above using broken lines.



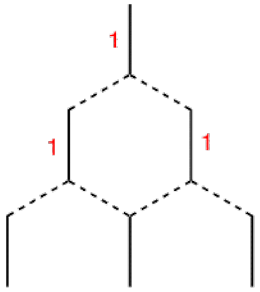
Step 4: Each of the two lines is connected to the single line above, which carries the number one. Therefore, write number one next to each line.



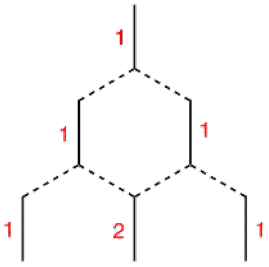
Step 5: Draw three vertical lines symmetrically underneath the two lines.



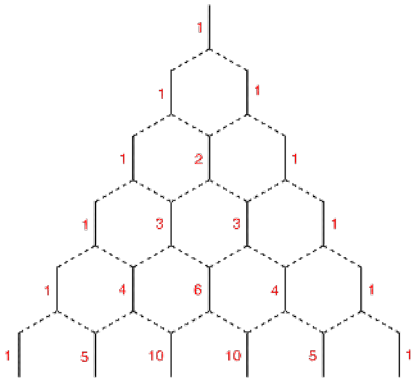
Step 6: Connect each of them to the nearest line(s) above.



Step 7: Each terminal line is connected to one line above, which carries the number one. Therefore, write number one next to each of them. The internal line is connected to two lines above, each carrying the number one. 1 + 1 = 2; write number two next to the internal line.



Continue the process as far down as necessary.



splitting pattern	the ratio of heights of lines in the peak
singlet	1
doublet	1:1
triplet	1:2:1
quartet	1:3:3:1
quintet	1:4:6:4:1
sextet	1:5:10:10:5:1

- see also (n+1) Rule, coupling constant

Contributors and Attributions

- Gamini Gunawardena from the OChemPal site (Utah Valley University)

Pascal's Triangle is shared under a CC BY-NC-SA 4.0 license and was authored, remixed, and/or curated by LibreTexts.

- **Pascal's Triangle** by Gamini Gunawardena is licensed CC BY 4.0.

SECTION OVERVIEW

5.8: Structural Assignment

(n 1) Rule

Background to C-13 NMR

Determine Structure with Combined Spectra

High Resolution Proton NMR Spectra

Integration in Proton NMR

Interpreting C-13 NMR Spectra

Introduction to Proton NMR

Low Resolution Proton NMR Spectra

More About Electronics

Multiplicity in Proton NMR

NMR11. More About Multiplicity

NMR14. More Practice with NMR Spectroscopy

NMR2. Carbon-13 NMR

NMR3. Symmetry in NMR

NMR4. 13C NMR and Geometry

NMR5. 13C NMR and Electronics

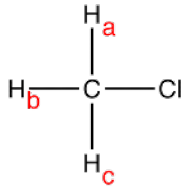
NMR8. Chemical Shift in 1H NMR

NMR Appendix. Useful Charts for NMR identification

5.8: Structural Assignment is shared under a CC BY-NC-SA 4.0 license and was authored, remixed, and/or curated by LibreTexts.

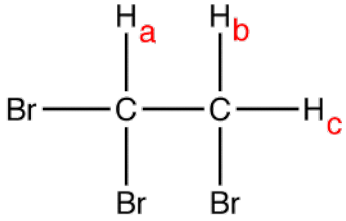
(n 1) Rule

The (n+1) Rule, an empirical rule used to predict the multiplicity and, in conjunction with Pascal's triangle, splitting pattern of peaks in ^{1}H and ^{13}C NMR spectra, states that if a given nucleus is coupled (see spin coupling) to n number of nuclei that are equivalent (see equivalent ligands), the multiplicity of the peak is n+1. eg. 1:



1

The three hydrogen nuclei in 1, H_a, H_b, and H_c, are equivalent. Thus, 1H NMR spectrum of 1 H_as only one peak. H_a, H_b, and H_c are coupled to no hydrogen nuclei. Thus, for H_a, H_b, and H_c, n=0; (n+1) = (0+1) = 1. The multiplicity of the peak of H_a, H_b, and H_c is one. The peak H_as one line; it is a singlet. eg. 2:



2

There are two sets of equivalent hydrogen nuclei in 2:

- Set 1: H_a
- Set 2: H_b, H_c

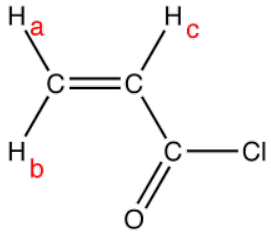
Thus, the 1H NMR spectrum of 2 H_as two peaks, one due to H_a and the other to H_b and H_c.

The peak of H_a: There are two vicinal hydrogens to H_a: H_b and H_c. H_b and H_c are equivalent to each other but not to H_a. Thus, for H_a, n=2; (n+1) = (2+1) = 3. The multiplicity of the peak of H_a is three. The peak H_as three lines; from the Pascal's triangle, it is a triplet.

The peak of H_b and H_c: There is only one vicinal hydrogen to H_b and H_c: H_a. H_a is not equivalent to H_b and H_c. Thus, for H_b and H_c, n=1; (n+1) = (1+1) = 2. The multiplicity of the peak of H_b and H_c is two. The peak H_as two lines, from the Pascal's triangle, it is a doublet.

To determine the multiplicity of a peak of a nucleus coupled to more than one set of equivalent nuclei, apply the (n+1) Rule independently to each other.

eg:



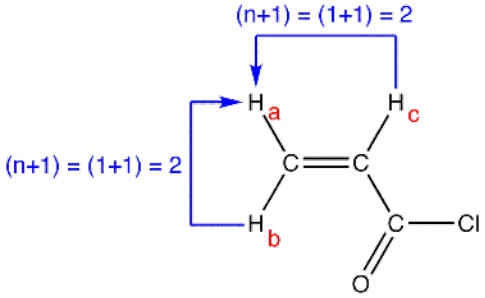
3

There are three set of equivalent hydrogen nuclei in 3:

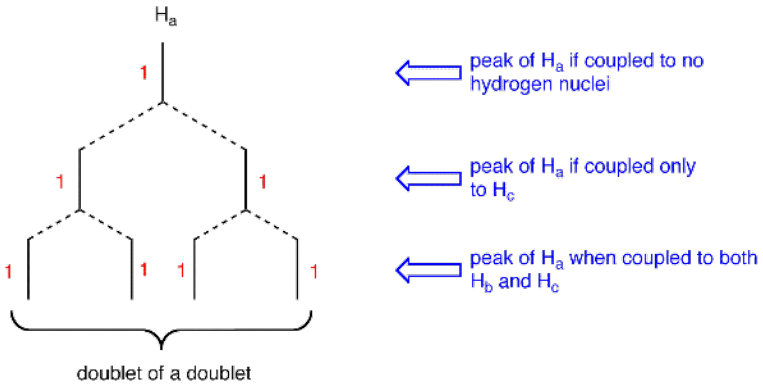
- Set 1: H_a
- Set 2: H_b
- Set 3: H_c

	H_a	H_b	H_c
H_a		geminal; coupling occurs	vicinal; coupling occurs
H_b	geminal; coupling occurs		vicinal; coupling occurs
H_c	vicinal; coupling occurs	vicinal; coupling occurs	

peak of H_a:

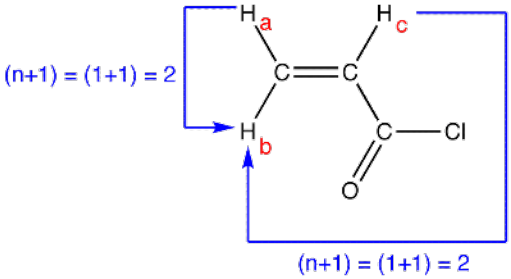


multiplicity of the peak of $H_a = 2 \times 2 = 4$. To determine the splitting pattern of the peak of H_a, use the Pascal's triangle, based on the observation that, for alkenyl hydrogens, $J_{cis} > J_{gem}$.

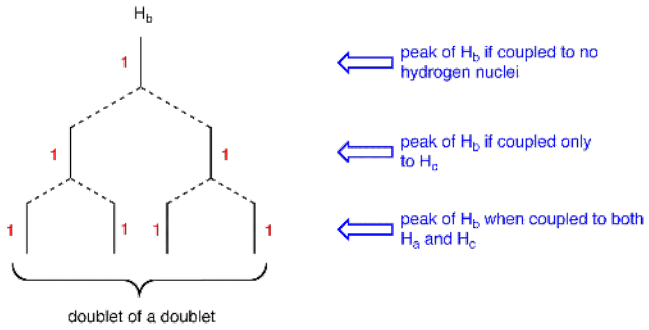


The peak of H_a is a doublet of a doublet.

peak of H_b:

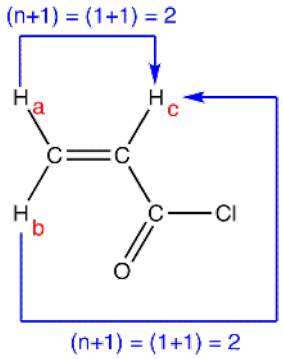


multiplicity of the peak of $H_b = 2 \times 2 = 4$. To determine the splitting pattern of the peak of H_b, use the Pascal's triangle, based on the observation that, for alkenyl hydrogens, $J_{trans} > J_{gem}$.

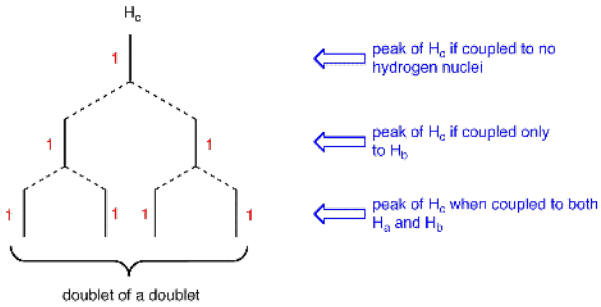


The peak of H_b is a doublet of a doublet.

peak of H_c:



multiplicity of the peak of $H_c = 2 \times 2 = 4$. To determine the splitting pattern of the peak of H_c, use the Pascal's triangle based on the observation that, for alkenyl hydrogens, $J_{trans} > J_{cis}$.



The peak of H_c is a doublet of a doublet.

(n 1) Rule is shared under a CC BY-NC-SA 4.0 license and was authored, remixed, and/or curated by LibreTexts.

- **(n+1) Rule** by Gamini Gunawardena is licensed CC BY 4.0.

Background to C-13 NMR

This page describes what a C-13 NMR spectrum is and how it tells you useful things about the carbon atoms in organic molecules.

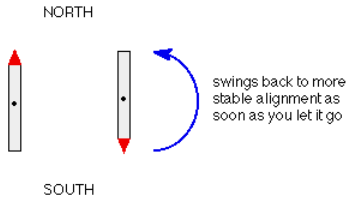
The background to C-13 NMR spectroscopy

Nuclear magnetic resonance is concerned with the magnetic properties of certain nuclei. On this page we are focussing on the magnetic behavior of carbon-13 nuclei.

Carbon-13 nuclei as little magnets

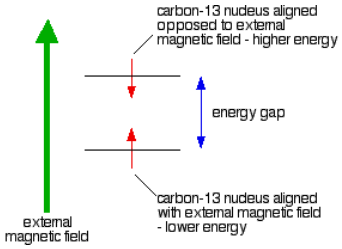
About 1% of all carbon atoms are the C-13 isotope; the rest (apart from tiny amounts of the radioactive C-14) is C-12. C-13 NMR relies on the magnetic properties of the C-13 nuclei. Carbon-13 nuclei fall into a class known as "spin ½" nuclei for reasons which don't really need to concern us at the introductory level this page is aimed at (UK A level and its equivalents). The effect of this is that a C-13 nucleus can behave as a little magnet. C-12 nuclei don't have this property.

If you have a compass needle, it normally lines up with the Earth's magnetic field with the north-seeking end pointing north. Provided it isn't sealed in some sort of container, you could twist the needle around with your fingers so that it pointed south - lining it up opposed to the Earth's magnetic field. It is very unstable opposed to the Earth's field, and as soon as you let it go again, it will flip back to its more stable state.



Because a C-13 nucleus behaves like a little magnet, it means that it can also be aligned with an external magnetic field or opposed to it.

Again, the alignment where it is opposed to the field is less stable (at a higher energy). It is possible to make it flip from the more stable alignment to the less stable one by supplying exactly the right amount of energy.

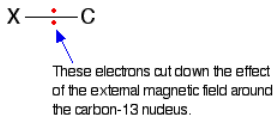


The energy needed to make this flip depends on the strength of the external magnetic field used, but is usually in the range of energies found in radio waves - at frequencies of about 25 - 100 MHz. (BBC Radio 4 is found between 92 - 95 MHz!) If you have also looked at proton-NMR, the frequency is about a quarter of that used to flip a hydrogen nucleus for a given magnetic field strength.

It's possible to detect this interaction between the radio waves of just the right frequency and the carbon-13 nucleus as it flips from one orientation to the other as a peak on a graph. This flipping of the carbon-13 nucleus from one magnetic alignment to the other by the radio waves is known as the resonance condition.

The importance of the carbon's environment

What we've said so far would apply to an isolated carbon-13 nucleus, but real carbon atoms in real bonds have other things around them - especially electrons. The effect of the electrons is to cut down the size of the external magnetic field felt by the carbon-13 nucleus.

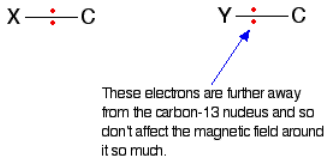


Suppose you were using a radio frequency of 25 MHz, and you adjusted the size of the magnetic field so that an isolated carbon-13 atom was in the resonance condition.

If you replaced the isolated carbon with the more realistic case of it being surrounded by bonding electrons, it wouldn't be feeling the full effect of the external field any more and so would stop resonating (flipping from one magnetic alignment to the other). The resonance condition depends on having exactly the right combination of external magnetic field and radio frequency.

How would you bring it back into the resonance condition again? You would have to increase the external magnetic field slightly to compensate for the shielding effect of the electrons.

Now suppose that you attached the carbon to something more electronegative. The electrons in the bond would be further away from the carbon nucleus, and so would have less of a lowering effect on the magnetic field around the carbon nucleus.



The external magnetic field needed to bring the carbon into resonance will be smaller if it is attached to a more electronegative element, because the C-13 nucleus feels more of the field. Even small differences in the electronegativities of the attached atoms will make a difference to the magnetic field needed to achieve resonance.

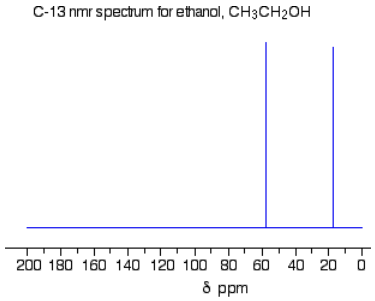
Summary

For a given radio frequency (say, 25 MHz) each carbon-13 atom will need a slightly different magnetic field applied to it to bring it into the resonance condition depending on what exactly it is attached to - in other words the magnetic field needed is a useful guide to the carbon atom's environment in the molecule.

Features of a C-13 NMR spectrum

The C-13 NMR spectrum for ethanol

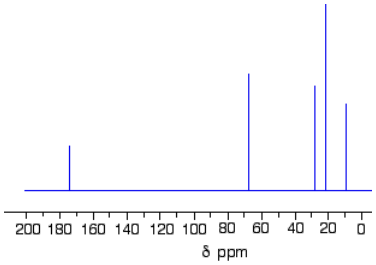
This is a simple example of a C-13 NMR spectrum. Don't worry about the scale for now - we'll look at that in a minute.



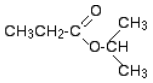
There are two peaks because there are two different environments for the carbons. The carbon in the CH_3 group is attached to 3 hydrogens and a carbon. The carbon in the CH_2 group is attached to 2 hydrogens, a carbon and an oxygen. The two lines are in different places in the NMR spectrum because they need different external magnetic fields to bring them in to resonance at a particular radio frequency.

The C-13 NMR spectrum for a more complicated compound

This is the C-13 NMR spectrum for 1-methylethyl propanoate (also known as isopropyl propanoate or isopropyl propionate).



This time there are 5 lines in the spectrum. That means that there must be 5 different environments for the carbon atoms in the compound. Is that reasonable from the structure?



Well - if you count the carbon atoms, there are 6 of them. So why only 5 lines? In this case, two of the carbons are in exactly the same environment. They are attached to exactly the same things. Look at the two CH_3 groups on the right-hand side of the molecule.

You might reasonably ask why the carbon in the CH_3 on the left isn't also in the same environment. Just like the ones on the right, the carbon is attached to 3 hydrogens and another carbon. But the similarity isn't exact - you have to chase the similarity along the rest of the molecule as well to be sure.

The carbon in the left-hand CH_3 group is attached to a carbon atom which in turn is attached to a carbon with two oxygens on it - and so on down the molecule.

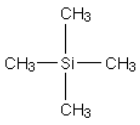
That's not exactly the same environment as the carbons in the right-hand CH_3 groups. They are attached to a carbon which is attached to a single oxygen - and so on down the molecule.

We'll look at this spectrum again in detail on the next page - and look at some more similar examples as well. This all gets easier the more examples you look at.

For now, all you need to realise is that each line in a C-13 NMR spectrum recognises a carbon atom in one particular environment in the compound. If two (or more) carbon atoms in a compound have exactly the same environment, they will be represented by a single line.

The need for a standard for comparison - TMS

Before we can explain what the horizontal scale means, we need to explain the fact that it has a zero point - at the right-hand end of the scale. The zero is where you would find a peak due to the carbon-13 atoms in tetramethylsilane - usually called TMS. Everything else is compared with this.



You will find that some NMR spectra show the peak due to TMS (at zero), and others leave it out. Essentially, if you have to analyse a spectrum which has a peak at zero, you can ignore it because that's the TMS peak.

TMS is chosen as the standard for several reasons. The most important are:

- It has 4 carbon atoms all of which are in exactly the same environment. They are joined to exactly the same things in exactly the same way. That produces a single peak, but it's also a strong peak (because there are lots of carbon atoms all doing the same thing).

- The net effect of this is that TMS produces a peak on the spectrum at the extreme right-hand side. Almost everything else produces peaks to the left of it.

The chemical shift

The horizontal scale is shown as δ (ppm). δ is called the chemical shift and is measured in parts per million - ppm. A peak at a chemical shift of, say, 60 means that the carbon atoms which caused that peak need a magnetic field 60 millionths less than the field needed by TMS to produce resonance. A peak at a chemical shift of 60 is said to be downfield of TMS. The further to the left a peak is, the more downfield it is.

Solvents for NMR spectroscopy

NMR spectra are usually measured using solutions of the substance being investigated. A commonly used solvent is $CDCl_3$. This is a trichloromethane (chloroform) molecule in which the hydrogen has been replaced by its isotope, deuterium.

$CDCl_3$ is also commonly used as the solvent in proton-NMR because it doesn't have any ordinary hydrogen nuclei (protons) which would give a line in a proton-NMR spectrum. It does, of course, have a carbon atom - so why doesn't it give a potentially confusing line in a C-13 NMR spectrum? In fact it does give a line, but the line has an easily recognizable chemical shift and so can be removed from the final spectrum. All of the spectra from the SDBS have this line removed to avoid any confusion.

Contributors and Attributions

Jim Clark (Chemguide.co.uk)

This page titled Background to C-13 NMR is shared under a CC BY-NC 4.0 license and was authored, remixed, and/or curated by Jim Clark.

- **Background to C-13 NMR** by Jim Clark is licensed CC BY-NC 4.0.

Determine Structure with Combined Spectra

There are a many ways we can use NMR spectroscopy to analyse compounds. One common application is in determination of an unknown structure. Given the MS, IR, ^{13}C and ^{1}H NMR spectra, what might be the structure of an unknown sample?

It is often easiest to start with the IR spectrum.

- identify at least three peaks in the IR spectrum. Which peaks seem to tell you the most information about this compound?
- don't think with your head; think with your hands. Write down ideas on the spectrum.
- if you are working on a formal proof of structure, on a class test or a lab report, you may be required to enter your data in a table correlating wavenumber with peak assignment:

cm^{-1}	asst

For example, a student might obtain the following IR spectrum.

From that information, she constructs the following table. She might even write this table, by hand, directly on her spectrum. She makes useful notes on the edges, and might even include some guesses, which she later crosses out, but does not erase. She is assisted in this task by consulting an IR table, that suggests what some of these peaks might mean.

Remember:

- make special note of what atoms are present in the compound: C, H, N, O...
- also note your initial ideas about specific functional groups that may be present.
- if you are unsure of an assignment, put a question mark beside it to signal this uncertainty.
- some data may need to be discarded later if it is not consistent with other data.

Look at the ^{13}C spectrum.

- How many different carbons are there, based on the number of peaks in the spectrum? This is the first step in estimating the molecular formula.
- Do you have reason to believe there is symmetry in the structure? In the entire compound or just part of it? Adjust the number of carbons you think you are dealing with.
- As in IR spectroscopy, begin assigning peaks, either on the spectrum or, if required, in a table:

ppm	asst

For example, a student might obtain the following ^{13}C NMR spectrum:

From that information, she puts together the following table:

Remember:

- you will be able to assign all peaks in the NMR spectrum, not just a few like in IR.

You can get more information on the formula from the ^{1}H NMR spectrum and the mass spectrum.

- In the ^{1}H NMR spectrum, what does the sum of the integrations suggest about the number of hydrogens?
- At this point you may have a formula, $C_xH_yO_z$. What would be the mass of a compound with this formula?
- Compare this mass to the mass spectrum. Does it match?
- If not, consider whether a common atom (such as oxygen) is missing from your formula, or if there might be symmetry that you have missed.
- Does the mass spectrum suggest the presence of a nitrogen (odd molecular weight) or chlorine or bromine (isotope pattern)?

Once you have the molecular formula, the number of possible structures is automatically limited. The number of units of unsaturation can help you narrow down the possibilities.

- The ratio of C : H in a saturated, acyclic hydrocarbon is n : 2n+2.
- Each pair of H missing from the formula corresponds to a multiple bond or a ring.
- The presence of oxygen (which is divalent) does not alter the C : H ratio.
- The presence of halogen (which is monovalent) means there is one H missing.
- The presence of a nitrogen (which is trivalent) means there is an extra H in the formula.
- In other words, C_4H_8O has one ring or double bond just like C_4H_8, and so do C_4H_7Br and C_4H_9N.

As in ^{13}C NMR, you should be able to assign all peaks in the ^{1}H NMR spectrum. You may be able to do so by making notes on the spectrum. If you think you know the structure, you may be able to draw it and note which peak belongs with which proton.

A formal proof of structure might require a table of assignments.

ppm	int	mult	partial structure	assignment

- This table demonstrates your ability to read the spectrum. Can you decide what ratio of protons is suggested by the integral line? Can you decide whether a peak is a quartet?
- The partial structure column should explain the shift, integration and multiplicity for the peak in that row. It should not show any other information from elsewhere in the structure. This restriction forces you to demonstrate a thorough understanding of the data in a way that "getting the right answer" does not.
- The partial structure column is best filled in with drawings, not words. The drawing is a partial structure.
- Because the partial structure will show the protons absorbing at the shift in that row as well the neighbouring protons, you need to distinguish between them in your picture. Most people circle or underline or make bold the protons that show up at the shift given in that row.
- When finished with the partial structure column, you should be able to link the partial structures together to make an entire structure in the assignment column.

An example of a spectrum and its accompanying data table is given below. Here is the spectrum:



Here is a data table:



Things to note:

- This student has used two integration columns instead of just one.
- The first column shows the integral measured from the spectrum. She probably used a ruler.
- The second column, which she called int(n), contains a convenient ratio taken from the raw data. This ratio is easier to use in her assignments.
- Also note that the peak at 9.7 ppm does not have a very good integral. There is either a "phasing" or a "level & tilt" problem here that can be corrected using the NMR software, but this is sometimes difficult to do. If she had taken an automatic printout of this integral measurement, she would have gotten a strange number; in this case, it would be about -5, because the end of the

integral line is lower than the start. It clearly isn't a negative number of hydrogens, though. She has instead measured the vertical rise in the integral and recorded that; it isn't perfect, but is a fair estimate in this case.

Contributors and Attributions

Chris P Schaller, Ph.D., (College of Saint Benedict / Saint John's University)

This page titled Determine Structure with Combined Spectra is shared under a CC BY-NC 3.0 license and was authored, remixed, and/or curated by Chris Schaller.

- **Determine Structure with Combined Spectra** by Chris Schaller is licensed CC BY 3.0.

High Resolution Proton NMR Spectra

This page describes how you interpret simple high resolution nuclear magnetic resonance (NMR) spectra. It assumes that you have already read the background page on NMR so that you understand what an NMR spectrum looks like and the use of the term "chemical shift". It also assumes that you know how to interpret simple low resolution spectra.

The difference between high and low resolution spectra

What a low resolution NMR spectrum tells you

- The number of peaks tells you the number of different environments the hydrogen atoms are in.
- The ratio of the areas under the peaks tells you the ratio of the numbers of hydrogen atoms in each of these environments.
- The chemical shifts give you important information about the sort of environment the hydrogen atoms are in.

High resolution NMR spectra

In a high resolution spectrum, you find that many of what looked like single peaks in the low resolution spectrum are split into clusters of peaks.

1 peak	a singlet
2 peaks in the cluster	a doublet
3 peaks in the cluster	a triplet
4 peaks in the cluster	a quartet

You can get exactly the same information from a high resolution spectrum as from a low resolution one - you simply treat each cluster of peaks as if it were a single one in a low resolution spectrum. But in addition, the amount of splitting of the peaks gives you important extra information.

Interpreting a high resolution spectrum

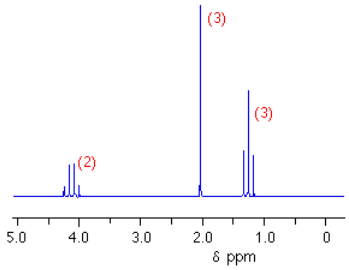
The n+1 rule

The amount of splitting tells you about the number of hydrogens attached to the carbon atom or atoms next door to the one you are currently interested in. The number of sub-peaks in a cluster is one more than the number of hydrogens attached to the next door carbon(s). So - on the assumption that there is only one carbon atom with hydrogens on next door to the carbon we're interested in.

singlet	next door to carbon with no hydrogens attached
doublet	next door to a CH group
triplet	next door to a CH_2 group
quartet	next door to a CH_3 group

Using the n+1 rule

What information can you get from this NMR spectrum?

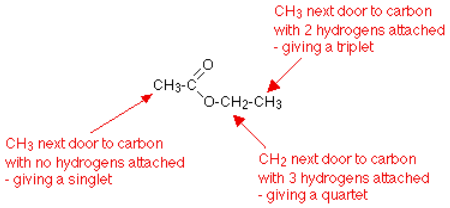


Assume that you know that the compound above has the molecular formula $C_4H_8O_2$.

Treating this as a low resolution spectrum to start with, there are three clusters of peaks and so three different environments for the hydrogens. The hydrogens in those three environments are in the ratio 2:3:3. Since there are 8 hydrogens altogether, this represents a CH_2 group and two CH_3 groups. What about the splitting?

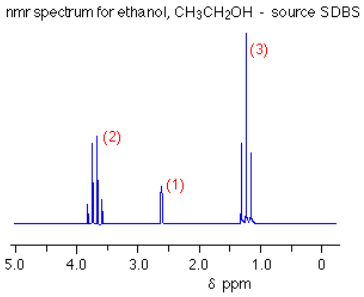
- The CH_2 group at about 4.1 ppm is a quartet. That tells you that it is next door to a carbon with three hydrogens attached - a CH_3 group.
- The CH_3 group at about 1.3 ppm is a triplet. That must be next door to a CH_2 group. This combination of these two clusters of peaks - one a quartet and the other a triplet - is typical of an ethyl group, CH_3CH_2. It is very common.
- Finally, the CH_3 group at about 2.0 ppm is a singlet. That means that the carbon next door doesn't have any hydrogens attached.

So what is this compound? You would also use chemical shift data to help to identify the environment each group was in, and eventually you would come up with:



Alcohols

Where is the -O-H peak? This is very confusing! Different sources quote totally different chemical shifts for the hydrogen atom in the -OH group in alcohols - often inconsistently. For example:



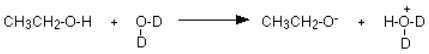
- The Nuffield Data Book quotes 2.0 - 4.0, but the Nuffield text book shows a peak at about 5.4.
- The OCR Data Sheet for use in their exams quotes 3.5 - 5.5.
- A reliable degree level organic chemistry text book quotes1.0 - 5.0, but then shows an NMR spectrum for ethanol with a peak at about 6.1.
- The SDBS database (used throughout this site) gives the -OH peak in ethanol at about 2.6.

The problem seems to be that the position of the -OH peak varies dramatically depending on the conditions - for example, what solvent is used, the concentration, and the purity of the alcohol - especially on whether or not it is totally dry.

A clever way of picking out the -OH peak

If you measure an NMR spectrum for an alcohol like ethanol, and then add a few drops of deuterium oxide, D_2O, to the solution, allow it to settle and then re-measure the spectrum, the -OH peak disappears! By comparing the two spectra, you can tell immediately which peak was due to the -OH group.

The reason for the loss of the peak lies in the interaction between the deuterium oxide and the alcohol. All alcohols, such as ethanol, are very, very slightly acidic. The hydrogen on the -OH group transfers to one of the lone pairs on the oxygen of the water molecule. The fact that here we've got "heavy water" makes no difference to that.



The negative ion formed is most likely to bump into a simple deuterium oxide molecule to regenerate the alcohol - except that now the -OH group has turned into an -OD group.



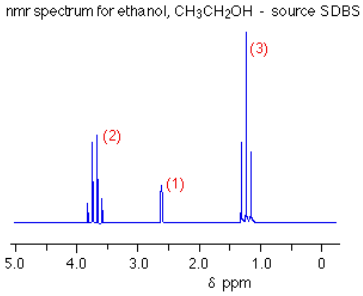
Deuterium atoms don't produce peaks in the same region of an NMR spectrum as ordinary hydrogen atoms, and so the peak disappears.

You might wonder what happens to the positive ion in the first equation and the OD^- in the second one. These get lost into the normal equilibrium which exists wherever you have water molecules - heavy or otherwise.



The lack of splitting with -OH groups

Unless the alcohol is absolutely free of any water, the hydrogen on the -OH group and any hydrogens on the next door carbon don't interact to produce any splitting. The -OH peak is a singlet and you don't have to worry about its effect on the next door hydrogens.

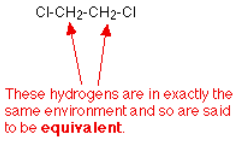


The left-hand cluster of peaks is due to the CH_2 group. It is a quartet because of the 3 hydrogens on the next door CH_3 group. You can ignore the effect of the -OH hydrogen. Similarly, the -OH peak in the middle of the spectrum is a singlet. It hasn't turned into a triplet because of the influence of the CH_2 group.

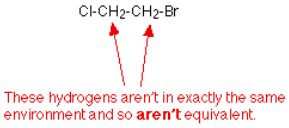
Equivalent hydrogen atoms

Hydrogen atoms attached to the same carbon atom are said to be equivalent. Equivalent hydrogen atoms have no effect on each other - so that one hydrogen atom in a CH_2 group doesn't cause any splitting in the spectrum of the other one.

But hydrogen atoms on neighboring carbon atoms can also be equivalent if they are in exactly the same environment. For example:



These four hydrogens are all exactly equivalent. You would get a single peak with no splitting at all. You only have to change the molecule very slightly for this no longer to be true.



Because the molecule now contains different atoms at each end, the hydrogens are no longer all in the same environment. This compound would give two separate peaks on a low resolution NMR spectrum. The high resolution spectrum would show that both peaks subdivided into triplets - because each is next door to a differently placed CH_2 group.

Contributors and Attributions

- Jim Clark (Chemguide.co.uk)

This page titled High Resolution Proton NMR Spectra is shared under a CC BY-NC 4.0 license and was authored, remixed, and/or curated by Jim Clark.

- **High Resolution Proton NMR Spectra** by Jim Clark is licensed CC BY-NC 4.0.

Integration in Proton NMR

Integration in Proton NMR

This page titled Integration in Proton NMR is shared under a CC BY-NC 3.0 license and was authored, remixed, and/or curated by Chris Schaller.

Interpreting C-13 NMR Spectra

This page takes an introductory look at how you can get useful information from a C-13 NMR spectrum.

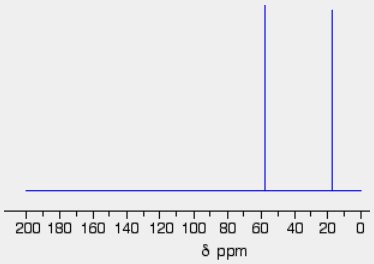
Typical chemical shifts in C-13 NMR spectra

In the table, the "R" groups won't necessarily be simple alkyl groups. In each case there will be a carbon atom attached to the one shown in red, but there may well be other things substituted into the "R" group.

carbon environment	chemical shift (ppm)
C=O (in ketones)	205 - 220
C=O (in aldehydes)	190 - 200
C=O (in acids and esters)	170 - 185
C in aromatic rings	125 - 150
C=C (in alkenes)	115 - 140
RCH_2OH	50 - 65
RCH_2Cl	40 - 45
RCH_2NH_2	37 - 45
R_3CH	25 - 35
CH_3CO-	20 - 30
R_2CH_2	16 - 25
RCH_3	10 - 15

If a substituent is very close to the carbon in question, and very electronegative, that might affect the values given in the table slightly. For example, ethanol has a peak at about 60 because of the CH_2OH group. It also has a peak due to the RCH_3 group. The "R" group this time is CH_2OH. The electron pulling effect of the oxygen atom increases the chemical shift slightly from the one shown in the table to a value of about 18.

Example 1: Ethanol

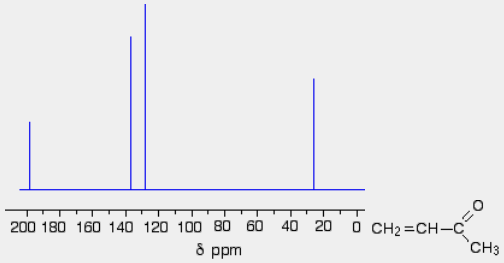


Remember that each peak identifies a carbon atom in a different environment within the molecule. In this case there are two peaks because there are two different environments for the carbons. The carbon in the CH_3 group is attached to 3 hydrogens and a carbon. The carbon in the CH_2 group is attached to 2 hydrogens, a carbon and an oxygen. So which peak is which?

You might remember from the introductory page that the external magnetic field experienced by the carbon nuclei is affected by the electronegativity of the atoms attached to them. The effect of this is that the chemical shift of the carbon increases if you attach an atom like oxygen to it. That means that the peak at about 60 (the larger chemical shift) is due to the CH_2 group because it has a more electronegative atom attached.

Example 2: But-3-en-2-one

This is also known as 3-buten-2-one (amongst many other things!)



Here is the structure for the compound:

You can pick out all the peaks in this compound using the simplified table above.

- The peak at just under 200 is due to a carbon-oxygen double bond. The two peaks at 137 and 129 are due to the carbons at either end of the carbon-carbon double bond. And the peak at 26 is the methyl group which, of course, is joined to the rest of the molecule by a carbon-carbon single bond.

If you want to use the more accurate table, you have to put a bit more thought into it - and, in particular, worry about the values which don't always exactly match those in the table!

- The carbon-oxygen double bond in the peak for the ketone group has a slightly lower value than the table suggests for a ketone. There is an interaction between the carbon-oxygen and carbon-carbon double bonds in the molecule which affects the value slightly. This isn't something which we need to look at in detail for the purposes of this topic.

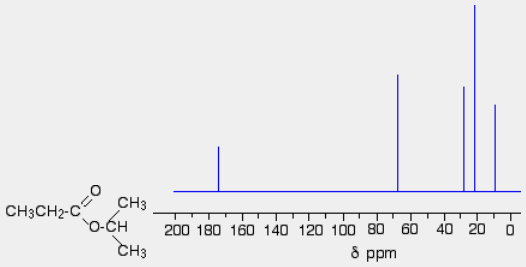
You must be prepared to find small discrepancies of this sort in more complicated molecules - but don't worry about this for exam purposes at this level. Your examiners should give you shift values which exactly match the compound you are given. The two peaks for the carbons in the carbon-carbon double bond are exactly where they would be expected to be. Notice that they aren't in exactly the same environment, and so don't have the same shift values. The one closer to the carbon-oxygen double bond has the larger value.

- And the methyl group on the end has exactly the sort of value you would expect for one attached to C=O. The table gives a range of 20 - 30, and that's where it is.

One final important thing to notice. There are four carbons in the molecule and four peaks because they are all in different environments. But they aren't all the same height. In C-13 NMR, you cannot draw any simple conclusions from the heights of the various peaks.

Example 3: Isopropyl propanoate

1-methylethyl propanoate is also known as isopropyl propanoate or isopropyl propionate.

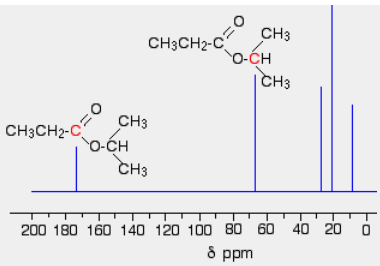


Here is the structure for 1-methylethyl propanoate:

Two simple peaks

There are two very simple peaks in the spectrum which could be identified easily from the second table above.

1. The peak at 174 is due to a carbon in a carbon-oxygen double bond. (Looking at the more detailed table, this peak is due to the carbon in a carbon-oxygen double bond in an acid or ester.)
2. The peak at 67 is due to a different carbon singly bonded to an oxygen. Those two peaks are therefore due to:



If you look back at the more detailed table of chemical shifts, you will find that a carbon singly bonded to an oxygen has a range of 50 - 65. 67 is, of course, a little bit higher than that.

As before, you must expect these small differences. No table can account for all the fine differences in environment of a carbon in a molecule. Different tables will quote slightly different ranges. At this level, you can just ignore that problem!

Before we go on to look at the other peaks, notice the heights of these two peaks we've been talking about. They are both due to a single carbon atom in the molecule, and yet they have different heights. Again, you can't read any reliable information directly from peak heights in these spectra.

The three right-hand peaks

From the simplified table, all you can say is that these are due to carbons attached to other carbon atoms by single bonds. But because there are three peaks, the carbons must be in three different environments. The more detailed table is more helpful.

The easiest peak to sort out is the one at 28. If you look back at the table, that could well be a carbon attached to a carbon-oxygen double bond. The table quotes the group as CH_3CO-, but replacing one of the hydrogens by a simple CH_3 group won't make much difference to the shift value.

The right-hand peak is also fairly easy. This is the left-hand methyl group in the molecule. It is attached to an admittedly complicated R group (the rest of the molecule). It is the bottom value given in the detailed table.

The tall peak at 22 must be due to the two methyl groups at the right-hand end of the molecule - because that's all that's left. These combine to give a single peak because they are both in exactly the same environment.

If you are looking at the detailed table, you need to think very carefully which of the environments you should be looking at. Without thinking, it is tempting to go for the R_2CH_2 with peaks in the 16 - 25 region. But you would be wrong!

The carbons we are interested in are the ones in the methyl group, not in the R groups. These carbons are again in the environment: RCH_3. The R is the rest of the molecule.

The table says that these should have peaks in the range 10 - 15, but our peak is a bit higher. This is because of the presence of the nearby oxygen atom. Its electronegativity is pulling electrons away from the methyl groups - and, as we've seen above, this tends to increase the chemical shift slightly.

Once again, don't worry about the discrepancies. In an exam, perhaps your examiners will just want you to have learnt the simple table above - in which case, they can't expect you to work out which peak is which in a complicated spectrum of this sort. Or they will give you tables of chemical shifts - in which case, they will give you values which match the peaks in the spectra.

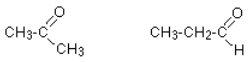
Working out structures from C-13 NMR spectra

So far, we've just been trying to see the relationship between carbons in particular environments in a molecule and the spectrum produced. We've had all the information necessary. Now let's make it a little more difficult - but we'll work from much easier examples!

In each example, try to work it out for yourself before you read the explanation.

Example 1

How could you tell from just a quick look at a C-13 NMR spectrum (and without worrying about chemical shifts) whether you had propanone or propanal (assuming those were the only options)?



https://chem.libretexts.org/@go/page/167072

Because these are isomers, each has the same number of carbon atoms, but there is a difference between the environments of the carbons which will make a big impact on the spectra.

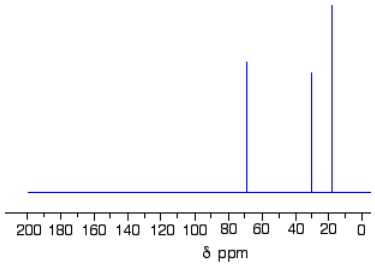
In propanone, the two carbons in the methyl groups are in exactly the same environment, and so will produce only a single peak. That means that the propanone spectrum will have only 2 peaks - one for the methyl groups and one for the carbon in the C=O group. However, in propanal, all the carbons are in completely different environments, and the spectrum will have three peaks.

Example 2

Thare are four alcohols with the molecular formula $C_4H_{10}O$.

A $CH_3CH_2CH_2CH_2OH$ **B** $CH_3CH_2CHCH_3$ (OH) **C** CH_3CHCH_2OH (CH_3) **D** CH_3CCH_3 (CH_3, OH)

Which one produced the C-13 NMR spectrum below?



You can do this perfectly well without referring to chemical shift tables at all.

In the spectrum there are a total of three peaks - that means that there are only three different environments for the carbons, despite there being four carbon atoms.

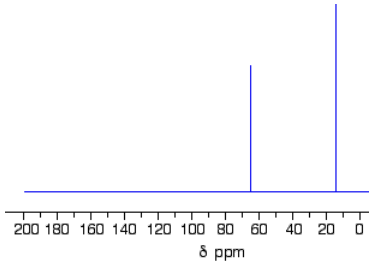
In A and B, there are four totally different environments. Both of these would produce four peaks.

In D, there are only two different environments - all the methyl groups are exactly equivalent. D would only produce two peaks.

That leaves C. Two of the methyl groups are in exactly the same environment - attached to the rest of the molecule in exactly the same way. They would only produce one peak. With the other two carbon atoms, that would make a total of three. The alcohol is C.

Example 3

This follows on from Example 2, and also involves an isomer of $C_4H_{10}O$ but which isn't an alcohol. Its C-13 NMR spectrum is below. Work out what its structure is.



Because we don't know what sort of structure we are looking at, this time it would be a good idea to look at the shift values. The approximations are perfectly good, and we will work from this table:

carbon environment	chemical shift (ppm)

C-C	0 - 50
C-O	50 - 100
C=C	100 - 150
C=O	150 - 200

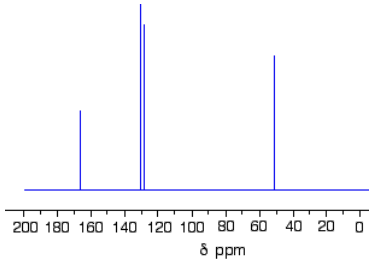
There is a peak for carbon(s) in a carbon-oxygen single bond and one for carbon(s) in a carbon-carbon single bond. That would be consistent with C-C-O in the structure. It isn't an alcohol (you are told that in the question), and so there must be another carbon on the right-hand side of the oxygen in the structure in the last paragraph.

The molecular formula is $C_4H_{10}O$, and there are only two peaks. The only solution to that is to have two identical ethyl groups either side of the oxygen.

The compound is ethoxyethane (diethyl ether), $CH_3CH_2OCH_2CH_3$.

Example 4

Using the simplified table of chemical shifts above, work out the structure of the compound with the following C-13 NMR spectrum. Its molecular formula is $C_4H_6O_2$.

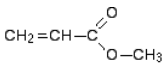


Let's sort out what we've got.

- There are four peaks and four carbons. No two carbons are in exactly the same environment.
- The peak at just over 50 must be a carbon attached to an oxygen by a single bond.
- The two peaks around 130 must be the two carbons at either end of a carbon-carbon double bond.
- The peak at just less than 170 is the carbon in a carbon-oxygen double bond.

Putting this together is a matter of playing around with the structures until you have come up with something reasonable. But you can't be sure that you have got the right structure using this simplified table.

In this particular case, the spectrum was for the compound:



If you refer back to the more accurate table of chemical shifts towards the top of the page, you will get some better confirmation of this. The relatively low value of the carbon-oxygen double bond peak suggests an ester or acid rather than an aldehyde or ketone.

It can't be an acid because there has to be a carbon attached to an oxygen by a single bond somewhere - apart from the one in the -COOH group. We've already accounted for that carbon atom from the peak at about 170. If it *was* an acid, you would already have used up both oxygens in the structure in the -COOH group.

Without this information, though, you could probably come up with reasonable alternative structures. If you were working from the simplified table in an exam, your examiners would have to allow any valid alternatives.

Contributors and Attributions

Template:ContribCalark

This page titled Interpreting C-13 NMR Spectra is shared under a CC BY-NC 4.0 license and was authored, remixed, and/or curated by Jim Clark.

- **Interpreting C-13 NMR Spectra** by Jim Clark is licensed CC BY-NC 4.0.

Introduction to Proton NMR

This page describes what a proton NMR spectrum is and how it tells you useful things about the hydrogen atoms in organic molecules.

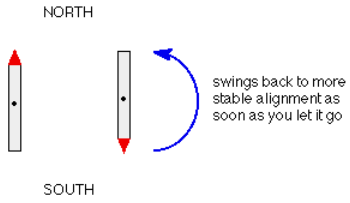
The background to NMR spectroscopy

Nuclear magnetic resonance is concerned with the magnetic properties of certain nuclei. On this page we are focusing on the magnetic behaviour of hydrogen nuclei - hence the term proton NMR or ^{1}H-NMR.^{1}H NMR spectroscopy is used more often than ^{13}C NMR, partly because proton spectra are much easier to obtain than carbon spectra. The ^{13}C isotope is only present in about 1% of carbon atoms, and that makes it difficult to detect. The ^{1}H isotope is almost 99% abundant, which helps make it easier to observe. Another advantage is that ^{1}H NMR spectroscopy gives more information than ^{13}C NMR, as you will find out later.

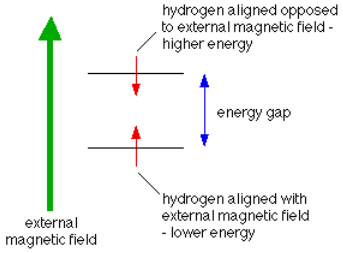
Note that in this discussion, the word "proton" is used for "hydrogen atom", because it is the proton in the nucleus of the ^{1}H isotope that is observed in these experiments. Although ^{2}H (deuterium) and ^{3}H (tritium) are also NMR-active, they absorb at frequencies that are different from the ones used in ^{1}H NMR. The ^{1}H isotope is also much more common than the other two, so ^{1}H NMR spectroscopy is more conveniently done than ^{2}H NMR spectroscopy.

Hydrogen atoms as little magnets

If you have a compass needle, it normally lines up with the Earth's magnetic field with the north-seeking end pointing north. Provided it isn't sealed in some sort of container, you could twist the needle around with your fingers so that it pointed south - lining it up opposed to the Earth's magnetic field. It is very unstable opposed to the Earth's field, and as soon as you let it go again, it will flip back to its more stable state.



Hydrogen nuclei also behave as little magnets and a hydrogen nucleus can also be aligned with an external magnetic field or opposed to it. Again, the alignment where it is opposed to the field is less stable (at a higher energy). It is possible to make it flip from the more stable alignment to the less stable one by supplying exactly the right amount of energy.

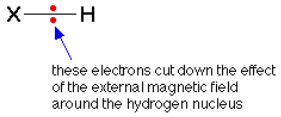


The energy needed to make this flip depends on the strength of the external magnetic field used, but is usually in the range of energies found in radio waves - at frequencies of about 60 - 100 MHz. (BBC Radio 4 is found between 92 - 95 MHz!)

It's possible to detect this interaction between the radio waves of just the right frequency and the proton as it flips from one orientation to the other as a peak on a graph. This flipping of the proton from one magnetic alignment to the other by the radio waves is known as the resonance condition.

The importance of the hydrogen atom's environment

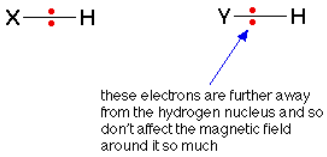
What we've said so far would apply to an isolated proton, but real protons have other things around them - especially electrons. The effect of the electrons is to cut down the size of the external magnetic field felt by the hydrogen nucleus.



Suppose you were using a radio frequency of 90 MHz, and you adjusted the size of the magnetic field so that an isolated proton was in the resonance condition.

If you replaced the isolated proton with one that was attached to something, it wouldn't be feeling the full effect of the external field any more and so would stop resonating (flipping from one magnetic alignment to the other). The resonance condition depends on having exactly the right combination of external magnetic field and radio frequency.

How would you bring it back into the resonance condition again? You would have to increase the external magnetic field slightly to compensate for the effect of the electrons. Now suppose that you attached the hydrogen to something more electronegative. The electrons in the bond would be further away from the hydrogen nucleus, and so would have less effect on the magnetic field around the hydrogen.



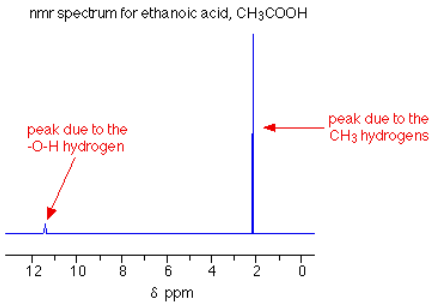
The external magnetic field needed to bring the hydrogen into resonance will be smaller if it is attached to a more electronegative element, because the hydrogen nucleus feels more of the field. Even small differences in the electronegativities of the attached atom or groups of atoms will make a difference to the magnetic field needed to achieve resonance.

Summary

For a given radio frequency (say, 90 MHz) each hydrogen atom will need a slightly different magnetic field applied to it to bring it into the resonance condition depending on what exactly it is attached to - in other words the magnetic field needed is a useful guide to the hydrogen atom's environment in the molecule.

Features of an NMR spectrum

A simple NMR spectrum looks like this:



The peaks

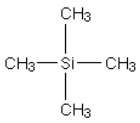
There are two peaks because there are two different environments for the hydrogens - in the CH_3 group and attached to the oxygen in the COOH group. They are in different places in the spectrum because they need slightly different external magnetic fields to bring them in to resonance at a particular radio frequency.

The sizes of the two peaks gives important information about the numbers of hydrogen atoms in each environment. It isn't the height of the peaks that matters, but the ratio of the areas under the peaks. If you could measure the areas under the peaks in the diagram above, you would find that they were in the ratio of 3 (for the larger peak) to 1 (for the smaller one).

That shows a ratio of 3:1 in the number of hydrogen atoms in the two environments - which is exactly what you would expect for CH_3COOH.

The need for a standard for comparison - TMS

Before we can explain what the horizontal scale means, we need to explain the fact that it has a zero point - at the right-hand end of the scale. The zero is where you would find a peak due to the hydrogen atoms in tetramethylsilane - usually called TMS. Everything else is compared with this.



You will find that some NMR spectra show the peak due to TMS (at zero), and others leave it out. Essentially, if you have to analyse a spectrum which has a peak at zero, you can ignore it because that's the TMS peak.

TMS is chosen as the standard for several reasons. The most important are:

- It has 12 hydrogen atoms all of which are in exactly the same environment. They are joined to exactly the same things in exactly the same way. That produces a single peak, but it's also a strong peak (because there are lots of hydrogen atoms).
- The net effect of this is that TMS produces a peak on the spectrum at the extreme right-hand side. Almost everything else produces peaks to the left of it.

The chemical shift

The horizontal scale is shown as δ (ppm). δ is called the chemical shift and is measured in parts per million - ppm. A peak at a chemical shift of, say, 2.0 means that the hydrogen atoms which caused that peak need a magnetic field two millionths less than the field needed by TMS to produce resonance. A peak at a chemical shift of 2.0 is said to be downfield of TMS. The further to the left a peak is, the more downfield it is.

Solvents for NMR spectroscopy

NMR spectra are usually measured using solutions of the substance being investigated. It is important that the solvent itself does not contain any simple hydrogen atoms, because they would produce confusing peaks in the spectrum. There are two ways of avoiding this. You can use a solvent such as tetrachloromethane, CCl_4, which does not contain any hydrogen, or you can use a solvent in which any ordinary hydrogen atoms are replaced by its isotope, deuterium - for example, $CDCl_3$ instead of $CHCl_3$. All the NMR spectra used on this site involve $CDCl_3$ as the solvent.

Deuterium atoms have sufficiently different magnetic properties from ordinary hydrogen that they do not produce peaks in the area of the spectrum that we are looking at.

Contributors and Attributions

Jim Clark (Chemguide.co.uk)

Chris P Schaller, Ph.D., (College of Saint Benedict / Saint John's University)

This page titled Introduction to Proton NMR is shared under a CC BY-NC 4.0 license and was authored, remixed, and/or curated by Jim Clark.

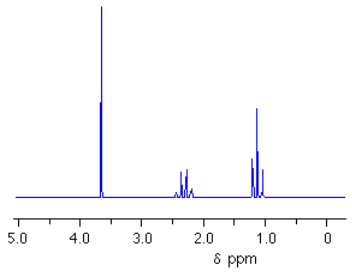
- **Introduction to Proton NMR** by Jim Clark is licensed CC BY-NC 4.0.

Low Resolution Proton NMR Spectra

This page describes how you interpret simple low resolution nuclear magnetic resonance (NMR) spectra. It assumes that you have already read the background page on NMR so that you understand what an NMR spectrum looks like and the use of the term "chemical shift".

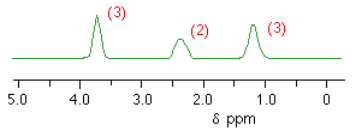
Difference between high and low resolution spectra

high resolution nmr spectrum for methyl propanoate, $CH_3CH_2COOCH_3$



A low resolution spectrum looks much simpler because it cannot distinguish between the individual peaks in the various groups of peaks.

low resolution nmr spectrum for methyl propanoate, $CH_3CH_2COOCH_3$



The numbers against the peaks represent the relative areas under each peak. That information is extremely important in interpreting the spectra.

Interpreting a low resolution spectrum

Using the total number of peaks

Each peak represents a different environment for hydrogen atoms in the molecule. In the methyl propanoate spectrum above, there are three peaks because there are three different environments for the hydrogens. Remember that methyl propanoate is $CH_3CH_2COOCH_3$. The hydrogens in the CH_2 group are obviously in a different environment from those in the CH_3 groups. The two CH_3 groups aren't in the same environment either. One is attached to a CH_2 group, the other to an oxygen.

Using the areas under the peaks

The ratio of the areas under the peaks tell you the ratio of the numbers of hydrogens in the various environments. In the methyl propanoate case, the areas were in the ratio of 3:2:3, which is exactly what you want for the two differently placed CH_3 groups and the CH_2 group.

You will probably be told the relative areas under the peaks - especially if you are only looking at low resolution spectra, but it is just possible that you might have to work them out. NMR spectrometers have a device which draws another line on the spectrum called an integrator trace (or integration trace). You can measure the relative areas from this trace.

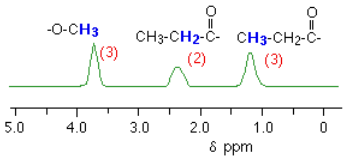
Using chemical shifts

The position of the peaks tells you useful things about what groups the various hydrogen atoms are in. The important shifts for the groups present in methyl propanoate are:

	chemical shift, δ
R-C**H**$_3$	0.7 - 1.6
-O-C**H**$_3$	3.3 - 4.3
R-C**H**$_2$-C(=O)-	2.0 - 2.9

Showing these groups on the low resolution spectrum gives:

low resolution nmr spectrum for methyl propanoate, $CH_3CH_2COOCH_3$



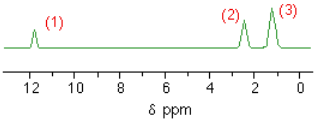
Questions

1. An organic compound was known to be one of the following. Use its low resolution NMR spectrum to decide which it is.

propanoic acid $CH_3-CH_2-C(=O)-O-H$

methyl ethanoate $CH_3-C(=O)-O-CH_3$

ethyl methanoate $H-C(=O)-O-CH_2-CH_3$

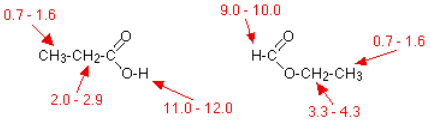


Notice that there are three peaks showing three different environments for the hydrogens. That eliminates methyl ethanoate as a possibility because that would only give two peaks - due to the two differently situated CH_3 group hydrogens.

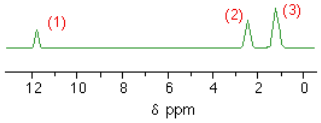
Does the ratio of the areas under the peaks help? Not in this case - both the other compounds would have three peaks in the ratio of 1:2:3. Now you need to look at the chemical shifts:

	chemical shift, δ
R-C**H**$_3$	0.7 - 1.6
R-C**H**$_2$-C(=O)-	2.0 - 2.9
-O-C**H**$_3$ or -O-C**H**$_2$-R	3.3 - 4.3
H-C(=O)-	9.0 - 10.0
-COO**H**	11.0 - 12.0

Checking the positions of the various hydrogens in the two possible compounds against the chemical shift table gives you this pattern of shifts:



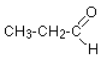
Comparing these with the actual spectrum means that the substance was propanoic acid, CH_3CH_2COOH.



2. How would you use low resolution NMR to distinguish between the isomers propanone and propanal?



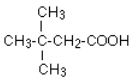
propanone



propanal

The propanone would only give one peak in its NMR spectrum because both CH_3 groups are in an identical environment - both are attached to $-COCH_3$. The propanal would give three peaks with the areas underneath in the ratio 3:2:1. You could refer to the chemical shift table above to decide where the peaks are likely to be found, but it isn't really necessary.

3. How many peaks would there be in the low resolution NMR spectrum of the following compound, and what would be the ratio of the areas under the peaks?



All the CH_3 groups are exactly equivalent so would only produce 1 peak. There would also be peaks for the hydrogens in the CH_2 group and the COOH group. There would be three peaks in total with areas in the ratio 9:2:1.

Contributors and Attributions

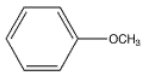
Jim Clark (Chemguide.co.uk)

This page titled Low Resolution Proton NMR Spectra is shared under a CC BY-NC 4.0 license and was authored, remixed, and/or curated by Jim Clark.

- **Low Resolution Proton NMR Spectra** by Jim Clark is licensed CC BY-NC 4.0.

More About Electronics

Methoxybenzene or anisole has six carbons, but only four peaks in the spectrum because of symmetry. These peaks are all above 100 ppm, but some peaks are as far downfield as 160 ppm.



methoxybenzene

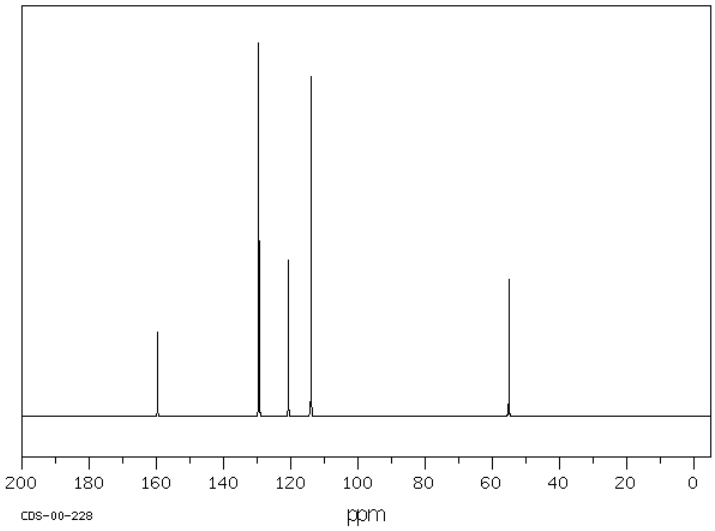
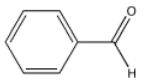


Figure NMR9.^{13}C NMR spectrum of methoxybenzene (anisole).

Source: SDBSWeb : http://riodb01.ibase.aist.go.jp/sdbs/ (National Institute of Advanced Industrial Science and Technology of Japan, 15 August 2008)

- Benzaldehyde has peaks between 130 and 140 ppm, as well as one near 190 ppm. Just as in the sp^3 region of the spectrum, when a carbon is attached to an electronegative element, it moves further downfield, and since the carbonyl (or C=O) carbon in the aldehyde has two bonds to oxygen, it shows up considerably downfield. The carbonyl carbon in some ketones can show up as far as 210 ppm.



benzaldehyde

Figure NMR10. ^{13}C NMR spectrum of benzaldehyde.

Source: SDBSWeb : http://riodb01.ibase.aist.go.jp/sdbs/ (National Institute of Advanced Industrial Science and Technology of Japan, 15 August 2008)

- Chris P Schaller, Ph.D., (College of Saint Benedict / Saint John's University)

This page titled More About Electronics is shared under a CC BY-NC 3.0 license and was authored, remixed, and/or curated by Chris Schaller.

- **More About Electronics** by Chris Schaller is licensed CC BY 3.0.

Multiplicity in Proton NMR

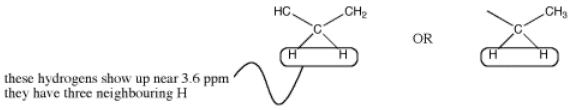
Another type of additional data available from ^1H NMR spectroscopy is called multiplicity or coupling. Coupling is useful because it reveals how many hydrogens are on the next carbon in the structure. That information helps to put an entire structure together piece by piece.

In ethanol, CH_3CH_2OH, the methyl group is attached to a methylene group. The ^1H spectrum of ethanol shows this relationship through the shape of the peaks. The peak near 3.5 ppm is the methylene group with an integral of 2H.

- The integral of 2H means that this group is a methylene, so it has two hydrogens. The carbon bearing these two hydrogens can have two other bonds.



There could be two hydrogens on one neighbouring carbon and one on another. Otherwise, all three hydrogens could be on one neighbouring carbon.

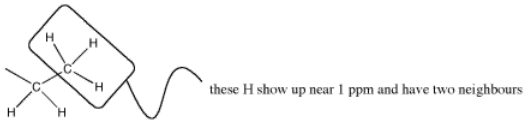


However, the shift of 3.5 ppm means that this carbon is attached to an oxygen. Mutliplicity usually only works with hydrogens on neighbouring carbons. If there is an oxygen on one side of the methylene, all three neighbouring hydrogens must be on a carbon on the other side.



Alternatively, look at the spectrum the other way around. The peak at 1 ppm is the methyl group with an integral of 3H.

- The neighbouring H could be on two different neighbouring carbons or both on the same one.



The number of lines in a peak is always one more than the number of hydrogens on the neighboring carbon. The triplet for the methyl peak means that there are two neighbors on the next carbon (3 - 1 = 2H); the quartet for the methylene peak indicates that there are three hydrogens on the next carbon (4 - 1 = 3H). Table NMR 1 summarizes coupling patterns that arise when protons have different numbers of neighbors.

# of lines	ratio of lines	term for peak	# of neighbors
1	-	singlet	0
2	1:1	doublet	1
3	1:2:1	triplet	2
4	1:3:3:1	quartet	3
5	1:4:6:4:1	quintet	4
6	1:5:10:10:5:1	sextet	5
7	1:6:15:20:15:6:1	septet	6
8	1:7:21:35:35:21:7:1	octet	7
9	1:8:28:56:70:56:28:8:1	nonet	8

The third peak in the ethanol spectrum is usually a "broad singlet." This is the peak due to the OH. You would expect it to be a triplet because it is next to a methylene. Under very specific circumstances, it does appear that way. However, coupling is almost always lost on hydrogens bound to heteroatoms (OH and NH). The lack of communication between an OH or NH and its neighbours is related to rapid proton transfer, in which that proton can trade places with another OH or NH in solution. This exchange happens quite easily if there are even tiny traces of water in the sample.

In summary, multiplicity or coupling is what we call the appearance of a group of symmetric peaks representing one hydrogen in NMR spectroscopy.

- There are limitations on coupling:
  - Chris P Schaller, Ph.D., (College of Saint Benedict / Saint John's University)

This page titled Multiplicity in Proton NMR is shared under a CC BY-NC 3.0 license and was authored, remixed, and/or curated by Chris Schaller.

- **Multiplicity in Proton NMR** by Chris Schaller is licensed CC BY 3.0.

NMR11. More About Multiplicity

The n + 1 rule (number of lines in a multiplet = number of neighboring H + 1) will work for the majority of problems you may encounter. Occasionally, you may see more complicated coupling. The spectrum of methyl acrylate is a good example. There are a couple of points to note in this spectrum, beginning with the number of peaks.

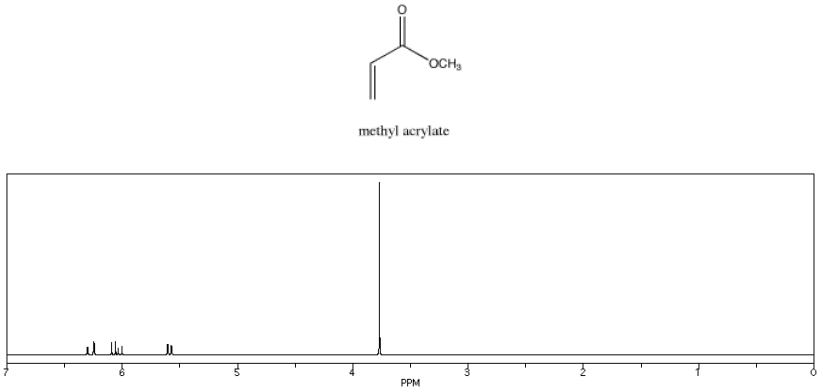


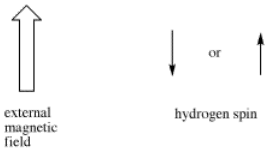
Figure NMR21.^{1}H NMR spectrum of methyl acrylate.

Source: Simulated spectrum.

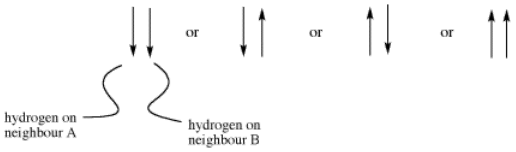
- In addition, there is a problem with coupling in the vinyl region.
  - This pattern is called a "doublet of doublets." The two symmetry-inequivalent neighbors on the other end of the double bond each act as if the other one isn't there. They couple to the proton next to the carbonyl independently, each one splitting the peak for this proton into a separate doublet.

    There are a few cases in which this independent coupling will occur rather than the (n+1) type coupling we saw first. Generally, independent coupling occurs when protons are not freely rotating. That can happen if one of the protons is attached to a double-bonded carbon, because we can't rotate around a double bond. It may also happen with protons that are directly attached to the carbons of a ring.

    - Sometimes coupling information is depicted as an arrow. This arrow stands for the coupling constant between two protons. The coupling constant is related to the spin of a hydrogen atom. The spin (related to magnetic moment) can be aligned with the external magnetic field (we will show it pointing up) or else against it; no other possibilities are allowed.

      If there are two neighboring hydrogens, both spins could be aligned with the external field, both could be aligned against it, or one could be aligned each way. That means there are three different magnetic combinations that will each have a different effect on the observed proton: increased magnetic field, decreased magnetic field, and no net effect (canceling out).

      These three combinations result in the observed proton absorbing at three different frequencies, because the frequency it absorbs is sensitive to the magnetic field it experiences. Note that there are two ways to arrive at the middle possibility, with one neighbour spin up and the other spin down. Statistically this possibility is twice as likely as either both spins up

or both spins down. It is thus twice as likely that the observed proton experiences that effect, and so the middle line in a triplet is twice as high as the other two lines.

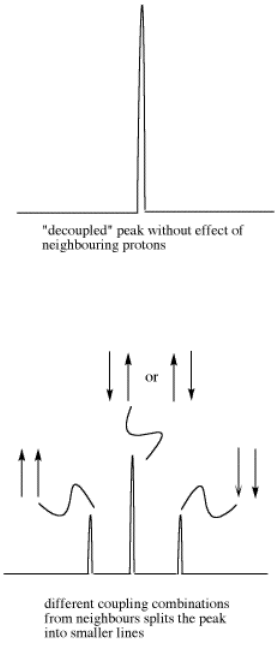
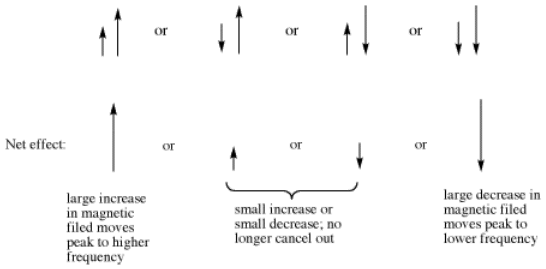


Figure NMR23. Effects of neighboring protons on an observed peak. This case assumes all the neighboring protons have an equivalent effect (they have the same coupling constant with the observed proton).

However, the size of that arrow, the coupling constant, is only the same for two neighboring hydrogens if they have the same spatial relationship with the observed hydrogen. That isn't always true.

- As a result, the two coupling constants are different. We can depict that situation using arrows of different lengths for the two neighboring proton spins. Each spin can be either up or down, but now two opposing spins do not cancel out. The result is four spin combinations of equal probability, not just three.



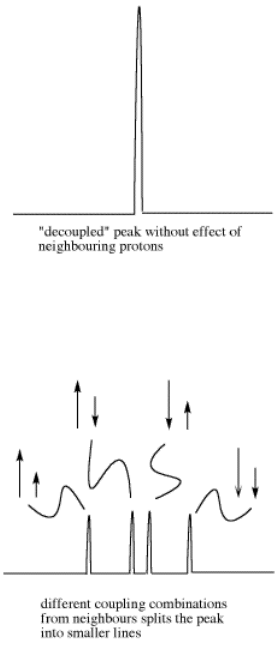


Figure NMR23. Effects of neighboring protons on an observed peak. This case assumes neighboring protons have inequivalent effects (they have differing coupling constants with the observed proton).

The dihedral angle is limited in only a few specific cases:

- Chris P Schaller, Ph.D., (College of Saint Benedict / Saint John's University)

This page titled NMR11. More About Multiplicity is shared under a CC BY-NC 3.0 license and was authored, remixed, and/or curated by Chris Schaller.

- **NMR11. More About Multiplicity** by Chris Schaller is licensed CC BY 3.0.

NMR14. More Practice with NMR Spectroscopy

Contributors and Attributions

Chris P Schaller, Ph.D., (College of Saint Benedict / Saint John's University)

This page titled NMR14. More Practice with NMR Spectroscopy is shared under a CC BY-NC 3.0 license and was authored, remixed, and/or curated by Chris Schaller.

- **NMR14. More Practice with NMR Spectroscopy** by Chris Schaller is licensed CC BY 3.0.

NMR2. Carbon-13 NMR

Contributors and Attributions

Chris P Schaller, Ph.D., (College of Saint Benedict / Saint John's University)

This page titled NMR2. Carbon-13 NMR is shared under a CC BY-NC 3.0 license and was authored, remixed, and/or curated by Chris Schaller.

- **NMR2. Carbon-13 NMR** by Chris Schaller is licensed CC BY 3.0.

NMR3. Symmetry in NMR

Butane shows two different peaks in the ^{13}C NMR spectrum, below. Note that:

the chemical shifts of these peaks are not very different from methane. The carbons in butane are in a similar environment to the one in methane.

- In the ^{13}C NMR spectrum of pentane (below), you can see three different peaks, even though pentane just contains methyl carbons and methylene carbons like butane. As far as the NMR spectrometer is concerned, pentane contains three different kinds of carbon, in three different environments. That result comes from symmetry.

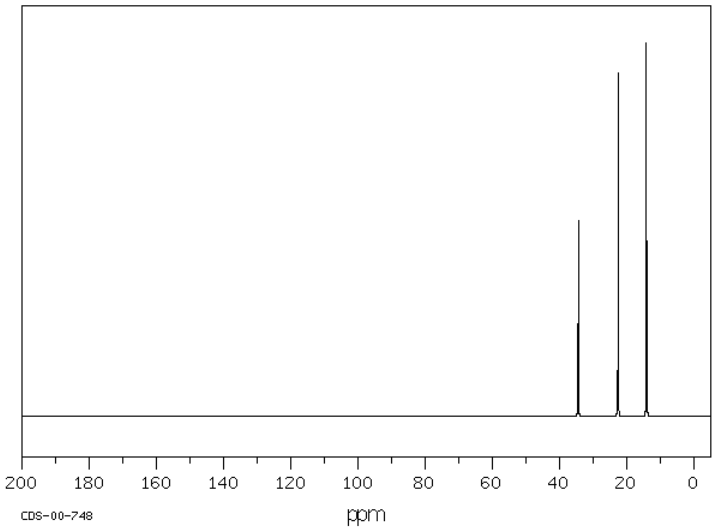


Figure NMR3.^{13}C NMR spectrum of pentane.

Source: SDBSWeb : http://riodb01.ibase.aist.go.jp/sdbs/ (National Institute of Advanced Industrial Science and Technology of Japan, 15 August 2008)

Symmetry is an important factor in spectroscopy. Nature says:

- To learn about symmetry, take a model of pentane and do the following:
  - Wire Frame
  - Ball & Stick

  Animation NMR1. A three-dimensional model of pentane. Grab the model with the mouse and rotate it so that you are convinced that the second and fourth carbons are symmetry-equivalent, but the third carbon is not.

  By the same process, you can see that the second and fourth carbons along the chain are also symmetry-equivalent. However, the middle carbon is not; it never switches places with the other carbons if you rotate the model. There are three different sets of inequivalent carbons; these three groups are not the same as each other according to symmetry.

Contributors and Attributions

Chris P Schaller, Ph.D., (College of Saint Benedict / Saint John's University)

This page titled NMR3. Symmetry in NMR is shared under a CC BY-NC 3.0 license and was authored, remixed, and/or curated by Chris Schaller.

- **NMR3. Symmetry in NMR** by Chris Schaller is licensed CC BY 3.0.

NMR4. 13C NMR and Geometry

Contributors and Attributions

Chris P Schaller, Ph.D., (College of Saint Benedict / Saint John's University)

This page titled NMR4. 13C NMR and Geometry is shared under a CC BY-NC 3.0 license and was authored, remixed, and/or curated by Chris Schaller.

- **NMR4. 13C NMR and Geometry** by Chris Schaller is licensed CC BY 3.0.

NMR5. 13C NMR and Electronics

Contributors and Attributions

Chris P Schaller, Ph.D., (College of Saint Benedict / Saint John's University)

This page titled NMR5. 13C NMR and Electronics is shared under a CC BY-NC 3.0 license and was authored, remixed, and/or curated by Chris Schaller.

- **NMR5. 13C NMR and Electronics** by Chris Schaller is licensed CC BY 3.0.

NMR8. Chemical Shift in 1H NMR

The trends here are exactly the same as in carbon spectra. Wherever the carbon goes, it takes the proton with it. By analogy with carbon spectra,

- Source: Simulated spectrum.

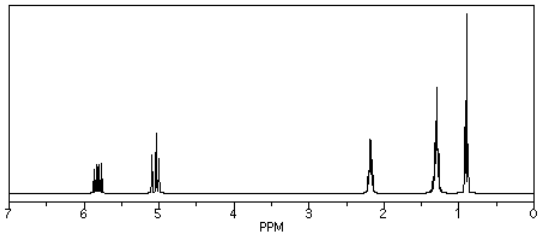


Figure NMR12.^{1}H NMR spectrum of 1-hexene.

Source: Simulated spectrum.

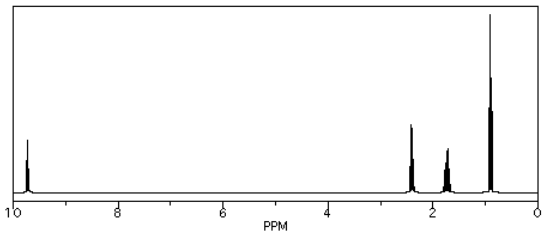


Figure NMR13.^{1}H NMR spectrum of butanal.

Source: Simulated spectrum.

As before, there are also hydrogens on linear carbons, although they are much less common than tetrahedral or trigonal carbons.

- Remember, these are general rules that you should know. There will occasionally be exceptions; the proton in a carboxylic acid may be seen at 12 ppm, and the proton in chloroform shows up at 7 ppm although it is attached to a tetrahedral carbon. (World-record shifts occur for hydrogens attached to transition metals: "late" metals like ruthenium or rhodium can move hydrogen peaks all the way up to -20 ppm, but "early" metals like tantalum can move them down as far as 25 ppm.)

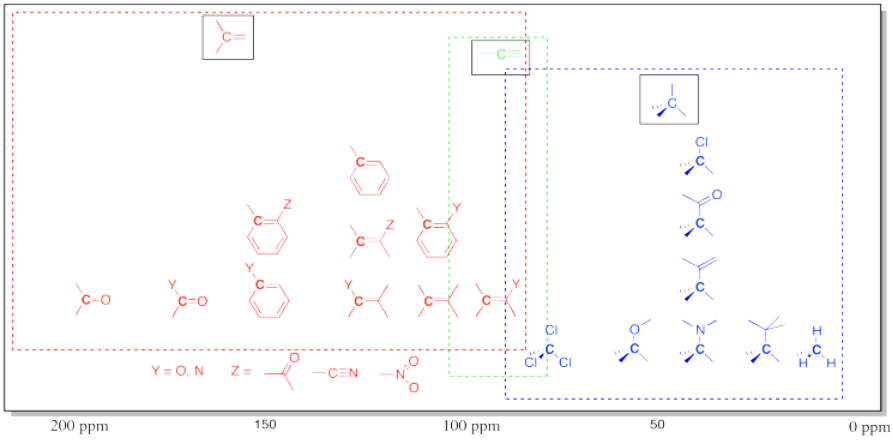
Contributors and Attributions

This page titled NMR8. Chemical Shift in 1H NMR is shared under a CC BY-NC 3.0 license and was authored, remixed, and/or curated by Chris Schaller.

- **NMR8. Chemical Shift in 1H NMR** by Chris Schaller is licensed CC BY 3.0.

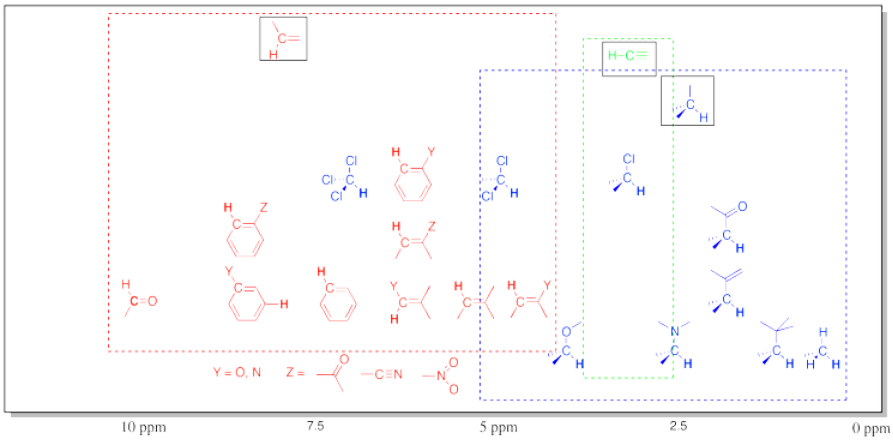
NMR Appendix. Useful Charts for NMR identification

Table of ^{13}C NMR Frequencies Common in Organic Compounds.



Note that effects are additive: two or more electron-withdrawing groups move the absorbance further to the left than just one group.

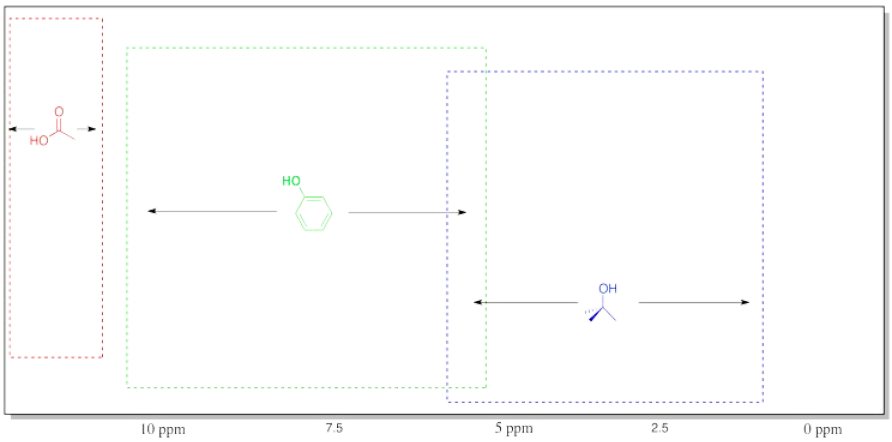
Table of ^{1}H NMR Frequencies Common in Organic Compounds.



This chart shows the frequancies of protons that are attached to carbons. In general, protons follow the trend seen in the carbon to which they are attached. Note again the additive effects of multiple attached groups.

This table does not include OH (or NH) protons. Protons attached to heteroatoms are more difficult to pinpoint because their locations in the spectrum are much less specific. Instead, they may be found across a very broad range.

Table of ^{1}H NMR Frequencies of OH Common in Organic Compounds.



Contributors and Attributions

Chris P Schaller, Ph.D., (College of Saint Benedict / Saint John's University)

This page titled NMR Appendix. Useful Charts for NMR identification is shared under a CC BY-NC 3.0 license and was authored, remixed, and/or curated by Chris Schaller.

- **NMR Appendix. Useful Charts for NMR identification** by Chris Schaller is licensed CC BY 3.0.

CHAPTER OVERVIEW

5.9: Active Learning with NMR

The goal of this unit is to develop introductory concepts on nuclear magnetic resonance (NMR) spectroscopy that are most relevant for undergraduate chemistry majors. Development of the concepts of NMR is accomplished through an examination of the normal hydrogen (^1H) nucleus. The unit is focused on understanding what occurs in molecules and within the NMR spectrometer that causes ^1H NMR spectra to look the way they do. There is less of an emphasis on interpreting NMR spectra, although the concepts developed herein provide students with the understanding needed to begin interpreting NMR spectra. Components of both a quantum mechanical and classical description of NMR spectroscopy are developed.

In-Class Questions

- Set 1 – Basic Concepts
- Set 2 – Energy Transition and Population
- Set 3 – Electron Shielding
- Set 4 – Nuclear Coupling
- Set 5 – Exchange Effects
- Set 6 – Classical Description

Instructor's Manual

Learning Objectives

Text

Contributors

- Dr. Thomas Wenzel (Bates College)

This page titled 5.9: Active Learning with NMR is shared under a CC BY-NC-SA 4.0 license and was authored, remixed, and/or curated by Thomas Wenzel.

SECTION OVERVIEW

In-Class Questions

Topic hierarchy

Set 1 – Basic Concepts

Set 2 – Energy Transition and Population

Set 3 – Electron Shielding

Set 4 – Nuclear Coupling

Set 5 – Exchange Effects

Set 6 – Classical Description

Template:HideTOC

This page titled In-Class Questions is shared under a CC BY-NC-SA 4.0 license and was authored, remixed, and/or curated by Thomas Wenzel.

Set 1 – Basic Concepts

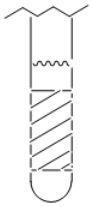
1. What makes up the nucleus of a hydrogen atom?
2. What are the allowable spin quantum numbers for an electron?
3. What do you think are the allowable spin quantum numbers for a proton?
4. What is the magnitude of I, the total nuclear spin, for a hydrogen nucleus?
5. What do you think is produced by the spinning, charged proton that is the hydrogen nucleus?
6. What happens when two magnetic fields (B_p and B_{APPL}) are in contact with each other?
7. What do you think are the two allowable orientations of B_p relative to B_{APPL}?
8. Do you think the two allowable orientations have the same or different energy?
9. Which of the two do you think is lower in energy?

This page titled Set 1 – Basic Concepts is shared under a CC BY-NC-SA 4.0 license and was authored, remixed, and/or curated by Thomas Wenzel.

- **Set 1 – Basic Concepts** by Thomas Wenzel is licensed CC BY-NC-SA 4.0. Original source: https://asdlib.org/activelearningmaterials/nuclear-magnetic-resonance-spectroscopy.

Set 2 – Energy Transition and Population

1. What frequency of electromagnetic radiation is needed to excite a nuclear spin flip?
2. Where is radiofrequency (RF) radiation on the energy scale of the electromagnetic spectrum?
3. Is the thermal energy at room temperature large or small compared to the energy of a π-π^* transition and to the energy of a nuclear spin flip?What are the consequences of your answers to these questions?
4. If thermal energy has sufficient energy to excite nuclear spin flips, why are there still more in the ground than excited state?
5. Can you think of two processes by which a specific excited state nucleus can get rid of its excess energy?
6. Do excited state nuclei have short or long relaxation times?
7. When the populations of the two levels are equal, can we continue to excite ground state nuclei up to the excited state such that the population of the excited state becomes larger than the population of the ground state, creating what is known as a population inversion?
8. What happens to the population distribution as the energy gap between the ground and excited state is increased?
9. Consider a sample in an NMR tube.The crosshatched region in the tube is the area over which signal is recorded.Why is it important that B_{APPL} be homogeneous over this entire region?



This page titled Set 2 – Energy Transition and Population is shared under a CC BY-NC-SA 4.0 license and was authored, remixed, and/or curated by Thomas Wenzel.

- **Set 2 – Energy Transition and Population** by Thomas Wenzel is licensed CC BY-NC-SA 4.0. Original source: https://asdlib.org/activelearningmaterials/nuclear-magnetic-resonance-spectroscopy.

Set 3 – Electron Shielding

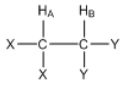
1. What “things” in a molecule generate magnetic fields that will influence B_o for a particular hydrogen nucleus?
2. Does electron density affect the magnitude of B_e? If so, what is the relationship?
3. Does a more highly shielded nucleus absorb higher frequency (higher energy) or lower frequency (lower energy) radiation?
4. Suppose the resonant frequency of the TMS singlet on a 400 MHZ NMR spectrometer is exactly 400 MHz.What is the chemical shift in ppm for a signal that has a resonant frequency of 400,000,400 Hz?
5. What is different as B_{APPL} is varied?

This page titled Set 3 – Electron Shielding is shared under a CC BY-NC-SA 4.0 license and was authored, remixed, and/or curated by Thomas Wenzel.

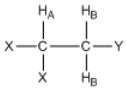
- **Set 3 – Electron Shielding** by Thomas Wenzel is licensed CC BY-NC-SA 4.0. Original source: https://asdlib.org/activelearningmaterials/nuclear-magnetic-resonance-spectroscopy.

Set 4 – Nuclear Coupling

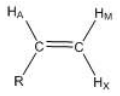
1. Consider the two hydrogen atoms H_A and H_B in the compound shown below.The X and Y groups are not hydrogen atoms and produce no magnetic fields.In particular, let's focus on the effect that H_B has on H_A.We can think of H_A "looking over" at H_B and ask ourselves about the magnetic field produced by H_B.



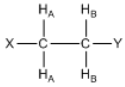
2. What do you know from earlier in this unit about the magnetic field produced by H_B?
3. Is the flip of H_B's spin between the "with" and "against" states rapid or slow?
4. What does the resonance for H_A look like in the NMR spectrum?
5. Which peak in the doublet corresponds to B_{HB} "with" and which corresponds to B_{HB} "against"?
6. Can you think of a way to decouple a hydrogen atom like H_B?
7. What would the H_B resonance look like?
8. What would the resonance for H_A look like in the compound shown below where there are two H_B protons?Provide a rationale for your answer.



9. Which peak of the triplet corresponds to the WW and which to the AA situation?
10. What factors do you think influence the magnitude of the coupling constant?
11. Predict the coupling constants that would occur between H_A, H_M and H_X and the mono-substituted alkene shown below and draw the shape of each resonance.



12. Consider the following compound in which J_{AB} = 10 Hz, δ_{HA} = 1.3 ppm and δ_{HB} = 1.2 ppm. Draw the resulting spectrum if the spectrum is recorded on a 100 MHz and 400 MHz spectrometer.

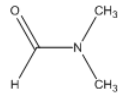


This page titled Set 4 – Nuclear Coupling is shared under a CC BY-NC-SA 4.0 license and was authored, remixed, and/or curated by Thomas Wenzel.

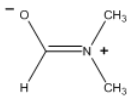
- **Set 4 – Nuclear Coupling** by Thomas Wenzel is licensed CC BY-NC-SA 4.0. Original source: https://asdlib.org/activelearningmaterials/nuclear-magnetic-resonance-spectroscopy.

Set 5 – Exchange Effects

1. Considering the spectrum of a compound such as methanol (CH_3OH).Using the rules for coupling we have established, predict the number of resonances and identify their multiplet structure.
2. However, in other situations the spectrum of methanol appears as two singlets, one of area three and the other of area one.Propose a reason why singlets are observed instead of coupled multiplets.
3. Another time-dependent aspect to consider about NMR spectra can be illustrated by considering the ^1H NMR spectrum of *N*,*N*-dimethylacetamide (DMA) shown below.



4. What does the NMR spectrum of DMA look like?
5. DMA has the following contributing resonance form.What would the NMR spectrum of DMA look like in this resonance form?



This page titled Set 5 – Exchange Effects is shared under a CC BY-NC-SA 4.0 license and was authored, remixed, and/or curated by Thomas Wenzel.

- **Set 5 – Exchange Effects** by Thomas Wenzel is licensed CC BY-NC-SA 4.0. Original source: https://asdlib.org/activelearningmaterials/nuclear-magnetic-resonance-spectroscopy.

Set 6 – Classical Description

1. What happens when an electrical current is run through a wire coil?
2. What happens to the nucleus after B_1 is turned off?
3. Suppose a wire coil is placed on the Y-axis.What happens in the wire coil as the magnetic field of the tipped nucleus is imparted on it?
4. Draw the current profile that would result in the wire coil on the X-axis as the tipped nucleus relaxes back to its ground state.
5. Draw the FID that would result if the nucleus had a much shorter relaxation time.
6. Do you see a problem with performing a FT on an FID with a very short relaxation time?If so, what would happen in the resulting frequency domain spectrum?
7. Where is the amplitude of peaks determined in the FID?
8. Why is a delay time incorporated into the sequence?
9. Why are the advantages and disadvantages of using 30° pulses instead of 90° pulses?
10. What is the advantage of recording several FIDs and adding them together?
11. Suppose the following pulse sequence is used to obtain the spectrum of a ^{13}C nucleus with a spin-lattice relaxation time of 100 seconds (90° pulse, 1 second collection of the FID, 1 second delay).Note, carbon atoms with no directly bonded hydrogen atoms can have relaxation times as long as 100 seconds.This pulse sequence is repeated four times.

    - Draw the position of the ^{13}C magnetization vector after each of the four pulses.
    - Draw the corresponding FID that would be obtained after each pulse.
    - Draw the composite FID obtained by adding the four individual FIDs together.
    - What do you observe for this carbon in the resulting frequency domain spectrum?

This page titled Set 6 – Classical Description is shared under a CC BY-NC-SA 4.0 license and was authored, remixed, and/or curated by Thomas Wenzel.

- **Set 6 – Classical Description** by Thomas Wenzel is licensed CC BY-NC-SA 4.0. Original source: https://asdlib.org/activelearningmaterials/nuclear-magnetic-resonance-spectroscopy.

SECTION OVERVIEW

Instructor's Manual

General Instructions about this Module:

The problem sets on NMR spectroscopy are meant to be used as in-class, collaborative learning exercises. Groups of 3-4 students work together in discussing and working through the problems. When using the problem sets in this manner, the instructor must actively facilitate and guide students through the material. This manual will guide instructors through each of the problem sets, identifying possible student responses to the questions and the response and activities of the instructor during the progression of the problem.

There is no perfect way to assemble groups for such collaborative learning activities. I gather information on the first day of class (year in college, major, prior chemistry courses) and then use this to set groups of 3-4 students that start on the second day of class. I try to make the groups as heterogeneous as possible and they work together for the entire semester. Another strategy is to assign groups for a shorter period of time that might encompass completion of a specific topic or unit, and to then create new groups for the next unit. One other possibility is to have different groups every day of class. Since it is important for groups to work well together, having new groups every day may be less successful than allowing groups to work together for more extended periods of time. I would recommend that the instructor assign groups rather than allowing the students to pick their own. This avoids the potential problem of friends who want to be in the same group but who then do not work well together or stay focused on the assigned task. It also avoids the problem of the student who is left without a group at the end of the selection process, something that can be especially problematic if it is a member of a minority group. When using collaborative groups, it is also important for the instructor to monitor the functioning of the groups and to step in to address either dysfunctional groups or the recalcitrant individual within a group. Peer-evaluation processes are often used by instructors who employ group activities as a way of assessing how well groups are working.

I also expect the groups to meet outside of class for any homework assignments, something that is aided because I am at a residential college. An alternative to this is to schedule a room on the evening before a homework assignment is due and encourage them to come to this place and work in any arrangement they wish on the homework. I have run such sessions for several years now and attend them as a facilitator (one result is that it has cut down considerably the individual traffic to my office seeking help on the homework problems) and it has been an excellent way to promote collaboration among the students.

The instructor has an especially important role to fulfill during such group activities. I have observed that the more engaged that I am in the process in helping to guide the students through the material, the more effective the learning that occurs. In most instances, it seems that the students are initially stumped by the question, that they begin to explore things that they do know that might apply to answering the question, and that help from the instructor either by letting them know that they are on the right track or by suggesting another direction in which to take their thinking is necessary. As they begin a question, I roam around the room listening in on conversations and looking over their shoulders at what might be written in their notebook. If I hear something interesting, I indicate that to the group. If I see that someone has written something interesting and relevant in their notebook, I tell other group members that they ought to talk with this individual about what they have written, and that the individual should explain to the other group members why they wrote that down. If I hear a group going entirely in the wrong direction, I probe them on why they are heading in that way and then offer suggestions about things to consider that will set them off in the right direction. When all groups have realized an important point, I call time out and summarize the concept at the board. Then I send them back to continue with the next part of the problem. Most of the problems are handled in such an iterative manner where the students work through some important part of the problem, I summarize it at the board when they have developed the concept, and then they return to the next part of the problem. Occasionally a group will just not see something, whereas every other group has gotten the point, and it may require a direct intervention from the instructor with that group to explain the concept. Similarly, there are times when I call their attention to the board to summarize a point when one of the groups still has not gotten the concept but waiting would slow down the remainder of the class to an unacceptable level.

When using these materials, I want the students to discuss and discover the concepts inherent in the problems, so they do not have the text when working on the problems. After they have completed a particular problem, I then make available to them a copy of that portion of the text. The text thoroughly goes through the thought process for solving each problem and I encourage the students

to read it over that evening to reinforce the concepts developed in class that day. I also give homework problems designed to reinforce the concepts developed in class.

Specific Instructions about the In-class NMR Problems:

I have developed in-class question sets for a number of modules on the ASDL site. With these other modules, it is typically the case that the sets of questions can be given to the students with minimal pre-lecturing from the instructor before they begin working on them. Also, in these other modules, later questions in the set may not give away the answer to earlier questions. Because of this, I give out hard copies of the entire question set to the students and they begin with the first question and we eventually work our way through the entire set.

Many of the questions in the NMR module are quite different. They often require a brief presentation by the instructor that sets the stage for the ensuing question. Also, in a number of cases the later questions in a particular set give away the answer to an earlier question.

I would recommend that an instructor using the in-class question sets with this NMR module put the questions into a Powerpoint presentation. Then when the topic is developed to the point that a question is now relevant for the students to consider, it can be projected for the groups to work on.

Specific answers to the questions below are given in the text that accompanies this module. Usually, students going through this module in an analytical chemistry course have some knowledge of NMR spectroscopy through an organic chemistry course.

Topic hierarchy

Template:HideTOC

This page titled Instructor's Manual is shared under a CC BY-NC-SA 4.0 license and was authored, remixed, and/or curated by Thomas Wenzel.

Learning Objectives

01 Learning Objectives

This page titled Learning Objectives is shared under a CC BY-NC-SA 4.0 license and was authored, remixed, and/or curated by Thomas Wenzel.

SECTION OVERVIEW

Text

The following textual material is designed to accompany a series of in-class problem sets that develop many of the fundamental aspects of NMR spectroscopy.

Template:HideTOC

This page titled Text is shared under a CC BY-NC-SA 4.0 license and was authored, remixed, and/or curated by Thomas Wenzel.

5.10: Chemical Shifts

Objectives

After completing this section, you should be able to

1. describe the delta scale used in NMR spectroscopy.
2. perform calculations based on the relationship between the delta value (in ppm), the observed chemical shift (in Hz), and the operating frequency of an NMR spectrometer (in Hz).

Key Terms

Make certain that you can define, and use in context, the key terms below.

- chemical shift
- delta scale
- upfield/downfield

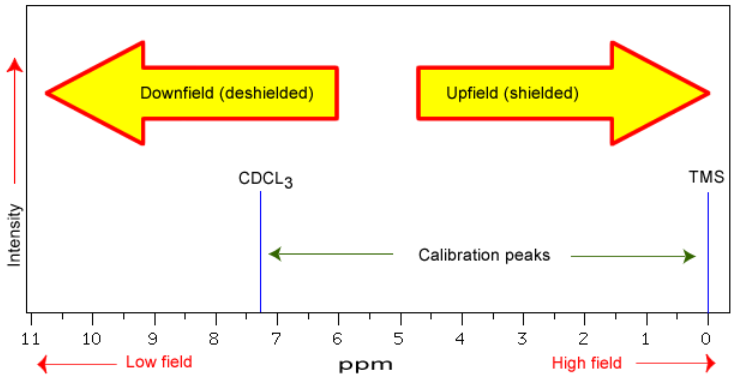
Study Notes

Although the calculations described in this section will help you understand the principles of NMR, it is the actual delta values, not the calculations, which are of greatest importance to the beginning organic chemist. Thus, we shall try to focus on the interpretation of NMR spectra, not the mathematical aspects of the technique.

In Section 13.9 we discuss ^{1}H NMR chemical shifts in more detail. Although you will eventually be expected to associate the approximate region of a ^{1}H NMR spectrum with a particular type of proton, you are expected to use a general table of ^{1}H NMR chemical shifts such as the one shown in Section 13.9.

Chemical Shifts

The NMR spectra is displayed as a plot of the applied radio frequency versus the absorption. The applied frequency increases from left to right, thus the left side of the plot is the low field, downfield or deshielded side and the right side of the plot is the high field, upfield or shielded side (see the figure below). The concept of shielding will be explained shortly.



The position on the plot at which the nuclei absorbs is called the **chemical shift**. Since this has an arbitrary value a standard reference point must be used. The two most common standards are TMS (tetramethylsilane, $(Si(CH_3)_4)$ which has been assigned a chemical shift of zero, and $CDCl_3$ (deuterochloroform) which has a chemical shift of 7.26 for ^{1}H NMR and 77 for ^{13}C NMR.

The scale is commonly expressed as parts per million (ppm) which is independent of the spectrometer frequency. The scale is the **delta (δ) scale**.

$$\delta = \frac{\text{frequency of signal - frequency of standard}}{\text{spectrometer frequency}} \times 10^{6}$$

The range at which most NMR absorptions occur is quite narrow. Almost all ^{1}H absorptions occur downfield within 10 ppm of TMS. For ^{13}C NMR almost all absorptions occurs within 220 ppm downfield of the C atom in TMS.

Shielding in NMR

Structural features of the molecule will have an effect on the exact magnitude of the magnetic field experienced by a particular nucleus. This means that H atoms which have different chemical environments will have different chemical shifts. This is what makes NMR so useful for structure determination in organic chemistry. There are three main features that will affect the shielding of the nucleus, electronegativity, magnetic anisotropy of π systems and hydrogen bonding.

Electronegativity

The electrons that surround the nucleus are in motion so they created their own electromagnetic field. This field opposes the the applied magnetic field and so reduces the field experienced by the nucleus. Thus the electrons are said to **shield** the nucleus. Since the magnetic field experienced at the nucleus defines the energy difference between spin states it also defines what the chemical shift will be for that nucleus. Electron with-drawing groups can decrease the electron density at the nucleus, deshielding the nucleus and result in a larger chemical shift. Compare the data in the table below.

Compound, CH_3X	**CH_3F**	**CH_3OH**	**CH_3Cl**	**CH_3Br**	**CH_3I**	**CH_4**	**$(CH_3)_4Si$**
Electronegativity of X	4.0	3.5	3.1	2.8	2.5	2.1	1.8
Chemical shift δ (ppm)	4.26	3.4	3.05	2.68	2.16	0.23	0

As can be seen from the data, as the electronegativity of X increases the chemical shift, δ increases. This is an effect of the halide atom pulling the electron density away from the methyl group. This exposes the nuclei of both the C and H atoms, "deshielding" the nuclei and shifting the peak downfield.

The effects are cumulative so the presence of more electron withdrawing groups will produce a greater deshielding and therefore a larger chemical shift, *i.e.*

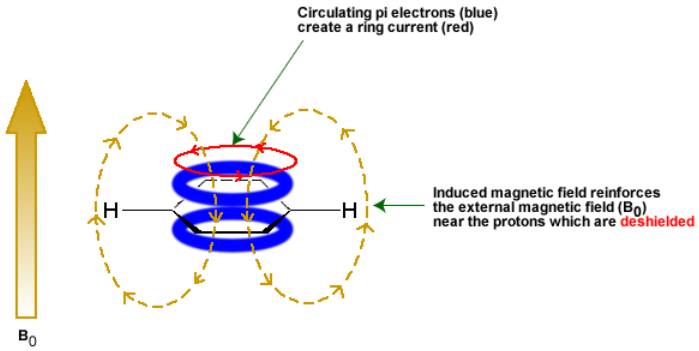
Compound	**CH_4**	**CH_3Cl**	**CH_2Cl_2**	**$CHCl_3$**
δ (ppm)	0.23	3.05	5.30	7.27

These **inductive effects** are not only felt by the immediately adjacent atoms, but the deshielding can occur further down the chain, *i.e.*

NMR signal	$-CH_2-CH_2-CH_2Br$
δ (ppm)	1.25 1.69 3.30

Magnetic Anisotropy: π Electron Effects

The π electrons in a compound, when placed in a magnetic field, will move and generate their own magnetic field. The new magnetic field will have an effect on the shielding of atoms within the field. The best example of this is benzene (see the figure below).

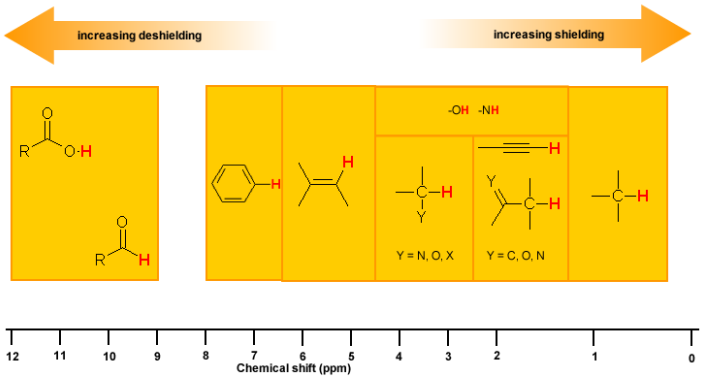


This effect is common for any atoms near a π bond, *i.e.*

Proton Type	Effect	Chemical shift (ppm)
C_6H_5-H	highly deshielded	6.5 - 8
C=C-H	deshielded	4.5 - 6
C≡C-H	shielded*	~2.5
O=C-H	very highly deshielded	9 - 10
* the acetylene H is shielded due to its location relative to the π system		

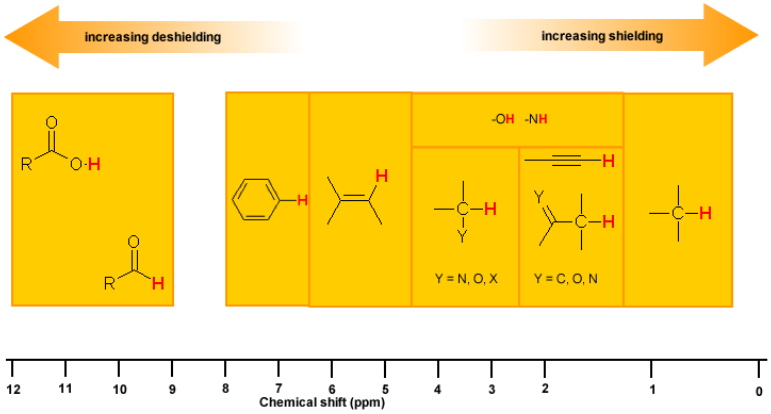
Hydrogen Bonding

Protons that are involved in hydrogen bonding (*i.e.*-OH or -NH) are usually observed over a wide range of chemical shifts. This is due to the deshielding that occurs in the hydrogen bond. Since hydrogen bonds are dynamic, constantly forming, breaking and forming again, there will be a wide range of hydrogen bonds strengths and consequently a wide range of deshielding. This as well as solvation effects, acidity, concentration and temperature make it very difficult to predict the chemical shifts for these atoms.



Experimentally -OH and -NH can be identified by carrying out a simple D_2O exchange experiment since these protons are exchangeable.

- run the normal H-NMR experiment on your sample
- add a few drops of D_2O
- re-run the H-NMR experiment
- compare the two spectra and look for peaks that have "disappeared"



Exercises

Exercise 5.10.1

The following peaks were from a H^1 NMR spectra from a 400 MHz spectrometer. Convert to δ units

A. $CHCl_3$ 1415 Hz

B. CH_3Cl 610 Hz

C. CH_3OH 693 Hz

D. CH_2Cl_2 1060 Hz

Answer

A. 3.627 ppm

B. 1.525 ppm

C. 1.732 ppm

D. 2.65 ppm

Exercise 5.10.2

Butan-2-one shows a chemical shit around 2.1 on a 300 MHz spectrometer in the H^1 NMR spectrum.

A. How far downfield is this peak from TMS in Hz?

B. If the spectrum was done with a 400 MHz instrument, would a different chemical shift be seen?

C. On this new 400 MHz spectrum, what would be the difference in Hz from the chemical shift and TMS?

Answer

A. Since TMS is at 0 δ = 0 Hz for reference, the difference between the two would be 630 Hz

B. No not a different chemical shift, but a different frequency would be seen, 840 Hz

C. 840 Hz

Questions

Q13.3.1

The following peaks were from a H^1 NMR spectra from a 400 MHz spectrometer. Convert to δ units

A. $CHCl_3$ 1451 Hz

B. CH_3Cl 610 Hz

C. CH_3OH 693 Hz

D. CH_2Cl_2 1060 Hz

Q13.3.2

Butan-2-one shows a chemical shift around 2.1 on a 300 MHz spectrometer in the H^1 NMR spectrum.

A. How far downfield is this peak from TMS in Hz?

B. If the spectrum was done with a 400 MHz instrument, would a different chemical shift be seen?

C. On this new 400 MHz spectrum, what would be the difference in Hz from the chemical shift and TMS?

Solutions

S13.3.1

A. 3.627 ppm

B. 1.525 ppm

C. 1.732 ppm

D. 2.65 ppm

S13.3.2

A. Since TMS is at 0 δ = 0 Hz for reference, the difference between the two would be 630 Hz

B. No not a different chemical shift, but a different frequency would be seen, 840 Hz

C. 840 Hz

Contributors and Attributions

- Dr. Dietmar Kennepohl FCIC (Professor of Chemistry, Athabasca University)
- Prof. Steven Farmer (Sonoma State University)
- Dr. Richard Spinney (The Ohio State University)

5.10: Chemical Shifts is shared under a CC BY-NC-SA 4.0 license and was authored, remixed, and/or curated by LibreTexts.

5.11: 1 H 1H NMR Spectroscopy and Proton Equivalence

Objectives

After completing this section, you should be able to

1. identify those protons which are equivalent in a given chemical structure.
2. use the ^{1}H NMR spectrum of a simple organic compound to determine the number of equivalent sets of protons present.

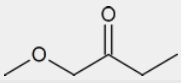
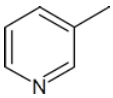
Key Terms

Make certain that you can define, and use in context, the key terms below.

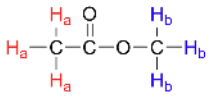
- diastereotopic
- enantiotopic
- homotopic

Study Notes

It is important at this stage to be able to identify equivalent protons in any organic compound given the structure of that compound. Once you know the number of different groups of equivalent protons in a compound, you can predict the number (before coupling) and relative strength of signals. Look at the following examples and make sure you understand how the number and intensity ratio of signals are derived from the structure shown.

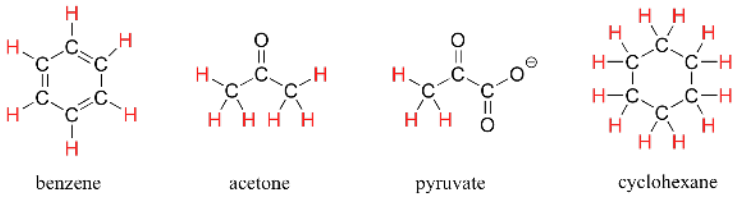
Structure	Number of Signals	Ratio of Signals	
$CH_3OCH_2CH_2Br$	3	A : B : C	3 : 2 : 2
	1		
	3	A : B : C	2 : 2 : 6 (or 1 : 1 : 3)
	3	A : B : C	2 : 4 : 2 (or 1 : 2 : 1)
	4	A : B : C : D	3 : 2 : 2 : 3
	5	A : B : C : D : E	3 : 1 : 1 : 1 : 1

If all protons in all organic molecules had the same resonance frequency in an external magnetic field of a given strength, the information in the previous paragraph would be interesting from a theoretical standpoint, but would not be terribly useful to organic chemists. Fortunately for us, however, resonance frequencies are not uniform for all protons in a molecule. *In an external magnetic field of a given strength, protons in different locations in a molecule have different resonance frequencies, because they are in non-identical electronic environments.* In methyl acetate, for example, there are two 'sets' of protons. The three protons labeled H_a have a different - and easily distinguishable – resonance frequency than the three H_b protons, because the two sets of protons are in non-identical environments: they are, in other words, chemically nonequivalent.

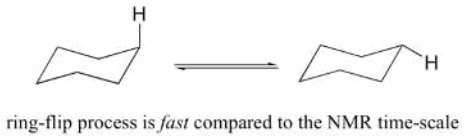


On the other hand, the three H_a protons are all in the same electronic environment, and are chemically equivalent to one another. They have identical resonance frequencies. The same can be said for the three H_b protons.

The ability to recognize chemical equivalency and nonequivalency among atoms in a molecule will be central to understanding NMR. In each of the molecules below, all protons are chemically equivalent, and therefore will have the same resonance frequency in an NMR experiment.



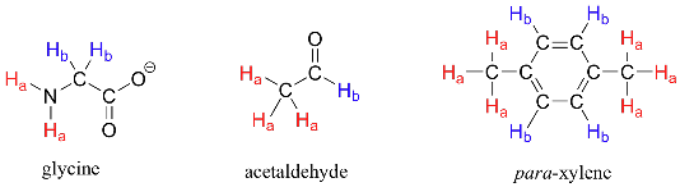
You might expect that the equitorial and axial hydrogens in cyclohexane would be non-equivalent, and would have different resonance frequencies. In fact, an axial hydrogen *is* in a different electronic environment than an equitorial hydrogen. Remember, though, that the molecule rotates rapidly between its two chair conformations, meaning that any given hydrogen is rapidly moving back and forth between equitorial and axial positions. It turns out that, except at extremely low temperatures, this rotational motion occurs on a time scale that is much faster than the time scale of an NMR experiment.



ring-flip process is *fast* compared to the NMR time-scale

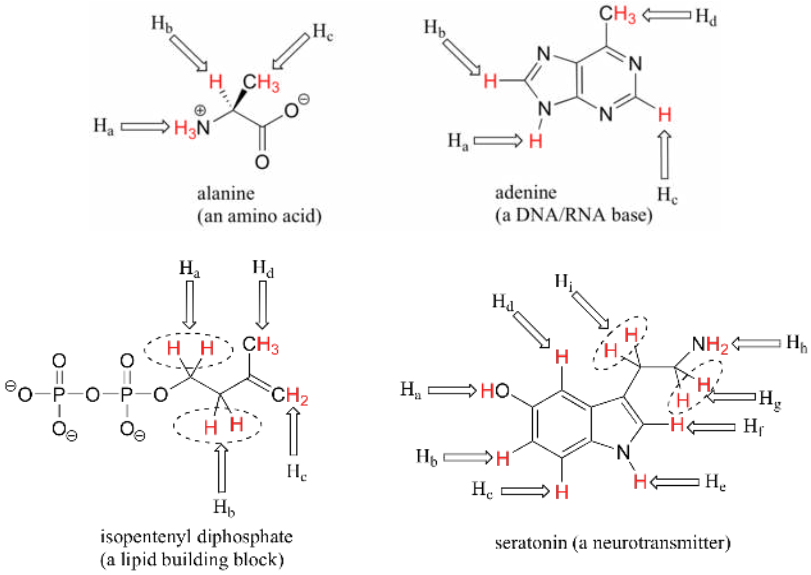
In this sense, NMR is like a camera that takes photographs of a rapidly moving object with a slow shutter speed - the result is a blurred image. In NMR terms, this means that all 12 protons in cyclohexane are equivalent.

Each the molecules in the next figure contains *two* sets of protons, just like our previous example of methyl acetate, and again in each case the resonance frequency of the H_a protons will be different from that of the H_b protons.



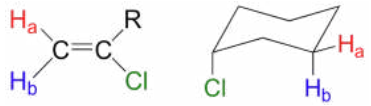
Notice how the symmetry of *para*-xylene results in there being only two different sets of protons.

Most organic molecules have several sets of protons in different chemical environments, and each set, in theory, will have a different resonance frequency in ^{1}H-NMR spectroscopy.

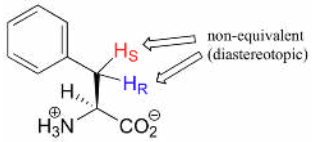


https://chem.libretexts.org/@go/page/167097

When stereochemistry is taken into account, the issue of equivalence vs nonequivalence in NMR starts to get a little more complicated. It should be fairly intuitive that hydrogens on different sides of asymmetric ring structures and double bonds are in different electronic environments, and thus are non-equivalent and have different resonance frequencies. In the alkene and cyclohexene structures below, for example, H_a is *trans* to the chlorine substituent, while H_b is *cis* to chlorine.

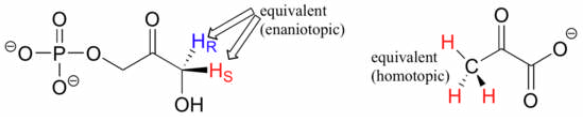


What is not so intuitive is that diastereotopic hydrogens (section 3.10) on chiral molecules are also non-equivalent:



phenylalanine

However, enantiotopic and homotopic hydrogens are chemically equivalent.

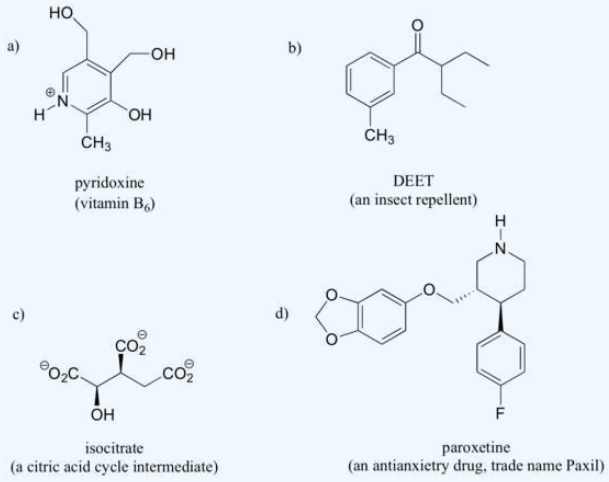


dihydroxyacetone phosphate

pyruvate

Example 13.8.1

How many different sets of protons do the following molecules contain? (count diastereotopic protons as non-equivalent).



pyridoxine (vitamin B_6)

DEET (an insect repellent)

isocitrate (a citric acid cycle intermediate)

paroxetine (an antianxietry drug, trade name Paxil)

Solution

a) 8 b) 8 c) 5 d) 18

Exercise

Exercise 5.11.1

How many non-equivalent hydrogen are in the following molecules; how many different signals will you see in a H^1 NMR spectrum.

A. $CH_3CH_2CH_2Br$

B. $CH_3OCH_2C(CH_3)_3$

C. Ethyl Benzene

D. 2-methyl-1-hexene

Answer

A. 3

B. 3

C. 5

D. 7

Questions

Q13.8.1

How many non-equivalent hydrogen are in the following molecules; how many different signals will you see in a H^1 NMR spectrum.

A. $CH_3CH_2CH_2Br$

B. $CH_3OCH_2C(CH_3)_3$

C. Ethyl Benzene

D. 2-methyl-1-hexene

Solutions

S13.8.1

A. 3; B. 3; C. 5; D. 7

Contributors and Attributions

- Dr. Dietmar Kennepohl FCIC (Professor of Chemistry, Athabasca University)
- Prof. Steven Farmer (Sonoma State University)
- Organic Chemistry With a Biological Emphasis by Tim Soderberg (University of Minnesota, Morris)

5.11: ^1H NMR Spectroscopy and Proton Equivalence is shared under a CC BY-NC-SA 4.0 license and was authored, remixed, and/or curated by LibreTexts.

5.12: Chemical Shifts in 1 H 1H NMR Spectroscopy

Objectives

After completing this section, you should be able to

1. state the approximate chemical shift (δ) for the following types of protons:
   a. aromatic.
   b. vinylic.
   c. those bonded to carbon atoms which are in turn bonded to a highly electronegative element.
   d. those bonded to carbons which are next to unsaturated centres.
   e. those bonded to carbons which are part of a saturated system.
2. predict the approximate chemical shifts of each of the protons in an organic compound, given its structure and a table of chemical shift correlations.

Study Notes

You should not attempt to memorize the chemical shifts listed in the table of this section, although it is probable that you will need to refer to it quite frequently throughout the remainder of this course. To fulfil Objective 1, above, you should be familiar with the information presented in the figure of chemical shift ranges for organic compounds. If you have an approximate idea of the chemical shifts of some of the most common types of protons, you will find the interpretation of ^{1}H NMR spectra less arduous than it might otherwise be. Notice that we shall not try to understand why aromatic protons are deshielded or why alkynyl protons are not deshielded as much as vinylic protons. These phenonomena can be explained, but the focus is on the interpretation of ^{1}H NMR spectra, not on the underlying theory.

^{1}H NMR Chemical Shifts

Chemical shift is associated with the Larmor frequency of a nuclear spin to its chemical environment. Tetramethylsilan[TMS; $(CH_3)_4Si$] is generally used for standard to determine chemical shift of compounds: δ_{TMS}=0ppm. In other words, frequencies for chemicals are measured for a ^{1}H or ^{13}C nucleus of a sample from the ^{1}H or ^{13}C resonance of TMS. It is important to understand trend of chemical shift in terms of NMR interpretation. The proton NMR chemical shift is affect by nearness to electronegative atoms (O, N, halogen.) and unsaturated groups (C=C,C=O, aromatic). Electronegative groups move to the down field (left; increase in ppm). Unsaturated groups shift to downfield (left) when affecting nucleus is in the plane of the unsaturation, but reverse shift takes place in the regions above and below this plane. ^{1}H chemical shift play a role in identifying many functional groups. Figure 1. indicates important example to figure out the functional groups.

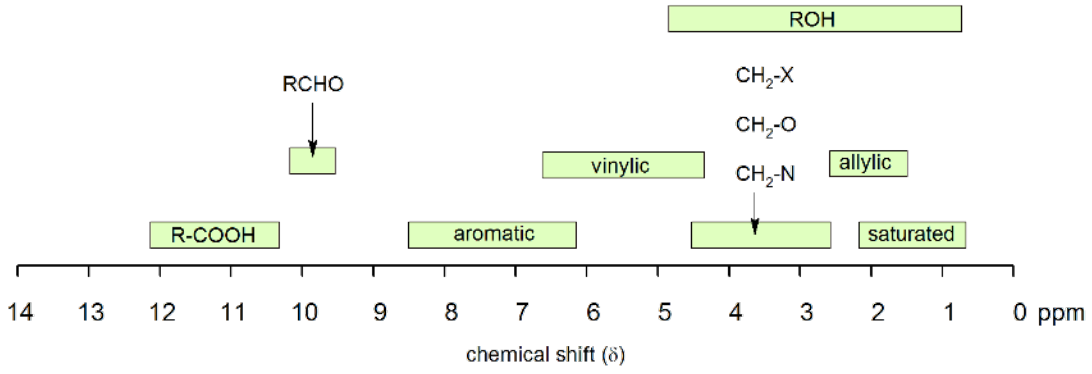
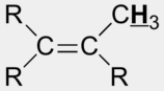
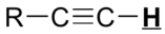
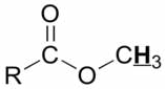
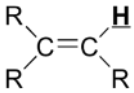
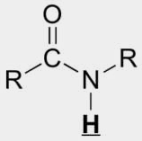
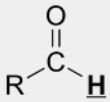
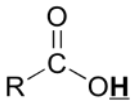


***Figure 1**. 1H chemical shift ranges for organic compounds*

Chemical shift values are in parts per million (ppm) relative to tetramethylsilane.

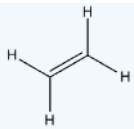
Hydrogen type	Chemical shift (ppm)

$RC\underline{H}_3$	0.9 - 1.0
$RC\underline{H}_2R$	1.2 - 1.7
$R_3C\underline{H}$	1.5 – 2.0
	2.0 – 2.3
	1.5 – 1.8
$RN\underline{H}_2$	1 - 3
$ArC\underline{H}_3$	2.2 – 2.4
	2.3 – 3.0
$ROC\underline{H}_3$	3.7 – 3.9
	3.7 – 3.9
$RO\underline{H}$	1 - 5
	3.7 – 6.5
	5 - 9
$Ar\underline{H}$	6.0 – 8.7
	9.5 – 10.0
	10 - 13

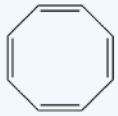
Exercises

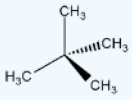
? Exercise 5.12.1

The following have one H^1 NMR peak. Predict where these peaks would be in a spectra. (MAY not be exact, but will be close)

A) 

B) 

C) 

D) 

Answer

A. 5.20 δ

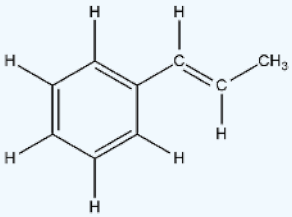
B. 1.50 δ

C. 6.40 δ

D. 1.00 δ

Exercise 5.12.2

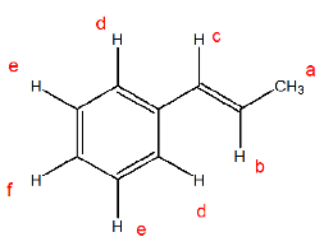
Identify the different protons in the following molecule and predict where they would be on a chemical spectrum.



Answer

There are 6 different protons in this molecule

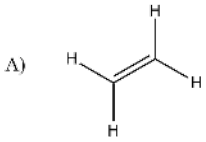
The shifts are (close) to the following: a. 2 δ; b. 6 δ; c. 6.5 δ; d. 7 δ; e. 7.5 δ; f. 7 δ

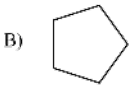


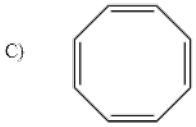
Questions

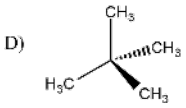
Q13.9.1

The following have one H^1 NMR peak. In each case predict approximately where this peak would be in a spectra.



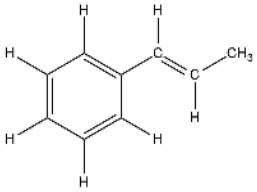






Q13.9.2

Identify the different equivalent protons in the following molecule and predict their expected chemical shift.



Solutions

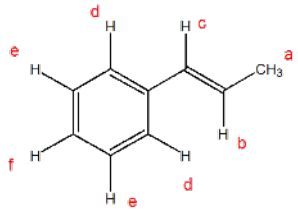
S13.9.1

A. 5.20 δ; B. 1.50 δ; C. 6.40 δ; D. 1.00 δ

S13.9.2

There are 6 different protons in this molecule

The shifts are (close) to the following: (a) 2 δ; (b) 6 δ; (c) 6.5 δ; (d) 7 δ; (e) 7.5 δ; (f) 7 δ



Contributors and Attributions

- Dr. Dietmar Kennepohl FCIC (Professor of Chemistry, Athabasca University)
- Prof. Steven Farmer (Sonoma State University)
- Organic Chemistry With a Biological Emphasis by Tim Soderberg (University of Minnesota, Morris)

5.12: Chemical Shifts in ^1H NMR Spectroscopy is shared under a CC BY-NC-SA 4.0 license and was authored, remixed, and/or curated by LibreTexts.

5.13: Integration of Proton Spectra

Objectives

After completing this section, you should be able to

1. explain what information can be obtained from an integrated ^{1}H NMR spectrum, and use this information in the interpretation of such a spectrum.
2. use an integrated ^{1}H NMR spectrum to determine the ratio of the different types of protons present in an organic compound.

Study Notes

The concept of peak integration is that the area of a given peak in a 1H NMR spectrum is proportional to the number of (equivalent) protons giving rise to the peak. Thus, a peak which is caused by a single, unique proton has an area which measures one third of the area of a peak resulting from a methyl (CH_3) group in the same spectrum.

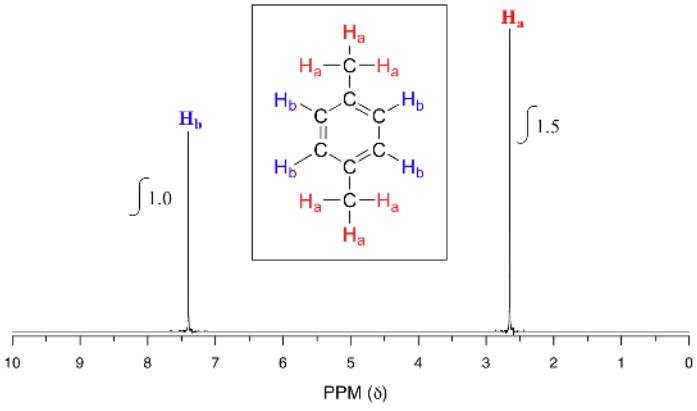
In practice, we do not have to measure these areas ourselves: it is all done electronically by the spectrometer, and an integration curve is superimposed on the rest of the spectrum. The integration curve appears as a series of steps, with the height of each step being proportional to the area of the corresponding absorption peak, and consequently, to the number of protons responsible for the absorption.

As it can be difficult to decide precisely where to start and stop when measuring integrations, you should not expect your ratios to be exact whole numbers.

Signal integration

The computer in an NMR instrument can be instructed to automatically integrate the area under a signal or group of signals. This is very useful, because *in ^{1}H-NMR spectroscopy the area under a signal is proportional to the number of hydrogens to which the peak corresponds*. The two signals in the methyl acetate spectrum, for example, integrate to approximately the same area, because they both correspond to a set of three equivalent protons.

Take a look next at the spectrum of *para*-xylene (IUPAC name 1,4-dimethylbenzene):



This molecule has two sets of protons: the six methyl (H_a) protons and the four aromatic (H_b) protons. When we instruct the instrument to integrate the areas under the two signals, we find that the area under the peak at 2.6 ppm is 1.5 times greater than the area under the peak at 7.4 ppm. This (along with the actual chemical shift values, which we'll discuss soon) tells us which set of protons corresponds to which NMR signal.

The integration function can also be used to determine the relative amounts of two or more compounds in a *mixed* sample. If we have a sample that is a 50:50 (mole/mole) mixture of benzene and acetone, for example, the acetone signal should integrate to the same value as the benzene sample, because both signals represent six equivalent protons. If we have a 50:50 mixture of acetone and cyclopentane, on the other hand, the ratio of the acetone peak area to the cylopentane peak area will be 3:5 (or 6:10), because the cyclopentane signal represents ten protons.

Example 5.13.1

You take a ^{1}H-NMR spectrum of a mixed sample of acetone ($CH_3(CO)CH_3$) and dichloromethane (CH_2Cl_2). The integral ratio of the two signals (acetone : dichloromethane) is 2.3 to 1. What is the molar ratio of the two compounds in the sample?.

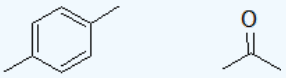
Solution

The acetone:dichloromethane molar ratio is 0.76:1. If the molar ratio was a 1:1 ratio, the signal integration ratio would be 3:1 because acetone has 6 protons while dichloromethane has 2. So, you need to divide the 2.3 integral value by a factor of 3 to get 0.76.

Example 5.13.2

You take the ^{1}H-NMR spectrum of a mixed sample of 36% *para*-xylene and 64% acetone in $CDCl_3$ solvent. How many peaks do you expect to see?

What is the expected ratio of integration values for these peaks? (set the acetone peak integration equal to 1.0)



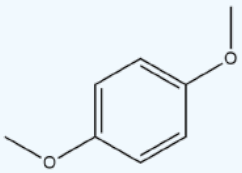
Solution

There are three peaks: two from *para*-xylene and one from acetone. The acetone peak and the *para*-xylene methyl peak both represent six protons, so the ratio of their integration values is simply 64 to 36 or 1 to 0.56. The ratio of the *para*-xylene methyl peak to the *para*-xylene aromatic peak is 6 to 4, or 0.56 to 0.37. So the final integral ratio of acetone:methyl:aromatic signals should be 1 to 0.56 to 0.37.

Exercise

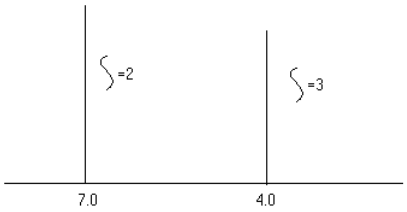
Exercise 5.13.1

Predict how many signals the following molecule would have? Sketch the spectra and estimate the integration of the peaks.



Answer

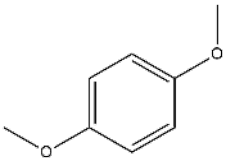
There will be two peaks in a ratio (integration) of 2 to 3 of benzene to methyl protons.



Questions

Q13.10.1

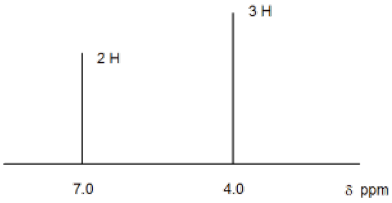
Predict how many signals the following molecule would have? Sketch the spectra and estimate the integration of the peaks.



Solutions

S13.10.1

There will be two peaks. Ideal general spectrum shown with integration.



Contributors and Attributions

- Dr. Dietmar Kennepohl FCIC (Professor of Chemistry, Athabasca University)
- Prof. Steven Farmer (Sonoma State University)
- Organic Chemistry With a Biological Emphasis by Tim Soderberg (University of Minnesota, Morris)

5.13: Integration of Proton Spectra is shared under a CC BY-NC-SA 4.0 license and was authored, remixed, and/or curated by LibreTexts.

5.14: Spin-Spin Splitting in 1 H 1H NMR Spectra

Objectives

After completing this section, you should be able to

1. explain the spin-spin splitting pattern observed in the ^{1}H NMR spectrum of a simple organic compound, such as chloroethane or 2-bromopropane.
2. interpret the splitting pattern of a given ^{1}H NMR spectrum.
3. determine the structure of a relatively simple organic compound, given its ^{1}H NMR spectrum and other relevant information.
4. use coupling constants to determine which groups of protons are coupling with one another in a ^{1}H NMR spectrum.
5. predict the splitting pattern which should be observed in the ^{1}H NMR spectrum of a given organic compound.

Key Terms

Make certain that you can define, and use in context, the key terms below.

- coupling constant
- multiplet
- quartet
- triplet
- doublet

Study Notes

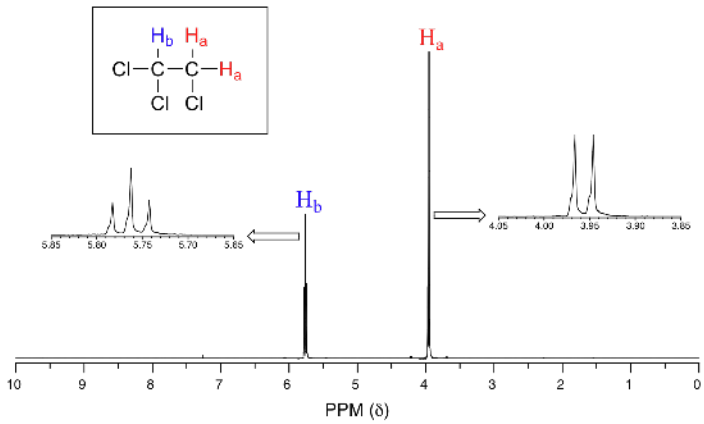
From what we have learned about ^{1}H NMR spectra so far, we might predict that the spectrum of 1,1,2-trichloroethane, $CHCl_2CH_2Cl$, would consist of two peaks—one, at about 2.5-4.0 δ, expected for CH_2-halogen compounds and one shifted downfield because of the presence of an additional electronegative chlorine atom on the second carbon. However, when we look at the spectrum it appears to be much more complex. True, we see absorptions in the regions we predicted, but these absorptions appear as a group of two peaks (a *doublet*) and a group of three peaks (a *triplet*). This complication, which may be disturbing to a student who longs for the simple life, is in fact very useful to the organic chemist, and adds greatly to the power of NMR spectroscopy as a tool for the elucidation of chemical structures. The split peaks (*multiplets*) arise because the magnetic field experienced by the protons of one group is influenced by the spin arrangements of the protons in an adjacent group.

Spin-spin coupling is often one of the more challenging topics for organic chemistry students to master. Remember the $n + 1$ rule and the associated coupling patterns.

The source of spin-spin coupling

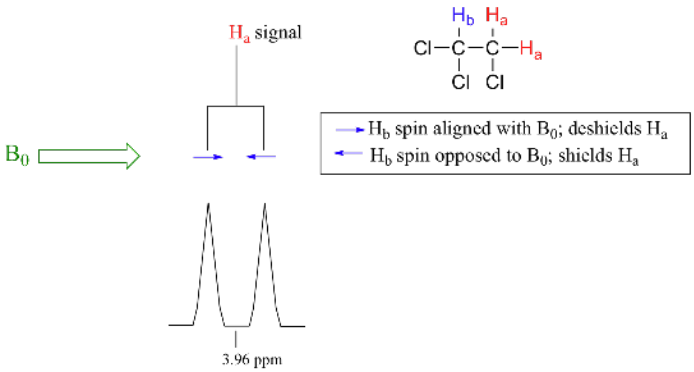
The ^{1}H-NMR spectra that we have seen so far (of methyl acetate and *para*-xylene) are somewhat unusual in the sense that in both of these molecules, each set of protons generates a single NMR signal. In fact, the ^{1}H-NMR spectra of most organic molecules contain proton signals that are 'split' into two or more sub-peaks. Rather than being a complication, however, this splitting behavior actually provides us with more information about our sample molecule.

Consider the spectrum for 1,1,2-trichloroethane. In this and in many spectra to follow, we show enlargements of individual signals so that the signal splitting patterns are recognizable.

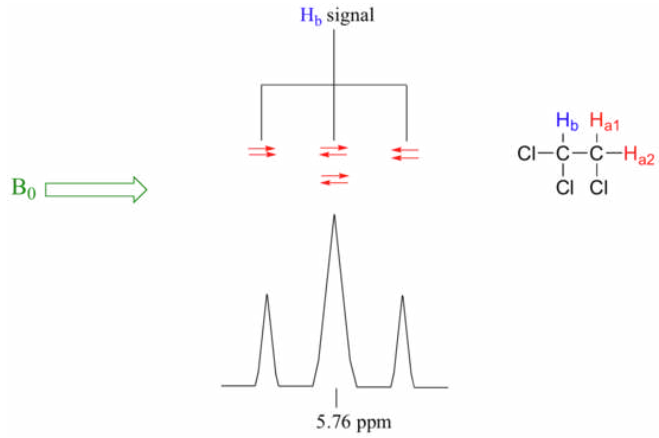


The signal at 3.96 ppm, corresponding to the two H_a protons, is split into two subpeaks of equal height (and area) – this is referred to as a **doublet**. The H_b signal at 5.76 ppm, on the other hand, is split into three sub-peaks, with the middle peak higher than the two outside peaks - if we were to integrate each subpeak, we would see that the area under the middle peak is twice that of each of the outside peaks. This is called a **triplet**.

The source of signal splitting is a phenomenon called **spin-spin coupling**, a term that describes the magnetic interactions between neighboring, non-equivalent NMR-active nuclei. In our 1,1,2 trichloromethane example, the H_a and H_b protons are spin-coupled to each other. Here's how it works, looking first at the H_a signal: in addition to being shielded by nearby valence electrons, each of the H_a protons is also influenced by the small magnetic field generated by H_b next door (remember, each spinning proton is like a tiny magnet). The magnetic moment of H_b will be aligned *with* B_0 in (slightly more than) half of the molecules in the sample, while in the remaining half of the molecules it will be opposed to B_0. The B_{eff} 'felt' by H_a is a slightly weaker if H_b is aligned against B_0, or slightly stronger if H_b is aligned with B_0. In other words, in half of the molecules H_a is *shielded* by H_b (thus the NMR signal is shifted slightly upfield) and in the other half H_a is *deshielded* by H_b(and the NMR signal shifted slightly downfield). What would otherwise be a single H_a peak has been split into two sub-peaks (a doublet), one upfield and one downfield of the original signal. These ideas an be illustrated by a **splitting diagram**, as shown below.

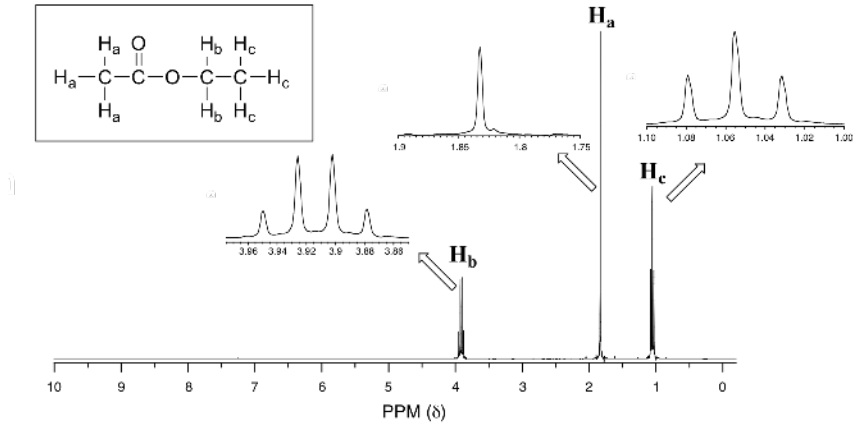


Now, let's think about the $H_b$signal. The magnetic environment experienced by H_b is influenced by the fields of both neighboring H_a protons, which we will call H_{a1} and H_{a2}. There are four possibilities here, each of which is equally probable. First, the magnetic fields of both H_{a1} and H_{a2} could be aligned with B_0, which would deshield H_b, shifting its NMR signal slightly downfield. Second, both the H_{a1} and H_{a2} magnetic fields could be aligned opposed to B_0, which would shield H_b, shifting its resonance signal slightly upfield. Third and fourth, H_{a1} could be with B_0 and H_{a2} opposed, or H_{a1}opposed to B_0 and H_{a2} with B_0. In each of the last two cases, the shielding effect of one H_a proton would cancel the deshielding effect of the other, and the chemical shift of H_b would be unchanged.



So in the end, the signal for H_b is a **triplet**, with the middle peak twice as large as the two outer peaks because there are *two* ways that H_{a1} and H_{a2} can cancel each other out.

Now, consider the spectrum for ethyl acetate:



We see an unsplit '**singlet**' peak at 1.833 ppm that corresponds to the acetyl (H_a) hydrogens – this is similar to the signal for the acetate hydrogens in methyl acetate that we considered earlier. This signal is unsplit because there are no adjacent hydrogens on the molecule. The signal at 1.055 ppm for the H_c hydrogens is split into a triplet by the two H_b hydrogens next door. The explanation here is the same as the explanation for the triplet peak we saw previously for 1,1,2-trichloroethane.

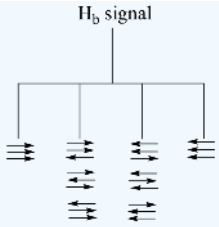
The $H_b$hydrogens give rise to a **quartet** signal at 3.915 ppm – notice that the two middle peaks are taller then the two outside peaks. This splitting pattern results from the spin-coupling effect of the *three* H_c hydrogens next door, and can be explained by an analysis similar to that which we used to explain the doublet and triplet patterns.

Example 13.11.1

a. Explain, using left and right arrows to illustrate the possible combinations of nuclear spin states for the H_c hydrogens, why the H_b signal in ethyl acetate is split into a quartet.
b. The integration ratio of doublets is 1:1, and of triplets is 1:2:1. What is the integration ratio of the H_b quartet in ethyl acetate? (Hint – use the illustration that you drew in part a to answer this question.)

Answer

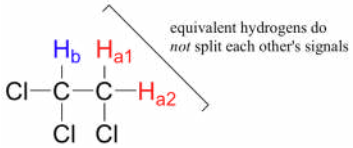
a)



b) The figure above demonstrates that the quartet subpeaks integrate to 1:3:3:1 (eg., there are three ways for two spins to be aligned with B_0 and one against B_0). As an analogy, if you flip three coins at once, you have a 1 in eight chance of getting all heads, 1 in 8 chance of all tails, a 3 in 8 chance of two heads and a tail, and a 3 in 8 chance of two tails and a head.

By now, you probably have recognized the pattern which is usually referred to as the ***n* + 1 rule**: if a set of hydrogens has *n* neighboring, non-equivalent hydrogens, it will be split into *n* + 1 subpeaks. Thus the two H_b hydrogens in ethyl acetate split the H_c signal into a triplet, and the three H_c hydrogens split the H_b signal into a quartet. This is very useful information if we are trying to determine the structure of an unknown molecule: if we see a triplet signal, we know that the corresponding hydrogen or set of hydrogens has two `neighbors`. When we begin to determine structures of unknown compounds using ^{1}H-NMR spectral data, it will become more apparent how this kind of information can be used.

Three important points need to be emphasized here. First, signal splitting only occurs between non-equivalent hydrogens – in other words, H_{a1} in 1,1,2-trichloroethane is *not* split by H_{a2}, and vice-versa.

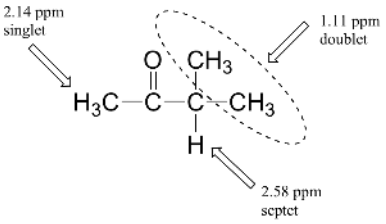


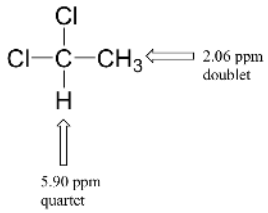
Second, splitting occurs primarily between hydrogens that are separated by three bonds. This is why the H_a hydrogens in ethyl acetate form a singlet– the nearest hydrogen neighbors are five bonds away, too far for coupling to occur.

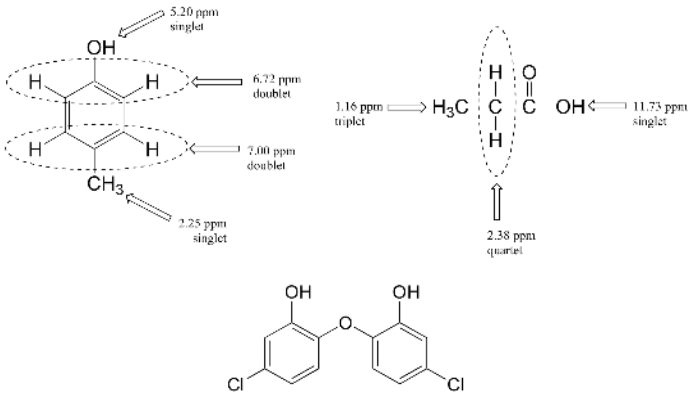


Occasionally we will see four-bond and even 5-bond splitting, but in these cases the magnetic influence of one set of hydrogens on the other set is much more subtle than what we typically see in three-bond splitting (more details about how we quantify coupling interactions is provided in section 5.5B). Finally, splitting is most noticeable with hydrogens bonded to carbon. Hydrogens that are bonded to heteroatoms (alcohol or amino hydrogens, for example) are coupled weakly - or not at all - to their neighbors. This has to do with the fact that these protons exchange rapidly with solvent or other sample molecules.

Below are a few more examples of chemical shift and splitting pattern information for some relatively simple organic molecules.







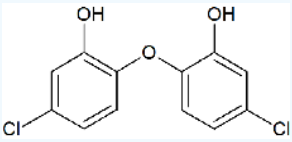
Multiplicity in Proton NMR

The number of lines in a peak is always one more (n+1) than the number of hydrogens on the neighboring carbon. This table summarizes coupling patterns that arise when protons have different numbers of neighbors.

# of lines	ratio of lines	term for peak	# of neighbors
1	-	singlet	0
2	1:1	doublet	1
3	1:2:1	triplet	2
4	1:3:3:1	quartet	3
5	1:4:6:4:1	quintet	4
6	1:5:10:10:5:1	sextet	5
7	1:6:15:20:15:6:1	septet	6
8	1:7:21:35:35:21:7:1	octet	7
9	1:8:28:56:70:56:28:8:1	nonet	8

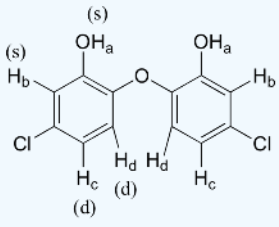
Example 13.11.2

How many proton signals would you expect to see in the ^{1}H-NMR spectrum of the structure shown below? For each of the proton signals, predict the splitting pattern. Assume that you see only 3-bond coupling.



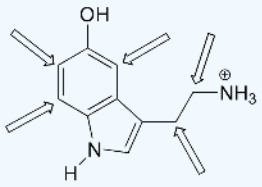
Answer

Because of the symmetry in the molecule, there are only four proton signals. Predicted splitting is indicated.

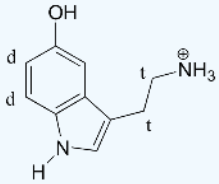


Example 13.11.3

Predict the splitting pattern for the ^{1}H-NMR signals corresponding to the protons at the locations indicated by arrows (the structure is that of the neurotransmitter serotonin).



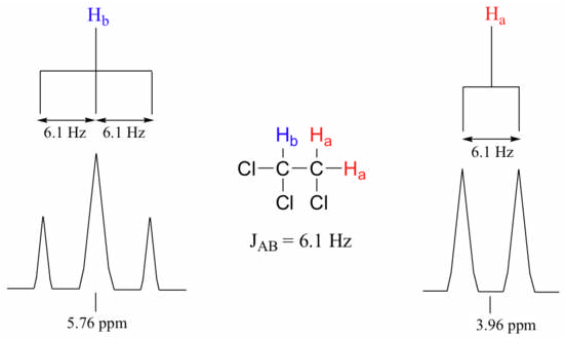
Answer



(recall that splitting is generally not seen with protons on heteroatoms)

Coupling constants

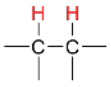
Chemists quantify the spin-spin coupling effect using something called the **coupling constant**, which is abbreviated with the capital letter *J*. The coupling constant is simply the difference, expressed in Hz, between two adjacent sub-peaks in a split signal. For our doublet in the 1,1,2-trichloroethane spectrum, for example, the two subpeaks are separated by 6.1 Hz, and thus we write $^3J_{a\text{-}b}$ = 6.1 Hz.



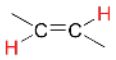
The superscript 3 tells us that this is a three-bond coupling interaction, and the a-b subscript tells us that we are talking about coupling between H_a and H_b. Unlike the chemical shift value, *the coupling constant, expressed in Hz, is the same regardless of the applied field strength of the NMR magnet*. This is because the strength of the magnetic moment of a neighboring proton, which is the source of the spin-spin coupling phenomenon, does *not* depend on the applied field strength.

When we look closely at the triplet signal in 1,1,2-trichloroethane, we see that the coupling constant - the `gap` between subpeaks - is 6.1 Hz, the same as for the doublet. This is an important concept! The coupling constant $^3J_{a\text{-}b}$ quantifies the magnetic interaction between the H_a and H_b hydrogen sets, and *this interaction is of the same magnitude in either direction*. In other words, H_a influences H_b to the same extent that H_b influences H_a. When looking at more complex NMR spectra, this idea of **reciprocal coupling constants** can be very helpful in identifying the coupling relationships between proton sets.

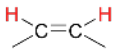
Coupling constants between proton sets on neighboring sp^3-hybridized carbons is typically in the region of 6-8 Hz. With protons bound to sp^2-hybridized carbons, coupling constants can range from 0 Hz (no coupling at all) to 18 Hz, depending on the bonding arrangement.



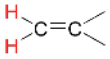
^3J = 6-8 Hz



vinylic *trans*: ^3J = 11-18 Hz

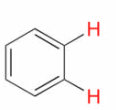


vinylic *cis*: ^3J = 6-15 Hz

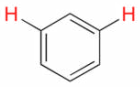


vinylic *gem*: ^2J = 0-5 Hz

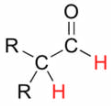
For vinylic hydrogens in a *trans* configuration, we see coupling constants in the range of ^3J = 11-18 Hz, while *cis* hydrogens couple in the ^3J = 6-15 Hz range. The 2-bond coupling between hydrogens bound to the same alkene carbon (referred to as geminal hydrogens) is very fine, generally 5 Hz or lower. *Ortho* hydrogens on a benzene ring couple at 6-10 Hz, while 4-bond coupling of up to 4 Hz is sometimes seen between *meta* hydrogens.



ortho-benzylic: ^3J = 6-10 Hz



meta-benzylic: ^4J = 0-4 Hz



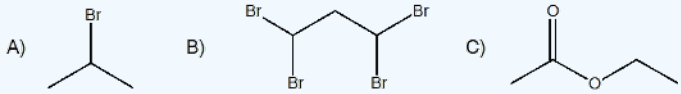
aldehyde: ^3J = 2-3 Hz

Fine (2-3 Hz) coupling is often seen between an aldehyde proton and a three-bond neighbor. Table 4 lists typical constant values.

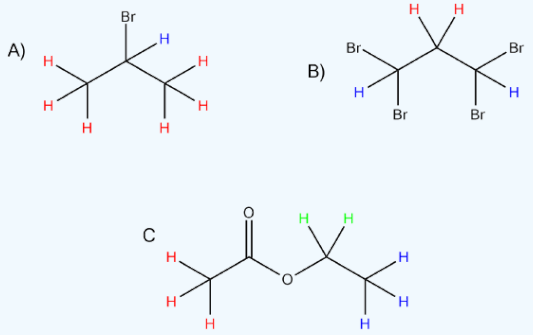
Exercises

? Exercise 5.14.1

Predict the splitting patterns of the following molecules.



Answer



A. H: Doublet. H: Septet

B. H: Triplet, H: Triplet

C. H: Singlet, H: Quartet, H: Triplet

Exercise 5.14.2

Draw the following according to the criteria given.

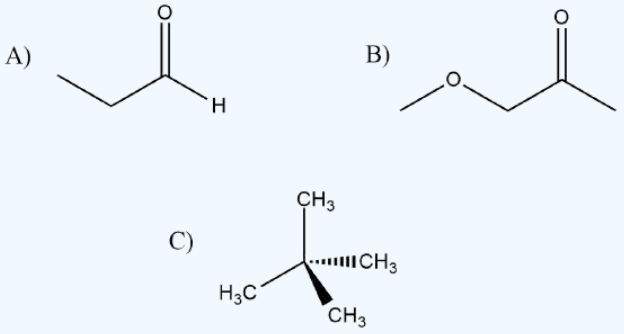
A. C_3H5O; two triplet, 1 doublet

B. $C_4H_8O_2$; three singlets

C. C_5H_{12}; one singlet

Answer

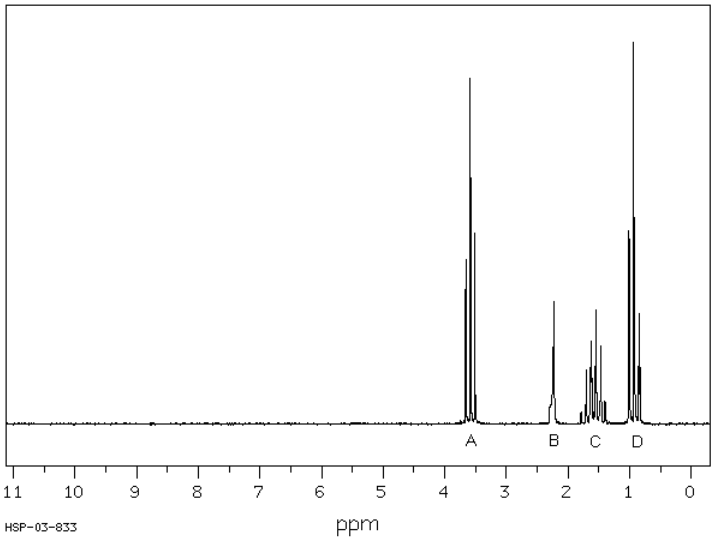
These are just some drawings, more may be possible.



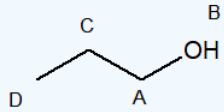
Exercise 5.14.3

The following spectrum is for C_3H_8O. Determine the structure.

A; triplet, B; Singlet, C; Sextet, D; Triplet



Answer



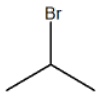
Propanol

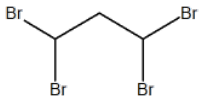
Note: Remember, chemically equivalent protons do not couple with one another to give spin-spin splitting.

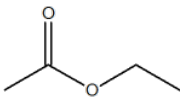
Questions

Q13.11.1

Predict the splitting patterns of the following molecules:

A) 

B) 

C) 

Q13.11.2

Draw the following according to the criteria given.

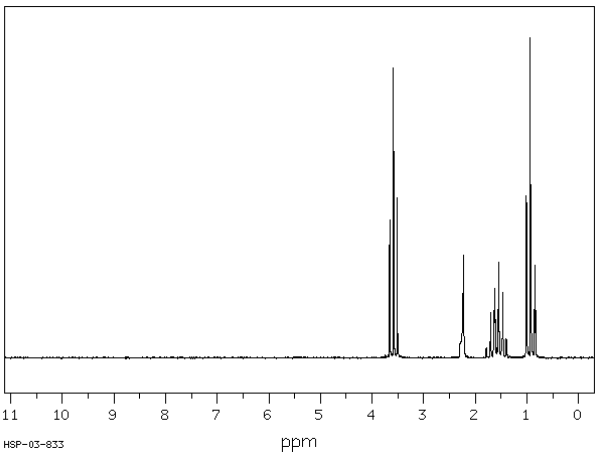
A. C_3H_5O; two triplet, 1 doublet

B. $C_4H_8O_2$; three singlets

C. C_5H_{12}; one singlet

Q13.11.3

The following spectrum is for C_3H_8O. Determine the structure.



A triplet; B singlet; C sextet; D triplet

Source: SDBSWeb : http://sdbs.db.aist.go.jp (National Institute of Advanced Industrial Science and Technology, 3 December 2016)

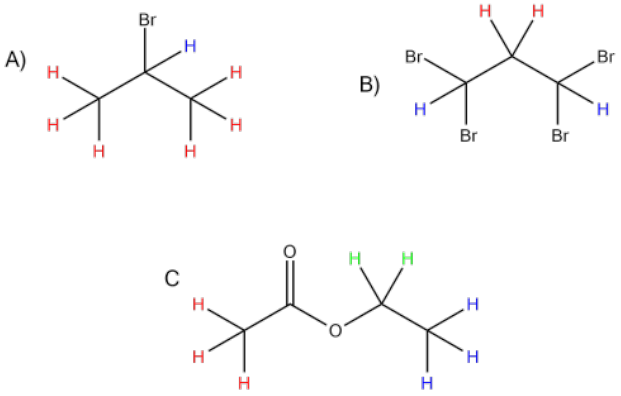
Solutions

S13.11.1

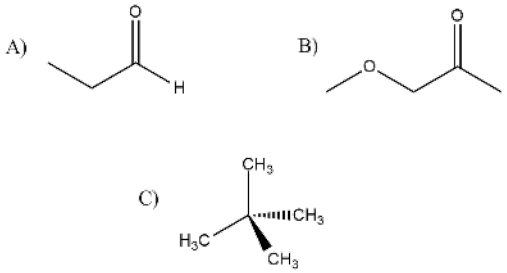
A. H: Doublet. H: Septet

B. H: Doublet, H: Triplet

C. H: Singlet, H: Quartet, H: Triplet

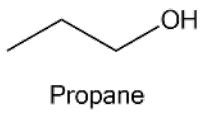


S13.11.2



These are just some drawings, more may be possible.

S13.11.3



Propane

Contributors and Attributions

- Dr. Dietmar Kennepohl FCIC (Professor of Chemistry, Athabasca University)
- Prof. Steven Farmer (Sonoma State University)
- Organic Chemistry With a Biological Emphasis by Tim Soderberg (University of Minnesota, Morris)
- Chris P Schaller, Ph.D., (College of Saint Benedict / Saint John's University)

5.14: Spin-Spin Splitting in ^1H NMR Spectra is shared under a CC BY-NC-SA 4.0 license and was authored, remixed, and/or curated by LibreTexts.

Welcome to the Chemistry Library. This Living Library is a principal hub of the LibreTexts project, which is a multi-institutional collaborative venture to develop the next generation of open-access texts to improve postsecondary education at all levels of higher learning. The LibreTexts approach is highly collaborative where an Open Access textbook environment is under constant revision by students, faculty, and outside experts to supplant conventional paper-based books.

5.16: More Complex Spin-Spin Splitting Patterns

Objectives

After completing this section, you should be able to

1. explain how multiple coupling can give rise to complex-looking ^{1}H NMR spectra.
2. predict the splitting pattern expected in the ^{1}H NMR spectrum of an organic compound in which multiple coupling is possible.
3. interpret ^{1}H NMR spectra in which multiple coupling is evident.

Key Terms

Make certain that you can define, and use in context, the key term below.

- tree diagram

Study Notes

We saw the effects of spin-spin coupling on the appearance of a ^{1}H NMR signal. These effects can be further complicated when that signal is coupled to several different protons. For example, $BrCH_2CH_2CH_2Cl$ would produce three signals. The hydrogens at C_1 and C_3 would each be triplets because of coupling to the two hydrogens on C_2. However, the hydrogen on C_2 "sees" two different sets of neighbouring hydrogens, and would therefore produce a triplet of triplets.

Another effect that can complicate a spectrum is the "closeness" of signals. If signals accidently overlap they can be difficult to identify. In the example above, we expected a triplet of triplets. However, if the coupling is identical (or almost identical) between the hydrogens on C_2 and the hydrogens on both C_1 and C_3, one would observe a quintet in the ^{1}H NMR spectrum. [You can try this yourself by drawing a tree diagram of a triplet of triplets assuming, first, different coupling constants, and then, identical coupling constants.] Keep this point in mind when interpreting real ^{1}H NMR spectra.

Also, when multiplets are well separated, they form patterns. However, when multiplets approach each other in the spectrum they sometimes become distorted. Usually, the inner peaks become larger than the outer peaks. Note the following examples:



Aromatic ring protons quite commonly have overlapping signals and multiplet distortions. Sometimes you cannot distinguish between individual signals, and one or more messy multiplets often appear in the aromatic region.

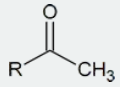
It is much easier to rationalize the observed ^{1}H NMR spectrum of a known compound than it is to determine the structure of an unknown compound from its ^{1}H NMR spectrum. However, rationalizations can be a useful learning technique as you try to improve your proficiency in spectral interpretation. Remember that when a chemist tries to interpret the ^{1}H NMR spectrum of an unknown compound, he or she usually has additional information available to make the task easier. For example, the chemist will almost certainly have an infrared spectrum of the compound and possibly a mass spectrum too. Details of how the compound was synthesized may be available, together with some indication of its chemical properties, its physical properties, or both.

In examinations, you will be given a range of information (IR, MS, UV data and empirical formulae) to aid you with your structural determination using ^{1}H NMR spectroscopy. For example, you may be asked to determine the structure of $C_6H_{12}O$ given the following spectra:

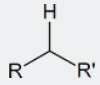
Infrared spectrum: 3000 cm^{-1} and 1720 cm^{-1} absorptions are both strong

^{1}H NMR	δ (ppm)	Protons	Multiplicity
	0.87	6	doublet
	1.72	1	broad multiplet
	2.00	3	singlet
	2.18	2	doublet

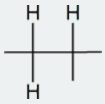
To answer this question, you note that the infrared spectrum of $C_6H_{12}O$ shows $C-H$ stretching (3000 cm^{-1}) and $C-O$ stretching (1720 cm^{-1}). Now you have to piece together the information from the ^{1}H NMR spectrum. Notice the singlet with three protons at 2.00 ppm. This signal indicates a methyl group that is not coupled to other protons. It could possibly mean the presence of a methyl ketone functional group.



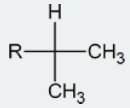
The signal at 1.72 ppm is a broad multiplet, suggesting that a carbon with a single proton is beside carbons with several different protons.



The doublet signal at 2.18 ppm implies that a $-CH_2-$ group is attached to a carbon having only one proton.

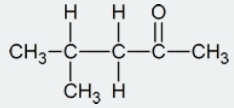


The six protons showing a doublet at 0.87 ppm indicate two equivalent methyl groups attached to a carbon with one proton.



Whenever you see a signal in the 0.7-1.3 ppm range that is a multiplet of three protons (3, 6, 9) it is most likely caused by equivalent methyl groups.

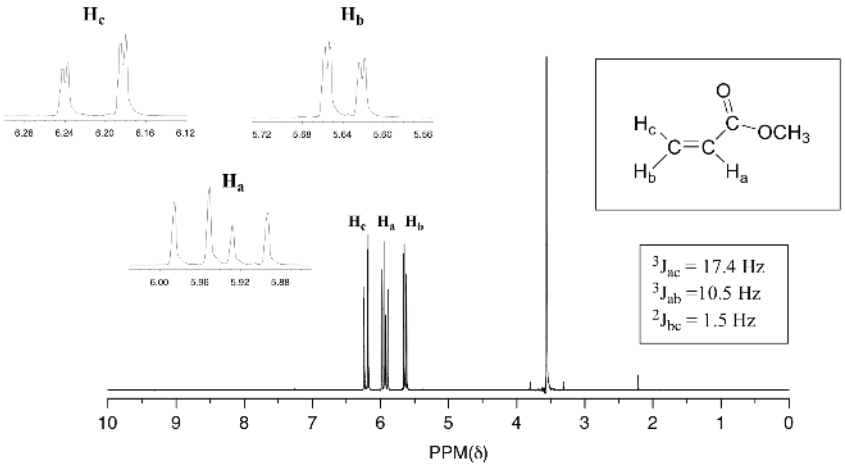
Using trial and error, and with the above observations, you should come up with the correct structure.



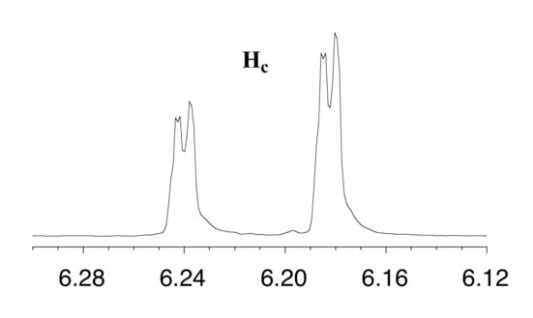
https://chem.libretexts.org/@go/page/167102

Complex coupling

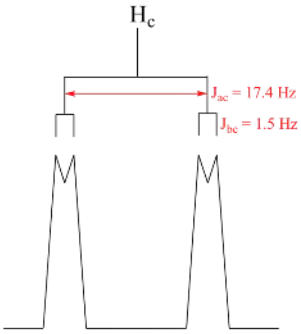
In all of the examples of spin-spin coupling that we have seen so far, the observed splitting has resulted from the coupling of one set of hydrogens to *just one* neighboring set of hydrogens. When a set of hydrogens is coupled to *two or more* sets of nonequivalent neighbors, the result is a phenomenon called **complex coupling**. A good illustration is provided by the ^{1}H-NMR spectrum of methyl acrylate:



First, let's first consider the H_c signal, which is centered at 6.21 ppm. Here is a closer look:

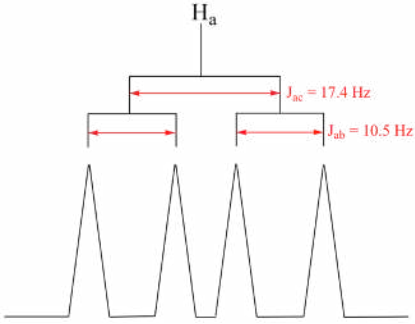


With this enlargement, it becomes evident that the Hc signal is actually composed of four sub-peaks. Why is this? H_c is coupled to both H_a and H_b , but with *two different coupling constants*. Once again, a splitting diagram (or tree diagram) can help us to understand what we are seeing. H_a is *trans* to H_c across the double bond, and splits the H_c signal into a doublet with a coupling constant of $^3J_{ac}$ = 17.4 Hz. In addition, each of these H_c doublet sub-peaks is split again by H_b (*geminal* coupling) into two more doublets, each with a much smaller coupling constant of $^2J_{bc}$ = 1.5 Hz.

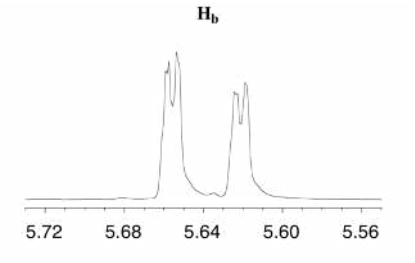


The result of this `double splitting` is a pattern referred to as a **doublet of doublets**, abbreviated `**dd**`.

The signal for H_a at 5.95 ppm is also a doublet of doublets, with coupling constants $^3J_{ac}$= 17.4 Hz and $^3J_{ab}$ = 10.5 Hz.



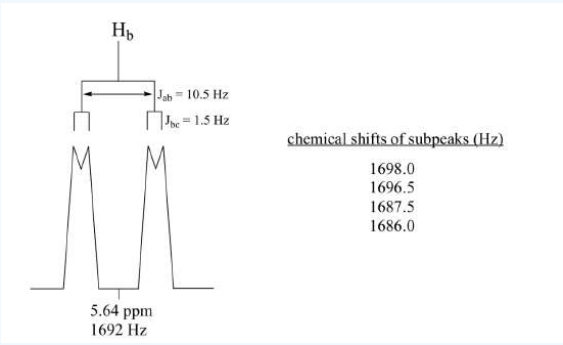
The signal for H_b at 5.64 ppm is split into a doublet by H_a, a *cis* coupling with $^3J_{ab}$ = 10.4 Hz. Each of the resulting sub-peaks is split again by H_c, with the same *geminal* coupling constant $^2J_{bc}$ = 1.5 Hz that we saw previously when we looked at the H_c signal. The overall result is again a doublet of doublets, this time with the two `sub-doublets` spaced slightly closer due to the smaller coupling constant for the *cis* interaction. Here is a blow-up of the actual $H_b$signal:



Example 5.16.1

Construct a splitting diagram for the H_b signal in the ^{1}H-NMR spectrum of methyl acrylate. Show the chemical shift value for each sub-peak, expressed in Hz (assume that the resonance frequency of TMS is exactly 300 MHz).

Solution:

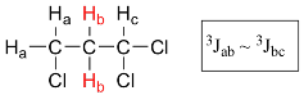


Note

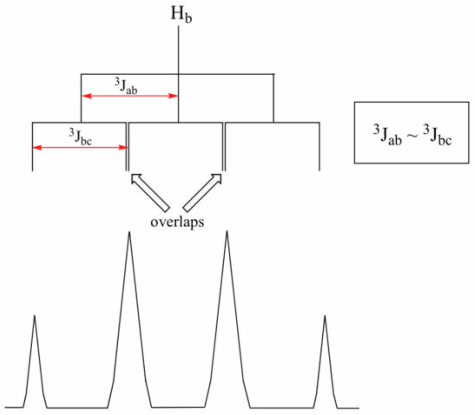
When constructing a splitting diagram to analyze complex coupling patterns, it is usually easier to show the larger splitting first, followed by the finer splitting (although the reverse would give the same end result).

When a proton is coupled to two different neighboring proton sets with identical or very close coupling constants, the splitting pattern that emerges often appears to follow the

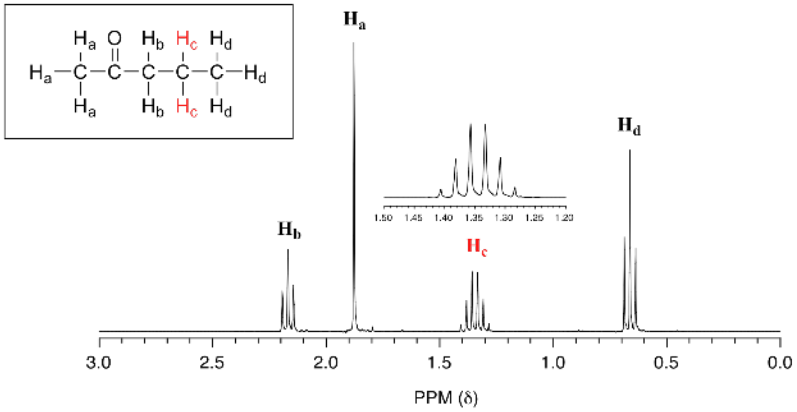
When a proton is coupled to two different neighboring proton sets with identical or very close coupling constants, the splitting pattern that emerges often appears to follow the simple `*n* + 1 rule` of non-complex splitting. In the spectrum of 1,1,3-trichloropropane, for example, we would expect the signal for H_b to be split into a triplet by H_a, and again into doublets by H_c, resulting in a 'triplet of doublets'.



H_a and H_c are not equivalent (their chemical shifts are different), but it turns out that $^3J_{ab}$ is very close to $^3J_{bc}$. If we perform a splitting diagram analysis for H_b, we see that, due to the overlap of sub-peaks, the signal appears to be a quartet, and for all intents and purposes follows the $n + 1$ rule.

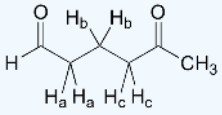


For similar reasons, the H_c peak in the spectrum of 2-pentanone appears as a sextet, split by the five combined H_b and H_d protons. Technically, this 'sextet' could be considered to be a 'triplet of quartets' with overlapping sub-peaks.



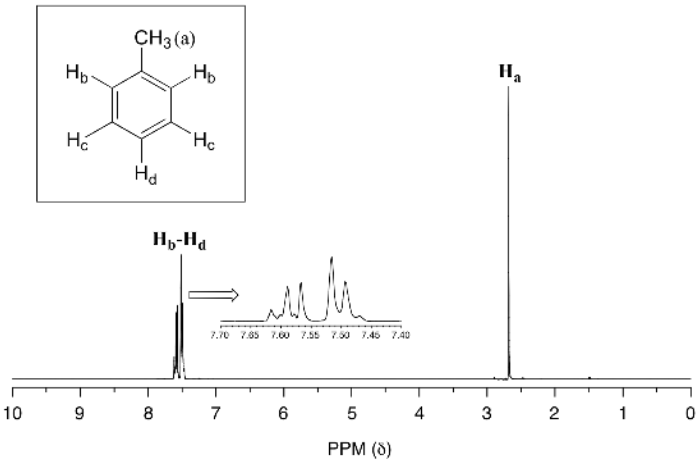
Example 5.16.2

What splitting pattern would you expect for the signal coresponding to H_b in the molecule below? Assume that $J_{ab} \sim J_{bc}$. Draw a splitting diagram for this signal, and determine the relative integration values of each subpeak.



Solution: We can think of this signal as being a triplet of triplets, but because the two coupling constants are very close, what we would actually see is a 1,2,3,2,1 pentet.

In many cases, it is difficult to fully analyze a complex splitting pattern. In the spectrum of toluene, for example, if we consider only 3-bond coupling we would expect the signal for H_b to be a doublet, H_d a triplet, and H_c a triplet.



In practice, however, all three aromatic proton groups have very similar chemical shifts and their signals overlap substantially, making such detailed analysis difficult. In this case, we would refer to the aromatic part of the spectrum as a **multiplet**.

When we start trying to analyze complex splitting patterns in larger molecules, we gain an appreciation for why scientists are willing to pay large sums of money (hundreds of thousands of dollars) for higher-field NMR instruments. Quite simply, the stronger our magnet is, the more resolution we get in our spectrum. In a 100 MHz instrument (with a magnet of approximately 2.4 Tesla field strength), the 12 ppm frequency 'window' in which we can observe proton signals is 1200 Hz wide. In a 500 MHz (~12 Tesla) instrument, however, the window is 6000 Hz - five times wider. In this sense, NMR instruments are like digital cameras and HDTVs: better resolution means more information and clearer pictures (and higher price tags!)

Exercises

1. Given the information below, draw the structures of compounds *A* through *D*.

   a. An unknown compound *A* was prepared as follows:

   $$CH_3{=}C(CH_2Cl)_2 \xrightarrow[THF]{Mg} A$$

   Mass spectrum:

   base peak *m*/*e* = 39
   parent peak *m*/*e* = 54

   ^{1}H NMR spectrum:

δ (ppm)	Relative Area	Multiplicity
1.0	2	triplet
5.4	1	quintet

   b. Unknown compound *B* has the molecular formula $C_7H_6O_2$.

   Infrared spectrum:

   3200 cm^{-1} (broad) and 1747 cm^{-1} (strong) absorptions

   ^{1}H NMR spectrum:

δ (ppm)	Protons
6.9	2
7.4	2

9.8	1
10.9	1

Hint: Aromatic ring currents deshield all proton signals just outside the ring.

c. Unknown compound *C* shows no evidence of unsaturation and contains only carbon and hydrogen.

Mass spectrum:

parent peak *m*/*e* = 68

^{1}H NMR spectrum:

δ (ppm)	Relative Area	Multiplicity
1.84	3	triplet
2.45	1	septet

Hint: Think three dimensionally!

d. Unknown compound *D* ($C_{15}H_{14}O$) has the following spectral properties.

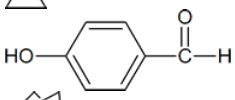
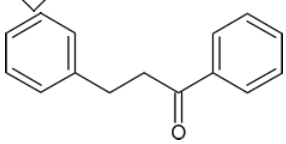
Infrared spectrum:

3010 cm^{-1} (medium)
1715 cm^{-1} (strong)
1610 cm^{-1} (strong)
1500 cm^{-1} (strong)

^{1}H NMR spectrum:

δ (ppm)	Relative Area	Multiplicity
3.00	2	triplet
3.07	2	triplet
7.1-7.9	10	Multiplets

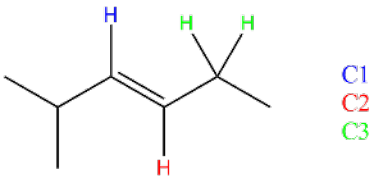
Answers

1. a.
   b. 
   c.
   d. 

Questions

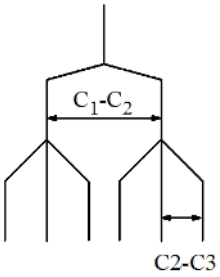
Q13.12.1

In the following molecule, the C2 is coupled with both the vinyl, C1, and the alkyl C3. Draw the splitting tree diagram.



Solutions

S13.12.1



Contributors and Attributions

- Dr. Dietmar Kennepohl FCIC (Professor of Chemistry, Athabasca University)
- Prof. Steven Farmer (Sonoma State University)
- Organic Chemistry With a Biological Emphasis by Tim Soderberg (University of Minnesota, Morris)

5.16: More Complex Spin-Spin Splitting Patterns is shared under a CC BY-NC-SA 4.0 license and was authored, remixed, and/or curated by LibreTexts.

- **13.7: More Complex Spin-Spin Splitting Patterns** by Dietmar Kennepohl, Steven Farmer, Tim Soderberg is licensed CC BY-SA 4.0.

5.17: Uses of 1 H 1H NMR Spectroscopy

Objective

After completing this section, you should be able to use data from ^{1}H NMR spectra to distinguish between two (or more) possible structures for an unknown organic compound.

There will be cases in which you already know what the structure might be. In these cases:

- You should draw attention to pieces of data that most strongly support your expected structure. This approach will demonstrate evaluative understanding of the data; that means you can look at data and decide what parts are more crucial than others.
- You should also draw attention to negative results: that is, peaks that might be there if this spectrum matched another, possible structure, but that are in fact missing.

One of the most complicated problems to deal with is the analysis of a mixture. This situation is not uncommon when students run reactions in lab and analyse the data.

- Sometimes the spectra show a little starting material mixed in with the product.
- Sometimes solvents show up in the spectrum.
- As you might expect, the minor component usually shows up as smaller peaks in the spectrum. If there are fewer molecules present, then there are usually fewer protons to absorb in the spectrum.
- In this case, you should probably make two completely separate sets of data tables for your analysis, one for each compound, or else one for the main compound and one for impurities.

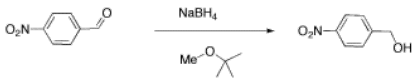
Remember that integration ratios are really only meaningful within a single compound. If your NMR sample contains some benzene (C_6H_6) and some acetone (CH_3COCH_3), and there is a peak at 7.15 that integrates to 1 proton and a peak at 2.10 ppm integrating to 6 protons, it might mean there are 6 protons in acetone and 1 in benzene, but you can tell that isn't true by looking at the structure. There must be six times as many acetone molecules as benzene molecules in the sample.

There are six protons in the benzene, and they should all show up near 7 ppm. There are six protons in acetone, and they should all show up near 2 ppm. Assuming that small integral of 1H for the benzene is really supposed to be 6H, then the large integral of 6H for the acetone must also represent six times as many hydrogens, too. It would be 36 H. There are only six hydrogens in acetone, so it must represent six times as many acetone molecules as there are benzenes.

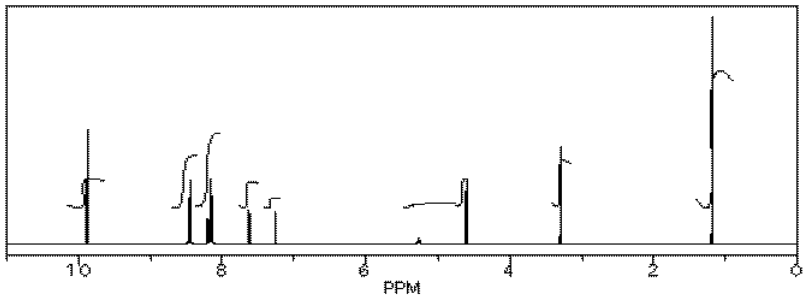
Similarly, if you have decided that you can identify two sets of peaks in the ^{1}H spectrum, analysing them in different tables makes it easy to keep the integration analysis completely separate too ; 1 H in one table will not be the same size integral as 1 H in the other table unless the concentrations of the two compounds in the sample are the same.

However, comparing the ratio of two integrals for two different compounds can give you the ratio of the two compounds in solution, just as we could determine the ratio of benzene to acetone in the mixture described above.

We will look at two examples of sample mixtures that could arise in lab. Results like these are pretty common events in the labIn the first example, a student tried to carry out the following reaction, a borohydride reduction of an aldehyde. The borohydride should give a hydride anion to the C=O carbon; washing with water should then supply a proton to the oxygen, giving an alcohol.

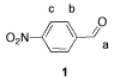
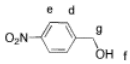


Her reaction produced the following spectrum.



(simulated data)

From this data, she produced the table below.

	shift	integration	int(n)	internal ratio	multiplicity	part structure	assignment
a	9.9 ppm	11 mm	2H	1H	singlet		
b	8.5 ppm	23 mm	4H	2H	doublet		 1
c	8.1 ppm	(20 mm?)	4H	2H	doublet		
d	8.2 ppm	(10 mm?)	2H	2H	doublet		
e	7.6 ppm	9 mm	2H	2H	doublet		 2
f	5.3 ppm	2 mm	0.4H	<1H	singlet	OH	
g	4.7 ppm	12 mm	2H	2H	singlet		
h	7.2 ppm	4 mm	0.8H	1H	singlet	$CHCl_3$	
i	3.3 ppm	8 mm	1.5H	3H	singlet		
j	1.2 ppm	24 mm	4.5H	9H	singlet		
			23.4H total				

Ratio of reactant **1** to product **2** is 2:1 based on peaks at 9.9 and 4.7 ppm (2H / 1H) : (2H / 2H); the reaction is 33% complete [2 / (2+1)]

Ratio of product **2** to TBME is 2:1 based on peaks at 4.7 and 3.3 ppm (2H / 2H) : (1.5H / 3H); the ratio of **1**:**2**:TBME is 2:1:0.5, so the sample is 57% **1** [2/(2+1+0.5)], 29% **2** and 14% TBME.

Notice how she calculated that ratio. She found a peak in molecule 1, the aldehyde, that she was pretty sure corresponded to the aldehydic hydrogen, the H attached to the C=O; in other words, the CH=O. She found another peak from molecule 2, the alcohol, that she was pretty sure represented the two hydrogens on the carbon attached to oxygen, the CH_2-O.

The integrals for those two peaks are equal. They are both 2H in her table. However, she notes that within each molecule, the first integral really represents 1H and the second represents 2H. That means there must be twice as many of molecule 1 as there are molecule 2. That way, there would be 2 x CH=O, and its integral would be the same as the 1 x CH_2-O in the other molecule.

One way to approach this kind of problem is to:

- choose one peak from each of the two compounds you want to compare.
- decide how many hydrogens each peak is supposed to represent in a molecule. Is it supposed to be a CH_2, a CH, a CH_3?
- divide the integral value for that peak by that number of hydrogens it is supposed to represent in a molecule.
- compare the two answers (integral A / ideal # H) vs (integral B / ideal # H).
- the ratio of those two answers is the ratio of the two molecules in the sample.

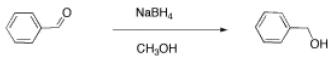
So there is twice as much aldehyde as alcohol in the mixture. In terms of these two compounds alone, she has 33% alcohol and 66% aldehyde. That's (1/(1+2)) x100% for the alcohol, and (2/(1+2)) x100% for the aldehyde. That calculation just represents

the amount of individual component divided by the total of the components she wants to compare.

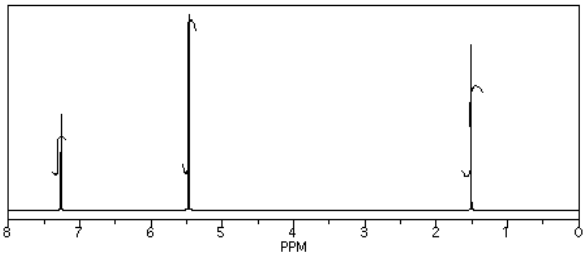
There are a number of things to take note of here.

- Her reaction really didn't work very well. She still has majority starting material, not product.
- She will get a good grade on this lab. Although the experiment didn't work well, she has good data, and she has analyzed it very clearly.
- She has separated her data table into different sections for different compounds. Sometimes that makes it easier to analyze things.
- She has noted the actual integral data (she may have measured the integral with a ruler) and also converted it into a more convenient ratio, based on the integral for a peak that she felt certain about.
- She went one step further, and indicated the internal integration ratio within each individual compound.
- She calculated the % completion of the reaction using the integral data for the reactant and product, and she made clear what part of the data she used for that calculation. A similar procedure could be done if a student were just trying to separate two components in a mixture rather than carry out a reaction.
- She also calculated the overall purity of the mixture, including a solvent impurity that she failed to remove.
- However, $CHCl_3$ is not included in her analysis of purity. $CHCl_3$ really isn't part of her sample; it was just present in the NMR solvent, so it doesn't represent anything in the material she ended up with at the end of lab.

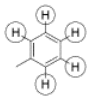
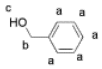
Another student carried out a similar reaction, shown below. He also finished the reaction by washing with water, but because methanol is soluble in water, he had to extract his product out of the water. He chose to use dichloromethane for that purpose.



He obtained the following data.



From this data, he constructed the following table.

	shift	integration	int(n)	multiplicity	partial structure	assignment
a	7.3 ppm	16 mm	5H	singlet		
b	5.4 ppm	64 mm	2H	singlet		
c	1.6 ppm	37 mm	1H	singlet	OH	

There are some things to learn about this table, too.

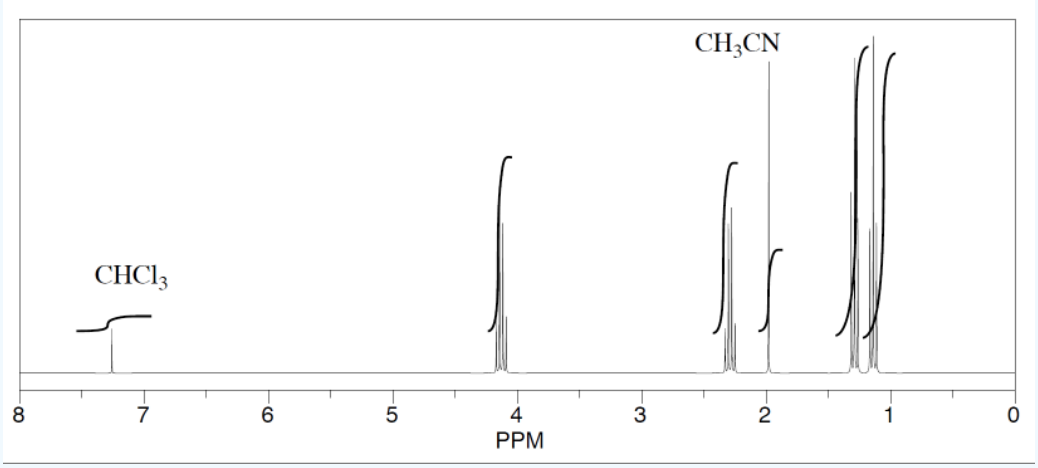
- Does the integration ratio really match the integral data? Or is this just wishful thinking?
- This table might reflect what he wants to see in the data. But what else could be in the data?
- $CHCl_3$ is often seen in NMR spectra if $CDCl_3$ is used for the NMR sample. It's there, at 7.2 ppm.
- "Leftover" or residual solvent is very common in real lab data. There it is, CH_2Cl_2 from the extraction, at 5.4 ppm.
- What about water? Sometimes people don't dry their solutions properly before evaporating the solvent. There is probably water around 1.5 to 1.6 ppm here.

This student might not get a very good grade; the sample does not even show up in the spectrum, so he lost it somewhere. But his analysis is also poor, so he will really get a terrible grade.

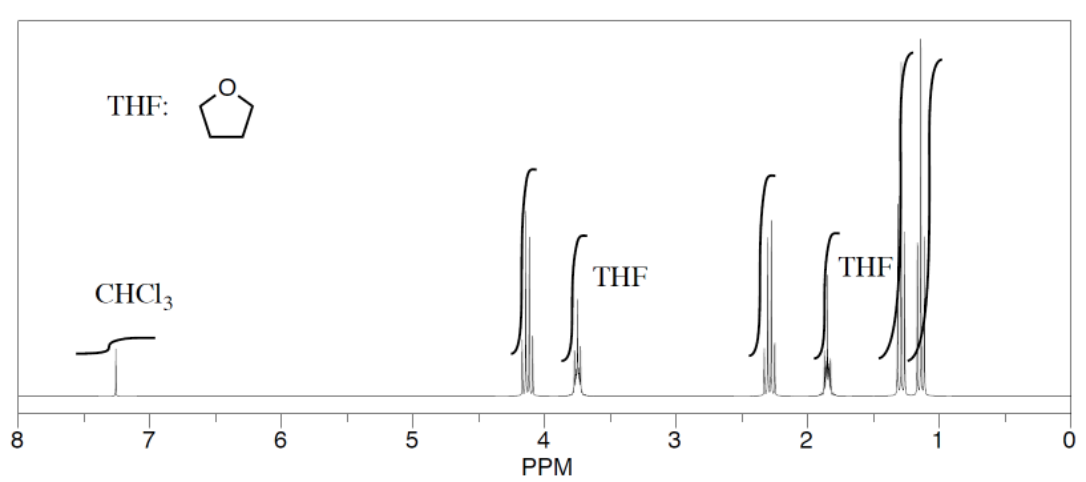
Example 13.13.1

Three students performed a synthesis of a fragrant ester, ethyl propanoate, $CH_3CH_2CO_2CH_2CH_3$. During their reactions, they each used a different solvent. The students were able to see peaks in the NMR spectrum for ethyl propanoate, as well as peaks for chloroform ($CHCl_3$, in the $CDCl_3$ they used to make their NMR samples).

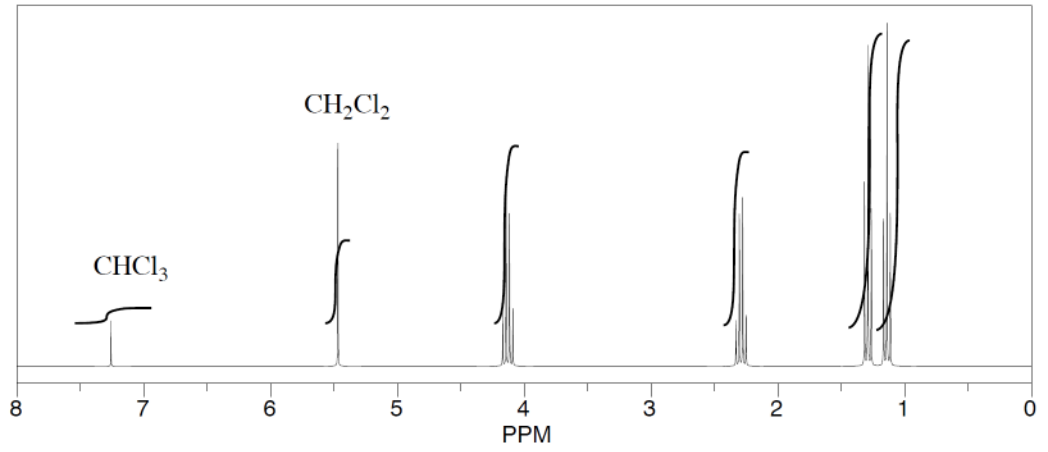
See the first student's spectrum:



See the second student's spectrum:



See the third student's spectrum:



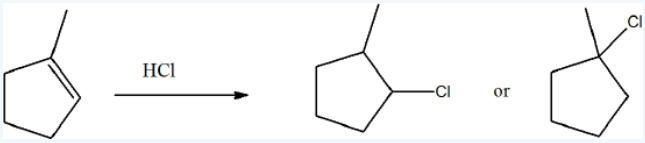
They were also able to determine that they had some leftover solvent in their samples by consulting a useful table of solvent impurities in NMR (which they found in Goldberg et. al., Organometallics 2010, 29, 2176-2179).

1. What is the ratio of leftover solvent to ethyl propanoate in each sample?
2. What is the percent of each sample that is leftover solvent

Exercise

? Exercise 5.17.1

How can H1 NMR determine products? For example, how can you tell the difference between the products of this reaction?



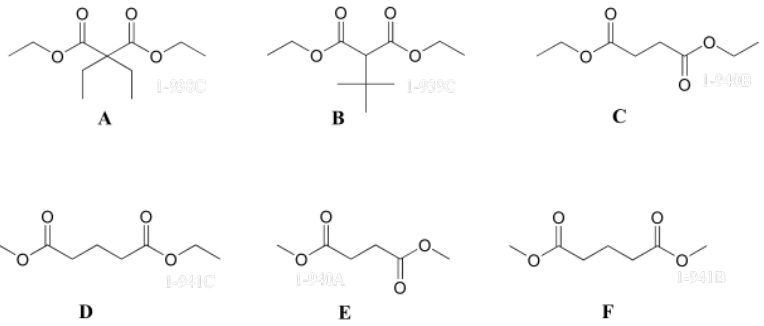
Answer

Yes, you are able to determine the difference in the spectra. For the 2-chloro compound will have multiple quartets while the 1-chloro compound will only have a quintet and a triplet for the signals in the ring.

Additional NMR Examples

Match spectra 1-6 below to their corresponding structures A-F.

Structures:



Spectrum 1

δ	splitting	integration
4.13	q	2
2.45	t	2
1.94	quintet	1
1.27	t	3

Spectrum 2

δ	splitting	integration
3.68	s	3
2.99	t	2
1.95	quintet	1

Spectrum 3

δ	splitting	integration
4.14	q	1
2.62	s	1
1.26	t	1.5

Spectrum 4

δ	splitting	integration
4.14	q	4
3.22	s	1
1.27	t	6
1.13	s	9

Spectrum 5

δ	splitting	integration
4.18	q	1

1.92	q	1
1.23	t	1.5
0.81	t	1.5

Spectrum 6

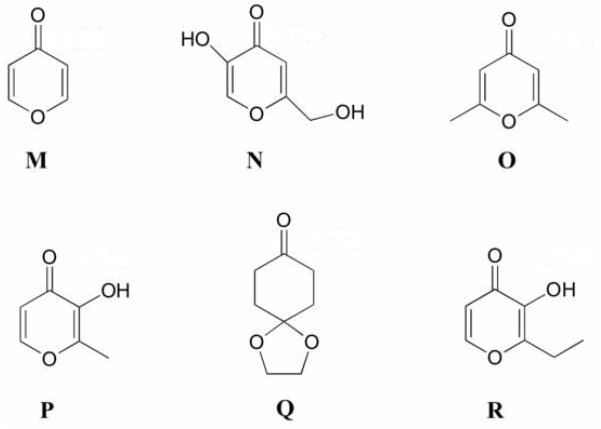
δ	splitting	integration
3.69	s	1.5
2.63	s	1

Solution:

Spectrum 1: structure D
Spectrum 2: structure F
Spectrum 3: structure C
Spectrum 4: structure B
Spectrum 5: structure A
Spectrum 6: structure E

Match the ^{1}H-NMR spectra 13-18 below to their corresponding structures M-R .

Structures:



Spectrum 13

δ	splitting	integration
8.15	d	1
6.33	d	1

Spectrum 14

δ	splitting	integration
6.05	s	1
2.24	s	3

Spectrum 15

δ	splitting	integration
8.57	s (b)	1
7.89	d	1
6.30	d	1
2.28	s	3

Spectrum 16

δ	splitting	integration
9.05	s (b)	1
8.03	s	1
6.34	s	1
5.68	s (b)	1
4.31	s	2

Spectrum 17

δ	splitting	integration
7.76	d	1
7.57	s (b)	1
6.44	d	1
2.78	q	2
1.25	t	3

Spectrum 18

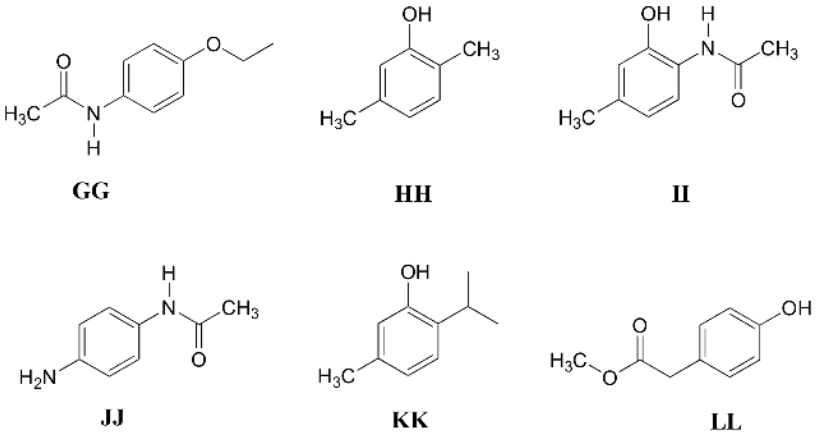
δ	splitting	integration
4.03	s	1
2.51	t	1
2.02	t	1

Solution:

Spectrum 13: structure M
Spectrum 14: structure O
Spectrum 15: structure P
Spectrum 16: structure N
Spectrum 17: structure R
Spectrum 18: structure Q

Match the ^{1}H-NMR spectra 31-36 below to their corresponding structures GG-LL

Structures:



Spectrum 31

δ	splitting	integration
6.98	d	1
6.64	d	1
6.54	s	1
4.95	s	1
2.23	s	3
2.17	s	3

Spectrum 32

δ	splitting	integration
7.08	d	1
6.72	d	1
6.53	s	1
4.81	s	1
3.15	7-tet	1
2.24	s	3
1.22	d	6

Spectrum 33

δ	splitting	integration
7.08	d	2
6.71	d	2
6.54	s	1

3.69	s	3
3.54	s	2

Spectrum 34

δ	splitting	integration
9.63	s	1
7.45	d	2
6.77	d	2
3.95	q	2
2.05	s	3
1.33	t	3

Spectrum 35

δ	splitting	integration
9.49	s	1
7.20	d	2
6.49	d	2
4.82	s	2
1.963	s	3

Spectrum 36

δ	splitting	integration
9.58	s(b)	1
9.31	s	1
7.36	d	1
6.67	s	1
6.55	d	1
2.21	s	3
2.11	s	3

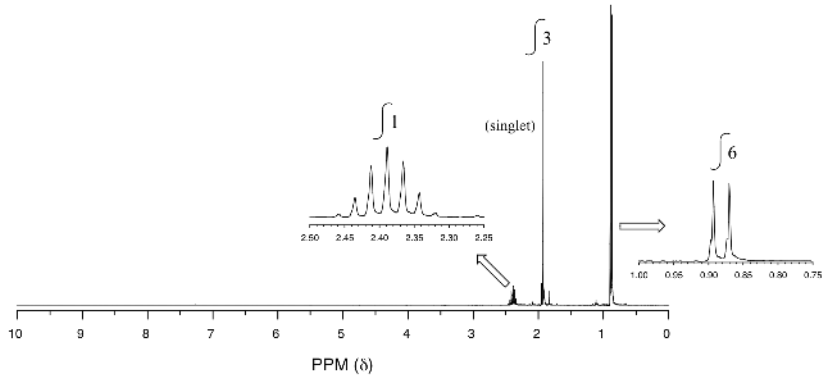
Solution:

Spectrum 31: structure HH
Spectrum 32: structure KK
Spectrum 33: structure LL
Spectrum 34: structure GG
Spectrum 35: structure JJ
Spectrum 36: structure II

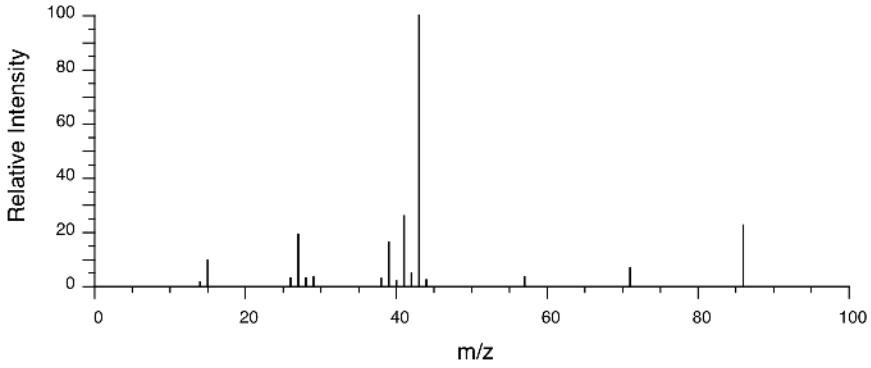
You obtain the following data for an unknown sample. Deduce its structure.

Combustion Analysis: C (69.7%); H (11.7%)

^{1}H-NMR:



Mass Spectrometry:



Solution: The structure is 3-methyl-2-butanone.

You take a ^{1}H-NMR spectrum of a sample that comes from a bottle of 1-bromopropane. However, you suspect that the bottle might be contaminated with 2-bromopropane. The NMR spectrum shows the following peaks:

δ	splitting	integration
4.3	septet	0.0735
3.4	triplet	0.661
1.9	sextet	0.665
1.7	doublet	0.441
1.0	triplet	1.00

How badly is the bottle contaminated? Specifically, what percent of the molecules in the bottle are 2-bromopropane?

Solution:

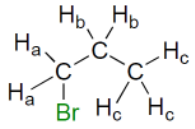
First, assign the peaks.

1-bromopropane: Ha is the triplet at 3.4 ppm, Hb is the sextet at 1.9 ppm, Hc is the triplet at 1.0 ppm.

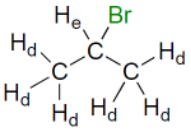
2-bromopropane: Hd is the doublet at 1.7 ppm, He is the septet at 4.3 ppm.

Now, just add up the integrations for each molecule and figure the percentage.
1-bromopropane: 0.661 + 0.665 + 1.00 = 2.326.
2-bromopropane: 0.0735 + 0.441 = 0.5145.
Percent 2-bromopropane is (0.5145)*100 / (0.5145 + 2.326) = 18.1%.

Notice that even if some peaks overlapped, you could still get this number as long as you could integrate one signal on each molecule: you could, for example, do the samecalculation (and get the same result) by comparing integrations of Hc and Hd signals, and just scale based on the fact that the Hc signal represents three protons while the Hd signal represents six protons.



H_c: 1.0 ppm (t)



H_d: 1.7 ppm (d)

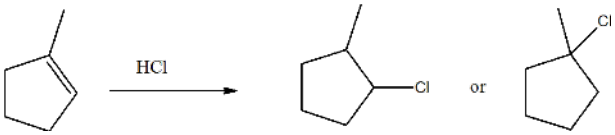
$$\text{integration: } \frac{1.00}{3 \text{ protons}} = 0.33 \qquad \text{integration: } \frac{0.441}{6 \text{ protons}} = 0.0735$$

$$\text{percent 2-bromopropane} = \left(\frac{0.0735}{0.0735 + 0.33}\right) \text{x } 100 = 18.2\ \%$$

Questions

Q13.13.1

How can H^1 NMR determine products? For example, how can you tell the difference between the products of this reaction?



Solutions

S13.13.1

Yes, you are able to determine the difference in the spectra. For the 2-chloro compound will have multiple quartets while the 1-chloro compound will only have a quintet and a triplet for the signals in the ring.

Contributors and Attributions

- Dr. Dietmar Kennepohl FCIC (Professor of Chemistry, Athabasca University)
- Prof. Steven Farmer (Sonoma State University)
- Organic Chemistry With a Biological Emphasis by Tim Soderberg (University of Minnesota, Morris)

Chris P Schaller, Ph.D., (College of Saint Benedict / Saint John's University)

5.17: Uses of ^1H NMR Spectroscopy is shared under a CC BY-NC-SA 4.0 license and was authored, remixed, and/or curated by LibreTexts.

CHAPTER OVERVIEW

6: Carbon-13 NMR Spectroscopy

13.4 \(^13C\) NMR Spectroscopy: Signal Averaging and FT-NMR

13.5 Characteristics of \(^13C\) NMR Spectroscopy

13.7 Uses of \(^13C\) NMR Spectroscopy

6.1: Interpreting C-13 NMR Spectra

6: Carbon-13 NMR Spectroscopy is shared under a CC BY-NC-SA 4.0 license and was authored, remixed, and/or curated by LibreTexts.

13.4 1 3C 13C NMR Spectroscopy: Signal Averaging and FT-NMR

The ^{12}C isotope of carbon - which accounts for up about 99% of the carbons in organic molecules - does not have a nuclear magnetic moment, and thus is NMR-inactive. Fortunately for organic chemists, however, the ^{13}C isotope, which accounts for most of the remaining 1% of carbon atoms in nature, has a magnetic moment just like protons. Most of what we have learned about ^{1}H-NMR spectroscopy also applies to ^{13}C-NMR, although there are several important differences.

The basics of ^{13}C-NMR spectroscopy

The magnetic moment of a ^{13}C nucleus is much weaker than that of a proton, meaning that NMR signals from ^{13}C nuclei are inherently much weaker than proton signals. This, combined with the low natural abundance of ^{13}C, means that it is much more difficult to observe carbon signals: more sample is required, and often the data from hundreds of scans must be averaged in order to bring the signal-to-noise ratio down to acceptable levels. Unlike ^{1}H-NMR signals, the area under a ^{13}C-NMR signal cannot be used to determine the number of carbons to which it corresponds. This is because the signals for some types of carbons are inherently weaker than for other types – peaks corresponding to carbonyl carbons, for example, are much smaller than those for methyl or methylene (CH_2) peaks. Peak integration is generally not useful in ^{13}C-NMR spectroscopy, except when investigating molecules that have been enriched with ^{13}C isotope (see section 5.6B).

The resonance frequencies of ^{13}C nuclei are lower than those of protons in the same applied field - in a 7.05 Tesla instrument, protons resonate at about 300 MHz, while carbons resonate at about 75 MHz. This is fortunate, as it allows us to look at ^{13}C signals using a completely separate 'window' of radio frequencies. Just like in ^{1}H-NMR, the standard used in ^{13}C-NMR experiments to define the 0 ppm point is tetramethylsilane (TMS), although of course in ^{13}C-NMR it is the signal from the four equivalent *carbons* in TMS that serves as the standard. Chemical shifts for ^{13}C nuclei in organic molecules are spread out over a much wider range than for protons – up to 200 ppm for ^{13}C compared to 12 ppm for protons (see Table 3 for a list of typical ^{13}C-NMR chemical shifts). This is also fortunate, because it means that the signal from each carbon in a compound can almost always be seen as a distinct peak, without the overlapping that often plagues ^{1}H-NMR spectra. The chemical shift of a ^{13}C nucleus is influenced by essentially the same factors that influence a proton's chemical shift: bonds to electronegative atoms and diamagnetic anisotropy effects tend to shift signals downfield (higher resonance frequency). In addition, sp^2 hybridization results in a large downfield shift. The ^{13}C-NMR signals for carbonyl carbons are generally the furthest downfield (170-220 ppm), due to both sp^2 hybridization and to the double bond to oxygen.

Example 13.4.1

How many sets of non-equivalent carbons are there in each of the molecules shown in exercise 5.1?

Solution

Example 13.4.2

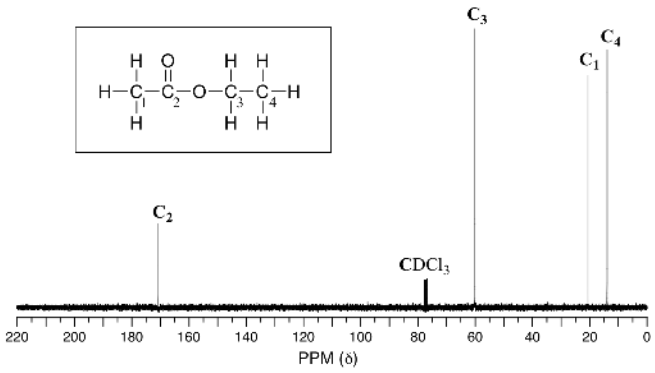
How many sets of non-equivalent carbons are there in:

a. toluene
b. 2-pentanone
c. para-xylene
d. triclosan

(all structures are shown earlier in this chapter)

Solution

Because of the low natural abundance of ^{13}C nuclei, it is very unlikely to find two ^{13}C atoms near each other in the same molecule, and thus *we do not see spin-spin coupling between neighboring carbons in a ^{13}C-NMR spectrum*. There is, however, **heteronuclear coupling** between ^{13}C carbons and the hydrogens to which they are bound. Carbon-proton coupling constants are very large, on the order of 100 – 250 Hz. For clarity, chemists generally use a technique called **broadband decoupling**, which essentially 'turns off' C-H coupling, resulting in a spectrum in which all carbon signals are singlets. Below is the proton-decoupled ^{13}C-NMR spectrum of ethyl acetate, showing the expected four signals, one for each of the carbons.



While broadband decoupling results in a much simpler spectrum, useful information about the presence of neighboring protons is lost. However, another modern NMR technique called DEPT (Distortionless Enhancement by Polarization Transfer) allows us to determine how many hydrogens are bound to each carbon. For example, a DEPT experiment tells us that the signal at 171 ppm in the ethyl acetate spectrum is a quaternary carbon (no hydrogens bound, in this case a carbonyl carbon), that the 61 ppm signal is from a methylene (CH_2) carbon, and that the 21 ppm and 14 ppm signals are both methyl (CH_3) carbons. The details of the DEPT experiment are beyond the scope of this text, but DEPT information will often be provided along with ^{13}C spectral data in examples and problems.

Contributors and Attributions

- Prof. Steven Farmer (Sonoma State University)
- Chris P Schaller, Ph.D., (College of Saint Benedict / Saint John's University)

13.4 $^{1}3C$ NMR Spectroscopy: Signal Averaging and FT-NMR is shared under a CC BY-NC-SA 4.0 license and was authored, remixed, and/or curated by LibreTexts.

13.5 Characteristics of 1 3C 13C NMR Spectroscopy

The ^{12}C isotope of carbon - which accounts for up about 99% of the carbons in organic molecules - does not have a nuclear magnetic moment, and thus is NMR-inactive. Fortunately for organic chemists, however, the ^{13}C isotope, which accounts for most of the remaining 1% of carbon atoms in nature, has a magnetic moment just like protons. Most of what we have learned about ^{1}H-NMR spectroscopy also applies to ^{13}C-NMR, although there are several important differences.

The basics of ^{13}C-NMR spectroscopy

The magnetic moment of a ^{13}C nucleus is much weaker than that of a proton, meaning that NMR signals from ^{13}C nuclei are inherently much weaker than proton signals. This, combined with the low natural abundance of ^{13}C, means that it is much more difficult to observe carbon signals: more sample is required, and often the data from hundreds of scans must be averaged in order to bring the signal-to-noise ratio down to acceptable levels. Unlike ^{1}H-NMR signals, the area under a ^{13}C-NMR signal cannot be used to determine the number of carbons to which it corresponds. This is because the signals for some types of carbons are inherently weaker than for other types – peaks corresponding to carbonyl carbons, for example, are much smaller than those for methyl or methylene (CH_2) peaks. Peak integration is generally not useful in ^{13}C-NMR spectroscopy, except when investigating molecules that have been enriched with ^{13}C isotope.

The resonance frequencies of ^{13}C nuclei are lower than those of protons in the same applied field - in a 7.05 Tesla instrument, protons resonate at about 300 MHz, while carbons resonate at about 75 MHz. This is fortunate, as it allows us to look at ^{13}C signals using a completely separate 'window' of radio frequencies. Just like in ^{1}H-NMR, the standard used in ^{13}C-NMR experiments to define the 0 ppm point is tetramethylsilane (TMS), although of course in ^{13}C-NMR it is the signal from the four equivalent *carbons* in TMS that serves as the standard. Chemical shifts for ^{13}C nuclei in organic molecules are spread out over a much wider range than for protons – up to 200 ppm for ^{13}C compared to 12 ppm for protons (see Table 3 for a list of typical ^{13}C-NMR chemical shifts). This is also fortunate, because it means that the signal from each carbon in a compound can almost always be seen as a distinct peak, without the overlapping that often plagues ^{1}H-NMR spectra. The chemical shift of a ^{13}C nucleus is influenced by essentially the same factors that influence a proton's chemical shift: bonds to electronegative atoms and diamagnetic anisotropy effects tend to shift signals downfield (higher resonance frequency). In addition, sp^2 hybridization results in a large downfield shift. The ^{13}C-NMR signals for carbonyl carbons are generally the furthest downfield (170-220 ppm), due to both sp^2 hybridization and to the double bond to oxygen.

Example 13.5.1

Exercise 5.11: How many sets of non-equivalent carbons are there in each of the molecules shown in exercise 5.1?

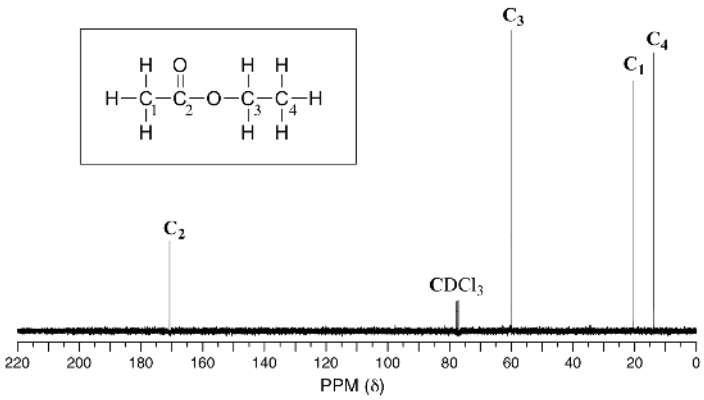
Exercise 5.12: How many sets of non-equivalent carbons are there in:

a. toluene
b. 2-pentanone
c. para-xylene
d. triclosan

(all structures are shown earlier in this chapter)

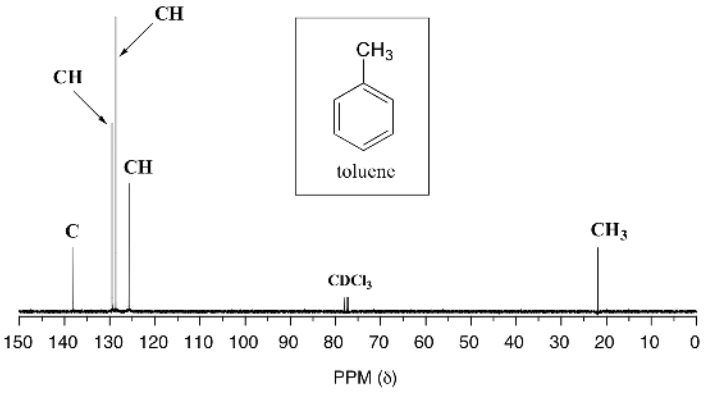
Solution

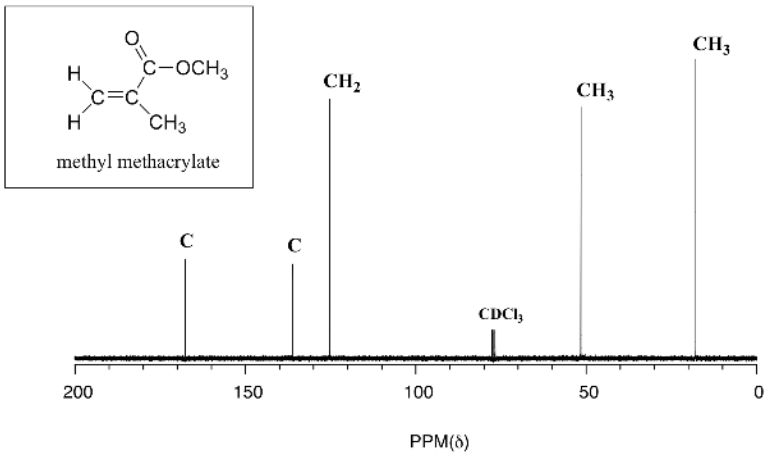
Because of the low natural abundance of ^{13}C nuclei, it is very unlikely to find two ^{13}C atoms near each other in the same molecule, and thus *we do not see spin-spin coupling between neighboring carbons in a ^{13}C-NMR spectrum*. There is, however, **heteronuclear coupling** between ^{13}C carbons and the hydrogens to which they are bound. Carbon-proton coupling constants are very large, on the order of 100 – 250 Hz. For clarity, chemists generally use a technique called **broadband decoupling**, which essentially 'turns off' C-H coupling, resulting in a spectrum in which all carbon signals are singlets. Below is the proton-decoupled^{13}C-NMR spectrum of ethyl acetate, showing the expected four signals, one for each of the carbons.



While broadband decoupling results in a much simpler spectrum, useful information about the presence of neighboring protons is lost. However, another modern NMR technique called DEPT (Distortionless Enhancement by Polarization Transfer) allows us to determine how many hydrogens are bound to each carbon. For example, a DEPT experiment tells us that the signal at 171 ppm in the ethyl acetate spectrum is a quaternary carbon (no hydrogens bound, in this case a carbonyl carbon), that the 61 ppm signal is from a methylene (CH_2) carbon, and that the 21 ppm and 14 ppm signals are both methyl (CH_3) carbons. The details of the DEPT experiment are beyond the scope of this text, but DEPT information will often be provided along with ^{13}C spectral data in examples and problems.

Below are two more examples of ^{13}C NMR spectra of simple organic molecules, along with DEPT information.



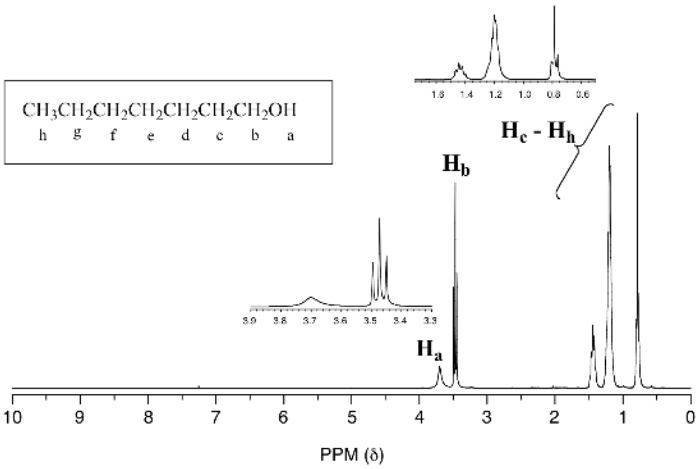


Example 13.5.2

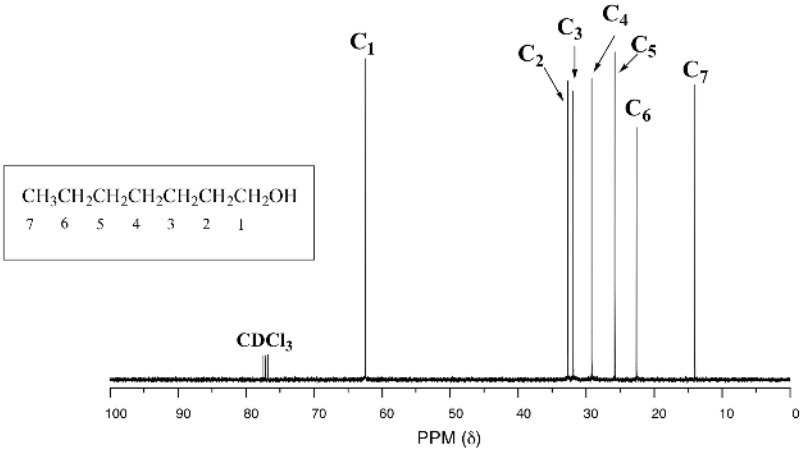
Give peak assignments for the ^{13}C-NMR spectrum of methyl methacrylate, shown above.

Solution

One of the greatest advantages of ^{13}C-NMR compared to ^{1}H-NMR is the breadth of the spectrum - recall that carbons resonate from 0-220 ppm relative to the TMS standard, as opposed to only 0-12 ppm for protons. Because of this, ^{13}C signals rarely overlap, and we can almost always distinguish separate peaks for each carbon, even in a relatively large compound containing carbons in very similar environments. In the proton spectrum of 1-heptanol, for example, only the signals for the alcohol proton (H_a) and the two protons on the adjacent carbon (H_b) are easily analyzed. The other proton signals overlap, making analysis difficult.



In the ^{13}C spectrum of the same molecule, however, we can easily distinguish each carbon signal, and we know from this data that our sample has seven non-equivalent carbons. (Notice also that, as we would expect, the chemical shifts of the carbons get progressively smaller as they get farther away from the deshielding oxygen.)

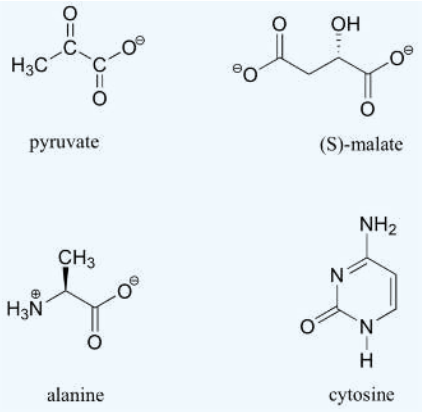


This property of ^{13}C-NMR makes it very helpful in the elucidation of larger, more complex structures.

Example 13.5.3

^{13}C-NMR (and DEPT) data for some common biomolecules are shown below (data is from the Aldrich Library of ^{1}H and ^{13}C NMR). Match the NMR data to the correct structure, and make complete peak assignments.

- spectrum a: 168.10 ppm (C), 159.91 ppm (C), 144.05 ppm (CH), 95.79 ppm (CH)
- spectrum b: 207.85 ppm (C), 172.69 ppm (C), 29.29 ppm (CH_3)
- spectrum c: 178.54 ppm (C), 53.25 ppm (CH), 18.95 ppm (CH_3)
- spectrum d: 183.81 ppm (C), 182. 63 ppm (C), 73.06 ppm (CH), 45.35 ppm (CH_2)



Solution

^{13}C NMR Chemical Shifts

The Carbon NMR is used for determining functional groups using characteristic shift values. ^{13}C chemical shifts are greatly affected by electronegative effects. If a H atom in an alkane is replaced by substituent X, electronegative atoms (O, N, halogen), ^{13}C signals for nearby carbons shift downfield (left; increase in ppm) with the effect diminishing with distance from the electron withdrawing group. Figure 13.5.1 shows typical ^{13}C chemical shift regions of the major chemical class.

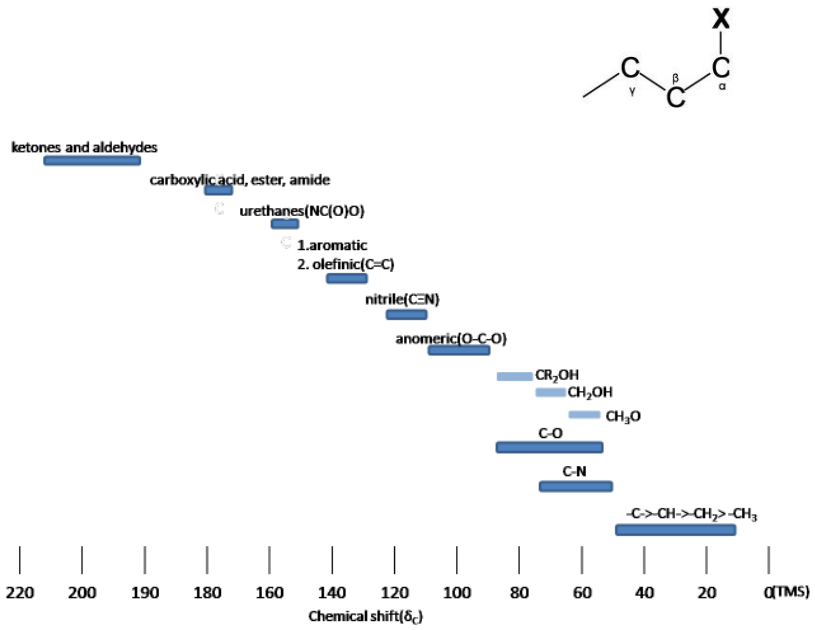


Figure 13.5.1: ^{13}C Chemical shift range for organic compound

Spin-Spin splitting

Comparing the ^{1}H NMR, there is a big difference thing in the ^{13}C NMR. The ^{13}C-^{13}Cspin-spin splitting rarely exit between adjacent carbons because ^{13}C is naturally lower abundant (1.1%)

- **^{13}C-^{1}H Spin coupling**: ^{13}C-^{1}H Spin coupling provides useful information about the number of protons attached a carbon atom. In case of one bond coupling ($^{1}J_{CH}$), -CH, -CH_2, and CH_3 have respectively doublet, triplet, quartets for the ^{13}C resonances in the spectrum. However, ^{13}C-^{1}H Spin coupling has an disadvantage for ^{13}C spectrum interpretation. ^{13}C-^{1}H Spin coupling is hard to analyze and reveal structure due to a forest of overlapping peaks that result from 100% abundance of ^{1}H.
- **Decoupling**: Decoupling is the process of removing ^{13}C-^{1}H coupling interaction to simplify a spectrum and identify which pair of nuclei is involved in the J coupling. The decoupling ^{13}C spectra shows only one peak(singlet) for each

unique carbon in the molecule (Figure 13.5.2). Decoupling is performed by irradiating at the frequency of one proton with continuous low-power RF.

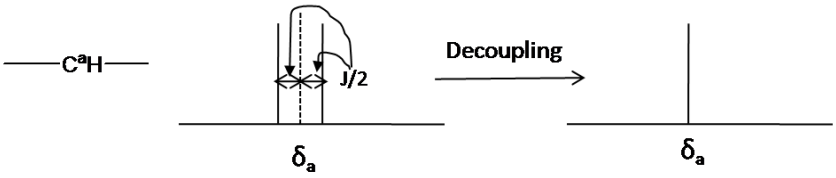


Figure 13.5.2. Decoupling in the ^{13}C NMR

Contributors and Attributions

- Prof. Steven Farmer (Sonoma State University)
- Organic Chemistry With a Biological Emphasis by Tim Soderberg (University of Minnesota, Morris)
- Chris P Schaller, Ph.D., (College of Saint Benedict / Saint John's University)

13.5 Characteristics of $^{1}3C$ NMR Spectroscopy is shared under a CC BY-NC-SA 4.0 license and was authored, remixed, and/or curated by LibreTexts.

13.7 Uses of 1 3C 13C NMR Spectroscopy

The interpretation of ^{13}C NMR spectra does not form a part of Chemistry 350; hence, you may omit Section 13.7. Interested students may wish to read this section for enrichment purposes.

Features of a C-13 NMR spectrum Edit section

Butane shows two different peaks in the ^{13}C NMR spectrum, below. Note that: the chemical shifts of these peaks are not very different from methane. The carbons in butane are in a similar environment to the one in methane.

- there are two distinct carbons in butane: the methyl, or CH_3, carbon, and the methylene, or CH_2, carbon.
- the methyl carbon absorbs slightly upfield, or at lower shift, around 10 ppm.
- the methylene carbon absorbs at slightly downfield, or at higher shift, around 20 ppm.
- other factors being equal, methylene carbons show up at slightly higher shift than methyl carbons.



***Figure NMR2**. Simulated ^{13}C NMR spectrum of butane (showing only the upfield portion of the spectrum).*

In the ^{13}C NMR spectrum of pentane (below), you can see three different peaks, even though pentane just contains methyl carbons and methylene carbons like butane. As far as the NMR spectrometer is concerned, pentane contains three different kinds of carbon, in three different environments. That result comes from symmetry.



***Figure NMR3**.^{13}C NMR spectrum of pentane. Source: SDBSWeb : http://riodb01.ibase.aist.go.jp/sdbs/ (National Institute of Advanced Industrial Science and Technology of Japan, 15 August 2008)*

Symmetry is an important factor in spectroscopy. Nature says:

- atoms that are symmetry-inequivalent can absorb at different shifts.
- atoms that are symmetry-equivalent must absorb at the same shift.

To learn about symmetry, take a model of pentane and do the following:

- make sure the model is twisted into the most symmetric shape possible: a nice "W".
- choose one of the methyl carbons to focus on.
- rotate the model 180 degrees so that you are looking at the same "W" but from the other side.
- note that the methyl you were focusing on has simply switched places with the other methyl group. These two carbons are symmetry-equivalent via two-fold rotation.

Animation NMR1. A three-dimensional model of pentane. Grab the model with the mouse and rotate it so that you are convinced that the second and fourth carbons are symmetry-equivalent, but the third carbon is not.

By the same process, you can see that the second and fourth carbons along the chain are also symmetry-equivalent. However, the middle carbon is not; it never switches places with the other carbons if you rotate the model. There are three different sets of inequivalent carbons; these three groups are not the same as each other according to symmetry.

Example 13.7.1

Determine how many inequivalent carbons there are in each of the following compounds. How many peaks do you expect in each ^{13}C NMR spectrum?

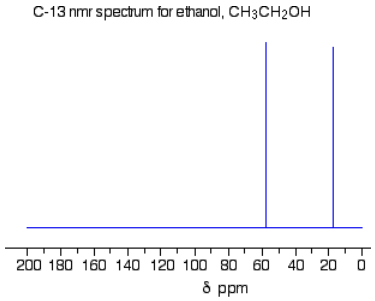


Practically speaking, there is only so much room in the spectrum from one end to the other. At some point, peaks can get so crowded together that you can't distinguish one from another. You might expect to see ten different peaks in eicosane, a twenty-carbon alkane chain, but when you look at the spectrum you can only see seven different peaks. That may be frustrating, because the experiment does not seem to agree with your expectation. However, you will be using a number of methods together to minimize the problem of misleading data.

The C-13 NMR spectrum for ethanol

Edit section

This is a simple example of a C-13 NMR spectrum. Don't worry about the scale for now - we'll look at that in a minute.



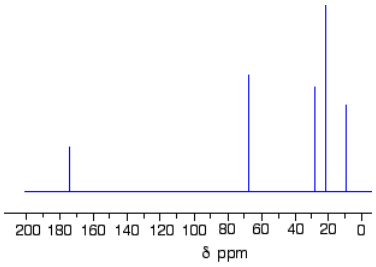
Note

Note: The NMR spectra on this page have been produced from graphs taken from the Spectral Data Base System for Organic Compounds (SDBS) at the National Institute of Materials and Chemical Research in Japan.

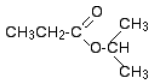
There are two peaks because there are two different environments for the carbons. The carbon in the CH_3 group is attached to 3 hydrogens and a carbon. The carbon in the CH_2 group is attached to 2 hydrogens, a carbon and an oxygen. The two lines are in different places in the NMR spectrum because they need different external magnetic fields to bring them in to resonance at a particular radio frequency.

The C-13 NMR spectrum for a more complicated compound

This is the C-13 NMR spectrum for 1-methylethyl propanoate (also known as isopropyl propanoate or isopropyl propionate).



This time there are 5 lines in the spectrum. That means that there must be 5 different environments for the carbon atoms in the compound. Is that reasonable from the structure?



Well - if you count the carbon atoms, there are 6 of them. So why only 5 lines? In this case, two of the carbons are in exactly the same environment. They are attached to exactly the same things. Look at the two CH_3 groups on the right-hand side of the molecule.

You might reasonably ask why the carbon in the CH_3 on the left is not also in the same environment. Just like the ones on the right, the carbon is attached to 3 hydrogens and another carbon. But the similarity is not exact - you have to chase the similarity along the rest of the molecule as well to be sure.

The carbon in the left-hand CH_3 group is attached to a carbon atom which in turn is attached to a carbon with two oxygens on it - and so on down the molecule. That's not exactly the same environment as the carbons in the right-hand CH_3 groups. They are attached to a carbon which is attached to a single oxygen - and so on down the molecule. We'll look at this spectrum again in detail on the next page - and look at some more similar examples as well. This all gets easier the more examples you look at.

For now, all you need to realize is that each line in a C-13 NMR spectrum recognizes a carbon atom in one particular environment in the compound. If two (or more) carbon atoms in a compound have exactly the same environment, they will be represented by a single line.

Note

You might wonder why all this works, since only about 1% of carbon atoms are C-13. These are the only ones picked up by this form of NMR. If you had a single molecule of ethanol, then the chances are only about 1 in 50 of there being one C-13 atom in it, and only about 1 in 10,000 of both being C-13.

But you have got to remember that you will be working with a sample containing huge numbers of molecules. The instrument can pick up the magnetic effect of the C-13 nuclei in the carbon of the CH_3 group and the carbon of the CH_2 group even if they are in separate molecules. There's no need for them to be in the same one.

Contributors and Attributions

- Prof. Steven Farmer (Sonoma State University)
- William Reusch, Professor Emeritus (Michigan State U.), Virtual Textbook of Organic Chemistry
- Organic Chemistry With a Biological Emphasis by Tim Soderberg (University of Minnesota, Morris)

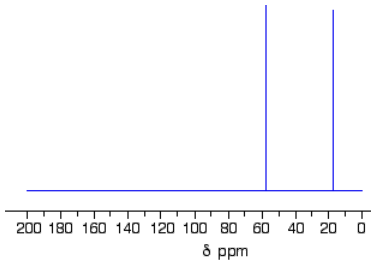
13.7 Uses of ^{13}C NMR Spectroscopy is shared under a CC BY-NC-SA 4.0 license and was authored, remixed, and/or curated by LibreTexts.

6.1: Interpreting C-13 NMR Spectra

This page takes an introductory look at how you can get useful information from a C-13 NMR spectrum.

Introduction

Taking a close look at three ^{13}C NMR spectra below. The ^{13}C NMR spectrum for ethanol



> The NMR spectra on this page have been produced from graphs taken from the Spectral Data Base System for Organic Compounds (SDBS) at the National Institute of Materials and Chemical Research in Japan.

Remember that each peak identifies a carbon atom in a different environment within the molecule. In this case there are two peaks because there are two different environments for the carbons. The carbon in the CH_3 group is attached to 3 hydrogens and a carbon. The carbon in the CH_2group is attached to 2 hydrogens, a carbon and an oxygen. So which peak is which?

You might remember from the introductory page that the external magnetic field experienced by the carbon nuclei is affected by the electronegativity of the atoms attached to them. The effect of this is that the chemical shift of the carbon increases if you attach an atom like oxygen to it. That means that the peak at about 60 (the larger chemical shift) is due to the CH2 group because it has a more electronegative atom attached.

> In principle, you should be able to work out the fact that the carbon attached to the oxygen will have the larger chemical shift. In practice, you always work from tables of chemical shift values for different groups (see below).
>
> What if you needed to work it out? The electronegative oxygen pulls electrons away from the carbon nucleus leaving it more exposed to any external magnetic field. That means that you will need a smaller external magnetic field to bring the nucleus into the resonance condition than if it was attached to less electronegative things. The smaller the magnetic field needed, the higher the chemical shift.

A table of typical chemical shifts in C-13 NMR spectra

carbon environment	chemical shift (ppm)
C=O (in ketones)	205 - 220
C=O (in aldehydes)	190 - 200
C=O (in acids and esters)	170 - 185
C in aromatic rings	125 - 150
C=C (in alkenes)	115 - 140
RCH2OH	50 - 65
RCH2Cl	40 - 45
RCH2NH2	37 - 45
R3CH	25 - 35

CH3CO-	20 - 30
R2CH2	16 - 25
RCH3	10 - 15

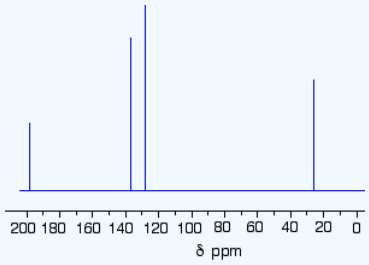
In the table, the "R" groups will not necessarily be simple alkyl groups. In each case there will be a carbon atom attached to the one shown in red, but there may well be other things substituted into the "R" group.

If a substituent is very close to the carbon in question, and very electronegative, that might affect the values given in the table slightly. For example, ethanol has a peak at about 60 because of the CH_2OH group. No problem! It also has a peak due to the RCH_3 group. The "R" group this time is CH_2OH. The electron pulling effect of the oxygen atom increases the chemical shift slightly from the one shown in the table to a value of about 18. A simplification of the table:

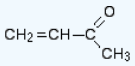
carbon environment	chemical shift (ppm)
C-C	0 - 50
C-O	50 - 100
C=C	100 - 150
C=O	150 - 200

This may, of course, change and other syllabuses might want something similar. The only way to find out is to check your syllabus, and recent question papers to see whether you are given tables of chemical shifts or not.

The ^{13}C NMR spectrum for but-3-en-2-one. This is also known as 3-buten-2-one (among many other things!)



Here is the structure for the compound:



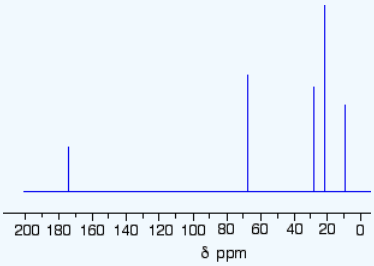
You can pick out all the peaks in this compound using the simplified table above.

- The peak at just under 200 ppm is due to a carbon-oxygen double bond. The two peaks at 137 ppm and 129 ppm are due to the carbons at either end of the carbon-carbon double bond. And the peak at 26 is the methyl group which, of course, is joined to the rest of the molecule by a carbon-carbon single bond. If you want to use the more accurate table, you have to put a bit more thought into it - and, in particular, worry about the values which do not always exactly match those in the table!
- The carbon-oxygen double bond in the peak for the ketone group has a slightly lower value than the table suggests for a ketone. There is an interaction between the carbon-oxygen and carbon-carbon double bonds in the molecule which affects the value slightly. This isn't something which we need to look at in detail for the purposes of this topic.
- You must be prepared to find small discrepancies of this sort in more complicated molecules - but do not worry about this for exam purposes at this level. Your examiners should give you shift values which exactly match the compound you are given.
- The two peaks for the carbons in the carbon-carbon double bond are exactly where they would be expected to be. Notice that they aren't in exactly the same environment, and so do not have the same shift values. The one closer to the carbon-oxygen double bond has the larger value.

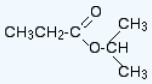
- And the methyl group on the end has exactly the sort of value you would expect for one attached to C=O. The table gives a range of 20 - 30, and that's where it is.

One final important thing to notice. There are four carbons in the molecule and four peaks because they are all in different environments. But they aren't all the same height. In C-13 NMR, you **cannot** draw any simple conclusions from the heights of the various peaks.

1-methylethyl propanoate is also known as isopropyl propanoate or isopropyl propionate.



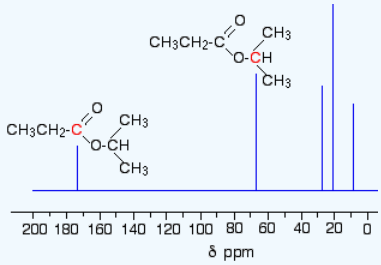
Here is the structure for 1-methylethyl propanoate:



Two simple peaks

There are two very simple peaks in the spectrum which could be identified easily from the second table above.

- The peak at 174 is due to a carbon in a carbon-oxygen double bond. (Looking at the more detailed table, this peak is due to the carbon in a carbon-oxygen double bond in an acid or ester.)
- The peak at 67 is due to a different carbon singly bonded to an oxygen. Those two peaks are therefore due to:



If you look back at the more detailed table of chemical shifts, you will find that a carbon singly bonded to an oxygen has a range of 50 - 65. 67 is, of course, a little bit higher than that.

As before, you must expect these small differences. No table can account for all the fine differences in environment of a carbon in a molecule. Different tables will quote slightly different ranges. At this level, you can just ignore that problem!

Before we go on to look at the other peaks, notice the heights of these two peaks we've been talking about. They are both due to a single carbon atom in the molecule, and yet they have different heights. Again, you can't read any reliable information directly from peak heights in these spectra.

The three right-hand peaks

From the simplified table, all you can say is that these are due to carbons attached to other carbon atoms by single bonds. But because there are three peaks, the carbons must be in **three** different environments.

The easiest peak to sort out is the one at 28. If you look back at the table, that could well be a carbon attached to a carbon-oxygen double bond. The table quotes the group as CH_3CO^-, but replacing one of the hydrogens by a simple CH3 group will not make much difference to the shift value.

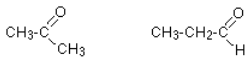
The right-hand peak is also fairly easy. This is the left-hand methyl group in the molecule. It is attached to an admittedly complicated R group (the rest of the molecule). It is the bottom value given in the detailed table.

The tall peak at 22 must be due to the two methyl groups at the right-hand end of the molecule - because that's all that's left. These combine to give a single peak because they are both in exactly the same environment.

If you are looking at the detailed table, you need to think very carefully which of the environments you should be looking at. Without thinking, it is tempting to go for the R_2CH2 with peaks in the 16 - 25 region. But you would be wrong! The carbons we are interested in are the ones in the methyl group, not in the R groups. These carbons are again in the environment: RCH3. The R is the rest of the molecule. The table says that these should have peaks in the range 10 - 15, but our peak is a bit higher. This is because of the presence of the nearby oxygen atom. Its electronegativity is pulling electrons away from the methyl groups - and, as we've seen above, this tends to increase the chemical shift slightly.

Working out Structures from C-13 NMR Spectra

So far, we have just been trying to see the relationship between carbons in particular environments in a molecule and the spectrum produced. We've had all the information necessary. Now let's make it a little more difficult - but we'll work from much easier examples! In each example, try to work it out for yourself before you read the explanation. How could you tell from just a quick look at a C-13 NMR spectrum (and without worrying about chemical shifts) whether you had propanone or propanal (assuming those were the only options)?

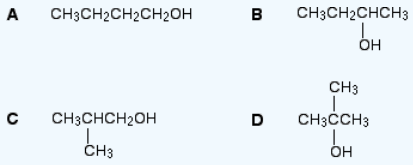


Because these are isomers, each has the same number of carbon atoms, but there is a difference between the environments of the carbons which will make a big impact on the spectra.

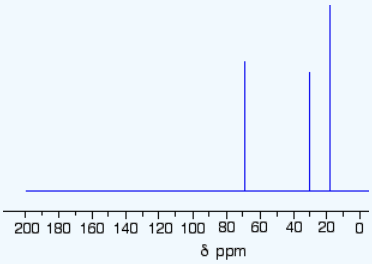
In propanone, the two carbons in the methyl groups are in exactly the same environment, and so will produce only a single peak. That means that the propanone spectrum will have only 2 peaks - one for the methyl groups and one for the carbon in the C=O group. However, in propanal, all the carbons are in completely different environments, and the spectrum will have three peaks.

Example 6.1.3: $C_4H_{10}O$

There are four alcohols with the molecular formula $C_4H_{10}O$.



Which one produced the C-13 NMR spectrum below?



You can do this perfectly well without referring to chemical shift tables at all.

In the spectrum there are a total of three peaks - that means that there are only three different environments for the carbons, despite there being four carbon atoms.

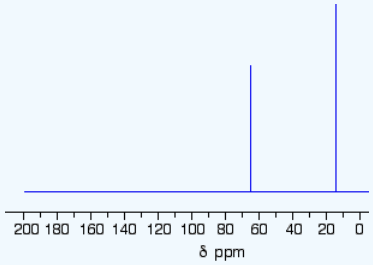
In A and B, there are four totally different environments. Both of these would produce four peaks.

In D, there are only two different environments - all the methyl groups are exactly equivalent. D would only produce two peaks.

That leaves C. Two of the methyl groups are in exactly the same environment - attached to the rest of the molecule in exactly the same way. They would only produce one peak. With the other two carbon atoms, that would make a total of three. The alcohol is C.

Example 6.1.4:

This follows on from Example 6.1.3, and also involves an isomer of $C_4H_{10}O$ but which isn't an alcohol. Its C-13 NMR spectrum is below. Work out what its structure is.



Because we do not know what sort of structure we are looking at, this time it would be a good idea to look at the shift values. The approximations are perfectly good, and we will work from this table:

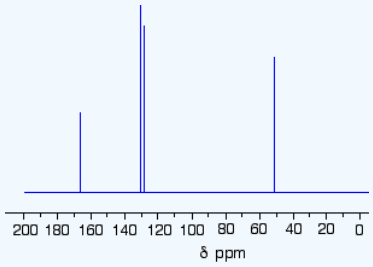
carbon environment	chemical shift (ppm)
C-C	0 - 50
C-O	50 - 100
C=C	100 - 150
C=O	150 - 200

There is a peak for carbon(s) in a carbon-oxygen single bond and one for carbon(s) in a carbon-carbon single bond. That would be consistent with C-C-O in the structure.

It is not an alcohol (you are told that in the question), and so there must be another carbon on the right-hand side of the oxygen in the structure in the last paragraph. The molecular formula is $C_4H_{10}O$, and there are only two peaks. The only solution to that is to have two identical ethyl groups either side of the oxygen. The compound is ethoxyethane (diethyl ether), $CH_3CH_2OCH_2CH_3$.

Example 6.1.5

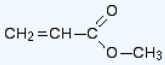
Using the simplified table of chemical shifts above, work out the structure of the compound with the following C-13 NMR spectrum. Its molecular formula is $C_4H_6O_2$.



Let's sort out what we've got.

- There are four peaks and four carbons. No two carbons are in exactly the same environment.
- The peak at just over 50 must be a carbon attached to an oxygen by a single bond.
- The two peaks around 130 must be the two carbons at either end of a carbon-carbon double bond.
- The peak at just less than 170 is the carbon in a carbon-oxygen double bond.

Putting this together is a matter of playing around with the structures until you have come up with something reasonable. But you can't be sure that you have got the right structure using this simplified table. In this particular case, the spectrum was for the compound:



If you refer back to the more accurate table of chemical shifts towards the top of the page, you will get some better confirmation of this. The relatively low value of the carbon-oxygen double bond peak suggests an ester or acid rather than an aldehyde or ketone.

It can't be an acid because there has to be a carbon attached to an oxygen by a single bond somewhere - apart from the one in the -COOH group. We've already accounted for that carbon atom from the peak at about 170. If it was an acid, you would already have used up both oxygen atoms in the structure in the -COOH group. Without this information, though, you could probably come up with reasonable alternative structures. If you were working from the simplified table in an exam, your examiners would have to allow any valid alternatives.

Contributors and Attributions

- Jim Clark (Chemguide.co.uk)

This page titled 6.1: Interpreting C-13 NMR Spectra is shared under a CC BY-NC 4.0 license and was authored, remixed, and/or curated by Jim Clark.

- **Interpreting C-13 NMR Spectra** by Jim Clark is licensed CC BY-NC 4.0.

CHAPTER OVERVIEW

7: Two-Dimensional NMR Spectroscopy

13.6: DEPT ^{13}C NMR Spectroscopy

7.1: 2D NMR

2D NMR Background

2D NMR Basics

2D NMR Experiments

2D NMR Introduction

Heteronuclear Correlations

Homonuclear Correlations

Indirect Detection

7.2 J-Resolved

7: Two-Dimensional NMR Spectroscopy is shared under a CC BY-NC-SA 4.0 license and was authored, remixed, and/or curated by LibreTexts.

13.6: DEPT ^{13}C NMR Spectroscopy

Distortions Enhancement by Polarization Transfer (DEPT)

DEPT is used for distinguishing between a CH_3 group, a CH_2 group, and a CH group. The proton pulse is set at 45°, 90°, or 135° in the three separate experiments. The different pulses depend on the number of protons attached to a carbon atom. Fig 13.6.1. is an example about DEPT spectrum.

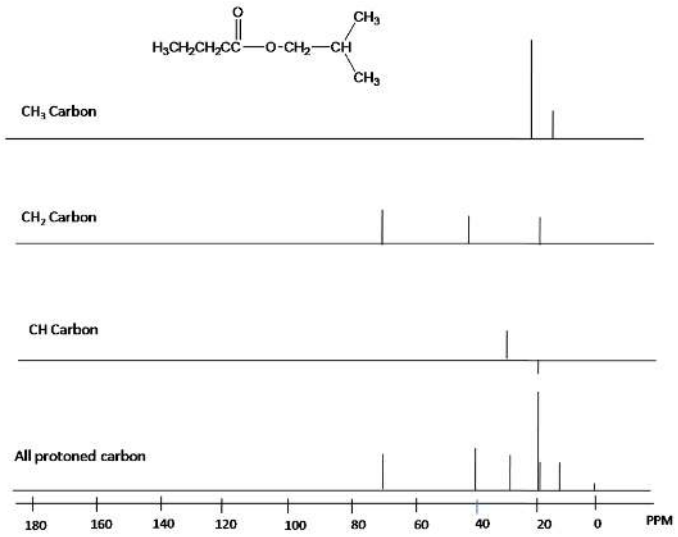
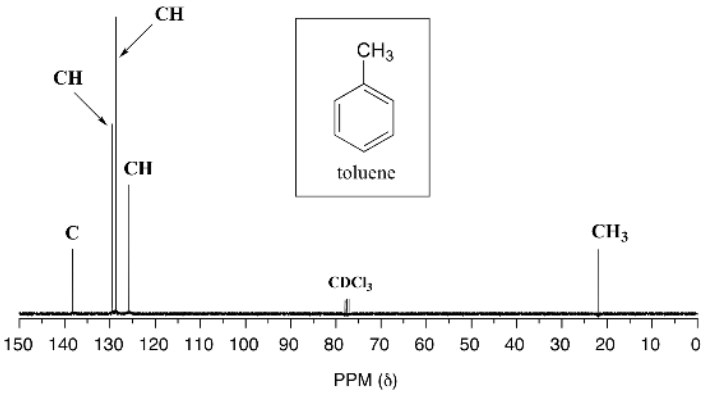
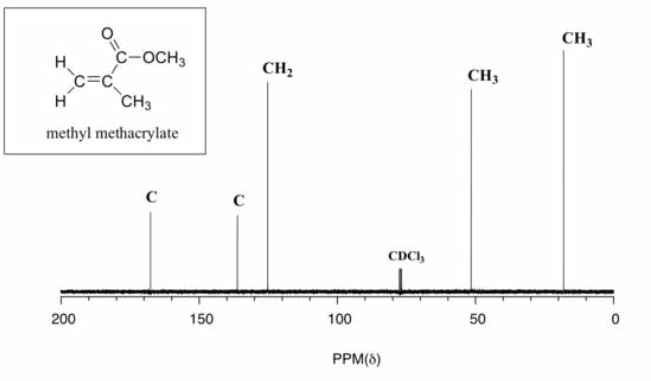


Fig 13.6.1. *DEPT spectrum of n-isobutlybutrate*

While broadband decoupling results in a much simpler spectrum, useful information about the presence of neighboring protons is lost. However, another modern NMR technique called DEPT (Distortionless Enhancement by Polarization Transfer) allows us to determine how many hydrogens are bound to each carbon. For example, a DEPT experiment tells us that the signal at 171 ppm in the ethyl acetate spectrum is a quaternary carbon (no hydrogens bound, in this case a carbonyl carbon), that the 61 ppm signal is from a methylene (CH_2) carbon, and that the 21 ppm and 14 ppm signals are both methyl (CH_3) carbons. The details of the DEPT experiment are beyond the scope of this text, but DEPT information will often be provided along with ^{13}C spectral data in examples and problems.

Below are two more examples of ^{13}C NMR spectra of simple organic molecules, along with DEPT information.





Contributors and Attributions

- Prof. Steven Farmer (Sonoma State University)
- Organic Chemistry With a Biological Emphasis by Tim Soderberg (University of Minnesota, Morris)
- Chris P Schaller, Ph.D., (College of Saint Benedict / Saint John's University)

13.6: DEPT ^{13}C NMR Spectroscopy is shared under a CC BY-NC-SA 4.0 license and was authored, remixed, and/or curated by LibreTexts.

SECTION OVERVIEW

7.1: 2D NMR

2D NMR Background

2D NMR Basics

2D NMR Experiments

2D NMR Introduction

Heteronuclear Correlations

Homonuclear Correlations

Indirect Detection

7.1: 2D NMR is shared under a CC BY-NC-SA 4.0 license and was authored, remixed, and/or curated by Marc Bria.

2D NMR Background

These atoms and some others behave, basically, as small magnets with a so called nuclear magnetic momentum quantified by a quantic value: the spin.

The spin ½ nuclei seen by the quantum mechanic

The example of the proton: The atomic physic teaches us that some nuclei have a kinetic momentum due to their spin state: P and also a magnetic momentum μ.[1] which is defined by the following relation:

$$\mu = \gamma P$$

where γ is the gyro magnetic ratio, thus μ/P characterizes a given nucleus. The quantum mechanic describes an atom with wave functions solution of the Schrödinger equation [2]. For a proton, nucleus with spin quantum number I = 1/2 or m_I = +/- ½ the own wave functions are the following: α for $m_I = \pm\frac{1}{2}\beta$ for m_I = -1/2.

m_I corresponds to the magnetic quantum number which characterizes the stationary state of the nucleus, which depends on the spin numbers I of the nucleus. The total number of the possible own stationary states of the nucleus is then equal to 2I+1. Thus the proton may exist from the point of view of its spin momentum in only two stationary states.

Without any magnetic field the α and β states have the same energy they are, so called, degenerated. It is only in a static homogenous magnetic field of value Bo and following the interaction between Bo and μ that this degeneracy is suppressed (Figure 1). The separation of energy then produced is proportional to the intensity of the field Bo and creates the necessary condition for the existence of spectroscopic transition and constitutes the basis of the spectroscopy by nuclear magnetic resonance.

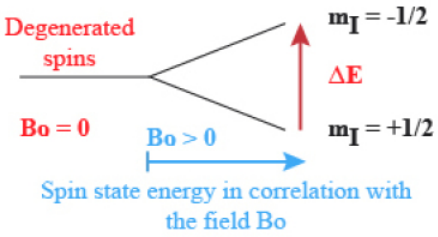


Figure 1: Energy of the spin states in correlation with the field B_o (2)

The proton will occupy the state (i.e., the weakest energy one) with a higher probability. The greater the B_o field amplitude, the more the difference of energy (or ΔE) between the two spin states increases. We describe the difference of occupancy between the basic state and the excited one with the Boltzmann law:

$$\left(\frac{N\beta}{N\alpha} = \exp\cdot\left(\frac{-\Delta E}{kT}\right)\right)$$

Where ΔE is the difference of energy between the two states, k the Boltzmann constant, T the absolute temperature in °K, **N** β the number of spins at the high energy level and Nα the number of spins at the low energy level.

At the equilibrium only a small excess of nuclei are at the fundamental state. For a field of 1.4 T at room temperature, **ΔE=0.02.J.mol^{-1}**. According to the theory the population excess determines the probability of excitation. However, this population excess does not reach more than 0.001%

The Nuclear Magnetic Resonance phenomena

According to the Bohr equation, $\Delta E = h\nu$, we need for inducing a transition towards the high level energy, an energy quantum with a value of $h\nu 0 = \gamma\hbar B_0$ (3) . This is a resonance condition, with $\nu 0$ which is the resonance frequency of the nucleus; ħ the Planck constant divided by $2\pi(\hbar = 1.05410^{-34} J.s.)$ and γ the gyro magnetic ratio. The resonance frequency of the nucleus, which is also called the Larmor frequency, is then proportional to the field Bo value following the equation $\nu 0 = \gamma B_0/2\pi$.

Its range is in the high frequencies:

$\gamma_H = 26.7510^7 rad.T^{-1}.s^{-1}$ in a field of 1.4T at the level of a frequency of $\nu 0$ =60 MHz.

This corresponds to an ultra short radio wavelength of $\lambda = 5m$

Schematic representation of the coherence

When the sample is in a field B_o we create a coherence at the thermal equilibrium (Figure 2). We create therefore also a magnetization along the Z axis [3].

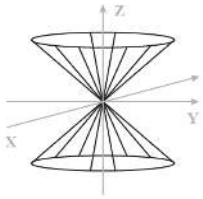


Figure 2: Scheme of the coherence.

This figure represents the spins precession movement which is induced by the field Bo. For example, we may consider the proton as a magnetic dipole whose component μz is either parallel or anti parallel to the z axis. The angular speed of the precession moment is $\omega 0 = \gamma B_0$

The rotating coordinates or rotating frame

It is convenient to figure only the magnetic momentum of the excess of the nuclei in their fundamental states (Figure 1).

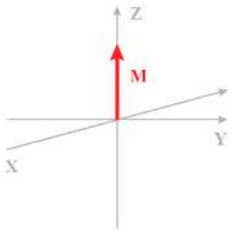


Figure 2: The magnetization M in the rotating frame K'.

M is the macroscopic magnetization as a result of the individual nuclear moment μ. The xy plane does not contain any magnetization component. In addition to the coordinate system K(x,y,z), another system K'(x,y,z) rotates around the z axis with the angular speed ω thus $B' = B_0 + \omega/\gamma$. In this figure, ω/γ is a virtual field B_f opposite to Bo, which is generated by the only relative rotation from one versus the other of the two coordinate systems K and K'. This means that the μ vector is static in the system K' which is called rotating frame, it happens when ω has the same sign and the same value than $\omega 0$. (3)

Requirements to get a resonance

The excitation of the nucleus is generated by a high frequency impulsion B_1 at a high power (50 watts) for a short time (10 to 50 μs). The field B_o is high and constant, the field B_1 is assumed to be weak, perpendicular to B_0 and rotates in the plane X_OY with an angular speed $\omega 1$ and in the same sense than μ [3].

Practically, a small coil put perpendicular in the field B_o is run by a current (Figure 4). This one causes an oscillatory induction along the axis of the coil. We may represent this induction Bx with two magnetic vectors rotating in opposite sense B(l) and B(r), one of which has the same rotation sense than the precession. The second vector is practically without any influence on the phenomenon.

The emitter coil on the x axis generates a weak electromagnetic field B_1 linearly polarized with a frequency ω and with an amplitude $2B_1$.

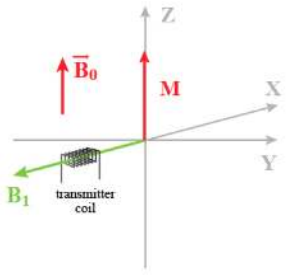


Figure 4: Requirements for the resonance condition.

The Fourier Transform

We may compare the NMR spectroscopy and the optic one. In the optical spectroscopy, the prism allows the monochromatic analysis of a polychromatic source interacting with the mater. In the NMR spectroscopy, the impulsion B_1 yield a broad frequency spectrum and the Fourier transform allows a "monochromatic" analysis of the interaction beam/nucleus. The technique is to treat the signal M(t) according to the following relationship (2):

$$F(v) = \int_0^\infty f(t) \exp(-2i\pi vt) dt$$

Since the pulse sequence last generally less than a second, we may achieve a great number of accumulations of data before to proceed to the Fourier transform. The signal to noise ratio thus improves (this ratio is proportional to $\sqrt{N}$ where S = number of scans).

Bibliography

1. La détection inverse en RMN ; M Boudonneu Analusis N°1, vol.18, 1990
2. La RMN concepts et méthodes; D. Canet inter éditions 1991
3. La spectroscope de RMN, H. Gunther MASSON 1994.
4. NMR in protein studies. M. P. Williamson. Chem. in Britain April 1991(335-337).
5. RMN 2D BRUKER 1993 Poly. 1, 2 et 3.
6. Resonance Magnétique Nucléaire; Evolution instrumentale et analyse de structure; J.P. Girault le technoscope de biofutur n°38 sept 90
7. Sensitivity enhancement by signal averaging in pulsed by Fourier transform NMR spectroscopy; D. L.Rabenteck; J. of Chem. Ed. Vol. 61, n°70, Oct 1984
8. Sequence Cosy Poly. BRUKER 1993.
9. Topic in chemical instrumentation part 3 and 4. 2 D Methods W. King and K. R. Williams J. of Chem. Educ. vol.67n°4.
10. Topics in chemical instrumentation (Definition) W. King and K. R. Williams
11. Two Dimensional NMR spectroscopy; Applications for chemists and biochemists; W. R. Crousmum, R. M. K. Carlson. Vol 9.
12. Two dimensional NMR Aspect 2000 - 3000 BRUKER
13. G. E. Reeman et Moms, J. ChemSoc, Chem.Comm, 684 (1978).
14. H. Kessler, W. Bernel and C. Giresinger, J. AM. Chem. Soc. 107, 1083 (1985).

2D NMR Background is shared under a CC BY-NC-SA 4.0 license and was authored, remixed, and/or curated by Marc Bria.

- **2D NMR Background** by Marc Bria is licensed CC BY 4.0.

2D NMR Basics

Durations

The 2D NMR experiment belongs as well to the Fourier transform spectroscopy than to the impulsion one and relies on a sequence of three time intervals: preparation, evolution and detection (3). In some experiment another time interval is added before the detection: the mixing time (Figure 1).

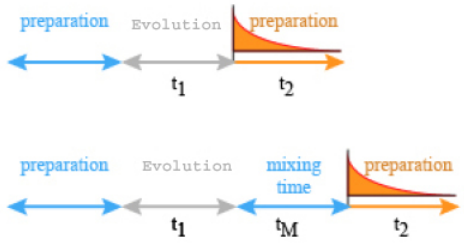


Figure 1: Scheme for time pulse in a 2 D NMR experiment (3)

The preparation time

Upon the preparation time the spin system under study is firstly prepared, for example it is submitted either to a decoupling experiment or just to a transverse magnetization by the means of a 90° impulsion. It allows the excited nuclei to get back their equilibrium state between two successively executed pulse sequence (5)

The evolution time t_1

During the evolution time t_1, the spin system is evolving under the effect of different factors, each coherence evolves at its own characteristic frequency as a function of the chemical shift and of the scalar coupling of the corresponding nucleus.

The Mixing time

It is made of a pulse sequence which achieves coherence transfers in such a way that different frequencies can be correlated.

The detection time

The acquisition of the modulated signal takes place during the detection period. The sequence we just described does not constitute by itself a 2D NMR experiment.

JEENER

The idea of Jeener consists in the stepwise increasing of the evolution time t_1. This will allow to get an NMR signal under the aspect of a sampling of free precession signals of the $s(t_2)$ type. These FID will differ from each other only by the t_1 period duration written under a matricial form $s(t_1, t_2)$ (5). The t_1 delay is the time between the first and the second pulse (Figure 2).

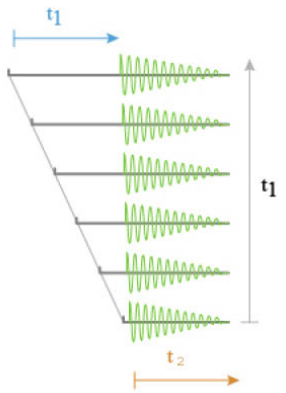


Figure 2: Sampling of signals of free precession of the type s(t2)

The first Fourier transform as a function of t_1 gives us an interferogram of the form $s(t_2, \omega_1)$(Figure 3).

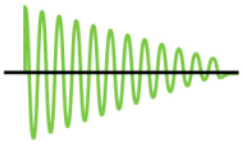


Figure 3: Interferogram of the form (t_2, ω_1)

A second Fourier transform, versus the second variable t_2, gives an NMR spectrum with two frequencies dimensions F_1 and F_2 (Figure 3). The result of this two fold Fourier transform does not get two spectra $s(\omega 1)$ and $s(\omega 2)$ but only one spectrum as a function of two independent frequencies, exhibiting a peak with the coordinates (Ω_1, Ω_2). Thus, an alimentation evolving with the frequency Ω_1 in the time course t_1 has been converted in another coherence evolving with the frequency $\Omega 2$ during the period t_2.

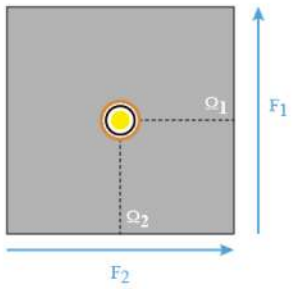


Figure 4: NMR spectrum in two dimensions following the second Fourier transform(4).

This double Fourier transform in both dimension yields thus a matrix $s(\omega_1, \omega_2)$. (Figure 3).

2D NMR Basics is shared under a CC BY-NC-SA 4.0 license and was authored, remixed, and/or curated by LibreTexts.

- **2D NMR Basics** by Marc Bria is licensed CC BY 4.0.

2D NMR Experiments

The experiment

When $\omega_1 \neq \omega_o$: There is no interaction between the field B_1 and μ (they are not in accord) and the precession is kept around the axis Oz.

When $\omega_1 \approx \omega_o$: B_1 and μ are in accordance. Thus the couple applied by B_1 modifies the angle α of μ with O_z, and then causes transitions between the magnetic sublevels.

There is resonance. The value of the z magnetization decreases and it appears, in the y direction, the transverse magnetization M_y.

The Rotating Coordinate System

Impulsion angle α and position of the $\vec{M}$ vector (Figure 1) is given by the following relation $\alpha = \gamma B_1 tp$, with B_1 which represents the amplitude or the power of the impulsion and t_p the width or duration of the impulsion. It is possible to make these two values vary together in such a way that particularly interesting rotation angles appear. One of these is the angle $\alpha = 90^o$.

In this case all the magnetization is orientated in the plane xy and the signal reaches its maximum of intensity. (7)

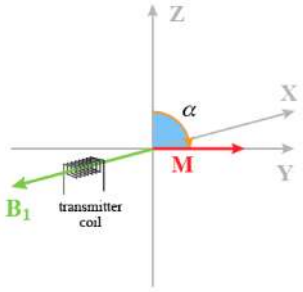


Figure 1: Location of the M vector after an impulsion time allowing anα angle of 90°

An other angle allows the inversion of the M vector by the application of an impulsion π or α = 180°. In this experiment, the vector M is orientated in –z. Practically, one uses the angle α = 45° in order to get a good compromise between measurement time/quality of the response.

The Free Induction Decay Signal

The signal given by the receiver coil is known under the name of interferogram: **Free Induction Decay** (FID). In opposition to the continue wavelength signal, the time dependent signal we monitor in this case is an emission signal, because the radiofrequency field B_1 is turned off upon the signal acquisition. The experiment gives us practically a variable field which is linear at high frequency following the y axis. In fact it is an oscillator or an emitter with the Larmor frequency of the nuclei under study (7) .

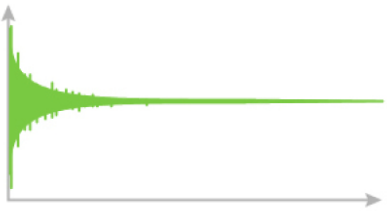


Figure 2: FID made of several superimposed damped sine wave.

The time signal S(t) generated in the receiver coil by the xy component of M weakens under the relaxation process.

The notion of phase cycle

The phase cycles or phase programs allow to:

- choose the relevant signals and to neglect these ones which do not contain information and which, eventually, are susceptible to hide some other useful signals.
- discriminate the sign of the frequencies in the fl dimension.

- compensate the inhomogeneity from one or several impulsion in the sequence,
- to achieve an optimal quadratic detection in the f2 axis. (5)

Any impulsion in a sequence has its own phase cycle which may be more or less complex. The ideal number of scans must be a multiple of the phase number of the longer cycle. For a better understanding of this method, a standard nomenclature has been defined (Fig. 7).

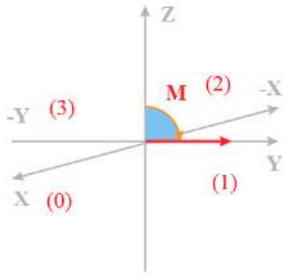


Figure 3: Standard nomenclature for the phase cycles.

Example 1: The Cyclops Cycle

Φ = x,y,-x,-y. 0,1,2,3. This cycle involves the accumulation of a multiple of 4 numbers between each free precession.

The first impulsion B_1 occurs around the x and the emission will occur in the y axis, the third impulsion along the - x and the reception in -y, etc.

There are other variations of this cycle like the following:

$$\Phi = x, -x, y, -y$$

or

$$\Phi = 0, 2, 1, 3.$$

or still:

$$\Phi = x, x, -x, -x, y, y, -y, -y$$

or

$$\Phi 0, 0, 2, 2, 1, 1, 3, 3.$$

This last one implies a multiple of eight transient cycles in the accumulation.

References

1. La détection inverse en RMN ; M Boudonneu Analusis N°1, vol.18, 1990
2. La RMN concepts et méthodes; D. Canet inter éditions 1991
3. La spectroscope de RMN, H. Gunther MASSON 1994.
4. NMR in protein studies. M. P. Williamson. Chem. in Britain April 1991(335-337).
5. RMN 2D BRUKER 1993 Poly. 1, 2 et 3.
6. Resonance Magnétique Nucléaire; Evolution instrumentale et analyse de structure; J.P. Girault le technoscope de biofutur n°38 sept 90
7. Sensitivity enhancement by signal averaging in pulsed by Fourier transform NMR spectroscopy; D. L.Rabenteck; J. of Chem. Ed. Vol. 61, n°70, Oct 1984
8. Sequence Cosy Poly. BRUKER 1993.
9. Topic in chemical instrumentation part 3 and 4. 2 D Methods W. King and K. R. Williams J. of Chem. Educ. vol.67n°4.
10. Topics in chemical instrumentation (Definition) W. King and K. R. Williams
11. Two Dimensional NMR spectroscopy; Applications for chemists and biochemists; W. R. Crousmum, R. M. K. Carlson. Vol 9.
12. Two dimensional NMR Aspect 2000 - 3000 BRUKER
13. G. E. Reeman et Moms, J. ChemSoc, Chem.Comm, 684 (1978).

14. H. Kessler, W. Bernel and C. Giresinger, J. AM. Chem. Soc. 107, 1083 (1985).

2D NMR Experiments is shared under a CC BY-NC-SA 4.0 license and was authored, remixed, and/or curated by Marc Bria.

- **2D NMR Experiments** by Marc Bria is licensed CC BY 4.0.

2D NMR Introduction

Some general principles and techniques used in two-dimensional NMR are discussed. Applications covered are mostly concerned with protein NMR, but additional 2D techniques and applications can be found in the references section.

Introduction

A two dimensional variation of NMR was first proposed by Jean Jeener in 1971; since then, scientists such as Richard Ernst have applied the concept to develop the many techniques of 2D NMR. Although traditional, one-dimensional NMR is sufficient to observe distinct peaks for the various funtional groups of small molecules, for larger, more complex molecules, many overlapping resonances can make interpretation of an NMR spectrum difficult. Two-dimensional NMR, however, allows one to circumvent this challenge by adding additional experimental variables and thus introducing a second dimension to the resulting spectrum, providing data that is easier to interpret and often more informative.

Basics of 2D NMR

Experimental Set-up

In traditional 1D Fourier transform NMR, a sample under a magnetic field is hit with a series of RF pulses, as seen in the pulse sequence below, and the Fourier transform of the outgoing signal results in a 1D spectra as a function chemical shift.

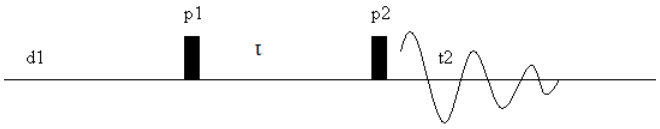


Figure 1: Pulse sequence of a typical FT-NMR experiment

A 2D NMR experiment, however, adds an additional dimension to the spectra by varying the length of time (τ)) the system is allowed to evolve following the first pulse. The result is an outgoing signal f (τ, t_2), which, when Fourier transformed, gives a 2D spectrum of F (ω_1, ω_2).

The use of two-dimensional NMR allows the researcher to better resolve signals which would normally overlap in 1D NMR. Depending on the size of your molecule, different variations or combinations of 2D and multidimensional NMR experiments are utilized.

The Spin Hamiltonian

The spin of a given nuclei during any NMR experiment is governmed by the spin Hamiltonian. If long-range spin interactions are ignored, the spin Hamilitonian for a one-spin system is given the equation

$$\hat{H} = \hat{H}^0 + \hat{H}_{RF}$$

The magnetic field along the z-axis, shielding, and J-coupling with nearby nuclei are all constant and are accounted for in H^0. H_{RF} is the induced magnetic field resulting from an RF pulse. For a system where two spins are coupled, the H^0 is

$$\hat{H} = \omega_1^0 \hat{I}_{1z} + \omega_2^0 \hat{I}_{2z} + 2\pi J_{12} \hat{I}_1 \hat{I}_2$$

Where ω is the Larmor frequency, **I** is the net magnetization vector of the given nucleus or nuclei, and **J** is the observed J coupling between nuclei. ω is directly related to the chemical shift (δ) by the equation

$$\omega_j^0 = -\gamma_j B^0 (1 + \delta_j^{iso})$$

Where γ is the gyromagnetic ratio of the given isotope. If nuclei 1 and 2 are of the same element and isotope, the system is referred to as homonuclear. If they are different, it is a heteronuclear spin system.

Correlation Spectroscopy (COSY)

The most basic form of 2D NMR is the 2D COSY (pulse sequence shown below) experiment, a homonuclear experiment with a pulse sequence similar to the procedure dicussed above. It consists of a 90° RF pusle followed by an evolution time and an additional 90° pulse. The resulting oscillating magnetization (symbolized by decaying the sinusoidal curve) is then acquired during t_2.

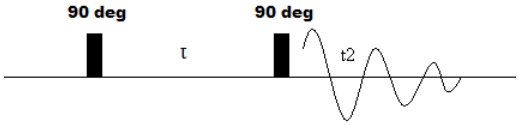


Figure 2: Pulse sequence of a 2D COSY experiment

The analysis of the acquired spectrum is discussed below, making it useful for determining the coupling between nuclei that are connected through one to three bond lengths. However, in macromolecules such as proteins, coupling through bonds alone is not sufficient to obtain substantial structural information. For this reason, the Nuclear Overhauser Effect (NOE) is often used in protein NMR to obtain information on the distance between nuclei through space rather than through bonds.

Nuclear Overhauser Effect (NOE)

Thus far, only the coupling of nuclei through bonds has been considered. In bond coupling, the magnetization of nuclei affect those closely bound to them through the electrons that make up those bonds; however, coupling directly between nuclei that are in close spatial proximity to each other also occurs. This is called the Nuclear Overhauser Effect, and it arises when the spin relaxation of nuclei A is felt by nearby nuclei B, stimulating a corresponding change in magnetization in B. In a typical NMR spectrum, the interference of electrons makes this coupling undetectable. However, a sample can be decoupled to “neutralize” the bond coupling through electrons, allowing the space coupling of the NOE to be detected. This is called NOESY (NOE correlation spectroscopy) and is another type of homonuclear NMR.

The pulse sequence for a NOESY NMR experiment is depicted below.

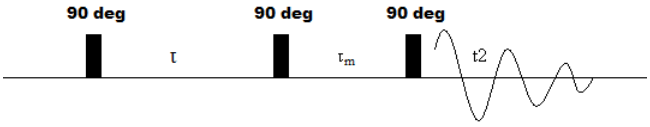


Figure 3: Pulse sequence of NOESY experiment

Like COSY, the first step is a 90° pulse followed by a variable evolution time. Unlike COSY, however, pulse two actually consists of two 90 degree pulses separated by a short delay. The first pulse converts the bulk magnetization from the transverse plane to the z-plane, eliminating the effect of electron-aided bond coupling. Then, during the τ_m, there is cross relaxation between spatially adjacent nuclei. Finally, the last 90 degree pulse converts the space coupling of nuclei into an observable transverse magnetization, which can be detected during t_2.

2D NMR Spectra

As discussed earlier, by performing multiple one dimensional experiments at varying lengths (τ) of the evolution period and performing a Fourier transformation on the signal which converts f (τ, t_2) to F(ω_1, ω_2), a two dimensional spectrum can be formed into a 3D contour map.

A more useful representation of 2D data is called a correlation map. The correlation map of the steroid progesterone is shown below.

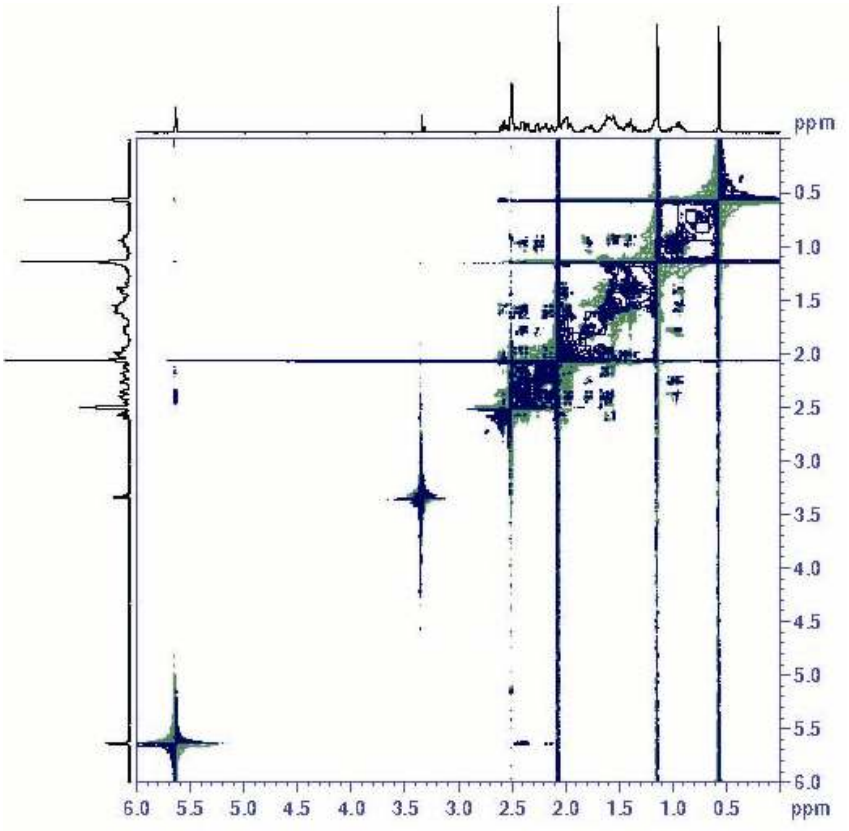


Figure 4: 2D COSY spectrum of progesterone

In this representation, the x- and y-axes correspond to the frequencies resulting from the Fourier transforms, and the intensity of shade at each frequency coordinate indicates the peak intensity. Two types of peaks are observed in a homonuclear correlation map—diagonal peaks and cross peaks. Diagonal peaks are found along the diagonal of the map where the x- and y-axes have equal frequency values and simply correspond to the absorptions from a one-dimensional NMR experiment. Because heteronuclear NMR does not involve the same isotope, diagonal peaks are not observed. Cross peaks, on the other hand, give information on the coupling of two nuclei and are seen in both homo- and heteronuclear spectra.

Applications in Protein NMR

As previously mentioned, the major advantage of 2D NMR over 1D NMR is the ability to distinguish between the overlapping signals that exist in larger molecules. Heteronuclear two-dimensional NMR is especially important in biological chemistry in the elucidation of the three-dimensional structure of proteins.

Heteronuclear Single Quantum Coherence (HSQC)

A protein is make-up of a series of amino acid monomers. Although there are 19 different amino acids each with a distinct side chain, the protein backbone is an invariable pattern of NH-C-CO as shown in Figure 5.

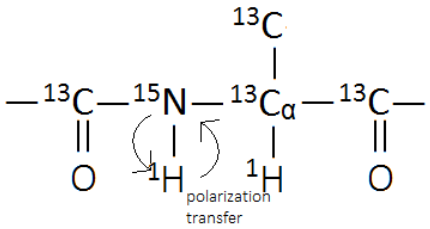


Figure 5: Structure of a amino acid chain with NMR active nuclei

When synthesized under the right conditions, a heavy atom protein can be produced which constains NMR active nuclei; however, a ^{15}N nucleus has a very low gyromagnetic ratio. According to the Hamiltonian operators discussed above, it will give a very weak

signal in traditional 2D NMR. Fortunately, the nucleus can be detected indirectly by transferring polarization through a ^{1}H nucleus. This method is used in HSQC NMR.

In protein NMR, each HSQC experiment has three steps:

1. An INEPT (insensitive nuclei enhanced by polarization transfer) transfers the polarization of a ^{1}H nuclei to the neighboring ^{15}N (see figure below)
2. The polarization is transferred back to the ^{1}H nuclei
3. Signal from the ^{1}H nuclei is recorded

The pulse sequence for a typical HSQC experiment is detailed below.

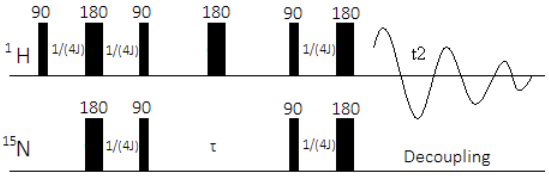


Figure 6: Pulse sequence of a HSQC experiment involving ^{1}H and ^{15}N nuclei

A 90^{o}^{1}H RF pulse creates a transverse polarization in ^{1}H nuclei. Following the pulse, the nuclei are allowed to evolve for a 1/(4J) time period, which is the longitudinal relaxation time. Next, a 180° ^{1}H and ^{15}N pulse are used at the same time. During the subsequent relaxation time, the ^{1}H nuclei develop a polarization that is antiphase to ^{15}N. Finally, a 90° ^{1}H and ^{15}N pulse, again simultaneous, enacts the INEPT transfer of antiphase magnetization from the ^{1}H nucleus to the ^{15}N nucleus. Following the INEPT transfer, the ^{15}N nuclei are allowed to evolve during τbefore a reverse INEPT transfer moves the ^{15}N polarization back to ^{1}H and a ^{15}N decoupled signal is recorded.

An example HSCQ spectrum from ubiquitin is shown below.

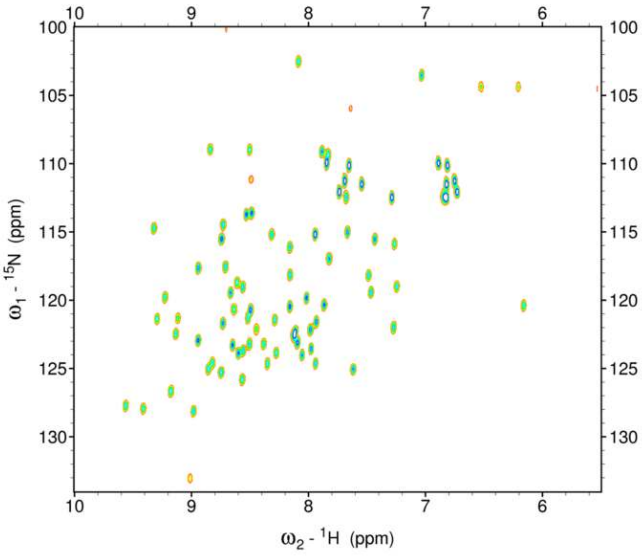


Figure 7: $^{1}H^{15}N$ HSQC spectrum of ubiquitin

Notice the greater clarity of spectra of the HSQC vs the COSY experiment. This is a strong advantage of heteronuclear NMR. In this diagram, each peak corresponds to a cross peak, showing coupling between sets of ^{1}H and ^{15}N nuclei. Each peak represents the ^{15}N—^{1}H of a unique amino acid along the backbone of the amino acid.

The 2D HSQC experiment which relates ^{1}H and ^{15}N is just the start on the long, complicated road of protein structural characterization using 2D and multidimensional NMR techniques. The next experiment is typically a 3D NMR technique in which coupling with ^{13}C is also including in the spectra—which will give information on which NH peaks are associated with which type of amino acid residue—followed by a NOE experiment—which gives spatial distances between nuclei. These multidimensional techniques are outside the scope of this module; however, the principles which were applied in the construction and analysis of the

2D spectra can be carried over to 3D and 4D NMR. The only difference, naturally, is the additional dimensions. By the time multiple experiments have been carried out, information regarding proximity of nuclei, the types of amino acid associated with each nuclei, and secondary structure has been amassed, and by carefully piecing all the data together, a 3D structure of a given protein can be constructed.

Other Applications of 2D NMR

2D NMR has many more applications beyond protein NMR, including characterization of pharmaceuticals, temperature dependence of carbohydrate conformations, and metabolomics, to just name a few. For more information on these applications and the 2D NMR techniques that are used in them, please see the "Further Reading" section.

? Exercise 1

What is the effect of the 90° pulse on the bulk magnetization of a sample?

Answer

A 90° pulse moves the bulk magnetization into the transverse plane

? Exercise 2

If a 90° pulse for a give sample is 4 fs long, how long is a 180° pulse on the same sample?

Answer

8 fs

? Exercise 3

The magnetic effect of which type of particle must be removed from an NMR experiment in order to observe an NOE?

Answer

electrons

References

1. Aue, W., E. Bartholdi, R.R. Ernst, *Two-dimensional spectroscopy. Application to nuclear magnetic resonance.* The Journal of Chemical Physics, 1976. **64**: p. 2229.
2. Gomathi, L., *Elucidation of secondary structures of peptides using high resolution NMR.* Current Science, 1996. **71**(7): p. 553.
3. Levitt, M.H., *Spin Dynamics: Basics of Nuclear Magnetic Resonance*. 2008: Wiley
4. Jacobsen, N.A., *NMR Spectroscopy Explained: Simplified Theory, Applications and Examples for Organic Chemistry and Structural Biology*. 2007: Wiley. 668.
5. Ames, J.B., Hamasaki, N., Molchanova, T., *Structure and calcium-binding studies of a recoverin mutant (E85Q) in an allosteric intermediate state*. Biochemistry, 2002. **41**(18): p. 5776. **DOI:** 10.1021/bi012153k
6. Clore, G.G., Angela M., *Determining structures of large proteins and protein complexes by NMR.* Biological Magnetic Resonance, 1998. **16**.

Further Reading

1. Ludwig, C., Viant, Mark R., *Two-dimensional J-resolved NMR spectroscopy: review of a key methodology in the metabolomics toobox.* Phytochemical Analysis, 2010. **21**(1): p. 22-32. **DOI**: 10.1002/pca.1186
2. Brown, S.P., *Applications of high-resolution 1H solid-state NMR.* Solida State Nuclear Magnetic Resonance, 2012. **41**: p. 1-27. **DOI:** 10.1016/j.ssnmr.2011.11.006
3. Shrot, Y.F., Lucio, *Ghost-peak suppression in ultrafast two-dimensional NMR.* Journal of Magnetic Resonance, 2003. **164**(2): p. 351-357. **DOI:** 10.1016/S1090-7807(03)00177-0

2D NMR Introduction is shared under a CC BY-NC-SA 4.0 license and was authored, remixed, and/or curated by LibreTexts.

- **2D NMR Introduction** by LibreTexts is licensed CC BY 4.0.

Heteronuclear Correlations

The heteronuclear correlation of chemical shifts by scalar coupling derives from the existence of heteronuclear scalar coupling all owing a magnetization transfer from the more sensitive nucleus (^{1}H) toward the less sensitive nucleus (^{13}C). The model experiment is the correlation $\delta(^{13}C)/\ \delta(^{1}H)$ which uses the large direct coupling $^{1}J_{(^{13}C-^{1}H)}$ comprised between more 100 Hz and 200Hz and which allows to correlate the signals from a proton to that of a ^{13}C to which it is bound (5).

The XHCORR sequence

This sequence allows to correlate the signals of the ^{1}H and of the ^{13}C bound to each other (13). Spectrum 11 (XHCORR), shows the correlations for the dihydrofuran (Fig. 31) between bound carbons and protons. The chemical shifts of the protons of these molecules are in the table 2, those of the carbon are in the table 3.

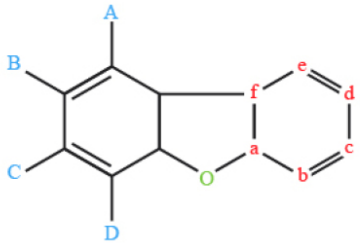


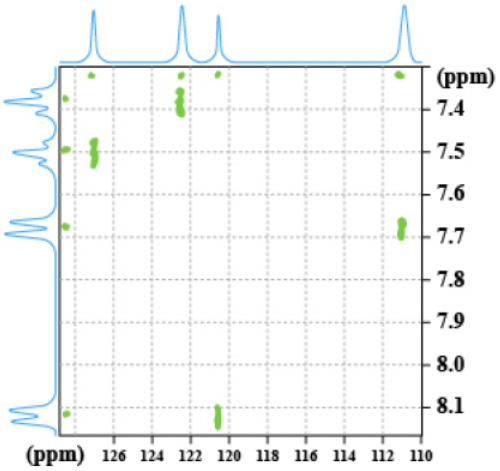
Fig. 31. The dibenzofuran (D.B.F.)

^{1}H	Shift (ppm)
A	8.15
B	7.4
C	7.5
D	7.7

Table 2: DBF protons chemical shift.

13C	Shift (ppm)
a	156.2
b	111.6
c	127.0
d	122.6
e	120.6
f	124.2

Table 3: DBF carbons chemical shift



https://chem.libretexts.org/@go/page/167117

Spectrum: XHCORR of the DBF

Within the XHCORR pulse sequence (Fig. 25), transverse magnetization is caused by a $\pi/2(^1H)$ impulsion which is evolving during the t_1 period. The π impulsion (^{13}C), located in the middle of this period refocuses the heteronuclear couplings.

The optimization of the $\Delta 1$ and $\Delta 2$ delays allows the selection of the long range heteronuclear couplings, this means that instead of seeing the correlation between ^{13}C and protons directly bound (H_B), we favor the appearance of the correlations spots between ^{13}C and non bound protons (H_{NB}).

For example, for a coupling constant J=10 Hz then $\Delta 1$ =50 ms and $\Delta 2$ =33 ms.

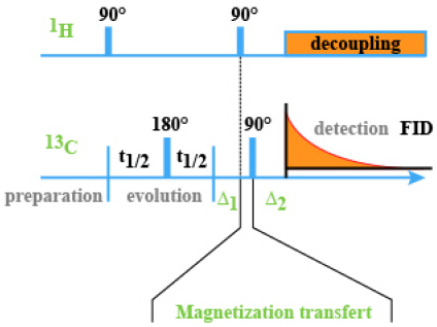


Fig. 25: The XHCORR pulse sequence.

The COLOC sequence (COrrelation via LOng range Coupling)

The sequence which is used (Fig. 26) allows generally a good correlation between the quaternary carbons and the neighbouring protons. On the spectrum 12 (COLOC), the correlation between the quaternary carbon (^{13}C = δ = 156. 2 ppm) and its vicinal proton (δ = 7.7 ppm) is named Cq. However, it does not give good results for long range correlations involving protonated carbons (14). This observation led to write a pulse sequence named XC ORFE (X nucleus proton CORrelation with Fixed Evolution time). This one is very closed to the COLOC sequence.

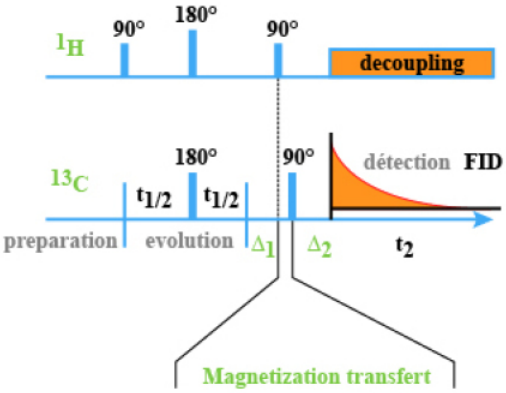
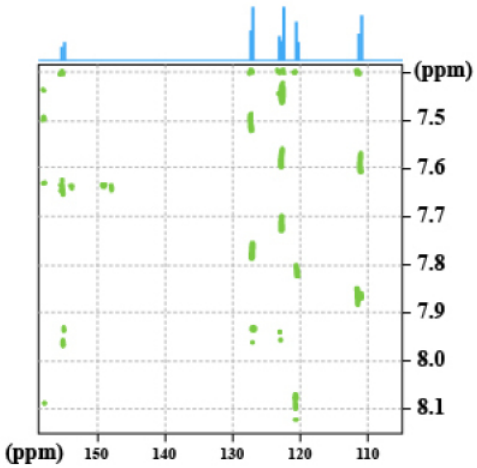


Fig. 26: The COLOC pulse sequence (14).

https://chem.libretexts.org/@go/page/167117



Spectrum 12: COLOC of DBF

Heteronuclear 2D J-resolved Pulse Sequence

In this experiment we observe the coupling J between the X nuclei (^{13}C, ^{15}N, ^{31}P ...etc) and the protons which are bound to them (Fig. 27). A coupled normal 1D spectrum XH may be very difficult to explain. This is due to the intercrossing of the multiplets (12). For simplifying the spectra, we will spread the coupling data in the Fl dimension and the informations arising from the chemical shifts in the F_2 dimension.

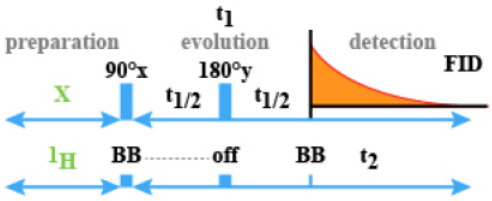
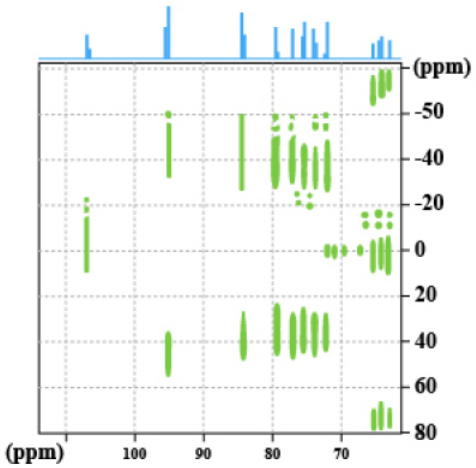


Fig. 27: The 2D J-resolved heteronuclear pulse sequence.

The results are given for the saccharine (Fig. 29). The F_2 carbon (108 ppm) is a quaternary one because we may observe only one spot devoid of coupling. The G_1 carbon (95 ppm) is a CH because there are two correlation spots. Moreover, the coupling constant between this ^{13}C and this ^{1}H is of 80 Hz approximately (Spectrum 13 and 14).



Spectrum 13: Heteronuclear 2D J-resolved

The Heteronuclear correlation of chemical shifts in inverse detection. What is the reverse detection? The reverse detection or indirect detection affords the NMR parameters (chemical shifts, t_1, ...) of a weakly sensitive X nucleus by observing it through a much more sensitive nucleus (generally the proton) (1.5).

Heteronuclear Correlations is shared under a CC BY-NC-SA 4.0 license and was authored, remixed, and/or curated by LibreTexts.

- **Heteronuclear Correlations** by Marc Bria is licensed CC BY 4.0.

Homonuclear Correlations

Homonuclear 2D J-resolved

This sequence allows to get the coupling constant along the Fl axis and the chemical shift of each uncoupled proton along the F2 axis (Spectrum 1 and 2). Of course, the couplings involving two different nuclei (^{3I}P, ^{19}P coupled to ^{1}H) are always found in the F2 dimension. One can thus determine the coupling between a proton within a multiplet of a coupled spectrum and phosphorus (8). For the 2D J-resolved sequence (Fig. 12), the pulse sequence used is a spin echo sequence. In our example we studied the saccharose molecule (Fig. 29). As in any "echo" experiment, the evolution period tl is divided into two equivalent parts. After the first impulsion of (90°)x, all the magnetization vectors begin to precess as a function of their chemical shifts and the coupling constants. The impulsion of (180°) on the y axis allows for each refocused spin to reassociate the vectors with their chemical shifts.

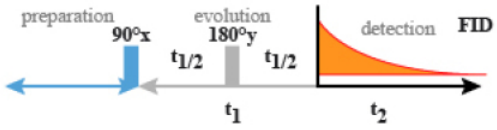
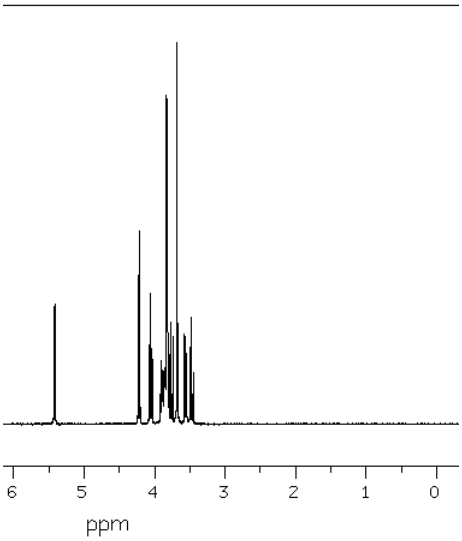


FIG. 12: The J-resolved 2D sequence.



Spectrum 1: 1D proton saccharin.

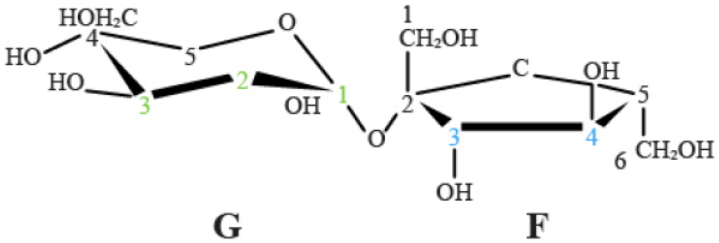
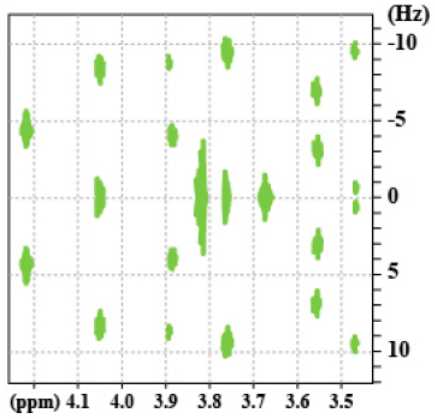


Fig 29: Saccharine Molecule.



Spectrum 2: J-resolved 2D.

The doublet which is located at 4.22 ppm, shows that the f3 proton has a neighboring proton. The coupling constant is directly seen on the F2 axis. The triplet f4 at 4.05 ppm shows that this one has two protons which are closed to him ... (and so on).

The COSY 90 pulse sequence (Correlated SpectroscopY)

The example under study is the saccharine (Fig. 29). The aim of this sequence is to correlate signals of identical nuclei with a scalar coupling. For an isolated nucleus, it is made of two $(\pi/2)_x$ impulsions on both side of the evolution period t_1 (Fig. 13).

The preparation begins with a relaxation delay allowing the magnetization to come back to its equilibrium, then the period t_1 occurs with a stepwise increase and finally the t_2 period is the acquisition time (8).

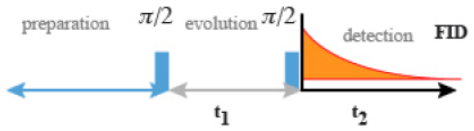


Fig. 13: The COSY experiment.

Following the double Fourier transform, we get a spectrum in chemical shift on the two axis. Moreover, the cross peaks indicate the nuclei which are coupled within each other and allow then a direct attribution of the neighboring protons.

We can understand the obtention of the diagonal and crossing signals of the COSY spectrum by the merely means of quantitative consideration. (8)

In fact, if we consider a singlet signal without scalar spin-spin coupling, the preparation allows to set the maximal amount of nuclei at their right position and the first impulsion $(\pi/2)_x$ generates a transverse magnetization M(A) which rotates around the Y axis (Fig. 14).

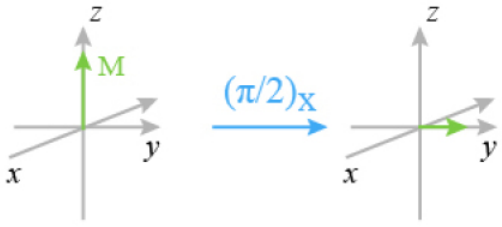


Fig. 14: After the first impulsion $(\pi/2)_x$

During the evolution period, the aimantation $M_{(A)}$ precesses with the frequency of the corresponding nucleus resonance $\Omega = 2\pi\nu$ in the rotating frame; there is thus a sharing of the spins between the x axis and the y axis (Fig. 15).

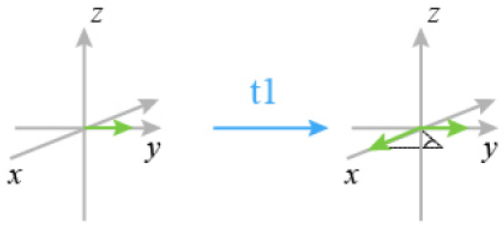


Fig. 15: Evolution of the magnetization during the time t_1

The components M_x and M_y of the transverse magnetization at the end of the evolution period in the O_x and O_y axis of the rotating frame are then:

$$M_x = M_0 \sin 2\pi\upsilon t_1 \exp(-t_1/T_2*)$$

$$M_y = M_0 \cos 2\pi\upsilon t_1 \exp(-t_1/T_2*)$$

Where M_0 is the aimantation contribution before the execution of the first impulsion and T_2^* the apparent transverse relaxation time of the corresponding nucleus.

The second impulsion $\pi/2$ allows to rotate the y component which stays in the xy plane, in the negative z part direction (-z). These last one will not be detected (Fig. 16). However, the x part, still in the xy plane will be taken into account.

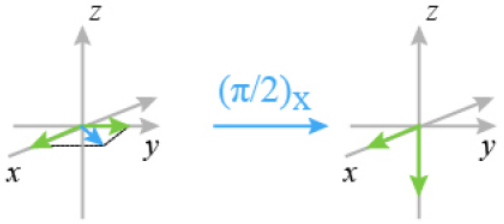


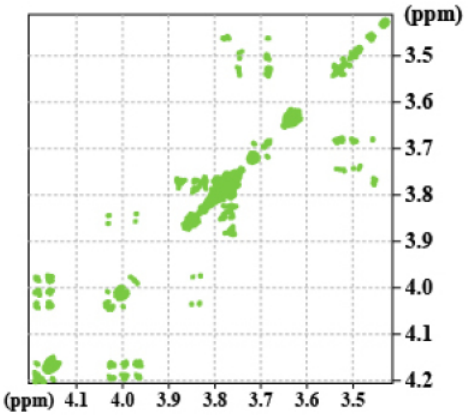
Fig. 16: Next to the second impulse $\pi/2$x

The magnetization which is going to be detected is of the form: $M_0 sin2\pi\upsilon t_1$, where as the magnetization along the –z axis followed the formula: $Mcos2\pi\upsilon t_1$.

The intensity of the signal to be recorded depends thus of the time dependent position of the M(A) vector at the very time of the end of the evolution period. This intensity is determined by the Larmor frequency of the A nucleus. The amplitude is modulated in t_1 versus this frequency and the Fourier transform yields in both dimensions the frequency υ_A and then a diagonal signal. In the case of a spin-spin coupling, the second impulsion $\pi/2$ does not only induce a change in the transverse A magnetization, but also changes of populations for other transitions in the spin system under study. Therefore, an exchange of magnetization occurs between all the nuclei which are coupled between each other. Their signals, in a set of experiments t_1, are in the same way modulated versus the neighboring nuclei.

This ends up with cross peaks of the 2D spectrum in (υ_A, υ_X) and (υ_X, υ_A) and allows us to get a spectrum in which the homonuclear scalar coupling constants are figure out by spots outside of the diagonal.

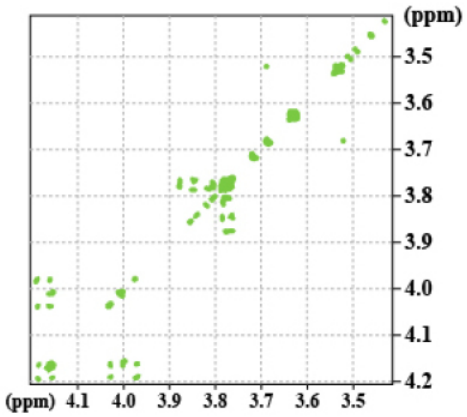
For example, we might see the coupling between the f3 and f4 protons at the crossing of 4.05 and 4.18 ppm (Spectrum 3).



Spectrum 3: COSY 90° Both impulsions are at 90°.

The COSY 45 pulse sequence

The example is given for the saccharose (Fig. 29). The second impulsion is of 45°. The drawback of this second pulse is to diminish the signal to noise ratio (Fig 17). However it allows a more easy attribution of the signals of the spectrum in the cases of strong AB type coupling. In fact, the correlations spots near the diagonal are no more susceptible to be hidden by the auto correlation peaks (Spectrum 4).



Spectrum 4: COSY 45°. We observe a strong diminution of the autocorrelation peaks.

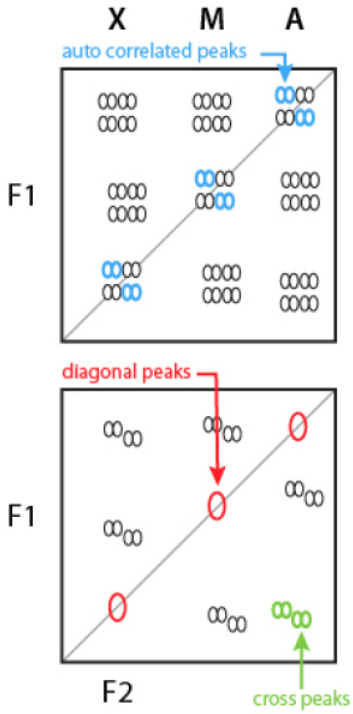


Fig 17: Comparison of the COSY spectrum (upper part) and COSY 45 of an AMX type system.

The long range coupling: COSY

This experiment allows the detection of the correlation peaks caused by weak coupling constant (less than one Hz) and which are not detectable with the COSY 9O° pulse sequence (8).

For the "long range" COSY sequence, we artificially increase the evolution and detection period by introducing a fixed Δ delay on both side of the mixing time (Fig. 18).

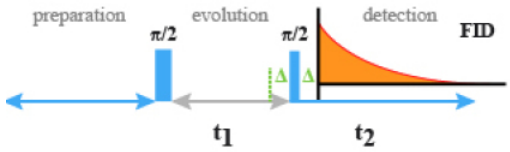
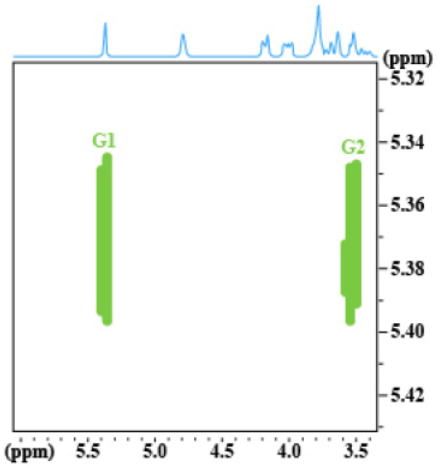


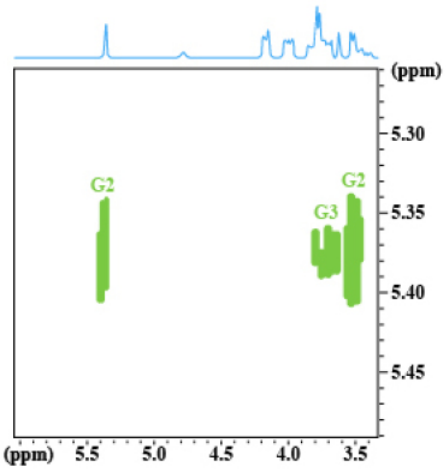
Fig 18: The long range COSY.

The chosen example is the saccharine molecule (see also Fig 29).

The spectrum 5 is a 90° COSY pulse sequence: The scalar coupling between neighboring protons G1 and G2 are clearly seen. The spectrum 6 is a L.R. COSY pulse sequence.:The long range couplings appear between the G1 proton and the G3 and G4 protons.



Spectrum 5: 90° COSY



Spectrum 6: LR COSY

The relayed COSY or one homonuclear step relayed COSY

A COSY spectrum may sometimes be inefficient to clearly identify all the signals, particularly if per chance two nuclei are equivalent. A typical example is that of peptides (Fig 19) where protons born by α carbon of different amino acids have closed chemical shifts; the COSY spectrum gives informations of the correlations between α proton and β protons in one hand and between α protons and NH protons on the other hand. Unfortunately, due to the overlapping of the α protons signals, the attribution for the β protons signals can not be deduced from the NH protons (or the other way around). To solve this problem, we should be able to correlate the NH proton signals to those of the β protons; such a correlation may be obtained either by a long range COSY if the 4J coupling is not too weak or, better, by a relayed COSY experiment which allows the correlation of the signal from two nuclei at the only requirement that both of them are coupled to a third one (8).

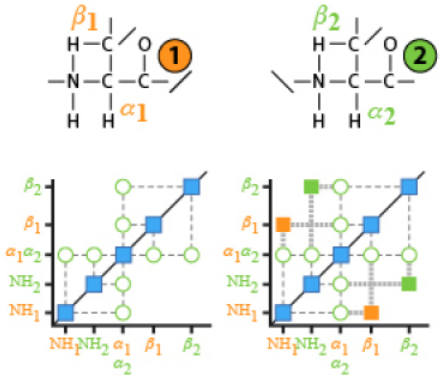


Fig. 19: Schematic representation of the spectra COSY (left) and relayed COSY with two AMX type systems (for ex.: NH-CH_a-CH_b) with Jax=0

This experiment allows the differentiation of the belonging of the NH versus the $CH_\beta 1$ or $CH_\beta 2$.

It is widely used for the sugar structure determination. The pulse sequence of the experiment is derived from the COSY sequence in which the mixing pulse is followed by a fixed time τ and by a 90° pulse (Fig. 20).

A 180° pulse, achieved in the middle of the new mixing period is also needed for the elimination of the evolution of the magnetization (refocalization) due to the chemical shifts during this additional delay.

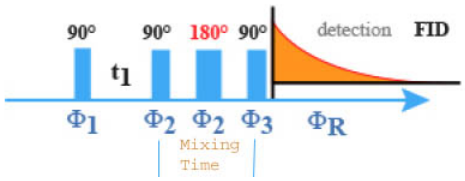


Fig. 20: The pulse sequence for the Relayed COSY.

Applied to the AMX type system, this pulse sequence achieves a first coherence transfer from A to M as that one observed in the COSY experiment. During the mixing time, the magnetization evolve in such a wav that ideally the different components of the magnetization of the M nucleus are in anti phase versus the J_{MX} coupling. The third impulsion at 90° achieves then the transfer from the M nucleus toward the X nucleus. The phase cycles of the impulsions and of the receiver is derived from that of the COSY experiment. However, it needs an additional base cycle for the elimination of the artifacts due to transfers of the NOESY type. This consists to inverse the phase of the second impulsion without modifying the reception phase. The result is a global cycle with 8 components:

$\Phi 1$ = 0, $\Phi 2$= 0 0 1 1 2 2 3 3 , $\Phi 3$ = 0 2 1 3, ΦR = 0 0 2 2

For optimizing the mixing time, we have to define the delay τ between each impulsion. This one is deduced from the following formula where J_{max} stands for the value of the biggest coupling constant:

$$\tau = \frac{1}{1 \bullet 6 J_{max}}$$

COSY experiment with a double quantum filter (DQF COSY)

The COSY sequence with double quantum filter affords some advantages compared to the conventional cosy (2). The diagonal spots and the correlation spots are not phase shifted to 90° and they have the same anti phase structure (Fig. 21). It is thus possible to phase as a whole all the peaks of the spectrum in positive or in negative absorption allowing thus an easier identification of the peaks whose correlations are the closest to the diagonal. These diagonal peaks correspond to singlet signals and are thus eliminated. Unfortunately the sensitivity is divided by 2.

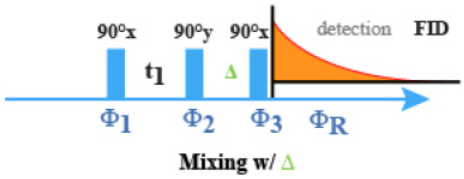
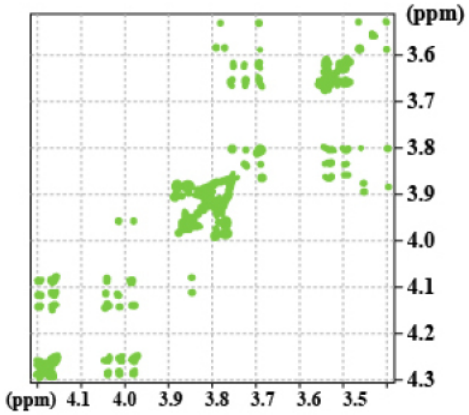


Fig. 21. The COSY DQF pulse sequence.

The molecule which is used as an example is the saccharine (Fig. 29). We may notice on the spectrum 7 (DQF COSY), a strong decrease of the singlet of the proton F1 which is located at 3.68 ppm compared to the spectrum 3.



Spectrum 7: DQF COSY.

The NOESY sequence (Nuclear Over Hauser Enhancement Spectroscopy)

It introduces the crossed relaxation swhich governs the Over Hauser effect (2). The NOESY spectroscopy is rather limited to the determination of the notion of crossed homonuclear relaxation. The pulse sequence scheme is given Figure 22.

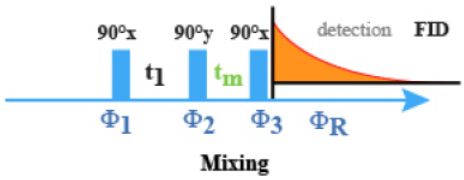


Fig. 22: The NOESY pulse sequence.

The correlation spots (peaks outside of the diagonal) indicate either a dipolar interaction, thus a given spatial vicinity (2 to 5 A°) between the spins under study, or a chemical shift. This experiment allows the determination of large molecules such as the proteins.

The spectrum 8 is a COSY 45° of the phenanthro-benzofurane (PBF) (Fig.30). The spectrum 9 is the corresponding NOESY spectrum We observe an additional correlation spot between the proton which is at 8.8 ppm and the proton which has a chemical shift of 8.6 ppm. This spot is termed A, it means a dipolar interaction between two protons **H_1** and **H_2**.

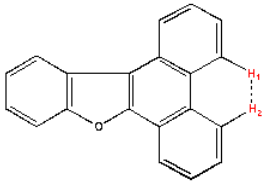
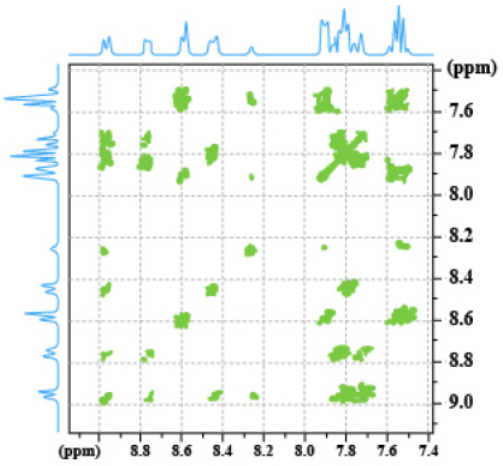
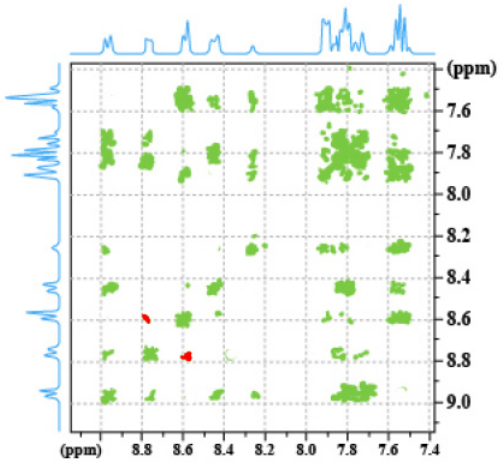


Fig. 30: The phenanthro-benzofurane. (PBF)



Spectrum 8: COSY spectrum of PBF



Spectrum 9: NOESY spectrum of PBF

Phase Sensitive COSY and NOESY

The TPPI technique (Time Proportional Phase incremantation) allows detection in a quadratic sequence. We may therefore solve the problem of the discrimination of the sign of the frequencies upon the detection of a free precession signal in an experiment of impulsional NMR There are other methods in the phase mode like the STATES technique where the detection is in simultaneous quadratic. It is easier to achieve a phased NOESY rather than a classical NOESY, because this technique is much more sensitive. Moreover, the correlation spots meaning a spatial vicinity are in the negative portion of the spectrum versus the correlation spots due to the spin-spin coupling. (5)

TOCSY and ROESY

These experiments are characterized by a mixing time during which the magnetization of a spin A, submitted to a radio wave frequency field B1 is transferred to a spin linked to A either by a dipolar coupling or by a scalar coupling. During the mixing time the magnetization is locked according to one direction of the space defined by the direction of the field B1 and the spin frequency shifting versus the main component. The block in the spin system is commonly named spin-lock (2).

TOCSY or HOHAHA

This method allows to demonstrate scalar couplings. The pulse sequence scheme is given Fig. 23. The first 90°x impulsion rotates the magnetization vectors in the xOy plane, in which they freely evolve during the time t1, under the influence of their chemical shift and the scalar coupling constants. We apply then a spin lock on the x axis, that means a low power impulsion or set of impulsions whose duration represents the mixing time tm. During this time, the spin coherence of the system is exchanged. By increasing the mixing time we increase the number of the visible transitions. That is to say that within the same experiment, we get the informations of a COSY, of a LR COSY and of a relayed COSY. The pulse sequence widely used is base upon the MLEV-17 sequence which contains a set of 17 pulses. (5).

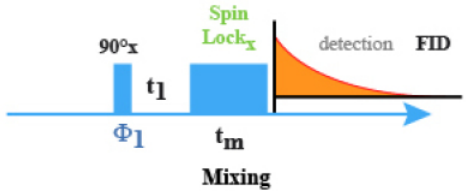
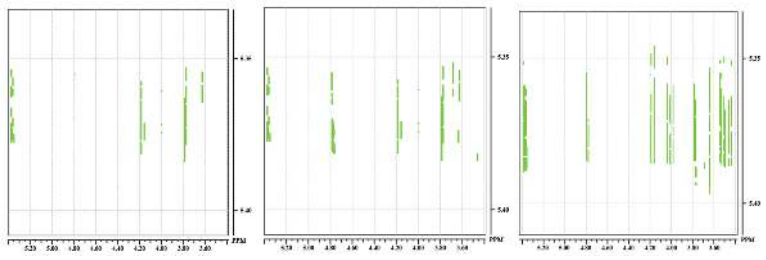


Fig 23: The pulse sequence TOCSY or HOHAHA

The spectrum 10 shows the result of three different mixing time for the saccharose (Fig. 29). These are given in milliseconds (20, 60, 100 ms). For each mixing time, we see the appearance of new correlation spots. There is thus an increase of the number of relays with the spin lock time. These ones correspond then to long range correlations.



Spectrum 10: 20 ms, 60 ms, 100 ms.

ROESY and CAMELSPIN

The aim of the dipolar correlation experiments in two dimensions is to take advantage of the vicinity in space of some nuclei. The result of this kind of experiment is a 2D map in which the signals outside of the diagonal arise from the Over Hauser enhancement effect between two space coupled nuclei (2) (Fig. 24).

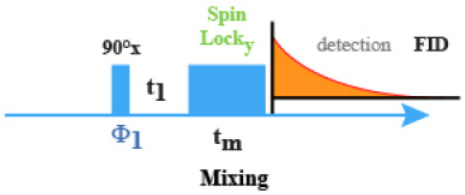


Fig. 24. The ROESY pulse sequence.

In this case, we apply a spin-lock onto the y axis. The correlation peaks arising from the ROE effect are on the opposite sign compared to the diagonal one their intensity is different from 0. However, the correlation peaks coming from a chemical exchange are of the same sign than the crossing one. The ROESY experiment allows by this way the separation of the contributions coming from the exchange and those coming from the dipolar interactions. The ROESY sequence is thus complementary of the NOESY one and it is more often used for the structural determination of the small molecules.

Homonuclear Correlations is shared under a CC BY-NC-SA 4.0 license and was authored, remixed, and/or curated by LibreTexts.

- **Homonuclear Correlations** by Marc Bria is licensed CC BY 4.0.

Indirect Detection

The advantages of the indirect detection

The reverse detection technique became increasingly popular due to the software improvements of the spectrometers from one hand and to the increase of the sensitivity of the detection of a X nucleus by the indirect way. In fact the reverse detection solves the problem of the low concentrations. Moreover, it allows to reach the NMR parameters such as chemical shifts, coupling constants and relaxation time spin lattice for nuclei impossible to study by the direct detection (Fig. 28).

For example it is not always obvious to get NMR spectra for nuclei such as ^{57}Fe, ^{183}W, ^{187}Os and sometimes even ^{15}N in direct observation. Consequently, the reverse detection becomes the only possible way either for ^{1}H-^{15}N correlation in the case of peptides or proteins or also for ^{1}H-X correlation in the case of organometallic compounds. In each of these examples the reverse detection allowed to determine the chemical shift of the heteronucleus together with the coupling constants $J_{(X-H)}$.

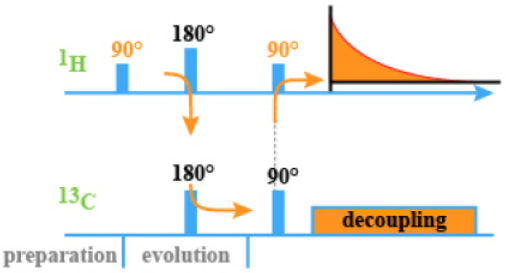


Fig. 28: Scheme for a reverse detection pulse sequence.

The arrows figure the magnetization transfer from the proton towards the ^{13}C and then from the ^{13}C towards the proton.

The available pulse sequences

The HSQC (*Heteronuclear Single Quantum Coherence*) is specially used for the structural determination of small proteins. The HMBC (*Heteronuclear Multiple Bond Coherence*) is optimized for long range couplings and works better than a COLOC.

Bibliography

1. La détection inverse en RMN ; M Boudonneu Analusis N°1, vol.18, 1990
2. La RMN concepts et méthodes; D. Canet inter éditions 1991
3. La spectroscope de RMN, H. Gunther MASSON 1994.
4. NMR in protein studies. M. P. Williamson. Chem. in Britain April 1991(335-337).
5. RMN 2D BRUKER 1993 Poly. 1, 2 et 3.
6. Resonance Magnétique Nucléaire; Evolution instrumentale et analyse de structure; J.P. Girault le technoscope de biofutur n°38 sept 90
7. Sensitivity enhancement by signal averaging in pulsed by Fourier transform NMR spectroscopy; D. L.Rabenteck; J. of Chem. Ed. Vol. 61, n°70, Oct 1984
8. Sequence Cosy Poly. BRUKER 1993.
9. Topic in chemical instrumentation part 3 and 4. 2 D Methods W. King and K. R. Williams J. of Chem. Educ. vol.67n°4.
10. Topics in chemical instrumentation (Definition) W. King and K. R. Williams
11. Two Dimensional NMR spectroscopy; Applications for chemists and biochemists; W. R. Crousmum, R. M. K. Carlson. Vol 9.
12. Two dimensional NMR Aspect 2000 - 3000 BRUKER
13. G. E. Reeman et Moms, J. ChemSoc, Chem.Comm, 684 (1978).
14. H. Kessler, W. Bernel and C. Giresinger, J. AM. Chem. Soc. 107, 1083 (1985).

Indirect Detection is shared under a CC BY-NC-SA 4.0 license and was authored, remixed, and/or curated by LibreTexts.

- **2D NMR: Indirect Detection** by Marc Bria is licensed CC BY 4.0.

7.2 J-Resolved

7.2 J-Resolved is shared under a CC BY-NC-SA 4.0 license and was authored, remixed, and/or curated by LibreTexts.

8: Multinuclear Magnetic Resonance Spectroscopy

8: Multinuclear Magnetic Resonance Spectroscopy is shared under a CC BY-NC-SA 4.0 license and was authored, remixed, and/or curated by LibreTexts.

Index

A

angular momentum
- 5.4: Theory

B

base peak
- Fragmentation Patterns in Mass Spectra

Bloch
- Bloch Equations

C

C13 NMR
- 6.1: Interpreting C-13 NMR Spectra

clark
- 6.1: Interpreting C-13 NMR Spectra

E

Electrospray Mass Spectrometry
- Electrospray Ionization Mass Spectrometry

energy level
- 5.2: Introduction

F

Fragmentation Pattern (Mass Spectroscopy)
- Fragmentation Patterns in Mass Spectra

Free Precession
- Bloch Equations

frequency
- Larmor Precession

I

Injection Stage (Mass Spec)
- Injection Stage

IR spectroscopy
- 3.2: IR Spectroscopy

Isotopomers
- 13C

L

Larmor
- Larmor Precession

Larmor Precession
- Larmor Precession

M

M+1 peak (mass spec)
- The M 1 Peak

Magnetization
- Bloch Equations

molecular ion
- Fragmentation Patterns in Mass Spectra
- The Molecular Ion (M^+) Peak

MRI
- 5.2: Introduction

N

NMR
- 5.2: Introduction
- 5.4: Theory

NMR spectroscopy
- 5.3: NMR Spectroscopy

Nuclear Shielding
- 5.2: Introduction

P

parent ion
- Fragmentation Patterns in Mass Spectra

Pascal's triangle
- Pascal's Triangle

Q

quadrupolar nuclei
- 5.2: Introduction

R

relaxation
- 5.2: Introduction
- Relaxation

S

selection rules
- 5.4: Theory

spin
- 5.2: Introduction
- 5.4: Theory

Spin Lattice Relaxation
- Relaxation

T

T1
- 5.2: Introduction
- Relaxation

T1rho
- Relaxation

T2
- 5.2: Introduction
- Relaxation

T2*
- Relaxation

Glossary

Sample Word 1 | Sample Definition 1

Detailed Licensing

Overview

Title: Introduction to Organic Spectroscopy

Webpages: 153

Applicable Restrictions: Noncommercial

All licenses found:

- CC BY-NC-SA 4.0: 61.4% (94 pages)
- CC BY-NC 3.0: 19.6% (30 pages)
- Undeclared: 7.8% (12 pages)
- CC BY-NC 4.0: 7.8% (12 pages)
- CC BY 4.0: 3.3% (5 pages)

By Page

- Introduction to Organic Spectroscopy - *CC BY-NC-SA 4.0*
  - Front Matter - *CC BY-NC-SA 4.0*
    - TitlePage - *Undeclared*
    - InfoPage - *Undeclared*
    - Table of Contents - *Undeclared*
    - Licensing - *Undeclared*
  - 1: Introduction to Organic Spectroscopy - *CC BY-NC-SA 4.0*
    - 1.1: 12.0 Introduction - *CC BY-NC-SA 4.0*
    - 1.2: 12.5 Spectroscopy and the Electromagnetic Spectrum - *CC BY-NC-SA 4.0*
    - 1.3: Electromagnetic Radiation - *CC BY-NC-SA 4.0*
    - 1.4: Introduction to Spectroscopy - *CC BY-NC-SA 4.0*
    - 1.5: The Power of the Fourier Transform for Spectroscopists - *CC BY-NC-SA 4.0*
    - 1.6: Time-resolved vs. Frequency Resolved - *CC BY-NC-SA 4.0*
  - 2: Mass Spectrometry - *CC BY-NC-SA 4.0*
    - 2.1: Introduction to Mass Spectrometry - *CC BY-NC 3.0*
    - 2.2: Mass Spectrometry - *CC BY 4.0*
    - 2.3: How the Mass Spectrometer Works - *CC BY-NC 4.0*
      - Electrospray Ionization Mass Spectrometry - *CC BY-NC-SA 4.0*
      - Injection Stage - *CC BY-NC-SA 4.0*
      - MALDI-TOF - *CC BY-NC-SA 4.0*
      - Mass Analyzers (Mass Spectrometry) - *CC BY-NC-SA 4.0*
    - 2.4: Interpretation of Mass Spectra - *CC BY-NC-SA 4.0*
      - 13C - *CC BY-NC 3.0*
      - Br and Cl - *CC BY-NC 3.0*
      - Fragmentation - *CC BY-NC 3.0*
      - Fragmentation Patterns in Mass Spectra - *CC BY-NC 4.0*
      - Molecular Ion and Nitrogen - *CC BY-NC 3.0*
      - Molecular Ions - *CC BY-NC 3.0*
      - Organic Compounds Containing Halogen Atoms - *CC BY-NC 4.0*
      - The M 1 Peak - *CC BY-NC 4.0*
      - The Molecular Ion (M^+) Peak - *CC BY-NC 4.0*
    - 2.5: Mass Spectrometry Problems - *CC BY-NC-SA 4.0*
      - LEGO Exercise - *CC BY-NC-SA 4.0*
    - 2.6: ESI-QTOF-MS Coupled to HPLC and its Application for Food Safety - *CC BY 4.0*
  - 3: Infrared Spectroscopy - *CC BY-NC-SA 4.0*
    - 3.1: Infrared Spectroscopy - *CC BY-NC-SA 4.0*
    - 3.2: IR Spectroscopy - *CC BY 4.0*
    - 3.3: Theory - *CC BY-NC-SA 4.0*
      - How an FTIR Spectrometer Operates - *CC BY-NC-SA 4.0*
      - Theory - *CC BY-NC-SA 4.0*
    - 3.4: ATR-FTIR - *CC BY-NC-SA 4.0*
    - 3.5: Instrumentation - *CC BY-NC-SA 4.0*
    - 3.6: Sample Handling - *CC BY-NC-SA 4.0*
    - 3.7: Interpreting Infrared Spectra - *CC BY-NC-SA 4.0*
    - 3.8: Interpreting Infrared Spectra - *CC BY-NC 3.0*
      - Carbon Nitrogen Bonds - *CC BY-NC 3.0*
      - IR Table of Organic Compounds - *CC BY-NC 3.0*
      - IR2. Hydrocarbon Spectra - *CC BY-NC 3.0*
      - IR3. Subtle Points of IR Spectroscopy - *CC BY-NC 3.0*
      - IR4. Carbon Carbon Multiple Bonds - *CC BY-NC 3.0*
      - IR5. Carbon Oxygen Single Bonds - *CC BY-NC 3.0*

        - IR6. Carbon Oxygen Double Bonds - *CC BY-NC 3.0*
        - IR8. More Complicated IR Spectra - *CC BY-NC 3.0*
        - IR9. Misleading Peaks - *CC BY-NC 3.0*
        - IR10. More Practice with IR Spectra - *CC BY-NC 3.0*
        - What Does an IR Spectrum Look Like? - *CC BY-NC 3.0*
    - 3.9: Interpretation - *CC BY-NC-SA 4.0*
    - 3.10: Identifying the Presence of Particular Groups - *CC BY-NC 4.0*
    - 3.11: Infrared Spectra of Some Common Functional Groups - *CC BY-NC-SA 4.0*
    - 3.12: Application - *CC BY-NC-SA 4.0*
- 4: Conjugated Compounds and Ultraviolet Spectroscopy - *CC BY-NC-SA 4.0*
    - Front Matter - *Undeclared*
        - TitlePage - *Undeclared*
        - InfoPage - *Undeclared*
    - 4.1: Chapter Objectives - *CC BY-NC-SA 4.0*
    - 4.2: 14.0 Introduction - *CC BY-NC-SA 4.0*
    - 4.3: Molecular Orbital Theory - *CC BY-NC-SA 4.0*
    - 4.4: Allylic Carbocations - *CC BY-NC-SA 4.0*
    - 4.5: 14.3 Kinetic vs. Thermodynamic Control of Reactions - *CC BY-NC-SA 4.0*
    - 4.6: 14.4 The Diels-Alder Cycloaddition Reaction - *CC BY-NC-SA 4.0*
    - 4.7: 14.5 Characteristics of the Diels-Alder Reaction - *CC BY-NC-SA 4.0*
    - 4.8: Natural and Synthetic Rubbers - *CC BY-NC-SA 4.0*
    - 4.9: Ultraviolet Spectroscopy - *CC BY-NC-SA 4.0*
    - 4.10: The Effect of Conjugation - *CC BY-NC-SA 4.0*
    - 4.11: 14.9 Conjugation, Color, and the Chemistry of Vision - *CC BY-NC-SA 4.0*
    - 4.12: UV-Visible Spectroscopy - *CC BY 4.0*
    - Back Matter - *Undeclared*
        - Index - *Undeclared*
- 5: Proton Nuclear Magnetic Resonance Spectroscopy (NMR) - *CC BY-NC-SA 4.0*
    - 5.1: Nuclear Magnetic Resonance Spectroscopy - *CC BY-NC-SA 4.0*
    - 5.2: Introduction - *CC BY-NC-SA 4.0*
    - 5.3: NMR Spectroscopy - *CC BY 4.0*
    - 5.4: Theory - *CC BY-NC-SA 4.0*
        - Bloch Equations - *CC BY-NC-SA 4.0*
        - Larmor Precession - *CC BY-NC-SA 4.0*
        - NMR Interactions - *CC BY-NC-SA 4.0*
        - Quantum Mechanic Treatment - *CC BY-NC-SA 4.0*
        - Relaxation - *CC BY-NC-SA 4.0*
        - Rotations and Irreducible Tensor Operators - *CC BY-NC-SA 4.0*
    - 5.5: The Nature of NMR Absorptions - *CC BY-NC-SA 4.0*
    - 5.6: Interpretation - *CC BY-NC-SA 4.0*
    - 5.7: Interpretation - *CC BY-NC-SA 4.0*
        - Integration in NMR - *CC BY-NC-SA 4.0*
        - Pascal's Triangle - *CC BY-NC-SA 4.0*
    - 5.8: Structural Assignment - *CC BY-NC-SA 4.0*
        - (n 1) Rule - *CC BY-NC-SA 4.0*
        - Background to C-13 NMR - *CC BY-NC 4.0*
        - Determine Structure with Combined Spectra - *CC BY-NC 3.0*
        - High Resolution Proton NMR Spectra - *CC BY-NC 4.0*
        - Integration in Proton NMR - *CC BY-NC 3.0*
        - Interpreting C-13 NMR Spectra - *CC BY-NC 4.0*
        - Introduction to Proton NMR - *CC BY-NC 4.0*
        - Low Resolution Proton NMR Spectra - *CC BY-NC 4.0*
        - More About Electronics - *CC BY-NC 3.0*
        - Multiplicity in Proton NMR - *CC BY-NC 3.0*
        - NMR Appendix. Useful Charts for NMR identification - *CC BY-NC 3.0*
        - NMR2. Carbon-13 NMR - *CC BY-NC 3.0*
        - NMR3. Symmetry in NMR - *CC BY-NC 3.0*
        - NMR4. 13C NMR and Geometry - *CC BY-NC 3.0*
        - NMR5. 13C NMR and Electronics - *CC BY-NC 3.0*
        - NMR8. Chemical Shift in 1H NMR - *CC BY-NC 3.0*
        - NMR11. More About Multiplicity - *CC BY-NC 3.0*
        - NMR14. More Practice with NMR Spectroscopy - *CC BY-NC 3.0*
    - 5.9: Active Learning with NMR - *CC BY-NC-SA 4.0*
        - In-Class Questions - *CC BY-NC-SA 4.0*
            - Set 1 – Basic Concepts - *CC BY-NC-SA 4.0*
            - Set 2 – Energy Transition and Population - *CC BY-NC-SA 4.0*
            - Set 3 – Electron Shielding - *CC BY-NC-SA 4.0*
            - Set 4 – Nuclear Coupling - *CC BY-NC-SA 4.0*
            - Set 5 – Exchange Effects - *CC BY-NC-SA 4.0*
            - Set 6 – Classical Description - *CC BY-NC-SA 4.0*
        - Instructor's Manual - *CC BY-NC-SA 4.0*
        - Learning Objectives - *CC BY-NC-SA 4.0*
        - Text - *CC BY-NC-SA 4.0*
    - 5.10: Chemical Shifts - *CC BY-NC-SA 4.0*

- 5.11: \(^1H\) NMR Spectroscopy and Proton Equivalence - *CC BY-NC-SA 4.0*
- 5.12: Chemical Shifts in \(^1H\) NMR Spectroscopy - *CC BY-NC-SA 4.0*
- 5.13: Integration of Proton Spectra - *CC BY-NC-SA 4.0*
- 5.14: Spin-Spin Splitting in \(^1H\) NMR Spectra - *CC BY-NC-SA 4.0*
- 5.15: Chemical Equivalence - *CC BY-NC-SA 4.0*
- 5.16: More Complex Spin-Spin Splitting Patterns - *CC BY-NC-SA 4.0*
- 5.17: Uses of \(^1H\) NMR Spectroscopy - *CC BY-NC-SA 4.0*

6: Carbon-13 NMR Spectroscopy - *CC BY-NC-SA 4.0*

- 6.1: Interpreting C-13 NMR Spectra - *CC BY-NC 4.0*
- 13.4 \(^13C\) NMR Spectroscopy: Signal Averaging and FT-NMR - *CC BY-NC-SA 4.0*
- 13.5 Characteristics of \(^13C\) NMR Spectroscopy - *CC BY-NC-SA 4.0*
- 13.7 Uses of \(^13C\) NMR Spectroscopy - *CC BY-NC-SA 4.0*

7: Two-Dimensional NMR Spectroscopy - *CC BY-NC-SA 4.0*

- 7.1: 2D NMR - *CC BY-NC-SA 4.0*
  - 2D NMR Background - *CC BY-NC-SA 4.0*
  - 2D NMR Basics - *CC BY-NC-SA 4.0*
  - 2D NMR Experiments - *CC BY-NC-SA 4.0*
  - 2D NMR Introduction - *CC BY-NC-SA 4.0*
  - Heteronuclear Correlations - *CC BY-NC-SA 4.0*
  - Homonuclear Correlations - *CC BY-NC-SA 4.0*
  - Indirect Detection - *CC BY-NC-SA 4.0*
- 7.2 J-Resolved - *CC BY-NC-SA 4.0*
- 13.6: DEPT ^{13}C NMR Spectroscopy - *CC BY-NC-SA 4.0*

8: Multinuclear Magnetic Resonance Spectroscopy - *CC BY-NC-SA 4.0*

Back Matter - *CC BY-NC-SA 4.0*

- Index - *Undeclared*
- Glossary - *Undeclared*
- Detailed Licensing - *Undeclared*